MendelNet

Conference Brno 2021

Editors:

Radim Cerkal

Natálie Březinová Belcredi

Lenka Prokešová

Proceedings of 28th
International PhD Students Conference

10 November 2021, Brno, Czech Republic

Mendel University in Brno
Faculty of AgriSciences

MendelNet 2021

Proceedings of 28th International PhD Students Conference
10 November 2021, Brno, Czech Republic

Editors: Radim Cerkal, Natálie Březinová Belcredi, Lenka Prokešová

The MendelNet 2021 conference would not have been possible without the generous support of The Special Fund for a Specific University Research according to the Act on the Support of Research, Experimental Development and Innovations and the **support of**:

BIOMIN Czech s.r.o.

kontroluje.me

PELERO CZ o.s.

Profi Press s.r.o.

Research Institute of Brewing and Malting, Plc.

All contributions of the present volume were peer-reviewed by two independent reviewers. Acceptance was granted when both reviewers' recommendations were positive.

ISBN 978-80-7509-821-4

Scientific Committee:

Assoc. Prof. Ing. Radim Cerkal, Ph.D. (Chair)
Prof. Ing. Radovan Pokorný, Ph.D.
Prof. Ing. Gustav Chládek, CSc.
Assoc. Prof. Ing. Radovan Kopp, Ph.D.
Assoc. Prof. Ing. Josef Suchomel, Ph.D.
Prof. Dr. Ing. Milada Šťastná
Assoc. Prof. Ing. Šárka Nedomová, Ph.D.
Assoc. Prof. Ing. Pavel Hanáček, Ph.D.
Prof. MVDr. Zbyšek Sládek, Ph.D.
Assoc. Prof. Ing. Vojtěch Kumbár, Ph.D.
Assoc. Prof. RNDr. Ondřej Zítka, Ph.D.

Organizing Committee:

Ing. Natálie Březinová Belcredi, Ph.D. (Chair)
Ing. Lucie Melišová, Ph.D.
Ing. Lenka Prokešová
Mgr. Patrik Vacek

PREFACE

Each year, the editors of the volume you are about to read are tasked with the responsibility of putting a coherent form to the proceedings from MendelNet, the international PhD Students Conference of the Faculty of AgriSciences of Mendel University in Brno.

The event which reached, this year, on November 10, 2021, its 28th edition, is traditionally aimed at both under and postgraduate students from the Czech Republic, Europe and beyond, and proudly welcomes the participants of various professional and cultural backgrounds. And while this time the people could not gather on-site due to globally-imposed covid-19 restrictions, the conference swiftly transformed itself into a virtual and fascinating beehive of results, opinions and brand new research paths and ideas.

Here in Brno, under the spell of great genetician G. J. Mendel and the guidance of skilled senior researchers and supervisors, students can introduce, defend and discuss their scientific results while those who do not feel confident enough to present and pen their paper in English are invited to join as spectators and follow-up discussion participants.

The best submissions are, after rigorous peer-review process, collected here and range from plant and animal production to fisheries and hydrobiology to wildlife research while agroecology and rural development, food technology, plant and animal biology, techniques and technology and applied chemistry and biochemistry also belong to the core areas being investigated.

The collection as varied and huge as this can succeed only as a team effort, both on authors' and editors' side, so we would like to express our thanks and gratitude to all committees and reviewers both for their outstanding work and invaluable comments and advice.

The Editors

TABLE OF CONTENTS

PLANT PRODUCTION

ANIMAL PRODUCTION

FISHERIES AND HYDROBIOLOGY

WILDLIFE RESEARCH

AGROECOLOGY AND RURAL DEVELOPMENT

FOOD TECHNOLOGY

PLANT BIOLOGY

ANIMAL BIOLOGY

TECHNIQUES AND TECHNOLOGY

APPLIED CHEMISTRY AND BIOCHEMISTRY

PLANT PRODUCTION

Comparing of observed and simulated field crop production in HERMES2Go model at Hněvčeves locality

Jakub Bohuslav[1,2], Kurt Christian Kersebaum[2,4], Mikulas Madaras[3], Petr Hlavinka[1,2], Miroslav Trnka[1,2], Zdenek Zalud[1,2]
[1]Department of Agrosystems and Bioclimatology
Mendel University in Brno
Zemedelska 1, 613 00 Brno
[2]Global Change Research Institute CAS
Belidla 986/4a, 603 00 Brno
[3]Crop Research Institute
Drnovska 507/73
161 06 Praha 6 – Ruzyne
CZECH REPUBLIC
[4]Research Platform "Data Analysis & Simulation"
Leibniz Centre for Agricultural Landscape Research (ZALF)
Eberswalder Straße 84
15374 Müncheberg
GERMANY

xbohusl4@mendelu.cz

Abstract: The main objective of this study was calibration and testing of crop growth model HERMES2Go under long–term field experiment in Hněvčeves locality (coordinate 50°18´N, 15°43´E, altitude 265 m.a.s.l.). Observed data of yields and the other parameters like a weather data, soil parameters, management practice, phenology phases etc. monitored in last 38 years was used for model calibration. Input parameters were available for 4 different fertilizer practices: i) control, ii) manure, iii) mineral fertilizer and iv) manure together with mineral fertilizer on each plot. Observed data are available for yields of main and by–product and above ground biomass. The main grown crops were sugar beet, spring barley, winter wheat, silage maize, oat and alfalfa. Outputs of the model for main product are relatively accurate, but values of by–product requires additional calibration parameters settings together with above–ground biomass.

Key Words: HERMES2Go, long–term experiments, simulation, yield, field crops

INTRODUCTION

Long–term experiments can help to identify effects of different management including temporal changes and trends in soil properties, nutrient availability as well as production aspects. Stability of the yields is very important parameter. Main factors, that can negative change both yield quantity and quality are adverse weather conditions, unsuitable soil conditions, insufficient water and nutrients and also pests and diseases.

Simulations are important for crop production assessment under various conditions including changes in management or climate. Moreover, comparing simulated and observed values could be conducted for different soil conditions. Only reliable crop growth model could be used for predictions of yields and properties during the next decades. For this purpose, successful calibration and testing of the model are necessary. And this is exactly what long–term experiments are used for.

The main aim of this study is calibration of relevant HERMES2Go parameters to estimate yields (main products and by–products), and above ground biomass under four different fertilization management. To test crop growth model HERMES2Go observed data from long–term field experiment was used. This experiment started in 1980 at Hněvčeves locality and data series end in 2017.

MATERIAL AND METHODS

Characterization of growing locality, management of growing field crops, HERMES2Go

The Hněvčeves experimental station is located in district of Hradec Králové at 50°18´ north latitude and 15°43´ east longitude, an altitude of 265 m.a.s.l. Part of the experimental plots is located on a plain, part slightly sloping to the south. The soil type is classified as Luvisol (Czech taxonomic soil classification system), clay–loamy, the based substrate is loess, about 2.34% of humus.

For calibration and testing data for the years 1980–2017 were used. The main goal of this experiment is to compare different fertilization methods. Specifically, there are 4 variants: i) control (without any fertilization), ii) only manure, iii) only mineral fertilization and iv) combination of manure and mineral fertilizer. Different crops are alternated on the experimental plots, the order of which is introduced in Table 1. For years with alfalfa and silage maize growing, by–product data are missing, because it has been used as fodder. In some cases, post–harvest residues were left in the field, in others removed. Catch crop (mustard) was sown in 2005, 2008, 2013 and killed by autumn tillage. Weather data was used from the meteorological station, situated in experimental station.

All plots were managed by convention tillage, to a depth of approximately 24 cm for all time of experiments. Before sowing of each crop seedbed preparation was carried out. Manure was applied every 3–5 years, with amount approximately 40 t/ha. Manure was usually plough into soil in same day or in earliest possible date. Application of mineral fertilizer was applicated in common amount for this locality. For sugar beet between 100–150 kg/ha N, for silage maize 120–160 kg/ha N, for winter wheat 100–125 kg/ha N, spring barley 60–90 kg/ha N for growing season.

The model HERMES2Go is a next type of the HERMES model (Kersebaum 2007). The new version is much faster and have a progressive potential for space simulations. The main fundamentals and the aim of the model is the simulation of soil water and nitrogen dynamics in different agricultural plant–soil–systems. HERMES2Go includes main processes such as evaporation and transpiration, nitrate and water transport in the soil, nitrogen mineralisation and denitrification, development of crop including biomass and yield formation. Simulation is mainly for annual crops, which are defined by external parameter files. This parameter files were calibrated and tested, using data from long–term field experiments in Hněvčeves while HERMES2Go simulations were conducted as uninterrupted runs from 1980 to 2017 for each variant.

Table 1 The list of cultivated crops

Harvest year	Name of crop	Harvest year	Name of crop
1980	sugar beet	1999	alfalfa
1981	spring barley	2000	winter wheat
1982	oat + alfalfa	2001	silage maize
1983	alfalfa	2002	winter wheat
1984	winter wheat	2003	spring barley
1985	silage maize	2004	sugar beet
1986	winter wheat	2005	spring barley
1987	spring barley	2006	spring barley + alfalfa
1988	sugar beet	2007	alfalfa
1989	spring barley	2008	winter wheat
1990	oat + alfalfa	2009	silage maize
1991	alfalfa	2010	winter wheat
1992	winter wheat	2011	spring barley
1993	silage maize	2012	sugar beet
1994	winter wheat	2013	spring barley
1995	spring barley	2014	spring barley + alfalfa
1996	sugar beet	2015	alfalfa
1997	spring barley	2016	winter wheat
1998	spring barley + alfalfa	2017	silage maize

RESULTS AND DISCUSSION

Results comparing observed and simulated values for main and by–product and above–ground biomass are contained in next figures. In Figure 1 for control, in Figure 2 for manure, in Figure 3 for mineral fertilizer and in Figure 4 for manure + mineral fertilizer variant. The model works in dependency on used fertilizers for all crops, where the lowest yields were observed for the control and next for manure, mineral fertilizer and their combinations variants. In general, HERMES2Go simulated the highest yields for the variant with a combination of both fertilizations.

In the future, it is necessary to better understand relationship between soil and crops, because soil quality is declining, despite improvements in genetic and agronomic technologies, including used fertilization (Macholdt et al. 2019b). Combination NPK and manure fertilization is very important for stable yields under certain conditions for winter wheat. Variant with manure produced higher yield stability of winter wheat. There is also next positive aspect of manure depending on support soil properties, like a nutrient, physical, chemical and biological properties. The time of degradability nutrients depends on the composition of material and to the other factors, for example weather conditions like a precipitation or temperature during the year (Macholdt et al. 2019a).

For lower production risk and higher stability of yields is needed contributed with intensified level of fertilization. The yields stability and reduction production risk support additional application of manure (Macholdt et al. 2019b). Dry matter and nitrogen content in grain was clearly affected for the amount of N in manure and speed of mineralization (Doltra et al. 2011). But the study Abyaneh et al. (2017) shows that it is necessary to provide water and nitrate fertilizer to achieve maximum yield.

The amount of yield by–product was measured only for cereals and sugar beet. For cereals are data more clearly, but for sugar beet is more complicated correct parameter setting, because fluctuation of yield is more common in some years. In some cases, the values do not correspond to observed data. Straw yields for spring barley are relatively good. Unfortunately, in 2016 year, the weight of the by–product for winter wheat is missing, but it is in the end of period. About amount of by–side product is necessary further development and improvement.

The values for total above–ground biomass contain different results compared to the observed values. This is also caused by a wrong by–product calculation. In the future, more focus is needed on the correct calibration yields of post–harvest residues, if data will be available.

Weaknesses and strengths for different performance model is identify by application unlike indices. Different results between models suggest another need of calibration, although for some parameters the outputs are sufficiently good (Kersebaum 2007).

Quality and quantity of all product is influenced by many different factors. Fertility and sustainability of the soil can be mirrored in the crop yields. Pests, crop disease, weeds in a greater extend can negatively reduce yields (Johnston and Poulton 2018). Observed data in some case have a difference in the amount of yield compared to the model. This can be caused by incorrect measurements or damage plants. The main factor, that can change yields of grain are primary fertilizer combination (43%), weather conditions in vegetable period (40%) a level of fertilization (17%) (Macholdt et al. 2019a).

But if we have a data for long period, years with considerable damage are more apparent. Model is necessary calibrated for annual values over the years. Change parameter files for each crop can help for better outputs of main product, by–product and a above ground biomass, depending on the observed data for individual phenological phases.

Overall results of the comparison of 15 models show, that it is better to compare longer period of simulation, instead of one–year simulation. In this case, the conditions of water, soil and nutrients can be more accurately predicted, because the system follows each other through daily outputs (Kollas et al. 2015).

In the next step is also very important to include catch crops. It is necessary to obtain more available data in the future, because in addicted to climate change, their necessary inclusion in sowing procedures can be expected. Especially for retain water in the soil, prevent wind and water erosion,

enrich the soil with biomass and subsequently improve conditions for major crops. Across different soil types and cropping system is possible effectively reduce N losses after condition using catch crop. Increasing N leaching from manure can be prevented by using suitable catch crops (Doltra et al. 2011).

It is necessary to use alternating systems of field crops and frequent measurement of soil conditions, especially for crops that have not been thoroughly researched so far (potatoes, sugar beets, oats, etc.) (Kersebaum and Nendel 2014).

Comparing many different models suggest urgency to use crop rotation altogether, in continuity, distribution resilience of cropping system to ecosystem services assuming change climate condition (Kollas et al. 2015).

Figure 1 Comparing observed and simulated values for control variant

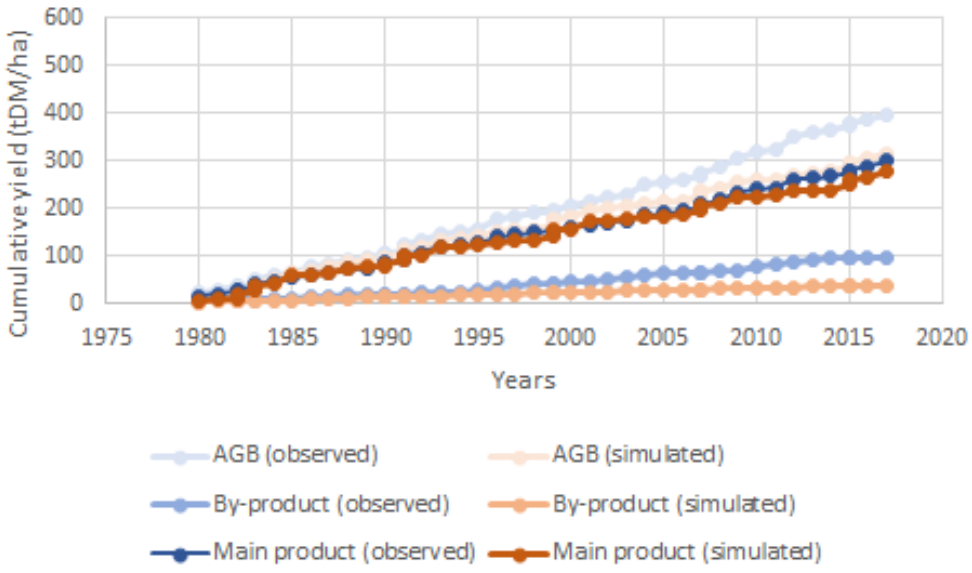

Figure 2 Comparing observed and simulated values for manure variant

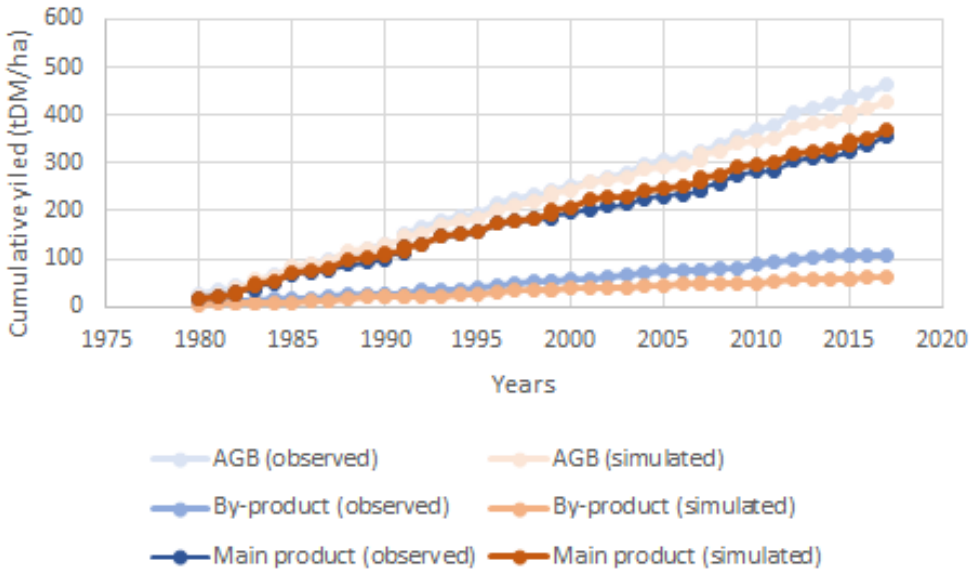

Figure 3 Comparing observed and simulated values for mineral fertilizer variant

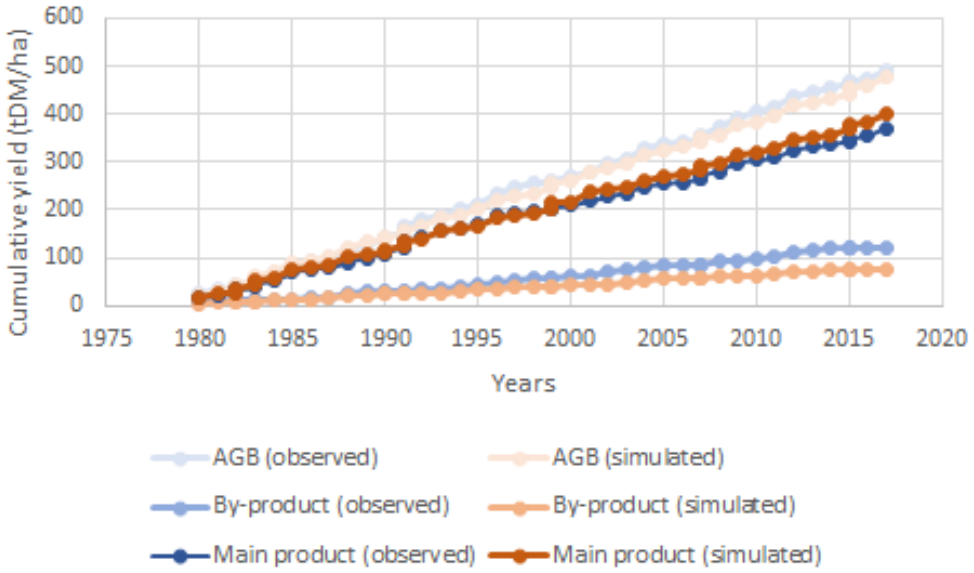

Figure 4 Comparing observed and simulated values for manure and mineral fertilizer variant

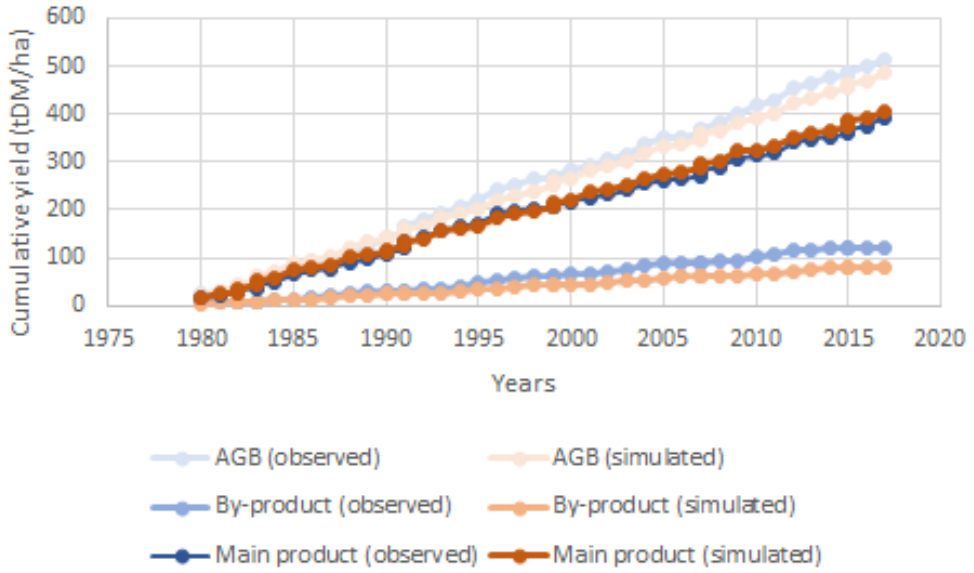

CONCLUSION

The HERMES model has undergone many significant changes over a long period of its development. Now, his parameters are constantly calibrated and validated according to the latest observed data and trends including to climate change or different management methods. In general, the parameters for the individual fertilization methods looks right, but this development also needs to be further improved. Especially for crops such as alfalfa, sugar beet or silage maize. Their rapid increase in biomass represent difficult parameters for the model in the form of correct determination of the weight of yields. Improving and developing model is addicted to high–quality experimental data. A properly set model is able to warn of the impending agronomic risk in the production of agricultural commodities and it is necessary to continue in model development.

The Hněvčeves locality is first locality for HERMES2Go calibration and testing in the Czech Republic, which is based on data from long–term field experiment. This is the beginning of the development system for adaptation measures in the Czech Republic. In the future, similar treatments within another 4 locations with long–term experiments will be conducted.

ACKNOWLEDGEMENTS

The research was financially supported by the SustES project – Adaptation strategies for sustainable ecosystem services and food security under adverse environmental conditions (CZ.02.1.01/0.0/0.0/16_019/0000797).

REFERENCES

Abyaneh, H.Z. et al. 2017. Effect of regulated deficit irrigation, partial root drying and N–fertilizer levels on sugar beet crop (*Beta vulgaris* L.). Agricultural Water Management, 194: 13–23.

Doltra, J. et al. 2011. Ceobserved yield and quality as affected by nitrogen availability in organic and conventional arable crop rotations: A combined modeling and experimental approach. European Journal of Agronomy, 34(2): 83–95.

Kersebaum, K.C. 2007. Modelling water and nutrient dynamics in soil–crop systems. Nutrient Cycling in Agroecosystems, 77: 39–52.

Kersebaum, K.C., Nendel, C. 2014. Site–specific impacts of climate change on wheat production across regions of Germany using different CO2 response functions. European Journal of Agronomy, 52: 22–32.

Kollas, C. et al. 2015. Crop rotation modelling—A European model intercomparison. European Journal of Agronomy, 70: 98–111.

Macholdt, J. et al. 2019a. Mineral NPK and manure fertilisation affecting the yield stability of winter wheat: Results from a long–term field experiment. European Journal of Agronomy, 102: 14–22.

Macholdt, J. et al. 2019b. Does fertilization impact production risk and yield stability across an entire crop rotation? Insights from a long–term experiment. Field Crops Research, 238: 82–92.

Modelling the onset of phenological phases of spring barley (*Hordeum vulgare* L.)

Petra Dizkova[1, 2], Lenka Bartosova [1, 2], Lenka Hajkova[2, 3], Jan Balek[1, 2], Monika Blahova[1, 2], Jakub Bohuslav[1, 2], Eva Pohankova[1, 2], Miroslav Trnka[1, 2], Zdenek Zalud[1, 2]

[1]Department of Agrosystems and Bioclimatology
Mendel University in Brno
Zemedelska 1, 613 00 Brno
[2]Global Change Research Institute CAS
Belidla 986/4a, 603 00 Brno
[3]Czech Hydrometeorogical Institute
Na Sabatce 2050/17, 143 06 Praha 4 – Komorany
CZECH REPUBLIC

xdizkova@mendelu.cz

Abstract: The onset of phenological phases of plant species is influenced mainly by air temperature. Each phenophase has its temperature limits (base temperature and temperature sum), which must be reached for each phase to occur. With knowledge of these limits, it is possible to predict the onset of phenological phases in localities where only meteorological data are available and also in future climate conditions. In this work, we used phenological ground-based data from 33 stations within the Czech Republic to calculate the most relevant meteorological predictors. PhenoClim software was used for phenological and meteorological data calibration and modelling. The smallest error that allows us to predict the term of the phenophases was found for the heading of spring barley (*Hordeum vulgare* L.), as the best predictor was the maximum daily temperature and the statistical error was 3.6 days.

Key Words: phenology, temperature, PhenoClim, climate parameters

INTRODUCTION

Spring barley (*Hordeum vulgare* L.) is one of the most cultivated field crops in the Czech Republic. The monitoring of field crops and the ability to detect and predict specific phenological phases can optimise agrotechnical interventions, such as fertiliser and pesticide applications or irrigation. This can help reduce the use of chemicals and lead to more sustainable management (Mercier et al. 2020).

The phenology of plants is influenced by solar radiation, precipitation totals and air humidity (Fu et al. 2020). However, the main factors influencing the onset of the phenological phases are air temperature, length of photoperiod and water availability (Oteros et al. 2015), with air temperature being the most significant (Fu et al. 2020). First of all, the plants need a certain minimum temperature for their growth and development (Středová et al. 2017). Below this temperature, the phenological development ceases; this is called the base temperature (T_b) (Salazar-Gutierrez et al. 2013) – in this paper indicated as T_{base}. Next, the onset of a certain phenological phase requires the sum of effective temperatures (SET) (Bartošová et al. 2010) which will be represented by T_{sum} in this paper. The importance of the use of temperature sums for modelling phenological phases or phenological periods of field crops can be noted in recent studies. For example, modelling based on temperature sums was performed in Denmark with a focus on predicting the historical harvest dates of winter wheat and spring barley (Pullens et al. 2021). In Argentina, they modelled the onset of the phenological phase grain filling of barley based on temperature sums (Otero et al. 2021).

Knowledge of the dynamics of the development of field crops is important in terms of proper agricultural technology and thus in achieving yields (Sujetoviene et al. 2018). Also, the knowledge of temperature thresholds (T_{base} and T_{sum}) for each phenophase allows us to calculate possible terms

of plant development phases for localities or years where no in-situ data is available; these calculations can then be used for remote sensing data verification. In response to the changing climate and the effort to adapt to future climatic conditions, there are a number of studies dealing with the prediction of the onset of phenological phases according to different scenarios of the future climate even in Central Europe, including the Czech Republic (e.g. Olesen et al. 2012 or Eitzinger et al. 2013).

For this reason, the aims of this study were: (1) to process all available phenological data for spring barley that were observed within various localities in the Czech Republic; (2) to use phenological data and daily meteorological parameters and set the model for each phenophase based on T_{base} and T_{sum} (using software Phenoclim); and (3) to evaluate the best model (based on statistical parameters) and calculate the terms of phenophases for the years with missing values (within the observed localities) and fill the phenological observations for the period 1961 to 2020.

MATERIAL AND METHODS

In this study, we analysed the onset of phenological phases (emergence, tillering, first node, second node, heading, yellow ripeness and ripening) of spring barely (*Hordeum vulgare* L.) in the period 1968 to 2012 from 33 localities. In-situ data sets were obtained from stations of the Czech Hydrometeorological Institute (CHMI) and the Central Institute for Supervising and Testing in Agriculture (CISTA) (Figure 1 and Table 1). Yellow ripeness and ripening were analysed individually, because each of institutes observed a different specific phase throughout the period of ripening. Data availability differs within each locality and phenophase (Table 1). For analysis, the software PhenoClim was used.

This software makes it possible to model the onset of phenological phases in localities or time periods where we only know the meteorological parameters (Bartošová et al. 2010) or (Černá et al. 2012). For this study, an optimization method called Calibration/Validation was used in PhenoClim software. The process of estimating the onset of phenological phases using this tool can be divided into several steps. First, in-situ phenological data are required for data calibration and validation. Phenological data were used together with meteorological data, namely daily values of minimum and maximum air temperature (°C), sum of precipitation (mm) and global solar radiation ($MJ/m^2/day$). For each of phenophases, each of the meteorological parameters was analysed individually. The variable was the use of different combinations of stations and time periods. By testing different software settings (different combinations), the strongest predictor is found for each phenological phase, i.e., meteorological parameter on the basis of which the software is able to model onset of phenological phases. For each of these parameters, the sum of effective temperatures (T_{sum}) (or the sum of precipitation or of radiation) above the selected base temperature was calculated. T_{sum} means the sum of the daily average (maximum, minimum) temperatures exceeding the threshold when the threshold value is subtracted. Base temperature (T_{base}) and the corresponding sum of effective temperatures (T_{sum}) (precipitation or radiation) are the values that are needed to reach a certain phenological phase. In modelling, T_{base} is the temperature from which the software begins to calculate T_{sum}, needed to reach a certain phenophase.

Other result parameters that complete the full interpretation of the result include mean bias error (MBE), root mean square error (RMSE), and coefficient of determination (R^2). RMSE gives the value of the error (number of days), which defines the accuracy of the model and its ability to calculate the terms of phenological phases. The MBE value indicates whether the shift in the onset of phenological phases will be to an earlier or later date. Finally, the value of R^2 is the value of the coefficient of determination, which indicates the strength of the relationship between a particular phenological phase and a meteorological parameter. Based on the smallest RMSE, the strongest meteorological parameter (i.e., predictor) was determined along with its corresponding T_{base} and T_{sum}. Using these values, the terms of onset of phenological phases were modelled for two time periods (1961–1968 and 2011–2020) for which we have only meteorological data at the input localities. The period with available ground observations is specific for each locality, therefore the modelled period is also specific for each locality and phenological phase.

Figure 1 Phenological experimental sites from the Czech Hydrometeorological Institute (blue dots) and from the Central Institute for Supervising and Testing in Agriculture (red dots)

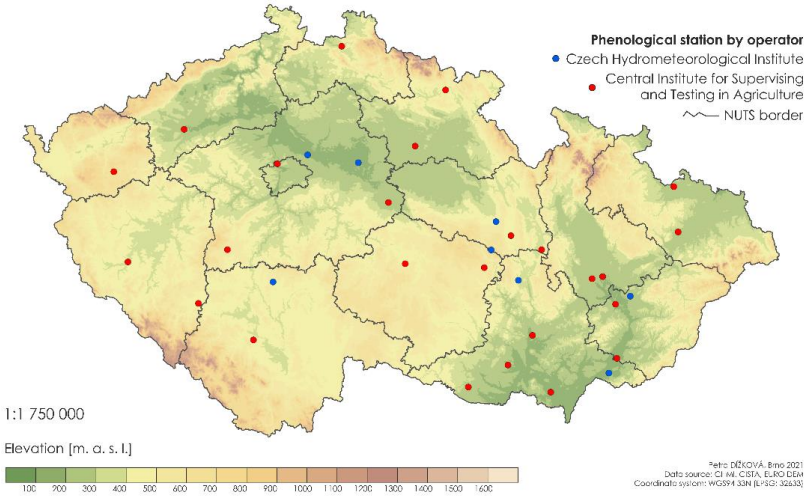

Table 1 Summary of basic information from two input data sets

	Czech Hydrometeorological Institute (CHMI)	Central Institute for Supervising and Testing in Agriculture (CISTA)
Number of stations	9	24
Available phenological phases	emergence, tillering, first node, second node, yellow ripeness	emergence, heading, ripening
Time period (years)	1984–2012	1968–2011
Altitude range (m.a.s.l.)	179–725	171–647

RESULTS AND DISCUSSION

Various model settings were tested for each phenological phase and each meteorological parameter (mean, maximum and minimum temperature, solar radiation and number of rainy days). An overview of all detected RMSE ranges and T_{base} and T_{sum} ranges is shown in Table 2, where the smallest RMSE values for each phenophase and each meteorological parameter are highlighted in grey. A smaller value of RMSE means a smaller deviation (greater accuracy) in modelling the onset of the phenological phase and therefore a more suitable predictor. For most phenophases, average and maximum daily air temperatures were found to be the best predictors.

The smallest uncertainty (errors of modelling) was found for the phenological phase of heading, when the predictor was the maximum air temperature with RMSE = 3.6 days, T_{base} = 6.1 °C and T_{sum} = 932.8 °C. For the first node, the predictor was solar radiation, and for the second node it was the minimum air temperature. The highest value of root mean square error, but still the best for this phenophase, was found in the phenological phase of emergence, where the predictor was the maximum air temperature with RMSE = 7.0 days, T_{base} = 6.0 °C and T_{sum} = 259.7 °C. The maximum air temperature was also found to be the strongest predictor for the phenological phases of yellow ripeness. For the phenological phases of tillering and ripening, the average air temperature was found to be the strongest predictor. RMSE = 5.9 days was found for tillering and RMSE = 4.3 days was found for ripening. In Germany, using a combination of genome-wide prediction and a phenology model, researches achieved RMSE values in the range of 3.1 to 5.6 days for modelling the phenophase heading of the spring barley (Uptmoor et al. 2017). Using calibration and cross-validation of the models, Pullens et al. (2021) reached RMSE = 5.5 days for maturity not only in spring barley but also in winter wheat.

Table 2 Overview of the range of RMSE, T_{base} and T_{sum} results for each phenological phase – the smallest RMSE values are highlighted in grey

		E (CHMI/CISTA)	T (CHMI)	FN (CHMI)	SN (CHMI)	H (CISTA)	YR (CHMI)	R (CISTA)
Tmean	RMSE (days)	8.8–10.1	5.9–9.9	6.7–9.8	6.4–9.8	4.1–8.5	5.7–10.6	4.3–9.4
	Tbase (°C)	0.0–3.6	0.5–5.3	0.8–6.2	0.4–6.4	0.0–5.0	0.0–5.2	0.0–4.7
	Tsum (°C)	144.6–349.0	181.2–512.1	299.1–753.3	365.7–891.0	537.4–1066.1	1006.4–1814.5	1173.9–1921.0
Tmax	RMSE (days)	7.0–9.3	6.7–10.4	7.1–11.2	7.1–11.7	3.6–8.7	5.5–14.0	4.6–9.1
	Tbase (°C)	3.4–7.9	4.3–7.8	0.7–9.1	0.1–8.8	1.7–8.3	0.0–6.2	1.8–7.1
	Tsum (°C)	184.4–400.0	328.1–579.3	464.6–1286.8	564.3–1493.6	730.2–1459.9	1607.1–2657.7	1635.0–2497.4
Tmin	RMSE (days)	12.2–14.3	7.2–12.6	7.2–11.9	6.2–11.2	6.1–10.7	6.4–9.1	6.7–14.3
	Tbase (°C)	0.0–6.1	0.0–2.7	0.0–3.9	0.0–5.3	0.0–0.9	0.0–3.8	0.0–0.4
	Tsum (°C)	4.9–126.8	85.9–226.8	163.1–367.6	133.3–446.8	410.2–524.7	583.1–1020.7	964.2–1096.1
Tmax–Tmin	RMSE (days)	11.6–18.7	9.8–25.0	11.7–29.7	12.1–31.0	12.9–17.6	13.2–53.3	13.8–18.9
	Tbase (°C)	0.0–5	0.0–6.8	0.0–6.4	0.0–4.6	0.0–4.4	0.0–2.3	0.0–0.9
	Tsum (°C)	306.7–742.5	286.3–967.8	417.0–1229.8	635.3–1303.3	761.7–1413.0	1354.6–1892.5	1823.1–2005.2
Srad	RMSE (days)	9.2–11.7	7.3–12.5	5.9–12.0	6.3–13.4	6.0–9.5	6.1–12.5	10.0–13.4
	Tbase (°C)	0.8–4.3	0.0–7.0	0.0–2.9	0.0–2.8	0.3–5.0	0.0–3.1	0.0–5.0
	Tsum (°C)	317.4–624.2	293.4–942.3	918.8–1320.4	973.7–1449.7	935.0–1654.2	1739.6–2371.1	1615.9–2676.3
Number of rainy days	RMSE (days)	26.0–32.6	24.8–32.1	24.4–31.4	23.6–31.3	23.0–30.9	23.7–49.4	30.6–43.6
	Tbase (°C)	0.0–0.0	0.0–8.8	0.0–8.4	0.0–7.5	0.0–5.9	0.0–6.4	0.0–0.0
	Tsum (°C)	48.2–54.9	2.8–59.7	4.5–70.8	6.2–74.5	8.8–87.0	13.2–106.5	112.7–120.9

Legend: E – emergence, T – tillering, FN – first node, SN – second node, H – heading, R – ripening, YR – yellow ripeness

Each station has its altitude and the total number of stations with available phenological data for heading was 11. By analysing the data observed and modelled for the phenological phase of heading, the value of R^2 has a decreases trend with increasing altitude, as shown by localities with different altitudes in Figure 2. This means that the correlation between the observed and modelled data decreases, which means that at higher altitudes, the model can make larger errors. Figure 3 shows randomly selected stations, which are only to be as an example of the specific relationship between the observed and modelled terms of the onset of heading on stations with different altitudes. However, there is still a strong relationship between the two parameters. High values of R^2 between the observed and predicted data for heading (R^2 = 0.72–0.83) of winter wheat were found in a study from the south-eastern USA (Salazar-Gutierrez et al. 2013).

Figure 2 The relationship between elevation and value of R^2 on stations with available data set for heading

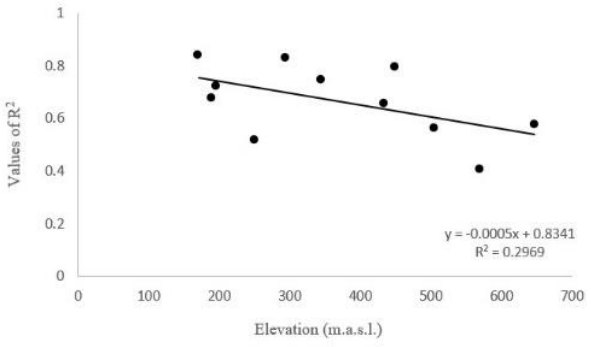

Figure 3 The relationship between selected observed and modelled terms of heading on stations at different elevations: Lednice (171 m.a.s.l.), Puste Jakartice (295 m.a.s.l.), Chrastava (345 m.a.s.l.), Lipa (505 m.a.s.l.)

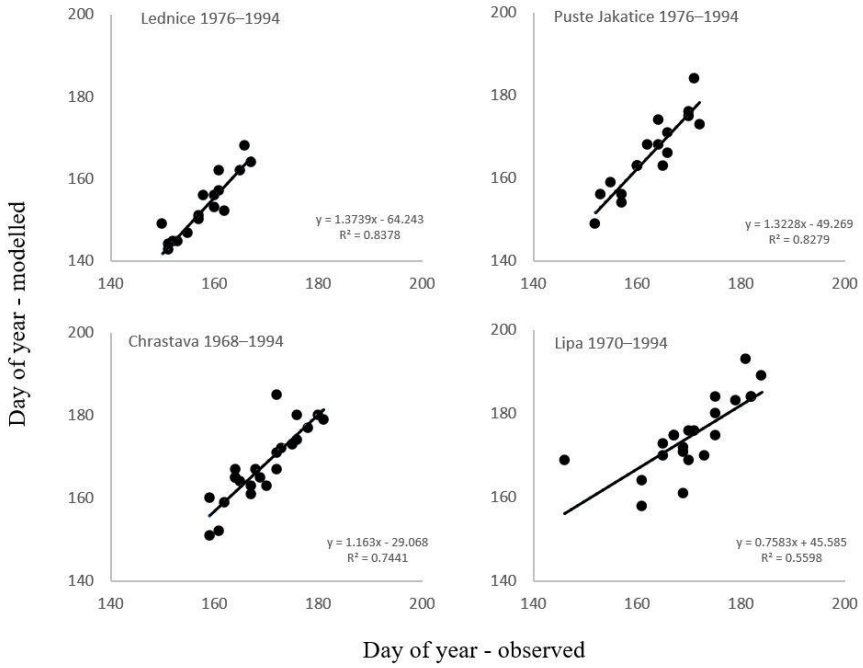

Based on the values of RMSE, T_{base} and T_{sum} of the best predictors, the onset of phenological phases were finally modelled for the years in which only meteorological data are known. We completed the whole period 1961 to 2020. Figure 4 shows an example of the onset of heading (observed and modelled) at four localities with different altitude in a given time period. The change in the onset of phenological phases (at all four experimental sites) show a shift to an earlier date by two to four days per decade (Lednice = 2.1 days, Puste Jakartice = 2.8 days, Chrastava = 2.9 days and Lipa = 3.5 days).

Figure 4 Course of observed and modelled terms of heading onset in the period 1961–2020 – using Tmax as a predictor of modelling with RMSE = 3.6 days, T_{base} = 6.1 °C and T_{sum} = 932.8 °C

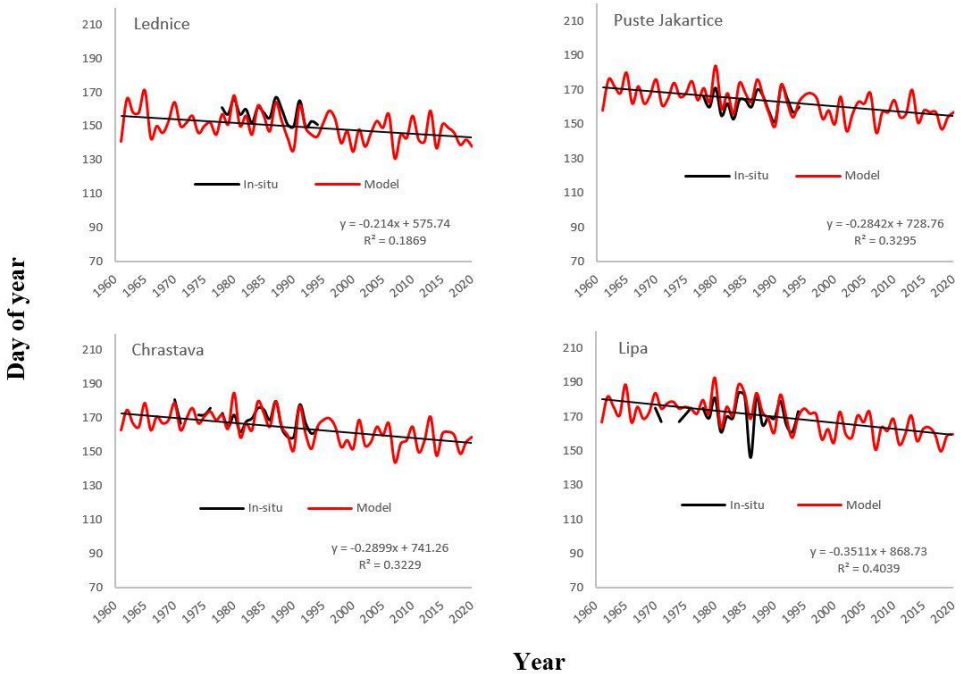

CONCLUSION

Ground-based phenological observations are still the most valuable in terms of data accuracy, but are limited by the demands on observers and provides information on a local scale. Based on the results of this study, it is possible to model the onset of phenological phases in localities and time periods where only meteorological data are available. Using the determined temperature limits, the PhenoClim software is able to model the onset of phenological phases with a relatively low error (depending on the given phenological phase) and to increase the spatial resolution of phenological observations. This study is the first step for follow-up work, which will address the possibility of determining the onset of phenological phases by combining multiple approaches: modelling based on temperature sums and the use of remote sensing data.

ACKNOWLEDGEMENTS

The research of the main author was financially supported by grant No. AF-IGA2021-IP036. The contributions of M. Trnka and J. Balek were funded by SustES project – Adaptation strategies for sustainable ecosystem services and food security under adverse environmental conditions (CZ.02.1.01/0.0/0.0/16_019/0000797), which also provided essential data and software access.

REFERENCES

Bartošová, L. et al. 2010. Klimatické faktory ovlivňující nástup a délku trvání fenofází vybraných rostlinných druhů na lokalitách jižní Moravy v letech 1961–2007. Acta Universitatis Agriculture et Silviculture Mendelianae Brunensis, 58(2): 1–10.

Černá, H. et al. 2012. The analysis of long-term phenological data of apricot tree (*Prunus armeniaca* L.) in southern Moravia during 1927–2009. Acta Universitatis Agriculture et Silviculture Mendelianae Brunensis, 60(3): 9–18.

Eitzinger, J. et al. 2013. Regional climate change impacts on agricultural crop production in Central and Eastern Europe – hotspots, regional differences and common trends. Journal of Agriculture Science, 151(6): 787–812.

Fu, Y. et al. 2020. Progress in plant phenology modeling under global climate change. Science China-Earth Sciences, 63(9): 1237–1247.

Mercier, A. et al. 2020. Evaluation of Sentinel-1 & 2 time series for predicting wheat and rapeseed phenological stages. ISPRS Journal of Photogrammetry and Remote Sensing, 163: 231–256.

Olesen, J.E. et al. 2012. Changes in time of sowing, flowering and maturity of cereals in Europe under climate change. Food Additives & Contaminants: Part A, 29(10): 1527–1542.

Otero, E.A. et al. 2021. Development of a precise thermal time model for grain filling in barley: A critical assessment of base temperature estimation methods from field-collected data. Field Crops Research, 260: 108003.

Oteros, J. et al. 2015. Variations in cereal crop phenology in Spain over the last twenty-six years (1986–2012). Climatic Change, 130: 545–558.

Pullens, J.W.M. et al. 2021. Temperature-based predictions of harvest date winter and spring cereals as a basis for assessing viability for growing cover crops. Field Crops Research, 264: 108085.

Salazar-Gutierrez, M.R. et al. 2013. Relationship of base temperature to development of winter wheat. International Journal of Plant Production, 7(4): 741–762.

Středová, H. et al. 2017. Long-term changes of vegetation season in context of spring barely phenology in South Moravia. Kvasný průmysl, 63(1): 11–15.

Sujetoviene, G. et al. 2018. Climate-change-related long-term historical and projected changes to spring barley phenological development in Lithuania. The Journal of Agriculture Science, 156(9): 1061–1069.

Uptmoor, R. et al. 2017. Combining genome-wide prediction and a phenology model to simulate heading date in spring barely. Field Crops Research, 202(15): 84–93.

The effect of milk thistle cultivation technology [*Silybum marianum* (L.) Gaertner] on the yield and contained compounds

Lucie Fojtikova[1], Marta Bradacova[1], Barbora Kudlackova[2], Marie Bjelkova[3], Helena Pluhackova[1]
[1]Department of Crop Science, Breeding and Plant Medicine
Mendel University in Brno
Zemedelska 1665/1, 613 00 Brno
[2]Institute of Analytical Chemistry of the Czech Academy of Sciences v.v.i.
Veveri 967/97, 602 00 Brno
[3]Agritec Plant Research,
Zemedelska 2520/16, 787 01 Sumperk
CZECH REPUBLIC

lucie.fojtikova@gmail.com

Abstract: The method of milk thistle cultivation can have a significant effect on both the yield and amount of contained compounds. The active complex of milk thistle is a mixture of flavonolignans composed of four compounds: silybin, isosilybinin, silychristin and silydianin. It is used as a cyto-protective agent for the treatment of liver disease, for the treatment and prevention of cancer and as a supportive medicine against green toadflax (*Amanita phalloides*) poisoning. Studies have also shown other therapeutic effects against cancer, diabetes, Alzheimer's and Parkinson's disease. Milk thistle is also significant by its oil content and composition. The aim of this study was to compare four cultivation variants with a treatment against dicotyledonous weeds using the registered product with selective postemergent effect and a wide spectrum efficacy against annual dicotyledonous weeds and certain other annual weeds with a combination of desmedifam active substances: desmedifam (4.35%), ethofumesate (6.94%), fenmedifam (5.56%) and lenacil (2.50%), in the text referred as “ethofumesate”, and combination with another product with the active substance chizalofop-p-ethyl. Weeding was also carried out in the plots and the importance of row width was evaluated. The results showed that the average yield of milk thistle achenes was 0.59–0.82 t/ha. The oil content varied in the range of 26.24–26.34% and the most important component of the silymarin complex was silychristin at the concentration 4.02–4.32 mg/g. Statistically significantly higher yield of achenes was found for variants 3 and 4. Higher average content of the silymarin complex was observed for variants 1 and 2. The oil content was higher in the achenes from experiment variants 3 and 4.

Key Words: milk thistle, oil, herbicide, cultivation technology, silymarin complex

INTRODUCTION

Milk thistle [*Silybum marianum* (L.) Gaertner] belongs to the Asteraceae family, it is a therapeutic medicinal herb with more than 2000 years long known history of use (Soleimani et al. 2019). The active complex of milk thistle is a mixture of flavonolignans composed of four compounds: silybin, isosilybinin, silychristin and silydianin. It is used as a cyto-protective agent for the treatment of liver disease, for the treatment and prevention of cancer (Rainone 2015).

Milk thistle achenes are able to keep the germination ability for up to 15 years, which leads to weeds in the subsequent crop. However, if a cereal crop follows the milk thistle, conventional herbicide control will reliably remove milk thistle weeds. Unsuitable follow-on crops are sunflower, root crops and rape (Habán et al. 2009).

In the autumn, medium tillage is carried out without organic fertiliser, only mineral fertilisers are added to the required level according to the soil chemistry. Early spring sowing is performed out at a soil temperature of 5°C (Karkanis et al. 2011). Optimum stands are those where the leaf rosette remains in the ground layer, the upper third of the plants are completely leafless, the plants have first

three flower heads at the same height, the leaf area dries out as the first flower heads mature, and the height of the stand is up to 150 cm. It is advisable to have 4–6 plants per linear meter, corresponding to a row width of 0.37 m to 0.40 m. The sowing rate is 8 kg/ha of seed, sown to a depth of 0.02–0.03 m. Weeder treatment can be carried out at the stage of 3–6 true leaves, rotary weeders can be used once the stand is established. Milk thistle is characterised by uneven ripening time of individual flower heads on the plant. Another disadvantage is the subsequent dropping of the hairy achenes from mature plants. The optimum harvest time must therefore be chosen, which is usually between July and September, when the fruit is at full biological maturity. The crop should have 30% overripe flower heads, recognisable in dry weather by the opening of the flower head and white fuzz. In wet weather the flower heads close, which is good for harvesting. It is done with a harvesting thresher with the suspensions of the thresher removed, cereal shakers are replaced with shakers for maize harvesting and the gap between the threshing basket and the drum is increased. The plants are still green at the time of harvest. The yield is based on the first 3–4 fully ripe flower heads on the plant. The achenes must be dried at a temperature of 45 °C at 12% humidity. The yield varies from 0.75 to 1 t/ha. The post-harvest residues can be crushed with a flail harvester or any other equipment capable of producing ploughable residues. Given the 20% post-harvest losses and the high germination rate of the pods, it is advisable to leave the seeds to germinate and to plough the field in the autumn after the plants have emerged as part of the autumn soil preparation (Andrzejewska et al. 2011).

The plant germinates at an optimum of 2–15 °C and the recommended sowing depth is 1–1.5 cm. Sowing takes place in autumn and spring and the row spacing is usually 40–75 cm, with 20–30 cm between plants in the row. Milk thistle is highly adaptable to many different growing conditions. The limiting factor in milk thistle production is weed interference. The nutrient requirements of this crop are low to medium, as it is adaptable to low quality soils. Milk thistle is considered drought tolerant and normal rainfall is often sufficient (Karkanis et al. 2011).

The active substances of milk thistle form the silymarin complex, a mixture of flavonolignans composed of four bioactive compounds: silybin, isosilybinin, silychristin and silydianin. Most food supplements are standardized according to their silibinin (often called silybin) content. Both silybin and isosilybinin are mixtures of two diastereomers, silybin A and B and isosilybinin A and B, respectively (Post-White et al. 2007).

MATERIAL AND METHODS

Variety and seeds

Mirel, purified and calibrated mercantile from the 2018 harvest with a germination rate of 94.5%. The Mirel variety has been legally protected since 2010, the rights holder is Moravol Ltd., based in Miroslavské Knínice. The seed used was mercantile from the 2018 trials (control variant) and was used with the consent of the sponsor of the trials, the Ministry of Agriculture of the Czech Republic.

Localisation and characteristics of the experimental site

The experiment was established at the site in Bratrušov (GPS coordinates: 49.990453N, 16.960289E). The locality of interest is characterized by a moderately warm climate with an average annual precipitation of 692 mm and an average annual temperature of 7.25°C. Precipitation is most frequently distributed in the months of June, July and August (Table 1).

Table 1 Weather course of Bratrušov locality in 2020 (January–October)

Meteorology data	April	May	June	July	August	September	October
Average temperature (°C)	9.9	11.6	16.9	17.1	18.6	13.9	9.5
Total precipitation (mm)	4.1	57.8	136.5	83.8	164.5	94.1	73.7

The area of Bratrušov is characterized by clay soil, illimerized, charred soil substrate with loess cover. The soil is well workable, moderately rich in nutrients, and has pH 5.4 with a medium humus content (Table 2). The average depth of the topsoil is 28 cm.

Table 2 Soil analyses from Bratrušov site

Sample identifier	N (Kjeldahl) [%]	P [mg/kg]	K [mg/kg]	Ca [mg/kg]	Mg [mg/kg]	pH
Bratrušov	0.135	55.1 (suitable)	120.94 (suitable)	1691	186.47 (good)	5.4

Experiment establishment

Smoothing: April 20th, 2020

Fertilisation: April 21st, 2020, NPK

Pre-sowing preparation: April 24th, 2020

Sowing: April 25th, 2020

Seed rate: 8 kg/ha

Table 3 Phenology phases: growth and development of milk thistle

Growth phase designation	Date:	Days from sowing
Emergence	May 6th	11
First pair of true leaves	May 21st	26
Leaf rosette	June 1st	37
Beginning of long-lived growth	June 19th	55
Butonisation	July 10th	76
Beginning of flowering	July 15th	81
10% of the growth still in bloom	August 6th	102
Blooming ended, beginning of ripening	August 15th	111
Maturity of the main flower head and first order flower heads	September 5th	133

The treatment during the growing season took place – first herbicide application: May 28th 2020, growth phase (first pair of true leaves), second herbicide application June 8st, 2020 growth phase (leaf rosette) (Table 3). Treatment against dicotyledonous weeds was performed on May 22nd, 2020 ethofumesat, dosage: 1.5 l/ha and June 1st, 2020 ethofumesat, dosage: 2 l/ha together with chizalofop-p-ethyl. A TECNOMA tractor mounted sprayer was used to apply herbicides. The insulation strips at the beginning and end of each plot were 0.5 m. The experiment was repeated four times and the total size of the experiment was 9 per 10 m, i.e. 90 m^2. For variant 1, commonly registered herbicides with a row range of 12.5 cm were used. For variant 2, double rows were used (range 25 cm), also with registered herbicides. Further, for variant 3, double rows were used (range 37 cm) together with registered herbicides and weeding at the emergence stage. Finally, for variant 4, double rows were used (range 37 cm) with registered herbicides and weeding at the beginning of leaf rose formation. The effect of experimental variant on yield-forming elements and quality parameters was studied.

The experiment with four different variants in four replications was established at the Bratrušov site in the Czech Republic. The yield of achenes was evaluated together with the weight of thousand seeds (WTS) and number of plants per linear meter. Furthermore, quality parameters were determined in obtained samples with respect to the variants of cultivation.

Date of harvest: September 15th, 2020. The experiment was harvested with a SAMPO Rosenlew small parcel harvester. Due to unfavourable weather conditions a large amount of moisture-increasing impurities was present in the harvested product at the time of harvest. Because of that, pre-cleaning was carried out immediately after the harvest and the harvested material was subsequently transferred to cold air drying. From each sample, 500 g was taken separately and the remaining part was cleaned.

Determination of was carried out according to ISO 461011 Part 28 (Testing of oilseeds - Determination of fat content), EN ISO 5509 (Preparation of fatty acid methyl esters), EN ISO 5508 (Analysis of methyl esters by gas chromatography) and EN ISO 542 (Oilseeds – Preparation of laboratory sample to analytical sample).

The silymarin complex content was determined by the means of ultrasonic extraction, sample weight 0.2 g weight, 5 min isooctane extraction to remove the oil followed by two 20 min extraction steps with 15 ml MeOH each. For HPLC analysis, following analytical method and conditions were used: Zorbax Eclipse C18 column, 150 x 4.6 mm i.d., 5 µm; isocratic elution, MeOH/Acetonitrile/

Water + 0.1% formic acid, 45/3/52 (v/v/v); mobile phase flow rate 0.7 ml/min; injection 5 µl; λ = 288 nm.

Statistical analysis

The obtained results were evaluated by single factor analysis of variance (ANOVA) followed by testing at a 95% ($P < 0.05$) level of significance using the Fisher LSD test. The data were processed using the STATISTICA CZ 12. Results are expressed as a mean value ± standard deviation (SD).

RESULTS AND DISCUSSION

Evaluation of selective effect of herbicides and weeding efficiency

First application was performed on May 28th. The cotyledons were fully developed and phytotoxicity was not detected, but gradual emergence of new weeds was observed. Second application was done on June 8th in the phase of four true leaves. Phytotoxicity was not detected, increase in new weeds was observed again, but these were subsequently overcome by milk thistle plants. The evaluation of weed infestation was carried out on June 26th. The weeds were present in limited numbers in the variants with wider rows, where there were more plants in a row per linear meter. In the variants with narrower rows and fewer plants per linear meter the weed infestation was greater. On July 29th the number of plants per linear meter was determined for all variants. Another evaluation of the experiment was carried out on August 9th. Plants in the variants with narrower rows (1 and 2) were higher and less branched. The average height was 2 to 2.5 m. In the variants with wider rows, the plants were shorter (1.7 m).

The effect of experimental variant on yield-forming elements and quality parameters

The yield of achenes was evaluated together with the WTS and number of plants per linear meter. Furthermore, quality parameters were determined in obtained samples with respect to the variants of cultivation.

Table 4 The effect of the treatment variant on yield, WTS and number of plants per m

Variant	1. (12.5 cm)	2. (25 cm)	3. (37 cm)*	4. (37 cm)**
Yield of achenes (t/ha)	0.59 ± 0.16 ^{a}	0.60 ± 0.18 ^{a}	0.82 ± 0.04 ^{b}	0.82 ± 0.09 ^{b}
WTS (g)	21.28 ± 3.99 ^{a}	23.02 ± 3.22 ^{a}	23.72 ± 2.90 ^{a}	23.25 ± 1.83 ^{a}
Number of plants per meter	1.90 ± 0.23 ^{a}	3.64 ± 0.30 ^{b}	4.21 ± 0.40 ^{c}	4.34 ± 0.31 ^{c}

*Legend: The average values marked with different letters in the rows differ statistically significantly at p = 0.05; *weeding at the emergence stage; **weeding at the beginning of leaf rose formation*

The results (Table 4) indicate that statistically significantly higher yield of achenes was found for variants 3 and 4, i.e. those with row width 37 cm (0.82 t/ha) with a lower standard deviation compared to variants 1 and 2 (0.59 and 0.60 t/ha). There were no statistically significant differences found among the weights of thousand seeds.

Table 5 The effect of treatment variant on oil content and fatty acid spectrum

Variant		1. (12.5 cm)	2. (25 cm)	3. (37 cm)*	4. (37 cm)**
Oil content (%)		26.24 ± 0.09 ^{b}	26.11 ± 0.09 ^{a}	26.34 ± 0.08 ^{b}	26.29 ± 0.06 ^{b}
Content [%]	Palmitic acid	10.75 ± 0.06 ^{b}	10.68 ± 0.17 ^{b}	10.45 ± 0.13 ^{a}	10.38 ± 0.10 ^{a}
	Stearic acid	5.40 ± 0.08 ^{b}	5.20 ± 0.29 ^{b}	4.93 ± 0.13 ^{a}	5.28 ± 0.13 ^{b}
	Oleic acid	23.58 ± 0.13 ^{a}	23.43 ± 0.17 ^{a}	24.58 ± 0.05 ^{b}	24.40 ± 0.08 ^{b}
	Linoleic acid	57.45 ± 0.06 ^{c}	57.43 ± 0.13 ^{c}	55.95 ± 0.13 ^{b}	55.33 ± 0.10 ^{a}
	Linolenic acid	0.53 ± 0.05 ^{a}	0.70 ± 0.08 ^{b}	1.45 ± 0.17 ^{c}	1.78 ± 0.05 ^{d}
	Octadecatetraenic acid	1.80 ± 0.08 ^{a}	1.98 ± 0.10 ^{b}	1.95 ± 0.06 ^{b}	2.13 ± 0.05 ^{c}
	Eicosenoic acid	0.55 ± 0.06 ^{a}	0.65 ± 0.06 ^{b}	0.73 ± 0.05 ^{b}	0.73 ± 0.05 ^{b}

*Legend: The average values marked with different letters in the rows differ statistically significantly at p = 0.05; *weeding at the emergence stage; **weeding at the beginning of leaf rose formation*

The oil content in the samples ranged from 26.11% to 26.34%. The most abundant fatty acid was linoleic acid, which was statistically significantly higher in the samples from variants 1 and 2 (57.45% and 57.43%, resp.). Samples from variants 1 and 2 also showed higher content of palmitic acid (10.75% and 10.68%, resp.). The stearic acid content in milk thistle samples varied in the range 4.93%–5.40%. On the other hand, the samples from variant 4 contained highest levels of linolenic and octadecatetraenoic acid (1.78% and 2.13%), resp. Both variant 3 and 4 showed higher amount of eicosenoic acid (0.73%) (Table 5).

Fathi-Achachlouei et al. (2009) reported an average oil content of 26–31% for milk thistle, which is consistent with the oil content observed in this work. The oil content can be influenced by several factors such as growing location and cultivation method, as well as storage conditions (Růžičková et al. 2011). Nasrollahi et al. (2016) compared the oil content in milk thistle samples obtained from different regions of Iran. These samples showed lower fat content of 21.28–25.61% compared to 26.11–26.34% in samples grown in Bratrušov.

Table 6 The effect of the treatment variant on content of the silymarin complex components (mg/g)

Variant	1. (12.5 cm)	2. (25 cm)	3. (37 cm)*	4. (37 cm)**
Silychristin	4.23 ± 0.37 ab	4.32 ± 0.30 b	4.01 ± 0.18 a	4.02 ± 0.17 a
Silydianin	0.23 ± 0.11 ab	0.32 ± 0.08 b	0.30 ± 0.11 b	0.19 ± 0.04 a
Silybin A	3.49 ± 0.31 a	3.53 ± 0.23 a	3.31 ± 0.15 a	3.33 ± 0.12 a
Silybin B	4.18 ± 0.36 b	4.27 ± 0.28 b	3.96 ± 0.17 a	3.99 ± 0.14 ab
Isosilybin A	1.44 ± 0.13 ab	1.51 ± 0.11 b	1.38 ± 0.07 a	1.37 ± 0.05 a
Isosilybin B	0.41 ± 0.03 ab	0.43 ± 0.03 b	0.41 ± 0.02 ab	0.39 ± 0.01 a

*Legend: The average values marked with different letters in the rows differ statistically significantly at p = 0.05; *weeding at the emergence stage; **weeding at the beginning of leaf rose formation*

Milk thistle is important not only for its spectrum of fatty acids, but especially for its flavonolignans. Silychristin was the most abundant of the silymarin complex components and its content was statistically significantly higher in variants 1 and 2 (4.23 and 4.32 mg/g, resp.). The content of silybin B was also higher in these variants (4.18 and 4.27 mg/g, resp.) (Table 6).

Quantitative and qualitative evaluation of silymarin complex compounds in milk thistle was also carried out by Habán et al. (2021). These authors reported that in 2015 and 2016 the content of silychristin was 3.18 ± 0.06 g/kg, silybin 0.91 ± 0.01 g/kg, silybin A 3.06 ± 0.06 and silybin B 7.04 ± 0.07. Albassam et al. (2017) reported the following contents of selected silymarin complex components: silybin A 10.39 ± 3.21 µg/ml, silybin B 26.53 ± 20.2 µg/ml, isosilybin A 8.77 ± 2.35 µg/ml and isosilybin B 2.67 ± 1.18 µg/ml. In this case silybin B was also the most significant constituent.

CONCLUSION

The results indicate that the highest yield of achenes was achieved in the variant where the milk thistle was grown in 0.37 m rows and the average number of plants per linear meter in a row was 4.2. The results showed a positive effect of wider rows on the weight of a thousand seeds. As for individual components of the silymarin complex, higher average content was observed for variants 1 and 2 of the experiment. As for the yield, however, variants 3 and 4 showed more favourable results. Unlike the silymarin complex, the oil content was higher in the achenes from experiment variants 3 and 4. Linoleic acid was found to be the most significant fatty acid contained in milk thistle achenes (55.3%–57.5%). This acid belongs to so called „omega-6“ fatty acids, a group of essential fatty acids which are an important dietary supplement. From the viewpoint of the use of oil cake as a priority raw material for pharmaceutical processing, it would be desirable to innovate the cultivation process to yield raw materials more suitable for pharmaceutical processing and for processing into food supplements.

ACKNOWLEDGEMENTS
The contribution has been supported by the programme of Regional Cooperation between the Regions and the Institutes of the Czech Academy of Sciences in 2021 (Project No. R200312101).

REFERENCES

Albassam, A.A. et al. 2017. The effect of milk thistle (*Silybum marianum*) and its main flavonolignans on CYP2C8 enzyme activity in human liver microsomes. Chemico-biological Interactions [Online], 271(1): 24–29. Available at: https://dx.doi.org/10.1016/j.cbi.2017.04.025. [2021-08-19].

Andrzejewska, J. et al. 2011. Effect of sowing date and rate on the yield and flavonolignan content of the fruits of milk thistle (*Silybum marianum* L. Gaertn.) on light soil in a moderate climate. Industrial Crops and Products [Online], 33: 463–468. Available at: https://doi.org/10.1016/j.indcrop.2010.10.027. [2021-10-09]

Fathi-Achachlouei, B. et al. 2009. Milk Thistle seed oil constituents from different varieties grown in Iran. Journal of the American Oil Chemists Society [Online], 86(7): 643–649. Available at: https://doi.org/10.1007/s11746-009-1399-y. [2021-08-19]

Habán, M. et al. 2009. Hodnotenie úrody a kvality drogy pestreca mariánskeho pestovaného v Zemedar, s. r. o. Poprad – Stráže. In Sborník příspěvků – 15. odborný seminár s medzinárodnou účasťou – Aktuální otázky pěstování léčivých, aromatických a kořeninových rostlin. December 14th, 2009, Brno, MZLU v Brně, pp. 83–90.

Habán, M. et al. 2021. Evaluation of variability of silymarin complex in Silybi mariani fructus harvested during two production years. European Pharmaceutical Journal [Online], 68(1): 40–45. Available at: https://doi.org/10.2478/afpuc-2020-0023. [2021-10-14].

Karkanis, A. et al. 2011. Cultivation of milk thistle (*Silybum marianum* L. Gaertn.), a medicinal weed. Industrial Crops and Products [Online], 34(1): 825–830. Available at: https://doi.org/10.1016/j.indcrop.2011.03.027. [2021-09-18].

Nasrollahi, I. et al. 2016. Study on *Silybum marianum* seed through fatty acids comparison, peroxide tests, refractive index and oil percentage. Pharmacognosy Journal [Online], 8(6): 595–597. Available at: https://doi.org/10.5530/pj.2016.6.13 [2021-09-18].

Post-White, J. et al. 2007. Advances in the Use of Milk Thistle (*Silybum marianum*). Integrative Cancer Therapies, 6(2): 104–109. Available at: https://doi.org/10.1177/1534735407301632. [2021-08-10]

Rainone, F. 2005. Milk thistle. American Family Physician [Online], 72(7): 1285–1292. Available at: https://www.aafp.org/afp/2005/1001/p1285.html. [2021-04-10].

Růžičková, G. et al. 2011. The yield and quality of milk thistle (*Silybum marianum* L. Gaertn.) seed oil from the perspective of environment and genotype - a pilot study. Acta Fytotechnica et Zootechnica, 14(1): 9–12.

Soleimani, V. et al. 2019. Safety and toxicity of silymarin, the major constituent of milk thistle extract: An updated review. Phytotherapy Research [Online], 33(6): 1627–1638. Available at: https://onlinelibrary.wiley.com/doi/10.1002/ptr.6361. [2021-09-15].

Yield formation parameters of winter wheat under two CO_2 levels in water sufficient and depleted environment

Marcela Hlavacova[1,4], Karel Klem[1,5], Barbora Vesela[5], Hana Findurova[5], Petr Hlavinka[1,4], Pavlina Smutna[3], Vladimira Horakova[6], Petr Skarpa[2], Miroslav Trnka[1,4]
[1]Department of Agrosystems and Bioclimatology
[2]Department of Agrochemistry, Soil Science, Microbiology and Plant Nutrition
[3]Department of Crop Science, Breeding and Plant Medicine
Mendel University in Brno
Zemedelska 1, 613 00 Brno
[4]Department of Climate Change Impacts on Agroecosystems
[5]Laboratory of Ecological Plant Physiology
Global Change Research Institute of the Czech Academy of Sciences
Belidla 986/4a, 603 00 Brno
[6]Central Institute for Supervising and Testing in Agriculture
Hroznova 65/2, 656 06 Brno
CZECH REPUBLIC

Marci.Hlava.22@gmail.com

Abstract: Agricultural production faces with ongoing climate that in Europe takes form of changing seasonal precipitation pattern with more frequent drought spells. These changes come on top of rising air temperature and did and will affect productivity as well as onset and duration of key developmental stages for yield formation of major staple crops such as wheat. In order to ensure stable agricultural production and satisfy demand of the increasing human population, it is crucial to know responses of major field crops to these abiotic stress factors to assess suitability of genotypes to specific environmental conditions. The aim of this study was to evaluate final yield formation parameters of five winter wheat genotypes cultivated in pots and exposed to two different levels of CO_2 concentrations (400 ppm as ambient and 700 ppm as elevated CO_2 concentrations) and two water treatments (well-watered control and drought-stressed plants). The experimental treatments were set up in growth chambers from the end of heading stage (BBCH 59) to the beginning of ripening stage (BBCH 71) to simulate the conditions under future climate. The results showed that elevated CO_2 concentration led to: (1) mitigation of reduction in final yield formation parameters of drought-stressed plants compared to those of control, (2) enhanced results of drought-stressed treatments compared to those of drought-stressed treatments exposed to the ambient CO_2 concentration. Pannonia NS was found out as the less responsive genotype to the exposition of CO_2 concentration (no statistically significant differences among ambient and elevated CO_2 concentrations in all yield formation parameters were identified). On contrary, harvest index of genotype Bohemia was identified as the most sensitive parameter in response to drought stress as well as to the atmospheric CO_2 concentration.

Key Words: drought stress, elevated CO_2, *Triticum aestivum* L., growth chamber, yield formation parameters

INTRODUCTION

Global climatic models predict occurrences of more frequent and more intense extreme weather events such as drought and heat spells (Aiqing et al. 2018) with changes in precipitation pattern towards much more intense precipitation but of lower number of precipitation events (Semenov and Stratonovitch 2015). Moreover, global atmospheric CO_2 concentrations are projected to increase from close to 400 ppm in 2015 to about 550 ppm in 2050 with increase in mean global temperature about 2 °C by 2050 according to RCP8.5 scenario (Stocker et al. 2013). Human population is continuously increasing when increase of about 50% is predicted by the year 2050 and intensification of crop production (Fischer et al. 2014) is expected as a solution. Wheat belongs to the most cultivated

crop world-wide, therefore, it is crucial to ensure its stable production also under changing climate. Reproductive and grain filling stages of wheat are considered as the most sensitive to drought stress resulting in significant losses of yields (Sehgal et al. 2018). Yield losses caused by drought-stress can be compensated by elevated CO_2 concentration enhancing growth and yields of C3 crops (Kimball et al. 2002, Leakey et al. 2009). Elevated CO_2 in the range of 450–800 ppm leaded to increases in grain yields of wheat by 24% (meta-analysis of 59 studies by Wang et al. 2013). A rise in wheat grain yield by 7–11% per 100 ppm increase in CO_2 with the highest enhancement of 30% at about 750 ppm was found out in plants grown in pots under controlled conditions (Amthor 2001, Pritchard and Amthor 2005).

MATERIAL AND METHODS

Five winter wheat (*Triticum aestivum* L.) genotypes (Bohemia, Elan, Pankratz, Pannonia NS and Tobak) were sown on 23 October 2018 into black plastic pots (10.5 × 10.5 × 21 cm) in the number of 2 seeds per each pot with total number of 16 pots per genotype ensuring later 4 replicates (pots) for each combination of factors (2 levels of CO_2 concentration × 2 levels of water availability). Soil used for pots filling was a topsoil (0–30 cm) coming from experimental station in Polkovice (199 m.a.s.l.) and it was analysed as Luvic Chernozem with silt-clay texture (21% clay, 70% loam and 9% sand). Chemical analyses of soil showed pH $CaCl_2$ 7.16 and following contents: total nitrogen 0.23%, total carbon 2.53%, 5701 mg/kg Ca, 247.33 mg/kg Mg, 427 mg/kg K and 84 mg/kg P. The pots were placed onto the concrete floor of the vegetation hall of Mendel University in Brno (235 m.a.s.l.; 49°12′36.62892“N, 16°36′48.64716“E) with a wire netting roof and surrounding walls where the plants were cultivated under ambient weather conditions until their transportation into two growth chambers of model FytoScope FS-SI 3400 (Photon Systems Instruments, spol. s.r.o., Brno, Czech Republic) of Global Change Research Institute of the Czech Academy of Sciences (Brno, Czech Republic) at the beginning of heading stage of development (BBCH 51). The plants were irrigated if needed to prevent drought-stress prior initiation of experimental part. The plants were also fertilized and protected both against frost (using expanded clay and/or non-woven fabric) and against pests and fungal diseases (Table 1).

Table 1 Applications of fertilizers and treatments against pests and fungal diseases on winter wheat plants (to be continued on the next page)

Date	Treatment	Substance name (form)	Dose/solution concentration	Active ingredients
5 April 2019	FA	Ammonium nitrate with dolomite (LAD 27%; GR)	45.4 kg N/ha (~ 0.2 g/1 pot)	27% N (13.5% N-NO_3^-, 13.5% N-NH_4^+), 7% CaO, 5% MgO
8 April 2019	F *	Boogie® Xpro (SF)	0.30%	bixafen, prothioconazole, spiroxamine
8 April 2019	I *	NURELLE D (SF)	0.20%	cypermethrin, chlorpyrifos
15 April 2019	FA	FERTILEADER Vital-954 (SF)	1.96%	9% N (urea nitrogen), 5% P_2O_5, 4% K_2O, 0.05% B, 0.1% Mn, 0.02% Cu, 0.01% Mo, 0.05% Zn, 0.02% Fe, max. 3% Cl^-
30 April 2019	I	PROTEUS® 110 OD (SF)	0.16%	thiacloprid, deltamethrin
30 April 2019	F	Boogie® Xpro (SF)	0.30%	bixafen, prothioconazole, spiroxamine
14 May 2019	FA	Ammonium nitrate with dolomite (LAD 27%; GR)	45.4 kg N/ha (~ 0.2 g/1 pot)	27% N (13.5% N-NO_3^-, 13.5% N-NH_4^+), 7% CaO, 5% MgO
14 May 2019	I *	PROTEUS® 110 OD (SF)	0.16%	thiacloprid, deltamethrin

Date	Treatment	Substance name (form)	Dose/solution concentration	Active ingredients
14 May 2019	F *	Boogie® Xpro (SF)	0.30%	bixafen, prothioconazole, spiroxamine

*Legend: FA – fertilizer application (GF – granular fertilizer, SF – solution form), F – fungicide treatment, I – insecticide treatment, * – combined fungicide and insecticide treatment applied*

The plants were left in the growth chambers for acclimation under ambient CO_2 protocols (see Table 2 for details) and optimal irrigation until the end of heading stage (BBCH 59) when stress treatments were launched. The plants were exposed to CO_2 and water availability treatments from the end of heading stage (BBCH 59) to the beginning of ripening stage (BBCH 71). Different level of CO_2 concentration was set up within each of two growth chambers: (1) ambient CO_2 with 400 ppm concentration and (2) elevated CO_2 concentration with 700 ppm. Two different water regimes within each growth chamber were set up: (1) drought-stressed treatment – plants were maintained at the level of ~20% of soil volumetric water content (field capacity was 43%) when pots were irrigated individually based on measurements of actual volumetric soil moisture using ThetaProbe Soil Moisture Sensor (Delta-T Devices Ltd, http://www.delta-t.co.uk), (2) control treatment – plants were maintained at full water capacity by capillary uptake of water from trays placed under the pots. Environmental conditions were set up as protocols via control computer within each growth chamber (Table 2) and these values changed continuously among two time points.

Table 2 Environmental conditions in growth chambers

Time	PAR (μmol/m^2/s)	t (°C)	RH (%)	CO_2 (ppm)	VPD (kPa)
00:00–04:00	0	20–18	85–90	AC/EC	0.351–0.206
04:00–06:00	0	18	90	AC/EC	0.206
06:00–12:00	0–1500	18–26	90–45	AC/EC	0.206–1.850
12:00–14:00	1500	26	45	AC/EC	1.85
14:00–20:00	1500–0	26–22	45–75	AC/EC	1.850–0.661
20:00–00:00	0	22–20	75–85	AC/EC	0.661–0.351

Legend: PAR – photosyntetically active radiation, t – temperature, RH – relative humidity, CO_2 – level of CO_2 concentration, VPD – vapour pressure deficit; AC – 400 ppm (ambient CO_2 concentration; also during acclimation of plants), EC – 700 ppm (elevated CO_2 concentration)

The pots were transported back to the vegetation hall after experimental part in the growth chambers was finished. The plants were manually harvested at full ripening stage (BBCH 92) and consequently, above-ground biomass was dried up at 105 °C for 12 hours. Yield formation parameters of grain number per spike (GN), grain weight per spike (GW), thousand grain weight (TGW; calculated using eq. 1) and harvest index (HI; calculated using eq. 2) were assessed per main spikes after drying following these equations (eq. 1–2):

$$TGW = \left(\frac{GW}{GN}\right) \times 1000 \quad (1)$$

$$HI = \frac{\mathrm{GW}}{\mathrm{GW+\,SLW}} \text{ where } SLW \text{ is a weight of straw and leaves of appropriate spike} \quad (2)$$

Statistical analyses (one-way and two-way ANOVA analyses with post-hoc Tukey's HSD tests) of each yield formation parameter under each treatment and treatments combination per each winter wheat genotype were performed using STATISTICA 12.0 software (StatSoft, Tulsa, USA).

RESULTS AND DISCUSSION

Based on results, responses to different level of CO_2 concentration and water treatment were specific for each genotype. Pannonia NS evinced to be the most resistant to both CO_2 concentration level and water treatment except for thousand grain weight that was susceptible for water treatment ($P < 0.001$). On contrary, three of four yield formation parameters of Bohemia and Elan were significantly affected by either level of CO_2 concentration (grain weight per spike in Bohemia and Elan: $P = 0.004$ and $P = 0.030$, respectively, harvest index in Bohemia: $P = 0.019$) or water treatment (thousand

grain weight in Bohemia and Elan: P < 0.001 and P = 0.004, respectively, harvest index in Bohemia: P = 0.005). Harvest index of Bohemia was significantly affected by level of CO_2 concentration as well as water treatment when assessed as single factors thus this parameter was identified as the most sensitive in response to these factors. Grain weight per spike and harvest index were significantly affected by water treatment in Tobak, while effect of CO_2 treatment as well as an interaction of water treatment and level of CO_2 concentration was found out as statistically insignificant. Grain number per spike was significantly affected by level of CO_2 concentration (P = 0.005) and thousand grain weight was significantly affected by water treatment (P = 0.041) in Pankratz. If genotypes were assessed all together, yield formation parameters were affected significantly by water treatment except for grain number per spike that was significantly affected by CO_2 concentration along with grain weight per spike (Table 3). This result is in accordance with findings of Krenzer and Moss (1975) who tested two hard red spring wheat genotypes (*Triticum aestivum* L.) in growth chambers and they found out that elevated CO_2 of 600 ppm resulted in higher grain number and grain size when it was applied at grain development stage from anthesis until maturity in the day/night temperature regimes of 25/20 °C. Sionit et al. (1981) who tested three CO_2 concentration levels (350, 675 and 1000 ppm) found out for semi-dwarf spring wheat (*Triticum aestivum* L., cv. GWO 1809) that grain weight per spike and grain number per spike were significantly higher with elevated CO_2 concentration under optimal environmental conditions set up in growth chambers. On contrary, Bourgault et al. (2013) found out insignificant response in final yield of 20 wheat lines (*Triticum aestivum* L.) to various levels of CO_2 set up in controlled environment of chambers and glasshouse where the levels of 420 ppm as ambient and 700 ppm as elevated CO_2 concentrations were set up. Combined effect of CO_2 concentration level and water treatment was found out as statistically insignificant in each yield formation parameter of each winter wheat genotype tested (Table 3, Figure 1). Generally, application of simultaneous drought-stress and ambient CO_2 concentration resulted in elevated grain number per spike in drought-stressed treatments compared to those of the control treatments (~ 8.79% increase), nevertheless, it led to decreased grain weight per spike (~ 15.38% reduction) as well as thousand grain weight (~ 25.01% drop) (Figure 1).

Figure 1 Yield formation parameters under ambient (AC)/elevated (EC) CO_2 concentrations in drought-stressed (DS)/control (WW) treatments (means are presented as columns, standard errors of these means are depicted as error bars) and statistical significances (P-values) of CO_2 concentration level (ambient/elevated – L), water treatment (drought-stressed/control – T) and their interactions (L × T) on individual yield formation parameters assessed with two-way ANOVA (α = 0.05, n ≥ 5) with post-hoc Tukey's HSD test (different letters denote statistically significant differences)

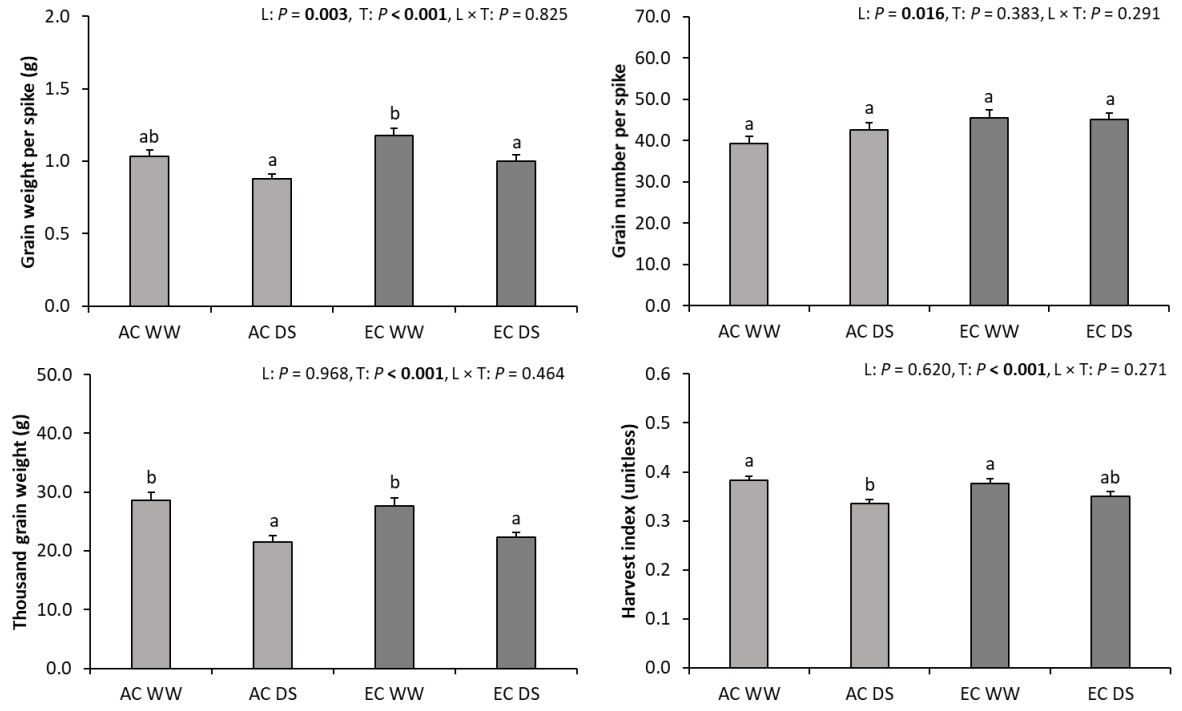

Table 3 Statistical significances (P-values) of CO_2 level (L), water treatment (T) and their interactions (L × T) on individual yield formation parameters of specific winter wheat genotypes separately and for data of all genotypes together tested by two-way ANOVA ($\alpha = 0.05$, $n \geq 5$)

Genotype	ANOVA factors	Grain number per spike	Grain weight per spike	Thousand grain weight	Harvest index
Bohemia	L	0.133	**0.004**	0.053	**0.019**
	T	0.307	0.054	**< 0.001**	**0.005**
	L × T	0.420	0.586	0.612	0.919
Elan	L	**< 0.001**	**0.030**	0.060	0.229
	T	0.161	0.110	**0.004**	0.072
	L × T	0.334	0.473	0.460	0.533
Pankratz	L	**0.005**	0.525	0.807	0.056
	T	0.979	0.078	**0.041**	0.134
	L × T	0.072	0.871	0.555	0.445
Pannonia NS	L	0.490	0.517	0.877	0.675
	T	0.312	0.268	**< 0.001**	0.137
	L × T	0.616	0.530	0.415	0.274
Tobak	L	0.233	0.093	0.114	0.219
	T	0.060	**0.034**	0.158	**0.005**
	L × T	0.377	0.808	0.194	0.784
All genotypes together	L	**0.016**	**0.003**	0.968	0.620
	T	0.383	**< 0.001**	**< 0.001**	**< 0.001**
	L × T	0.291	0.825	0.464	0.271

Elevated CO_2 concentration level enhanced final yield formation parameters in drought-stressed treatments compared to the drought-stressed plants under ambient CO_2 concentration. On the other hand, thousand grain weight and harvest index parameters in control treatments under elevated CO_2 concentration reached lower values of 3.36% and 1.49%, respectively, in elevated CO_2 compared to those in ambient CO_2 concentration. Decline in harvest index (HI) under elevated CO_2 concentration was found out earlier in soybean by Allen (1991). On contrary, no response and higher HI were observed in two genotypes of durum wheat under elevated CO_2 of 700 ppm (pot experiment led by Aranjuelo et al. 2013). In the case of grain weight per spike and grain number per spike parameters, elevated CO_2 concentration with sufficient water amount led to increases values of these parameters compared to those of ambient CO_2 concentration. Yield formation parameters of plants in environment of elevated CO_2 concentration evinced less declines in drought-stressed treatments compared to the appropriate control treatments than in cases of plants under ambient CO_2 concentration where these declines were higher (0.13% in grain weight per spike, 5.25% in harvest index and 5.54% in thousand grain weight, except for grain number per spike where the higher mean value was reached in drought-stressed treatments) (Figure 1).

CONCLUSION

Final values of yield formation parameters of all tested winter wheat genotypes in drought-stressed treatments were enhanced by increased CO_2 concentration at the level of 700 ppm and thus the negative effect of drought stress was alleviated by 3.75% in thousand grain weight, by 4.23% in harvest index, by 5.41% in grain number per spike and by 12.14% in grain weight per spike. While Pannonia NS showed the lowest effect caused by different levels of CO_2 concentration and drought-stress conditions, harvest index of Bohemia was identified as the most sensitive parameter to these factors. Final values of yield formation parameters of wheat exposed to various levels of CO_2 concentration and water treatments at the range of BBCH 59–71 developmental stages differed among specific genotypes.

ACKNOWLEDGEMENTS

The research was financially supported by the SustES – Adaptation strategies for sustainable ecosystem services and food security under adverse environmental conditions (CZ.02.1.01/0.0/0.0/16_019/0000797).

REFERENCES

Aiqing, S. et al. 2018. Heat stress during flowering affects time of day of flowering, seed set, and grain quality in spring wheat. Crop Science Society of America [Online], 58: 380–392. Available at: https://doi.org/10.2135/cropsci2017.04.0221. [2021-09-17].

Allen, L.H. Jr. 1991. Effects of increasing carbon dioxide levels and climate change on plant growth, evapotranspiration, and water resources. In Proceedings of a colloquium on managing water resources in the west under conditions of climatic uncertainty. Scottsdale, 14–16 November 1990, AZ: National Research Council, National Academy Press, Washington DC, pp. 101–147.

Amthor, J.S. 2001. Effects of atmospheric CO_2 concentration on wheat yield: review of results from experiments using various approaches to control CO_2 concentration. Field Crops Research, 73: 1–34.

Aranjuelo, I. et al. 2013. Harvest index, a parameter conditioning responsiveness of wheat plants to elevated CO_2. Journal of Experimental Botany [Online], 64(7): 1879–1892. Available at: https://doi.org/10.1093/jxb/ert081. [2021-09-17].

Bourgault, M. et al. 2013. Genotypic variability in the response to elevated CO_2 of wheat lines differing in adaptive traits. Functional Plant Biology, 40: 172–184.

Fischer, R.A. et al. 2014. Crop yields and global food security: Will yield increase continue to feed the world? ACIAR Monograph No. 158, Canberra: Australian Centre for International Agricultural Research.

Kimball, B.A. et al. 2002. Responses of agricultural crops to free-air CO_2 enrichment. Advances in Agronomy, 77: 293–368.

Krenzer, E.G. Jr., Moss, D.N. 1975. Carbon dioxide enrichment effects upon yield and yield components in wheat. Crop Science Society of America, 15: 71–74.

Leakey, A.D.B. et al. 2009. Elevated CO_2 effects on plant carbon, nitrogen, and water relations: six important lessons from FACE. Journal of Experimental Botany, 60(10): 2859–2876.

Pritchard, S.G., Amthor, J.S. 2005. Crops and environmental change. An introduction to effects of global warming, increasing atmospheric CO_2 and O_3 concentrations, and soil salinization on crop physiology and yield. Birmingham, New York: Food Product Press, The Haworth Press.

Sehgal, A. et al. 2018. Drought or/and heat-stress effects on seed filling in food crops: Impacts on functional biochemistry, seed yields, and nutritional quality. Frontiers in Plant Science [Online], 9: 1705. Available at: https://doi.org/10.3389/fpls.2018.01705. [2021-09-17].

Semenov, M.A., Stratonovitch, P. 2015. Adapting wheat ideotypes for climate change: accounting for uncertainties in CMIP5 climate projections. Climate Research, 65: 123–139.

Sionit, N. et al. 1981. Effects of different concentrations of atmospheric CO_2 on growth and yield components of wheat. The Journal of Agricultural Science, 97(2): 335–339.

Stocker, T.F. et al. 2013. Technical summary. In Climate change 2013: The physical science basis. Contribution of working group I to the fifth assessment report of the Intergovernmental Panel on Climate Change. Cambridge, UK and New York, NY, USA: Cambridge University Press, pp. 33–115.

Wang, L. et al. 2013. Effects of elevated atmospheric CO_2 on physiology and yield of wheat (*Triticum aestivum* L.): A meta-analytic test of current hypotheses. Agriculture, Ecosystems and Environment, 178(15): 57–63.

Use of unmanned aerial remote sensing for in-season diagnosis of winter wheat nitrogen status

Igor Horniacek[1], Vojtech Lukas[1], Lubomir Neudert[1], Renata Duffkova[2], Jiri Mezera[1], Vladimir Smutny[1]
[1]Department of Agrosystems and Bioclimatology
Mendel University in Brno
Zemedelska 1, 613 00 Brno
[2]Research Institute for Soil and Water Conservation
Zabovreska 250, 156 27 Praha
CZECH REPUBLIC

igor.horniacek@mendelu.cz

Abstract: Unmanned aerial survey allows more precise diagnosis of the plants in the site-specific crop management by the ultra-high spatial resolution of raster data. This study is focused on the selection of the most suitable sampling size by analysis of multispectral UAV images and its comparison with Sentinel-2 satellite data, both aimed on the diagnosis of the nutritional status of winter wheat. The data used for this study were collected in 2020 from the field experiment located in Kojčice (Pelhřimov, Czech Republic) on two plots with the area of 16.2 ha and 12.1 ha. The survey was realized by plant sampling in irregular grid for estimation of N content, total biomass, Nitrogen uptake (Nupt) and Nitrogen Nutrition Index (NNI) in two vegetation stages important for the application of nitrogen fertilizers to cereals (BBCH 31, BBCH 51). Simultaneously, aerial imaging was carried out by UAV equipped with a MicaSense Altum multispectral camera. The results of statistical evaluation by correlation and regression analysis showed a significant relationship between the monitored crop parameters and vegetation indices from UAV survey and from Sentinel-2 images. Higher sensitivity to the amount of aboveground biomass was proved by the NDVI and SRI indices, on the other hand, the NDRE and RENDVI indices showed higher correlations to the Nupt. The comparison of different buffer zone analysis of UAV data showed the improvement of the estimation accuracy by the increase of the sampling size to the 10 m. Explanation of this result requires further study concentrating on the detailed investigation of the micro-variability of crop parameters within the sampling site.

Key Words: crop status diagnosis, plant sampling, remote sensing, vegetation index, UAV, precision agriculture

INTRODUCTION

Other benefits of precision farming include more precise hybrid selection, better orientation in leases by reconciling actual farm conditions, better planning for the use of fertilizers with potential crop yields, lower costs for the procurement of chemicals and fuels, and last but not least, field crossings. and thus the reduction of environmental pollution. Thanks to precision agriculture, companies can create high-tech jobs to be served by the necessary technologies (Mulla 2013).

The use of unmanned aerial vehicles (UAV) in precision agriculture is not new in today's world. UAV can be used for different types of measurements; it only depends on the use of a suitable sensor. We can use them, for example, to make crop zone management. With such a divided plot of land, the farmer has the maximum chance to intervene in a timely and targeted manner on a specific problem. Unmanned systems can be further used for crop health monitoring, disease detection, weed management and detection, growth monitoring and yield estimation (Tsouros et al. 2019).

In agriculture, remote sensing is performed on the principles of non-contact measurements of emitted solar radiation reflected from agricultural fie lds. Intensity of rest from the properties of the investigated plants. Most of the monitored parameters are light reflectance from the leaf surface, fluorescence from chlorophyll, and light transmission through the leaves (Demotes-Mainard 2008).

The aim of this study was the selection of the most suitable size of the evaluated area (buffer) from multispectral images from UAV in comparison with freely available satellite images, for the diagnosis of the nutritional status of winter wheat.

MATERIAL AND METHODS

Study site

The field experiment with winter wheat was established in 2020 at locality Kojčice (Pelhřimov, Czech Republic) on two field plots – see Table 1 with detailed information.

Table 1 Informations about experimental site

Company	Year	Field	Area	Crop	Altitude	Slope
ZD Kojčice	2020	Makyti	12.1 ha	Winter wheat	487.6 m.a.s.l.	3.5°
ZD Kojčice	2020	U Moucek	16.2 ha	Winter wheat	543.9 m.a.s.l.	3.7°

Plant sampling

Field monitoring consists of plant sampling realized in two important vegetation stages – stem elongation (BBCH 31) and heading (BBCH 51), both sampled at 41 points in irregular grid on both field plots. Plant samples were taken from two 0.5 × 0.5 m squares per sampling point. Plant samples were analyzed in the laboratory to determine the nitrogen content [%] and the total amount of above-ground dry biomass [t/ha]. These two parameters were the input for the calculation of the Nitrogen uptake (Nupt) and Nitrogen Nutrition Index (NNI) based on the Lemaire calculation. NNI represents the nitrogen status of plants, NNI <1 indicates insufficient fertilization N, NNI> 1 excessive nitrogen fertilization (Lemaire 2008).

UAV survey

At the same time as the plant sampling, Skymaps company s.r.o. (Brno, Czech republic) carried out a multispectral aerial survey using a UAV equipped with a MicaSense Altum multispectral camera. Camera records image data in the visible (RGB), red-edge (RE) and near infrared (NIR) part of spectrum, including measurement of incoming radiation by DLS to normalize lighting conditions. Before each flight, camera was calibrated with reflectance panel according to the standard routine recommended by camera producer. The acquired images were processed by photogrametric software Agisoft Metashape to obtain the orthomosaic with a spatial resolution of 18 cm per pixel. A set of seven broadband vegetation indices was calculated in ESRI ArcGIS; this study includes two of them: NDVI and NDRE. Due to the high spatial resolution of the images, the average value of all pixel values within the 2 m, 5 m, 10 m sampling size (buffer zone) around each sampling point was calculated. Statistical evaluation of the relationship between plant parameters and aerial survey was performed by correlation analysis and calculation of the regression equation in the software statistical program Tibco Statistica.

Sentinel-2 satellite data

The Sentinel-2 images were downloaded from public available ESA Scihub repository in the form of atmospherically corrected raster data (Level L2A). Individual scenes were selected to be acquired close to the date of field monitoring while keeping lowest cloud occurrence. Images were resampled to 10m spatial resolution by using ESA SNAP tool and set of vegetation indices was calculated by an automated algorithm in ESRI ArcGIS. The pixel values were obtained at the sampling points and exported as table data. Subsequently statistical evaluation of the relationship between plant parameters and satellite survey was performed by correlation analysis and regression equation in Tibco Statistica.

RESULTS AND DISCUSSION

Descriptive statistics of the results of laboratory analysis of plant samples for both monitored fields “Makyti”, “U Moucek” and two phenological stages (BBCH 31 and 51) are shown in Table 2.

Coefficients of variability (CV) show the highest variability in the field "U Moucek" (BBCH 31), which corresponds to the higher spatial area of this field (16.2 ha) compared to the field "Makyti" (12.1 ha). Higher variability of plant parameters was achieved in phase (BBCH 51), with all monitored parameters there was an increase in variability by 5–10% in fields with winter wheat. In the case of the experimental area "Makyti", there was a higher increase in dry biomass between the first and second sampling of plants.

Table 2 Descriptive statistics of monitored localities

Makyti	BBCH 31				BBCH 51			
	Biomass [t/ha]	N [%]	NNI	Nupt [kg/ha]	Biomass [t/ha]	N [%]	NNI	Nupt [kg/ha]
Average	1.80	3.00	0.72	54.13	8.05	1.67	0.78	135.78
Median	1.72	3.00	0.71	50.76	8.19	1.60	0.74	136.35
Std.	0.39	0.26	0.09	12.64	1.71	0.33	0.19	43.42
Min.	1.11	2.42	0.54	34.08	5.18	1.18	0.52	77.53
Max.	2.44	3.69	0.89	78.29	12.16	2.37	1.21	230.71
Count	20.00	20.00	20.00	20.00	20.00	20.00	20.00	20.00
CV [%]	21.53	8.61	12.39	23.36	21.19	19.95	24.06	31.98
U Moucek	BBCH 31				BBCH 51			
Average	1.91	3.15	0.78	60.24	7.83	1.90	0.88	150.94
Median	1.93	3.14	0.77	58.82	7.48	1.98	0.90	148.35
Std.	0.44	0.33	0.12	15.78	2.16	0.30	0.20	52.77
Min.	1.03	2.60	0.58	35.95	3.80	1.37	0.58	66.90
Max.	2.86	3.88	1.04	89.58	13.41	2.32	1.25	275.16
Count	21.00	21.00	21.00	21.00	21.00	21.00	21.00	21.00
CV [%]	23.25	10.48	15.09	26.20	27.56	15.55	22.45	34.96

As we can see from Table 3, correlations between unmanned survey, satellite survey and crop parameters are statistically significant in most cases. This proved the usability of both remote sensing methods for diagnosis of plant nitrogen status, which can be implemented for variable rate application of nitrogen during the crop vegetation (Elbl et al. 2019). Similar to Lukas et al. (2016), the second survey in late crop development (BBCH 51) showed lower values of correlation coefficients in comparison to the survey in stem elongation (BBCH 31). This could be also used for prediction of crop yield, as proved Duan et al. (2017) in their study, where the plant diagnosis by UAV monitoring in late phenological stages achieved higher correlation between NDVI and final crop yield.

Considering both UAV and satellite sensing methods and the sampling size variants of UAV, the best values were achieved by correlations with unmanned survey at the size of the monitored area of 10 m (buff10 m). The lowest values were achieved by correlations with the 2 m (buff2 m) monitored area and correlations with satellite images. The increase of sampling size of UAV led to improvement of the relationship of vegetation indices to the plant parameters (e.g. Biomass, Nupt). In some cases, it was achieved higher correlation of UAV than with the Sentinel-2 (UAV buff10 m). This confirms the survey of Mukherjee et al. (2019) that unmanned aerial sensing are more feasible and preferred for crop mapping in precision agriculture. As identified by Wilke et al. (2021), ultra-high spatial resolution of the UAV raster data allows also an estimation the plant density of cereals even at the very early vegetation stages. However, the usage of UAV imagery for diagnosis of plant nutrient status requires specific analysis of raster data to cover extended size of observed area. Explanation of these effect in further research are needed as well as the study of integration of UAV observation into robust growth models rather to transfer this technology to everyday practice in precision farming (Maes and Steppe 2019).

Negative correlations of crop parameters with Sentinel-2 vegetation indices at field Makyti in BBCH51 (Table 3) are caused by atmospheric effects of satellite image. The weather condition

in the May and June 2020 in the region of interest was not appropriate for satellite imagery – the images were often cloudy. Analysed scene from 30. May was mostly clear for the field "U Mouček" but there occurred clouds and their shadows over the "Makyti" field. However, UAV images were not influenced by these effect because of low altitude survey (up to 300 m).

Table 3 Correlation coefficients between crop parameters and vegetation indices calculated from unmanned aerial survey and Sentinel-2 survey. Colored background shows the level of correlation (minimal-maximal values as red-green gradient), red values are statistically significant at 95% probability.

		UAV buff 2 m				UAV buff 5 m				UAV buff 10 m				SENTINEL — 2			
Location	Crop parameters	NDRE	NDVI	RENDVI	SRI	NDRE	NDVI	RENDVI	SRI	NDRE	NDVI	RENDVI	SRI	NDRE	NDVI	RENDVI	SRI
Makyti (BBCH 31)	Biomass [t/ha]	0.782	0.703	0.715	0.768	0.696	0.563	0.601	0.765	0.797	0.716	0.722	0.780	0.741	0.846	0.636	0.845
	N [%]	-0.020	-0.109	-0.095	0.022	0.145	0.041	0.048	0.020	0.310	0.258	0.229	0.254	0.106	0.017	-0.183	0.038
	NNI	0.624	0.505	0.519	0.631	0.641	0.467	0.501	0.619	0.825	0.728	0.715	0.779	0.642	0.687	0.416	0.698
	Nupt [kg/ha]	0.742	0.638	0.652	0.740	0.703	0.538	0.577	0.736	0.860	0.764	0.762	0.831	0.726	0.814	0.577	0.820
Makyti (BBCH 51)	Biomass [t/ha]	0.582	0.556	0.618	0.642	0.701	0.673	0.639	0.694	0.709	0.691	0.663	0.691	0.118	0.076	0.357	0.289
	N [%]	-0.026	-0.069	-0.004	0.029	0.226	0.229	0.228	0.209	0.256	0.312	0.292	0.206	-0.384	-0.505	-0.462	-0.423
	NNI	0.242	0.194	0.269	0.308	0.460	0.446	0.428	0.439	0.483	0.518	0.488	0.433	-0.285	-0.401	-0.246	-0.235
	Nupt (kg/ha)	0.402	0.357	0.439	0.478	0.589	0.569	0.548	0.575	0.608	0.628	0.601	0.570	-0.160	-0.256	-0.034	-0.045
U Moucek (BBCH 31)	Biomass [t/ha]	0.548	0.552	0.553	0.553	0.846	0.786	0.735	0.806	0.873	0.805	0.782	0.849	0.808	0.739	0.861	0.755
	N [%]	0.169	0.174	0.189	0.190	0.274	0.182	0.158	0.293	0.180	0.079	0.056	0.253	-0.123	-0.164	0.177	-0.098
	NNI	0.515	0.531	0.545	0.533	0.799	0.707	0.653	0.775	0.759	0.656	0.624	0.782	0.524	0.464	0.732	0.505
	Nupt [kg/ha]	0.563	0.574	0.583	0.575	0.876	0.791	0.735	0.846	0.869	0.774	0.744	0.873	0.701	0.629	0.847	0.664
U Moucek (BBCH 51)	Biomass [t/ha]	0.541	0.577	0.530	0.557	0.585	0.618	0.585	0.581	0.640	0.617	0.623	0.659	0.639	0.593	0.699	0.641
	N [%]	0.286	0.284	0.235	0.283	0.347	0.300	0.311	0.391	0.764	0.744	0.704	0.762	0.238	0.265	0.428	0.357
	NNI	0.480	0.510	0.468	0.499	0.565	0.545	0.540	0.597	0.880	0.883	0.826	0.885	0.518	0.508	0.675	0.599
	Nupt [kg/ha]	0.532	0.565	0.517	0.551	0.597	0.597	0.593	0.624	0.778	0.766	0.772	0.811	0.607	0.576	0.734	0.660

Graphs of relationship between vegetation index NDRE and Nitrogen uptake (Figure 1) shows that the values of the NDRE index for nitrogen uptake have an increasing tendency. This trend can also be seen for other parameters and indices in Table 3, such as the NDVI index for Biomass. This information confirms, that the different sampling size affects the resulting correlation values calculated from UAV images.

Figure 1 Set of regression graphs comparing nitrogen uptake and NDRE index, calculated from unmanned aerial survey, at different sampling sizes (2 m, 5 m, 10 m) from the locality „UMoucek_BBCH51“

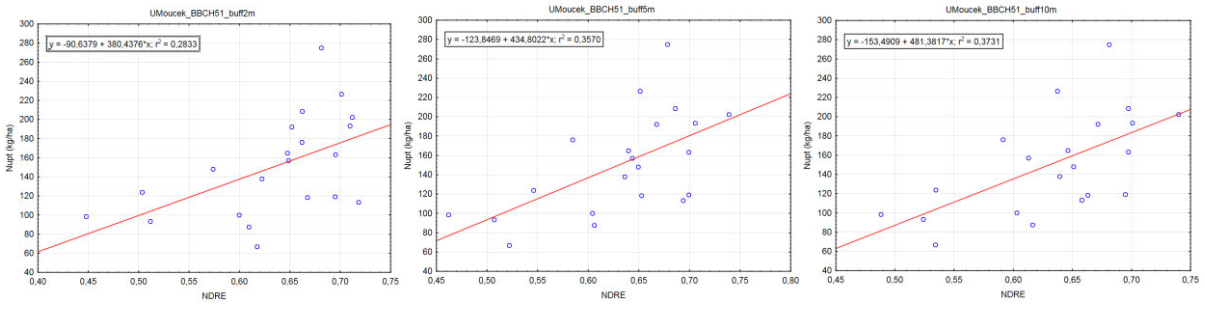

Figure 2 shows aerial photographs obtained by the unmanned survey. The images are from the period of the first sampling (April 26, 2020) made by a multispectral sensor Altum from the company MicaSense. In the pictures, white circles shows the buffer zones around the sampling points. Images represent the higher spatial variability of the crop stand within both experimental fields.

Figure 2 Images of the experimental sites "Makyti" (left), "U Moucek“ (right)

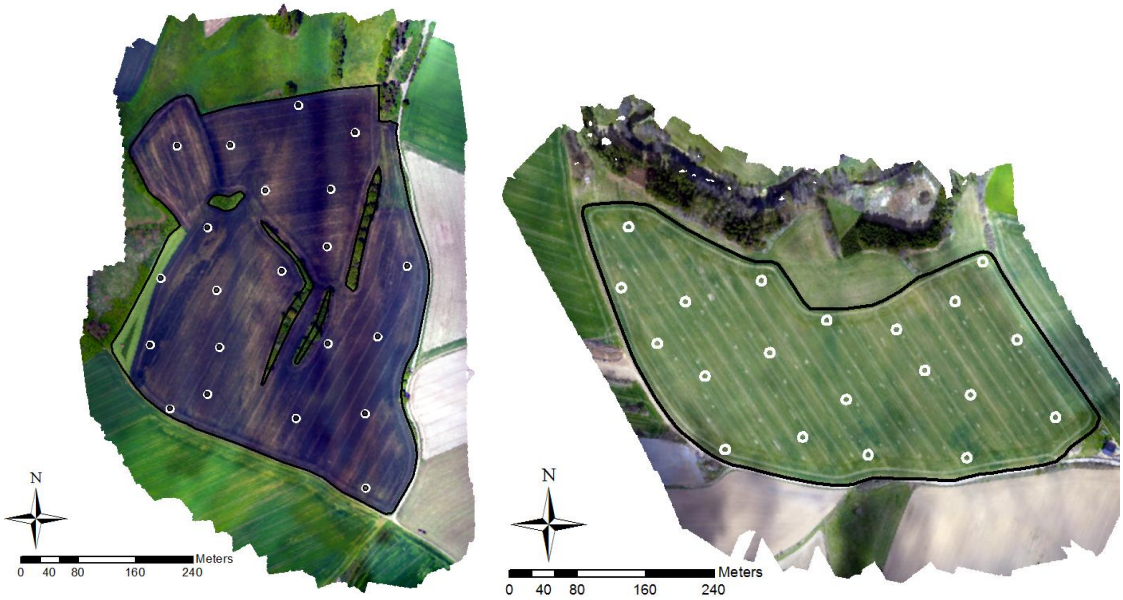

CONCLUSIONS

The results of this study showed that UAV imaging can be used to diagnose the condition of winter wheat. The best correlations with unmanned survey reached the values of dry aboveground biomass and nitrogen uptake. These crop parameters show statistically significant correlations in almost all cases in both monitored plots and in both terms.

The results of this study also showed that a change in the sampling size demonstrably changes the values of the obtained indices. The change in the size of the monitored area helped most significantly on the U Moucek plot in the second phase of monitoring, where all indices showed higher correlations with crop parameters. On the other hand, the smallest effect of improvement using a 10 meter buffer can be observed at the Makyti field in the second phase of imaging.

It should also be emphasized, that increasing the monitored area to 10 meters, resulted in an improvement in the correlation values compared to the values from the Sentinel-2 satellite, whose data are freely available and thus often preferred for diagnosing crop conditions in precision agriculture. Images obtained from UAVs have many times higher resolution than images obtained from satellite surveys. The photos thus carry detailed information about the monitored areas, which could be useful for field inspections. Correlation analysis of sampling sizes showed higher sensitivity with 10-meter buffer, mainly calculated from red-edge spectral bands (NDRE, RENDVI). The cause of the observed effect of an increase in index values with an increase in sampling sizes can be affected by many factors and therefore requires furthermore extensive study.

ACKNOWLEDGEMENTS

This study was supported by Internal Grant Agency of Faculty of AgriSciences at Mendel University in Brno as the research project AF-IGA2021-IP088.

REFERENCES

Demotes-Mainard, S. et al. 2008. Stimu Scienta Horticulture, 115(4): 377–385.

Duan, T. et al. 2017. Dynamic monitoring of NDVI in wheat agronomy and breeding trials using an unmanned aerial vehicle. Field Crops Research, 210(15): 71–80.

Elbl, J. et al. 2019. Evaluation of flat and variable rate nitrogen application effect on winter wheat yield on the basis of yield maps. In Proceeding of 19th International Multidisciplinary Scientific Geoconference, SGEM 2019, International Multidisciplinary Scientific Geoconference, pp. 823–830.

Lemaire, G. et al. 2008. Diagnosis tool for plant and crop N status in vegetative stage. Theory and practices for crop N management. European Journal of Agronomy, 28(4): 614–624.

Lukas, V. et al. 2016. The combination of UAV survey and landsat imagery for monitoring of crop vigor in precision agriculture. The International Archives of the Photogrammetry. Remote Sensing and Spatial Information Sciences, 41(B8): 953–957.

Maes, W.H., Steppe, K. 2019. Perspectives for Remote Sensing with Unmanned Aerial Vehicles in Precision Agriculture. Trends in Plant Science, 24(2): 152–164.

Mukherjee, A. et al. 2019. A survey of unmanned aerial sensing solutions in precision agriculture. Journal of Network and Computer Applications, 148(15): 102461.

Mulla, D.J. 2013. Twenty five years of remote sensing in precision agriculture: Key advances and remaining knowledge gaps. Biosystems Engineering, 114(4): 358–371.

Tsouros, D. et al. 2019. A Review on UAV-Based Applications for Precision Agriculture. Information, 10(11): 349.

Wilke, N. et al. 2021. Assessment of plant density for barley and wheat using UAV multispectral imagery for high-throughput field phenotyping. Computers and Electronics in Agriculture, 189: 106–380.

Seed vigour effected by total polyphenols content

Ivana Jovanovic[1], Jhonny Edison Alba-Mejia[1], Vratislav Psota[2], Tomas Streda[1]
[1]Department of Crop Science, Breeding and Plant Medicine
Mendel University in Brno
Zemedelska 1, 613 00 Brno
[2]Research Institute of Brewing and Malting
Malting Institute Brno
Mostecka 971/7, 613 00 Brno
CZECH REPUBLIC

ivana.jovanovic@mendelu.cz

Abstract: Phenolic compounds are important products of secondary metabolism in plants and cannot be synthesized in the human body, so they are mainly taken from food. For the performance of crop seeds a key is the complex trait of seed vigour. It defines their ability to emerge across diverse environmental conditions. It was published, an increase in total phenolic content correlated with enhanced seed vigour in some plant species. The aim of this work was to investigate whether higher content of total polyphenols in seeds affects seed vigour. For the purpose of this study four varieties of spring barley from four localities were tested. Seed vigour was conducted in two ways: in the first one, seeds were placed between two layers of germinating paper in the germinating box, whereas in the second barley kernels were placed in Petri dishes without filter paper under the same environmental conditions. Effect of drought and temperature stress (10°C) was simultaneously induced. Drought stress -0.5 MPa was induced using polyethylene glycol (PEG 6000). Evaluated parameters for seed vigour were root and plumula length and surface area performed through digital image analysis with WinRhizo software. The content of total polyphenols in the grains was determined spectrophotometrically from the previously prepared extract. The total polyphenols content (TPC) was significantly affected both by variety and locality. The statistically significant correlation between total polyphenols content and seed vigour was found.

Key Words: total polyphenols, human health, emergency, drought stress, cold stress

INTRODUCTION

Barley (*Hordeum vulgare* L.) is an ancient and important cereal crop, mainly used for beer production. Moreover, there is a renewed interest in barley food, because of its nutritional value. Barley grain provides low fat, complex carbohydrates (mainly starch), proteins, minerals, vitamins (especially vitamin E) and other antioxidants, mostly phenolic compounds. More than 50% of polyphenols in barley have been reported to be present in a conjugated form linked to the cell wall materials of the grain Arigò et al. (2018).

Germination is defined as the protrusion of the radicle through the seed envelopes in favorable conditions. However, unfavorable germination environment can impose stress on the seeds, which can delay or prevent germination Saux et al. (2020). Germination is widely used to improve the nutritional value of seeds for human consumption. Several studies have proved that content of folic acid, γ-aminobutyric acid, phenolic compounds can greatly enhance during the germination process Li et al. (2019), Tang et al. (2021). Also, the level of total phenolics in germinated seeds and sprouts can be changed during germination while having a distinct impact on bound phenolics Gan et al. (2017).

In some species, an increase in total phenolic content correlated with enhanced seed vigour Burguieres et al. (2007), Chloupek et al. (2008). Seed vigour reflects properties of a seed to germinate in a wide range of environmental conditions. Although, high vigour seeds are expected to perform better under environmentally stressed conditions than low vigour seeds, even if standard germination test results can be comparable Ullmannová et al. (2013), Bodner et al. (2013). Since then, the International Seed Testing Association (ISTA) brought a more specific definition that considers not only those properties that determine the activity and level of performance of seeds of acceptable germination

in a wide range of environments but also the performance after storage. However, the vigour of seeds can decline owing to improper storage, resulting in incalculable direct and indirect economic losses in terms of breeding work Feng et al. (2021).

The amount and composition of polyphenols similarly to most other compounds in barley grain depends on the genetic characteristics of the variety, growing and climatic conditions. As the protein content of the grain increases, the polyphenol content decreases Basařová et al. (2015). Nitrogen application significantly affects the protein concentration in barley grain and therefore it is important to adjust the nitrogen dose.

Based on this knowledge, the aim of this study was to determine and explain the interaction between seed vigour and the total polyphenols content in four varieties of barley grown from four localities of Czech Republic.

MATERIALS AND METHODS

Plant material

The collection of four barley varieties was cultivated with of using common agricultural practices in the four localities, carried out during the 2020 growing season and under observation of Central Institute for Supervising and Testing in Agriculture and Research Institute of Brewing and Malting which provided the seeds. Varieties (Bojos, Overture, Laudis 550, KWS Amadora) were selected based on the content of nitrogen compounds, germination parameters (germination energy, germination capacity) and resilience in the field under different environmental conditions. Additionally, the aim was to maintain variability within the variety.

Table 1 Overview of meteorological conditions in 2020

	Air temperature (°C)							
	March		April		May		June	
	1991–2020	2020	1991–2020	2020	1991–2020	2020	1991–2020	2020
Lednice	5.3	6.2	11.1	11.2	15.6	13.8	19.2	18.6
Uherský Ostroh (Strážnice)	4.6	5.5	10.1	10.0	14.7	12.7	18.2	18.0
Čáslav	4.6	5.0	9.8	9.5	14.5	11.9	17.9	17.4
Chrastava (Liberec)	3.0	3.4	8.2	9.0	12.6	10.3	15.9	16.3
	Precipitation totals (mm)							
	March		April		May		June	
	1991–2020	2020	1991–2020	2020	1991–2020	2020	1991–2020	2020
Lednice	31.8	16.3	29.3	8.9	54.2	72.9	63.2	117.1
Uherský Ostroh (Strážnice)	31.5	18.0	32.7	16.4	60.1	68.5	69.0	127.1
Čáslav	37.8	42.1	31.7	22.3	67.6	55.4	72.3	152.9
Chrastava (Liberec)	61.4	45.7	41.3	3.6	75.6	86.9	89.0	140.2

Localities (Čáslav, Chrastava, Uherský Ostroh, Lednice) were selected based on their variable agroecological conditions. Data from the stations of the Czech Hydrometeorological Institute were used to evaluate weather conditions of the year (Lednice, data from station Strážnice for Uherský Ostroh, Čáslav, data from station Liberec for Chrastava). Air temperatures in 2020 were close to normal except for May, which was significantly colder in all regions. In terms of precipitations, in 2020, April was subnormal, and June was above normal (Table 1).

Seed vigour determination

To evaluate the barley seeds vigour percentage after seven and fourteen days experiment was conducted. Samples were stored under controlled laboratory conditions before any manipulation.

The first step was sorting of the seeds and after, those seeds were soaked in 3% sodium hypochlorite solution and then washed with distilled water three times. The seed vigour of harvested seeds was then tested after the seeds had broken dormancy (i.e., six months after harvest). Fifty barley seeds were chosen (four varieties, four regions, three replicates) and placed between two layers of germinating paper, previously labeled, and placed in the germinating box. The seeds with germ length at least half the length of the seed and at least three embryonic roots were considered properly germinated.

Seed vigour of barley as the germination percentage under drought (-0.5 MPa) and temperature stress (10 °C) was evaluated. Drought stress -0.5 MPa was induced using polyethylene glycol (PEG 6000) at a concentration of 193 g/l. After germinating boxes were prepared, they were put into plastic bags, to prevent evaporation. Additionally, six seeds of each variety were placed in a Petri dish, with 10 ml of PEG inside. Also labeled and put into plastic bags. After that both germinating boxes and Petri dishes were placed in a climate box under 10°C. After seven and fourteen days germinated seeds from germinating boxes were counted. Germinated seeds from Petri dish were scanned and analyzed in WinRhizo (Régent Instruments Inc., Quebec, Kanada). Seed vigour germinating boxes were used in order to have seed vigour evaluated as number of germinated seed. Seed vigour under drought in Petri dish was evaluated as Len 7; Len 14 (length of germ and roots after seven and fourteen days) and as S.A. 7; S.A. 14 (surface area of 7 and 14 days). Usage of PEG in Petri dish without filter paper might be a useful tool since filter paper can cause problems with breaking the root architecture during samples manipulation.

Preparation of the extract

Twenty grams of barley grains from each variety was grounded finely on a 1 mm sieve barley grinder. After that, 5 g of ground barley was weighed into a 200 ml tall beaker. Then, 100 ml of 75% dimethylformamide solution was added. Shortly afterwards, the mixer head was immersed in the beaker and mixed for ninety seconds. The mixture was supposed to be left from twelve to fifteen minutes and the whole procedure was repeated three times in each sample. After the last mixing, the solution was poured into a centrifuge tube. Samples were centrifuged at 3000 rpm for 10 min. From the centrifuged solution 25 ml of the solution was pipetted into a 100 ml volumetric flask and made up to the mark line with deionized water. The solution was poured into a centrifuge tube and for the last time samples were centrifuged at 15000 rpm for 30 min. The pure solution has been used for the determination of the polyphenols content.

Preparation of a blank solution

Twenty ml of extract was pipetted into a 50 ml volumetric flask. After that, 0.10 ml ammonium ferric citrate was added. The solution was mixed thoroughly and made up to the mark line with deionized water. Then it was let to stand for 10 min and the clarity of the solution was observed.

Determination of polyphenols

Twenty ml of extract was pipetted into a 50 ml volumetric flask, then 16 ml of ethylenediaminetetraacetic sodium hydroxide (CMC/EDTA) was added. To the solution was also added 0.10 ml ammonium ferric citrate and the content was shaken. Then, 0.10 ml of ammonium solution was added, made up to the mark line with deionized water and mixed thoroughly. The absorbance was measured spectrophotometrically in 10 mm cuvette at a wavelength of 525 nm against a blank solution.

Calculation and evaluation of total polyphenol content (TPC)

The calculation was performed according to the formula for calculating the content of polyphenols in the original solution as previously published Jovanovic et al. (2020).

Correlation and ANOVA

Correlation between gained parameters was calculated based on Pearson correlation coefficient r on the level of significance $p = 0.05$ for $n = 16$. The results were statistically analyzed by the analysis of variance (ANOVA) method. The differences between mean values were evaluated by the Fishers LSD test in STATISTICA 12 Software (Statsoft Inc. Tulsa, OK, USA) at the level of significance $p = 0.05$.

RESULTS AND DISCUSSION

The total polyphenol content ranged from 0.14–0.23% DM (dry matter). Seed vigour evaluated as Len ranged from 11.43–133.37 mm, while seed vigour evaluated as S.A. ranged from 7.51–44.59 mm^2 (value for six seeds from Petri dish).

Figure 1 Differences of total polyphenols content among studied varieties and regions; effect of variety (Bojos, Overture, Lauids 550, KWS Amadora) ***a)*** *and localities (Čáslav, Chrastava, Uherský Ostroh, Lednice)* ***b)*** *Eror bars show standard deviation, and letters indicate significant differences ($p < 0.05$).*

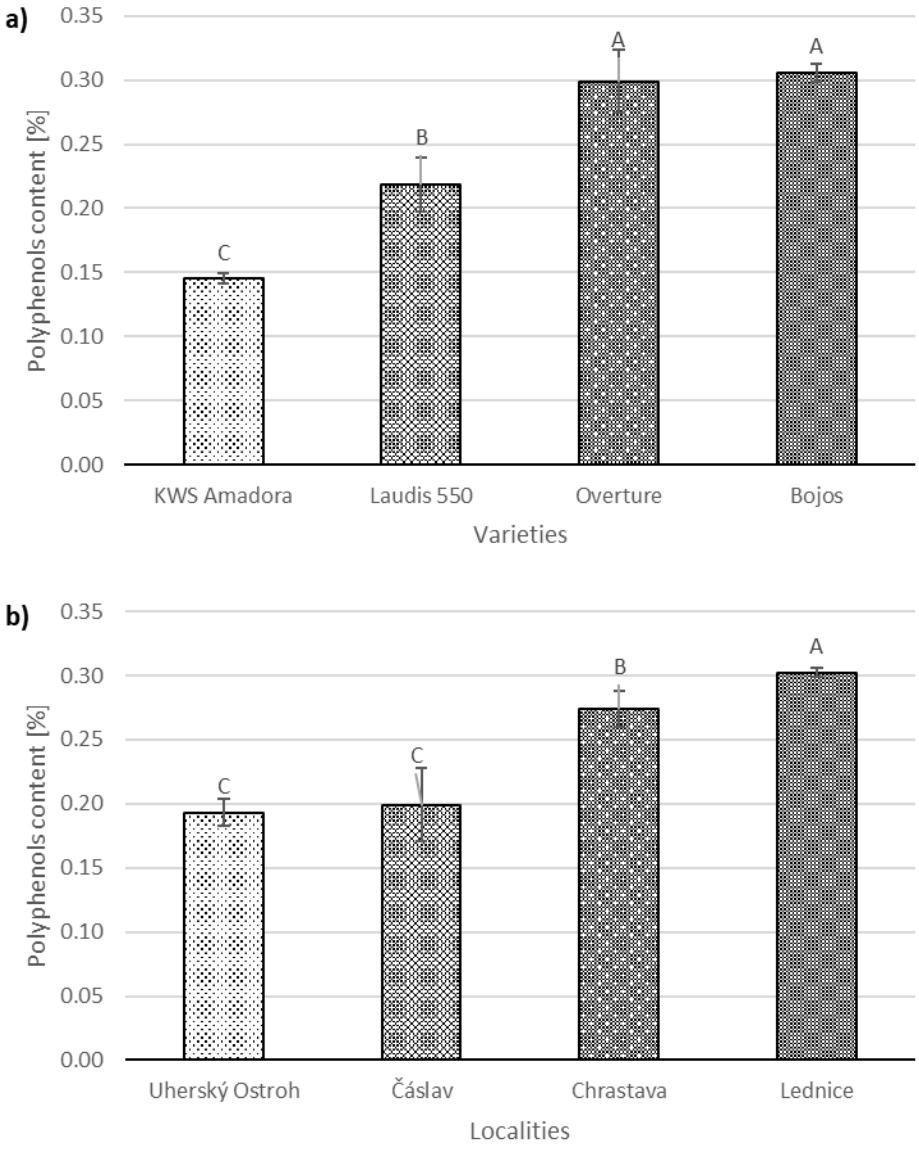

As previously mentioned, the Pearson correlation coefficient was used to explain how strong the correlation between TPC and seed vigour evaluated as S.A. and Len after seven and fourteen days was. Results have shown that there was statistically significant correlation between TPC and seed vigour evaluated as S.A.14 ($r = 0.536$; $n = 16$). It can be concluded that higher TPC leads to vigorous seeds. Higher content of TPC according to Basařová et al. (2015), is related to lower amount of nitrogen in soil. There was no statistically significant correlation between seed vigour evaluated as (Len 7, Len 14, and S.A. 7) TPC. Higher values of negative correlation coefficients were found for the relationship of seed vigour evaluated as number of sprouted seeds and TPC ($r = - 0.615$; $n = 16$). There is a dependency among these parameters, which implicates that with higher TPC the number of vigorous seeds is lower. This result is in contrast with the previous one, which can be caused by some deviation within environmental conditions. Other possible reason can actually be in compliance

with findings of Chon (2013), Gan et al. (2017), which concluded that some phenolic compounds have been modified during germination.

The results of ANOVA related to four varieties of spring barley grown in four different localities and their TPC is presented in Figure 1 a) and b). Analysis of variance confirmed that the TPC in seeds was significantly affected by variety and localities. However, differences in the effect of individual factors were thoroughly observed. Accordingly, varieties Bojos and Overture had the highest level of polyphenols content. Nevertheless, there was not a statistically significant difference among those two varieties. Statistically significant difference was observed in variety Laudis 550 and KWS Amadora (Figure 1 a). The differences for the TPC of barley varieties might be due to different characteristics of the variety as well as differences in environmental conditions as previously published in a similar study by Zrcková et al. (2019). From the Figure 1 b) it can be seen that the effect of the locality was significant for the total polyphenols content in studied varieties. Within the localities Lednice a Chrastava a statistically significant difference was observed. On the other hand, there was no statistically significant difference among localities Čáslav and Uherský Ostroh. It is known that many antioxidants in plants are produced as response to abiotic stress, like water stress and heat stress Lu et al. (2015). According to that, differences in temperature, precipitations among different localities can be the possible cause of different impact each locality had on the polyphenols content in tested varieties.

CONCLUSION

As results have shown the TPC content was significantly correlated to seed vigour. Also, the effect of variety and localities was statistically significant regarding TPC in studied varieties. Based on this research it can be concluded that, there is a strong correlation between TPC and seed vigour, but as mentioned it also depends on environmental conditions. Therefore, further studies on this subject need to be carried out to make a clear conclusion.

ACKNOWLEDGEMENTS

The work was supported by the project from Czech Ministry of Agriculture QK1910197 „The strategy for minimizing the impact of drought on sustainable production and barley malting quality“.

REFERENCES

Arigò, A. et al. 2018. Development of extraction method for characterization of free and bonded polyphenols in barley (Hordeum vulgare L.) grown in czech republic using liquid chromatography-tandem mass spectrometry. Food Chemistry, 245(15): 829–837.

Basařová, G. et al. 2015. Sladařství: Teorie a praxe výroby sladu. 1st ed., Praha, Czech Republic.

Bodner, G. et al. 2013. Prospects of selection for barley seed vigour as a precondition for stand emergence under dry condition. Kvasný průmysl, 59(9): 238–241.

Burguieres, E. et al. 2007. Effect of vitamin C and folic acid on seed vigour response and phenolic-linked antioxidant activity. Bioresource Technology, 98(7): 1393–1404.

Chloupek, O. et al. 2008. Better Bread from Vigorous Grain? Czech Journal of Food Sciences, 26(6): 402–412.

Chon, S-U. 2013. Total Polyphenols and Bioactivity of Seeds and Sprouts in Several Legumes. Current Pharmaceutical Design, 19(34): 6112–6124.

Feng, L. et al. 2021. Assessment of rice seed vigour using selected frequencies of electrical impedance spectroscopy. Biosystems Engineering, 209: 53–63.

Gan, R.Y. et al. 2017. Bioactive compounds and bioactivities of germinated edible seeds and sprouts: An updated review. Trends in Food Science & Technology, 59: 1–14.

ISTA Vigour Test Committee. Chapter 15 Seed vigour testing. In International Rules for Seed Testing; International Seed testing Association: Zurich, Switzerland, 2015.

Jovanovic, I. et al. 2020. Polyphenols content and seed vigor interaction in spring barley (Hordeum vulgare L.). In Proceedings of International PhD Students Conference MendelNet 2020 [Online]. Brno, Czech Republic, 11–12 November, Brno: Mendel University in Brno, Faculty of AgriSciences, pp. 38–43. Available at: https://mnet.mendelu.cz/mendelnet2020/mnet_2020_full.pdf. [2021-08-29].

Li, W. et al. 2019. Rapid evaluation of γ-aminobutyric acid in foodstuffs by direct real-time mass spectrometry. Food Chemistry, 277: 617–623.

Lu, Y.J. et al. 2015. Genotype, environment, and their interactions on the phytochemical compositions and radical scavenging properties of soft winter wheat bran. LWT – Food Science and Technology, 60(1): 277–283.

Saux, M. et al. 2020. A Correlative Study of Sunflower Seed Vigor Components as Related to Genetic Background. Plants, 9(3): 386.

Tang, Y. et al. 2021. Impact of germination pretreatment on the polyphenol profile, antioxidant activities, and physicochemical properties of three color cultivars of highland barley. Journal of Cereal Science, 97: 103152.

Ullmannová, K. et al. 2013. Use of barley seed vigour to discriminate drought and cold tolerance in crop years with high seed vigour and low trait variation. Plant Breeding, 132(3): 295–298.

Zrcková, M. et al. 2019. Variation of the total content of polyphenols and phenolic acids in einkorn, emmer, spelt and common wheat grain as a function of genotype, wheat species and crop year. Plant, Soil and Environment, 65(5): 260–266.

A variety of transpiration in the young spruce stands with different thinning management

Ina Kyselova[1,2], Justyna Szatniewska[1,3], Lukas Vagner[1], Jan Krejza[1], Marian Pavelka[1]
[1]Global Change Research Institute CAS
Belidla 986/4a, 603 00 Brno
[2]Department of Forest Ecology
[3]Department of Silviculture
Mendel University in Brno
Zemedelska 1, 613 00 Brno
CZECH REPUBLIC

Kyselova.i@czechglobe.cz

Abstract: Managing the spruce forest growing beyond its favourable conditions is trading between water consumption and increasing biomass. We examined tree transpiration in four stands with different thinning intensities in a 40-year-old spruce forest in South Moravia. Tree transpiration was significantly higher under moderate and heavy intensity compared to low intensity and control plots. Tree transpiration differed also among trees of different sizes within the treatments and also between the treatments. The stem increment was visibly increasing with the intensity of treatment, particularly for suppressed trees. The findings show an ecological tree response two years after the thinning.

Key Words: Norway spruce, tree size, water consumption, sap flow, biomass production, thinning treatment

INTRODUCTION

The increasing frequency, intensity and duration of a period with extreme weather conditions have already led to a decrease in forest productivity (Allen et al. 2015). This emphasises a need for silvicultural approaches for existing forest stands that have not reached economic maturity, suitable short-term adaptation strategies to achieve a higher forest resistance and resilience to extreme climatic events (Brang et al. 2014, Lasch et al. 2002). Moreover, still prevailing spruce forest growing beyond its ecological suitable conditions is more vulnerable in terms of water deficit conditions, which is increasing with climate change (Brázdil et al. 2015). Hence, the essential assumption for an examination of the future of spruce-dominated forestry is the estimation of spruce water demand. The thinning is suggested as an approach to climate adaptation in the short term and has a positive impact of thinning on the growth performance of trees during drought. This has been shown in several studies from America (D'Amato et al. 2013, Hsiao 1973), Israel (Tsamir et al. 2019) and Europe (Elkin et al. 2015, Nilsen and Strand 2008). However, a response of trees to any sudden long-lasting conditions varies with a taxonomic class (conifer or broadleaved), species' potential to occupy newly available growing space, thinning intensities, time since the last thinning and stand age (Elkin et al. 2015), not to mention the meteorological conditions. In this study, we evaluated the response of tree and stand transpiration and diameter increment to the thinning treatments of different intensities.

MATERIAL AND METHODS

Study site description

The study site is located close to Rájec–Němčice (49°26'37"N, 16°41'47"E) at an altitude of 625 m.a.s.l. The mean annual temperature from May until September in 2020 was 17 °C (long-term annual average is 7.8 °C) and the amount of precipitation over the same period was 495 mm (long-term average annual sum is 679 mm). It is 40 years old Norway spruce managed forest. The study area was divided into four equally large plots, of an area of 625 m^2 and lastly managed in spring 2018 with three thinning intensity treatments from below (low, moderate, heavy) and a control plot without thinning

treatment (Table 1). The distribution of all trees' diameter in breast height (1.3 m, further DBH) varied between thinning intensities especially considering suppressed trees (Figure 1).

Figure 1 Distribution of the tree classes within the managed plots (625 m^2)

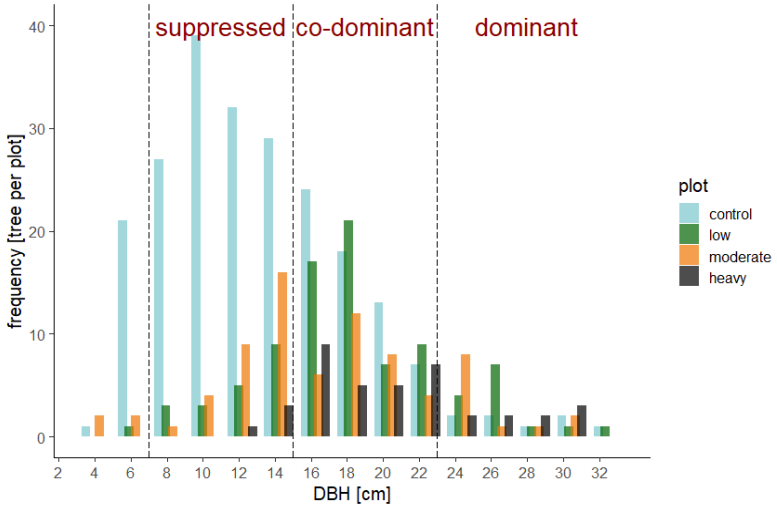

Legend: DBH – diameter breast height (cm), suppressed trees: 7–14 cm in DBH, co-dominant trees: 15–23 cm in DBH, dominant trees: above 23 cm in DBH

Table 1 Characteristics of the spruce stand in the different treatments

Thinning intensity	Stand density [tree/ha]	Stand BA [m^2/ha]	BA reduction [%]	Mean DBH ± SD [cm]	LAI [-]	Mean sap flow ± SD [kg/year/tree]	T_{stand} [l/year/ha]
Control	3504	3.506	0	13 ± 5.2	5	1139 ± 518	399
Low	1424	2.514	28	18 ± 5.1	4	1602 ± 902	228
Moderate	1216	1.914	45	17 ± 5.7	3	1686 ± 389	205
Heavy	624	1.358	61	20 ± 5.2	3	2145 ± 1106	134

Legend: BA – basal area, SD – standard deviation, LAI – leaf area index, T_{stand} – stand transpiration

Sap flow measurement

The water consumption was calculated based on the measurement of the tree transpiration by the sap flow modules EMS81 (EMS Brno, CZ), based on the tissue heat balance method from (Čermák et al. 2004). Data were measured in 2 minutes intervals, stored in 10 minutes averages and then aggregated to daily values. The growth increment was measured by band automatic dendrometers (DR 26, EMS Brno, CZ). We selected trees of similar diameter at breast height (DBH) in each plot in four DBH classes representing co-dominant and dominant trees (DBH18, DBH20, DBH23, DBH26). A software Mini32 (Environmental Measuring Systems s.r.o. Brno, CZ) was used for sap flow and dendrometers' data pre-processing. For data analysis, we used a selection of data of the main growing season, from 8 May 2020 until 30 September 2020, and excluded days with precipitation above 10 mm/day (moderate rain), according to the declining regression curve between sap flow and precipitation. For the statistical analysis were used the standardized sap flow data, expressed as mass flow from one centimetre of tree circumference [kg/day/cm]. Statistical analyses and graphs were conducted in R (R Core Team 2019). The sap flow of an average tree (calculated according to stand inventory data of DBH classes' distribution) was calculated for each plot to represent the stand density. The whole stand transpiration (T_{stand}) was calculated as the multiplication of the average tree sap flow and the number of trees in each treatment. As the assumptions to meet the requirement of homogeneity and normality were in most cases violated, we used the Kruskal-Wallis test and post hoc tests: Dunn's test for multiple groups means comparisons and the Median test for median comparison. Statistical significance for all analyses was set at $p \leq 0.05$ for α=0.05.

RESULTS AND DISCUSSION

Effect of thinning on the tree and stand transpiration

The yearly transpiration of the single average tree increased by 41% in the low thinned plot, by 48% in the moderated, and by 88% in the heavily thinned in comparison with the average tree at the control plot (Table 1), which corresponds with the findings of Tsamir et al. (2019). The highest increase of tree sap flow was in a heavily thinned stand which is comparable with the results of Park et al. (2018) and McJannet and Vertessy (2001). In our study, an increased thinning intensity led to a reduction of total stand transpiration (Table 1), as also shown by Gebhardt et al. (2014) and Wang et al. (2019). Annual stand transpiration was reduced by 43% in the low thinned plot, by 49% in moderated and 66% in the heavy thinned plot compare to the control plot (Table 1). The proportional decrease of stand transpiration concerning the reduction of the basal area through thinning agreed with the findings of Morikawa et al. (1986) and Breda et al. (1995).

Figure 2 Variation of the sap flow among thinning intensity

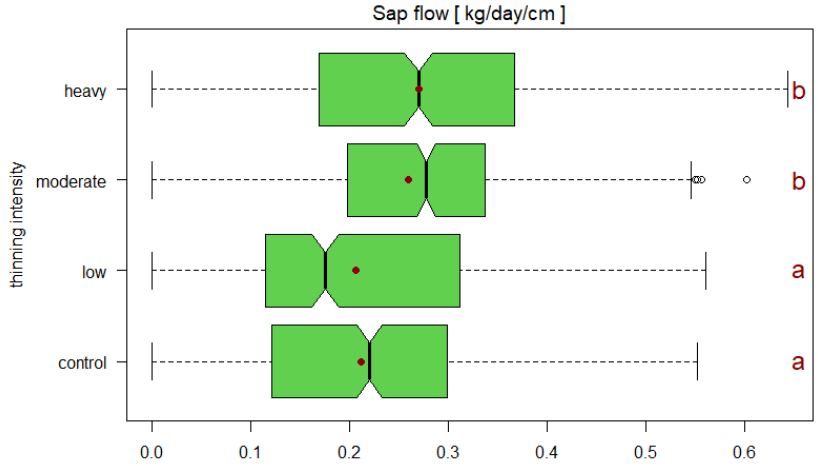

Legend: Different letters indicate significant differences in means of sap flow (red points) and notches in boxes show a 95% confidence interval for the median (black lines)

We were expecting an increase of sap flow with increasing tree size in each treatment in comparison to the un-thinned stand. According to the study of Lagergren et al. (2008), we were expecting higher transpiration within the same tree size range of DBH in heavy thinning compared to the control plot.

In our study sap flow differed significantly among treatments as well as among trees from the same DBH classes (from now on the number in the DBH class name corresponds to the mean DBH within class of 2 cm interval). The most contrasting mean transpiration was in heavy and moderate thinning intensity when compared to the control plot and low intensity thinning (Figure 2). The observed increase in tree sap flow after thinning can be related to various factors such as the increase in incoming radiation to the lower crown layers, increase in tree leaf area and higher soil water availability (Jiménez et al. 2008).

Comparing thinning intensity on selected DBH classes, we found that the heavy thinning had a significant effect on the sap flow of the dominant trees (DBH23 and DBH26) compared to the control (Figure 3). Despite the fact, that the mean tree transpiration of the control plot did not differ from low thinning (Figure 2), there was a significant effect of thinning when the separate DBH classes were considered. The most variance was among the trees in the DBH23 class, where all trees were different from the control (Figure 3).

We were expecting sap flow to increase with the tree size according to Wang et al. (2019). The largest differences in sap fluxes were shown in heavy thinning among all tree DBH variations (Figure 4). Besides moderate intensity, the lowest tree and the largest (DBH26) are transpiring significantly different. With moderate treatment, all trees were transpired very similarly, except for the tree with DBH23.

Figure 3 Tree sap flow response of various DBH classes to thinning management

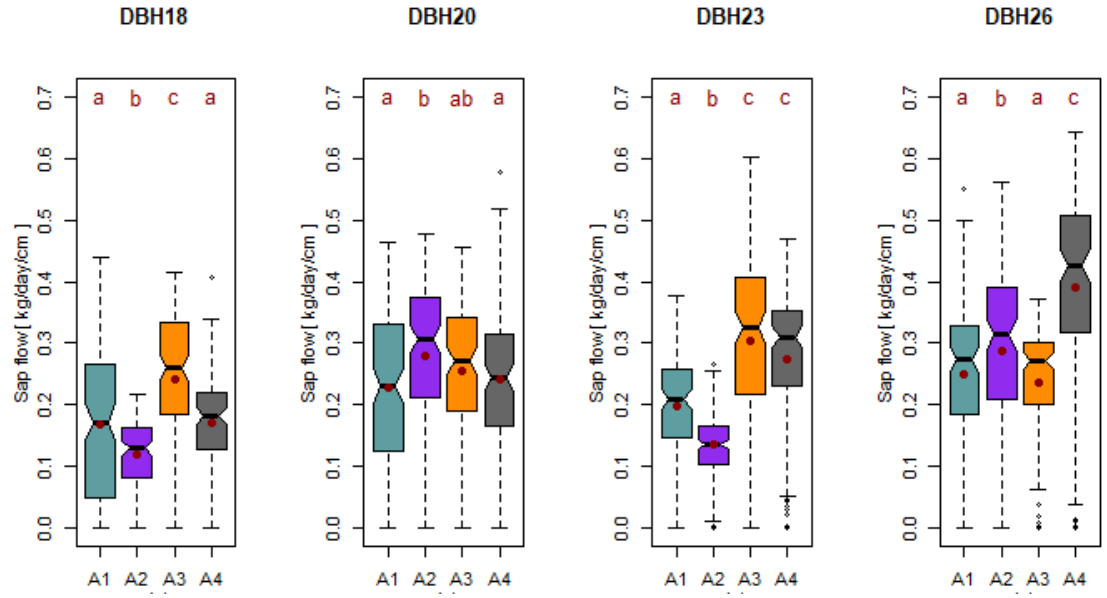

Legend: Different letters indicate significant differences (α=0.05) in means of sap flow (red points). A1 – control, A2 – low intensity, A3 – moderate intensity, A4 – heavy intensity

Figure 4 Comparison of the tree sap flow among variance of large trees within plots

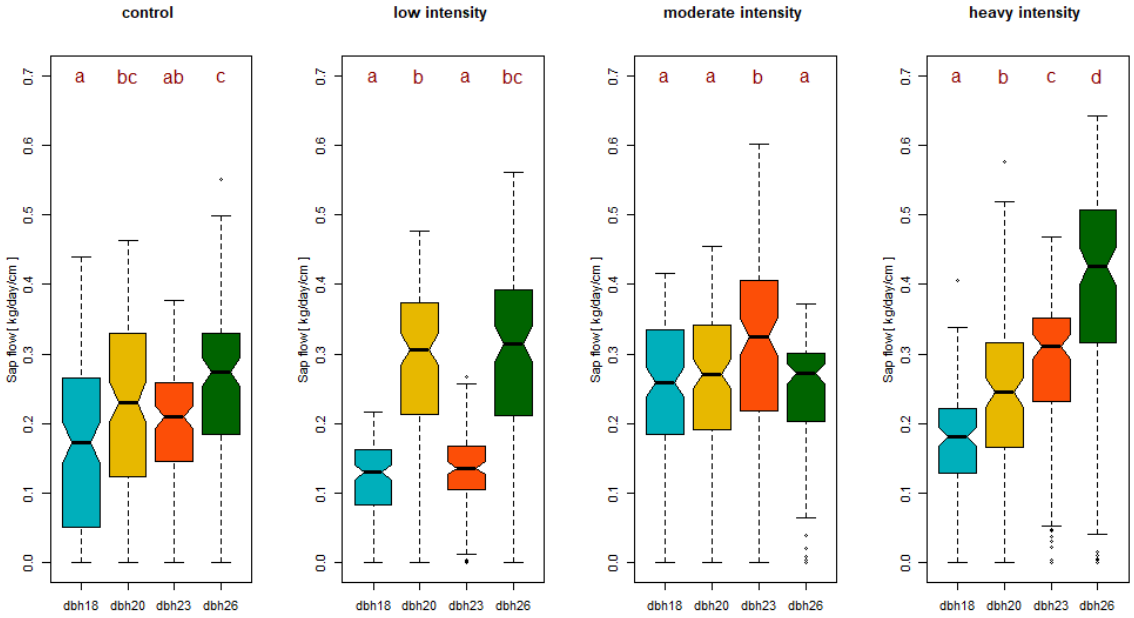

Legend: Different letters indicate significant differences (α=0.05) in means of the tree sap flow. Boxplot shows variation for a single tree in time. The tree with DBH of 18 cm (blue), the tree with DBH of 20 cm (yellow), the tree with DBH of 23 cm (red), the tree with DBH of 26 cm (green)

Biomass

We did not find any statistically significant differences in increments among the plots nor the tree classes from averages of stem radial increment. Visually, the highest average radial stem increment was in the heavy thinning only for the suppressed and co-dominant trees (Figure 5), which is probably caused by an increase of the light availability for the crowns of the trees in lower social positions (Breda et al. 1995). A similar trend of increased diameter increment along with increased thinning intensity was found in other studies (Manrique-Alba et al. 2020). On the contrary, Breda et al. (1995) reported significantly higher stem circumference increment of dominant trees. The low thinning intensity supported the higher growth only of dominant trees. Our results generally agree with other studies

showing that thinning can greatly increase tree radial growth while stand transpiration decreases due to the reduction of stand density (Wang et al. 2019).

Figure 5 Average values of stem radial increment for the social status of the trees growing on plots with various thinning intensities

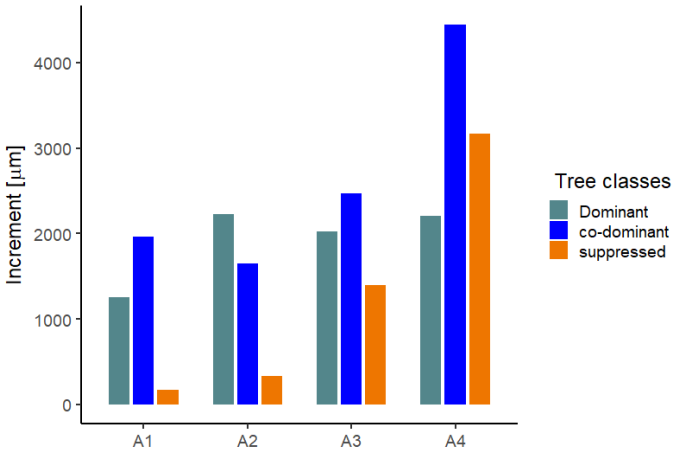

Legend: A1 – control, A2 – low intensity, A3 – moderate intensity, A4 – heavy intensity

CONCLUSION

The study confirmed the effect of thinning on the whole stand and mean tree transpiration. The results showed a significant effect of the heavy intensity thinning on tree transpiration for all measured tree DBH classes, where the tree transpiration increased in all thinning intensities compared to the control. On the other hand, the stand transpiration decreased in all thinning intensities. However, the transpiration of the dominant trees was primarily increased by the heavy thinning intensity, the stem increment was not affected so much. Contrarily, the effect of thinning on co-dominant trees sap flow was not consistent with diameter increment. Moreover, the highest stem radial increment was measured on the suppressed trees which could not be connected with the sap flow measurements. Given the limitation of sampling set and potential influence of other biometric and stand structural factors further studies are recommended.

ACKNOWLEDGEMENTS

The research was financially supported This research was supported by SustES—Adaptation strategies for sustainable ecosystem services and food security under adverse environmental conditions, project no. CZ.02.1.01/0.0/0.0/16_019/0000797.

This work is based on the use of Large Research Infrastructure CzeCOS supported by the Ministry of Education, Youth and Sports of CR within the CzeCOS program, grant number LM2018123

REFERENCES

Allen, C.D. et al. 2015. On underestimation of global vulnerability to tree mortality and forest die-off from hotter drought in the Anthropocene. Ecosphere, 6(8): 129.

Brang, P. et al. 2014. Suitability of close-to-nature silviculture for adapting temperate European forests to climate change. Forestry, 87(4): 492–503.

Brázdil, R. et al. 2015. Sucho v Českých zemích: minulost, současnost, budoucnost. 1. ed., Brno: Centrum výzkumu globální změny Akademie věd České republiky, v.v.i.

Breda, N. et al. 1995. Effects of thinning on soil and tree water relations, transpiration and growth in an oak forest (Quercus petraea (Matt.) Liebl.). Tree Physiology, 15(5): 295–306.

Čermák, J. et al. 2004. Sap flow measurements with some thermodynamic methods, flow integration within trees and scaling up from sample trees to entire forest stands. Trees, 18(5): 529–546.

D'Amato, A.W. et al. 2013. Effects of thinning on drought vulnerability and climate response in north temperate forest ecosystems. Ecological Applications, 23(8): 1735–1742.

Elkin, C. et al. 2015. Short- and long-term efficacy of forest thinning to mitigate drought impacts in mountain forests in the European Alps. Ecological Applications, 25(4): 1083–1098.

Gebhardt, T. et al. 2014. The more, the better? Water relations of Norway spruce stands after progressive thinning. Agricultural and Forest Meteorology, 197: 235–243.

Hsiao, T.C. 1973. Plant Responses to Water Stress. Annual Review of Plant Physiology, 24(1): 519–570.

Jiménez, E. et al. 2008. Effects of pre-commercial thinning on transpiration in young post-fire maritime pine stands. Forestry, 81(4): 543–557.

Lagergren, F. et al. 2008. Thinning effects on pine-spruce forest transpiration in central Sweden. Forest Ecology and Management, 255(7): 2312–2323.

Lasch, P. et al. 2002. Regional impact assessment on forest structure and functions under climate change—the Brandenburg case study. Forest Ecology and Management, 162(1): 73–86.

Manrique-Alba, À. et al. 2020. Long-term thinning effects on tree growth, drought response and water use efficiency at two Aleppo pine plantations in Spain. Science of The Total Environment, 728: 138536.

McJannet, D., Vertessy, R. 2001. Effects of thinning on wood production, leaf area index, transpiration and canopy interception of a plantation subject to drought. Tree Physiology, 21(12–13): 1001–1008.

Morikawa, Y., et al. 1986. Transpiration of a 31-year-old Chamaecyparis obtusa Endl. stand before and after thinning. Tree Physiology, 2(1–2–3): 105–114.

Nilsen, P., Strand, L.T. 2008. Thinning intensity effects on carbon and nitrogen stores and fluxes in a Norway spruce (Picea abies (L.) Karst.) stand after 33 years. Forest Ecology and Management, 256(3): 201–208.

Park, J. et al. 2018. Effects of thinning intensities on tree water use, growth, and resultant water use efficiency of 50-year-old Pinus koraiensis forest over four years. Forest Ecology and Management, 408: 121–128.

Tsamir, M. et al. 2019. Stand density effects on carbon and water fluxes in a semi-arid forest, from leaf to stand-scale. Forest Ecology and Management, 453: 117573.

Wang, Y. et al. 2019. Juvenile thinning can effectively mitigate the effects of drought on tree growth and water consumption in a young Pinus contorta stand in the interior of British Columbia, Canada. Forest Ecology and Management, Elsevier, 454(12): 117667.

Estimation of winter wheat nitrogen status and prediction of crop yield by satellite and proximal sensing

Jiri Mezera, Vojtech Lukas, Jakub Elbl, Lubomir Neudert, Igor Horniacek, Vladimir Smutny
Department of Agrosystems and Bioclimatology
Mendel University in Brno
Zemedelska 1, 613 00 Brno
CZECH REPUBLIC

jiri.mezera@mendelu.cz

Abstract: Remote and proximal sensing of crop has been widely used in the last decades for agricultural applications, both for assessing vegetation condition and for subsequent yield prediction. In this work, we take advantage of vegetation indices for an advanced monitoring of spatial variability of winter wheat biophysical parameters, nitrogen status and prediction of crop yield estimation. Input data were obtained from farm field trials with winter wheat in 2019 and 2020 at Zdounky and Rašovice (Czech Republic) with a total area of 136 ha. To estimate the crop parameters, a plant sampling was realized in the stem elongation vegetation phase and later the grain sampling before harvest. Spectral properties were obtained from the satellite imagery of Sentinel-2 as the set of broadband vegetation indices (GNDVI, NDRE, NDVI, NRERI, RENDVI) and proximal crop sensor systems (Fritzmeier ISARIA, AgLeader OptRx). Spatial data were processed and analyzed using tools of geographic information systems and then statistically evaluated relationships between variables by using correlation analysis. The finding of high level of correlation between in-vegetation crop sensing and grain yield showed the possibility to identify yield spatial variability by both sensing systems in early stage of crop growth. This can be implemented for development of decision support tools for yield zoning in site specific crop management – precision farming.

Key Words: precision agriculture, vegetation indices, crop sensing, Sentinel-2, grain yield

INTRODUCTION

Site-specific crop management is one of the main drivers of precision agriculture. Spatial and temporal variability can be used to support decision-making in agronomy and can thus lead to improved profitability and sustainability of agricultural production, taking advantage of sensors, information and communications technologies (Fountas et al. 2016). Soil, vegetation or yield properties can be used to define homogeneous management zones in order to apply site-specific management. The identification within field variability is not an easy task and can be obtained by various technologies (Shaddad et al. 2016). Today are used the advantages of proximal, remote and yield sensors in practice, on the basis of which it is possible to obtain information on variability and subsequent data for decision in the agronomy and plant production (De Benedetto et al. 2013). Assessment of plant status and crop biophysical parameters is important information for decision support in agronomy to correct the crop management practices, especially for application of nitrogen fertilizers (Vizzari et al. 2019, Lukas et al. 2016). Vegetation index values can be obtained from several sources, e. g. ground sensors, UAV (unmanned air vehicles), airborne and satellite sensors. These sources differ in spatial resolution, but also in the design of the sensor and the range of wavelengths (Gozdowski et al. 2020).

The aim of the study was to verify the use of proximal sensing and satellite imaging to estimate agronomically relevant biophysical parameters and nitrogen status of winter wheat crop stand and to predict differences in crop yield.

MATERIAL AND METHODS

Study area

Data were acquired in year 2019 and 2020 from two experimental localities with winter wheat in locality Zdounky and Rašovice (Czech Republic). The total area of the observation was 136 ha, the overview of field trials is described in Table 1.

Table 1 Description of localities

Locality	Area [ha]	Altitude [m.a.s.l.]	Slope [°]	District	Coordinates	Sampling date	Satellite image date
Zdounky	95.84	275	6.45	Kroměříž	49.297N, 17.393E	6. 5. 2019	1. 5. 2019
Rašovice	40	277–323	3.37–4.13	Vyškov	49.120N, 16.948E	28. 4. 2020	25. 4. 2020

Field sampling

Field survey consisted of plant sampling during the vegetation (stem elongation, BBCH 32–39) and crop sampling before harvest (BBCH 91). The number of sampling points was 20 in Zdounky respectively 21 in Rašovice (Table 3, Table 4). Samples were taken from 0.5 x 0.5 m squares per each sampling point localised by RTK-GPS. Plant samples were analysed in laboratory for estimation of nitrogen content [%], total amount of aboveground dry biomass [t/ha], respectively number of ears [n/m^2], thousand seed weight [g], density [kg/m^3] and yield (marked as Yield S) [t/ha] in case of harvest sampling. To complete the determination of nutritional status of plants, a nitrogen uptake (Nupt, [kg/ha]) was calculated from nitrogen content and dry biomass as multiplication of N concentration by dry biomass.

Proximal sensing

Proximal sensing was realized by using two crop sensing systems – Fritzmeier ISARIA (locality Zdounky) and AgLeader OptRx (locality Rašovice) during second topdressing nitrogen application (Figure 1). Nutrient status of plants is evaluated based on the spectral measurement of reflectance by active LED lighting in near infrared, red and red-edge part of spectrum. The system ISARIA calculated two vegetation indices – Isaria Reflectance Measurement Index (IRMI), which is related to chlorophyll content, and Isaria Biomass Index (IBI) related to crop biomass. The system AgLeader OptRx calculated vegetation index NDRE (Normalized Difference Red Edge Index). From both systems, data records of vegetation indices were downloaded from board computers as the spatial point data in shapefile format.

Figure 1 Nitrogen application by crop sensing system Fritzmeier ISARIA (left) and AgLeader OptRx (right) on the field. Photo by J. Mezera

Remote sensing by satellite platform Sentinel-2

The Sentinel-2 images were selected with the minimum of clouds occurrence and acquired near to the date of field sampling. The datasets were downloaded from ESA open hub database as surface reflectance product produced by sen2cor algorithm (Level L2A, Lantzanakis et al. 2017) and filtered through a cloud mask derived with L2A scene classification dataset. Set of five vegetation indices was calculated from multispectral bands by the automatized workflow in ArcGIS (see the list in Table 2).

Table 2 List of Sentinel-2 vegetation indices used in the study (Klem et al. 2014)

GNDVI	Green Normalized Difference Vegetation index
NDRE	Normalized Difference Red Edge Index
NDVI	Normalized Difference Vegetation Index
NRERI	Normalized Red Edge Index
RENDVI	Red Edge NDVI

The results of crop mapping by plant sampling and datasets from Sentinel-2 were processed in Geographic Information System ArcMap 10.6.1 (ESRI, Redlands, USA). For each sampling point, the pixel value of Sentinel-2 vegetation indices was obtained by overlay analysis. The data was then exported to Microsoft Excel (Microsoft Corporation, Redmond, USA) and subsequently to Statistica 12 (Tibco, USA) for correlation and regression analysis.

Yield data recording

Crop yield maps were recorded during the harvest of winter wheat in 2019 and 2020 for both experimental localities. Data were acquired by grain harvesters equipped with sensor system for estimation of grain flow, grain moisture and DGPS receiver. Outliers and error values were filtered in ArcGIS, followed by spatial interpolation using the kriging technique to smooth out the differences at small scale level. The final raster dataset contains information about crop yield (marked as Yield H) in 5 m spatial resolution.

RESULTS AND DISCUSSION

Basic statistical characteristics of results from online sensors, laboratory analysis of plant samples taken from two locations are shown in Table 3 and Table 4. High values of the coefficient of variation (CV) indicate high variability within the fields, the highest CV was reached for Nupt in Zdounky (18.06%) and for number of ears in Rašovice (36.47%).

Table 3 Basic statistics of plant sampling results in Zdounky, 20 samples

	N plant [%]	Biomass [t/ha]	Nupt [kg/ha]	IRMI	IBI	Yield H [t/ha]	Number of ears [n/m^2]	Yield S [t/ha]	TSW [g]	Density [kg/m^3]	N grain [%]
Average	2.70	7.26	196.71	23.86	3.38	6.78	628.8	10.29	47.75	818.26	13.81
Median	2.73	7.27	204.84	24.00	3.42	6.98	622.5	10.25	47.93	819.84	13.97
Minimum	2.10	4.98	108.03	21.10	2.82	4.92	420.0	7.65	43.82	801.23	10.78
Maximum	3.37	9.38	282.39	25.77	3.82	7.88	840.0	13.49	52.85	834.42	17.09
Std	0.31	0.99	35.52	1.16	0.26	0.80	100.8	1.71	2.23	9.19	1.53
CV (%)	11.32	13.59	18.06	4.84	7.60	11.81	16.0	16.62	4.67	1.12	11.07

Legend: Std – standard deviation; CV – coefficient of variation; N – nitrogen content; Nupt – nitrogen uptake; Yield H – yield harvest; Yield S – yield sample; TSW – thousand seed weight

Table 4 Basic statistics of plant sampling results in Rašovice, 21 samples

	N plant [%]	Biomass [t/ha]	Nupt [kg/ha]	NDRE OptRx	Yield H [t/ha]	Number of ears [n/m^2]	Yield S [t/ha]	TSW [g]	Density [kg/m^3]	N grain [%]
Average	2.45	7.53	186.58	0.37	9.62	924.52	15.4	47.64	785.39	12.79
Median	2.53	7.59	200.48	0.39	9.71	890.00	15.6	47.23	784.38	13.24
Minimum	2.02	3.79	81.97	0.23	7.95	440.00	9.6	35.74	761.18	9.68
Maximum	3.01	10.44	275.52	0.44	10.51	1610.00	27.6	53.56	816.06	15.25
Std	0.29	1.83	55.37	0.05	0.65	337.18	4.4	4.69	15.36	1.36
CV (%)	11.69	24.24	29.67	14.02	6.73	36.47	28.7	9.85	1.96	10.60

Legend: Std – standard deviation; CV – coefficient of variation; N – nitrogen content; Nupt – nitrogen uptake; Yield H – yield harvest; Yield S – yield sample; TSW – thousand seed weight

Table 5 Correlation coefficients between crop parameters, vegetation indices and harvest parameters for locality Zdounky. Red values represent statistically significant results at 95% of probability

	N plant [%]	Biomass [t/ha]	Nupt [kg/ha]	IRMI	IBI	NoE [n/m^2]	TSW [g]	Density [kg/m^3]	N grain [%]	Yield S [t/ha]	Yield H [t/ha]
N plant [%]	1.000	0.018	0.700	0.546	0.572	0.491	-0.246	0.561	0.597	0.370	0.460
Biomass [t/ha]	0.018	1.000	0.594	0.175	0.211	0.105	-0.274	-0.126	0.160	0.311	0.335
Nupt [kg/ha]	0.700	0.594	1.000	0.526	0.620	0.384	-0.304	0.444	0.509	0.472	0.508
IRMI	0.546	0.175	0.526	1.000	0.926	0.338	-0.036	0.141	0.090	0.669	0.444
IBI	0.572	0.211	0.620	0.926	1.000	0.373	-0.208	0.244	0.183	0.557	0.490
GNDVI	0.501	0.259	0.583	0.844	0.894	0.405	-0.235	0.211	0.140	0.693	0.650
NDRE	0.372	0.377	0.580	0.803	0.810	0.449	-0.066	0.110	-0.084	0.734	0.740
NDVI	0.429	0.188	0.415	0.887	0.889	0.200	-0.090	-0.023	0.008	0.520	0.490
NRERI	0.431	0.448	0.618	0.857	0.831	0.306	-0.123	0.020	-0.020	0.611	0.647
RENDVI	0.457	0.433	0.624	0.867	0.835	0.299	-0.122	0.032	0.018	0.603	0.618
Yield H [t/ha]	0.460	0.335	0.508	0.444	0.490	0.666	-0.206	0.217	-0.012	0.639	1.000
NoE [n/m^2]	0.491	0.105	0.384	0.338	0.373	1.000	-0.451	0.496	0.116	0.638	0.666
Yield S [t/ha]	0.370	0.311	0.472	0.669	0.557	0.638	-0.054	0.167	0.027	1.000	0.639
TSW [g]	-0.246	-0.274	-0.304	-0.036	-0.208	-0.451	1.000	-0.328	-0.131	-0.054	-0.206
Density [kg/m^3]	0.561	-0.126	0.444	0.141	0.244	0.496	-0.328	1.000	0.506	0.167	0.217
N grain [%]	0.597	0.160	0.509	0.090	0.183	0.116	-0.131	0.506	1.000	0.027	-0.012

Legend: Std – standard deviation; CV – coefficient of variation; N – nitrogen content; Nupt – nitrogen uptake; Yield H – yield harvest; NoE – number of ears; Yield S – yield sample; TSW – thousand seed weight

The relationship between crop parameters, Sentinel-2 satellite indices and harvest parameters was evaluated using the Spearman correlation coefficient (Table 5, Table 6). Attention was paid to the sensitivity of vegetation indices from satellite and proximal sensing to the crop vegetation parameters. Recent studies have shown the finding of relationship between the Nupt and red-edge vegetation indices (e.g. NDRE, NRERI, RENDVI) from Sentinel-2 imagery and/or proximal sensing (Lukas et al. 2019, Mezera et al. 2020). Both sites achieved showed moderate to strong level of correlation between selected vegetation indices and Nupt, except NDVI at Zdounky. As shown by Elbl et al. (2019), this outcome can be used as a basis for variable fertilizer application and grain quality monitoring in precision farming.

Table 6 Correlation coefficients between crop parameters, vegetation indices and harvest parameters for locality Rašovice. Red values represent statistically significant results at 95% of probability

	N plant [%]	Biomass [t/ha]	Nupt [kg/ha]	NDRE OptRx	NoE [n/m^2]	TSW [g]	Density [kg/m^3]	N grain [%]	Yield S [t/ha]	Yield H [t/ha]
N plant [%]	1.000	0.410	0.662	0.558	0.568	-0.411	0.005	0.785	0.493	0.415
Biomass [t/ha]	0.410	1.000	0.919	0.825	0.596	-0.739	-0.097	0.604	0.419	0.844
Nupt [kg/ha]	0.662	0.919	1.000	0.830	0.624	-0.734	-0.152	0.743	0.475	0.823
NDRE OptRx	0.558	0.825	0.830	1.000	0.695	-0.836	-0.171	0.703	0.490	0.703
GNDVI	0.605	0.812	0.858	0.917	0.665	-0.796	-0.148	0.744	0.516	0.706
NDRE	0.542	0.869	0.875	0.942	0.695	-0.818	-0.171	0.727	0.538	0.743
NDVI	0.609	0.804	0.830	0.923	0.637	-0.830	-0.231	0.723	0.455	0.713
NRERI	0.594	0.821	0.845	0.938	0.755	-0.734	-0.029	0.804	0.626	0.626
RENDVI	0.581	0.803	0.826	0.921	0.753	-0.716	0.013	0.816	0.630	0.581
Yield H [t/ha]	0.415	0.844	0.823	0.703	0.418	-0.718	-0.322	0.419	0.282	1.000
NoE [n/m^2]	0.568	0.596	0.624	0.695	1.000	-0.531	0.127	0.800	0.937	0.418
Yield S [t/ha]	0.493	0.419	0.475	0.490	0.937	-0.313	0.295	0.719	1.000	0.282
TSW [g]	-0.411	-0.739	-0.734	-0.836	-0.531	1.000	0.390	-0.531	-0.313	-0.718
Density [kg/m^3]	0.005	-0.097	-0.152	-0.171	0.127	0.390	1.000	0.104	0.295	-0.322
N grain [%]	0.785	0.604	0.743	0.703	0.800	-0.531	0.104	1.000	0.719	0.419

Legend: Std – standard deviation; CV – coefficient of variation; N – nitrogen content; Nupt – nitrogen uptake; Yield H – yield harvest; NoE – number of ears; Yield S – yield sample; TSW – thousand seed weight

The spatio-temporal variability of crop growth and differences of yield formation at both experimental sites were observed by the statistical evaluation of the results of crop yield mapping (Yield S – sampled yield, Yield H – yield data from harvester sensor). Both localities resulted in statistically significant moderate relationship among harvested and sampled yield and vegetation indices from proximal sensors and from the Sentinel-2 satellite. Yang and Anderson (2000) have found strong correlation coefficients (r = 0.90–0.95) between the NDVI index and crop yield when assessing the relationship between grain yields of sorghum and spectral variability. The highest correlation coefficient in this study was achieved for the NDRE vegetation index (r = 0.740 and 0.741), which concluded in the high potential of early stage in-vegetation sensing to predict the main spatial differences in crop yield, for example for yield zoning (Řezník et al. 2020). As shown by Reyniers et al. (2006), there are differences in ground-truth and aerial NDVI measurement and its relation to crop yield variables compared. This was not confirmed by the experiment, both crop sensing systems achieved similar correlation to the satellite sensing. More detailed results of the analysis of linear relationship and regression equation between Yield harvest and Sentinel-2 NDRE vegetation index is documented by scatter plots (Figure 3). The low level of the correlation between harvested and sampled yield implies from the differences of the measurement area and precision. In addition, the crop stand at Rašovice was partially affected by lodging, which could also influence the field sampling. The investigation of the main driven factor for crop yield formation differs at observed location. Results from experimental site in Zdounky identified only moderate influence of plant nitrogen status (Nupt) to the crop yield values, while in Rašovice it proved almost the highest level of correlation (r = 0.823). Sampling of crop yield parameters highlighted the number of ears as the main factor for yield formation at both sites.

Figure 2 Sentinel-2 NDRE image (up) and yield maps (below) of the experimental fields, black crosses represent sampling points

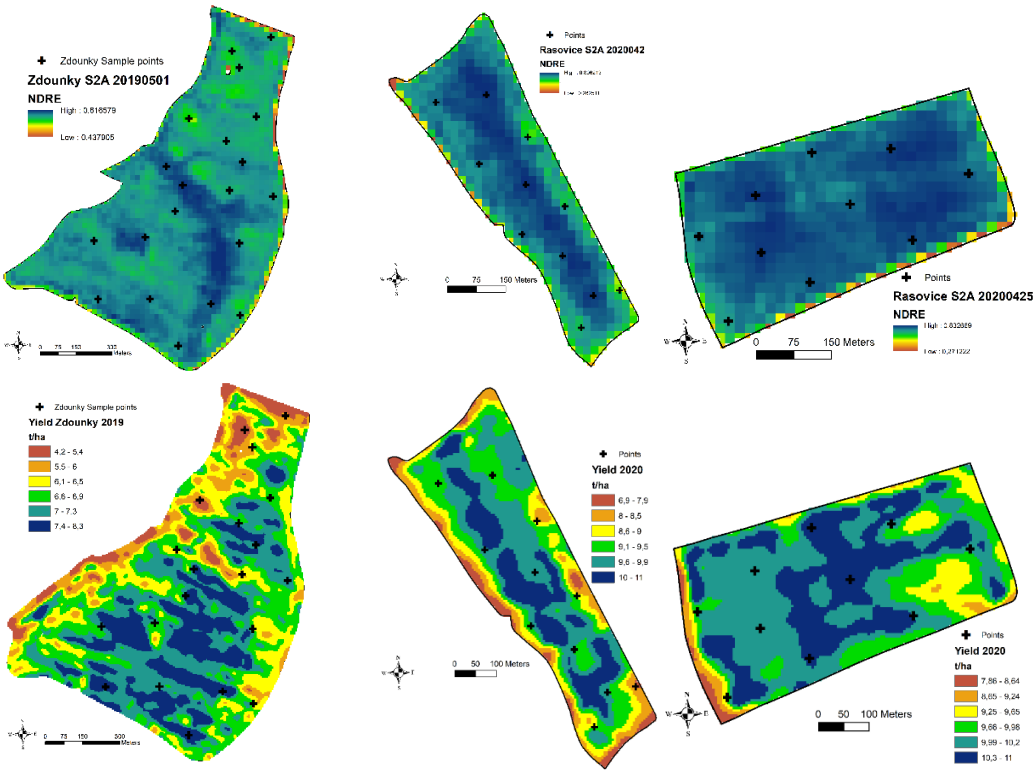

Figure 3 Scatterplot of Yield harvest and Sentinel-2 NDRE vegetation index Zdounky (left) and Rašovice (right)

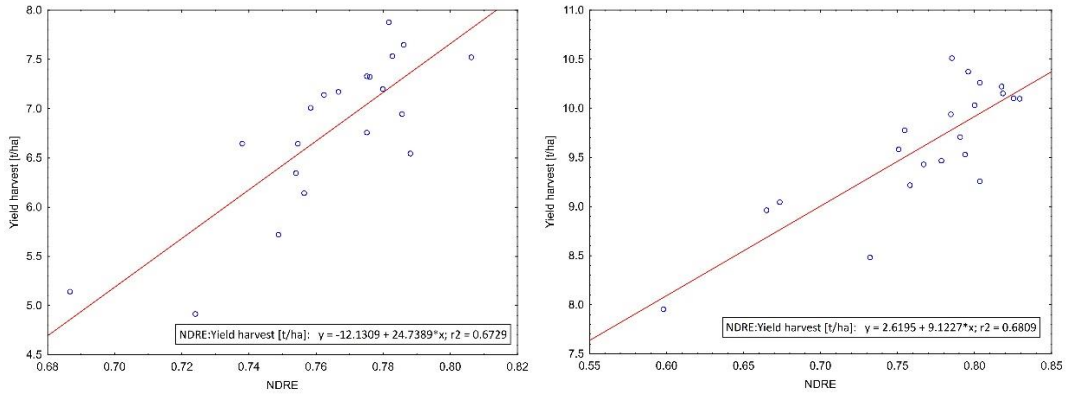

CONCLUSIONS

The relationships between vegetation indices from the online sensors, Sentinel-2 satellite, diagnostics of the nutritional status and harvest parameters of the winter wheat crop stand was investigated in this study. The evaluation was performed in 2019 and 2020 at the Zdounky and Rašovice localities. When evaluating the relationships between the parameters of winter wheat crop stands and yield, moderately strong dependences between crop yield and vegetation indices from proximal sensors and Sentinel-2 satellite data were found for both observed. The strongest correlation coefficient was achieved for the vegetation index NDRE (Sentinel-2). The NDRE index thus proved to be a universal index for delineation of spatial differences in crop yield at an early stage of in-vegetation mapping regardless the sensing system (proximal or satellite). This can be implemented for yield zoning products for precision farming. Despite the free availability of Sentinel-2 data for users, their main disadvantage in comparison to the proximal crop sensors is the occurrence of clouds and other atmospherically objects in the provided image. Final analysis of yield formation parameters highlighted the number of ears as the most important factor for both localities. It has been found that

the grain yield taken from the samples and the yield measured by harvester may differ, which needed to be considered in the further studies.

ACKNOWLEDGEMENTS

This study was supported by Internal Grant Agency of Faculty of AgriSciences at Mendel University in Brno as the research project AF-IGA2021-IP073.

REFERENCES

De Benedetto, D. et al. 2013. Field partition by proximal and remote sensing data fusion. Biosystems Engineering, 114(4): 372–383.

Elbl, J. et al. 2019. Evaluation of flat and variable rate nitrogen application effect on winter wheat yield on the basis of yield maps. In Proceedings of 19th International Multidisciplinary Scientific GeoConference. Informatics, Geoinformatics and Remote Sensing [Online]. Albena, Bulgaria, 28 June–7 July, Sofie: STEF92 Technology Ltd., pp. 823–830. Available at: https://www.sgem.org/index.php/elibrary-research-areas?view=publication&task=show&id=5565. [2021-08-30].

Fountas, S. et al. 2016. Precision Agriculture. In Supply Chain Management for Sustainable Food Networks. UK: John Wiley & Sons, pp. 41–65.

Gozdowski, D. et al. 2020. Comparison of winter wheat NDVI data derived from Landsat 8 and activeoptical sensor at field scale. Remote Sensing Applications: Society and Environment, 20: 100409.

Klem, K. et al. 2014. Využití měření spektrální odrazivosti a odvozených specializovaných vegetačních indexů v pěstební technologii jarního ječmene. Metodika pro zemědělskou praxi. Kroměříž, Brno, Havlíčkův Brod.

Lantzanakis, G. et al. 2017. Comparison of physically and image based atmospheric correction methods for Sentinel-2 satellite imagery. In Perspectives on Atmospheric Sciences [Online]. Switzerland: Springer International Publishing, pp. 255–261. Available at: 10.1007/978-3-319-35095-0_3. [2021-09-10].

Lukas, V. et al. 2016. The combination of UAV survey and Landsat imagery for monitoring of crop vigor in precision agriculture. In Proceedings International Archives of Photogrametry, Remote Sensing and Spatial Information Sciences. XXIII ISPRS Congress [Online]. Prague, Czech Republic, 12–19 July, Göttingen: Copernicus GmbH, pp. 953–957. Available at: http://dx.doi.org/10.5194/isprsarchives-XLI-B8-953-2016. [2021-08-15].

Lukas, V. et al. 2019. Estimation of winter wheat parameters for site-specific crop management by unmanned aerial multispectral imaging. In Proceedings of 19th International Multidisciplinary Scientific GeoConference. Informatics, Geoinformatics and Remote Sensing [Online]. Albena, Bulgaria, 28 June–7 July, Sofie: STEF92 Technology Ltd., pp. 533–540. Available at: https://www.sgem.org/index.php/elibrary?view=publication&task=show&id=5529. [2021-08-30].

Mezera, J. et al. 2020. Assessment of spatial heterogeneity of winter wheat canopy stand by Sentinel-2 satellite imagery. In Proceedings of International PhD Students Conference MendelNet 2020 [Online]. Brno, Czech Republic, 11–12 November, Brno: Mendel University in Brno, Faculty of AgriSciences, pp. 44–49. Available at: https://mnet.mendelu.cz/mendelnet2020/mnet_2020_full.pdf. [2021-08-15].

Reyniers, M. et al. 2006. Comparison of an aerial-based system and an on the ground continuous measuring device to predict yield of winter wheat. European Journal of Agronomy, 24(2): 87–94.

Řezník, T. et al. 2020. Prediction of Yield Productivity Zones from Landsat 8 and Sentinel-2A/B and Their Evaluation Using Farm Machinery Measurements. Remote Sensing, 12(12): 1917.

Shaddad, S. et al 2016. Data fusion techniques for delination of site-specific management zones in field in UK. Precision Agriculture, 17(2): 200–217.

Vizzari M. et al. 2019. Sentinel 2-based bitrogen VRT fertilization in wheat: comparison between traditional and simple precision practices. Agronomy, 9(6): 278.

Yang, C., Anderson G.L. 2020. Mapping Grain Sorghum Yield Variability Using Airborne Digital Videography. Precision Agriculture, 2: 7–23.

Influence of vermicompost on growth parameters and content of chlorophylls in maize during vegetation

Jakub Neupauer, Peter Kovacik
Department of Agrochemistry and Plant Nutrition
Slovak University of Agriculture in Nitra
Tr. A. Hlinku 2, 949 76 Nitra
SLOVAK REPUBLIC

xneupauer@uniag.sk

Abstract: The influence of vermicompost on the growth parameters of cultivated crops is the subject of research by many authors around the world. In the present work was observed the effect of the increasing dose of vermicompost (vermicompost at dose of 170 kg/ha N; 10% and 20% of vermicompost in the substrate). During vegetation was recorded the effect of vermicompost on plant height, stem perimeter, growth phase, weight and content of chlorophyll *a* and *b* in maize (*Zea mays* L.). The results show that increasing the dose of vermicompost had a positive effect on the measured parameters. The highest plants with the largest stem perimeter were found in the variant with the highest amount of vermicompost in the soil substrate. The 10 and 20% proportion of vermicompost in the substrate resulted in an earlier onset of growth phases compared to the control variant. The weights of the plants were significantly the highest in the variant with the highest proportion of vermicompost 20%. The content of chlorophyll *a* and chlorophyll *b* was the highest in the variant with the content of vermicompost 10%. The lowest content of chlorophylls was recorded in the control variant without vermicompost. However, it showed the highest ratio of chlorophylls *a*/*b*.

Key Words: growth parameters, earthworm, leaf dyes, corn

INTRODUCTION

The history of growing maize (*Zea mays* L.) dates in continental Europe to the end of the 15th century when it was imported from North America. During the 16th century began expansion of cultivation throughout Europe. From that period, it began to be consumed as boiled, roasted, in the form of popcorn, flour, beer and as fodder for cattle. It is also a renewable source of raw material for industry (Smith et al. 2004). Maize is a crop with high demands on nutrients. Its average yields are higher than crops type wheat or barley and then it need an adequate supply of nutrients in the soil. Nutrients enter the soil through inorganic and organic fertilizers, to which maize responds very well (Petrová et al. 2006).

Vermicompost is a material, that is obtained in the process of vermicomposting. Vermicomposting is a simple biotechnological process of composting, which uses certain types of earthworms. They improve the process of converting waste into a product of better quality (Adhikary 2012). In our region, the most used earthworm is *Eisenia fetida* (Kováčik and Kmeťová 2017). The earthworms' casts become part of vermicompost and they are able to improve soil health and nutritional status (Adhikary 2012). The raw materials entering the vermicomposting process can be a mixture of leaves, straw, fruit peels, soil (Kováčik and Ryant 2019), waste from the industry (Sharma and Garg 2018). The effect of increased dose of vermicompost on cultivated crops was observed by several authors (Arancon et al. 2008, Kováčik and Kmeťová 2017), who presented findings on the effect of increased content of available macro and microelements in it. The aim of the work was to assess how the dose of vermicompost affects the growth parameters of maize during vegetation and to confirm the suitability of using vermicompost for fertilizing maize.

MATERIAL AND METHODS

The experiment pots were located in a vegetation cage in areal of the Slovak University of Agriculture in Nitra. The soil was taken from the top layer of soil from a depth of 0.0–0.3 m from

the locality Dolné Krškany and it was medium soil (Haplic Chernozems). The soil was sieved through sieves of diameter 0.03 x 0.03 m. Vermicompost was obtained through a purchase from VermiVital s. r. o. Four experimental variants were created. Variant 1 (S) contained 20 kg of soil without vermicompost, variant 2 (Vc_{Nin}) contained 20 kg of soil and vermicompost (Vc) in a dose of 170 kg/ha N (14.2 g/pot Vc;), variant 3 (Vc_{10}) contained 18 kg of soil and 2 kg of vermicompost with a ratio of 9:1 (10% of vermicompost) and variant 4 (Vc_{20}) contained 16 kg of soil and 4 kg of vermicompost with a ratio of 4:1 (20% of vermicompost). The dose 170 kg/ha N is the maximum permitted dose of nitrogen in the form of organic manure for the growing season in vulnerable areas (91/676/EHS). The agrochemical parameters of the used soil and vermicompost are shown in Table 1. The following analytical procedures were used to determine these parameters: $N\text{-}NH_4^+$ colorimetrically using Nessler's agent; $N\text{-}NO_3^-$ colorimetrically with phenol 2,4-disulfonic acid; $N_{min} = N\text{–}NH_4^+ + N\text{–}NO_3^-$. The contents of available P, K and Mg were determined after extraction of the substrates with Mehlich 3 acidic extract (Mehlich 1984). The content of phosphorus was determined colorimetrically, potassium photometrically and calcium spectrophotometrically. The percentage of C_{ox} was determined oxidometrically and pH_{KCl} potentiometrically.

Table 1 Agrochemical properties of the soil and vermicompost used in the experiment

Substrate		$N\text{-}NH_4^+$	$N\text{-}NO_3^-$	N_{min}	P	K	Mg	pH_{KCl}	C_{ox}
Description	Mark	mg/kg							%
Soil	S	1.8	8.7	10.5	7	185	397	6.8	1.2
Vermicompost	Vc	0	974.5	974.5	5,150	27,250	3,314	7.6	24.5

The experiment was established according to the method of random arrangement of pots with the triple repetition. The model crop was maize (*Zea mays* L.) cultivar P9241. The sowing was carried out on April 29th, 2021 and 12 seeds were sown in the pot. During the vegetation, the field water capacity was maintained at 75%. For 5 weeks were performed measurements of individual height, stem perimeter and growth phase. The first measurement was performed one month after seed emergence on 6 June 2021 and then were taken weekly interval of measurements (15th June, 22nd June, 29th June, and 6th July 2021). The height of the observed plants and perimeter of stem were measured using a measure tape. The growth phase was determined based on the BBCH methodology (Meier 2001). Samples were taken twice (7th June and 6th July) and was determined the weight of the individuals. The content of chlorophyll *a*, chlorophyll *b* and total chlorophylls was determined based on the methodology of Šesták and Čatský (1966) by the first sampling. The plant material was used from the 3rd fully developed leaf. Absorbances wavelengths 663 (chlorophyll *a*) and 647 (chlorophyll *b*) were measured using acetone solution. We calculated the concentrations according to the following equations (Lichtenthaler 1987):

$$Cl\ a = (12.25 * A_{663} - 2.79 * A_{647}) * D \quad [mg/l]$$

$$Cl\ b = (21.5 * A_{647} - 5.10 * A_{663}) * D \quad [mg/l]$$

$$Cl\ a + b = (7.15 * A_{663} + 18.71 * A_{647}) * D \quad [mg/l]$$

Where D is the thickness of the cuvette (D = 1.000).

All measured data were statistically evaluated in the computer program Statgraphics 5.1 using analysis of variance (ANOVA). Differences between variants were subsequently evaluated using the LSD test at a significance level of 95% ($\alpha \leq 0.05$).

RESULTS AND DISCUSSION

Table 2 presents the values of plant height during vegetation. The measurements show that with increasing dose of vermicompost, the height of maize is also increased. In each measurement was demonstrated a statistically significant difference between control and Vc_{10} and Vc_{20} variants. Variants Vc_{10} and Vc_{20} showed a significant statistical difference in each measurement also compared to variant Vc_{Nin}, in which vermicompost was at a dose of 170 kg N per hectare. Except for one measurement, a dose of 170 kg N per hectare, in the form of vermicompost, slightly increased the overall height of the plants but was observed no statistically significant difference compared to the control variant. The height of maize was in the variant with the highest amount of vermicompost (20% Vc content on the substrate) 52% higher after the last measurement than in the control variant. The highest average

weekly increase was achieved in the variant with the highest dose of vermicompost, up to 11.3 cm per week. Kováčik and Kmeťová (2017) also recorded a significant increase in the amount of maize due to vermicompost.

Table 2 Influence of vermicompost on plant height during vegetation

Treatment		Date					Average increase
		June 7	June 15	June 22	June 29	July 6	
n	Mark	cm/plant					
1	S	21.2 a	26.5 a	35.2 a	45.2 a	53.2 a	8.0 a
2	Vc_{Nin}	23.0 a	28.5 a	35.2 a	46.3 a	55.9 a	8.2 a
3	Vc_{10}	35.1 b	44.2 b	55.4 b	71.7 b	78.2 b	10.8 b
4	Vc_{20}	40.2 c	51.6 c	61.6 c	76.8 b	85.4 c	11.3 b
$LSD_{0.05}$		3.98	3.78	4.50	5.43	3.57	1.26

Legend: n – number; $LSD_{0.05}$ – least significant difference at the level $\alpha \leq 0.05$

Similar to the height of maize, vermicompost also affected the stem perimeter. The strength of influence increased with increasing amount of vermicompost in the substrate (Table 3). The Vc_{10} variant showed a significant increase in stem perimeter compared to the control and the N 170 kg per hectare variant. The variant with the highest vermicompost content (4:1) achieved significant statistical differences between all other variants. There was also statistical significance between variants Vc_{10} and Vc_{20}, but in the later stages of growth the significance was lost, thus reducing the effect of fertilization on the stem perimeter. These findings confirm the well-known fact that nutrient deficiency in maize is manifested by reduced plant height and reduced stem perimeter (Gutiérez-Miceli et al. 2008). The dose of 170 kg N per hectare caused an increase in stem perimeter compared to the control, but apart from one measurement, no statistically significant difference was demonstrated between them.

The positive effect of vermicompost on the height of plants and the perimeter of the stem is caused by the increased content of accessible nutrients in it. The exudates of earthworms have an increased content of nutrient and are enriched with microbial life (Adhikary 2012). Vermicompost, compared to conventional composts, contain larger amounts of total nutrients and higher percentage of acceptable forms (Kováčik and Ryant 2019). The total content of nitrogen in the vermicomposting process can increase 2–3 times (Sharma and Garg 2018).

Table 3 Influence of vermicompost on the stem perimeter maize during vegetation

Treatment		Date					Average increase
		June 7	June 15	June 22	June 29	July 6	
n	Mark	cm/plant					
1	S	1.9 a	2.2 a	2.4 a	2.9 a	3.0 a	0.3 a
2	Vc_{Nin}	2.1 a	2.3 a	2.9 b	3.0 a	3.1 a	0.3 a
3	Vc_{10}	3.3 b	3.5 b	4.2 c	4.5 b	5.0 b	0.4 b
4	Vc_{20}	3.8 c	4.2 c	4.9 d	5.1 c	5.2 b	0.4 b
$LSD_{0.05}$		0.33	0.27	0.41	0.37	0.39	0.10

Legend: n – number; $LSD_{0.05}$ – least significant difference at the level $\alpha \leq 0.05$

Vermicompost accelerated the onset of growth phases. Plants in variants Vc_{10} and Vc_{20} reached growth phase approximately 2 weeks earlier than plants in variants 1 and 2 (Figure 1). At the beginning of measure, plants in variants S and Vc_{Nin} were found mainly in the growth phase BBCH 14 and in variants Vc_{10} and Vc_{20} BBCH 16. Two weeks later we observe the development of plants in variant S on BBCH 16 and in variant Vc_{Nin} on BBCH 17. Vermicompost promotes faster and more even germination seeds (Arancon et al. 2008), in this respect there is also a faster onset of growth phases. Kováčik and Ryant (2019) report that the effect of vermicompost results in faster germination of seeds by approximately 10 to 30 days. Agricultural crops need a significant amount of phosphorus in the early stages of growth. Its supply is provided from germinating seeds as well as from easily

acceptable forms of soil solution (Kováčik and Ryant 2019). Vermicompost has an increased content of phosphorus, because the process of vermicomposting increases its content by 36 to 166%, depending on the used type of raw material. Higher values of phosphorus, but also of potassium, in vermicompost, can be attributed to the degradation of labile organic compounds by the release of CO_2 and the activity of earthworms (Sharma and Garg 2018).

Figure 1 Effect of vermicompost on the growth phases of maize

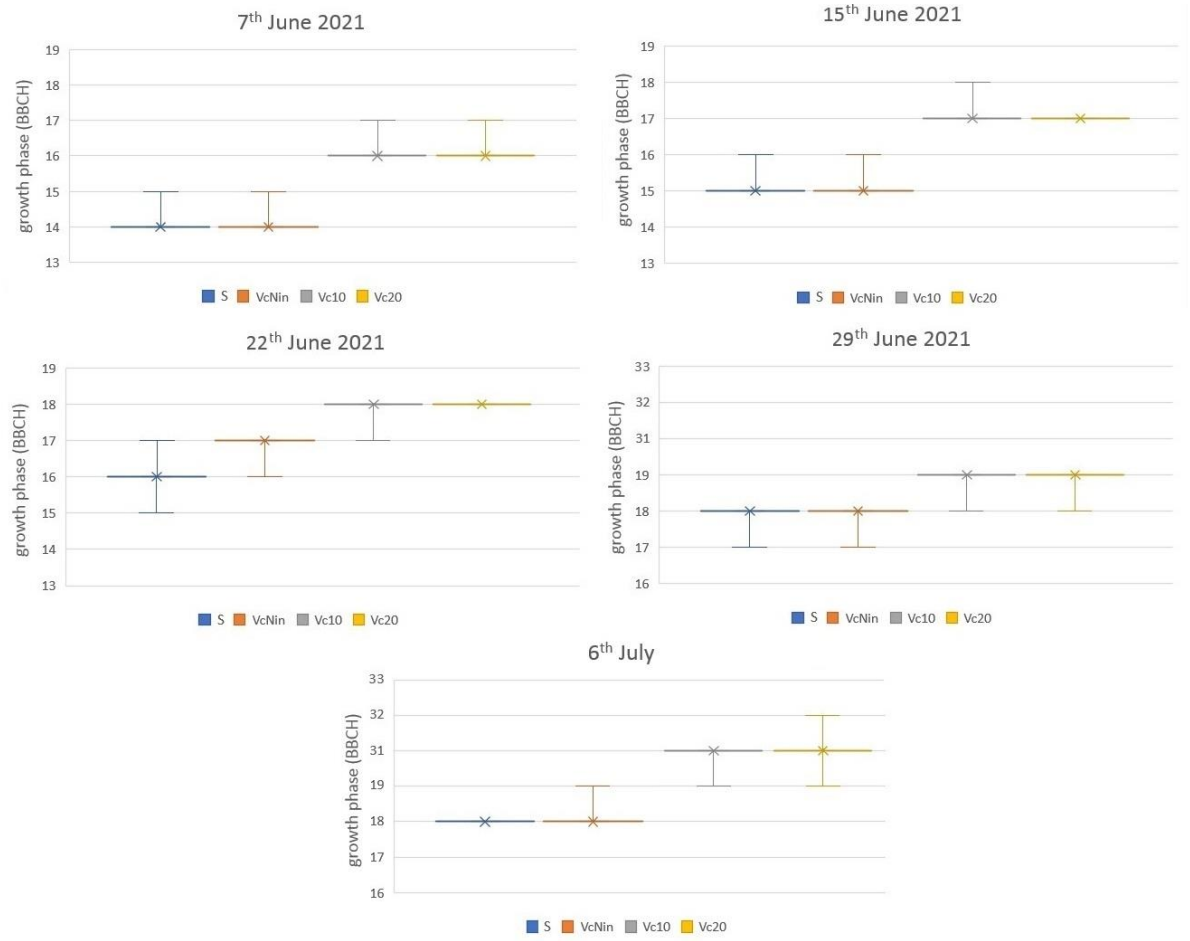

With increasing dose of vermicompost also increased the total weight of individuals. Vermicompost significantly increased the weight of maize plants compared to the control, in the variant with the highest dose by up to 1,059% in the first measurement and by 550% in the second measurement (Table 4). In this variant was also achieved the highest average increase. The Vc_{10} variant achieved statistically significant increases the weight in compare with the control variant and the Vc_{Nin} variant in both measurements. There was no significant difference in the second measurement between the Vc_{10} and Vc_{20} variants, which suggests that the effect of vermicompost decreases during vegetation. A dose of 170 kg N per hectare increased the total weight compared to the control, but there was no statistically significant difference between them. As mentioned earlier, vermicompost increases the proportion of acceptable nutrients for the plant that receive them, and they increase the total weight. The positive effect of vermicompost is also conditioned by the increased content of humic acids and fulvic acids with a predominance of humic acids, increased activity of microscopic bacteria, fungi, and enzymes such as dehydrogenase and urease (Goméz-Fernández et al. 2011).

The vermicompost changed contents of chlorophyll in variants. The lowest values of chlorophyll *a* were recorded in the control variant (Table 5). The vermicompost increased its content but only to the Vc_{10} variant, where was recorded the highest value of chlorophyll *a*. Additional increases the dose

of vermicompost resulted in a decrease in content of chlorophyll *a*, but its content was higher than in the control variant and variant Vc_{Nin}. The content of chlorophyll *b* had the same dynamics as the content of chlorophyll *a*. However, statistical significance was demonstrated only between the control and other variants. They showed an increase content of chlorophyll *b*. The highest chlorophyll *a*/*b* ratio was recorded in the control variant. In the variant with a dose of N 170 kg per hectare was recorded the lowest ratio. The *a*/*b* ratio was lower in variants Vc_{10} and Vc_{20} than in the control, and therefore we can agree with the findings of Tóth et al. (2002), who found that with increasing supply of soil nitrogen, the ratio *a*/*b* decreased.

Table 4 Influence of vermicompost on plant weight during vegetation (fresh matter)

Treatment		Date				Increase	
		June 7		July 6			
n	Mark	g/plant	rel. 100%	g/plant	rel. 100%	g/plant	rel. 100%
1	S	1.57 a	100	14.23 a	100	12.67 a	100
2	Vc_{Nin}	1.99 a	128	15.00 a	105	13.01 a	103
3	Vc_{10}	12.56 b	805	66.67 b	468	54.11 b	427
4	Vc_{20}	16.53 c	1,060	78.33 b	550	61.80 b	488
$LSD_{0.05}$		2.50		22.50		28.90	

Legend: n – number; $LSD_{0.05}$ – least significant difference at the level $\alpha \leq 0.05$

Table 5 Influence of vermicompost on the content of leaf pigments

Treatment		Chlorophyll *a*	Chlorophyll *b*	Total chlorophylls	Ratio *a*/*b*
n	Mark	mg/m^2			
1	S	151.0 a	52.9 a	203.9 a	2.9 b
2	Vc_{Nin}	163.1 a	71.6 b	234.7 ab	2.3 a
3	Vc_{10}	213.0 b	80.7 b	293.7 c	2.6 ab
4	Vc_{20}	192.0 b	75.7 b	267.7 bc	2.5 ab
$LS_{0.05}$		26.80	17.53	0.36	36.02

Legend: n – number; a – chlorophyll a; b – chlorophyll b; $LSD_{0.05}$ – least significant difference at the level $\alpha \leq 0.05$

In our presented experiment, the content of total chlorophylls varied from 203.9 to 293.7 mg/m^2. The lowest values were recorded in the control variant and the highest in the Vc_{10} variant. In the experiment Kováčik and Kmeťová (2017) the content of total chlorophylls in the growth phase BBCH 18 varied in the range of 147.7 to 249.7 mg/m^2. Elevated values of total chlorophylls may be due to an earlier growth stage or selection of the test leaf because the difference contents of chlorophyll also differ by selecting a suitable leaf material.

CONCLUSION

The results of the experiment indicate a positive effect of vermicompost on the monitored parameters. The highest dose of vermicompost 20% of growing substrate showed a significant increase in the total height of plants and the stem perimeter of maize. Compared to the control, vermicompost doses of 10% and 20% accelerated the onset of growth phases by approximately 2 weeks. During the measurements was observed a more pronounced effect of vermicompost in the early vegetation period, and in the later period the effect of vermicompost decreased. The total weight of the plants and the highest increase were at the highest dose of vermicompost. As the dose of vermicompost increased, the content of chlorophyll *a* and chlorophyll *b* also increased, but only to the variant with 10% vermicompost in the substrate. The highest dose of vermicompost had a negative effect on contents of chlorophylls, without statistical significance, but the content was higher than in the control and in the variant with a nitrogen dose of 170 kg per hectare. The dose of 170 kg N per hectare in the form of vermicompost increased the monitored parameters in comparison with the control variant but were not statistically significantly. The results show that vermicompost is a suitable organic fertilizer to increase the growth parameters of maize.

ACKNOWLEDGMENTS
This research was supported by the project VEGA no. 1/0378/20.

REFERENCES

Adhikary, S. 2012. Vermicompost, the story of organic gold: A review. Agricultural Sciences [Online], 3(7): 905–917. Available at: http://dx.doi.org/10.4236/as.2012.37110. [2021-07-26].

Arancon, N. et al. 2008. Influences of vermicomposts, produced by earthworms and microorganisms from cattle manure, food waste and paper waste, on the germination, growth and flowering of petunias in the greenhouse. Applied soil ecology [Online], 39(1): 91–99. Available at: https://doi.org/10.1016/j.apsoil.2007.11.010. [2021-07-28].

Goméz-Fernández, M.J. et al. 2011. Role of vermicompost chemical composition, microbial functional diversity, and fungal community structure in their microbial respiratory response to three pesticides. Bioresource Technology [Online], 102(20): 9638–9645. Available at: https://doi.org/10.1016/j.biortech.2011.07.113. [2021-07-29].

Gutiérez-Miceli, F.A. et al. 2008. Sheep manure vermicompost supplemented with a native diazotrophic bacteria and mycorrhizas for maize cultivation. Bioresource technology [Online], 99: 7020–7026. Available at: 10.1016/j.biortech.2008.01.012. [2021-07-28].

Kováčik, P., Kmeťová, M. 2017. Vplyv vermikompostu na fytomasu kukurice siatej. 1st ed., Nitra: Slovenská poľnohospodárska univerzita.

Kováčik, P., Ryant, P. 2019. Agrochémia (princípy a prax). 1st ed., Nitra: Slovenská poľnohospodárska univerzita.

Lichtenthaler, H.K. 1987. Chlorophylls and carotenoids: Pigments of photosynthetic biomembranes. Methods in Enzymology [Online], 148: 350–382. Available at: https://www.sciencedirect.com/science/article/abs/pii/0076687987480361. [2021-07-24].

Mehlich, A. 1984. Mehlich 3 soil test extractant: A modification of Mehlich 2 extractant. Communication in Soil Science and Plant Analysis [Online], 15(12): 1409–1416. Available at: https://www.tandfonline.com/doi/abs/10.1080/00103628409367568. [2021-07-25].

Meier, U. 2001. Growth stages of mono and dicotyledonous plants. 3rd ed., Berlin: Federal Biological Research Centre for Agriculture and Forestry.

Petrová, J. et al. 2006. Úroda zrna kukurice siatej (*Zea mays*) ovplyvnená organickým odpadom bioplynovej jednotky v Bátke. Aktuálne problémy riešené v agrokomplexe. Nitra: Slovenská poľnohospodárska univerzita.

Sharma, K., Garg, V.K. 2018. Comparative analysis of vermicompost quality produced from rice straw and paper waste employing earthworm *Eisenia fetida* (Sav.). Bioresource Technology [Online], 250: 708–705. Available at: https://doi.org/10.1016/j.biortech.2017.11.101. [2021-07-25].

Šesták, Z., Čatský, J. 1966. Metody studia fotosyntetické produkce rostlin. Praha: Academia.

SMERNICA RADY (91/676/EHS) z 12. decembra 1991 o ochrane vôd pred znečistením dusičnanmi z poľnohospodárskych zdrojov. Smith, C.W. et al. 2004. Corn: Origin, History, Technology and Production. 1st. London: John Wiley & Sons.

Tóth, R. et al. 2002. Effects of the available nitrogen on the photosynthetic activity and xanthophyll cycle pool of maize in field. Journal of Plant Physiology [Online], 159(6): 627-634. Available at: https://doi.org/10.1078/0176-1617-0640. [2021-07-29].

Interactive effects of adaptation technology, based on no-till sowing into the mulch of cover crop residues, and nitrogen nutrition on photosynthetic performance of maize under drought stress

Emmanuel Opoku[1,2], Petr Holub[1], Hana Findurova[1,2], Barbora Vesela[1], Karel Klem[1,2]
[1]Laboratory of Ecological Plant Physiology
Global Change Research Institute CAS
Belidla 986/4a, 603 00 Brno
[2]Department of Agrosystems and Bioclimatology
Mendel University in Brno
Zemedelska 1, 613 00 Brno
CZECH REPUBLIC

opoku.e@czechglobe.cz

Abstract: The aim of this study was to evaluate the interactive effect of adaptation technology based on no-till sowing into cover crop mulch and nitrogen nutrition on photosynthetic performance of maize under short term drought stress induced by rain-out shelters. The experiment was established in two locations in the same climatic condition but differing in soil fertility. The negative effect of drought on CO_2 assimilation rate was modulated by nitrogen nutrition. However, while nitrogen nutrition led to alleviating effect at the location with higher fertility, the opposite effect was found at the site with lower fertility. Adaptation technology had only a minor impact on photosynthetic response to drought, but it generally increased CO_2 assimilation rate at the site with higher soil fertility and decreased at the site with lower soil fertility. We can conclude that adaptation technology, despite of assumptions, did not significantly change the resilience of maize to drought, and probably longer use of such technology is required to improve soil water retention and thus also balanced supply of water to plants. At the same time, we did not find a negative impact of adaptation technology on photosynthesis which can be related to cooler soil during maize emergence and slower mineralization, although the use of adaptation technology seems to be more effective in soils with higher fertility.

Key Words: climate change adaptation, cover crops, drought, nitrogen nutrition, photosynthetic rate

INTRODUCTION

Global climate is associated with a rise in the atmospheric CO_2 concentration resulting in extreme weather events such as a rise in temperature, heat waves, or changes in precipitation patterns. This resulted in changes in the structure and functions of the terrestrial ecosystem, water and carbon balance as well as general agricultural production (IPCC 2013).

Global average temperatures over the years have increased by 1.41 ºC taking into considerations periods between 1850–1900, which is the pre-industrial era and 1998 to 2018. This has caused a shift in the hot and cold, day and night patterns, with the latter falling whilst the former has risen in number (Ye et al. 2018). The earth surface has successively been warmer with time, showing 0.85 °C increase in the average surface temperature of land and ocean globally from 1880 to 2012.

Climate change is leading to extreme weather conditions and weather events, which significantly contribute to the reduction in food production. Some crop species and regions of the high latitude may benefit from events such as warming with regards to crop production, but globally, extreme climate events have resulted in the decline of crop production. Climate change impact on agricultural production may thus significantly affect food security (IPCC 2014). Carbon dioxide (CO_2) as the primary source of carbon for terrestrial ecosystems, and the building block of organic compounds, has risen over

the years in concentration which is also affecting (mostly stimulating) its fixation by the terrestrial plants.

However, the positive effect of elevated CO_2 concentration on plants is usually overcome by negative impacts such as heat and drought stress, which are tightly linked to climate change. Plants being sessile are generally heavily affected by such adverse environmental conditions. Water availability is a major limiting factor to the growth and development of plants. Climate change will likely increase the scarcity of water as rainfall patterns changes and evapotranspiration increases due to rising temperatures. Globally, the functions and productivity of plants and ecosystems are limited by drought. Although plants are subjected to several stress factors during growth, reduced water availability is currently the prominent plant stress factor globally (Jenks and Hasegawa 2014).

Weather and climate changes have a direct impact on agriculture; irrespective of the regional differences in the impact of climate change, its impact at one place affects significantly global market prices of food and other agricultural products (Uleberg et al. 2014). Because these changes are mostly inevitable, and we can only expect moderation of these trends, if climate change mitigation measures are successful, effective adaptation measures in crop production are necessary. However, the environmental conditions that influence plant growth and development also contribute to the effectiveness of adaptation measures and strategies, and potentially the adaptation measures or the whole system of agronomic practices have to be adjusted according to specific environmental conditions. This is the basic task of research in the coming years so as to maximize the effectiveness of adaptation measures and, conversely, eliminate any losses caused by this transition on agricultural production and provided ecosystem services.

The aim of this study was to test the effect of adaptation technology, based on no-till sowing into cover crop mulch on photosynthetic performance of maize under drought stress and to evaluate the interactions with nitrogen nutrition. We hypothesized, that adaptation technology increase water infiltration and retention and thus will alleviate the drought impacts on photosynthesis. On the other hand, we expected slower nitrogen mineralization under adaptation technology and thus also higher requirements for nitrogen supply.

MATERIALS AND METHODS

Experimental site and design

The experimental sites were in the Czech Republic near the Banin municipality. The experiment was carried out at two experimental sites Babicka (less fertile soil) 49 40.4’N 16 27.5’E, 460 m.a.s.l. and Vetrolam (more fertile soil) 49 39.9’N, 16 28.4’E, 475 m.a.s.l during the 2021 growing season. The mean annual temperature and precipitation are 7.6 °C and 629 mm respectively at this location (long term average 2000–2012). According to the FAO soil groups, the soil type is classified as Retisols. The area of plots was 12.5 m^2 (2.5*5m). Maize (*Zea mays*, Variety Jaipur, FAO 240) was sown on May 10th, 2021, using the ED-6000-2C sowing machine (Amazone).

Immediately after sowing the nitrogen was applied as calcium saltpetre to the fertilized variants in dose 75 kg/ha N (N75). Two treatments of nitrogen fertilization were established: 0 kg/ha N which was left unfertilized (N0) and fertilized with calcium saltpetre 75 kg/ha N (N75). In the conventional technology (CT) variant, the soil was cultivated before sowing to the depth of 6-8 cm using seedbed cultivator with shoe coulters.

A 2 m buffering strips sown with maize were used to separate the plots representing nitrogen fertilization and drought treatment within the block, and the blocks were separated by 3 m grass strips. The blocks were further split lengthwise into conventional technology (CT) where after harvest of preceding crop (spring barley) the shallow soil cultivation and then ploughing on depth 22 cm was done, and adaptation technology (AT), where directly after harvest of preceding crop the no-till sowing of species rich cover crops was done and no more cultivated as in (see Figure 1).

The cover crop mixture comprised 25 kg/ha Fitsoil Nitro (consisting of *Avena strigosa, Vicia benghalensis, Vicia villosa, Trifolium incarnatum,Trifolium alexandrinum, Raphanus sativus, Brassica juncea, Phacelia tanacetifolia, Linum usitatissimum*), 15 kg/ha Greening 5 (consisting of *Phacelia tanacetifolia, Trifolium alexandrinum, Vicia sativa, Pisum sativum var. arvense, Fagopyrum exculentum*) and 15 kg/ha *Lupinus angustifolius*.

Figure 1 Sowing of maize using the sowing machine Amazone ED-6000-2C (left) and rain-out shelters for induction of drought stress (right). The split plots with conventional technology based on ploughing and no cultivation of cover crop (CT), and adaptation technology with no-till sowing into cover crop mulch (AT) are visible on the left picture.


Physiological measurements

Light saturated CO_2 assimilation rate (A_{max}), stomatal conductance (G_{Smax}) and transpiration rate (E), were determined under ambient CO_2 concentration (400 ppm), photosynthetically active radiation intensity 1200 µmol/m^2/s, leaf temperature 25 °C, and relative humidity 55% using gas exchange system Li 6800 (LiCOR Biosciences, USA). The water use efficiency (WUE) was calculated as ratio between A_{max} and E.

RESULTS AND DISCUSSION

Four-way ANOVA (Table 1) across all factors, including the location, showed a significant effect of nitrogen application on A_{max} and G_{Smax} but not on WUE, while location showed a significant effect on G_{Smax} and WUE but not on A_{max}. On the other hand, the technology effect was significant only for A_{max}. Drought showed highly significant effects in all three gas exchange parameters evaluated, A_{max}, G_{Smax} and WUE. Two-way interactions were significant for A_{max} in case of interactions nitrogen x location, nitrogen x technology and location x technology. For G_{Smax} the interactions were significant in case of nitrogen x location, location x technology, and location x drought. For WUE the two-way interaction was not significant at all. Three-way interactions were significant for A_{max} in case of nitrogen x location x drought and for WUE in case of nitrogen x location x technology.

The interactive effects, which are important mainly for location x technology, are evident also in Figure 2. While in the location Babicka (which is characteristic with lower soil fertility) is observed rather a negative effect of adaptation technology (AT) on Amax and GSmax rather, in location Vetrolam (higher soil fertility) shows rather positive or no effect of AT. The role of fertility for the success of AT is also evident from the nitrogen application effect. Nitrogen application (N75) completely alleviated the negative effect of AT at site Babicka and stimulated the positive effect of AT at site Vetrolam.

The availability of nitrogen and probably also other nutrients seems, therefore, to be key for achieving high physiological performance of maize and thus also its productivity. The effect of technology on the physiological impact of drought was, despite the expectations, rather negligible and insignificant. This is also evident from the interaction between technology and drought. Also, nitrogen fertilization did not affect the drought response of maize significantly. WUE was affected

mainly by drought, while drought increases WUE. The effects of drought on WUE were higher at location Vetrolam.

Table 1 Results of four-way ANOVA indicating the significance (p-values) of individual factors, and their interactions. Significant effects (p<0.05) are indicated in bold for the main gas exchange parameters (A_{max} – light saturated CO_2 assimilation rate, G_{Smax} – light saturated stomatal conductance, WUE – water use efficiency calculated as ratio of light saturated CO_2 assimilation and transpiration rate).

Treatment	A_{max}	G_{Smax}	WUE
Nitrogen (N)	**0.000**	**0.000**	0.067
Location (L)	0.084	**0.013**	**0.018**
Technology (T)	**0.047**	0.214	0.963
Drought (D)	**0.000**	**0.000**	**0.000**
N x L	**0.000**	**0.020**	0.648
N x T	**0.002**	0.052	0.790
L x T	**0.000**	**0.000**	0.163
N x D	0.494	0.077	0.114
L x D	0.193	**0.006**	0.200
T x D	0.358	0.919	0.366
N x L x T	0.166	0.181	**0.034**
N x L x D	**0.015**	0.180	0.226
N x T x D	0.267	0.401	0.361
L x T x D	0.167	0.091	0.201
N x L x T x D	0.284	0.618	0.657

Plants responses to drought can be observed as a result of changes in their physiological processes such as photosynthesis, respiration and transpiration (Knauer et al. 2017). Mechanisms such as stomatal closure, as indicated by (Liu et al. 2018), affect the related physiological processes mentioned above, and by this means, plants can restrain water loss due to suppression of transpiration under this mechanism. Within this experiment, WUE was affected mainly by drought and slightly also by location and the interaction location x nitrogen x technology.

The interaction of nitrogen application has had some diverging views, and there have been many uncertainties regarding the interaction of water deficit and N deficiency on leaf gas exchange, respiration and WUE (Xing et al. 2021). According to (Song et al. 2019), water stress was alleviated, and resistance to drought improved when nitrogen supply was increased, whilst other studies from (Araus et al. 2020), revealed that nitrogen application could weaken crops with limited water supply.

AT, which employs no-tillage, avoids frequent soil disturbance, and this is notable for its role in crop residue maintenance on the soil surface (Soane et al. 2012). This technology is known to increase organic matter content in the long term under tropical and temperate conditions, as recorded by (Miranda et al. 2016, Kinoshita et al. 2017). Zhou et al. (2011) also reported the positive effect of organic mulch on soil surface on maize yield under drought stress. Similarly, to our results, they did not reveal the interactive effect of nitrogen nutrition with drought.

Figure 2 Effects of nitrogen nutrition, technology and simulated drought by rain-out shelter during the main elongation stage, on the main gas exchange parameters

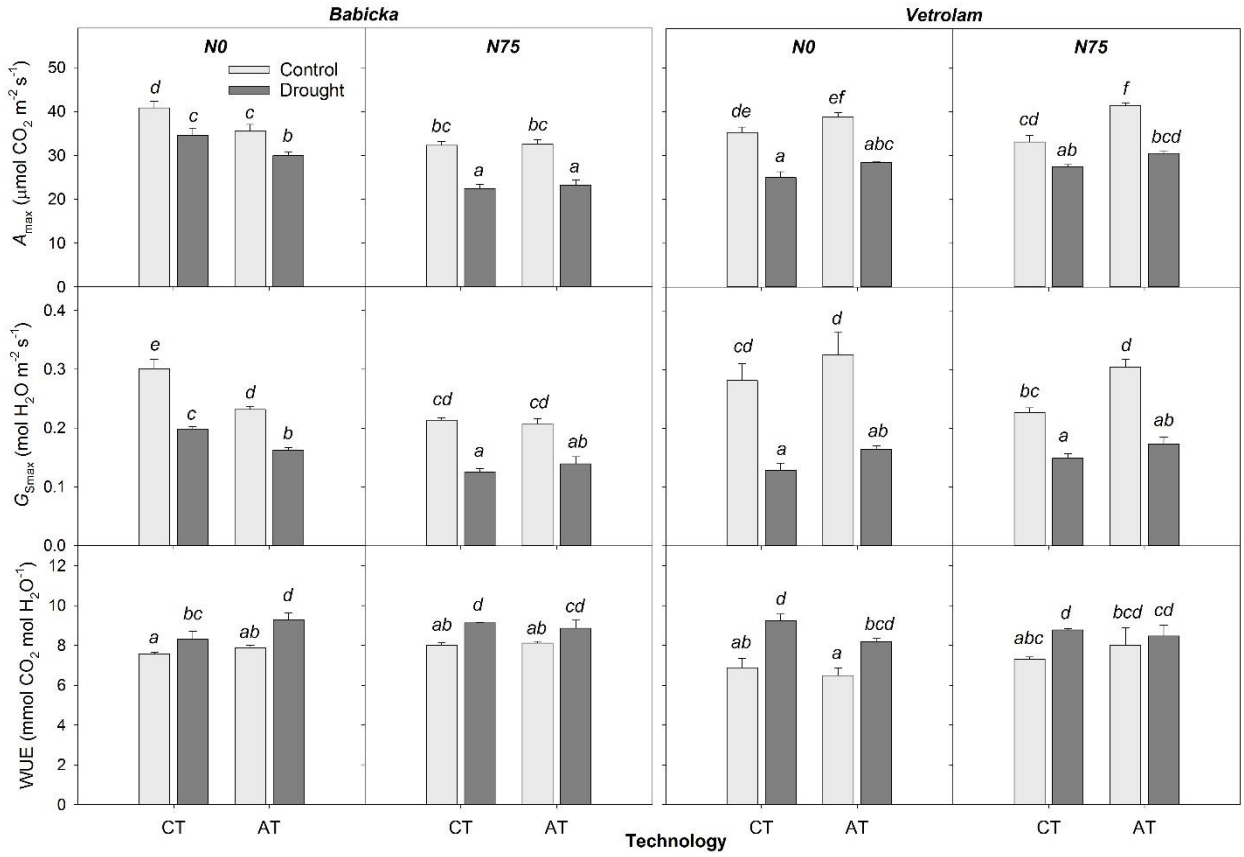

Legend: N0 – without N fertilisation, N75 – 75 kg N applied after sowing in the form of calcium saltpetre, CT – conventional technology with ploughing and no cultivation of cover crops, AT adaptation technology with no-till sowing of crop into mulch of cover crops, Control – no rain-out shelters, Drought - exclusion of rainfall by rain-out shelters, A_{max} – light saturated CO_2 assimilation rate, G_{Smax} – light saturated stomatal conductance, WUE – water use efficiency calculated as ratio of light saturated CO_2 assimilation and transpiration rate.

CONCLUSION

We can conclude that the application of AT has to be considered from the perspective of soil conditions, and in the case of less fertile soils, the possible adverse effects of AT should be compensated by a higher nitrogen rate. We did not find any positive effect of AT on drought impact, which probably requires a longer period of using AT to reach the improved soil water infiltration and retention, allowing to help the plants to cope with drought stress better than in conventional technologies, which are typical with damaged soil structure, sealing of soil to infiltration by forming a crust on soil surface after heavy rain, and higher sensitivity to soil compaction.

ACKNOWLEDGEMENTS

This study was supported by the SustES project – Adaptation strategies for sustainable ecosystem services and food security under adverse environmental conditions (CZ.02.1.01/0.0/0.0/16_019/0000797).

REFERENCES

Araus, V. et al. 2020. A balancing act: how plants integrate nitrogen and water signals. Journal of Experimental Botany, 71: 4442–4451

IPCC. ©2014. Climate Change 2014: Impacts, adaptation and vulnerability. [Online]. Available at: http://www.ipcc.ch/report/ar5/wg2. [2021-08-20].

IPCC. ©2013. Climate Change 2013: The Physical Science Basis. [Online]. Available at: http://www.ipcc.ch/report/ar5/wg1. [2021-08-20].

Jenks, M.A., Hasegawa, P.M. 2014. Plant Abiotic Stress. 2. ed., Ames, Iowa: John Wiley & Sons, Inc.

Kinoshita, R. et al. 2017. Quantitative soil profile-scale assessment of the sustainability of long-term maize residue and tillage management. Soil and Tillage Research, 174: 34–44.

Knauer, J. et al. 2017. The response of ecosystem water-use efficiency to rising atmospheric CO_2 concentrations: Sensitivity and large-scale biogeochemical implications. New Phytologist, 213(4): 1654–1666.

Liu, C. et al. 2018. Variation of stomatal traits from cold temperate to tropical forests and association with water use efficiency. Functional Ecology, 32(1): 20–28.

Miranda, E. et al. 2016. Long-Term Changes in Soil Carbon Stocks in the Brazilian Cerrado Under Commercial Soybean. Land Degradation & Development, 27: 1586–1594.

Song, Y. et al. 2019. Nitrogen increases drought tolerance in maize seedlings. Functional Plant Biology, 46: 350–359.

Soane, B.D. et al. 2012. No-till in northern, western and south-western Europe: A review of problems and opportunities for crop production and the environment. Soil and Tillage Research, 118: 66–87.

Uleberg, E. et al. 2014. Impact of climate change on agriculture in Northern Norway and potential strategies for adaptation. Climatic Change, 122(1): 27–39.

Xing, H. et al. 2021. Excessive nitrogen application under moderate soil water deficit decreases photosynthesis, respiration, carbon gain and water use efficiency of maize. Plant Physiology and Biochemistry, 166: 1065–1075.

Ye, J. et al. 2018. Which Temperature and Precipitation Extremes Best Explain the Variation of Warm versus Cold Years and Wet versus Dry Years? Journal of Climate, 31(1): 45–59.

Zhou, J.B. et al. 2011. Effect of water saving management practices and nitrogen fertilizer rate on crop yield and water use efficiency in a winter wheat–summer maize cropping system. Field Crops Research, 122(2): 157–163.

A comparison of the efficiency of pheromone lures on the *Cydia pomonella* (codling moth)

Zaneta Prazanova, Hana Sefrova
Department of Crop Science, Breeding and Plant Medicine
Mendel University in Brno
Zemedelska 1, 613 00 Brno
CZECH REPUBLIC

xprazano@mendelu.cz

Abstract: In May 2021–August 2021, the effectiveness of differently aged pheromone lures from Propher and Pherobank on *Cydia pomonella* L., 1758 (codling moth) was compared. Monitoring was carried out in the gardens of two villages in Malá Lhota and Újezd u Černé Hory. A total of six green delta traps were put up by Propher. Pheromone lures from Propher from the years 2013, 2015, 2019 and 2020 were used. Pheromone lures from Pherobank with normal and increased pheromone content were used from 2020. A total of 220 male *Cydia pomonella* was captured. *Cydia pomonella* was recorded in all traps. The greatest number of individuals were captured in the trap with 2019´s pheromone lure, with 66 in total. The 2013´s lure from Propher captured the lowest number of imagoes, with a total of seven. A total of three non-target species were recorded, all of them *Agrotis segetum*. Based on the monitoring, the effectiveness of two-year-old lures (2019, 2020) on *Cydia pomonella* was demonstrated.

Key Words: codling moth, *Cydia pomonella,* pheromone lure, monitoring, orchard

INTRODUCTION

Pheromones are the most important category of chemicals used for insect communication (Hrdý 2006a). W. J. Roelofs pioneered the discovery of a sexual attractant for the *Cydia pomonella*. The main component of this pheromone (codlemon) is (E,E)-8,10-dodecadien-1-ol (abbreviated E8E10-12OH). In later years, another 8–12 components for this pheromone were identified (Hrdý 2006b). Currently, three commercial preparations based on these pheromones are registered for *Cydia pomonella* in the Czech Republic (CISTA 2021). A considerable advantage of pheromones is that non-target organisms are not adversely affected by pheromones (Witzgall et al. 2010).

Cydia pomonella is the most important pest of apple trees in many countries (Pajač et al. 2011). The first record of *Cydia pomonella* damage came from the Netherlands in 1635 (Geest and Evenhuis 1991). This species belongs to the family Tortricidae; its caterpillars cause apple blight and can also damage pear and walnut trees (Razowski 2001). In our conditions (Czech Republic), it usually has two generations (Hluchý 2011, Pražanová 2016), while in Europe, it can have up to three generations (Razowski 2001). In our study, we tested the effect of the age of pheromone lures on their efficiency and selectivity.

MATERIALS AND METHODS

Defining the study areas

The monitoring of *Cydia pomonella* took place in 2021 in the gardens of Malá Lhota and Újezd u Černé Hory from May to August. These villages are located in the South Moravian Region in the Blansko District at an altitude of up to 400 m above sea level. They are about 3.5 km away from each other. The gardens are cultivated with fruit trees, mainly apple and plum trees, and less commonly, pear trees. The fruit trees have not been chemically treated since 2017. The characteristics of the study areas are stated in Table 1.

Table 1 Description of study areas Malá Lhota and Újezd u Černé Hory (https://www.google.cz/maps)

Study area	Malá Lhota	Újezd u Černé Hory
Coordinates	49.3933722N, 16.5455886E	49.3709506N, 16.5431967E
Fauna square	6665	6665
Altitude	387 m	365 m
Area	2600 m^2	3700 m^2
Type of fruit tree	apple, pear, plum	apple, plum

Material

Green pheromone traps of the delta type from Propher (Figure 1) and pheromone lures from Propher and Pherobank were used to monitor the *Cydia pomonella*. White sticky inserts were inserted into the traps, which were included in the package. A total of six variants of pheromone traps were put up. Several pheromone lures from different years of manufacture were used. From Propher, lures CZ 2013, CZ 2015, CZ 2019, and CZ 2020 were used, and from Pherobank, which provided two types of lures, one conventional (NL 2020) and one so-called super lure (NL super 2020) for *Cydia pomonella* (Figure 2). The super lure should contain more attractant than the classic lure. The composition of lures and the ratios of attractants used are trade secrets of manufacturers and distributors.

Monitoring

The traps were placed in the gardens of Malá Lhota and Újezd u Černé Hory on 24 April 2021. The traps were placed on trees at a height of approximately 1.6 m above ground and were spaced approximately 25 m apart. In Malá Lhota, four traps were placed (CZ 2013, CZ 2015, CZ 2019, CZ 2020), and in Újezd u Černé Hory, two traps (NL 2020, NL super 2020) were placed. In Malá Lhota, individuals were observed flying into Propher lures, and in Újezd u Černé Hory, Pherobank lures were placed. The traps were shifted after a week, rotated by one position each time, to partially reduce exposure conditions. The sticky inserts were checked weekly and replaced as needed, usually once every 14 days.

Figure 1 Green delta trap with sticky insert from Propher

Figure 2 Pheromone lures of Cydia pomonella from two producers (Propher, Pherobank)

RESULTS AND DISCUSSION

Cydia pomonella

Cydia pomonella was recorded in all traps set out (Figure 3). A total of 220 male *Cydia pomonella* was captured. A total of 90 and 130 imagoes of *Cydia pomonella* was captured in Malá Lhota and Újezd u Černé Hory, respectively. Most of the imagoes were captured in a trap with a Propher lure from 2019, with a total of 66. The Pherobank lure from 2020, type super, had a comparable effect. Here, only three fewer individuals were recorded. The fewest adults were captured in the oldest 2013 Propher lure, with only seven imagoes.

Figure 3 Numbers of Cydia pomonella males using different old pheromone lures from two producers for tortricid moths

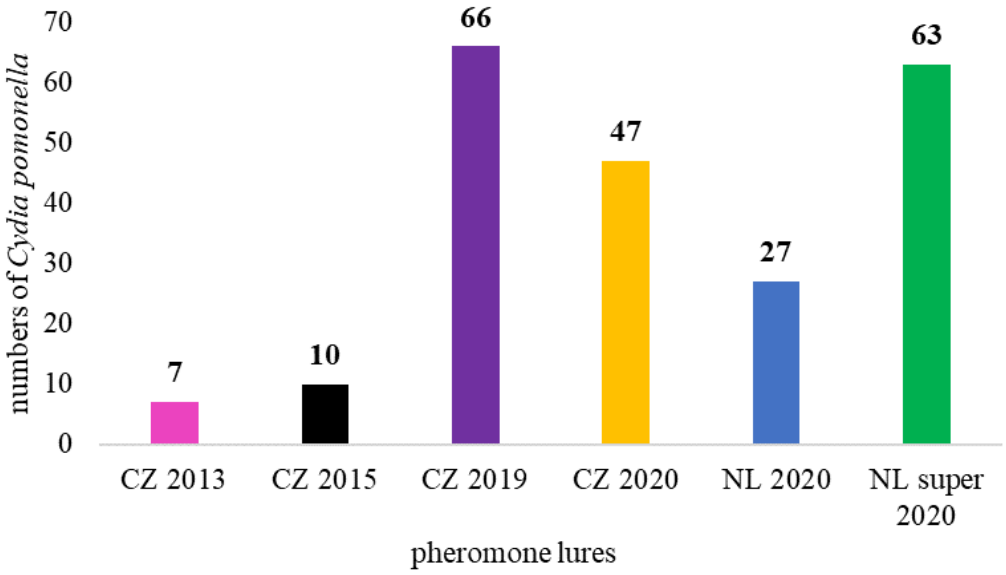

The first *Cydia pomonella* record was from the week of 17. 5. to 23. 5. in almost all traps. The first imago was registered one week later in the trap with lure NL 2020 and two weeks later in the trap with lure CZ 2013. The graph shows two distinct flight waves of *Cydia pomonella* (Figure 4). The number of captures increased around mid-June, and a second surge of individuals took place in early July. These findings are consistent with results from 2015 in the same study area (Pražanova 2016). The number of captured *Cydia pomonella* individuals slightly decreased since the beginning of August. Several other Czech authors have also monitored the occurrence of *Cydia pomonella* (Hrdý 2006b, Hluchý 2011, Spáčilová 2011, Vymětal 2013, Kohoutová 2020). In these investigations, the first occurrences of *Cydia pomonella* were detected in May, and the number of catches decreased from mid-August onwards. The first flight maximum was captured from the end of May to mid-June. A second flight maximum was recorded from mid to late July.

Figure 4 Flight period of Cydia pomonella males in traps using different old pheromone lures for tortricid moths

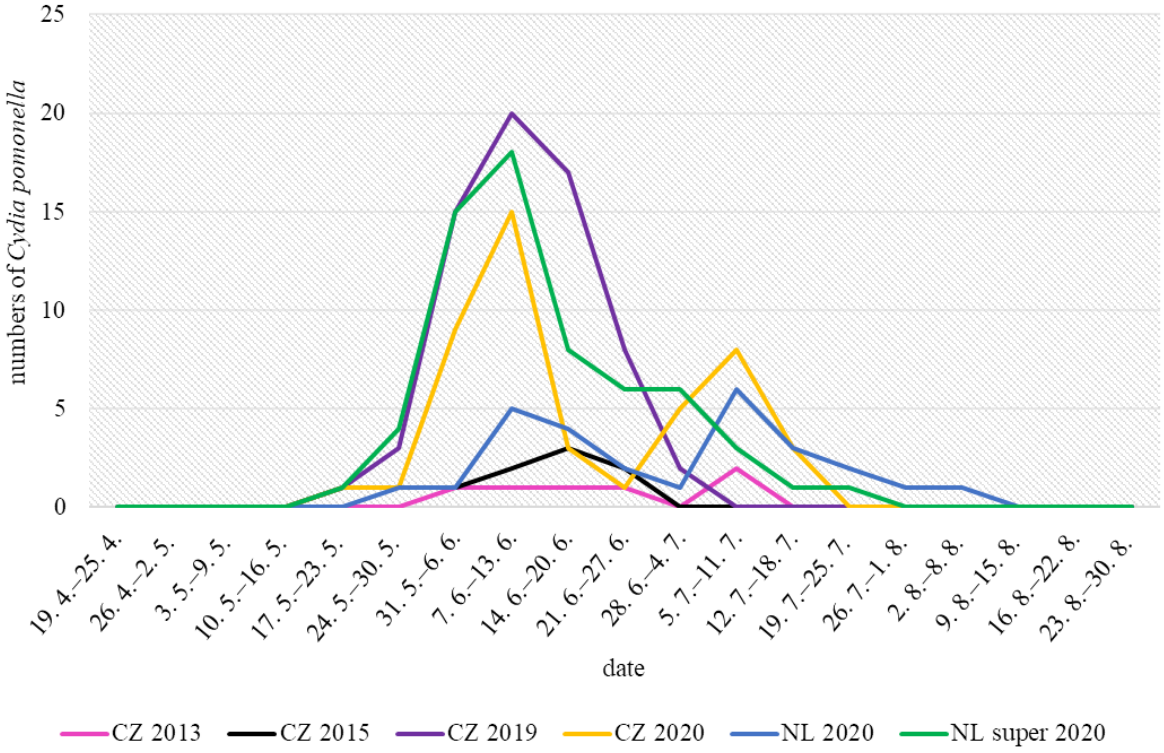

Non-target species

A total of three non-target species were recorded. Two *Agrotis segetum* imagoes were recorded in a trap with a lure from 2013 and one imago in a trap with a lure from 2020. Both of these were Propher lure. *Agrotis segetum* was recorded in the traps at the beginning of July and August. The observation is confirmed by the literature (Nowacki 1998). This species was caught earlier on the pheromone lure *Grapholita funebrana* (Hrudová 2005). It is well known that the lures on the *Cydia pomonella* are selective. Monitoring with older pheromone lures has shown that the lure continues to retain its selectivity.

CONCLUSION

All traps, with all pheromone lures, recorded a male *Cydia pomonella*. According to the results, I dare to say that older pheromone lures can be used to monitor this pest, and two-year-old pheromones can be used without a decrease in effectiveness. The purchase price of Propher's lures is lower than that of Pherobank. Propher pheromone lures perform comparably to Pherobank pheromone lures. Two-year-old pheromones maintain their selectivity. Almost no non-target species were captured.

REFERENCES

CISTA (Central Institute for Supervising and Testing in Agriculture), The register of plant protection products. 2021. [Online]. Available at: http://eagri.cz/public/app/eagriapp/POR/. [2021-09-16].

Geest, L.P.S. van der, Evenhuis H.H. 1991. Tortricid pests: their biology, natural enemies, and control. Amsterdam, Netherlands: Elsevier Science Publishers.

Hluchý, Š. 2011. Necílové druhy obalečů (Tortricidae) ve feromonových lapácích v ochraně jabloňových sadů, jejich letová dynamika a bionomie. Diploma thesis (in Czech), Mendel University in Brno.

Hrdý, I. 2006a. Feromony v integrované ochraně rostlin I. Repetitorium. Živa, 1: 25–27.

Hrdý, I. 2006b. Feromony v integrované ochraně rostlin II. Obaleč jablečný. Živa, 2: 73–76.

Hrudová, E. 2005. Nontarget lepidoptera species found in the pheromone traps for selected tortricid species in 2002 and 2003. Acta Universitatis Agriculturae et Silviculturae Mendelianae Brunensis, 53(1): 35–44.

Kohoutová, M. 2020. Škůdci jabloní v závislosti na intenzitě pěstování. Diploma thesis (in Czech), Mendel University in Brno.

Nowacki, J. 1998. The Noctuids (Lepidoptera, Noctuidae) of Central Europe. Bratislava: F. Slamka.

Pajač, I. et al. 2011. Codling Moth, Cydia pomonella (Lepidoptera: Tortricidae) – Major Pest in Apple Production: an Overview of its Biology, Resistance, Genetic Structure and Control Strategies. Agriculturae Conspectus Scientificus, 76(2): 87–92.

Pražanová, Ž. 2016. Škodlivost obalečů na slivoních a jabloních na ošetřovaných a neošetřovaných dřevinách. Bachelor thesis (in Czech), Mendel University in Brno.

Razowski, J. 2001. Die Tortriciden (Lepidoptera, Tortricidae) Mitteleuropas. Bestimmung – Verbreitung – Flugstandort – Lebensweise der Raupen. Bratislava: F. Slamka.

Spáčilová, E. 2011. Výskyt obaleče jablečného (Cydia pomonella) na Olomoucku. Bachelor thesis (in Czech), Mendel University in Brno.

Vymětal, M. 2013. Zhodnocení účinnosti různých metod monitoringu obaleče jablečného (Cydia pomonella). Diploma thesis (in Czech), Mendel University in Brno.

Witzgall, P. et al. 2010. Sex pheromones and their impact on pest management. Journal of Chemical Ecology, 36(1): 80–100.

Evaluation of nutritional potential of selected sorghum varieties in relation to different types of soil localities

Michal Rihacek[1], Jakub Novotny[1], Dana Zalesakova[1], Lucie Horakova[1], Eva Mrkvicova[1], Leos Pavlata[1], Ondrej Stastnik[1], Vladimir Smutny[2], Michal Rabek[2]
[1]Department of Animal Nutrition and Forage Production
[2]Department of Agrosystems and Bioclimatology
Mendel University in Brno
Zemedelska 1, 613 00 Brno
CZECH REPUBLIC

xrihace2@mendelu.cz

Abstract: The aim of this study was to evaluate selected sorghum varieties and their nutritional potential in relation to different types of soil locations. The comparison was done at the Field Experimental Station in Žabčice at two different locations Obora (clay loam soil – fluvial soil) and Písky (light sandy soil). Sorghum varieties were analysed for basic laboratory parameters – ash, fat, crude protein, acid detergent fibre (ADF), neutral detergent fibre (NDF) and digestibility of dry matter and organic matter using in vitro pepsin by cellulase method. The analyses were performed according to the relevant standards. The results of this research prove that the differences in selected nutritional parameters between the compared locations are not very high. A statistically significant difference (P> 0.05) were found for crude protein at Písky location.

Key Words: sorghum, nutritional values, climate change

INTRODUCTION

Sorghum is one of the most important cereals grown mainly in warmer and drier climates. In global production, sorghum is the fifth most widespread cereal in the world after wheat, corn, rice and barley (Ratnavathi et al. 2012). Due to global warming, the possibility of using sorghum as feed, but also use in human nutrition for gluten-free diet, interest in growing sorghum is extending. With rising summer temperatures reaching up to 40 °C is possible to grow sorghum in the Czech Republic and other Central and Estern European countries. However, the problem of growing sorghum in the temperate climate of the Czech Republic and Central and Eastern Europe may be spring ground frost and low temperatures in the morning.

Sorghum is considered as flexible crop with natural ability for adaptation to different temperatures, day lengths, light and soil. This adaptability is futher used in breeding to increase resistance to diseases, pests or stress (Chobotová and Prokeš 2013). This sorghum varieties can be a high guarantee of economic profitability in their cultivation (Bogaň 2013).

A positive quality of sorghum is adaptability to different types of soils. Sorghum is also much more tolerant to shallow soil and drought than corn, althought it grows the best on deep, fertile and well-drainded clay soils. Sorghum is grown on soils with an optimal pH > 6.5.

Environmental requirements are quite low, for germination minimal temperature is 12–15 °C and the annual requirement for the sum of temperatures is 2500–3000 °C. The lenght of the vegetation period without frosts requires 120–180 days. Sorghum can grow without irrigation in areas with an average total precipitation of 400–700 mm (Hermuth et al. 2012). The average dry matter yield of forage sorghum variety is 24.4 t/ha and BMR of varieties 21.1 t/ha (Marsalis et al. 2010). The resistance of sorghums to dry conditions is supported by an extensive root system and a waxy layer on the surface of the leaves. From this point of view, there is a reduction of water loss and the ability to stop growing in times of drought and subsequently resume their growth under appropriate conditions (Brink et al. 2006).

MATERIAL AND METHODS

Characterization of experimental location

Experimental part was perfomed on the Field Experimental Station in Žabčice located 179 meter above sea level in maize production area of South Moravia in the Czech Republic. The annual average temperature is 9.2 °C and the thirty-year annual average precipitation is 480 mm. Two habitats were used for the experiment, Obora and Písky, differing in soil quality. While Písky are locations with lighter, sandy and dry soils (chernozem), Obora is a location characterized by heavier soils with higher groundwater levels (fluvisol). All varieties were grown in both localities.

Characterization of selected varieties

Six varieties were chosen: Triunfo BMR, Nutri Honey, Latte, KWS Freya, KWS Sole, KWS Sammos (*S. bicolor* x *S. sudanense*). Seeds of these varieties were provided by SEED Service and KWS companies.

Characterization of experimental design

To achieve optimal agrotechnical requirements during sowing, the rows distance was 45 cm and the sowing depth 3 cm. Harvest area was always 5 meters in one row and repeated 3 times. The dimensions and size of the harvest area were 2.25 m^2 (5 m x 0.45). The sowing was done on 22nd of May 2020. The harvest date was determined by the value of the dry matter from samples of plants (28% of dry matter and above) as the important indicator. Sampling of sorghums varieties were performed on September (4th, 11th, 18th), 2 kg of fresh matter was obtained from each variety. Then the samples were chopped (VIKING GE 375), pre-dried in oven Venticell 707 (BMT Medical Technology s.r.o., CZ) at the temperature 65 °C for 24 hours and grinded FRITSCH (Pulverisette, Germany) through a 1 mm sieve. Laboratory dry matter, ash, crude protein, fat, fibre, acid-detergent fibre (ADF), neutral detergent fibre (NDF) and *in vitro* digestibility of dry matter (DMD – dry matter digestibility) and *in vitro* digestibility of organic matter (OMD – organic matter digestibility) were determined for all varieties.

According to commision regulation (EC) No. 152/2009 for determination of methods used in sampling and laboratory testing for the official control of feeding stuffs, the analysis are carried out according to current methodics of Central Agricultural Inspection and Testing Institute. The dry matter was determined at 103 ± 2 °C. Ash (macro-elements and micro-elements) can be determined from the dry matter by incineration at temperature of 550 ± 20 °C to constant weight in a muffle furnace. Crude protein was determined by the Kjeldahl method and then multiplied by factor of 6.25, expressed as nitrogen content. After hydrolysis, the fibre remains in diluted sulfuric acid and diluted lye of potassium hydroxide. After washing of the fibre with an organic solvent and after deducting the value of the ash was determined. The method of Henneberg and Stohmann is used to determine the value. The nitrogen-free extractives are determined by calculation after deducting the values of fat, crude protein, ash and fibre obtained from dry matter. The fat was determined according to the Soxhlet reaction, in which the sample is extracted by diethyl ether. The digestibility of dry matter and organic matter was determined by the pepsin cellulase method *in vitro* using an ANKOM Daisy Analyzer incubator (Ankom Technology, NY) was monitored. The digestibility of dry matter and organic matter by pepsin cellulas method *in vitro* is based on incubation of the sample in acidic pepsin solution, the hydrolysis of starch at elevated temperature and the subsequent incubation in a buffered cellulase solution.

Statistical analyses

The results of the experiment were processed using Microsoft Office (USA) and STATISTICA version 12 (USA). Gathered values were tested using by one-way analyses of variance (ANOVA) and post-hoc Sheff´s test, where $P < 0.05$ value was considered as statistically significant difference.

RESULTS AND DISCUSSION

The following table (Table 1) presents a comparison of the achieved laboratory values of sorghum at both sites – Obora and Písky.

Table 1 Overview of average values of laboratory parameters of sorghum at both localities

Location	Obora			Písky		
n	6			6		
	Mean ± SE					
Laboratory dry matter (%)	94.24	±	0.12	93.81	±	0.23
Ash (%)	7.68	±	0.55	7.40	±	0.23
Crude protein (%)	7.88	±	0.12[b]	9.15	±	0.35[a]
Fat (%)	2.26	±	0.07	2.21	±	0.06
Fibre (%)	27.25	±	1.40	28.49	±	0.85
ADF (%)	37.39	±	1.65	38.29	±	0.72
NDF (%)	53.91	±	2.18	59.43	±	1.44
DMD (%)	49.25	±	3.85	47.92	±	1.58
OMD (%)	46.12	±	4.30	44.18	±	2.06

Legend: [a,b] means differ significantly at P < 0.05; n – number of cases; SE – standard error; ADF – acid detergent fibre; NDF – neutral detergent fibre; DMD – dry matter digestibility; OMD – organic matter digestibility

A statistically significant difference (P > 0.05) was found for crude protein. At Písky, the value was higher (9.15%) in comparison to the other locality Obora (7.88%). This was also proved in study of Baholet et al. (2018). They compared sorghum varieties in the same locations, while individual sorghum varieties reached higher values (8.38–14.2%) at Písky. Even though this site was not fertilized. This may correspond with the fact that the soil is well supplied with nitrogen. However, low values are not a problem, due to crude proteins can be increased in crop by higher fertilization. According to Doležal (2014) range of crude protein in sorghum is from 13% to 18%. This corelates with the study of Rajčáková (2005), where the range of crude proteins was 13.1–18.6%.

There were not found any statistically significant differences among other parameters (P > 0.05). According to Rajčáková (2005) the range of values NDF was from 54–55.2%. In the research of Baholet et al. (2018) values of neutral detergent fibre were found in varieties of sorghum from 41.72% to 54.12%. These results show large differences between selected varieties, differences between the habitats are not very high. Similar values were also found in the study of Rihacek et al. (2020) for selected sorghum varieties in both habitats. The results of acid detergent fibre at both habitats also correspond with the study of Baholet et al. (2018). According to a study of Hermuth et al. (2012), sorghum has higher NDF (48–62%), ash (6–12%), crude fibre (32–44%) and higher DMY, in comparison to maize.

According to Assefa and Ledin (2001) both NDF (hemicelluloses, cellulose, and lignin) and ADF (cellulose and lignin) are considered to be important indicators of forage quality. Better forage quality exhibits low content of NDF and ADF because these indicators are negatively correlated with the ruminants' nutrient intake and food digestibility (Guretzky et al. 2011, Bean et al. 2013). According to a study of Hermuth et al. (2012), sorghum has higher NDF (48–62%), ash (6–12%), crude fibre (32–44%), in comparison to maize.

Digestibility of dry matter and organic matter belong to important parameter in animal nutrition. Statistically significant differences were found among tested varieties (DMD 73.21 ± 1.57%, OMD 70.58 ± 2.12%) in the study of Koláčková et al. (2020), of Ruzrok (DMD 73.99 ± 3.11%, OMD 71.46 ± 3.71%) and KWS Sole varieties (DMD 74.13 ± 2.03%, OMD 71.91 ± 2.48%). The highest digestibility was observed in Triumfo BMR (DMD 79.57 ± 0.72%, OMD 77.90 ± 0.64%), Sweet Susana (DMD 82.11 ± 0.94%, OMD 80.62 ± 0.97%) and DSM 45-480 (DMD 86.70 ± 1.22%, OMD 85.67 ± 1.41).

The average digestibility of organic matter is in the range of 45–60% (Přikryl 2014). Sriagtula et al. (2017) claims that the digestibility of organic matter was affected by mutant lines of sorghum. In their study BMR sorghum achieved higher digestibility of organic matter (66.59%). Traditional varieties without BMR mutation contained lower digestibility of organic matter (60.59%).

Average temperature in June 2020 was 18.3 °C and normal temperature 17.7 °C. Extremely high temperatures were measured in August (21.7 °C) and normal (18 °C). These findings may indicate a high

potential for future agricultural use of sorghum in higher and lower production systems in areas affected by climate change.

CONCLUSION

The results of this research prove that the differences in selected nutritional parameters between the compared localities are not very high. A statistically significant difference (P> 0.05) was found for crude protein at Písky location. This parameter is therefore influenced by habitat conditions and fertilization. We can state that both locations are suitable for growing sorghum. The main advantage of this crop above all is the ability to withstand and even thrive in poor soil conditions without much maintenance. Therefore selected varieties can be included among common agricultural crops. Then the ideal variety for animal nutrition is the form of sorghum, which is important.

ACKNOWLEDGEMENTS

The research was financially supported by the Internal Grant Agency of Faculty of AgriSciences (Mendel University in Brno) no. AF-IGA2021-IP067. Publication has been summarizing with project“MendelFarm – Integrated plant protection in a company operating in dry conditions” 9. F. m – Demonstrační farmy. Supported by Ministry of Agriculture of the Czech Republic.

REFERENCES

Assefa, G., Ledin, I. 2001. Effect of variety, soil type and fertiliser on the establishment, growth, forage yield, quality and voluntary intake by cattle of oats and vetches cultivated in pure stands and mixtures. Animal Feed Science Technology, 92: 95–111.

Baholet, D. et al. 2018. Comparison of nutrient composition of sorghum varieties depending on different soil types. In Proceedings of 25th International PhD Students Conference MendelNet 2018 [Online], Brno, Czech Republic, 7–8 November, Brno: Mendel University in Brno, Faculty of AgriSciences, 159–164. Available at: https://mendelnet.cz/pdfs/mnt/2020/01/29.pdf. [2021-09-10].

Bean, B.W. et al. 2013. Comparison of sorghum classes for grain and forage yield and forage nutritive value. Field Crop Research, 142: 20–26.

Bogaň, J. 2013. Energetický čirok – plodina s velkou budoucností. Úroda, 61(2): 13.

Brink, M. et al. 2006. Plant resources of tropical Africa 1: Cereals and pulses. 1st ed., Wageningen, Netherlands: PROTA Foundation.

Chobotová, M., Prokeš, K. 2013. Čirok, plodina s budoucností. Farmář, (2): 24–26.

Doležal, P. 2014. Má čirok budoucnost jako energetická plodina – ano, nebo ne? Úroda [Online], Available at:
https://www.uroda.cz/ma-cirok-budoucnost-jako-energeticka-plodina-ano-nebo-ne. [2021-09-10].

Guretzky, J.A. et al. 2011. Switchgrass for forage and bioenergy: harvest and nitrogen rate effects on biomass yields and nutrient composition. Plant Soil, 339: 69–8.

Hermuth, J. et al. 2012. Čirok obecný Sorghum bicolor (L.) Moench, možnosti využitı́ v podmínkách České republiky: Methodology for Practice [Online], Praha-Ruzyně: Výzkumný ústav rostlinné výroby, v.v.i. Available at: http://invenio.nusl.cz/record/124035/files/nusl-124035_1.pdf. [2021-09-14].

Koláčková, I. et al. 2020. Effect of Variety, Sowing Date and Location on Yield and Nutritional Characteristics of Sorghum. Acta Universitatis Agriculture Silviculture Mendelianae Brunensis, 68(3): 529–537.

Marsalis, M.A. et al. 2010. Dry matter yield and nutritive value of corn, forage sorghum, and BMR forage sorghum at different plant populations and nitrogen rates. Field Crops Research [Online], 116(1–2): 52–57. Available at: https://doi.org/10.1016/j.fcr.2009.11.009. [2021-09-8].

Přikryl, J. 2014. Čirok nebo kukuřice. Úroda, 62(4): 13.

Rajčáková, L. 2005. Pestovanie ciroku sudánského v suchom postihovaných oblastiach. Krmivářství, 9(4): 36–37.

Ratnavathi, C.V. et al. 2012. Natural occurrence of aflatoxin B1 in sorghum grown in different geographical regions of India. Journal of the Science of Food and Agriculture [Online], 92(12): 2416–2420. Available at: https://www.ncbi.nlm.nih.gov/pubmed/22419387. [2021-09-7].

Rihacek, M. et al. 2020. Nutritional evaluation of selected varieties of sorghum. In Proceedings of 27th International PhD Students Conference MendelNet 2020 [Online], Brno, Czech Republic, 11 November, Brno: Mendel University in Brno, Faculty of AgriSciences, 159–164. Available at: https://mendelnet.cz/pdfs/mnt/2020/01/29.pdf. [2021-09-10].

Sriagtula, R. et al. 2017. Nutrient changes and in vitro digestibility in generative stage of M10–BMR sorghum mutant lines. Media Peternakan, 40(2): 111–117.

The effect of biochar co-application with soil prebiotic on biomass production and soil basal respiration

Daniel Ruzicka, Vojtech Polach, Jaroslav Zahora
Department of Agrochemistry, Soil Science, Microbiology and Plant Nutrition
Mendel University in Brno
Zemedelska 1, 613 00 Brno
CZECH REPUBLIC

xruzick6@mendelu.cz

Abstract: One of the most important problems of this century is an increase in abundance of atmospheric CO_2. Because of this phenomenon, slowing down the climate change through sequestration of carbon in soil has been a popular topic of discussion during the last decade. At the same time, we are as a society dealing with another urgent problem of soil degradation. The goal of this contribution is to assess co-application of biochar combined with soil prebiotic in context of its biomass production and basal respiration influence. Two kinds of biochar were used to conduct the pot experiment (composted biochar – beech wood feedstock and fresh sewage sludge biochar). Co-application of composted biochar with soil prebiotic resulted in decrease of shoot biomass meanwhile no significant change in root biomass occurred compared to composted biochar treatment with no prebiotic applied. Co-application of fresh sewage sludge biochar with prebiotic leaded to significant decrease in root biomass meanwhile there was no significant difference in shoot biomass observed compared to the control whatsoever. Application of both types of biochar in combination with soil prebiotic significantly decreased soil basal respiration in comparison with only biochar addition.

Key Words: biochar, soil prebiotic, biochar co-application

INTRODUCTION

One of the most important problems of this century is an increase in abundance of atmospheric CO_2 (Lal 2009). Because of this phenomenon, slowing down the climate change through sequestration of carbon in soil has been a popular topic of discussion during the last decade (Powlson et al. 2021). At the same time, we are as a society dealing with another urgent problem of soil degradation. Gomiero (2016) in his study defined soil degradation as a global pandemic, because it is a world problem. One of the many forms of soil degradation is a depletion of organic matter (DeLong et al. 2015).

There are many tools to achieve sustainability and all of them shall be included as part of a solution for this global crisis, because there is no silver bullet. For example, biochar as a soil amendment is one proposed tool and, while it is getting a lot of attention, it is still crucial to promote the role of soil biology, particularly soil microbiology, which is key for soil fertility, quality, and health sustainability (Lehman et al. 2015). The goal of this contribution is to assess co-application of biochar combined with soil prebiotic in context of its biomass production and basal respiration influence.

MATERIAL AND METHODS

The pot experiment was conducted on 21 May 2021–10 July 2021 in the vegetation hall which belongs to the pavilion M of Mendel University in Brno (49.2101792N, 16.6136814E), in the South Moravian Region, Czech Republic.

Containers made of polyvinylchloride (volume of 0.6 dm^3) were used for this pot experiment. The soil for the experiment was taken from the conventionally managed area at coordinates 49.6643967N, 16.4728317E from an altitude of 479 m. The soil was removed with a spade from the upper 10 centimetres of the soil profile. This soil was classified as luvizem modal. The soil was dried at room temperature and then homogenized on 2mm sieves and then mixed with appropriate additives and poured into containers (see Table 1).

Two different kinds of biochar were obtained for the experiment. First one was made from sewage sludge. The second used biochar was obtained by mixing biochar from beech wood into the compost stack in a ratio of 1:10. Soil prebiotic is manufactured by Gaïago, which presents this product as NUTRIGEO®. It's distributed on the czech market by BIOCONT LABORATORY, spol. s r.o., according to available materials, the mechanism of its influence is to promote the abundance of organisms involved in the humification of organic residues. It contains polysaccharides, organic acids, and microelements. The model plant that was planted to pot experiment to ensure the supply of root exudates to the soil was *Lactuca sativa* L. var. *Capitata* L.

Basal soil respiration was determined by the capture of respirated CO_2 on natrocalcite according to the methodology of Keith and Wong (2006). Incubation was conducted at room temperature for 24 h. For the measurement of basal respiration 4 soil samples were collected for each variant.

The extracted underground and aboveground biomass of the model plants was dried at 105 °C to constant weight, and then weighed. For measurement 4 plants (root + shoot) out of each variant were collected. Values of root to shoot ratio are represented as a shoot biomass values divided by root biomass values.

Obtained data were processed by data-analytical program STATISTICA. Analysis of variance (one-way ANOVA) with subsequent testing of the significance of differences between variants by Tukey's HSD test at level of significance $P < 0,05$ were conducted.

Table 1 Variants of the vegetation pot experiment

Variant	Treatment	Biochar dose [Mg/ha]	Prebiotic dose [dm^3/ha]
A	Composted biochar (beech feedstock)	20	-
B	Composted biochar (beech feedstock) + prebiotic	20	40
C	Biochar (sewage sludge feedstock)	2	-
D	Biochar (sewage sludge feedstock) + prebiotics	2	40
E	Prebiotics	-	40
F	Control	-	-

RESULTS AND DISCUSSION

Biomass of the lettuce planted in experimental pots

Significant increase in shoot biomass (Figure 1a, variant A) was observed compared to the control variant with no treatment. Kaye and Hart (1997) in their study confirmed that in a N-poor soils heterotrophic organisms can outcompete plants in a context of N utilization. It can be assumed that significant difference between variant A and B (Figure 1) could be caused by favourable soil conditions for soil microorganisms due to the soil prebiotic addition. This assumption can be also supported by the value of root to shoot ratio (Figure 2, variant A, B). Kuzyakov and Xu (2013) in their study describes a factor contributing to increased competition between microorganisms and root in the sense of nutrient uptake. Available carbon in root zone leads to an increase in abundance of soil microorganisms and microbial activity in rhizosphere. Due to this phenomenon depletion zones occur. When uptake of limiting nutrient per unit of root mass decreases plant starts to develop its root system at the expense of shoot biomass (Shipley and Meziane 2002).

Figure 1 The effect of biochar co-application with soil prebiotic on biomass

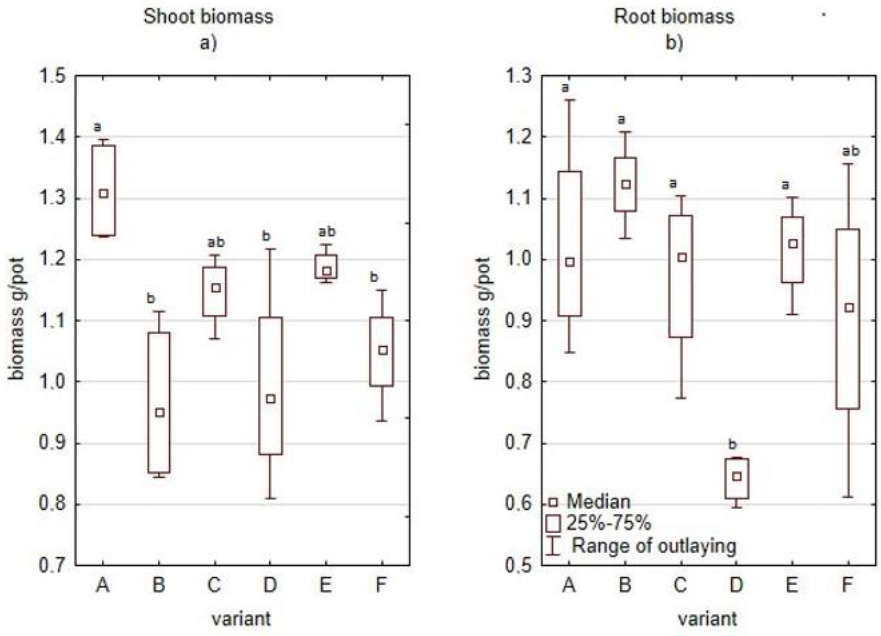

Another interesting significant difference occurred in root biomass (Figure 1b, variant C, D), meanwhile no significant change occurred in shoot biomass of those treatments. As we can see, there is no significant difference between variants C, E (Figure 1b), neither sewage sludge biochar nor soil prebiotics didn't decrease root biomass itself.

It can be assumed that plant was able to obtain more nutrients per unit of root mass because of an interaction between sewage sludge biochar and soil prebiotics.

Figure 2 The effect of biochar co-application with soil prebiotic on root to shoot ratio

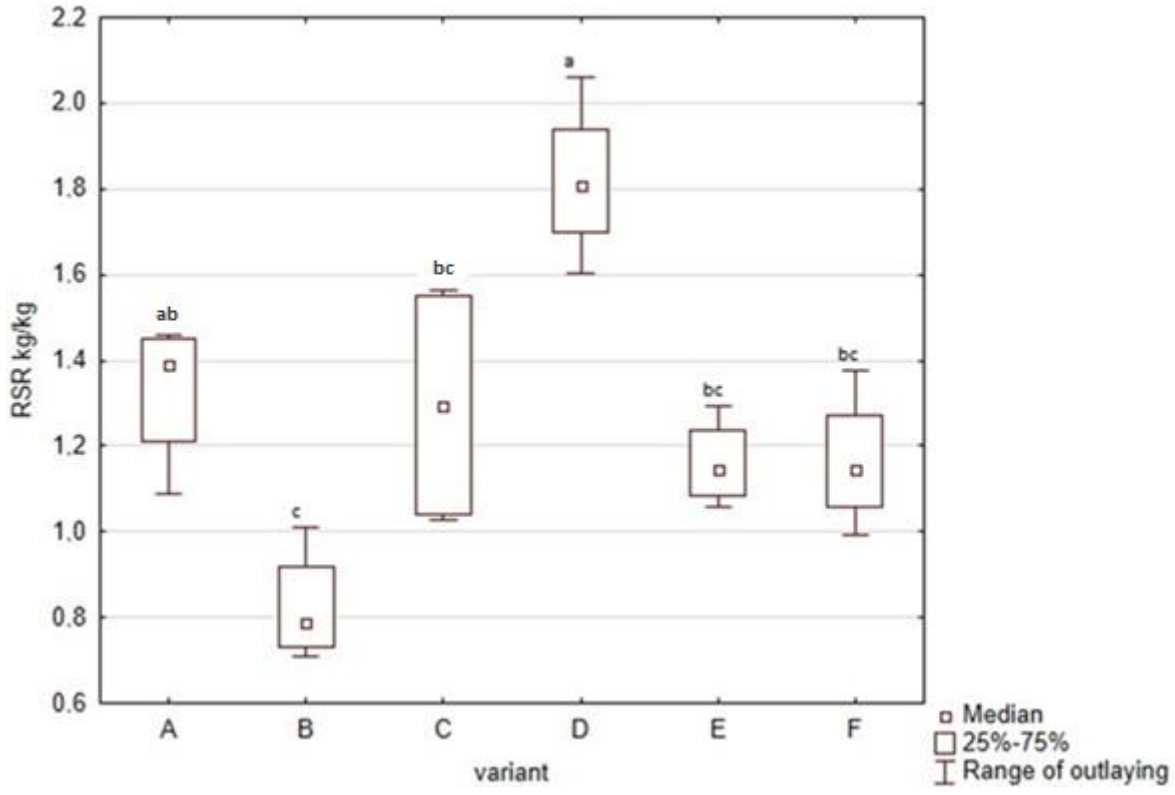

Influence of treatments on soil basal respiration

According to the results (Figure 3), co-application of both types of biochar with soil prebiotic resulted in a decreased basal respiration compared to their paired variants with no soil prebiotics added. This phenomenon could be attributed to higher efficiency of available carbon utilization (Zimmerman et al. 2011). However, SOM content was not measured for this contribution.

No significant difference in soil basal respiration occurred within all present variants when compared to control variant.

Figure 3 The effect of biochar co-application with soil prebiotic on basal respiration

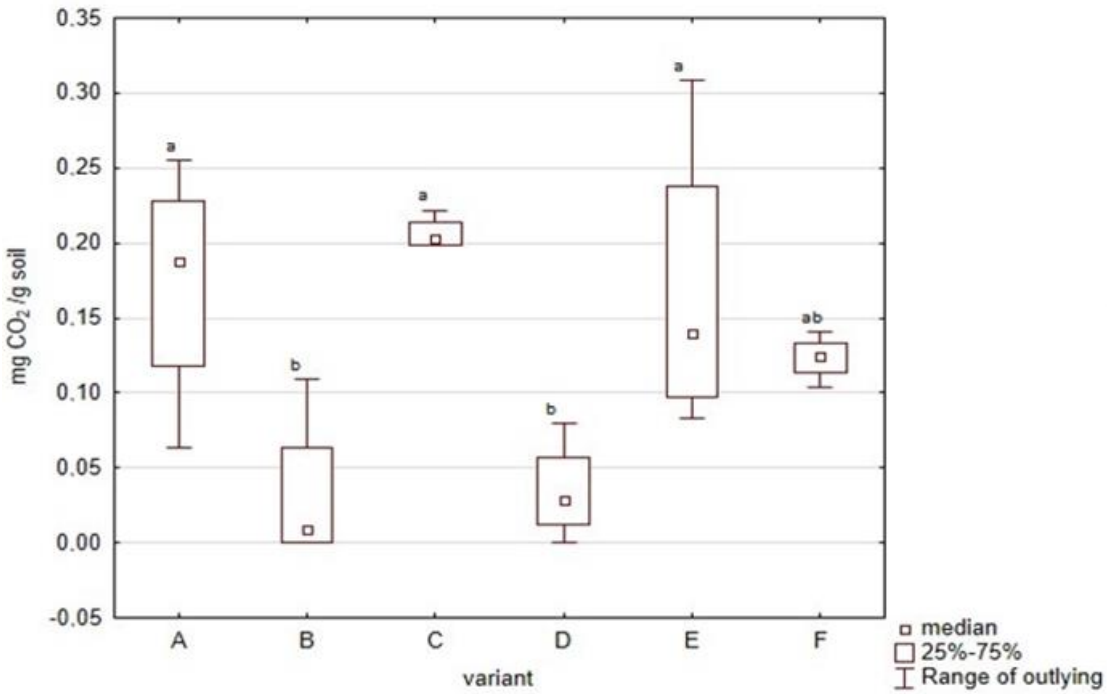

CONCLUSION

Co-application of composted biochar with soil prebiotic resulted in decrease of shoot biomass meanwhile no significant change in root biomass occurred compared to composted biochar treatment with no prebiotic applied. Co-application of fresh sewage sludge biochar with prebiotic leaded to significant decrease in root biomass meanwhile there was no significant difference observed compared to the control whatsoever. Application of both types of biochar in combination with soil prebiotic significantly decreased soil basal respiration when compared to both types of biochar additions without soil prebiotics.

ACKNOWLEDGEMENTS

Contribution was supported by Internal grant agency of Mendel University in Brno. (AF-IGA2021 IP077)

REFERENCES

DeLong, C. et al. 2015. The Soil Degradation Paradox: Compromising Our Resources When We Need Them the Most. Sustainability, 7(1): 866–879.

Gomiero, T. 2016. Soil Degradation, Land Scarcity and Food Security: Reviewing a Complex Challenge. Sustainability, 8(3): 281.

Kaye, J.P., Hart, S.C. 1997. Competition for nitrogen between plants and soil microorganisms. Trends in Ecology & Evolution, 12(4): 139–143.

Keith, H., Wong, S. 2006. Measurement of soil CO2 efflux using soda lime absorption: both quantitative and reliable. Soil Biology and Biochemistry, 38(5): 1121–1131.

Kuzyakov, Y., Xu, X. 2013. Competition between roots and microorganisms for nitrogen: mechanisms and ecological relevance. New Phytologist, 198(3): 656–669.

Lal, R. 2009. Challenges and opportunities in soil organic matter research. European Journal of Soil Science, 60(2): 158–169.

Lehman, R. et al. 2015. Understanding and Enhancing Soil Biological Health: The Solution for Reversing Soil Degradation. Sustainability, 7(1): 988–1027.

Powlson, D.S. et al. 2011. Soil carbon sequestration to mitigate climate change: a critical re-examination to identify the true and the false. European Journal of Soil Science, 62(1): 42–55.

Shipley, B., Meziane, D. 2002. The balanced-growth hypothesis and the allometry of leaf and root biomass allocation. Functional Ecology, 16(3): 326–331.

Zimmerman, A.R. et al. 2011. Positive and negative carbon mineralization priming effects among a variety of biochar-amended soils. Soil Biology and Biochemistry, 43(6): 1169–1179.

Effect of elevated CO_2 concentration and nitrogen nutrition on mais response to short-term high temperature and drought stress

Jan Simor[1], Karel Klem[1,2]
[1]Department of Agrosystems and Bioclimatology
Mendel University in Brno
Zemedelska 1, 613 00 Brno
[2]CzechGlobe – Global Change Research Institute, CAS
Belidla 986/4a, 603 00 Brno
CZECH REPUBLIC

jan.simor@gmail.com

Abstract: Within an experiment conducted in open top chambers in which two mais genotypes differing in stay-green trait were cultivated under elevated atmospheric CO_2 concentration (EC) in comparison with ambient CO_2 concentration (AC), and in two contrast levels of nitrogen nutrition, the effect of acclimation to these factors on photosynthetic performance and water use efficiency, and subsequent response to short-term high temperature and drought stress was studied. Although EC improved water use efficiency, this effect did not alleviate the response to drought stress, and under some combinations of factors even led to a decrease in CO_2 assimilation rate under drought stress. Differences in the stay-green trait between genotypes did not have a major effect on the response to high temperature and drought stress. Differences between genotypes were manifested mainly in the interaction with nitrogen nutrition, while in the Korynt genotype, non fertilised variants showed a lower response of CO_2 assimilation rate to drought. Slight alleviating effect of higher nitrogen dose was found under EC conditions, while no nitrogen fertilisation rather increased drought resilience under AC conditions.

Key Words: mais, elevated carbon dioxide, nitrogen nutrition, drought stress

INTRODUCTION

Climate change is one of the world's most significant problems today. This phenomenon is not a question of a distant future, but it is actually affecting our lives. Crop growth and development are influenced continuously by changing environmental conditions related to climate change causing numerous biotic and abiotic stresses. Between the abiotic stresses, drought belongs to most frequent across world regions, which often synchronises with higher (or extreme) temperature leading to increasing severity of drought stress (Barnabas et al. 2008.) and could cause a negative impact on crop production (Field et al. 2012). Raising the CO_2 concentration in the atmosphere is another factor which is related to climate change. Anthropogenic activities between the pre-industrial period and year 2000 caused an increase in CO_2 concentration by 90 ppm (House et al. 2002). The current state (September 2021) of CO_2 concentration in the atmosphere is 413 ppm, with an average increase of more than 2 ppm per year (NOAA 2021). These factors determine the growth and yield of crops significantly and thus can result in food shortage and compromise food security of the world (Mosley 2015). For this reason, understanding the interactions between the effect of elevated CO_2 concentration, drought stress and its timing, nitrogen nutrition and other factors associated with climate change is crucial for predicting future food security. The aim of this study was to analyse the impacts of mais acclimation to elevated CO_2 concentration and nitrogen nutrition on the response to subsequent high temperature and drought stress.

MATERIAL AND METHODS

The multifactorial field experiment was carried out in Open Top Chamber (OTC) facility in experimental station Domanínek near Bystřice nad Pernštejnem (Figure 1). The experiment consists of 24 OTCs, in which two very early mais genotypes (FAO < 250) but differing in the stay-green trait (Korynt, stay-green type, FAO 240; Nestor, dry-down type). The sowing was done manually on April 29th in density 7 grains/m^2 into rows with distance 0.75 m. Directly after sowing the nitrogen

fertilisation of split plots was done using calcium saltpeter at dose 200 kg/ha (N+ treatment) and the second split plot was left unfertilised with nitrogen (N- treatment). From the growth stage of first leaf (DC 11) the plants were also exposed to two levels of CO_2 concentration: ambient (AC, ca 400 ppm), elevated (EC, ca 700 ppm). Until the stage of 6-8th leaf (DC 16–18, acclimation phase) all variants were regularly watered using the irrigation system with amount of water 15 mm per week. At the end of acclimation phase, gas exchange parameters (light saturated CO_2 assimilation rate, A_{max}; transpiration rate, E) were measured using the instrument Li-6800 (Li-COR, Nebraska, USA) on the first fully developed leaf from the top. Gas exchange parameters were measured under environmental conditions of given variant, including the CO_2 concentration. Water use efficiency after acclimation was calculated as WUE = A_{max}/E.

After acclimation period the short term (14 days) high temperature stress was applied to all chambers and drought stress to one half of chambers with randomisation of this treatment within experiment. The temperature increase was set to +7 °C compared to ambient temperature and was regulated automatically by passive warming (closing the lamellar roof and reducing the active air exchange). The drought stress was ensured by omitting irrigation, while the control variants were regularly irrigated by 15 mm of water per week. At the end of high temperature and drought stress treatment, the measurement of gas exchange parameters was conducted again with instrument Li-6800.

Figure 1 Open top chambers for manipulation of CO_2 concentration and water availability (left) and the detail of gas exchange measurement with the instrument Li-6800 (right).

RESULTS AND DISCUSSION

ANOVA revealed significant effect of both acclimation factors, CO_2 concentration and nitrogen nutrition on light saturated CO_2 assimilation rate (A_{max}) in both genotypes, but only CO_2 concentration had significant effect on WUE (Table 1). The interactive effects of both acclimation factors were also found only for A_{max}. Such interactive effect was more pronounced in genotype Korynt ($p<0.05$).

The acclimation to elevated CO_2 concentration (EC) significantly increased A_{max} in both genotypes (Table 1). Such increase was higher in variant without nitrogen fertilisation (N-), particularly in the genotype Korynt. While the effect of nitrogen fertilisation was positive or neutral in genotype Korynt, it was negative in genotype Nestor. WUE significantly increased under EC conditions in the acclimation phase, and such increase was slightly higher in genotype Nestor. Nitrogen showed no effect on WUE in both genotypes tested (Figure 2).

Table 1 Results of two-way ANOVA indicating the significance of effects (p-values) of individual factors and their interaction after acclimation phase on A_{max} – light saturated CO_2 assimilation rate and WUE – water use efficiency calculated as ratio of light saturated CO_2 assimilation and transpiration rate. Significant effects ($p<0.05$) are indicated in bold.

	Korynt		Nestor	
	A_{max}	WUE	A_{max}	WUE
CO_2	**<0.001**	**<0.001**	**<0.001**	**<0.001**
Nitrogen	**<0.001**	0.704	**<0.001**	0.462
CO_2 x Nitrogen	**<0.001**	0.127	**0.033**	0.212

Figure 2 Effects of atmospheric CO_2 concentration (AC – ambient CO_2 concentration ~400ppm, EC – elevated CO_2 concentration ~700ppm) and nitrogen fertilisation (N- no nitrogen fertilisation, N+ fertilisation with 200 kg/ha nitrogen applied after sowing in the form of calcium saltpetre) on the light saturated CO_2 assimilation rate (A_{max}), and water use efficiency calculated as ratio of light saturated CO_2 assimilation and transpiration rate (WUE) in two mais hybrids, Korynt and Nestor, after acclimation phase (before applied short term heat and drought stress). Means (columns) and standard errors (error bars) are presented (n=6). Different letters indicate significant differences ($p \leq 0.05$) between means based on Fischers's LSD ANOVA post-hoc test.

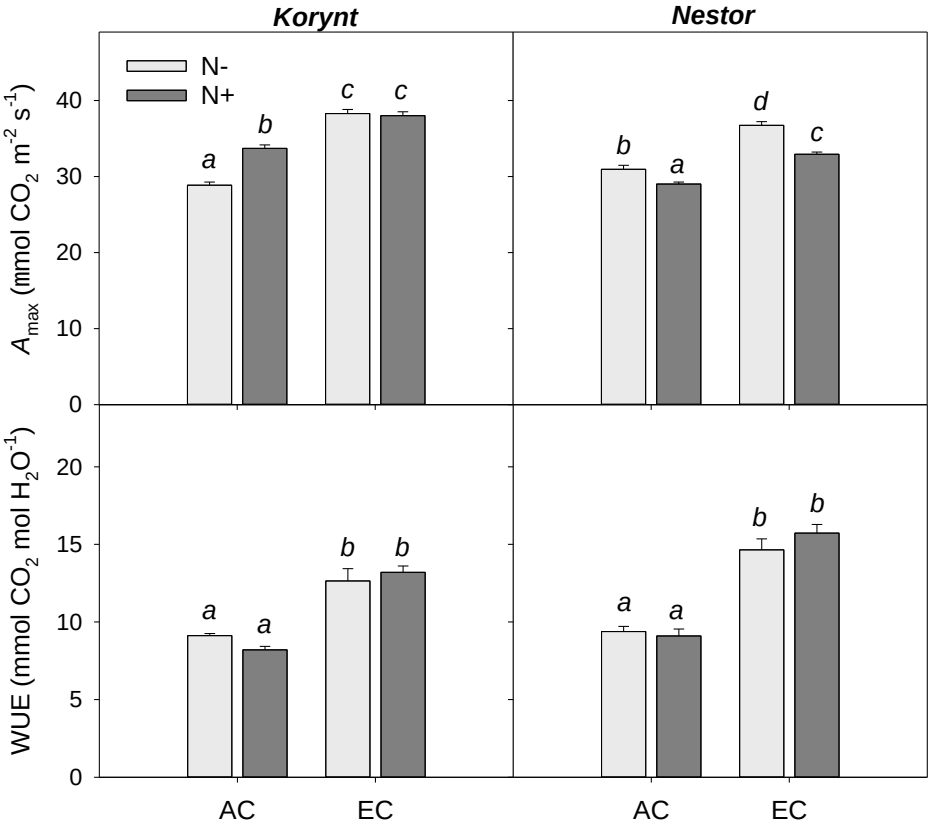

Table 2 Results of three-way ANOVA indicating the significance of effects (p-values) of individual factors and their interaction after short term heat and drought stress on A_{max} – light saturated CO_2 assimilation rate and WUE – water use efficiency calculated as ratio of light saturated CO_2 assimilation and transpiration rate. Significant effects ($p<0.05$) are indicated in bold.

	Korynt		Nestor	
	A_{max}	WUE	A_{max}	WUE
Drought	**<0.001**	**<0.001**	**<0.001**	**0.003**
CO_2	0.069	**<0.001**	0.319	**<0.001**
Nitrogen	0.097	**0.018**	0.084	**0.027**
Drought x CO_2	0.119	**0.047**	0.824	0.311
Drought x Nitrogen	**0.013**	**0.002**	0.222	0.136
CO_2 x Nitrogen	0.420	0.105	**0.033**	0.207
Drought x CO_2 x Nitrogen	0.140	**0.001**	**0.042**	**0.036**

According to ANOVA results, after short term high temperature and drought stress, drought has a significant effect on A_{max} and WUE in both genotypes. On the contrary, atmospheric CO_2 concentration and nitrogen fertilisation affected WUE significantly in both genotypes; however, this effect was more pronounced ($p<0.01$) for the CO_2 effect. Significant interactive effects were found in genotype Korynt

for interactions drought x CO_2 (in case of WUE), drought x nitrogen (in case of both A_{max} and WUE), and for interaction drought x nitrogen x CO_2 (in case of WUE). In genotype Nestor, significant interactive effects were found for interaction CO_2 x nitrogen (in case of A_{max}) and for interaction drought x nitrogen x CO_2 (in case of both A_{max} and WUE).

After short-term high temperature and drought stress, the positive effect of EC on A_{max} disappeared, or A_{max} was even lower compared to AC in response to high temperature. The combination of drought and high temperature showed the highest reduction of A_{max} under AC N+ in genotype Korynt and under EC N- in genotype Nestor.

WUE was significantly increased after short term high temperature and drought stress in response to EC and drought. On the contrary, nitrogen fertilisation and genotype did not affect WUE.

The importance of interactions between atmospheric CO_2 concentration and nitrogen nutrition on mais response to drought stress were documented by (Markelz et al. 2011). They found no stimulation of CO_2 assimilation rate be EC when water availability was sufficient, but under drought stress EC alleviated its negative impacts on photosynthetic performance. Limiting nitrogen supply exacerbated the drought impacts (Table 2).

In our experiment limited nitrogen availability effect on drought was genotype-specific, but in contrary to Markelz et al. (2011), it rather reduced the impact of drought on CO_2 assimilation, particularly in stay-green genotype Korynt.

Although the effects were mostly insignificant, our results also indicate that mais plants acclimated to EC were more sensitive to high temperature stress and the stimulation of CO_2 assimilation rate, which was observed after the acclimation phase mostly disappeared after short-term heat stress (Figure 3).

Figure 3 Light saturated CO_2 assimilation rate (A_{max}, upper), and water use efficiency calculated as ratio of light saturated CO_2 assimilation and transpiration rate (WUE) after short term high temperature (light grey) and combined high temperature and drought stress (dark grey) in two mais hybrids, Korynt and Nestor, following the acclimation to atmospheric CO_2 concentration (AC – ambient CO_2 concentration ~400ppm, EC – elevated CO_2 concentration ~700ppm) and nitrogen fertilisation (N- no nitrogen fertilisation, N+ fertilisation with 200 kg/ha nitrogen applied after sowing in the form of calcium saltpetre). Means (columns) and standard errors (error bars) are presented (n=6). Different letters indicate significant differences ($p \leq 0.05$) between means based on Fischers's LSD ANOVA post-hoc test.

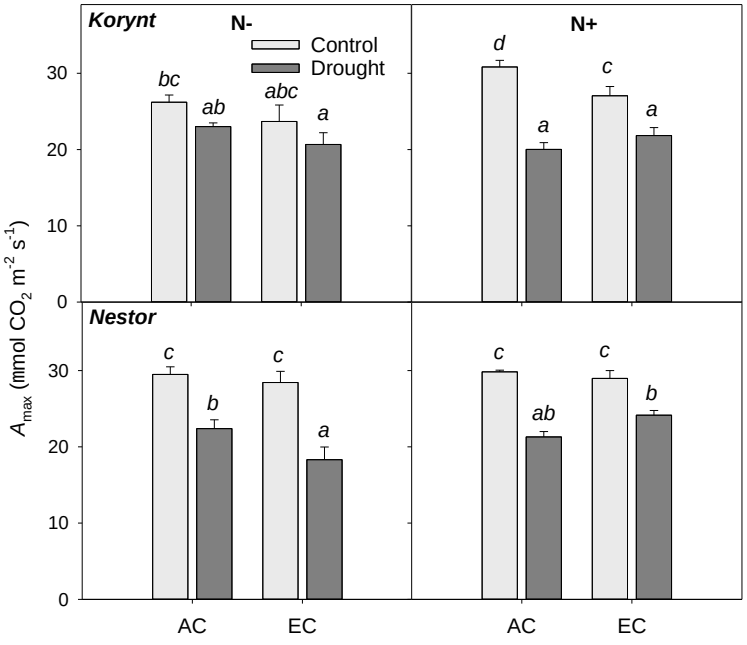

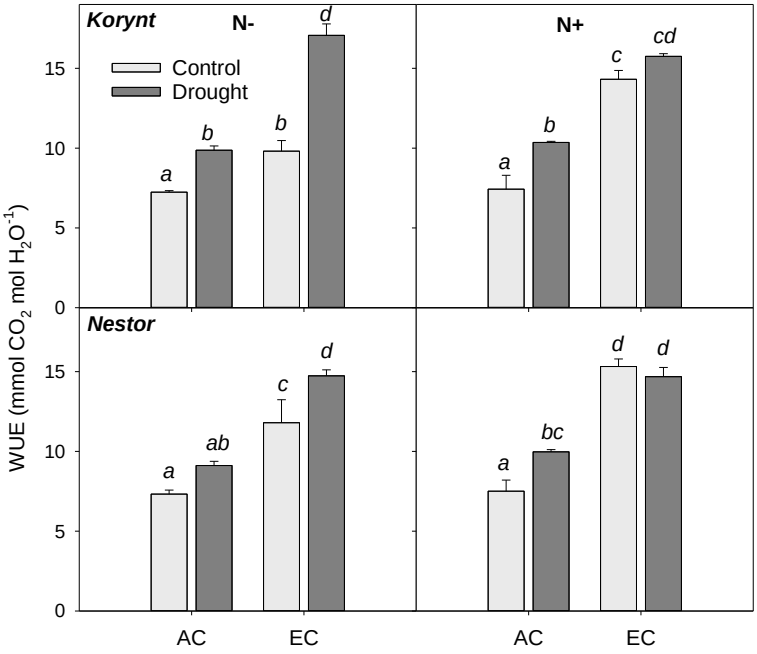

The response of plants with C4 photosynthetic metabolism to EC is generally lower compared to C3 plants (Poorter and Navas 2003), however, recent work shows that C3 and C4 plants can show also reversal response in this comparison (Reich et al. 2018). The mechanisms for such reversal are not yet known, but it is expected that such change in favour of C4 plants is mainly caused by rising temperatures and reduced water availability in last years (Boretti and Florentine 2019).

CONCLUSION

In our experiment, we found that although acclimation to elevated CO_2 concentration increases WUE significantly in mais, this effect was not reflected in the mitigating effect of elevated CO_2 concentration on CO_2 assimilation rate under drought stress. Nitrogen nutrition only slightly modulates the response to drought. Alleviating effect of higher nitrogen dose was found under EC conditions, while no nitrogen fertilisation rather increased drought resilience under AC conditions.

ACKNOWLEDGEMENTS

This study was supported by research projects IGA - AF-IGA2021-IP084 (Impact of climate change factors in interaction with nitrogen nutrition on physiology and yield of mais). KK was supported by the SustES project - Adaptation strategies for sustainable ecosystem services and food security under adverse environmental conditions (CZ.02.1.01/0.0/0.0/16_019/0000797).

REFERENCES

Barnabas, B. et al. 2008. The effect of drought and heat stress on reproductive processes in cereals. Plant Cell Environ, 31: 11–38.

Boretti, A., Florentine, S. 2019. Atmospheric CO_2 concentration and other limiting factors in the growth of C3 and C4 plants. Plants, 8(4): 92.

Field, C.B. et al. 2012. Observed and Projected Impacts on the Natural Physical Environment. In Managing the Risks of Extreme Events and Disasters to Advance Climate Change Adaptation: Special Report of the Intergovernmental Panel on Climate Change. University Press, 167–175.

House, J.I. et al. 2002. Maximum impacts of future reforestation or deforestation on atmospheric CO_2. Global Change Biology, 8(11): 1047–1052.

Markelz, R.C. et al. 2011. Impairment of C4 photosynthesis by drought is exacerbated by limiting nitrogen and ameliorated by elevated [CO_2] in mais. Journal of Experimental Botany, 62(9): 3235–3246.

Mosley, L.M. 2015. Drought impacts on the water quality of freshwater systems; review and integration. Earth-Science Reviews, 140: 203–214.

NOAA (National and Oceanic Administration), 2021. Recent Global CO_2 [Online], Available at: http://www.esrl.noaa.gov/gmd/ccgg/trends/global.html. [2021-09-01].

Poorter, H., Navas, M.L. 2003. Plant growth and competition at elevated CO_2: on winners, losers and functional groups. New Phytologist, 157(2): 175–198.

Reich, P.B. et al. 2018. Unexpected reversal of C3 versus C4 grass response to elevated CO_2 during a 20-year field experiment. Science, 360(6386): 317–320.

Estimation of winter wheat yield using machine learning from airborne hyperspectral data

Marian Svik[1,2], Miroslav Pikl[1], Ruzena Janoutova[1], Barbora Vesela[1], Lukas Slezak[1,2], Karel Klem[1], Lucie Homolova[1]
[1]Global Change Research Institute of the Czech Academy of Sciences
Belidla 986/4a, 603 00 Brno
[2]Department of Geography, Masaryk University
Kotlarska 2, 611 37 Brno
CZECH REPUBLIC

svik.m@czechglobe.cz

Abstract: Methods based on optical remote sensing allow nowadays to assess crop conditions over larger areas. The assessment of crop conditions and potential estimation of crop yields in the early growth stages can help farmers to better target their management practice such as application of fertilizers. In this study we analysed airborne hyperspectral images acquired several times during the growing season over two experimental sites in the Czech Republic (Ivanovice and Lukavec). The field experiments on winter wheat included 12 levels of fertilisation (combination of organic and mineral fertilisers). Such an experiment design and the possibility of combining the data from two sites together increased the variability in our wheat yield dataset, which varied between 2.8 and 10.0 t/ha. Further, we used a machine learning method – namely gaussian process regression from the ARTMO toolbox to train two variants of models: a) combining the spectral data from both sites and from the multiple acquisition days and b) combining the spectral data from both sites for individual acquisition days. The results showed that it was feasible to predict wheat yield already at the beginning of April with $R^2 > 0.85$. This promising result, however, requires more thorough validation and therefore we plan to include more data from other sites in the next steps.

Key Words: hyperspectral, machine learning, remote sensing, winter wheat, yield

INTRODUCTION

Wheat (*Triticum aestivum* L.) is the dominant crop in the Czech Republic, and it plays an important role in the food security in the world especially in Europe. Due to still more frequent weather extremes and expected climate changes (Palmer et al. 2021), increased attention is nowadays paid to identification of varieties more resilient especially to drought.

The field experiments where varieties are tested are also excellent data sources for development of remote sensing (RS) approaches predicting crop yields (Raya-Sereno et al. 2021). Early yield prediction is useful both for farmers but also in the connected food production industry.

Yield prediction is traditionally based on the process-based models parameterized primarily by climatic and soil variables. With rapidly increasing temporal resolution of RS data with mid- to high spatial resolution new approaches of yield prediction solely from RS data or combination of RS data and process-based models are emerging (Migdall et al. 2009, Dong et al. 2020). Tools such as ARTMO toolbox (Caicedo et al. 2014) allow to evaluate several empirical approaches and can help researchers to develop solely RS-based methods more effectively. Therefore, in this study we tested machine learning methods to develop a model to predict winter wheat yield from airborne hyperspectral images.

MATERIAL AND METHODS

Experiment sites and field data

Airborne and field data were collected at two sites Lukavec (49°33’23”N, 14°58’39”E, 620 m.a.s.l.) and Ivanovice (49°18’40’’N, 17°05’45’’E, 225 m.a.s.l.) that are part of the Czech stationary long-term crop rotation experiment. Different amounts of fertilizers (N, P, K, Mg) were

applied to each subplot within the study site (white polygons in Figure 1) with four independent replicates. Detailed information about the site conditions and experiment design are provided by Kunzová and Hejcman (2009) and Hejcman and Kunzová (2010). To eliminate the edge effect, only the central 5 m × 5 m area of each 8 m × 8 m experimental plot was used for the determination of yield sample collection.

Figure 1 Location of two study sites Lukavec and Ivanovice. Both sites contain fertilization experiments with 12 levels of combinations of different approaches. Each experiment has four repetitions.

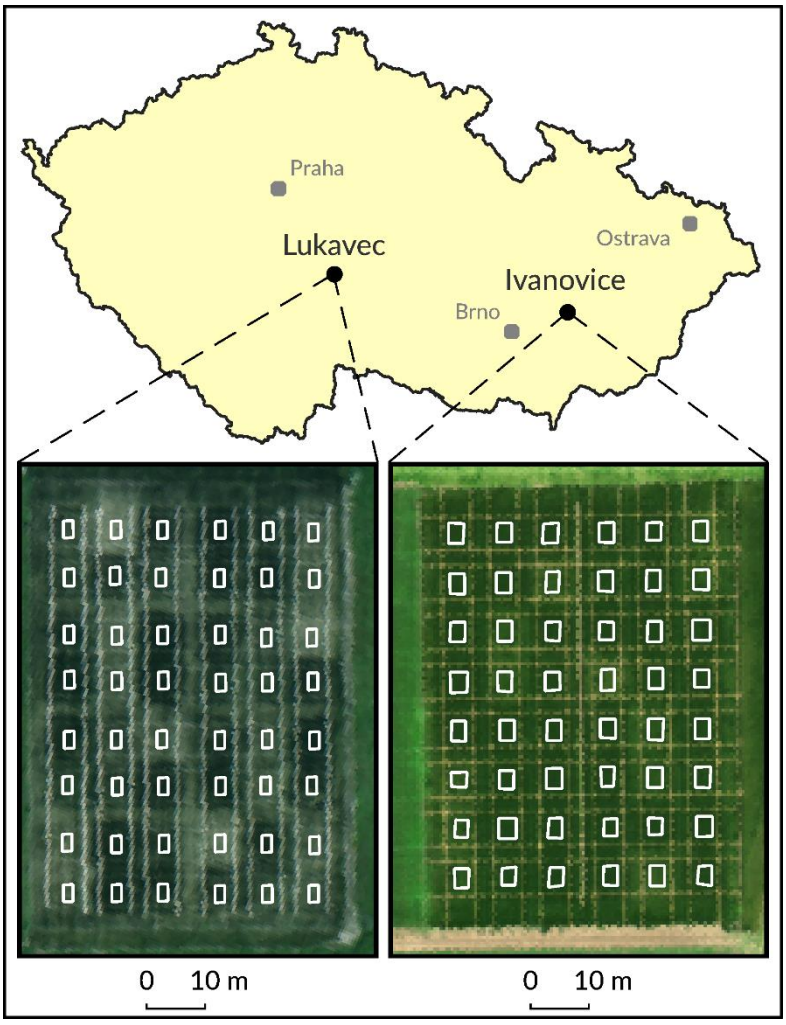

Remote sensing data

Airborne hyperspectral images were acquired at several days of year (DOY) along the vegetation season of winter wheat from April to July in 2020 (corresponding DOY and BBCH stages are shown in Table 1). The images were acquired with a CASI sensor (Itres Research, Calgary, AB, Canada) in the range of 383–1053 nm (48 bands with spectral sampling distance of 14.25 nm and pixel size of 0.5 m) and with a SASI sensor (Itres, Research, Calgary, AB, Canada) in the range of 957–2442 nm (100 bands with spectral sampling distance of 15 nm and pixel size of 1.25 m). Corrections of the hyperspectral images were carried out in a data processing chain established at the CzechGlobe institute (Hanuš et al. 2016). Radiometric corrections were performed using the factory calibration coefficients in the post-processing software developed by the sensors' producer. Geometric corrections (i.e. image orthorectification and geo-referencing) were performed using the GeoCorr software provided also by the sensors' manufacturer. Atmospheric corrections were made using ATCOR-4 software (Richter and Schläpfer 2002). The mean spectral information was extracted for each field, so that all the pixels contain only pixels from a given polygon (Figure 1) and for each sensor separately.

Table 1 Summary of remote sensing acquisitions in day of year (DOY) and corresponding BBCH stages on Ivanovice and Lukavec

Lukavec			Ivanovice		
Date	DOY	BBCH	Date	DOY	BBCH
2 April	93	23-24	7 April	98	24-25
23 April	114	25-27	23 April	114	27-30
18 May	139	31-32	18 May	139	32
2 June	154	57-59	1 June	153	61-65
22 June	174	71-75	13 June	165	77-79
10 July	192	83-85	10 July	192	85-87

Models and retrievals

For creating yield estimations an ARTMO toolbox (Caicedo et al. 2014), specifically its machine learning regression algorithms (MLRA) toolbox, was used. Firstly, data from both CASI and SASI sensors were joined together in order to obtain better representation of spectral behaviour.

We made two variants of models. For the first variant (called "Pooled DOY" in further text), data from both sites and all the suitable RS acquisition dates were pooled together into one dataset with paired yields and spectra. For the second variant (called "Individual DOY" in further text), data from both sites but from pairs of individual RS acquisitions (e.g. DOY 93 on Lukavec and DOY 98 on Ivanovice) were used. For both variants the data were first randomly split into calibration (70%) and validation (30%) datasets. For calibration of the Pooled DOY model we excluded data from Ivanovice DOY 192 because the grain was lying down due to strong wind and rain.

From a large number of machine learning algorithms provided by ARTMO, we decided to use gaussian process regression (GPR) which was shown to have good estimation power by Verrelst et al. (2013). Furthermore, GPR not only computes estimate but it also provides associated uncertainty values, expressed as the standard deviation (SD) around the mean estimate. In order to reduce number of correlated spectral bands, we first applied principal component analysis to compress the full spectral information (CASI and SASI bands) into components. First five components were then used for model training.

After the training of the models, they were then used for the estimation of winter wheat yield: a) on the validation datasets and b) directly on two hyperspectral images for each pixel. To evaluate model performance, we computed basic statistics – coefficient of determination (R^2) and root mean square error (RMSE) for model calibration and validation.

RESULTS AND DISCUSSION

The performance for all six pairs of acquisition dates and for both model variants is shown in Table 2. From these six pairs of acquisitions, three (DOY 93/98, DOY 139 and DOY 192) were chosen to show in the form of a scatterplot (Figure 2). The results show that estimation of yields even in the early stage (at the beginning of April) of the winter wheat growth is feasible. Both from Pooled DOY model (R^2 = 0.78, 0.92, and 0.92 for Lukavec, Ivanovice, and both sites together respectively, Figure 2 – upper graphs) and from Individual DOY model (R^2 = 0.68, 0.82, and 0.87 for Lukavec, Ivanovice, and both sites together respectively, Figure 2 – bottom graphs). Although in the case of Pooled DOY model, the GPR are trained on a dataset containing the same values of yields for different spectral information, the algorithm estimates yield accurately and is able to cope with this ambiguity. As Table 2 shows, high R^2 between estimated and measured yield values was observed for all other dates, except the last DOY 192 (R^2 = 0.70) at the Ivanovice site in the case of Pooled DOY model (grain was lying down). The reason for difference in the estimation power between model variants is discussed in the next section.

Table 2 Calibration and validation statistics (R^2 and RMSE) of models used for wheat yield estimation

	Pooled DOY model				Individual DOY models			
	R^2_{cal}	R^2_{val}	$RMSE_{cal}$	$RMSE_{val}$	R^2_{cal}	R^2_{val}	$RMSE_{cal}$	$RMSE_{val}$
DOY 93/98	0.92	0.92	0.46	0.53	0.90	0.87	0.53	0.67
DOY 114		0.89		0.63	0.95	0.93	0.39	0.48
DOY 139		0.84		0.81	0.94	0.93	0.39	0.49
DOY 153/154		0.95		0.53	0.94	0.93	0.34	0.51
DOY 165/174		0.93		0.54	0.93	0.93	0.44	0.51
DOY 192		0.70		1.25	0.91	0.87	0.49	0.68

Figure 2 Scatter Plot of measured vs estimated values of winter wheat yield (t/ha) on Ivanovice (blue) and Lukavec (red) sites in three image acquisition dates (indicated by day of year – DOY). Estimates from Pooled DOY model are on the upper graphs, estimates from Individual DOY models are on the bottom graphs. Coefficient of determination (R^2) and regression line for each site is included. Value of R^2 is also shown for both sites together (black).

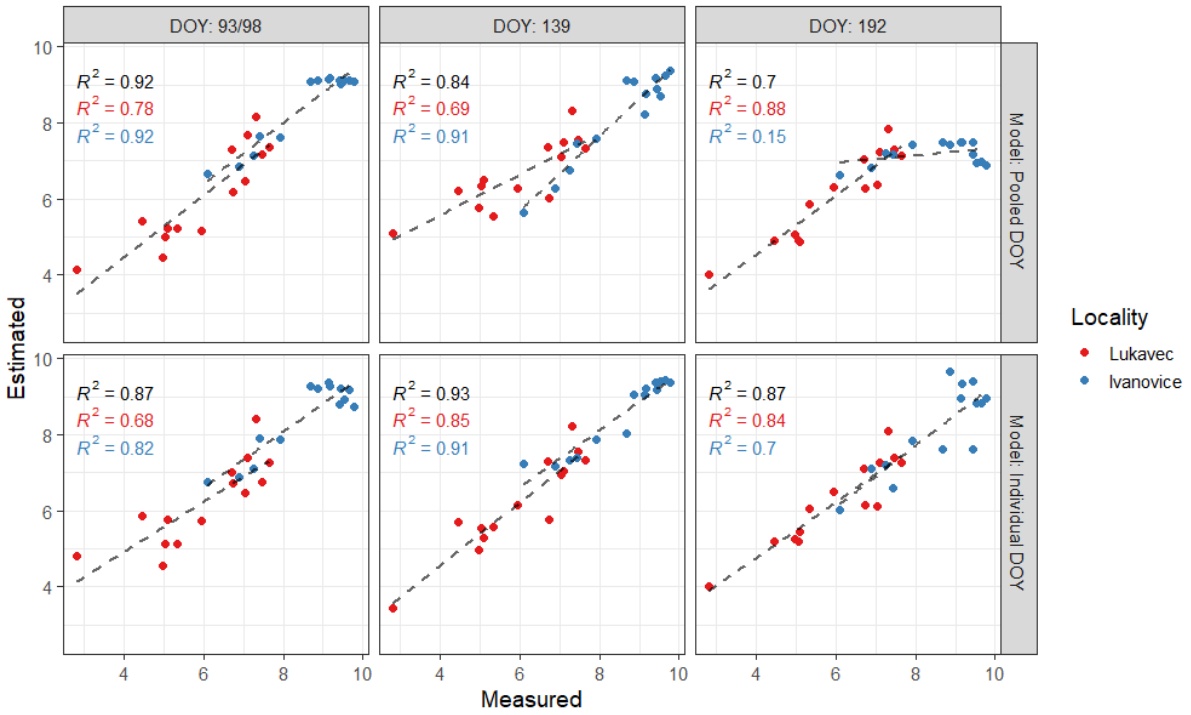

Pooled DOY model is more robust, but it can give worse estimations when an unexpected event is introduced in the data. In the case of Ivanovice DOY 192 for example, the grain was lying down due to the strong wind and rain which affected the spectral information. Individual DOY model is able to handle these cases by using training data only from the same DOY, but this means that the model is biased and cannot be used for yield estimation of wheat in stable condition. Furthermore, our goal is to make Pooled DOY model even more robust by using DOY or BBCH stage as one of its input parameters.

High values of R^2 as soon as in the beginning of April can be attributed to the fact that the spectral information is sufficiently distinguishable even at those early stages of crop growth (Raya-Sereno et al. 2021). But the spectral information is only a part of the equation. The other part, equally as important, are other variables like irrigation, fertilization, weather conditions etc. Even if the spectral information is the same at the same DOY, those other variables can have a huge impact on the resulting yields. Therefore, we have to be careful when interpreting these high values of R^2 and if possible, take those other variables into account in further developments of the model.

Spatial retrieval of the wheat yield for each site is tested at both sites from Pooled DOY model on 18 May (DOY 139, Figure 3 – left panels) and it shows that the yield prediction varies according to fertilisation levels. The uncertainty of estimated yields is rather low (0–1σ) and stable across all the fields (Figure 3 – right panels).

Figure 3 Prediction of wheat yields (t/ha) and corresponding uncertainty (σ) for Lukavec and Ivanovice sites from hyperspectral airborne images acquired on 18 May (DOY 139)

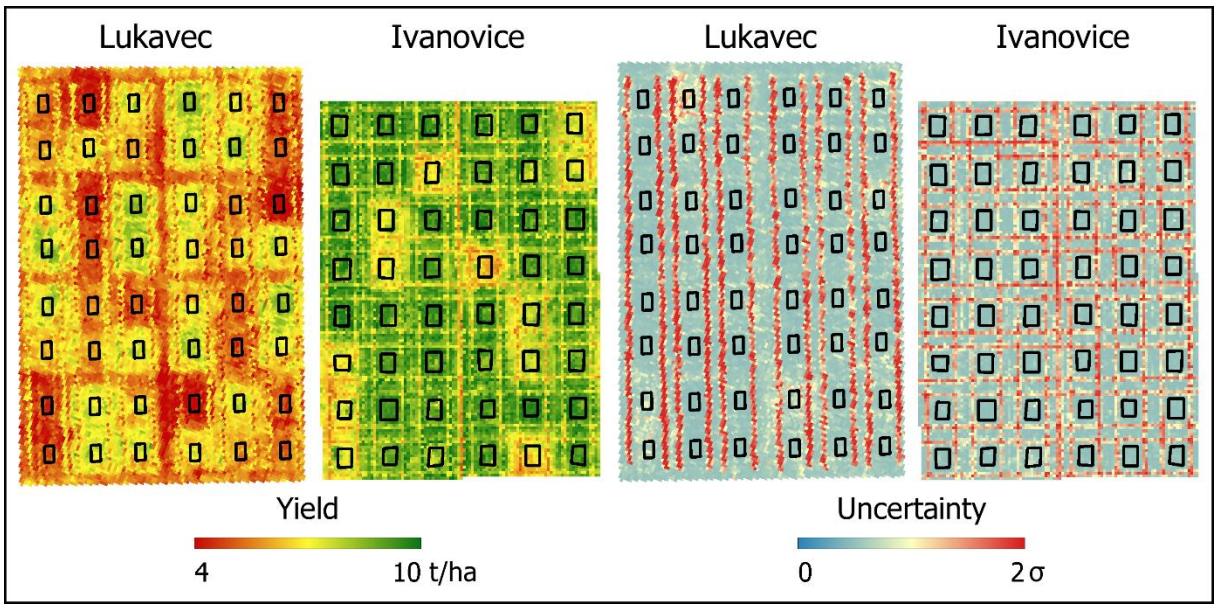

Despite the fact that the atmospheric correction of the airborne imagery might introduce some uncertainty (without any reference spectral data, we were unfortunately not able to quantify this uncertainty), no bias was observed when the model was applied on different dates (Figure 2). As the processing chain of hyperspectral RS images is not able to remove all atmospheric and other influences, the overall improvement of results could be done by smoothing the data across the DOYs as proposed for instance by Magney et al. (2016).

The next step is to extend the estimations to other study sites with other crop experiments run under various conditions to better evaluate the robustness of the proposed retrieval approach. It is expected to introduce slight modifications to cover any possible variability, which was not part of experiments at Lukavec and Ivanovice study site. The model could be simplified to use only a given vegetation index or list of indices (Magney et al. 2016, Prey and Schmidhalter 2020). The same approach would be tested among other crops typically grown in the Czech Republic such as maize, rapeseed, or barley.

CONCLUSION

In this study, we trained and compared two variants of models using hyperspectral data from CASI and SASI sensors and field data of winter wheat yield on two study sites (Lukavec, Ivanovice) during multiple days of the year 2020. Combining both sites together expanded the variability in the training dataset, which allowed to develop a robust model for winter wheat yield prediction. Individual DOY models yielded better estimates than Pooled DOY model on average because they were tuned to each specific acquisition period, but these models are less robust and hardly transferable to other sites and dates. Application of the models showed that it was feasible to predict wheat yield already at the beginning of April (DOY 93 and 98) with $R^2 > 0.85$. However, we must admit that these predictions might have been only possible to obtain because of the relatively stable conditions over the study area during the study period and adverse events like drought might negatively affect the estimation power of the models. Therefore, further data from different growing seasons will be needed to account for those different conditions. For further research, we plan to develop and evaluate even more robust model which would take DOY/BBCH as an input parameter and test the models both on year 2021 growing season and on different research sites.

ACKNOWLEDGEMENTS

The research was financially supported by the SustES – Adaptation strategies for sustainable ecosystem services and food security under adverse environmental conditions (CZ.02.1.01/0.0/0.0/16_019/0000797).

REFERENCES

Caicedo, J.P.R. et al. 2014. Toward a Semiautomatic Machine Learning Retrieval of Biophysical Parameters. IEEE Journal of Selected Topics in Applied Earth Observations and Remote Sensing, 7(4): 1249–1259.

Dong, J. et al. 2020. Estimating winter wheat yield based on a light use efficiency model and wheat variety data. ISPRS Journal of Photogrammetry and Remote Sensing, 160: 18–32.

Hanuš, J. et al. 2016. Potential of airborne imaging spectroscopy at CzechGlobe. ISPRS - International Archives of the Photogrammetry, Remote Sensing and Spatial Information Sciences, 41: 15–17.

Hejcman, M., Kunzová, E. 2010. Sustainability of winter wheat production on sandy-loamy Cambisol in the Czech Republic: Results from a long-term fertilizer and crop rotation experiment. Field Crops Research, 115(2): 191–199.

Kunzová, E., Hejcman, M. 2009. Yield development of winter wheat over 50 years of FYM, N, P and K fertilizer application on black earth soil in the Czech Republic. Field Crops Research, 111(3): 226–234.

Magney, T.S. et al. 2016. Proximal NDVI derived phenology improves in-season predictions of wheat quantity and quality. Agricultural and Forest Meteorology, 217: 46–60.

Migdall, S. et al. 2009. Inversion of a canopy reflectance model using hyperspectral imagery for monitoring wheat growth and estimating yield. Precision Agriculture, 10(6): 508–524.

Palmer, T.E. et al. 2021. How does the CMIP6 ensemble change the picture for European climate projections? Environmental Research Letters, 16(9): 094042.

Prey, L., Schmidhalter, U. 2020. Deep Phenotyping of Yield-Related Traits in Wheat. Agronomy, 10(4): 603.

Raya-Sereno, M.D. et al. 2021. High-Resolution Airborne Hyperspectral Imagery for Assessing Yield, Biomass, Grain N Concentration, and N Output in Spring Wheat. Remote Sensing, 13(17): 1373.

Richter, R., Schläpfer, D. 2002. Geo-atmospheric processing of airborne imaging spectrometry data. Part 2: Atmospheric/topographic correction. International Journal of Remote Sensing, 23(13): 2631–2649.

Verrelst, J. et al. 2013. Gaussian processes uncertainty estimates in experimental Sentinel-2 LAI and leaf chlorophyll content retrieval. ISPRS Journal of Photogrammetry and Remote Sensing, 86: 157–167.

The effect of different technical details of drip irrigation on fruit yield and annual increments of "Gala" apple

Lukas Vastik[1], Vladimir Masan[1], Patrik Burg[1], Pavel Zemanek[1], Pavel Hic[2]
[1]Department of Horticultural Machinery
[2]Department of Post-Harvest Technology of Horticultural Products
Mendel University in Brno
Zemedelska 1, 613 00 Brno
CZECH REPUBLIC

xvastik@mendelu.cz

Abstract: The entire Earth's climate system is changing which causes significant changes in precipitation conditions in the various seasons within Central Europe. The dry season in the summer months is growing, while forcing fruit and vegetable growers to think about the economic and ecological water consumption used for irrigation and to make the best use of it. Therefore, the experiment deals with various technical details of implementing the drip irrigation in an orchard. Four variants of technical details were monitored: IR+F-A (drip hose placed on the wire – common method), IR+F-B (drip hose placed on the auxiliary structure from the left and right side of trees, 0.5 m above the soil surface), IR+F-C (drip hose located on the left and right side of trees, 0.3 m below the soil surface), NON-IR (without irrigation). A drip hose with a drip flow of 2.1 l/h and a drip distance of 0.75 m from each other was used to irrigate the variants. The best results were found in the IR+F-C variant and demonstrably the worst in the NON-IR variant, where the importance of irrigation and fertilization of fruit plantations was shown. The highest weight was found for the IR+F-C variant of 178 g and the lowest for the NON-IR variant of 148 g. The largest diameter of apples was achieved with the IR+F-C variant 73.7 mm and the smallest with the NON-IR variant 66.4 mm. Also, when measuring the length of annual increments, the longest increments of shoots were measured for the IR+F-C variant, namely 797.1 mm, demonstrably the shortest increments were measured for the NON-IR variant of 501.2 mm.

Key Words: drip flow, irrigation, fertigation, apple tree, orchard

INTRODUCTION

The areas of orchards are gradually increasing worldwide. In 2008, for example, around 48,000 ha of orchards were registered in Germany (Blanke 2008). In 2016, more than 2,200,000 ha of fruit orchards were registered in Brazil, making it third largest fruit producers in the world (Blanke 2017). While the intensive planting care is required to achieve the highest possible yields.

Intensive orchards are characterized by a high degree of intensive care, agrotechnical measures and used are the latest technologies in establishment and cultivation (Blanke 2008). Technological factors such as irrigation, fertilization, integrated pest management and the use of quality nursery sprouts and rootstocks, which eliminate the negative impact of ecological factors on production, should be used to increase yield per unit area when growing, as in all other areas of agricultural cultivation (Ucar et al. 2016).

During the growing season, the orchard must fight diseases and pests. Among the most famous pests are aphids (*Aphis pomi*), which suck on young shoots of trees, the shoots stun and deform, which reduces the quality of trees in the upcoming years. Another important pest is the codling moth (*Cydia pomonella*), which damages in the form of a larva. The larva gets from the surface of the apple to the nucleolus, which eats. The fruits then fall and rot. An important disease is also sunburn. Sunburn is a physiological damage to the fruit that has a major impact on the quality of fruit and reduces its value. The change occurs mainly on the surface or in the upper layers of the fruit. Later, phytopathogenic fungi may appear on the fetuses due to infection of the injured skin. This disease reduces the value of fruit and therefore fruits are not suitable for sale (Racskó et al. 2005).

Intensive orchards are characterized by regular irrigation and fertilization, which are, in addition to protection against diseases and pests, another important agrotechnical operations (Radivojevic et al. 2020). Drip irrigation is characterized by its slow dosing of water directly to the roots of fruit trees and thus avoids unnecessary irrigation of the grassy surroundings. In areas with a lack of water during the summer months (Israel), drip irrigation is located below the soil surface. Water with fertilizers thus reaches directly to the roots and surface evaporation is prevented (Fallahi 2017).

The aim of this experiment was to evaluate four variants of technical details of the implementation of drip irrigation in an orchard and its impact on the weight and diameter of fruits and annual increments.

MATERIAL AND METHODS

The growing conditions

The experiment is based on previous measurements, which were performed in the Plantex company fruit orchard and are described in the article by Mašán et al. (2018). The company called Plantex is located in the village of Veselé, 10 km south of Piešťany (latitude: 48 ° 33'4.25 "N, longitude: 17 ° 43'57.78" E). The experiment examined 16 year old Gala apples, a Schniga clone grown on low-growing M9 rootstocks. The trees were grown in the shape of a slender spindle. The stem strip was maintained with herbicides and the intercrop was grassed and mowed regularly. The trees were planted in a clip 3.6 × 1 m.

Irrigation and fertigation

The orchard was irrigated by drip irrigation with fertigation. Drip irrigation is mounted on the bottom row of the wire. Droppers are located in the so-called in-line pipeline. The distance of the drippers is 0.75 m. The diameter of the drip hose is 22 mm and the flow rate of the drip tray is 2.1 l/h of water. Four methods of irrigation were observed in the experiment: IR+F-A (drip hose placed on the wire – conventional method), IR+F-B (drip hose placed on the auxiliary structure from the left side and the right side of the trees, 0.5 m above the soil surface), IR+F-C (drip hose located on the left side and the right side of the trees, 0.3 m below the soil surface), NON-IR (without irrigation and fertigation). For variants IR+F-B and IR+F-C, the irrigation was performed alternately after two weeks. First from the left side of the trees and then from the right side (Table 1). Fully water-soluble fertilizers from Haifa Chemicals (Israel) were used for fertilization: ammonium sulfate, iron chelate 6% EDDHA, Humifirst, KNO3 Multi K, K2SO4 Solupotasse, MKP. Irrigation with fertigation in the orchard was performed by an automatic irrigation system.

The evaluation of experiment

When experimenting, the weight of fruits was determined on an accurate KERN PCB 1000-2 scale (England). The weight of apples determined was recorded and then averaged. One hundred apples from each variant were randomly selected for weighing.

The diameter of the fruit was measured by using plastic scales with circular holes, the diameter of which was gradually increased by 5 mm. These scales are a commonly used part of harvesting technology to separate the size gauges of apples. The measured fruit diameter was recorded in a table and then averaged. To measure the diameter, 100 apples from each variant were randomly selected.

At the end of vegetation, the length of annual increments was measured. One hundred shoots were randomly selected from each variant. The length of shoots was measured from the terminal bud scale scar from the previous vegetation to the terminal bud of the measured shoot. The measured shoots were selected evenly, between the wires of the supporting structure. To measure the length of annual increments, a steel tape measure was used.

Statistical analysis

One hundred apples and one hundred shoots from each variant were selected for statistical analysis. Data are reported as mean ± standard deviation. SHD test and one-way ANOVA with interaction ($P < 0.05$) were used to determine differences. Statistical analyses were performed with "Statistica 12.0" software (StatSoft Inc., USA).

Table 1 The amount of precipitation and the amount of irrigation during the year of 2020 in Plantex Veselé orchard

Month	Precipitation (mm)	Irrigated variants (mm)	
		No irrigation	With irrigation
I.	15.8	0	15.8
II.	55.1	0	55.1
III.	71.7	10.5	82.2
IV.	16.7	100.8	117.5
V.	38.4	113.4	151.8
VI.	15.6	79.8	95.4
VII.	58.1	50.4	108.5
VIII.	61.9	81.9	146.8
IX.	135.3	0	135.3
X.	132.1	0	132.1
XI.	21.4	12.6	34
XII.	58.8	0	58.8
∑	703.8	675.2	1 379

RESULTS AND DISCUSSION

Fruit weight

The highest average fruit weight was found in the IR+F-C variant, namely 178 g. This was followed by the IR+F-B variant, where the average fruit weight was about 171 g. The IR+F-A variant had the lowest average fruit weight among the irrigated variants, more precisely 167 g. The lowest average fruit weight among all variants was found for the NON-IR variant, where it was 148 g, which was expected because it is an non-irrigated and unfertilized variant (Figure 1). Nazari et al. (2021) reports significant differences between underground (IR+F-C) and aboveground (IF+F-A) irrigation of approximately 7%, which also agrees with our results. Wang et al. (2019) reported for the irrigated (IR+F-A) and non-irrigated (NON-IR) variants approximately the same results as found in this experiment. The results point to the advantage of underground irrigation, which supplies water and fertilizers directly to the root zone of apple trees and thus prevents surface evaporation of water. These results are from the second year after the start of the experiment, and it is assumed that the following year the differences between the variants will increase even more (Robinson 2006).

Figure 1 Impact of irrigation on "Gala" apple fruit weight in Plantex Veselé orchard, 2020

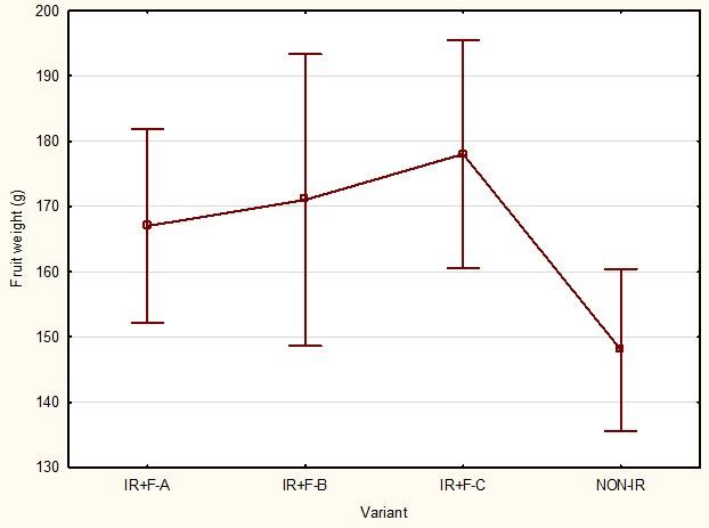

Legend: vertical columns indicate 0.95 confidence intervals

Fruit diameter

The classification into quality classes and subsequently the price of apples depends on the average fruit. According to the ČSN 46 3010 standard (Czech Standards Institute 1995), apples of a diameter of 70+ mm with dyed flesh of at least 80% belong to the selected quality, apples of diameter 55–69 mm with dyed flesh of at least 40% belong to the I. class, and apples below 55 mm in size and less than 40% dyed flesh belong to the II. class. Apples of selected quality are the most valuable for the producer. The largest fruit diameter was found in the IR+F-C variant with a diameter of 73.7 mm. This was followed by the IR+F-B variant, where the fruit diameter was found to be 72.2 mm, and the IR+F-A variant with a fruit diameter of 71.6 mm. The presumed smallest fruit diameter was found for the NON-IR variant, namely 66.4 mm. The difference in the diameter of the apples was demonstrated only between the variants IR+F-C and NON-IR (Figure 2). The share of apples in the selection quality was the largest in the IR+F-C variant, namely 68.4%. In the I. class the largest share was 36.7% in the variant IR+F-A and in the II. class was the largest proportion of apples in the NON-IR variant, namely 20% (Table 2). Nazari et al. (2021) shows approximately the same results as the IR+F-C variant. Wang et al. (2019) show the fruit diameter 10 mm larger in the IR+F-A variant. Mert et al. (2007) report an apple diameter 15 mm smaller than that found for the NON-IR variant. The results of the fruit average are closely related and point to the importance and need for fruit collection. If the fruit is insufficiently harvested on the trees, this subsequently affects the fruit diameter. It is recommended to load the tree with apples in the number of 100–120 pieces.

Figure 2 Impact of irrigation on "Gala" apple fruit diameter in Plantex Veselé orchard, 2020

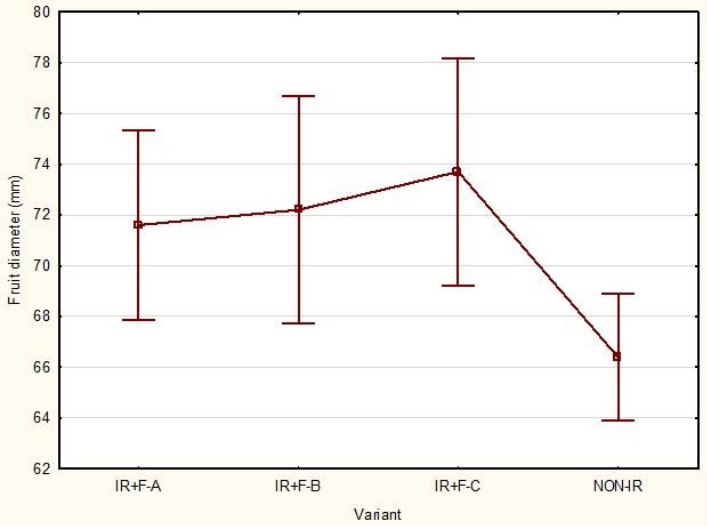

Legend: vertical columns indicate 0.95 confidence intervals

The length of annual increments

Annual increments on apple trees represent the basic vegetation element on which leaf – vegetative and flower – generative buds are differentiated. From the leaf buds new shoots continue to develop in the following vegetation, while from the flower buds flowers develop and subsequently after pollination and fertilization the fruits. In general, the more horizontal the growing shoots, the sooner the flower buds differentiate on them. In order to maintain a balance between the vegetative and generative parts of apples, there should be approximately 30 leaves per apple (Webster et al. 2000). Root pruning also plays an important role in the length of annual increments. The demonstrably longest average annual increments were found in the IR+F-C variant, namely 797.1, followed by the IR+F-B variant of 665.7 mm. For the IR+F-A variant, the average length of the annual increments was 582 mm. Demonstrably the most beautiful average annual increments were measured with the NON-IR variant 501.2 mm (Figure 3). Nazari et al. (2021) states shorter increments for underground irrigation. Neilsen and Neilsen (2002) report longer increments in the IR+F-C variant, which is caused by higher doses of nitrogen during vegetative growth. Another factor that affected the length of annual growth was the total precipitation during the month of May, when the growth of shoots is intense. The shortest annual increments were as long as Iancu et al. (2011). Longer annual increments bring the possibility of better generation of generative buds and thus can bring more crops

Figure 3 Impact of irrigation on length of annual increments on "Gala" apple in Plantex Veselé orchard, 2020

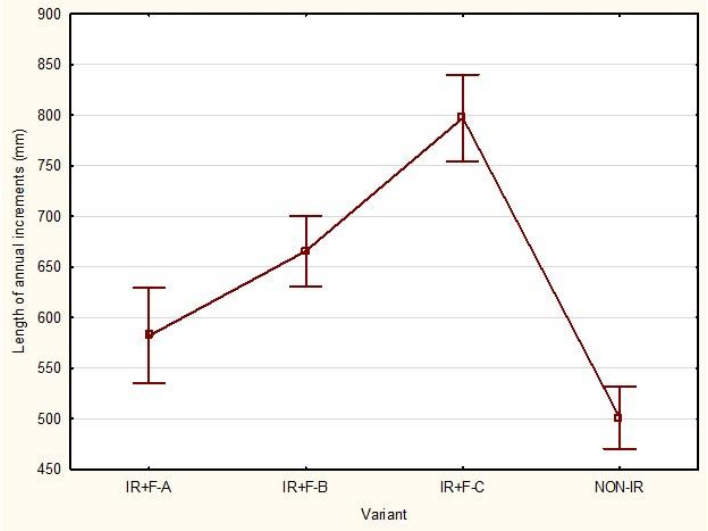

Legend: vertical columns indicate 0.95 confidence intervals

Table 2 Proportion of quality classes for individual irrigation variants on "Gala" apple in Plantex Veselé orchard, 2020

Variant	IR+F-A	IR+F-B	IR+F-C	NON-IR
Selective quality (%)	57.1	60.7	68.4	26
I. class (%)	36.7	34.9	29.1	54
II. class (%)	6.2	4.4	2.5	20

CONCLUSION

Intensive fruit orchards are characterized by high level of agricultural technology – regular care in the form of chemical treatment, annual pruning, fertilization and, last but not least, drip irrigation, which is an integral part of every intensive fruit orchard. Thanks to high level of agricultural technology, it is possible to achieve higher yields, better fruit quality and keep the trees in the best possible vitality. The highest fruit weight was found in the underground variant of irrigation IR+F-C 178 g. Variants with above-ground irrigation had a gradually lower fruit weight. The lowest fruit weight was found for the NON-IR variant of 148 g. The difference was shown only between the IR+F-C and NON-IR variants. The largest fruit diameter was found in the IR+F-C variant, namely 73.7 mm. The smallest diameter reached the NON-IR variant 66.4 mm. Both in terms of fruit weight and on average, the difference was demonstrated only between the IR+F-C and NON-IR variants. The demonstrably longest annual increments were measured for the IR+F-C variant (797.1 mm), while the demonstrably shortest increments were measured for the NON-IR variant (501.2 mm). The results of the experiment point to the importance of irrigation, while the influence of underground irrigation compared to above-ground irrigation can be observed. This is the second year of the experiment, and it is possible to expect an increase in the differences in individual variants in the upcoming year. From the results it is possible to evaluate that in intensive orchards it is suitable to build underground drip irrigation. However, in order to demonstrate the suitability of building such irrigation, it is necessary to continue research.

ACKNOWLEDGEMENTS

This paper was supported by the project CZ.02.1.01/0.0/0.0/16_017/0002334 Research Infrastructure for Young Scientists, this is co-financed from Operational Programme Research, Development and Education.

REFERENCES

Blanke, M.M. 2008. Perspectives of fruit research and apple orchard management in germany in a changing climate. Acta Horticulturae [Online], 772: 441–446. Available at: https://doi.org/10.17660/ActaHortic.2008.772.75. [2020-11-09].

Blanke, M. 2017. Apfel oder Acai: Brasiliens Obstbau im ökonomischen und klimatischen Wandel. Erwerbs-Obstbau [Online], 59(4): 245–252. Available at: https://doi.org/10.1007/s10341-017-0328-8. [2020-11-09].

Czech Standards Institute. 1995. Fresh Fruits. Red chokeberries, Apples, Pears, Rowanberries, Quinces, Medlars. CSN 46 3010 (463010). Praha: Czech Standards Institute.

Fallahi, E. 2017. Long-Term Influence of Irrigation Systems on Postharvest Fruit Quality Attributes in Mature 'Autumn Rose Fuji' Apple Trees. International Journal of Fruit Science [Online], 18(2): 177–187. Available at: https://doi.org/10.1080/15538362.2017.1389329. [2021-07-02].

Iancu, M. et al. 2011. Influence of the groundcover management system and drip irrigation on behavior of the 'Golden Spur' apple cultivar grafted on MM106 rootstock. Acta Horticulturae [Online], 889: 265–271. Available at: https://doi.org/10.17660/ActaHortic.2011.889.31. [2021-07-09].

Mašán, V. et al. 2018. Effects of Irrigation and Fertigation on Yield and Quality Parameters of 'Gala' and 'Fuji' Apple. Acta Universitatis Agriculturae et Silviculturae Mendelianae Brunensis [Online], 66(5): 1183–1190. Available at: https://acta.mendelu.cz/66/5/1183/. [2021-08-14].

Mert, C. et al. 2007. The King Fruit versus Lateral Fruit Thinning Effects on Yield and Fruit Quality in Apple. International Journal of Fruit Science [Online], 7(1): 37–46. Available at: https://doi.org/10.1300/J492v07n01_04. [2021-07-10].

Nazari, E. et al. 2021. Measurement and simulation of the water flow and root uptake in soil under subsurface drip irrigation of apple tree. Agricultural Water Management [Online], 255: 106972. Available at: https://doi.org/10.1016/j.agwat.2021.106972. [2021-09-07].

Neilsen, D., Neilsen, G.H. 2002. Efficient Use of Nitrogen and Water in High-density Apple Orchards. HortTechnology [Online], 12(1): 19–25. Available at: https://doi.org/10.21273/HORTTECH.12.1.19. [2021-07-09].

Racskó, J. et al. 2005. Schadwirkung des Sonnenbrands auf das Gewebe des Apfels (Malus domestica Borkh.). Gesunde Pflanzen [Online], 57: 47–52. Available at: https://doi.org/10.1007/s10343-005-0067-x. [2021-08-09].

Radivojevic, D. et al. 2020. Comparison of metamitron efficiency for postbloom thinning of young 'Gala' and 'Golden Delicious' apple trees. Turkish Journal of Agriculture and Forestry [Online], 44(1): 83–94. Available at: http://journals.tubitak.gov.tr/agriculture/issues/tar-20-44-1/tar-44-1-9-1902-22.pdf. [2021-07-02].

Robinson, T.L. 2006. Interaction of fertilization, rootstock and irrigation on growth, thinning efficiency, yield and fruit quality of 'empire' apple. Acta Horticulturae [Online], 721: 41–47. Available at: https://doi.org/10.17660/ActaHortic.2006.721.4. [2021-07-10].

Ucar, Y. et al. 2016. Quality Response of Young 'Gala, Galaxy' Trees under Different Irrigation Regimes. Erwerbs-Obstbau [Online], 58(3): 159–167. Available at: https://doi.org/10.1007/s10341-016-0269-7. [2021-08-09].

Wang, Y. et al. 2019. Effects of soil water stress on fruit yield, quality and their relationship with sugar metabolism in 'Gala' apple. Scientia Horticulturae [Online], 258: 108753. Available at: https://doi.org/10.1016/j.scienta.2019.108753. [2021-07-02].

Webster, A.D. et al. 2000. Interactions between root restriction, irrigation and rootstock treatments on the growth and cropping of 'Queen Cox' apple trees: Effects on orchard growth and cropping. Journal of Horticultural Science and Biotechnology [Online], 75(2): 181–189. Available at: https://doi.org/10.1080/14620316.2000.11511220. [2021-07-02].

ANIMAL PRODUCTION

Different selenium sources in medium-slow growing broiler chicken's diets and their influence on blood biochemical and performance parameters

Lucie Horakova, Jakub Novotny, Dana Zalesakova, Michal Rihacek, Andrea Roztocilova, Ondrej Stastnik, Eva Mrkvicova, Leos Pavlata
Department of Animal Nutrition and Forage Production
Mendel University in Brno
Zemedelska 1, 613 00 Brno
CZECH REPUBLIC

xhorak34@mendelu.cz

Abstract: The aim of the present study was to investigate the influence of different dietary sources of selenium on blood biochemical parameters in medium-slow growing broiler chickens. The study was conducted on 54 male Hubbard JA 57 broiler chickens which were divided into three groups. The Control group was fed a diet without the addition of selenium (Se), the Organic group was fed diet with a natural Se content in the feeds and organic source of Se (*Saccharomyces cerevisiae* CNCM I-3060), the Inorganic group was containing a natural source of Se and the addition of sodium selenite. No influence on the feed consumption and body weight was found at the end of trial (50 days of age). However, the effect of selenium sources was reflected in several biochemical parameters of blood: aspartate aminotransferase (AST), Se and glutathionperoxidase (GPx). One of the significant differences was for the AST between the Organic and Inorganic group, where its value in the Organic group reached 2.73 µkat/l and in the Inorganic group 2.39 µkat/l. Other significant difference was for the Se between Control vs Organic and Inorganic groups, where its value in the Control group reached 0.10 mg/l, in the Organic group 0.17 mg/l and in the Inorganic group 0.18 mg/l. Another significant difference was for the GPx also between Control vs Organic and Inorganic groups, where its value in the Control group reached 120.54 U/gHb, in the Organic group 207.46 U/gHb and in the Inorganic group 211.56 U/gHb. In conclusion, the addition of organic and inorganic selenium sources to the diet can increase selenium levels and glutathione peroxidase activity in the blood of broilers.

Key Words: Saccharomyces cerevisiae, sodium selenite, Hubbard JA 57, broiler nutrition

INTRODUCTION

Selenium (Se) is an essential micronutrient required for normal growth and normal functioning in poultry. The major biological forms include sulfur analogs of selenium such as selenomethionine, selenocysteine and selenocystine. Selenium plays a number of essential roles in the body, including the regulation of glutathione peroxidase activity, thyroid hormones, strengthens the role of vitamin E, has a positive effect on immune and reproductive functions and protects against heavy metals such as mercury and cadmium (Shlig 2009, Surai 2002). It is well understood that selenium deficiency has a negative effect on the performance of broiler chickens. The amount of selenium in poultry feed is different. This fact depends on the plant additives in the feed ration and the properties selenium of the soils in which the plants were grown. According to Mahan (1995) and NRC (1994), the recommended concentration of selenium in broiler feed ranges from 0.01 mg/kg to 0.15 mg/kg and selenium is supplied to the feed as an inorganic complex in the form of sodium selenite (Na_2SeO_3) or the organic form such as selenomethionine derived from selenized yeast. However, the efficiency of using organic and inorganic sources of selenium is different.

The aim of the present study was to investigate the influence of different sources of selenium on growth performance and blood biochemical parameters in medium-slow growing chickens.

MATERIAL AND METHODS

Characterization of the experiment

The experiment was performed in the experimental stables of Mendel University in Brno and the animal procedures were reviewed and approved by the Animal Care Committee and by the Ministry of Education, Youth and Sports (MSMT-21593/2020-3). The microclimatic conditions and light regime were set and controlled according to the requirements for the actual age of the chickens.

Animals and experimental diets

The total of 54 male medium-slow growing (Hubbard JA 57) broiler chickens were used in our experiment. The trial started at 1st day of the age and finished 50th day of the age of broiler chickens. Broiler chickens were fed experimental starter diets until 21st day of age and with experimental grower diets until 35th day of their age. The last feed mixture was experimental finisher diet from 36th day of age until the end of the experiment. At the first day of age broilers were divided by body mass into three groups with two replicates per treatment, i.e., there were placed 18 broilers in one experimental treatment. Three types of diets were used in this experiment: control and two experimental (Organic and Inorganic). The Control group (n=18) was fed a diet without addition of selenium (selenium was supplied only with its natural content in the feeds), the Organic group (n=18) was fed the natural content of selenium in the feeds and organic source of selenium (Sel-Plex – *Saccharomyces cerevisiae* CNCM I-3060). The last experimental group (Inorganic; n=18) was fed the natural content of selenium in the feeds and inorganic source of selenium (Sodium selenite – Na_2SeO_3). Diets were designed to be isoenergic and isonitrogenous. The broiler chickens had free access to water, and they were fed *ad libitum.*

Ingredient and chemical composition of used diets are shown in Table 1, Table 2 and Table 3 for starter, grower and finisher, respectively. The chemical compositions were determined for dry matter, crude protein, crude fat, crude fibre, and ash according to the EC Commission Regulation (Commission Regulation 152/2009).

Table 1 Ingredient and chemical composition of starter diets

Component	Unit	Control	Organic	Inorganic
Maize	g/kg	330.0	330.0	330.0
Soybean meal	g/kg	341.0	341.0	341.0
Wheat	g/kg	252.2	252.2	252.2
Rapeseed oil	g/kg	33.6	33.6	33.6
Premix*	g/kg	30.0	30.0	30.0
Limestone milled	g/kg	0.8	0.8	0.8
Monocalcium phosphate	g/kg	10.0	10.0	10.0
DL-Methionine	g/kg	2.4	2.4	2.4
Sodium selenite	g/kg	-	-	0.0078
Saccharomyces cerevisiae	g/kg	-	0.155	-
Dry matter	**%**	**88.00**	**88.00**	**88.00**
ME_N*	MJ/kg	12.29	12.29	12.29
Crude protein	%	20.26	20.32	20.51
Ether extract	%	5.53	5.34	5.40
Crude fibre	%	2.15	1.98	2.00
Crude ash	%	5.69	5.60	5.69

*Legend: *One kg of premix contained: L-lysine 2.34 g; DL-Methionine2.4g;Threonine 0.99 g; calcium 5.25 g; phosphorus 1.95 g; sodium 1.44 g; copper 15 mg;iron 84 mg; zinc 99 mg; manganese 99 mg; iodin 0.99 mg; retinol 13,500 IU (international units); calciferol 5, 001 IU; tocopherol 45 mg; phylloquinone 1.5 mg; thiamine 4.2 mg; riboflavin 8.4 mg; pyridoxin 6 mg; cobalamin 30 µg; biotin 0.21 mg; niacinamid 36 mg; folic acid 1.8 mg; calcium pantothenate 13.5 mg; cholin chloride 180 mg. *ME_N – Apparent metabolizable energy.*

Table 2 Ingredient and chemical composition of grower diets

Component	Unit	Control	Organic	Inorganic
Maize	g/kg	357.6	357.6	357.6
Soybean meal	g/kg	295.0	295.0	295.0
Wheat	g/kg	272.0	272.0	272.0
Rapeseed oil	g/kg	37.6	37.6	37.6
Premix*	g/kg	30.0	30.0	30.0
Monocalcium phosphate	g/kg	5.6	5.6	5.6
DL-Methionine	g/kg	2.20	2.20	2.20
Sodium selenite	g/kg	-	-	0.008
Saccharomyces cerevisiae	g/kg	-	0.155	-
Dry matter	**%**	**88**	**88**	**88**
ME_N*	MJ/kg	12.64	12.62	12.62
Crude protein	%	19.62	20.11	19.34
Ether extract	%	6.11	5.81	6.08
Crude fibre	%	1.68	1.72	1.87
Crude ash	%	5.32	5.16	5.16

*Legend: *One kg of premix contained: L-lysine 2.58 g; DL-Methionine 2.52 g; Threonine 1.47 g; calcium 5.04 g; phosphorus 1.65 g; sodium 1.38 g; copper 15 mg; iron 75 mg; zinc 99 mg; manganese 99 mg; iodine 0.9 mg; retinol 9,900 IU (international units); calciferol 5,001 IU; tocopherol 45 mg; phylloquinone 1.5 mg; thiamine 4.2 mg; riboflavin 8.4 mg; pyridoxin 6 mg; cobalamin 28.8 µg; biotin 0.18 mg; niacinamid 36 mg; folic acid 1.71 mg; calcium pantothenate 13.35 mg; cholin chloride 180 mg. *ME_N – Apparent metabolizable energy.*

Table 3 Ingredient and chemical composition of finisher diets

Component	Unit	Control	Organic	Inorganic
Maize	g/kg	399.1	399.1	399.1
Soybean meal	g/kg	252	252	252
Wheat	g/kg	272.5	272.5	272.5
Rapeseed oil	g/kg	40	40	40
Premix*	g/kg	30	30	30
Monocalcium phosphate	g/kg	4.90	4.9	4.9
DL-Methionine	g/kg	1.5	1.5	1.5
Sodium selenite	g/kg	-	-	0.0083
Saccharomyces cerevisiae	g/kg	-	0.16	-
Dry matter	**%**	**88**	**88**	**88**
ME_N*	MJ/kg	12.85	12.85	12.85
Crude protein	%	17.49	17.45	17.94
Ether extract	%	6.33	6.29	6.32
Crude fibre	%	1.45	1.63	1.42
Crude ash	%	4.89	4.96	4.94

*Legend: *One kg of premix contained: L-lysine 2.58 g; DL-Methionine 2.52 g; Threonine 1.47 g; calcium 5.04 g; phosphorus 1.65 g; sodium 1.38 g; copper 15 mg; iron 75 mg; zinc 99 mg; manganese 99 mg; iodine 0.9 mg; selenium 0.36 mg; retinol 9,900 IU (international units); calciferol 5,001 IU; tocopherol 45 mg; phylloquinone 1.5 mg; thiamine 4.2 mg; ri-boflavin 8.4 mg; pyridoxin ; cobalamin 28.8 µg; biotin 0.18 mg; niacinamid 36 mg; folic acid 1.71 mg; calcium pantothenate 13.35 mg; cholin chloride 180 mg. *ME_N – Apparent metabolizable energy*

Blood sample collection

The blood samples were collected into heparinized tubes after the slaughtering. Plasma was collected after centrifugation (10 minutes, 3,000 rpm) till 2 hours after blood collection and then it was frozen (-20 °C) until biochemical examination. Biochemical parameters were determined using Erba Lachema commercial sets on the Ellipse biochemical analyzer in plasma samples. Following parameters

were measured: AST – aspartate aminotransferase, GMT – gamma-glutamyltransferase, ALT – alanine aminotransferases, ALP – alkaline phosphatase, LD – lactate dehydrogenase, Tbili – total bilirubin, TG – triglycerides, cholesterol, urea, CK – creatine kinase, creatinine, TP – total protein, albumin, Se – selenium, GSH-Px – glutathione peroxidase. The content of globulins (total protein minus albumin) was calculated.

Statistical analysis

All measured data has been processed by Microsoft Excel (USA) and StatSoft Statistica version 12 (USA) was used to perform one-way analysis of variance (ANOVA). The Scheffe´s test was used to determine the significant differences among respective groups, where the differences among evaluated groups were considered significant at $P < 0.05$.

RESULTS AND DISCUSSION

Feed consumption and live weights of chickens

The average feed consumption per day and whole trial is shown in Table 4. The value of feed conversion ratio (FCR) is also shown here.

Table 4 Feed consumption and FCR of fattened chickens in respective dietary groups

	Control	Organic	Inorganic
Average consumption per trial/bird (g)	4315.58	4330.22	4163.83
Average consumption per day/bird (g)	88.07	88.37	84.98
FCR (kg/kg)	1.67	1.68	1.64

Legend: FCR – feed conversion ratio

The calculated FCR in Control group was 1.67; 1.68 in Organic and 1.64 in Inorganic group. FCR reached satisfactory values in all groups. The experiment Wang et al. (2008) also did not find statistically significant differences in FCR values in diets containing selenium. The Figure 1 shows live weight of broiler chickens.

Figure 1 Live weights of broiler chickens in respective dietary groups

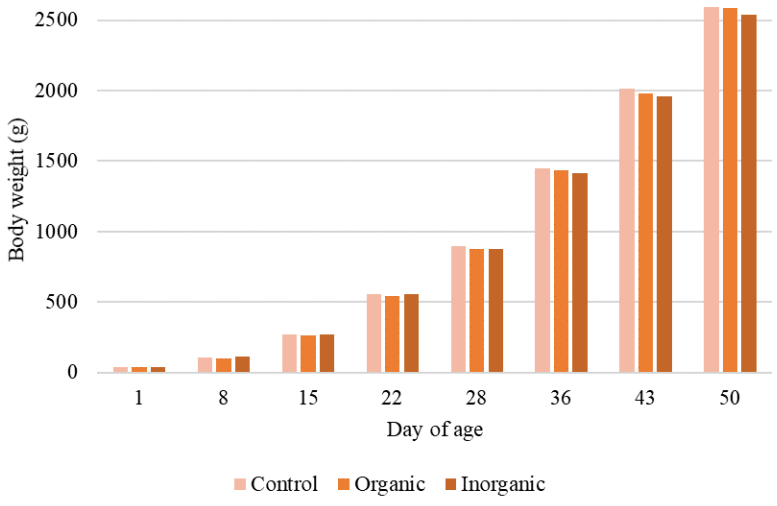

Legend: There were no significant differences (P > 0.05) among the respective groups.

The average live weight was 2590 g in the Control group, 2583 g in the Organic group and 2539 g in the Inorganic group, i.e. the weights were quite similar in all groups during the trial. There was not found any statistically significant differences ($P > 0.05$) in average live weights of chickens. In the experiment of Skřivan et al. (2008) was found that the addition of selenomethionine to feed had positive effect on the live weight of the broilers whose weight has increased by 3%. In contrast, Dalia et al. (2017) found in their study that various sources of selenium did not significantly affect the growth performance of broilers.

Blood biochemical parameters of chickens

The results of biochemical examination of blood are presented in Table 5.

Table 5 Blood biochemical parameters of broilers in relation to dietary treatment

Group		Control	Organic	Inorganic
n		6	6	6
Parameter	Unit	Mean ± Standard error		
ALT	µkat/l	0.09 ± 0.02	0.08 ± 0.01	0.06 ± 0.01
AST	µkat/l	2.49 ± 0.07	2.73 ± 0.03 [a]	2.39 ± 0.07 [b]
GGT	µkat/l	0.25 ± 0.07	0.32 ± 0.02	0.30 ± 0.06
ALP	µkat/l	17.93 ± 2.72	18.54 ± 2.08	30.09 ± 6.11
LD	µkat/l	46.64 ± 1.19	52.39 ± 4.51	47.77 ± 3.69
CK	µkat/l	187.58 ± 18.91	213.69 ± 29.31	211.55 ± 69.94
Tbili	µmol/l	6.33 ± 0.54	6.50 ± 0.32	7.10 ± 0.47
Urea	µmol/l	1.41 ± 0.03	1.43 ± 0.09	1.46 ± 0.05
Creat	µmol/l	29.27 ± 1.25	29.17 ± 1.77	33.30 ± 1.22
UA	µmol/l	329.60 ± 82.00	241.77 ± 40.05	248.63 ± 3.58
TP	g/l	34.00 ± 1.57	34.43 ± 1.07	34.67 ± 1.23
Alb	g/l	19.04 ± 1.13	18.96 ± 0.45	17.28 ± 1.08
Glob	g/l	14.96 ± 0.59	15.47 ± 1.47	17.38 ± 0.16
Glu	mmol/l	13.65 ± 0.36	14.05 ± 0.72	13.86 ± 0.75
Chol	mmol/l	3.48 ± 0.21	3.28 ± 0.10	3.35 ± 0.14
TG	mmol/l	0.83 ± 0.08	0.86 ± 0.04	0.85 ± 0.10
Se	mg/l	0.10 ± 0.00 [b]	0.17 ± 0.02 [a]	0.18 ± 0.01 [a]
GPx	U/gHb	120.54 ± 2.84 [b]	207.46 ± 26.39 [a]	211.56 ± 11.09 [a]

Legend: Means in the row not sharing a common letter (a – b) are statistically different (P < 0.05); n – number of cases per group. ALT – alanine aminotransferase, AST – aspartate aminotransferase, GGT – gamma glutamyl transferase, ALP – alkaline phosphatase, LD – lactate dehydrogenase, CK – creatine kinase, Tbili – total bilirubin, Creat – creatinine, UA – uric acid, TP – total protein, Alb – albumin, Glob – globulin, Glu – glucose, Chol – cholesterol, TG – triglycerides, GPx – glutathione peroxidase.

In the analysis of biochemical blood parameters were found statistically significant differences ($P < 0.05$) in the parameters of AST, Se and GPx. For the AST, a significant difference was found between the Organic and Inorganic group, where its value in the Organic group reached 2.73 µkat/l and in the Inorganic group 2.39 µkat/l. In another study, inorganic and organic selenium were found to significantly affect serum ALT and AST activity and creatinine concentration (Dalia et al. 2017). In the Control group was measured only 0.10 mg/l Se, in the experimental groups this value was much higher (Organic=0.17; Inorganic=0.18 mg/l). It was similar with the GPx value, where the lowest value was shown by the Control group (120.24 U/gHb). According to Arnaut et al. (2021) GPx levels in chicken blood increased after diets containing selenium yeast, higher values were also observed in chickens fed sodium selenite.

CONCLUSION

In our experiment, no significant differences in average live weight were found between the control and organic or inorganic group of broiler chickens. The addition of selenium to the diet in our experiment had no influence on the total feed consumption at the end of trial. However, a statistically significant differences were observed in the evaluation of blood biochemical parameters among assessed dietary groups, specifically for the parameters of AST, Se and GPx. In conclusion, the addition of organic and inorganic selenium sources to the diet can increase selenium levels and glutathione peroxidase activity in the blood of broilers.

ACKNOWLEDGEMENTS
The research was supported by the Internal Grant Agency of Faculty of AgriSciences (Mendel University in Brno) no. AF-IGA2020-TP012.

REFERENCES

Arnaut, P.R. et al. 2021. Selenium source and level on performance, selenium retention and biochemical responses of young broiler chicks. BMC Veterinary Research, 17(1): 151.

Commission regulation (EC) 152/2009. Laying down the methods of sampling and analysis for the official control of feed. Brussels: The commission of the European Communities.

Dalia, A.M. et al. 2017. The effect of dietary bacterial organic selenium on growth performance, antioxidant capacity, and Selenoproteins gene expression in broiler chickens. BMC Veterinary Research, 13(1): 254.

Mahan, D.C. 1995. Selenium metabolism in animals: what role does selenium yeast have? In Proceedings of the 15th Annual Symposium. Biotechnology in the Feed Industry. Nottingham, UK: Nottingham University Press, 257–267.

National Research Council (NRC). 1994. Nutrient Requirements of Poultry 9th. Washington DC: National Academy Press.

Shlig, A.A. 2009. Effect of vitamin E and selenium supplement in reducing aflatoxicosis on performance and blood parameters in broiler chicks. Iraqi Journal of Veterinary Sciences, 23(3).

Skřivan, M. et al. 2008. Effect of dietary selenium on lipid oxidation, selenium and vitamin E content in the meat of broiler chickens. Czech Journal of Animal Science, 53(7): 306–311.

Surai, P.F. 2002. Selenium in poultry nutrition: a new look at an old element. 1. Antioxidant properties, deficiency and toxicity. World's Poultry Science Journal, 58(3): 333–347.

Wang, Y.-B. et al. 2008. Effect of different selenium source (sodium selenite and selenium yeast) on broiler chickens. Animal Feed Science and Technology, 144(3–4): 306–314.

The influence of organic and inorganic selenium sources on the metabolism of broiler chickens

Lucie Horakova, Jakub Novotny, Dana Zalesakova, Michal Rihacek, Ondrej Stastnik, Eva Mrkvicova, Leos Pavlata
Department of Animal Nutrition and Forage Production
Mendel University in Brno
Zemedelska 1, 613 00 Brno
CZECH REPUBLIC

xhorak34@mendelu.cz

Abstract: The aim of the present study was to investigate the effect of organic and inorganic forms of selenium addition to the diet and their effect on the metabolism of broiler chickens. The study was conducted on 84 Ross 308 male broiler chickens which were divided into three groups. It was evaluated the average live weight, feed consumption, carcass yield and biochemical blood parameters in the study. Control group was fed a diet containing only natural content of selenium in the feed. Organic group was fed the organic source of selenium (*Saccharomyces cerevisiae* CNCM I-3060). Inorganic group was fed the inorganic source of selenium (sodium selenite – Na_2SeO_3). The selenium was added to its total content of 0.5 mg/kg of feed in both groups. The addition of selenium to the diets had no influence on average live weight, feed consumption at the end of trial and on the carcass, breast and legs yields. The analysis of blood biochemical parameters revealed a statistically significant difference ($P<0.05$) in glutathione peroxidase activity between the control and experimental groups. No significant differences in assessed traits of broilers were found between groups fed by organic and inorganic forms of selenium.

Key Words: organic selenium, broiler chickens, *Saccharomyces cerevisiae*, sodium selenite

INTRODUCTION

Selenium (Se) is an essential microelement required for the normal functioning of living organisms (Chen et al. 2014). Sufficient Se in animal nutrition is important for maintaining their good health and performance. Thanks to the higher concentration of Se in meat, milk and eggs, its intake into the human diet can also be increased (Otrubová 2018). This microelement is well known for its importance for growth, feather development, antioxidant and immune systems, and also for reproduction (Zhou and Wang 2011). Selenium deficiency in poultry reduces their growth, muscular dystrophy and lower lipid absorption (Zuberbuehler et al. 2006). Selenium plays an important role in regulating various metabolic processes in the body (Olson and Palmer 1976). Together with vitamin E, it is involved in protecting cell membranes from oxidative damage (World health organization 2004). The aim of the present study was to investigate the effect of organic and inorganic forms of selenium with their different content in the poultry diet and to monitor their effect on the metabolism of broiler chickens.

MATERIAL AND METHODS

Experimental conditions

The animal procedures were reviewed and approved by the Animal Care Committee of Mendel University in Brno and by the Ministry of Education, Youth and Sports (MSMT-21593/2020-3).

Animals and diets

The experiment was performed with 84 Ross 308 male broiler chickens and started at the 1st day of their age. Broiler chickens were divided into three equal groups with four replicates in each. The broilers had access to water and feed *ad libitum.* Control group (n=28) was fed a diet containing only natural content of selenium in the feed. First experimental (Organic) group (n=28) was fed

the organic source of selenium (*Saccharomyces cerevisiae* CNCM I-3060). The second experimental (Inorganic) group (n=28) was fed the inorganic source of selenium (sodium selenite – Na_2SeO_3). In Organic and Inorganic group, selenium was supplied with its natural content in the feed plus selenium was added that its total content was 0.5 mg/kg in both groups. The three isocaloric and isonitrogenous diets were formulated according to the recommended nutrients content for Ross 308 broiler chickens with use 2-phase feeding program.

The health status of broiler chickens was monitored daily. The live weight was measured periodically, and two deaths were recorded during the trial. At the end of the experiment at the 35th days of age of broiler chickens, all animals were weighed and slaughtered by decapitation. After slaughter, the yield of the main meat parts of the chickens was evaluated. Yield was calculated from live body weight. Blood of two birds per group was collected into the heparinized tubes and centrifuged for 15 minutes at 3,000 rpm. The blood plasma was stored frozen (-20 °C) until biochemical examination.

The chemical compositions of diets were determined for dry matter, crude protein, crude fat, crude fibre, and ash according to the EC Commission Regulation (Commission Regulation 152/2009). Ingredient and chemical composition of used starter and grower diets are shown in Table 1 and Table 2, respectively.

Table 1 Ingredient and chemical composition of used starter diets

Component	Unit	Control	Organic	Inorganic
Maize	g/kg	297.5	297.5	297.5
Wheat	g/kg	190.0	190.0	190.0
Rapeseed oil	g/kg	45.0	45.0	45.0
Soybean meal	g/kg	424.0	424.0	424.0
Premix*	g/kg	30.0	30.0	30.0
Limestone milled	g/kg	5.5	5.5	5.5
Monocalcium phosphate	g/kg	8.0	8.0	8.0
Saccharomyces cerevisiae	g/kg	-	0.03	-
Sodium selenite	g/kg	-	-	0.013
Dry matter	**g/kg**	**100**	**100**	**100**
ME_N*	MJ/kg	12.24	12.24	12.24
Crude protein	g/kg	26.48	26.21	25.07
Ether extract	g/kg	7.22	6.93	7.13
Crude fibre	g/kg	4.29	4.9	4.37
Crude ash	g/kg	7.27	7.32	7.23

*Legend: *Premix added to 1 kg of feed contained: L-lysine 2.34 g; DL-Methionine 2.4 g; Threonine 0.99 g; calcium 5.25 g; phosphorus 1.95 g; sodium 1.44 g; copper 15 mg; iron 84 mg; zinc 99 mg; manganese 99 mg; iodin 0.99 mg; retinol 13,500 IU (international units); calciferol 5, 001 IU; tocopherol 45 mg; phylloquinone 1.5 mg; thiamine 4.2 mg; riboflavin 8.4 mg; pyridoxin 6 mg; cobalamin 30 µg; biotin 0.21 mg; niacinamid 36 mg; folic acid 1.8 mg; calcium pantothenate 13.5 mg; cholin chloride 180 mg. *ME_N – Apparent metabolizable energy.*

Statistical analysis

All detected values has been processed by Microsoft Excel (USA) and the StatSoft Statistica version 12 (USA) was used to evaluate the data, in which one-way analysis of variance (ANOVA) was used. The Scheffe´s test was used to determine the significant differences among respective groups. The differences among evaluated groups were considered significant at $P< 0.05$.

Table 2 Ingredient and chemical composition of used grower diets

Component	Unit	Control	Organic	Inorganic
Maize	g/kg	292.0	287.0	287.0
Wheat	g/kg	250.0	250.0	250.0
Rapeseed oil	g/kg	45.0	45.0	45.0
Soybean meal	g/kg	370.0	375.0	375.0
Premix*	g/kg	30.0	30.0	30.0
Limestone milled	g/kg	4.0	4.0	4.0
Monocalcium phosphate	g/kg	6.0	6.0	6.0
Saccharomyces cerevisiae	g/kg	-	0.25	-
Sodium selenite	g/kg	-	-	0.01
Chromium oxide	g/kg	3.0	3.0	3.0
Dry matter	**g/kg**	**100**	**100**	**100**
ME_N*	MJ/kg	12.40	12.38	12.38
Crude protein	g/kg	24.18	25.61	25.19
Ether extract	g/kg	7.13	7.26	7.29
Crude fibre	g/kg	4.25	4.12	4.25
Crude ash	g/kg	7.02	6.94	6.9

*Legend: *Premix added to 1 kg of feed contained: L-lysine 2.34 g; DL-Methionine 2.4 g; Threonine 0.99 g; calcium 5.25 g; phosphorus 1.95 g; sodium 1.44 g; copper 15 mg; iron 84 mg; zinc 99 mg; manganese 99 mg; iodine 0.99 mg; retinol 13,500 IU (international units); calciferol 5,001 IU; tocopherol 45 mg; phylloquinone 1.5 mg; thiamine 4.2 mg; riboflavin 8.4 mg; pyridoxin 6 mg; cobalamin 30 µg;biotin 0.21 mg; niacinamid 36 mg; folic acid 1.8 mg; calcium pantothenate 13.5 mg; cholin chloride 180 mg. *ME_N – Apparent metabolizable energy.*

RESULTS AND DISCUSSION

Evaluation of broiler chickens live weight and feed consumption

The live weight of broiler chickens is shown in Figure 1. The average live weight was 2325 g in the Control group, 2340 g in the Organic group and 2251 g in the Inorganic group at the end of the trial. No statistically significant differences were found (P>0.05) in average live weights of chickens during the experiment. In the experiment of Dlouhá et. al (2008) was found that the addition of 0.3 mg/kg Se-chlorella had the positive effect on the live weight of the broilers.

Figure 1 Average live weight (g) of broiler chickens during the experiment

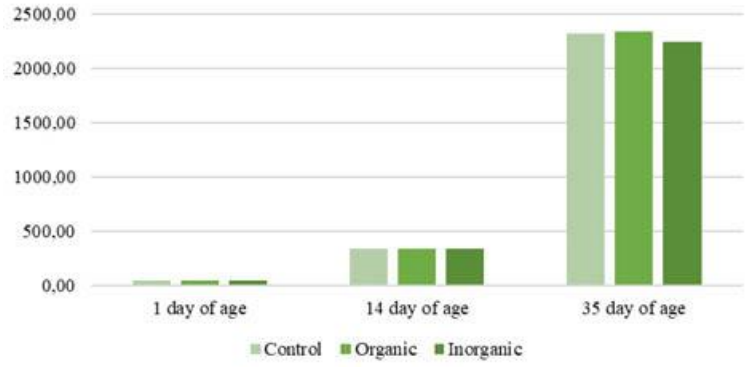

Legend: There were found no significant differences (P > 0.05) among the respective groups.

The average feed consumption per whole experiment was 3093 g for the Control group, 3056 g for Organic group and 2919 g for Inorganic group. The average total feed consumption per a day was 88 g for the Control group, 87 g for Organic group and 83 g for Inorganic group. The calculated feed conversion ratio (FCR) was 1.33 for the Control group, 1.31 for Organic group and 1.30 for Inorganic group, respectively. FCR reached satisfactory values in all groups. This fact is evidenced

by the guidelines for Ross 308 (Aviagen group 2019), where they consider 1.473 to be the optimal FCR value. The measured results show that no statistically significant differences (P>0.05) were found among evaluated groups. Wang and Bao-Hua (2008) also did not find statistically significant differences in FCR values in their experiment studying different selenium sources.

Table 3 shows the carcass weight and yield of main meat parts of broilers at the end of the trial.

Table 3 Carcass weight and yields of main meat parts of broilers in relation to the dietary group of broilers

Group	**Control**	**Organic**	**Inorganic**
n	**8**	**8**	**8**
	Mean ± Standard error		
Carcass weight (g)	1629.52 ± 67.10	1619.60 ± 43.63	1606.99 ± 37.47
Carcass yield (%)	71.03 ± 0.56	69.64 ± 0.65	70.24 ± 0.61
Breast (%)	32.16 ± 0.76	32.84 ± 0.50	32.41 ± 0.47
Leg meat (%)	21.75 ± 0.55	20.83 ± 0.67	20.89 ± 0.39

Legend: There was not found statistically significant differences (P > 0.05) among dietary groups; n – number of cases per group.

Blood biochemical parameters of broilers

The results of the biochemical analysis are presented in Table 4.

Table 4 Blood biochemical parameters of 35-day old broilers in relation to the dietary group

Group		**Control**	**Organic**	**Inorganic**
n		**8**	**8**	**8**
Parameter	**Unit**	Mean ± Standard error		
ALT	µkat/l	0.05 ± 0.00	0.04 ± 0.00	0.05 ± 0.01
AST	µkat/l	5.23 ± 0.55	4.89 ± 0.51	5.30 ± 0.56
GMT	µkat/l	0.27 ± 0.03	0.21 ± 0.02	0.23 ± 0.02
ALP	µkat/l	98.61 ± 13.77	84.30 ± 14.91	67.41 ± 08.11
LD	µkat/l	25.57 ± 5.30	23.30 ± 2.65	24.53 ± 2.71
CK	µkat/l	328.51 ± 38.68	327.66 ± 49.06	376.09 ± 45.50
Tbili	µmol/l	1.34 ± 0.42	1.11 ± 0.20	1.60 ± 0.36
Urea	µmol/l	0.83 ± 0.05	0.89 ± 0.06	0.97 ± 0.05
Creat	µmol/l	36.00 ± 2.29	32.79 ± 0.95	33.91 ± 1.93
UA	µmol/l	173.64 ± 19.26	129.56 ± 17.45	184.06 ± 22.71
TP	g/l	26.50 ± 2.15	25.23 ± 0.98	25.45 ± 1.19
Alb	g/l	12.58 ± 1.09	12.25 ± 0.50	12.33 ± 0.46
Glob	g/l	13.93 ± 1.06	12.98 ± 0.48	13.12 ± 0.73
Glu	mmol/l	12.76 ± 0.85	12.27 ± 0.50	12.97 ± 0.34
Chol	mmol/l	2.68 ± 0.24	2.42 ± 0.09	2.37 ± 0.12
TG	mmol/l	0.48 ± 0.08	0.37 ± 0.03	0.54 ± 0.09
GPx	U/gHb	47.83 ± 2.77 [b]	190.26 ± 11.82 [a]	192.08 ± 14.15 [a]

Legend: Means in the row not sharing a common letter (a – b) are statistically different (P < 0.05); n – number of cases per group. ALT – alanine aminotransferase, AST – aspartate aminotransferase, GMT – gamma glutamyl transferase, ALP – alkaline phosphatase, LD – lactate dehydrogenase, CK – creatine kinase, Tbili – total bilirubin, Creat – creatinine, UA – uric acid, TP – total protein, Alb – albumin, Glob – globulin, Glu – glucose, Chol – cholesterol, TG – triglycerides, GPx – glutathione peroxidase.

Chen et al. (2013) conducted a study examining the effect of adding different levels of selenium-enriched yeast on growth factor, performance parameters, immune system, oxidation resistance, meat quality and selenium content in broiler tissue. A total of 540 one-day-old Arbor Acres broilers were used in their study and fed diets supplemented with 0.0, 0.3, 0.5, 1.0 and 2.0 mg of organic selenium/kg

of feed. The experiment lasted 42 days. The results showed that the effect of different levels of selenium on growth factor, immune system, etc., did not differ significantly (P>0.05) among different selenium dietary levels. However, serum glutathione peroxidase (GSH-Px) activity and selenium content were significantly increased (P<0.05) at the end of the study. The results showed that organic selenium had no apparent effect on the performance of broilers, but significantly affected the oxidative resistance of broilers.

CONCLUSION

At the end of the experiment, no significant differences in average live weight were found between the control and experimental groups of broiler chickens. The addition of selenium to the diet in our experiment had no influence on feed consumption at the end of trial, carcass yield and yields of breast and leg meat. However, a statistically significant difference was observed in the GPx activity, which showed differences between the control group and the experimental groups with added selenium.

ACKNOWLEDGEMENTS

The research was supported by the project AF-IGA2021-IP063.

REFERENCES

Aviagen Group 2019. Broiler ROSS: Performance Objectives. Available at: http://eu.aviagen.com/tech-center/download/1339/Ross308-308FF-BroilerPO2019-EN.pdf. [2021-08-27].

Chen, G. et al. 2014. Effect of different selenium sources on production performance and biochemical parameters of broilers. Journal of Animal Physiology and Animal Nutrition, 98(4): 747–754.

Commission regulation (EC) 152/2009. Laying down the methods of sampling and analysis for the official control of feed. Brussels: The commission of the European Communities.

Dlouhá, G. et al. 2008. Effect of dietary selenium sources on growth performance, breast muscle selenium, glutathione peroxidase activity and oxidative stability in broilers. Czech Journal of Animal Science, 53(6): 265.

Olson, O.A., Palmer L.S. 1976. Seleno amino acids in tissues of rats administered inorganic selenium. Metabolism, 25(3): 299–306.

Otrubová, M. 2018. Selen ve výživě skotu. Agropress.cz [Online]. Available at: https://www.agropress.cz/selen-ve-vyzive-skotu/. [2020-11-20].

Wang, Y.-B., Bao-Hua, X.-O. 2008. Effect of different selenium source (sodium selenite and selenium yeast) on broiler chickens. Animal Feed Science and Technology, 144(3–4): 306–314.

World health organization. 2004. Vitamin and mineral requirements in human nutrition. 2nd ed., Rome: World Health Organization and Food and Agriculture Organization of the United Nations.

Zhou, X., Wang, Y. 2011. Influence of dietary nano elemental selenium on growth performance, tissue selenium distribution, meat quality, and glutathione peroxidase activity in Guangxi Yellow chicken. Poultry Science, 90(3): 680–686.

Zuberbuehler, C.A. et al. 2006. Effects of selenium depletion and selenium repletion by choice feeding on selenium status of young and old laying hens. Physiology & Behavior, 87(2): 430–440.

The effect of stage and number of lactations on the incidence of milking success when using Automatic Milking Systems

David Jenik[1], Daniel Falta[1], Tomas Kopec[1], Milan Vecera[1], Francois Lategan[2], Gustav Chladek[1]
[1]Department of Animal Breeding
[2]Department of Regional and Business Economics
Mendel University in Brno
Zemedelska 1, 613 00 Brno
CZECH REPUBLIC

david.jenik@mendelu.cz

Abstract: One of the characteristics of automatic milking systems is that cows can visit the Automatic Milking System (AMS) voluntarily for milking. This leads to variations in the frequency of visits of cows to the AMS. The number of visits, rejections and volume of milk produced were studied using data from the private farm ZD Libín, located in the South Bohemian region. The dairy herd under observation consisted of 147 Montbeliarde cows. Data were collected from 1 January to 7 December 2020, creating a total of 23 389 data records. The average daily milk yield during the observation period was 33.7 kg milk per cow with a maximum of 59.3 kg milk per cow. Each cow in the herd was milked on average, 2.6 times per day. Only in rare cases were some cows milked less than twice or more than four times per day. Results show that high producing cows go to the AMS more often. During the first stage of lactation the cows produced an average of 35.9 kg of milk per day and were milked on average 2.8 times a day. Data further shows that 44.3% of cows were never rejected by the AMS because they were ready to be milked.

Key Words: dairy cows, automatic milking system, rejection, Montbeliarde

INTRODUCTION

The increasing demand for investment in livestock production due to higher workloads, higher material costs and increased organizational complexity, compel livestock breeders to continuously intensify production and strive to meet optimum biological and economic objectives and increase the economic profitability of livestock production systems using the genetic potential of animals (Bouška 2006, Kuczaj et al. 2020).

Current knowledge of Automatic Milking Systems (AMS) does not claim to be a milking management solution for all types of herds in all production conditions since the effectiveness of their application is determined by a number of operational and economic factors (Kuczaj et al. 2020). Research suggests that AMS is a suitable system for herds of 60 to 240 cows and, under certain conditions with controlled movement of animals, for herds of 300 to 400 cows (Vacek and Smutný 2021).

The benefit of AMS lies in the fact that it allows for the natural extraction of milk. Milking becomes a natural process that the cow seeks out of own accord, to allow for the cow´s biological processes and avoid stress. AMS represents not only a new milking system but also a new way of milking management. The AMS is positioned in the stable and contributes to improving the welfare of dairy cows. Cows are allowed to determine when they need to be milked, rested or graze (Madsen et al. 2009). During milking they do not have to lose visual contact with the rest of the herd, so it never feels separated from the herd. At the same time, due to the increasing frequency of milking, it improves udder health (Machálek et al. 2011).

MATERIAL AND METHODS

The Automatic Milking System Lely Astronaut was used as experimental automatic milking system for the purpose of this study. The feed composition was typical for the region (460 meters above

sea level) and a mineral premix was also included. Nutrient levels in the feed were optimized to maintain daily milk production and the feed ration was fed in the form of total mixed ratio (TMR). The cows were fed twice a day and excess feed regularly pushed closer to the animals. The cows were housed in cubicles using mattresses replacing bedding material. Cows entered the AMS voluntarily but twice daily the herd was monitored for animals avoiding the AMS. This was done in order to prevent milking mastitis or other health complications associated with skipped milkings.

Data were collected by means of an electronic recognition device, which was part of the AMS. This device recognizes individual cows, each with an unique ID. The AMS records the date, the milking yield, number of milkings per day and number of rejections per day. Rejections were registered when cows were refused entry by the AMS. This rejection occured when cows attempted to enter the AMS more often than permitted. The AMS settings only allowed cows for milking more than 3 hours after the last milking. Cows were also rejected when they tried to enter the AMS more than 7 times a day. In this way a total of 23,389 data recordings were created.

Data were collected at the private farm ZD Libín in the South Bohemian Region where Montbeliarde cows are kept. Data collection took place from 1 January to 7 December 2020. The herd consisted of 147 dairy cows, which, on average produce 8,809 kg of milk per lactation. The cows calved the first time at the age of 26 months.

All data from sick cows and cows in heat were discarded. Cows that were lactating for 306 or more days were excluded from the results. The data were statistically analyzed using Statistica CZ 12 software. The significance of the effects and the differences between the means were tested using the analysis of variance and Schéffe test. Statistical significance was tested at a significance level of $\alpha = 0.01$.

According to their stage in lactation, cows were divided into three groups. The first stage (I) 1–100 days in milk (DIM), the second stage (II) 101–200 DIM and the third stage (III) 201–305 DIM. Cows were also sorted according to their number of lactations. The first lactation (36.9% of the cows), in the second lactation (24.5% of the cows), in the third lactation (17.2% of the cows) and in their fourth lactation or higher (21.3% of the cows).

RESULTS AND DISCUSSION

Descriptive analysis of the observed herd showed the following frequencies of distribution of cows in different lactation stages. In DIM stage I were 52.4% of the cows, in DIM stage II 32.4%, and in DIM stage III 15.2% of the cows. Figure 1 shows the distribution of successful milkings per cow per day. The average number of milkings per cow per day was 2.6 for the whole herd. A herd maximum of 7 milkings per day per cow (4 observations only) was recorded at the peak of their lactations. Machálek et al. (2011) state that the average number of milkings per day in the range of 2.5–3 is satisfactory, which was also proved by this measurement. Closer reflection indicates that more than 95% of the herd was milked more than once per day. This is in contrast with comparative manual milking systems where generally 100% cows in lactation are milked twice per day.

Table 1 shows the distribution of milk yields, successful milkings and rejections by lactation stages. Results suggest that cows achieved the highest milk production in the first stage of lactation. This is confirmed by Žižlavský and Mikšík (2005) and Žižlavský et al. (2008), who stated that milk production gradually increases (ascending) immediately after calving and continues for about 30–60 days. After reaching the highest daily milk yield, the milk production decreases until the end of the lactation. Furthermore, we can observe the same tendency in changes of milk production with changes in the number of the milkings per day. The opposite tendency is observed between the changes in rejections with changes in DIM stages. In the first DIM stage, when the highest average milk yield is 35.9 kg per day, the cows are milked on average 2.8 times a day. At the same time the least rejections by the AMS is reccorded (1.7 times a day). In subsequent stages this number gradually increases.

Figure 1 Ilustration of the frequency of milkings per day

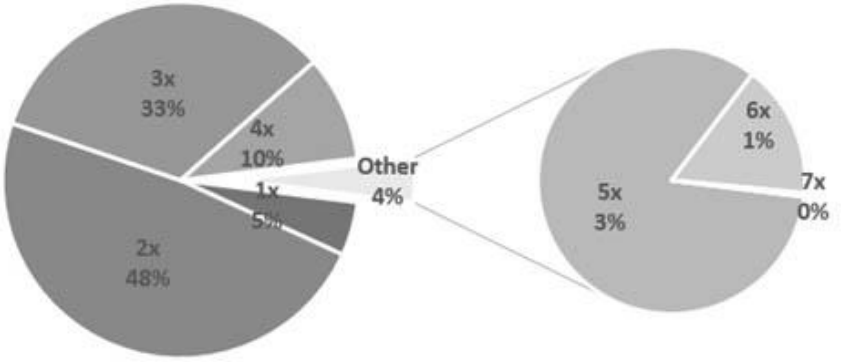

Table 1 Milk yield and milkings and rejection numbers by lactation stages

DIM stage	x̄ milk yield (kg)	Max	Min	Std
I. (0–100)	35.9 ^{A}	59.3	4.3	8.173
II. (101–200)	33.0 ^{B}	54.4	11.6	6.707
III. (201–305)	28.3 ^{C}	48.1	1	6.506
	x̄ milkings (times a day)	Max	Min	Std
I. (0–100)	2.8 ^{A}	7	1	0.924
II. (101–200)	2.5 ^{B}	7	1	0.870
III. (201–305)	2.2 ^{C}	6	1	0.713
	x̄ rejection (times a day)	Max	Min	Std
I. (0–100)	1.7 ^{A}	48	0	2.815
II. (101–200)	1.8 ^{B}	31	0	2.982
III. (201–305)	2.2 ^{C}	90	0	4.101

Legend: Values in the same columns marked with different letters (A to C) are statistically different (P < 0.01).

Table 2 Milk yield and milkings and rejection numbers by number of lactations

Lactation	x̄ milk yield (kg)	Max	Min	Std
1st	28.5 ^{A}	50.3	1	5.928
2nd	34.0 ^{B}	54.5	0.8	7.329
3rd	38.1 ^{C}	59.2	2	7.833
4th +	37.9 ^{C}	59.3	0.4	7.909
	x̄ milkings (times a day)	Max	Min	Std
1st	2.2 ^{A}	5	1	0.561
2nd	2.7 ^{B}	6	1	0.880
3rd	3.0 ^{C}	7	1	1.081
4th +	2.9 ^{D}	7	1	0.931
	x̄ rejection (times a day)	Max	Min	Std
1st	1.3 ^{A}	31	0	2.239
2nd	2.2 ^{B}	90	0	3.806
3rd	2.5 ^{C}	48	0	3.725
4th +	1.9 ^{D}	35	0	3.023

Legend: Values in the same columns marked with different letters (A to D) are statistically different (P < 0.01).

Table 2 shows the distribution of milk yields, successful milkings and rejections by number of lactation. Momani and Šáda (2010) stated that milk yield increases with increase in the number

of lactations, with apex production in the third lactation. It is then kept at the same level for one to two lactations and then gradually decreases. This tendency is strongly supported and confirmed in Table 2. The same tendency as with milk yield per lactations can be seen with the number of milkings per lactation. This tendency is also true for the number of rejections per lactation. Findings suggest that cows with higher milk yields tend to enter the AMS successfully more often. The higher rate of rejections could possibly be because of the higher number of entrances to the AMS. This may be an indication of the increased need to be milked due to higher production. This could be an important theme for the further investigation.

CONCLUSION

Looking at the basic indicators of milking success findings suggest that the use of artificial intelligence in the optimization of milking systems has positive prospects for improving the animal welfare status of dairy production without negative consequences for dairy production systems. It allows for dairy cows to move freely throughout the day while voluntarily participates in the milking activities with the minimum force and stress. This creates a more stable, relaxed and conducive environment for optimum milk production by cows. The absence of a rigid milking routine associated with conventional milking parlours contributes largely to a more relaxed and productive milking session. Normal activities associated with the management and control of milking parlours (manure removal and feeding) have a far less disturbing effect on dairy cows. The hygienic procedures associated with the AMS before, during and after milking eliminates human error and negligence. This improves and protects the general health status of the mammary glands of the dairy cow. In conclusion it can therefore be stated that the AMS not only improves the welfare of the animals but also saves breeders time, manpower and costs.

REFERENCES

Bouška, J. 2006. Chov dojeného skotu. 1st ed., Praha: Profi Press.

Hulsen, J. 2005. Cow signals: a practical guide for dairy farm management. Zutphen, Netherlands: Roodbont Publishers.

Kuczaj, M. et al. 2020. Relationships between Selected Physiological Factors and Milking Parameters for Cows Using a Milking Robot. Animals (Basel) [Online], 10(11): 2063. Available at: https://doi.org/10.3390/ani10112063. [2021-09-05].

Machálek, A. et al. 2011. Analýza a metodika hodnocení interakcí systému člověk - zvíře - robot na farmách dojnic. Praha: Výzkumný ústav zemědělské techniky, v.v.i., 49 pp. Certified methodology, ISBN 978-80-86884-63-9. Available at: www.vuzt.cz/svt/publ/P2011/085.PDF. [2021-09-01].

Madsen. J. et al. 2009. Concentrate composition for Automatic Milking Systems – Effect on milking frequency. Livestock Science [Online], 127(1): 45–50. Available at: https://doi.org/10.1016/j.livsci.2009.08.005. [2021-09-09].

Momani, M.S., Šáda, I. 2010. Základy chovu zvířat v TS I. 1st ed., Praha: Česká zemědělská univerzita.

Vacek, M., Smutný, L. 2021. Ekonomika robotického dojení. Náš chov [Online], 6: 75. Available at: https://www.naschov.cz/ekonomika-robotickeho-dojeni. [2021-09-01].

Žižlavský, J., Mikšík, J. 2005. Chov skotu. Brno: Mendelova zemědělská a lesnická univerzita v Brně.

Žižlavský, J. et al. 2008. Chov hospodářských zvířat. 2nd ed., Brno: Mendelova zemědělská a lesnická univerzita v Brně.

Evaluation of reproductive parameters at a farm specializing in breeding of Czech Fleckvieh dairy cows

Kristyna Kocianova, Radek Filipcik, Zuzana Reckova, Vojtech Pesan
Department of Animal Breeding
Mendel University in Brno
Zemedelska 1, 613 00 Brno
CZECH REPUBLIC

kriskoci12@seznam.cz

Abstract: The aim of this study was to evaluate the level of selected reproductive parameters at a farm specializing in breeding Czech Fleckvieh dairy cows. The study was carried out at the farm AZOS, s. r. o. Zakřany. Reproductive parameters were assessed in 291 cows in the years 2017, 2018 and 2019. The longest calving interval was 400 days for cows on the 4th lactation and there was not a statistically conclusive ($p>0.05$) difference. The shortest calving interval of 378 days was found in cows at 2nd lactation and there was not a statistically conclusive ($p>0.05$) difference. Cows had more difficult calvings when they had twins than when they had one offspring. It was also established that the length of gestation was shorter in twin pregnancies. There was a statistically conclusive ($p\leq0.01$) difference in gestation length for cows with a single offspring, where the length of gestation was 285 days, and cows with twins, which were pregnant for 279 days.

Key Words: Czech Fleckvieh cattle, reproduction, reproductive parameters

INTRODUCTION

The reproductive performance of cows together with the yield achieved are among the most important factors influencing the output and economic results of breeding farms. Ensuring regular reproduction is thus the main condition for successful breeding, because reproduction is the cornerstone of profitable breeding (Coufalík 2013). With increasing demands on the yield of dairy cows comes a deterioration in the reproductive rate (Rodriguez-Martinez et al. 2008). One of the main problems is the low heat detection rate and the prolongation of postpartum anoestrus (Coufalík 2013). Other complications may include the higher incidence of ovarian abnormalities (Royal et al. 2000), shorter oestrus and lower intensity of oestrus symptoms (Lopez et al. 2004) or increased incidence of early or late embryonic mortality (Humblot et al. 2009). Nowadays, many synchronization programmes (e.g. Ovsynch, Cosynch etc.) are used to improve reproductive efficiency. However, these programmes are costly and do not address the causes of the problems. The main condition for the resumption and physiological functioning of the sexual cycle after parturition is that each cow be healthy after calving with a trouble-free puerperium (Coufalík 2013).

MATERIAL AND METHODS

The study assessed reproductive indicators in the selected Czech Fleckvieh cattle farm for the years 2017, 2018 and 2019. These parameters were assessed in a total of 291 cows. The individual values were acquired from farm records, breeding cows' cards and monthly yield recording results.

At the farm in question, insemination is carried out using semen from both proven and genomic bulls. As a last resort, insemination doses from beef sires are employed when dairy cows have problems conceiving. Visual checks for oestrus are conducted twice a day. If oestrus is not detected in a cow or if she is found to be infertile during a pregnancy examination, oestrophan is used to induce heat. Diagnosis of pregnancy is carried out rectally two months after service. Dairy cows are dried off for at least two months before the expected calving date and are moved to a group maternity pen three weeks prior to calving.

As part of performance monitoring, the average milk yield achieved at the farm was 7641 kg in 2017, 8279 kg in 2018 and 8624 kg in 2019.

At the selected breeding farm, the following factors were assessed: the effect of year (2017, 2018, 2019), number of offspring (singleton, twins) and lactation order (2, 3, 4, 5, 6 and above) on the length of calving interval, length of gestation and difficulty of parturition (1 = easy delivery, 2 = assistance required during delivery). Statistical analysis of the data was performed using the statistical programme STATISTICA 12.0, with variance analysis being employed. An HSD test was used to determine significance among the levels of the individual factors.

RESULTS AND DISCUSSION

Table 1 summarizes the results for the effect of year, number of offspring and lactation order on gestation length, difficulty at parturition and length of calving interval.

Table 1 Effect of year, number of offspring and lactation order on gestation length, calving interval and difficulty at parturition

		N	Gestation length (days)		Difficulty at parturition		Calving interval (days)	
			$\bar{x}$	s_x	$\bar{x}$	s_x	$\bar{x}$	s_x
Total		291	285	5.27	1.26	0.44	388	54.07
Year	2017	104	284^{a}	5.46	1.20^{A}	0.4	385	53.07
	2018	95	285	5.02	1.20^{A}	0.4	385	50.94
	2019	92	286^{b}	5.21	1.38^{B}	0.49	394	58.23
No. of offspring	1	269	285^{A}	5.02	1.25	0.44	388	53.25
	2	22	279^{B}	4.59	1.32	0.48	392	64.24
Lactation order	2.	88	284	4.99	1.28	0.45	378	41.47
	3.	71	285	5.38	1.24	0.43	382	51.95
	4.	58	283.43	5.06	1.18	0.39	400	60.2
	5.	39	285.79	6.03	1.32	0.47	398	60.83
	6. +	35	285.49	4.93	1.31	0.47	392	62.84

Legend: the different letters (a,b; A,B) denote separately statistically significant differences between years, numbers of calves and lactation order. a, b= p≤0.05, A, B= p≤0.01.

The analysis of the data revealed a statistically significant (p≤0.05) difference in gestation length between the years 2017 and 2019. In 2017 the average gestation length was 284 ± 5.46 days, and in 2019 it was 286 ± 5.21 days. In 2018 the average gestation length was 285 days with a variability of ± 5.02 days. For the effect of the number of offspring on gestation length, it was statistically proven (p≤0.01) that if the cow was carrying twins, gestation was significantly shorter. The average gestation length was 285 ± 5.02 days for cows with a single offspring and 279 ± 4.59 days for cows with twins. In the case of twins, gestation was thus shortened by almost 7 days, which is also confirmed by Coufalík (2013), who stated that in twin pregnancies gestation is shortened by 5–10 days. In their study, Bezdíček and Louda (2009) report a gestation length of 281 days for Czech Fleckvieh cows with twins and a shortening of gestation by 5.84 days compared to single pregnancies.

When assessing the difficulty of parturition, it was found that in the years 2017 and 2018 there were easier births at the farm (1.20 ± 0.40 points). In 2019 there was a significant (p≤0.01) deterioration in this indicator (1.38 ± 0.49 points). The average calving difficulty was 1.25 ± 0.44 points for a single pregnancy and 1.32 ± 0.48 points for a twin pregnancy. Grummer et al. (2008) stated in their study that cows with twins are more likely to require assistance during delivery. The most difficult births were in cows on the 5th lactation and above. Jakubec et al. (2012) stated that the age of the cow and birth weight of the calf are the most important traits influencing the difficulty of parturition.

The average length of calving interval was 385 ± 53.07 days in 2017, 385 ± 50.94 days in 2018 and 394 ± 58.23 days in 2019. The length of the calving interval was 388 ± 53.25 days for cows

with a single offspring and 392 ± 64.24 days for cows with twins. The shortest calving interval was 378 ± 41.47 days for cows on the 2nd lactation, and the longest calving interval belonged to cows on the 4th lactation, where the average length was 400 ± 60.20 days. According to Kvapilík et al. (2019), the optimal length of calving interval is up to 385 days, but an extension of up to 400 days is tolerated in high-producing cows. Chagas et al. (2007) stated that an extension of the calving interval may result from a prolonged postpartum anoestrus. According to Coufalík (2013), a calving interval longer than 380 days is a sign of poor reproductive efficiency. In 2017, according to Kvapilík et al. (2018), the average length of calving interval for cows in the Czech Republic was 401 days, and in 2018, according to Kvapilík et al. (2019), it was 397 days. Andrýsek et al. (2018) stated that in 2017 the average length of calving interval for Czech Fleckvieh cows was 391 days, and in 2018, according to Andrýsek et al. (2019), it was 390 days. Bucek and Kučera (2019) stated from the results of milk yield recording that in 2019 the calving interval for cows in the Czech Republic was 396 days long, and 391 days long for Czech Fleckvieh cows. The cows assessed at the farm in 2017 and 2018 achieved more favourable values than the national average. In 2019 the length of calving interval was calculated to be 393 ± 58.23 days, which points to a slight deterioration in the conception rate among dairy cows compared to previous years. In their study, Řehák et al. (2012) determined the length of calving interval among Czech Fleckvieh cattle to be 382 days. Of the assessed cows, the only ones to achieve better results are those on the 2nd lactation, the figure being 378 ± 41.47.

CONCLUSION

It was determined that among the cows there was a statistically significant ($p \leq 0.05$) difference in gestation length between the years 2017 and 2019, when the length of gestation was extended by 1.85 days. Furthermore, a statistically conclusive ($p \leq 0.01$) difference was found in gestation length for cows with a single offspring, where the length of gestation was 285 days, and cows with twins, which were pregnant for 279 days. For cows with twins, there was thus a shortening of gestation by an average of six days.

There was also found to be a statistically significant ($p \leq 0.01$) deterioration in the difficulty of parturition between the assessed years. In the years 2017 and 2018, the mean calving difficulty was 1.2, and in 2019 it was 1.38. Twin births were more difficult than births of a single offspring, with the average value being 1.25 for single pregnancies and 1.32 points for twin pregnancies.

In 2019 there was a prolongation of the average length of calving interval by 8.6 days.

At the selected farm, relatively good results were achieved for reproduction: in the majority of cases, the individual reproductive parameters correspond to optimal values, and for the most part the values are superior to the average for the Czech Republic.

ACKNOWLEDGEMENTS

We are grateful to AZOS, s. r. o. for providing information for our research.

REFERENCES

Andrýsek, J. et al. 2018. Rozbor plnění šlechtitelského programu českého strakatého skotu v roce 2017. Zpravodaj Svazu chovatelů a plemenné knihy českého strakatého skotu, 1.

Andrýsek, J. et al. 2019. Rozbor plnění šlechtitelského programu českého strakatého skotu v roce 2018. Zpravodaj Svazu chovatelů a plemenné knihy českého strakatého skotu, 1.

Bezdíček, J., Louda, F. 2009. Analýza délky březosti při vícečetných porodech u českého strakatého a holštýnského skotu. Acta Universitatis Agriculturae et Silviculturae Mendelianae Brunensis, 57(5): 27–32.

Bucek, P., Kučera, J. 2019. Výsledky kontroly mléčné užitkovosti skotu v roce 2019. Náš chov, 79(12): 22–25.

Chagas, L.M. et al. 2007. Invited review: New perspectives on the roles of nutrition and metabolic priorities in the subfertility of high-producing dairy cows. Journal of Dairy Science, 90(9): 4022–4032.

Coufalík, V. 2013. Současné problémy v reprodukci skotu. Olomouc: Agriprint.

Grummer, R.R. et al. 2008. Změna doby stání na sucho a postupů k minimalizaci negativní bilance energie; dopad na mléčnou produkci a reprodukční aktivitu. In Nové pohledy na řízení okoloporodního období dojnic: sborník příspěvků: 18. června 2008, Větrný Jeníkov u Jihlavy. Brno: Veterinární a farmaceutická univerzita, pp. 19–23.

Humblot, P. et al. 2009. Epidemiology of embryonic mortality in cattle; practical implications for AI and embryo production. In Proceedings of Canadian Embryo Transfer association and American Embryo Transfer Association Joint Convention, 17.–19. September 2009, Montréal, Canada, 17–32.

Jakubec, V. et al. 2012. Šlechtění a management genetických zdrojů zvířat. Rapotín: Agrovýzkum.

Kvapilík, J. et al. 2018. Ročenka: Chov skotu v České republice: Hlavní výsledky a ukazatele za rok 2017 [Online]. Praha: Českomoravská společnost chovatelů. Available at: https://www.cmsch.cz/plemenarska-prace/ku-kontrola-uzitkovosti/rocenky/rocenky-chovu-skotu/. [2020-8-14].

Kvapilík, J. et al. 2019. Ročenka: Chov skotu v České republice: Hlavní výsledky a ukazatele za rok 2018 [Online]. Praha: Českomoravská společnost chovatelů. Available at: https://www.cmsch.cz/plemenarska-prace/ku-kontrola-uzitkovosti/rocenky/rocenky-chovu-skotu/. [2020-8-14].

Lopez, H. et al. 2004. Relationship between level of milk production and estrous behavior of lactating dairy cows. Animal Reproduction Science, 81: 209–223.

Rodriguez-Martinez, H. et al. 2008. Reproductive performance in high-producing dairy cows: can we sustain in under current practice? IVIS Reviews in Veterinary Medicine. International Veterinary Information Service, Ithaca, NY, USA.

Royal, M.D. et al. 2000. Declining fertility in dairy cattle: changes in traditional and endocrine parameters of fertility. Animal Science, 70(3): 487–501.

Řehák, D. et al. 2012. Relationships among milk yield, body weight, and reproduction in Holstein and Czech Fleckvieh cows. Czech Journal of Animal Science, 57(6): 274–282.

Determination of the effectiveness of disinfectants containing organic acids for bovine footbaths

Lucie Langova[1], Miroslav Machacek[2], Zdenek Havlicek[1], Petra Nemcova[1], Ivana Novotna[1]
[1]Department of Animal Morphology, Physiology and Genetics
Mendel University in Brno
Zemedelska 1, 613 00 Brno
[2]Department of Animal Protection and Welfare and Veterinary Public Health
University of Veterinary Sciences Brno
Palackeho tr. 1, 612 42 Brno
CZECH REPUBLIC
xlangov2@mendelu.cz

*Abstract***:** Disinfection footbaths are a common practice for controlling and preventing the spread of infectious diseases causing lameness (dermatitis digitalis, footrot) in dairy cows. On the market there exists many disinfectants for cattle footbaths, but their effectiveness on farms is often disputable. In vitro tests were performed to verify the effectiveness of disinfection according to ČSN EN 1656. The effect of different disinfectants on bacteria in various concentrations at a specified temperature of 20 °C was verified. The aim was to determine their effectiveness even at temperatures of 10 and 5 °C, which are really in lavage baths on farms. Effectiveness verification of the disinfectant consists of ideal conditions of two steps, tests of the effectiveness of the disinfectant in the laboratory and controlled field conditions. Three disinfectants with organic acids (A) organic acids (lactic, propionic, formic), zinc, aloe vera, aldehyde, glycerin, (B) organic acid (lactic), zinc, copper and (C) iodine, organic acid (lactic) were tested in the laboratory by dilution-neutralization method and membrane filtration method. Laboratory tests have shown better bactericidal effects of organic acids in selected bacteria with another active substance (zinc, copper in disinfection B and iodine in disinfection C), colony-forming units were reduced by at least by 5 logs at low temperatures.

Key Words: disinfection, organic acids, footbaths, dairy cow, lameness, effectiveness

INTRODUCTION

The antibacterial mechanisms of organic acids are based primarily on lowering the pH of the environment, accumulating cellular anions, and lowering cellular pH (Wang et al. 2019). Organic acids can cross bacterial membranes and dissociate into protons and organic anions in the cytoplasm. Organic acid molecules vary in the length of the carbon chains and the number and nature of attached acidic and other chemical groups. A study by Wales et al. (2013) yielded conflicting findings regarding the relative antibacterial activity of different organic acids, probably due to many different conditions (humidity, pH, and bacterial physiological conditions) that may affect measurements (Wales et al. 2013). Efficient penetration of bacterial cells occurs when organic acid molecules are in an electrically neutral, undissociated state. So, their activity is markedly increased in an acidic environment, where most weak acid molecules are undissociated (Ricke 2003). Carrique-Mas et al. (2007) demonstrated the "masking" of viable bacterial cells due to organic acids lowering the pH of the culture medium (Carrique-Mas et al. 2007), with the aldehyde / organic acid mixture showing little masking compared to products containing only organic acids. This effect could potentially overestimate the apparent efficacy of organic acids. Masking would probably not overestimate the effect of products associated with a low or moderate reduction (up to about 3 log units) in bacterial counts (Wales et al. 2013).

Low temperature reduces the disinfecting effect against many bacteria, which can be significant, especially in colder periods (Wales et al. 2013).

Among organic acids, lactic acid and acetic acid have disinfectant effects and are commonly used (Ölmez and Kretzschmar 2009). Lactic acid is a better antimicrobial agent in reducing the number of aerobic mesophilic bacteria, *Listeria monocytogenes* and *Escherichia coli* O157: H7 compared

to acetic acid (Wang et al. 2019). Furthermore, citric, and malic acids have confirmed antimicrobial properties (Park et al. 2011). Phytic acid also shows high antimicrobial activity (Kim and Rhee 2016). The disinfectant consists of citric and lactic acid inactivated *Yersinia enterocolitica*, *L. monocytogenes* and *E. coli* (Virto et al. 2006). Propionic, acetic, lactic, malic, and citric acid also inactivated *E. coli* O157: H7, *S. Typhimurium* and *L. monocytogenes* (Park et al. 2011).

The combination of different organic acids shows more effective disinfection results. Individual and/or combined disinfection with citric, malic and phytic acid inactivated *Escherichia coli* and *Staphylococcus aureus* depending on concentration and time. At one selected concentration, the mixture of these acids effectively reduced the viability of *E. coli* and *S. aureus* by approximately 99.9% in 10 minutes. The combined application of the three organic acids led to a higher bactericidal activity, indicating a synergistic effect between the acids. Combined acid treatment disrupted the integrity of the bacterial membrane and increased intracellular reactive oxygen species. The inactivation efficiency of said mixture of organic acids is also effective on *Salmonella Typhimurium*, *Pseudomonas aeruginosa* and *Listeria monocytogenes* (Seo et al. 2021).

The combined use of an organic acid with an oxidizing agent is more effective than a single organic acid disinfectant alone, as dissociated acid and oxidizing agent molecules can cause protein agglutination and membrane destruction. Organic acids and ozone show increased efficiency in disinfection against *E. coli* O157: H7, *Shigella* spp. and *L. monocytogenes* (Singla et al. 2011). The antimicrobial reduction has also been observed using organic acid and electrolyzed water, as well as with hydrogen peroxide (Zhang and Yang 2017). A mixture of sodium chloride and various organic acids (acetic, citric, lactic, malic and phytic) was effective against *E. coli* O157: H7 (Kim and Rhee 2016). The bactericidal activity of organic acids is generally dependent on the acid composition and requires a high concentration, increased costs, odour, and corrosion. Therefore, it would be interesting to explore new combinations of organic acids to achieve effectiveness with lower amounts and higher safety (Seo et al. 2021).

The disinfectant efficacy observed with organic acids is relatively variable and sometimes disappointing (Wales et al. 2013). This study aimed to determine the effectiveness of individual combinations of organic acids with other active substances in temperature conditions that mimic field applications.

MATERIAL AND METHODS

Disinfectants were tested by dilution-neutralization and membrane filtration methods according to ČSN EN 1656 (665208) Chemical disinfectants and antiseptics - Quantitative suspension test to determine the bactericidal effect of chemical disinfectants and antiseptics used in veterinary care – Test method and requirements.

The tested microorganisms were bacteria used for testing disinfection by neutralization and membrane method (*Enterococcus hirae* CCM 4533, *Staphylococcus aureus* CCM 2022, *Pseudomonas aeruginosa* CCM 7930, *Proteus hauseri* CCM7011) according to ČSN EN 1656. Bacteria were from the Czech University gelatin discs or lyophilized. A bacterial suspension was prepared to a value of $1.5x10^8$–$5x10^8$ CFU/ml (optical density around 0.5 McFarland).

Three tested disinfectants contained organic acids as active compounds in combination with other active ingredients. Disinfection (A) contains organic acids (lactic, propionic, formic), zinc, aloe vera, aldehyde, glycerin, (B) organic acid (lactic), zinc, copper and (C) iodine, organic acid (lactic).

RESULTS AND DISCUSSION

Organic acid-based disinfectants were tested at 20, 10 and 5 °C. The disinfectant has a bactericidal effect if the defined CFUs (colony forming units) have been reduced by at least 5 logs. The effect can be considered bacteriostatic if the defined CFU is reduced by 3–5 logs.

For disinfection A containing organic acids (lactic, propionic, formic), zinc, aloe vera, aldehyde and glycerin, the test results are in Table 1. A demonstrable bactericidal effect (by 5 logs) was only in *Pseudomonas aeruginosa*. For the other bacteria (*Proteus hauseri*, *Enterococcus hirae*

and *Staphylococcus aureus*), the efficacy was less than the reduction of 3 logs, which did not correspond to the bacteriostatic effect and the product was evaluated as ineffective.

Table 1 Results of disinfection testing containing organic acids, zinc, aloe vera, aldehyde, glycerin in concentrations of 1, 3 and 5% (A)

Bacteria/ Temperature	20 °C			10 °C	5 °C
Pseudomonas aeruginosa	1%	3%	5%	1%	1%
Proteus hauseri	1%	3%	5%	5%	5%
Enterococcus hirae	1%	3%	5%	5%	5%
Staphylococcus aureus	1%	3%	5%	5%	5%

Legend: tinted green - reduction by more than 5 logs, bactericidal efficacy; tinted red - no bactericidal or bacteriostatic effect

Formic acid has the best disinfecting effect of all organic acids. Propionic acid is not very effective against bacteria, and its use is more limited against fungi (Škaloud 2013). Aldehydes are unstable in the environment depending on the temperature. Ricke (2003) found that denaturation of acid-sensitive proteins is an antibacterial mode of action of organic acids. This result is consistent with the results of Wang et al. (2015). Wang et al. (2019) hypothesized that due to the different structures of cellular proteins and extracellular polysaccharides of different bacteria, the binding sites of lactate, propionate anions are different, making some specific bacteria resistant to disinfection. Through the combined action of lactate and propionate anions, the disinfection efficiency can be improved by affecting multiple protein sites. Overall, these results suggest that the mixture of acids and individual acids have different effects on the bacteria tested.

Table 2 Results of disinfection testing containing organic acids, zinc, copper in concentrations of 1, 3 and 5% (B)

Bacteria/ Temperature	20 °C			10 °C	5 °C
Pseudomonas aeruginosa	1%	3%	5%	1%	1%
Proteus hauseri	1%	3%	5%	1%	1%
Enterococcus hirae	1%	5%	5%	5%	5%
Staphylococcus aureus	1%	3%	5%	3%	3%

Legend: tinted green - CFU reduction by more than 5 logs, battery efficiency; tinted light green - bacteriostatic effect, CFU reduction between 3 and 5 logs; tinted red - no bactericidal or bacteriostatic effect

The results of the disinfection tests B containing lactic acid, zinc, copper, given in Table 2, show that it has poorer efficacy in cocci and *Proteus hauseri* at reduced temperatures. It is bactericidal in *Staphylococcus aureus* only at 20 °C and higher temperatures. At lower temperatures, it behaves bacteriostatic ally, or the efficacy is not proven. Lactic acid is effective for disinfection in concentrations of 1 and 2% (Škaloud 2013). The results of the study by Michaels et al. (2005) examining the disinfecting effects of copper compounds show a bactericidal effect on E. coli O157: H7 for ninety minutes at room temperature (20 °C) (Michaels et al. 2005). At cold temperatures (4 °C), copper inactivates more than 99.9% of *E. coli* O157: H7 within 270 minutes (Wilks et al. 2005). Since we followed ČSN EN 1656, the exposure time of disinfection with bacteria was 5 minutes which is not enough for the oligodynamic effect of copper.

Table 3 Results of disinfection testing containing organic acid (lactic), iodine 0.5, 0.75 and 1% (C)

Bacteria/ Temperature	20 °C			10 °C	5 °C
Pseudomonas aeruginosa	0.5%	0.75%	1%	0.5%	0.5%
Proteus hauseri	0.5%	0.75%	1%	0.5%	0.5%
Enterococcus hirae	0.5%	0.75%	1%	0.5%	0.5%
Staphylococcus aureus	0.5%	0.75%	1%	0.5%	0.5%

Legend: tinted green - reduction by more than 5 logs, battery efficiency; tinted red - no bactericidal or bacteriostatic effect

The disinfection C had the best results (Table 3) in in vitro testing. The disinfection had bactericidal effects at all temperatures and in all bacteria tested. The iodine content of this disinfection

is much higher, and the organic acid was in second place in the composition. It is possible that disinfection would be effective even without organic acids. The combined use of an organic acid and an oxidizing agent is advantageous in terms of the action of the dissociated acid molecule, and the oxidizing agent can cause protein agglutination and membrane destruction (Seo et al. 2021).

CONCLUSION

In vitro tests and trials of footbath products at various concentrations would help to develop an optimal strategy for the control and prevention of infectious diseases of the limbs and to make the use of disinfectants more effective. Laboratory tests have shown that organic acids in combination with other active substances (zinc, copper, and iodine) are effective with selected bacteria even at low temperatures. Given the different modes of action, the combination of organic acids and oxidative disinfectants may be a promising approach to controlling infectious diseases of cattle limbs.

ACKNOWLEDGEMENTS

Research reported in this publication was supported by grant no. AF-IGA2021-IP009.

REFERENCES

Carrique-Mas, J.J. et al. 2007. Organic acid and formaldehyde treatment of animal feeds to control Salmonella: efficacy and masking during culture. Journal of Applied Microbiology [Online], 103(1): 88–96. Available at: https://doi.org/10.1111/j.1365-2672.2006.03233.x. [2021-10-05].

Kim, N.H., Rhee, M.S. 2016. Phytic Acid and Sodium Chloride Show Marked Synergistic Bactericidal Effects against Nonadapted and Acid-Adapted Escherichia coli O157:H7 Strains. Applied and Environmental Microbiology Journal [Online], 82(4): 1040–1049. Available at: https://doi.org/10.1128/AEM.03307-15. [2021-10-05].

Michaels, H.T. 2005. Copper alloys for human infectious disease control. Materials Science and Technology, 1: 3–13.

Ölmez, H., Kretzschmar, U. 2009. Potential alternative disinfection methods for organic fresh-cut industry for minimizing water consumption and environmental impact. LWT-Food Science and Technology [Online], 42(3): 686–693. Available at: https://doi.org/10.1016/j.lwt.2008.08.001.[2021-10-05].

Park, S.H. et al. 2011. Use of organic acids to inactivate Escherichia coli O157:H7, Salmonella Typhimurium, and Listeria monocytogenes on organic fresh apples and lettuce. Journal of Food Science [Online], 76(6): M293–M298. Available at: https://doi.org/10.1111/j.1750-3841.2011.02205.x. [2021-10-05].

Ricke, S.C. 2003. Perspectives on the use of organic acids and short chain fatty acids as antimicrobials. Poultry Science [Online], 82(4): 632–639. Available at: https://doi.org/10.1093/ps/82.4.632. [2021-10-05].

Seo, Y. S. et al. 2021. Combinatorial treatment using citric acid, malic acid, and phytic acid for synergistical inactivation of foodborne pathogenic bacteria. Korean Journal of Chemical Engineering [Online], 38(4): 826–832. Available at: https://doi.org/10.1007/s11814-021-0751-2. [2021-10-05].

Škaloud, J. 2013. Příručka veterinární dezinfekce. 2nd ed., Praha.

Singla, R. et al. 2011. An effective combined treatment using malic acid and ozone inhibits Shigella spp. on sprouts. Food Control [Online], 22(7): 1032–1039. Available at: https://doi.org/10.1016/j.foodcont.2010.12.012. [2021-10-05].

Virto, R. et al. 2006. Application of the Weibull model to describe inactivation of Listeria monocytogenes and Escherichia coli by citric and lactic acid at different temperatures. Journal of the Science of Food and Agriculture [Online], 86(6): 865–870. Available at: https://doi.org/10.1002/JSFA.2424. [2021-10-05].

Wales, A. et al. 2013. Assessment of the anti-Salmonella activity of commercial formulations of organic acid products, Avian Pathology [Online], 42(3): 268–275. Available at: https://doi.org/10.1080/03079457.2013.782097. [2021-10-05].

Wang, C. et al. 2015. Antibacterial mechanism of lactic acid on physiological and morphological properties of Salmonella Enteritidis, Escherichia coli and Listeria monocytogenes. Food Control [Online], 47: 231–236. Available at: https://doi.org/10.1016/j.foodcont.2014.06.034. [2021-10-05].

Wang, J. et al. 2019. Disinfection of lettuce using organic acids: An ecological analysis using 16S rRNA sequencing. RSC advances [Online], 9(30): 17514–17520. Available at: https://doi.org/10.1039/C9RA03290H. [2021-10-05].

Wilks, S.A. et al. 2005. "The survival of Escherichia coli O157 on a range of metal surfaces". International Journal of Food Microbiology [Online], 105 (3): 445–454. Available at: https://doi.org/10.1016/j.ijfoodmicro.2005.04.021. [2021-10-05].

Zhang, J., Yang, H. 2017. Effects of potential organic compatible sanitisers on organic and conventional fresh-cut lettuce (Lactuca sativa Var. Crispa L). Food Control [Online], 72: 20–26. Available at: https://doi.org/10.1016/j.foodcont.2016.07.030. [2021-10-05].

The effect of breed on body indices in draft horses in Czech Republic

Alzbeta Matuskova[1], Veronika Coudkova[2], Radek Filipcik[1], Miroslav Marsalek[1]
[1]Department of Animal Breeding
Mendel University in Brno
Zemedelska 1, 613 00 Brno
[2]Department of Zootechnical Sciences
University of South Bohemia
Studentska 1668, 370 05 Ceske Budejovice
CZECH REPUBLIC

xmatusk5@mendelu.cz

Abstract: Growth of cold-blooded horses is rarely monitored, but the numbers of horses of breeds bred in Czech Republic are rapidly decreasing. Body indices are useful tools to monitor and evaluate horses' built and quality of growth. Thirteen body measurements of horses on four farms were taken every three months (227 sets of measurements) and five hippometric indices were calculated for 3 draft horses breeds: Czech-Moravian Belgian (CMB), Noriker (N) and Silesian Noriker (SN). The effect of breed on these indices was analyzed. The index of compactness (CI) and massiveness (MI) showed as affected by breed ($p<0.001$), when the value 114.17 of CI was significantly the lowest in SN and value 123.78 of MI was significantly the highest in N. The index of boniness ($p<0.1$) and skeletal strength ($p<0.1$) indicated statistical significance of breed effect. The index of body frame didn't prove statistically significant effect of breed at all ($p>0.05$). Populations of these horses are small, with more data would be possible to get clearer results and analysis of the effect of age would be a viable option.

Key Words: draft horse, hippometric index, growth, colt, stallion

INTRODUCTION

There are three breeds of cold-blooded horses in Czech Republic – Czech-Moravian Belgian (CMB), Noriker (N) and Silesian Noriker (SN). Two of these three breeds (CMB, SN) are in national genetic resources program, so their breeding is financially supported by the state, Noriker on the other hand is the black sheep. Counts of all these horses are usually going down every year, Noriker especially. They are being bred by people working in forestry, agriculture or by people with passion for these breeds. There is no guarantee of work for the trained horse, more often there is no work for them. There are few competitions for these breeds and their special skills, but the prizes are mostly symbolic, so again, there are not opportunities to get financial revenue in sports etc.

Head counts for every breed are interesting. Breeding mares are the foundation of every breed. In 2001, CMB studbook included 900 breeding mares, N studbook 800 mares, and SN studbook 400 mares. In 2019, there were 750 CMB mares, 520 N mares and 507 SN mares. According to these numbers, it is obvious that counts of cold-blooded horses are lowering in general, biggest fall is in numbers of Noriker horses, exception are SN horses which are rising (Maršálek 2020).

Dušek et al. (1999) define "draft horses" as pulling horses, who use mainly walk while working. These horses are supposed to be more massive in size, bulky, with heavy less pronounced head shape, but with wide, barrel-like chest. These definitions are often connected with skeletal strength, tighter and tougher constitution. Characteristics like these are needed for pulling large loads either on wheels (in a cart) or by slide (forestry work).

Dušek et al. (1999) characterize the most common Czech breed of cold-blooded horses – Czech-Moravian Belgian – as of early development, body of these horses should have square frame, meaning these horses should have height at withers approximately the same as length of their body (this ration is expressed as body format index). They usually have large chest circumference in comparison

to the rest of these breeds. This breed description by Dušek et al. (1999) is in agreement with breed description in Code of studbook of CMB breeders' association (Asociace svazů chovatelů koní České republiky 2010). Maršálek and Civišová (2016) add that CMB mature fairly early and that allows them to work at approximately two years of age.

Silesian Noriker is described best in "Goal of breeding" chapter of Code of studbook of SN breeders' association (Asociace svazů chovatelů koní České republiky 2008). The ideal Silesian Noriker horse should be a little bit of "late bloomer" and should reach adulthood between five and six years of age. The horse should have slightly longer body, i.e., rectangular form, unlike CMB. This breed has its origin in Noriker breed, but was regionally specified, in this case is the region Silesia in Czech Republic.

Noriker is supposed to have large rectangular body frame with large chest and maturing rather late (Štrupl et al. 1983). Bílek et al. (1957) describe Noriker as heavy, wide, and tough and highlights his endurance and modesty. In Czech Republic is now being officially founded Czech Noriker as a breed, so Czech breeders can have autonomy and don't have to be under Austrian breeders association.

Studies from Poland are the closest to horse breeding in Czech Republic, because Poland is one of a few countries, where are cold-blooded horses bred as work horses and some breeds are in genetic resources conservations program, same as in Czech Republic. Polak (2019) was studying genetic variability using pedigree analysis of such horses, focusing on Sztumski and Sokólski breeds. Those breeds are part of the genetic resources' conservation program. The study included 4 718 horses. Both populations were bred by imported stallions, but over 40% of Polish founders-mares had no documented origin, which once again shows the overlook of pedigrees of breeding mares, which is common, only in warmblood horse breeding are dam lines slowly getting more attention. This trend has yet to arrive to draft horse breeding.

While individual studbooks have chapters regarding description of breeding goals, including basic body measurements and some directions for visual assessment and evaluation, the values are often outdated. The evaluation of these horses is depending mostly on subjective evaluation and assessment, but even these definitions can't be properly used on today's horses. This statement is confirmed in study by Polak and Lewczuk (2017).

Polak and Lewczuk (2017) published study concerning cold-blooded horses, focusing on stability of conformation and movement traits evaluation in cold-blooded horses of different endangerment status. Authors wanted to analyze the stability of traits assessment at draft horse show by individual judges, analyzing the factors influencing the results. Ninety-three horses of different endangerment status were part of the analysis of variance, these horses were assessed by six judges at the same horse show. The fixed effects of sex, breed of the sire and dam, type of breeder (state, national) and age were considered. Results showed significant effects of parents' breed on individual judges scores. Evaluation of body condition showed as the most difficult. The „trot" was also the trait most dependent on genetic endangerment status of horses' pedigree. These results show that definitions of these traits are outdated and should be newly established, especially for the needs of conservation programs, where the breeding is the most sensitive because of small populations of these horses, and visual evaluation is the first phase of the selection process. Introducing body indices into the process of selection and evaluation could be very helpful and practical tool.

At present time, only breeding plan of the Noriker breed has defined values for index of body frame. The rest of the breeds have nothing of this sort, even though these breeds are endangered and put in conservation program and they should pay the most attention to these details.

Growth of these horses is not often monitored, but in this work were young growing stallions periodically measured in rearing stations since the age of approximately 10 months until the end of basic training, which occurs at 2.5 years of age. Fourteen measurements and weight were taken every three months. The three-month period between measuring was chosen to accommodate possible effect of season and other environmental circumstances. He et al. (2020) focused in their work on the effect of season on growth of muscle and fat in 16 horses under 4 years of age. Their research proved that season influenced fat deposition the most in fall ($p=0.05$) but had virtually no effect on growth of muscles.

Indices calculated from these body measurements can provide a lot of additional information about individual breeds, and their growth.

Bílek et al. (1957) describe "hippometric indices" as important for comparison and evaluation of physical build of more individuals or comparison between breeds. Authors also define indices as expression of individual body measurements and their anatomical or physiological relations.

MATERIAL AND METHODS

Data collection

Measurements of draft horses were performed on four farms in a year and a half (February 2020–August 2021). All four groups were living in herds, of which one group resided solely on a pasture, other groups were stabled overnight, still in groups. Their feed rations were composed of unlimited pasture, and hay, especially during winter months. All groups had unlimited access to water. Horses were measured every three months. A total 227 sets of measurements of draft horses at 10 to 24 months of age were recorded. The biggest group was consisted of measurements of 132 CMB stallions, followed by 71 SN stallions, and 24 N stallions. The age ratio was the same in composition of all breed groups. In total, 15 variables including 13 body measurements (height at withers measured by stick, height at withers measured by tape, saddle height, croup height, dock height, cannon circumference, chest circumference, sternum height, shoulder width, chest width, anterior pelvis width, central pelvis width, pelvis length, body length), and weight, and five indices (body frame, compactness, massiveness, boniness, and skeletal strength) were determined.

Selected indices were calculated using the following formulas:

$$body\ frame\ index = \frac{body\ length}{stick\ height\ at\ withers} \times 100$$

$$compactness\ index = \frac{chest\ circumference}{body\ length} \times 100$$

$$massiveness\ index = \frac{chest\ circumference}{stick\ height\ at\ withers} \times 100$$

$$boniness\ index = \frac{cannon\ circumference}{stick\ height\ at\ withers} \times 100$$

$$skeletal\ strength\ index = \frac{cannon\ circumference}{chest\ circumference} \times 100$$

Statistical Analysis

MS Office and Statistica.12 (Tibco®, Prague, Czech Republic) were used for data processing. The effect of breed was assessed using analysis of variance followed by the Tukey test for multiple comparisons. Statistical significance was set at $P < 0.001$ (***), $P < 0.01$ (**) and $P < 0.05$ (*) and tendencies were defined as $0.05 < P < 0.10$ (+). Data are presented as means ± standard error of the mean (SEM) unless otherwise indicated.

RESULTS

Table 1 shows the significant effect of breed on indices of compactness and massiveness. The results of multiple comparisons using the Tukey HSD test demonstrate, that breed SN differ from CMB and N in compactness index with the highest value 119.16. In case of massiveness index, breed N differ from CMB and SN with the highest value 123.78.

Table 1 The effect of breed on body indices assessed by analysis of variance (means ± standard error of the mean)

Breed/Index	CMB (N = 132)	SN (N = 71)	N (N = 24)	p-value	significance
Body frame	98±1.68	95.79±2.30	103.96±3.95	0.204	–
Compactness	117.65±0.45[a]	114.17±0.62[b]	119.16±1.06[a]	0.000	***
Massiveness	118.89±0.37[a]	119.51±0.50[a]	123.78±0.86[b]	0.000	***
Boniness	18.10±1.80	24.03±2.45	15.98±4.22	0.098	+
Skeletal strength	15.23±1.52	20.11±2.06	12.91±3.55	0.094	+

Legend: N – number of observations; CMB – Czech-Moravian Belgian; SN – Silesian Noriker; N – Noriker
Data are presented as statistical significance P<0.001 (***), P< 0.01 (**), P< 0.05 (*), tendencies were declared at P< 0.10 (+), P> 0.10 (–).
[a,b] Different superscripts in a row indicate significant differences among breeds (P<0.05).

Graphic form of these results can be seen in Figure 1. Tendencies of significant effect of breed was observed in case of boniness and skeletal strength indices. The highest boniness index was observed in SN (24.03). In case of skeletal strength index the lowest value was in N (12.91) and the highest in SN (20.11).

Figure 1 Graphic results of analysis of variance which asses the effect of breed on compactness and massiveness indices.

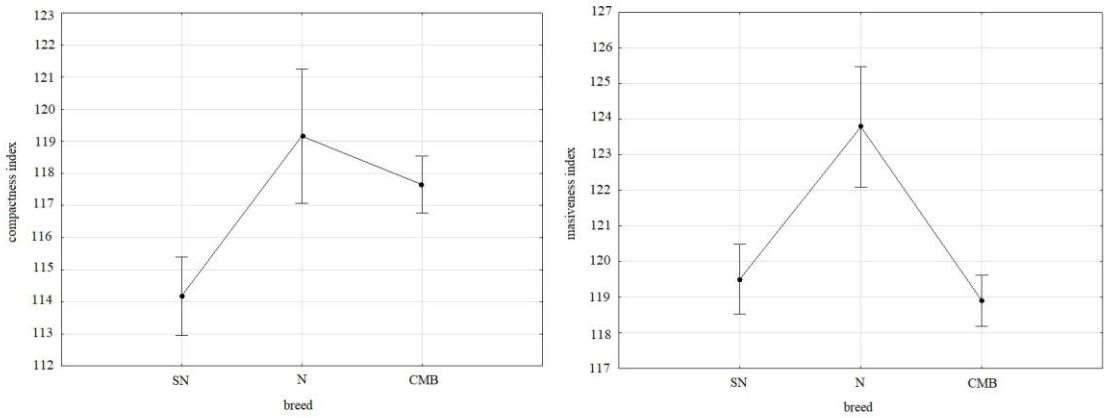

Legend: CMB – Czech-Moravian Belgian; SN – Silesian Noriker; N – Noriker

DISCUSSION

The body frame index represents the ratio between body length and stick height at wither, value 100 means the body is perfect square, values under 100 indicates longer body – rectangle laying on the long side. In Table 1 is visible that Noriker horses, who are supposed to be of a longer frame are meeting this requirement. On the other hand, Silesian Norikers, who should also have longer body frame, are going against this rule, that confirms the fact, that there wasn't found effect of breed. CMB horses, who are supposed to be square framed are close to the ideal value. The standard errors of means are probably corresponding with population size in individual breed group, meaning higher value of the standard error of means is evidence of bigger effect of each individual in the group (as seen in Noriker group). The large population of CMB horses shows more balanced values. Oravcova et al. (2014) compared basic body dimensions and hippo-metrical indices of Hucul horses around Slovakia and Hungary. Authors wanted to discover differences between these countries in terms of age, gender, line, and environment. The effect of gender and environment showed as the most statistically significant. Out of nine body measurements and indices, six proved as highly significant. Interestingly, age wasn't statistically significant factor. Matoušová-Malbohanová et al. (2004) are one of the few publications with significant population of horses. They measured 17 body measurements and analyzed 11 indices on 209 breeding Hucul horses and analyzed influence of country of origin, sex, age, and sire line. For purposes of this contribution says the effect of age

and sex the most. Authors describe as surprising the fact, that the effect of sex was proved only in seven out of 17 measurements. On the other hand, age plays a major role in 10 out of 17 body measurements and in 10 out of 11 indices.

The compactness index is the ratio between chest circumference and body length. This index is affected by breed, as indicated in the significance column. Again, values over 100 shows larger chest than body length, which visually presents as bulkiness of the horse. In lighter warmblood horses is this index going to be clearly lower than in horses of "respiratory" type build. Norikers should have large chest and look more massive, Silesian Noriker should give off a lighter impression and value of this index corresponds. Since CMB are more square-bodied, their index of compactness should be lower, which contradicts the results above. Possible reason for this is their early maturity, so they get more "compact" earlier than N and SN. Again, standard error of the mean is higher in Norikers, probably because smaller population, but still shows pretty balanced composition in all three herds. Kostukova et al. (2015) studied morphological parameters in donkeys in Czech Republic. They gathered 23 body measurements and six indices were calculated. Their sample group included 70 donkeys, of which were 23 stallions and 47 mares. The most significant influence had gender on five measurements. Even more interesting was statistically significant difference in the length of scapula influenced by age, because previous study by Oravcova et al. (2014) didn't find age as statistically significant influence.

The index of massiveness is fairly balance in all three breeds. This value is lower in lighter horses and heavier the horse, higher the value. In the results above are numbers again corresponding with description of breeds themselves. This also confirms the finding of effect of breed on this value. The value is higher in Norikers, who should present as heavier and bulky horses, while CMB should be lighter. Silesian Norikers are in the middle values, which also corresponds with the requirement of lighter horse than Noriker. The fact SN horses have value closer to CMB is up for debate, depending on how much lighter they should be in comparison with N horses.

The boniness index represents how heavily is horse built. This value should be the lowest in light horses as thoroughbreds, cold-blooded horses should be heavier and stronger, and this value reflects that. As seen in significance column, there is indication of proven effect of breed. It is interesting, that this value is significantly highest in SN horses and after a big gap follows CMB and Noriker is last. The results of CMB are probably again because of their early maturing age, Norikers are late bloomers, so their value of this index probably grows with age.

The index of skeletal strength, like boniness index, shows indication of affection by breed. To calculate this index, cannon and chest circumference is used. Cannon circumference is considered indication of bone strength of a horse in breeders' circles. Chest circumference is the most unbalanced in all horse breeds, because it's affected by body condition and nutrition of the individual horse, and shows horse breeds, that more of a "respiratory" type. The skeletal index combines the two, so the ratio shows not only build of a horse, but also heaviness of his build, which is essential in cold-blooded horses. It's interesting, that this index is the highest in SN stallions, the lowest in N stallions and CMB horses are in the middle. The significant difference between both Noriker breeds is again up to debate, since SN should be slightly lighter, but still similar to N.

CONCLUSION

Body measurement and assessment of horses are two of the most common a most practical tools in monitoring growth and overall exterior quality of horses and is used to adjust breeding plans. Hippo metric indices provide even more clarity in overall body composition and potential deficiencies in practical sense.

Repeated observation would provide more conclusive results and more detailed information about body conformation of young stallions. The effect of breed on hippo metric indices and inter-breed differences are obvious, but because of lesser amount of data wasn't possible to include the effect of age. It is recommended to repeat this experiment when more data is available and analyze the effect of age on body development of young stallions for the future contributions.

REFERENCES

Asociace svazů chovatelů koní České republiky, 2008. Řád PK Slezského norika. Svaz chovatelů chladnokrevných koní [Online]. Available at: https://www.schchk.cz/clanky/slezsky-norik/rad-pk/. [2021-09-01].

Asociace svazů chovatelů koní České republiky, 2010. Řád PK ČMB. Svaz chovatelů chladnokrevných koní [Online]. Available at: https://www.schchk.cz/clanky/ceskomoravsky-belgik/rad-pk/. [2021-09-01].

Bílek, F. et al. 1957. Speciální zootechnika - díl druhý: Chov koní. 2. ed., Praha: Státní zemědělské nakladatelství Praha.

Dušek, J. et al. 1999. Chov koní. 3. ed., Praha: Nakladatelství Brázda, s.r.o..

He, Y. et al. 2020. The Effect of Season on Muscle Growth, Fat Deposition, Travel Patterns, and Hoof Growth of Domestic Young Horses. Journal of Equine Veterinary Science, 85: 1–10.

Kostukova, M. et al. 2015. Characteristics of morphological parameters of donkeys in the Czech Republic. Acta Universitatis Agriculturae et Silviculturae Mendelianae Brunensis, 63(2): 419–424.

Maršálek, M. 2020. Historie chovu norických koní v Čechách a na Moravě. Svaz chovatelů a přátel norika [Online]. Available at: https://svaznorika.org/history/historie-chovu-norickych-koni-v-cechach-a-na-morave/. [2021-09-01].

Maršálek, M. et al. 2016. Šlechtění chladnokrevných koní a jejich uplatnění. České Budějovice: Jihočeská univerzita v Českých Budějovicích.

Matoušová-Malbohanová, Z. et al. 2004. Porovnání exteriéru huculských koní chovaných v České republice a Polsku. Acta Universitatis Agriculturae et Silviculturae Mendelianae Brunensis, 52(1): 153–158.

Oravcova, I. et al. 2014. The comparison of selected breedings of Hucul horses bred in the Slovak republic and Hungary. In Proceedings of International PhD Students Conference MendelNet 2014. Brno, Czech Republic, 19–20 November, Brno: Mendel University in Brno, Faculty of Agronomy, pp. 172–177.

Polak, G. 2019. Genetic variability of cold-blooded horses participating in genetic resources conservations programs, using pedigree analysis. Annals of Animal Science, 19(1): 49–60.

Polak, G. et al. 2017. The stability of conformation and movement traits evaluation tested in cold-blooded horses of different endangerment status. Journal of Applied Animal Research, 46(1): 547–551.

Štrupl, J. et al. 1983. Chov koní. Praha: Státní zemědělské nakladatelství v Praze.

Methods for assessing the health of the limbs and their relationship to the duration of treatment for footrot: a pilot study

Petra Nemcova, Zdenek Havlicek, Lucie Langova, Ivana Novotna
Department of Animal Morphology, Physiology and Genetics
Mendel University in Brno
Zemedelska 1, 613 00 Brno
CZECH REPUBLIC

xnemcov6@mendelu.cz

Abstract: Footrot is an infectious disease with a major impact on the health of dairy cows, their performance, reproduction and breeding economics. The timeliness of the diagnosis of footrot is therefore important in terms of treatment and prevention of the disease. The work aimed to verify and compare methods of identification of lame dairy cows by locomotion scoring and by infrared thermography. The study included 24 cows with footrot. It was found that the infrared thermography revealed a change in the health status of 25% of lame cows of patients with footrot in the preclinical phase, that is before of clinical symptoms were expressed. In dairy cows with a disease diagnosed by infrared thermography, the treatment time was shorter by 3.7 days, as the treatment time was 21.2 days in lame cows, compared to non-lame cows, but with an increased temperature score of 17.5 days. Due to the small number of animals, these differences were not statistically tested.

Key Words: cow, footrot, locomotion score, thermal score, infrared thermography, lameness

INTRODUCTION

The lameness of cattle has a heavy impact on milk production, the prosperity and profitability of farms. Limb disease harms milk yield (Charfeddine and Perez-Cabal 2017, Langova et al. 2020), reproductive performance, high treatment costs for affected cows and high risk of forced slaughter (Charfeddine and Perez-Cabal 2017). Previous studies have found that the presence of a hoof lesion has been associated with increased locomotor scores and behavioural changes (Thomsen et al. 2012).

In addition to the evaluation of locomotion score used so far, new approaches are being sought, including the method of infrared thermography, which has been successfully used in various veterinary medicine applications, for example, to test early oestrus detection, to diagnose mastitis etc. However, little information is available on the use of infrared thermography to detect lameness in dairy cows (Alsaaod and Büscher 2012). It is a non-invasive, non-radiation, rapidly evolving diagnostic method. For veterinary applications, the recommended resolution range for studies in Equidae, cattle and birds is 320 x 240 to 640 x 480 pixels. Image quality and resolution are directly proportional to the number of pixels (LokeshBabu et al. 2018). One of the main functions of infrared thermography is the detection of temperature changes in the body caused by changes in superficial blood circulation. This principle can also be used to measure the surface temperature of dairy limbs (Alsaaod et al. 2015). The limb with the lesion has a higher surface temperature than a healthy one (Novotna et al. 2019). The thermal imager should always be at the same angle and distance from the animal being monitored. Thermograms should be created at the same time of day and in a place free from direct sunlight and drafts (LokeshBabu et al. 2018). Thus, the disease can be diagnosed before the animals become lame and experience pain (Alsaaod et al. 2015).

Often, lesions caused by footrot (necrobacillosis) are identified for the first time in the overall treatment of the hoofs, indicating shortcomings in the assessment of the health of the dairy limbs. Footrot is an acute and highly infectious disease of cattle characterized by swelling and lameness. This extremely painful condition can become chronic if treatment is not provided, allowing other foot structures to become affected. Therefore, there is a need for alternative methods of diagnosing hoof disease (Thomsen et al. 2012) that can detect hoof abnormalities earlier than in the evaluation using the subjective locomotion score (Alsaaod and Büscher 2012, Novotna et al. 2019). In addition to the above methods of locomotion scoring and thermographic (infrared) scoring, many technologies

are currently being tested to help breeders detect lameness in herds (Dutton-Regester et al. 2020, Alsaaod et al. 2015), by hand/visually based traditional techniques, such as monitoring changes in gait (Leach et al. 2012), to fully automated technologies that include force plate evaluation and infrared thermography (Alsaaod and Büscher 2012).

One of the major diseases that can be diagnosed based on changes in locomotion score and temperature score determined by infrared thermography is the footrot (Havlíček et al. 2021). In general, footrot occurs as a sporadic disease in cattle. The frequency or prevalence has been reported being 0.2–5% in herds, but some other reports of earlier outbreaks of footrot exist where the incidence may be as high as 31.42%. It can arise from several causes and has serious economic consequences. It significantly reduces daily milk production, and intensive preventive measures must be implemented on the farm to prevent spread (Osová et al. 2017).

MATERIAL AND METHODS

Evaluation of limb health was evaluated for four months by the locomotion scoring (Hulsen 2011, Havlíček et al. 2021) once a week, always after morning milking. At each pass to the milking parlour, the health of the limbs was assessed by the infrared thermography. The camera was in the passage corridor to the milking parlour. The measurement process took place automatically without any animal restrictions. For the evaluation was used the Thermo-veterinary system from the company "TMVSS", which assigns the result of the temperature score in the range of 1–4 based on changes in the temperature fields of the limbs.

Animals with an increased value of the temperature score, which had an increased value of the locomotion score, were included for examination by a veterinarian to diagnose footrot disease. The experiment included dairy cows in which the veterinarian diagnosed necrobacillosis with swelling and erythema of the soft tissues of the interdigital space and the adjacent coronary stripe. The skin of the interdigital space was discoloured; it later fragmented into exudate formation. An unpleasant odour was characteristic. All sick animals that were treated were included in the experiment. Was carried out common treatments include rubbing a sterilized rope or twine between the animal's toes to remove the necrotic tissue, followed by applying a topical antimicrobial and simply keeping the foot clean and dry. All animals included in the experiment were treated with parenteral antibiotics.

In the footrot, the time from the first changes in temperature score to the first clinical signs of lameness was monitored. The time required for healing (average length of treatment) was then monitored in all animals (for cows, who started treatment within three days of changes in locomotion score, for cows, who started treatment from four to seven days after the change in locomotion score and for cows who were treated only based on changes in temperature score, without symptoms of limb pain, i.e. lameness). Due to the small number of animals, these differences were not statistically tested.

RESULTS AND DISCUSION

From May to August, the incidence of footrot was monitored, which was diagnosed based on lameness in dairy cows, i.e. with an increased locomotion score and with regular overall hoof adjustment. Of the 24 cases of footrot found (Table 1), signs of an altered locomotion score above 1 were identified in 18 cases that were treated within 3.9 days. While in the study by Leach et al. (2012), cows were not treated until after 14 days of observation of the locomotion score. In 6 animals that showed changes in temperature score, without signs of lameness, the disease was diagnosed with regular hoof trimming. The increase in the surface temperature of the diseased limb when the lesion occurred was confirmed by Alsaaod and Büscher (2012).

Table 1 Evaluation of temperature and locomotion score for limb health

Lameness	n	Duration of treatment		Time of LS change to treatment		Time of TS change to treatment	
		x	SD	x	SD	x	SD
NO	6	17.5	5.54	0	0	4.2	2.71
YES	18	21.2	5.97	3.9	2.82	5.2	5.61

Legend: n – number of dairy cows, x – mean duration of treatment, SD – standard deviation, LS – locomotion score, TS – thermal score

The temperature score was increased for 4.2 days before veterinary service organized treatment. In the case of lame animals, the treatment of the disease lasted on average 21.2 days, i.e. when found in a cage, with the absence of clinical signs of lameness, it was 17.5 days. Differences in the duration of treatment were found (Table 2). In the case of dairy cows without a change in locomotion score, the average healing of footrot was found to be 17.5 days, with the dairy cows included in the treatment recovering the fastest within three days after the change in temperature score (15.7 days).

Table 2 Evaluation of treatment duration based on changes in locomotion and temperature scores

Lameness	Change of temperature score	n	x	SD
NO	within 3 days	3	15.7	5.51
	4–7 days	2	19.0	8.49
	without temperature changes	1	20.0	–
YES	within 3 days	6	21.2	5.67
	4–7 days	8	21.3	6.39
	without temperature changes	4	21.3	7.27

Legend: n – number of dairy cows, x – mean duration of treatment, SD – standard deviation

In the case of later treatment in the period from 4 to 7 days of increased temperature score, the duration of the disease was 19 days. In dairy cows, without clinical signs of a change in locomotion score and without a change in temperature score, which was one case, the treatment lasted 20 days. The results cannot be assessed in terms of statistical significance of differences, as this is a pilot study, so far with a small number of sick dairy cows. Despite this, lagging cows have been treated for more than 21 days.

The results shown in Tables 1 and 2 show that the infrared thermography can be used for the early detection of footrot, as 25% of the animals included in the cage treatment did not show changes in the movement expressed by the locomotion score, in contrast to the Renn et al. (2014), which states that 97% of cows were lame on at least one leg. In the case of lame dairy cows, a change in temperature score was observed as a manifestation of the disease 1.3 days before the first signs of pain expressed by locomotion score appeared. The study by Schaefer et al. (2007) confirmed that infrared thermography was able to identify animals in the early stages of the disease, often several days to more than a week before clinical signs appeared.

In the case of the system used to assess the health of the limbs based on visual analysis of animal movement, expressed by a change in locomotion score (Table 3), the hypothesis of a positive effect of early treatment of the patient's hoof with footrot was confirmed, as the duration of treatment increased with later treatment.

Table 3 Duration of footrot treatment depending on the timeliness of treatment with LS changes

Treatment of dairy cows	n	x	SD
within 3 days	13	19.9	5.06
4–7 days	5	24.6	7.40
regular treatment of hooves– without changes in LS	6	17.5	5.54

Legend: n – number of dairy cows, x – mean duration of treatment, SD – standard deviation, LS – locomotion score

This is evidenced by the treatment period of 6 dairy cows of 17.5 days, in case of finding this disease with the regular preventive general treatment of the limbs. If the dairy cows were treated within three days of the first lameness, the treatment lasted 19.9 days, and if the treatment was up to one week, the treatment lasted 24.6 days. A study by Leach et al. (2012) shows a median duration of treatment of 65 days, which is 2.6 times more than in our study after treatment over 7 days. The same study states that dairy farmers prefer to treat cows with an LS higher than 3, suggesting a tendency towards insufficient measures.

CONCLUSION

Due to the severity of the disease by necrobacillosis and the known costs caused by this disease, we should take measures that reduce the likelihood of its occurrence and the success of treatment.

It is primarily a matter of creating good conditions for the animal, and early diagnosis of the disease is also important. The results of the study showed that it is appropriate to use automated methods for assessing the health of the limbs by infrared thermography, which seems promising from the point of view of the future. With this tool, up to 25% of cases of footrot can be detected in the preclinical phase, i.e. before the onset of clinical symptoms expressed by lameness, because out of a total of 24 sick cows, necrobacillosis was diagnosed in 6 animals only by the infrared method, without a change in the locomotor score. It was further confirmed that early treatment of the limbs affects the effectiveness of treatment expressed by a shorter duration of treatment, and thus a shorter duration of pain in the limbs of dairy cows. In dairy cows included in the treatment on the basis of early diagnosis with an Infrared Thermography, recovery occurred within 20 days, and in dairy cows with clinical symptoms in 21.3 days. This is the original first work of this type, so far with a small number of animals. Therefore, it is necessary to continue the work and perform a statistical analysis based on a sufficient number of animals.

ACKNOWLEDGEMENTS
Research reported in this publication was supported by grant no. AF-IGA2021-IP078.

REFERENCES

Alsaaod, M., Büscher, W. 2012. Detection of hoof lesions using digital infrared thermography in dairy cows. Journal of Dairy Science [Online], 95(2): 735–742. Available at: https://doi.org/10.3168/jds.2011-4762. [2021-10-05]

Alsaaod, M. et al. 2015. The role of infrared thermography as a non-invasive tool for the detection of lameness in cattle. Sensors [Online], 15(6): 14513–14525. Available at: https://doi.org/10.3390/s150614513. [2021-10-05].

Charfeddine, N., Pérez-Cabal, M.A. 2017. Effect of claw disorders on milk production, fertility, and longevity, and their economic impact in Spanish Holstein cows. Journal of Dairy Science [Online], 100(1): 653–665. Available at: https://doi.org/10.3168/jds.2016-11434. [2021-10-05].

Dutton-Regester, K.J. et al. 2020. Lameness in dairy cows: farmer perceptions and automated detection technology. Journal of Dairy Research [Online], 87(S1): 67–71. Available at: https://doi.org/10.1017/S0022029920000497. [2021-10-05].

Havlíček, Z. et al. 2021. Inovační způsob diagnostiky onemocnění končetin dojnic. Brno: Mendelova univerzita v Brně. Nmetc-Metodika certifikovaná oprávněným orgánem. Č: 4564/2021-ČPI. 12.07.2021. ISBN 978-80-7509-791-0.

Hulsen, J. 2011. Cow signals. Praha: Profi Press. ISBN 978-80-86726-44-1.

Langova, L. et al. 2020. Impact of nutrients on the hoof health in cattle. Animals [Online], 10(10): 1824. Available at: https://doi.org/10.3390/ani10101824. [2021-10-05].

Leach, K.A. et al. 2012. The effects of early treatment for hindlimb lameness in dairy cows on four commercial UK farms. The Veterinary Journal [Online], 193(3): 626–632. Available at: https://doi.org/10.1016/j.tvjl.2012.06.043. [2021-10-05].

LokeshBabu, D.S. et al. 2018. Monitoring foot surface temperature using infrared thermal imaging for assessment of hoof health status in cattle: A review. Journal of Thermal Biology [Online], 78: 10–21. Available at: https://doi.org/10.1016/j.jtherbio.2018.08.021. [2021-10-05].

Novotna, I. et al. 2019. Risk factors and detection of lameness using infrared thermography in dairy cows – A Review. Annals of Animal Science [Online], 19(3): 563–578. Available at: https://doi.org/10.2478/aoas-2019-0008. [2021-10-05].

Osova, A. et al. 2017. Interdigital phlegmon (foot rot) in dairy cattle-an update. Wien Tiearztl Monatsschr. Veterinary Medicine Austria, 104(7–8): 209–220.

Renn, N. et al. 2014. Digital infrared thermal imaging and manual lameness scoring as a means for lameness detection in cattle. Veterinary Clinical Sciences, 2: 16–23.

Schaefer, A.L. et al. 2007. The use of infrared thermography as an early indicator of bovine respiratory disease complex in calves. Research in Veterinary Science [Online], 83(3): 376–384. Available at: https://doi.org/10.1016/j.rvsc.2007.01.008. [2021-10-05].

Thomsen, P.T. et al. 2012. Locomotion scores and lying behaviour are indicators of hoof lesions in dairy cows. The Veterinary Journal [Online], 193(3): 644–647. Available at: https://doi.org/10.1016/j.tvjl.2012.06.046. [2021-10-05].

The influence of different feed particle size in broiler diets on the performance parameters and digestive viscosity

Jakub Novotny[1], Lucie Horakova[1], Dana Zalesakova[1], Michal Rihacek[1], Vojtech Kumbar[2], Ondrej Stastnik[1], Leos Pavlata[1]
[1]Department of Animal Nutrition and Forage Production
[2]Department of Technology and Automobile Transport
Mendel University in Brno
Zemedelska 1, 613 00 Brno
CZECH REPUBLIC

jakub.novotny@mendelu.cz

Abstract: The effect of different feed particle size used in broiler chickens' diet on performance parameters and chyme viscosity was evaluated. Broilers were divided into three different groups based on the structure of particles (coarse vs. medium vs. fine). Geometric Mean Diameter (GMD) (1,109.95 vs. 953.00 vs. 732.58) and Geometric Standard deviation (GSD) (1,067.75 vs. 845.23 vs. 611.70) of particles size were calculated. In the experiment were not observed statistically significant differences ($P > 0.05$) among dietary groups in the final live weight (2,415.50 g vs. 2,373.56 g vs. 2,423.17 g), feed intake (83.56 g/bird/day vs. 82.12 g/bird/day vs. 87.82 g/bird/day), carcass yield (64.70% vs. 68.55% vs. 68.49%) and viscosity of chyme (5.46 mPa.s vs. 4.66 mPa.s vs. 5.36 mPa.s).

Key Words: poultry nutrition, Geometric Mean Diameter, Geometric Standard Deviation, Ross 308

INTRODUCTION

The feed industry strives to produce a homogeneous feed, however, it is stated that various factors including particle size, shape, density, electrostatic charge, dustiness, hygroscopicity and flowability can significantly affect the quality of the compound feed (Axe 1995, Behnke 1996, Schofield 2005). The nature of the particles, especially their size, is one of the most controversial problems not only in poultry nutrition. From the economic point of view, the optimal size distribution should be adapted to the physiological needs of the animal, which allows optimal utilization of nutrients and increases the performance parameters. However, the recommendations regarding the optimum particle size are contradictory, as shown by feeding experiments. These are influenced by several factors, including the physical form of the feed, the composition of the diet, the type of grain, the hardness of the endosperm, the method of grinding, the quality of the pellets and the particle size distribution (Amerah et al. 2007, Vukumirović et al. 2017). It is generally stated that finer grinding increase energy consumption during grinding and reduces the capacity of the grinding equipment, increases dust problems and, most importantly, too fine particles are associated with a negative effect on the health and function of the gastrointestinal tract. Thanks to their mechanoreceptors located in the beak, birds are able to distinguish the particle size of the feed they receive (Denbow 1994). Chickens have been found to prefer larger particle sizes in diets. With increasing age, these preferences deepen (Schiffman 1968, Nir et al. 1994). Therefore, it is desirable for the particles in compound feeds to gradually increase with age. This could achieve optimum poultry performance. Evenly formulated feed mixtures save the energy that poultry would consume when searching for and selecting larger particles (Amerah et al. 2007).

Non-starch polysaccharides forms gels in the digestive tract, which significantly increases the viscosity of the chyme (Kiarie et al. 2013, Zarghi 2018). That leads to impaired digestibility of nutrients and minerals (especially Na, P, Ca), their accessibility to digestive enzymes and mechanical inhibition of diffusion and movement of nutrients to the intestinal wall. This is negatively reflected in lower increments and other disorders as greasy feces and limb burns, so-called "hock burns", which are common in broiler chickens (Rada and Havlík 2010).

The aim of this study is to determine the influence of different feed particle size in diet on performance parameters and chyme viscosity of broiler chickens.

MATERIAL AND METHODS

Animals and diets

The total of 54 male broiler chickens Ross 308 were randomly divided into 3 different experimental groups (Coarse group, Medium and Fine group – 6 birds per cage, 3 replicates). The lighting program, temperature and humidity was set according to the technological instruction (Aviagen 2018). Till 10 days of age, the starter diets were used. After that, chickens were fed experimental grower diets from 11th day until 35th day of age. The chickens were fed *ad libitum* and animals had free access to water. The feed intake of each group was daily recorded. The body weight was regularly noticed. The experiment lasted 35 days. At the end of the trial, broilers were slaughtered, the chyme was collected, and the selected yields were evaluated.

There were used three diets of the same composition differing in the particle size (Coarse, Medium, and Fine group named by using particle size in diet). The compounds and chemical composition of used diets shows Table 1.

Table 1 Ingredient and chemical composition of used diets on the dry matter basis

	STARTER			GROWER		
Component	**Coarse**	**Medium**	**Fine**	**Coarse**	**Medium**	**Fine**
Maize (g/kg)	331.65	331.65	331.65	366.4	366.4	366.4
Soybean meal (g/kg)	438.0	438.0	438.0	396.0	396.0	396.0
Wheat (g/kg)	130.0	130.0	130.0	153.2	153.2	153.2
Rapeseed oil (g/kg)	52.0	52.0	52.0	40.0	40.0	40.0
Premix (g/kg)	30.0	30.0	30.0	30.0	30.0	30.0
Limestone milled (g/kg)	5.5	5.5	5.5	4.0	4.0	4.0
Monocalcium phosphate (g/kg)	7.7	7.7	7.7	5.9	5.9	5.9
DL-Methionine (g/kg)	2.0	2.0	2.0	1.5	1.5	1.5
Wheat gluten (g/kg)	3.1	3.1	3.1	-	-	-
Chromium oxide (g/kg)	-	-	-	3	3	3
ME_N (MJ/kg)*	12.42	12.42	12.42	12.3	12.3	12.3
Crude protein (g/kg)	231.9	239.6	234.4	215.4	215.1	209.9
Ether extract (g/kg)	71.2	72.4	71.7	73.7	73.1	73.5
Crude fibre (g/kg)	38.2	36.1	36.6	47.6	46.9	42.4
Crude ash (g/kg)	62.7	65.9	64.7	61.3	60.2	60.6

Legend: ***Premix for starter contains*** *(per kg): L-lysine 2.34 g; DL-Methionine 2.4 g; Threonine 0.99 g; calcium 5.25 g; phosphorus 1.95 g; sodium 1.44 g; copper 15 mg; iron 84 mg; zinc 99 mg; manganese 99 mg; iodine 0.99 mg; selenium 0.18 mg; retinol 13,500 IU (international units); calciferol 5,001 IU; tocopherol 45 mg; phylloquinone 1.5 mg; thiamine 4.2 mg; ri-boflavin 8.4 mg; pyridoxin 6 mg; cobalamin 30 µg; biotin 0.21 mg; niacinamid 36 mg; folic acid 1.8 mg; calcium pantothenate 13.5 mg; cholin chloride 180 mg.* ***Premix for grower contains*** *(per kg): L-lysine 2.58 g; DL-Methionine 2.52 g; Threonine 1.47 g; calcium 5.04 g; phosphorus 1.65 g; sodium 1.38 g; copper 15 mg; iron 75 mg; zinc 99 mg; manganese 99 mg; iodine 0.9 mg; selenium 0.36 mg; retinol 9,900 IU (international units); calciferol 5,001 IU; tocopherol 45 mg; phylloquinone 1.5 mg; thiamine 4.2 mg; ri-boflavin 8.4 mg; pyridoxin 6 mg; cobalamin 28.8 µg; biotin 0.18 mg; niacinamid 36 mg; folic acid 1.71 mg; calcium pantothenate 13.35 mg; cholin chloride 180 mg.* ******* *Apparent metabolize energy, calculated value.*

The feed particle size was evaluated by dry sieving on a separator (Retch AS 200 Control) using a representative sample of 100 g for 10 minutes. The amplitude was set on 1.8 mm/g. The samples were passed through the set of sieves with different mesh size (3 mm–0.3 mm). The amount of particles on each sieve was determined and the GSD and GMD were calculated using formulas according to Asabe (2008).

Samples and analysis

The feed consumption and body weight of broilers during the trial were evaluated. The carcass yield was calculated as the carcass weight/slaughter live weight * 100 from 6 bird per group. Yield of breast meat and leg meat were calculated as their proportion from the carcass weight. FCR (Feed

Conversion Ratio) was determined as average consumption/average weight body gain. The chyme was collected in test tubes and then centrifuged for 10 minutes at 3500 rpm. The resulting supernatant was pipetted into eppendorf tubes. The samples were analysed to determine the dynamic viscosity on an RST instrument (Brookfield, MA, USA) at a constant shear rate of 50 s-1 with geometrical spindle cone arrangement (RCT-50-2; α = 2°) including duplicator for tempering sample. The measurement was performed in 10 replicates at 40 °C and the sample volume was approx. 2 ml. The obtained data were evaluated by specialized software Rheo300 (Brookfield; MA, USA). This software allows you to program measurements, acquire and process data on rheological and viscosity properties of substances. It also allows statistical evaluation and inserting appropriate mathematical models.

Statistical analysis

Data has been processed by Microsoft Excel (USA) and StatSoft Statistica 12 (USA). It was used one-way analysis of variance (ANOVA). To evaluate differences among groups, the Sheffé´s test was used. $P < 0.05$ was a significance level determine a statistically significant difference.

RESULTS AND DISCUSSION

Diets analysis

Figure 1 shows the differences between particle size distribution in the Coarse, Medium and Fine grower diet.

Figure 1 Particle size distribution used in grower diets

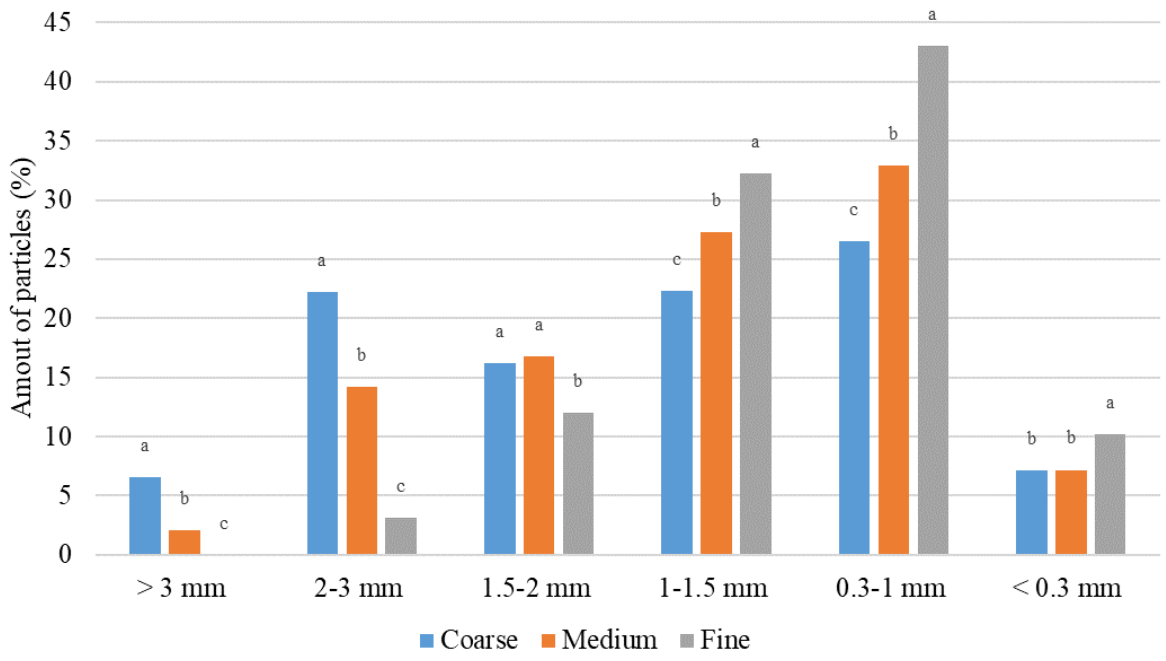

Legend: [a,b,c] means with different superscript letters differ significantly at P < 0.05

Feed particle size in diets were determined by dry sieving. It is obvious that there are statistically significant differences in feed particle size among used diets. Differences in amount of particles on sieve were found on each sieve ($P < 0.05$). That proves variety of used mixtures.

According to the weight fraction on individual sieves the Geomitric Mean Diameter (GMD) and Geometric Standard Deviation (GSD) were calculated (see Figure 2).

There were found statistically significant differences between GMD for coarse, medium and fine diet ($P < 0.05$). Values of GMD correspond to values in the study of Ege et al. (2019) which dealt with the similar issue. They calculated values of GMD were 707 µm vs. 1096 µm. The GSD, which is a homogeneity indicator of diet also showed the statistically significant differences ($P < 0.05$) among respective assessed groups. That means the diet with the fine particle size is more homogenous.

Figure 2 GMD and GSD of grower diets

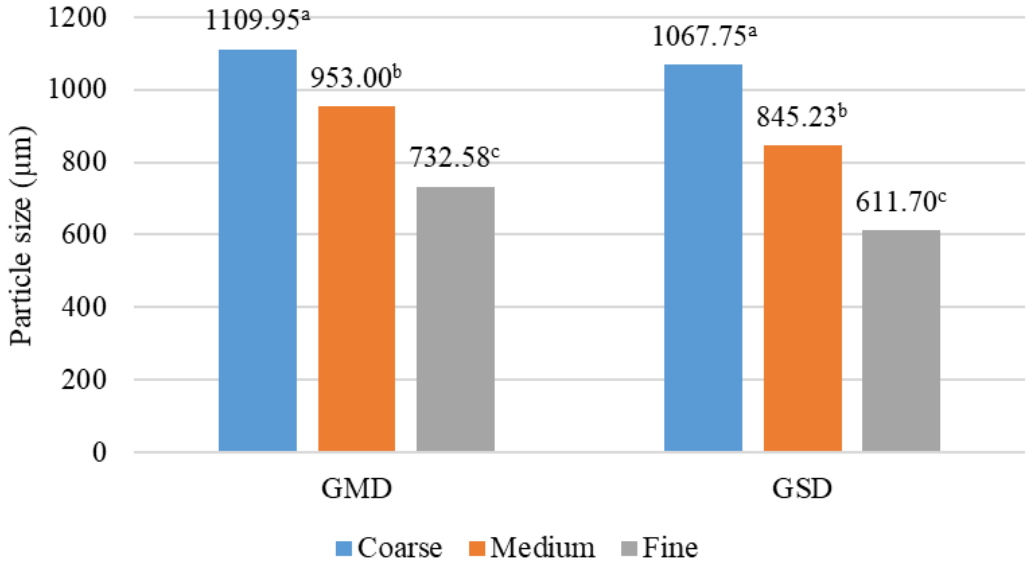

Legend: [a,b,c] means with different superscript letters differ significantly at P < 0.05; GMD – Geometric Mean Diameter; GSD – Geometric Standard Deviation

Feed consumption, body weight and carcass characteristics

Table 2 shows values for feed consumption. There were not found statistically significant differences among values for feed consumption (P > 0.05) in chickens.

Table 2 Feed consumption of broilers (g/bird) in relation to physical properties of diets (per day)

	Coarse	Medium	Fine
		Mean ± SE (g/bird)	
Starter	22.30 ± 1.03	23.16 ± 0.24	22.95 ± 0.68
Grower	108.07 ± 9.78	105.71 ± 8.35	113.76 ± 4.50
Trial	83.56 ± 7.27	82.12 ± 5.92	87.82 ± 3.40

Legend: There was not found statistically significant differences (P > 0.05) among evaluated dietary groups; SE – standard error

The body weight (Figure 3) of all three broiler groups were similar during the trial. The highest weight at the end of the experiment was recorded for the Fine group (2,423.17 g), but the Coarse group had a minimal difference (2,415.50 g). The lowest average body weight had the Medium group (2,373.56 g), but no statistically significant differences were found among all three groups (P > 0.05).

Table 3 shows values of carcass yield and yield of main meat parts. There were found no statistically significant differences among the evaluated carcass traits (P > 0.05). The highest value of FCR had the Fine group (1.34 ± 0.01), then Medium group (1.34 ± 0.01) and the lowest FCR had the Coarse group (1.36 ± 0.02). No statistically significant difference (P > 0.05) was found among the respective groups.

Nir et al. (1995) stated that broiler chickens fed a coarse mixture of wheat and sorghum had a higher body weight and better feed conversion compared to broilers fed a finely ground mixture. Amerah et al. (2007) confirmed that chickens fed a mixture with finely ground wheat had reduced weight gain and lower feed intake than groups given a diet with a high proportion of medium and coarse particles.

Viscosity of the chyme

In Table 4, there are shown values concerning the viscosity and the density of chyme. There were not found any statistically significant differences among groups (P > 0.05).

Figure 3 Live weight of broilers during the trial

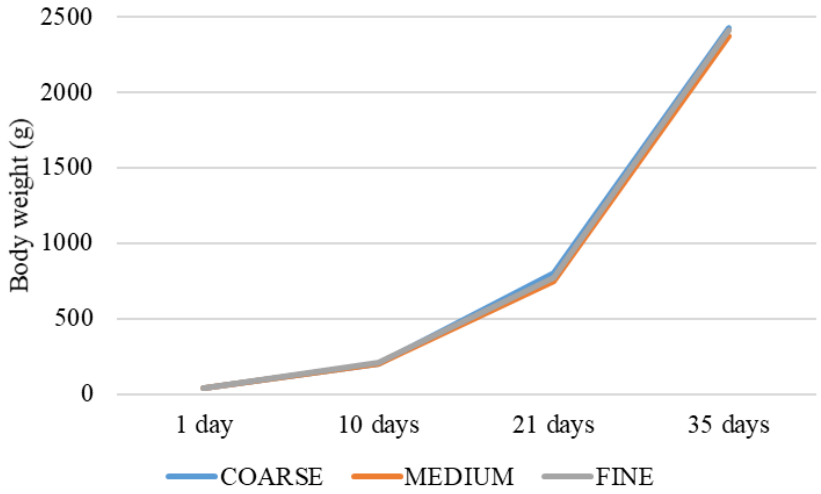

Legend: There was not found statistically significant differences (P > 0.05) among evaluated dietary groups

Table 3 Carcass characteristics of broilers in relation to physical properties of diets

	Coarse	**Medium**	**Fine**
n	6	6	6
		Mean ± SE	
Slaughter weight (g)	2,348.00 ± 217.06	2,211.33 ± 146.10	2,542.00 ± 147.22
Carcass weight (g)	1,516.85 ± 179.72	1,514.63 ± 97.98	1,746.47 ± 120.24
Carcass yield (%)	64.70 ± 4.40	68.55 ± 0.79	68.49 ± 0.91
Breast meat (%)	33.56 ± 2.66	29.83 ± 0.71	30.99 ± 0.76
Leg meat (%)	25.38 ± 2.73	23.03 ± 0.27	22.95 ± 0.20

Legend: There was not found statistically significant differences (P > 0.05) among evaluated dietary groups; n – number of cases; SE – standard error

Table 4 Viscosity and density of chyme in relation to physical properties of broiler diets

Particles of diet		**Viscosity (mPa·s)**	**Density (kg/m^3)**
	n	Mean ± SE	
Coarse	6	5.46 ± 0.16	1,034.52 ± 17026
Medium	6	4.66 ± 0.18	1,029.57 ± 0.87
Fine	6	5.36 ± 0.47	1,031.05 ± 1.85

Legend: There was not found statistically significant differences (P > 0.05) among evaluated dietary groups; n – number of cases; SE – standard error

In contrast to our experiment, Yasar (2003) recorded a high value of chyme viscosity in birds fed a fine mixture compared to feeds containing medium or coarse wheat particles in diets.

CONCLUSION

In the present study, broiler performance parameters and viscosity of chyme were evaluated. The diets with a different particle size (coarse, medium, and fine) showed no influence on feed consumption, body weight, and yield of carcass, breast meat and leg meat. The chyme viscosity was also monitored, while no significant differences in its values were found among the respective dietary groups containing a different particle size.

ACKNOWLEDGEMENTS

The research was financially supported by the Internal Grant Agency of Faculty of AgriSciences (Mendel University in Brno) no. AF-IGA2021-IP026.

REFERENCES

Amerah, A. et al. 2007. Feed particle size: Implications on the digestion and performance of poultry. World´s Poultry Science Journal, 63(3): 439–455.

Asabe. 2008. Method of determining and expressing fineness of feed materials by sieving. S319.3. St. Joseph, US: American Society of Agricultural and Biological Engineers.

Aviagen Group. 2018. Technological procedure for broiler Ross. Available at: http://eu.aviagen.com/language-mini-site/show/cz. Last modified July 24, 2019.

Axe, D.E. 1995. Factors affecting unimormity of a mix. Animals Feed Science and Technology, 53(2): 211–220.

Behnke, K.C. 1996. Feed manufacturing technology: current issues and challenges. Animal Feed Science and Technology, 62(1): 49–57.

Denbow, D.M. 1994. Peripheral regulation of food intake in poultry. The Journal of Nutrition, 124(8): 1349–1354.

Ege, G. et al. 2019. Influence of feed particle size and feed form on productive performance, egg quality, gastrointestinal tract traits, digestive enzymes, intestinal morphology, and nutrient digestibility of laying hens reared in enriched cages. Poultry Science, 98(9): 3787–3801.

Kiarie, E. et al. 2013. The role of added feed enzymes in promoting gut health in swine and poultry. Nutrition Research Reviews, 26(1): 71–88.

Nir, I. et al. 1994. Effect of feed particle size on performance: 1. Corn. Poultry Science, 73(1): 45–49.

Nir, I. et al. 1995. Effect of particle size on performance: 3. Grinding pelleting interactions. Poultry Science, 74(5): 771–783.

Rada, V., Havlík, J. 2010. Vědecký výbor výživy zvířat: Enzymy ve výživě hospodářských zvířat. Praha: Výzkumný ústav živočišné výroby.

Schiffman, H.R. 1968. Texture preference in the domestic chick. Journal of Comparative and Physiological Psychology, 66(2): 540.

Schofield, E.K. 2005. Feed Manufacturing Technology. V. Arlington, VA: American Feed Industry Association.

Vukumirović, Đ. et al. 2017. Importance of feed structure (particle size) and feed form (mash vs. pellets) in pig nutrition – A review. Animal Feed Science and Technology, 233: 133–144.

Yasar, S. 2003. Performance, gut size and ileal digesta viscosity of broiler chickens fed with a whole wheat added diet and the diets with different wheat particle size. International Journal of Poultry Science, 2(1): 75–82.

Zarghi, H. 2018. Application of xylanase and β-glucanase to improve nutrient utilization in poultry fed cereal base diets: Used of enzymes in poultry diet. Insights in Enzyme Research, 2(1): 11–17.

The effect of cumin (*Carum carvi* L.) on broiler chickens performance parameters

Jakub Novotny[1], Lucie Horakova[1], Dana Zalesakova[1], Michal Rihacek[1], Eva Mrkvicova[1], Helena Pluhackova[2], Ondrej Stastnik[1], Leos Pavlata[1]
[1]Department of Animal Nutrition and Forage Production
[2]Department of Crop Science, Breeding and Plant Medicine
Mendel University in Brno
Zemedelska 1, 613 00 Brno
CZECH REPUBLIC

jakub.novotny@mendelu.cz

Abstract: The effect of the addition of cumin (*Carum carvi* L.) on broilers performance parameters were evaluated. The male Ross 308 broiler chickens were used in the experiment and divided into two groups (Control and Cumin group). The control diet did not contain the cumin, while the Cumin group consumed diet with 1% of cumin. No influence on feed consumption, feed conversion ratio, final body weight, carcass yield and on breast and leg meat yields was found. The addition of 1% cumin in diet had no positive neither negative effect on performance parameters assessed in broilers.

Key Words: poultry nutrition, phytoadditives, carcass yield, caraway

INTRODUCTION

Cumin is known for its positive effect on digestion, helping with stomach cramps and bloating (Rausch et al. 2014). It is the only one of about 30 species of the genus *Carum* that has a medicinal effect and can be used in the food industry (Jahodář 2010). Plants of the genus *Apiaceae* have real use in food production. The essential oils contained in cumin give a taste and stimulate digestive enzymes and thus improve nutrient digestibility. The benefits that result from this are better productivity, quality, and quantity of broiler chicken meat (Lee et al. 2004).

Khajeali et al. (2012) investigated the addition of cumin to the diets of broiler chickens. With the addition of 1–1.5% of cumin, the body weight of the chickens was significantly increased. Conversely, if the cumin in the diet was 2%, the body weight was lower, probably due to the bitterness of the cumin and thus the reduced palatability and lower feed intake. Simultaneously with the increase in chicken weight in the 1 and 1.5% cumin groups, a lower feed intake was recorded, indicating that cumin has a positive effect on nutrient digestibility. In another experiment, where different amounts of cumin added to the feed ration for broilers were compared, the effect of these doses on growth, feed conversion and serum parameters was studied. The addition of 1% cumin to the feed ration appeared to be the best for these parameters (Gandkanlo et al. 2011).

Also in Japanese quails, the addition of cumin has been shown to be beneficial. In an experiment in which 1, 1.5 and 2% of cumin were included in the diet, the results showed that the addition of cumin to the quail feed mixture had significant effects on performance, carcass characteristics and blood biochemical parameters. The highest daily gain and the best feed conversion was achieved in the group with 2% of cumin. The highest daily feed intake was recorded in the group with an intake of 1.5% of cumin. Total serum cholesterol and triglyceride levels were significantly lower in the 1.5 and 2% groups compared to the control group (Jafari 2011).

The aim of present study is to determine the influence of cumin in 1% addition in diet on performance parameters of broiler chickens.

MATERIAL AND METHODS

The animal procedures were reviewed and approved by the Animal Care Committee of Mendel University in Brno and by the Ministry of Education, Youth and Sports (MSMT-21593/2020-2). The experiment was performed at the experimental stables of Mendel University.

Animals and diets

The total of 46 male broiler chickens Ross 308 were used in the experiment. At the first day of age broilers were divided by body mass into two equal groups (23 birds in one experimental pen). The trial lasted from one day to 35th day of chicken's age. Broilers were fed experimental starter diets until 10 days of age. Chickens were fed experimental grower diets from 11th day until 35th day of age. The chickens were fed *ad libitum* and animals had free access to water. The feed intake of each group was daily recorded. During the experiment, the microclimatic conditions and the light regime was controlled according to the requirements for actual age of chickens (Aviagen Group 2018). A conventional system of deep litters with wood shavings was used as the bedding material. The body weight was regularly and individually noticed. The experiment lasted 35 days and after slaughtering some carcass traits were evaluated.

There were used two diets in the experiment in meal form. The Control group (n = 18) was fed a diet without addition *Carum carvi*. The experimental group (Cumin group, n = 18) was fed a diet containing 1% achenes of *Carum carvi*. The compounds and chemical composition of used diets shows Table 1. Diets were formulated as isoenergic and isonitrogenous according to the Broiler nutrition specifications (Aviagen group 2019). The chemical compositions of both diets (starter and grower) were determined for dry matter, crude protein, crude fat, crude fibre, and ash according to the EC Commission Regulation (Commission Regulation 152/2009).

Table 1 Composition and chemical analysis of used diets in 88% dry matter

	STARTER		GROWER	
Component	**Control**	**Cumin**	**Control**	**Cumin**
Maize (g/kg)	300.0	300.0	370.0	370.0
Soybean meal (g/kg)	436.0	436.0	395.5	391.83
Wheat (g/kg)	176.7	168.5	151.7	145.37
Rapeseed oil (g/kg)	40.0	40.0	40.0	40.0
Premix (g/kg)	30.0	30.0	30.0	30.0
Limestone milled (g/kg)	5.5	5.5	3.3	3.3
Monocalcium phosphate (g/kg)	8.0	8.0	8.0	8.0
DL-Methionine (g/kg)	2.0	2.0	1.5	1.5
Wheat gluten (g/kg)	1.8	-	-	-
Cumin (g/kg)	-	10.0	-	10.0
ME_N (MJ/kg)*	12.1	12.1	12.3	12.3
Crude protein (g/kg)	233.9	243.4	222.4	221.3
Ether extract (g/kg)	58.9	63.6	61.1	61.2
Crude fibre (g/kg)	35.7	36.3	36.4	33.6
Crude ash (g/kg)	65.9	66.2	61.0	62.5

*Legend: Premix for starter contains (per kg): L-lysine 2.34 g; DL-Methionine 2.4 g; Threonine 0.99 g; calcium 5.25 g; phosphorus 1.95 g; sodium 1.44 g; copper 15 mg; iron 84 mg; zinc 99 mg; manganese 99 mg; iodine 0.99 mg; retinol 13,500 IU (international units); calciferol 5,001 IU; tocopherol 45 mg; phylloquinone 1.5 mg; thiamine 4.2 mg; riboflavin 8.4 mg; pyridoxin 6 mg; cobalamin 30 µg; biotin 0.21 mg; niacinamid 36 mg; folic acid 1.8 mg; calcium pantothenate 13.5 mg; cholin chloride 180 mg. Premix for grower contains (per kg): L-lysine 2.58 g; DL-Methionine 2.52 g; Threonine 1.47 g; calcium 5.04 g; phosphorus 1.65 g; sodium 1.38 g; copper 15 mg; iron 75 mg; zinc 99 mg; manganese 99 mg; iodine 0.9 mg; retinol 9,900 IU (international units); calciferol 5,001 IU; tocopherol 45 mg; phylloquinone 1.5 mg; thiamine 4.2 mg; ri-boflavin 8.4 mg; pyridoxin 6 mg; cobalamin 28.8 µg; biotin 0.18 mg; niacinamid 36 mg; folic acid 1.71 mg; calcium pantothenate 13.35 mg; cholin chloride 180 mg. * Apparent metabolize energy, calculated value.*

Samples and analysis

The feed intake and body weight of broilers during the experiment were evaluated. The carcass yield was calculated as the carcass weight/slaughter live weight * 100. Yield of breast meat and leg meat were calculated as their proportion from the carcass weight. The Feed Conversion Ratio (FCR) was determined as total feed consumption/ weight body gain.

Statistical analysis

Data has been processed by Microsoft Excel (USA) and StatSoft Statistica 12 (USA). It was used a one-way analysis of variance (ANOVA). To evaluate the differences between groups, the Sheffé´s test was used. $P < 0.05$ was a significance level determine statistically significant difference.

RESULTS AND DISCUSSION

Feed consumption, body weight and carcass characteristics

Table 2 shows the average feed consumption of a broiler per day and whole trial. There is also recorded FCR.

Table 2 Feed consumption and feed conversion ratio of broilers in relation to the dietary group

	Control	Cumin
Average consumption per trial (g/bird)	2,696.22	2,715.49
Average consumption per day (g/bird)	79.30	79.87
FCR (g/g)	1.34	1.33

Legend: FCR – Feed Conversion Ratio

It was found in both groups of broilers a good feed conversion ratio. According to the guidelines for Ross 308 chickens (Aviagen group 2019), the conversion on day 35 is 1.473. Khajeali et al. (2012) in his study achieved an improvement in feed conversion in the cumin experimental group compared to the control group. The feed conversion ratio in the experimental group was significantly worse than FCR in the control group (1.71 vs. 1.87, respectively) in their trial.

Figure1 Live weight of broilers during the trial

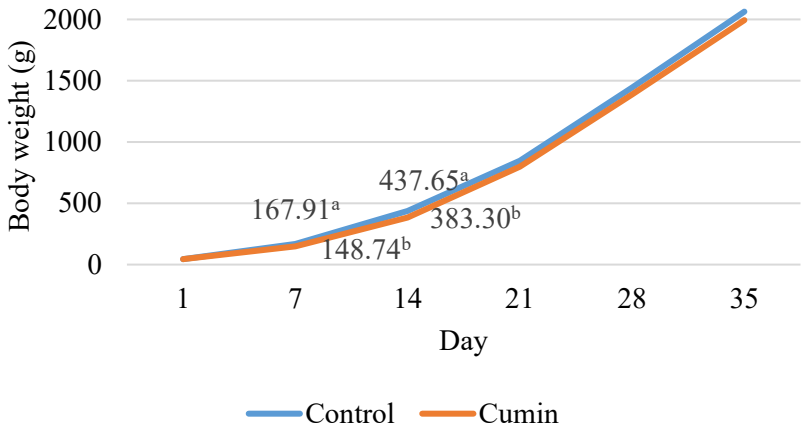

Legend: [a,b] means with different superscript significantly at P < 0.05

Live body weight curve during the trial is shown in Figure 1. The average live weight at the end of the trial was 2,064 g in the Control group and 1,994 g in the Cumin group. The live weights of broilers were in both dietary groups quite similar during the trial. There was found statistically significant differences ($P < 0.05$) between live weights only in 7th and 14th day of age. After that, there were no statistically significant differences in live weights ($P > 0.05$).

In the experiment of Khajeali et al. (2012) was found out that addition of 1% of cumin had a positive effect on body weight, while their trial lasted till 42 days of age. The better weight gain in the group with 1% of cumin in the diet during the whole trial proved also Gandkanlo et al. (2011).

Table 3 is concerning about evaluated carcass traits. There were not found any statistically significant differences in values of carcass yield and yields of main meat parts between dietary groups of chickens ($P > 0.05$).

Table 3 Carcass characteristics of broilers in relation to the dietary group

Trait	Control	Cumin
n	6	6
	Mean ± SE	
Carcass weight (g)	1,495.04 ± 45.03	1,541.85 ± 72.84
Carcass yield (%)	67.69 ± 0.65	69.24 ± 0.48
Breast meat (%)	29.35 ± 0.80	31.20 ± 0.82
Leg meat (%)	21.54 ± 0.43	21.50 ± 0.57

Legend: There was not found statistically significant differences (P > 0.05) between dietary groups; n – number of cases; SE – standard error

CONCLUSION

In the trial the effect of addition of cumin on broilers performance parameters were evaluated. The diet with addition of 1% cumin (*Carum carvi*) had no influence on feed consumption, final body weight, carcass yield, and breast and leg meats yields of chickens. The cumin had no positive neither negative effect on performance parameters in broiler chickens in this trial.

ACKNOWLEDGEMENTS

The research was financially supported by the Internal Grant Agency of Faculty of AgriSciences (Mendel University in Brno) no. AF-IGA2020-TP012.

REFERENCES

Aviagen Group. 2018. Technological procedure for broiler Ross. Available at: http://eu.aviagen.com/language-mini-site/show/cz. [2019-07-24].

Aviagen Group 2019: Broiler nutrition specifications. Available at: http://eu.aviagen.com/language-mini-site/show/cz. [2019-05-23].

Commission regulation (EC) 152/2009. Laying down the methods of sampling and analysis for the official control of feed. Brussels: The commission of the European Communities.

Gandkanlo, M. et al. 2011. The effects of different dietary levels of Black Caraway (Carum carvi L.) seeds on performance and some blood indices in broiler chickens. Animal Sciences Journal (Pajouhesh & Sazandegi), 93: 26–33.

Jafari, B. 2011. Influence of caraway on improve performance and blood parameters of Japanese quails. Annals of Biological Research, 2(6): 474–478.

Jahodář, L. 2010. Léčivé rostliny v současné medicíně: (co Mathioli ještě nevěděl). 1. ed., Praha: Havlíček Brain Team.

Khajeali, Y. et al. 2012. Effect of use different levels of caraway (Carum carvi L.) powder on performance, some blood parameters and intestinal morphology on broiler chickens. World Applied Sciences Journal, 19(8): 1202–1207.

Lee, K.W. et al. 2004. Essential oils in broiler nutrition. International Journal of Poultry Science, 3(12): 738–752.

Rausch, A. et al. 2014. Bylinky: nejznámější bylinky od A do Z: kuchyně, kosmetika, zdraví. Česlice: Rebo.

Determination of optimal insemination time in sheep by assessing cervical mucus arborization

Vojtech Pesan, Martin Hosek, Radek Filipcik, Katarina Souskova, Martina Pesanova Tesarova
Department of Animal Breeding
Mendel University in Brno
Zemedelska 1, 613 00 Brno
CZECH REPUBLIC

vojtech.pesan@mendelu.cz

Abstract: Insemination and estrus synchronization are one of the most used biotechnological reproductive methods used in sheep breeding, but also in most other livestock species. Subsequent insemination values are influenced by several factors such as age, condition, health, hereditary establishment of the animals, quality of the insemination doses and the quality of the performance of the insemination itself. Another way to optimise the insemination values is to determine the optimal time for insemination, which varies between livestock species but may also vary slightly within the individuality of the individuals within the breed. One way of determining the optimal time for insemination is to assess the arborisation of cervical mucus, which forms different types of structures after crystallisation at different stages of estrus. Changes in the arborisation structures are influenced by endocrine changes, by the action of oestrogen on the cervical glands, where electrolytes are concentrated and which, after association with mucin and subsequent crystallisation, form typical structures. The experiment took place from September 2020 (synchronization of estrus and insemination) to March 2021 (end of lambing). In this experiment, it was found that the type of crystallization structures at the time of insemination has a conclusive effect on the subsequent pregnancy rate. Animals with "V" type crystallization achieved the best pregnancy rate (80%).

Key Words: arborization, cervical mucus, insemination, sheep, Zwartbles

INTRODUCTION

Small ruminants are generally seasonally polyestrous animals. Sexual activity is influenced by the length of the light day and its shortening affects the onset of the reproductive season. In tropical animals, reproductive activity is not affected by seasonal variation and estrus can occur throughout the calendar year. The methods used to synchronize estrus or induce estrus depend on the season: ither breeding season, transitional period and nonbreeding season (Romano 2021).

Synchronisation of estrus (whether using natural or artificial methods) is used mainly to save time, reduce labour intensity and the associated economic demands of breeding, because of more accurate recording of animals, facilitating the assessment of health status and the possibility of scheduling births into a targeted period, which is associated, for example, with greater seasonal sales of lambs or dairy or meat products. The synchronisation of estrus results in turntable lambing, which allows group weaning and subsequent rearing in larger and more balanced groups of lambs (Štolc et al. 2007, Whitley and Jackson 2004).

Thanks to the subsequent breeding of the sheep (natural breeding, insemination or a combination of both, for example by forming harems after insemination) we are able to select the best males, shorten the period of breeding and know the approximate date of birth, thanks to the synchronisation of estrus, we can situate it in a suitable period to be able to produce lambs at Easter and Christmas, when demand is highest, or to focus on off-season production of lambs for slaughter (Kuchtík et al. 2007, Štolc et al. 2007).

After the synchronization of estrus, the choice of the method of insemination is important. Due to the lower labour, time and economic requirements (compared to the laparoscopic method) and the good results of insemination, which are around 60%, vaginal insemination with vaginal speculum and intracervical deposition is mainly used (Kuchtík et al. 2007). Due to the very complex

structure of the cervical septum, intracervical deposition of the insemination dose is only possible to a depth of one to three centimetres (Leethongdee 2010). The success rate of insemination increases significantly with greater depth of penetration. However, this is influenced by cervical openness, breed affiliation and age of the ewe (Eppleston and Maxwell 1995). (Eppleston and Maxwell (1995) reported that, on average, it is possible to insert the insemination pipette to a cervical depth of 1 cm in 31% of animals, 2 cm in 31% of animals, 3 cm in 30% of animals and only 8% of inseminated animals to a depth exceeding 4 cm.

Therefore, determining the optimal stage of estrus and the optimal time of insemination is essential for insemination. The activity of the females, changes in the genital organs (swelling, redness, quantity and quality of cervical mucus, openness of the cervix, etc.) are monitored.

The average length of an estrus cycle is 17 days and estrus lasts 24 to 36 hours in ewes. Ovulation occurs towards the end of estrus (24 to 27 hours after the start of estrus). The ovulation rate is between 1 and 3 eggs per cycle and increases with age, peaking between 3 and 6 years of age and then gradually decreasing. After ovulation, the egg is capable of fertilization for 10 to 25 hours (Gimenez and Rodning 2007). Čunát et al. (2013) state that in ewes with natural onset of estrus, insemination is best performed 12 to 18 hours after the onset of estrus and in ewes synchronized with intravaginal sponges 50 to 60 hours after removal.

One of the methods of determining the optimal insemination time is to assess the arborization (crystallization) of cervical mucus, which forms different types of structures after crystallization in the different stages of estrus. Changes in arborization structures are influenced by endocrine changes, namely the action of estrogen on the cervical glands/epithelium, where electrolytes are concentrated and form typical structures after association with mucin and subsequent crystallization (Cortés et al. 2014).

Several authors have addressed this issue in cattle. There are not many publications with results of arborization evaluation in sheep (or goats), especially studies related directly to the determination of the appropriate time of admission/insemination. Recent studies include, for example, the evaluation of cervical mucus in goats – Fonseca et al. (2017), Maddison et al. (2017), or the evaluation of crystallization forms from saliva smears in sheep – Gonçalves et al. (2020).

MATERIAL AND METHODS

A total of 51 Zwartbles sheep were monitored in this experiment. The age of the sheep ranged from 2 to 8 years with a BCS (body condition score) of 3. The sheep were housed on the family farm of Mr. Ing. Martin Hošek Ph.D. in Mohelno. The experiment itself was conducted from September 2020, when estrus synchronization was performed using intravaginal sponges, until March 2021, when the lambing of the group of animals under study ended. Before the actual insemination (mid-October 2020), the collection of the rams' ejaculate, its evaluation and dilution were carried out. Pregnancy diagnosis was carried out in mid-December 2020.

Inseminated ewes and breeding rams used for ejaculate collection and insemination doses were fed on silage from stale forage and hay ad libitum. As flushing, 200 g of fodder potatoes and 400 g of cereals per head were used one month before insemination and one and a half months after insemination. Flushing was mainly used to modify the condition of the animals, improve ejaculate quality, accentuate estrus symptoms and improve pregnancy rates.

To synchronise the estrus, which took place at the end of September and the beginning of October 2020, intravaginal sponges (tampons) (Ovigest - medroxyprogesterone acetate 60 mg, Laboratorios Hipra, Spain) were used, which were injected into the sheep vagina for 14 days. After their subsequent removal, sheep were injected intramuscularly with lyophilized serum gonadotropin (PMSG – 0.2 ml/sheep = Sergon 200 IU, Bioveta Ivanovice, CZ).

Ejaculate was collected from rams into an artificial vagina on the day of insemination (Minitübe, Germany) after the ejection on an ewe in heat (fixed on a fixation pad). In case of a smaller quantity of collected ejaculate, a second jump was performed. The ejaculate was then macroscopically and microscopically evaluated and diluted to the required amount according to sperm concentration and motility. The diluted ejaculate ready for insemination was stored in plastic containers cooled to 3 °C in a refrigerated box until the time of insemination.

For each inseminated ewe, several parameters (colour and amount of cervical mucus, cervical openness, genital blood supply and behavioural activity – willingness to mate) were monitored before insemination and a cervical mucus sample was taken for arborization examination. Prior to insemination, the external genitalia were cleaned and disinfected, and the vagina was inspected using an ovine vaginal speculum. Each insemination dose of cooled dilute ejaculate was injected in a quantity of 0.4 ml through the vaginal speculum using a plastic loader into the cervix to a depth of approximately 1 to 2 centimetres.

The cervical mucus sample was collected using a plastic loader through the vaginal speculum before insemination. This sample was transferred to a microscope slide immediately after collection and then smeared at an angle of 45 °. Once the cervical mucus had sufficiently dried on the slide, it was labelled (date and time of collection, ewe number) and placed in a plastic box. The smears were then examined microscopically (Olympus BX51TF; Olympus Optical CO., LTD, Tokyo, Japan). At 200× magnification and their crystallization type were evaluated (examples of crystallization types in Figure 1). The procedure of smear formation, their evaluation and crystallization types were determined according to standard methodologies for assessing cervical mucus arborization in cattle (Cortés et al. 2014, Stádník et al. 2013). The individual samples were divided into different groups according to the type of crystallization (V: twigg-shaped, V + P: twigg-shaped-clubmosses, P: clubmosses, P + K: clubmosses-fern frond, K: fern frond, Z: swollen, C: cellularization).

Sequence of crystallization types during estrus is: Type "V" (pre-estrus period), type "V+P", type "P" (beginning of estrus), type "P+K" (half of estrus), type "K" (second half of estrus). The undesirable structures include type "Z" (swollen crystallization - post-estrus period) and "C" (cellularization - occurring during inflammation) (Stádník et al. 2013).

Type "V" is characterised by fine structures that resemble twigs, type "P" is characterised by branching structures that resemble plants of the genus Lycopodium (clubmosses), type "K" is characterised by a shape that resembles palm leaves or fern frond. The swollen crystallisation of type "Z" produces enlarged branched crystals. Type "C" crystallizes into simple forms composed of several short segments.

Figure 1 Examples of crystallization types

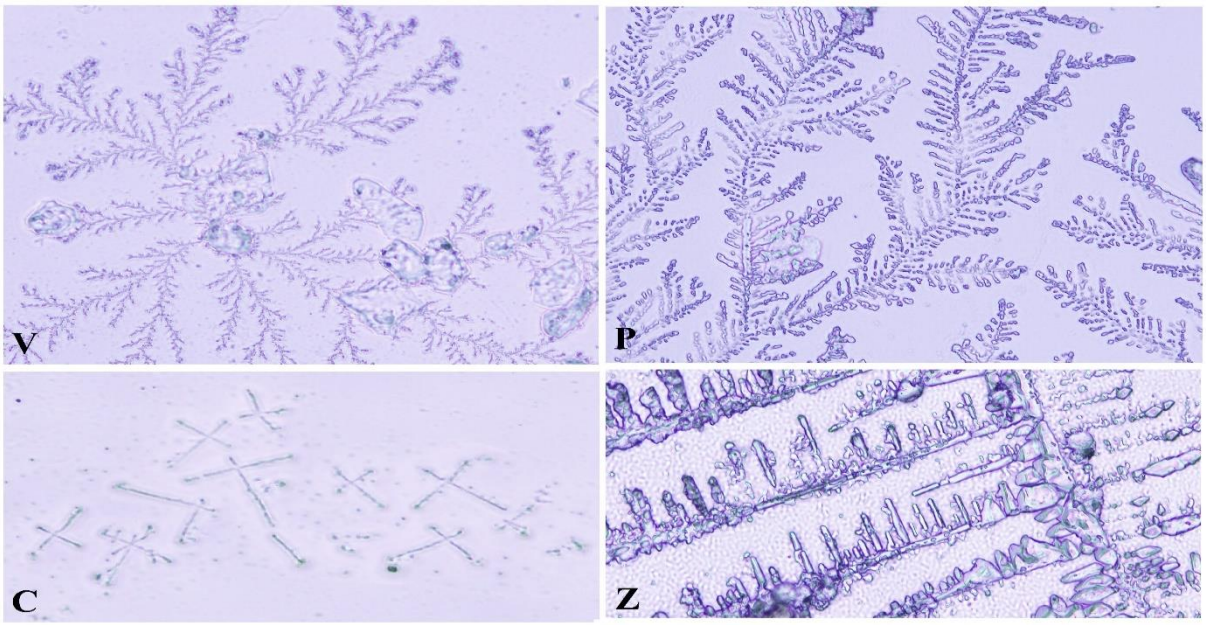

In Figure 1 are the examples of crystallization types: type V (twigg-shaped: pre-estrus), type P (clubmosses: beginning of estrus), type C (cellularization: occurring during inflammation) and type Z (swollen: post-estrus).

Preliminarily, the value of pregnancy rate was determined during pregnancy diagnosis and control, which took place on days 43 and 83 after insemination using OVI-SCAN ultrasound (BCF technology, Scotland. The exact value of the pregnancy rate was determined by recording the date and time of insemination and insemination. Subsequently, trimming values were compared with each type of cervical mucus crystallisation: post-estrus period).

STATISTICA 12.0 was used for statistical evaluation of the results.

RESULTS AND DISCUSSION

The cervical mucus samples were divided into several groups according to the type of crystallization. These types of crystallization structures change during estrus.

Table 1 Total frequency of crystallization structures

Type of crystallisation	Number of samples (n)	Frequency (%)	Sx	Vx
V	15	29.4		
V+P	16	31.4		
P	7	13.7	10.05181023	0.66067239
P+K	6	11.8		
Z	3	5.9		
C	4	7.8		

Legend: Sx – Standard deviation, Vx – Coefficient of variation

Table 1 shows the frequency of the individual crystallization structures. Most of the inseminated sheep (60.8%) had "V" type crystallization (29.4%) and a mixed form of "V"+"P" type crystallization (31.4%). In 25.5% of inseminated sheep, "P" and mixed forms of "P"+"K" crystallization occurred. Crystallisation of the "K" type did not occur in the animals studied. In 5.9% of the inseminated sheep, a swollen crystallization of the "Z" type occurred, and in 7.8% of the animals, a crystallization of the "C" type occurred.

Table 2 Influence of crystallization type on pregnancy rate

Type of crystallisation	Number of samples (n)	Number of pregnant sheep (n)	Pregnancy rate (%)
V	15	12	80.0
V+P	16	7	43.8
P	7	4	57.1
P+K	6	3	50.0
Z	3	2	66.7
C	4	0	0.0
			P = 0.002858
∑	51	28	54.9

Legend: P < 0.01 = high statistically significat differences

According to Stádník et al. (2013), the optimal form of crystallization structures (suitable time for insemination) is the "P"+"K" and "K" type, which occurs in cattle in the second half of estrus. According to the results shown in Table 1, it can be assumed that most of the inseminated animals were inseminated prematurely around the beginning of estrus (type "V", "V"+"P", "P").

Table 2 and Figure 2 show the effect of crystallization types on the pregnancy rate. The highest value of pregnancy (80.0%) was found in animals that had a "V" type crystallization pattern. For the "V+P", "P" and "P+K" types, a total of 48.3% (14 pregnancies out of 29 inseminated) were crystallized. The type of crystallization structures "V", "V"+"P", "P" and "P"+"K" had a highly statistically significant effect (P = 0.002858) on the pregnancy rates.

In cattle, the highest values of pregnancy at insemination are reached at the time of crystallization structures "P" to "K". On the contrary, the lowest values of pregnancy are achieved by animals with atypical crystallization (Ježková et al. 2007, Ježková et al. 2008, Stádník et al. 2013).

The value of pregnancy in inseminated animals with "Z" type crystallization was 66.7%. As this is a structure occurring in cattle at the end of estrus/postpartum, the higher values (compared to similar observations - see Stádník et al. (2013): 20.0%) are probably due to the low number of animals with this type of crystallisation. The lowest values of pregnancy were found for crystallization type "C" (0.0%), which occurs in inflammation.

Figure 2 Influence of crystallization type on pregnancy rate

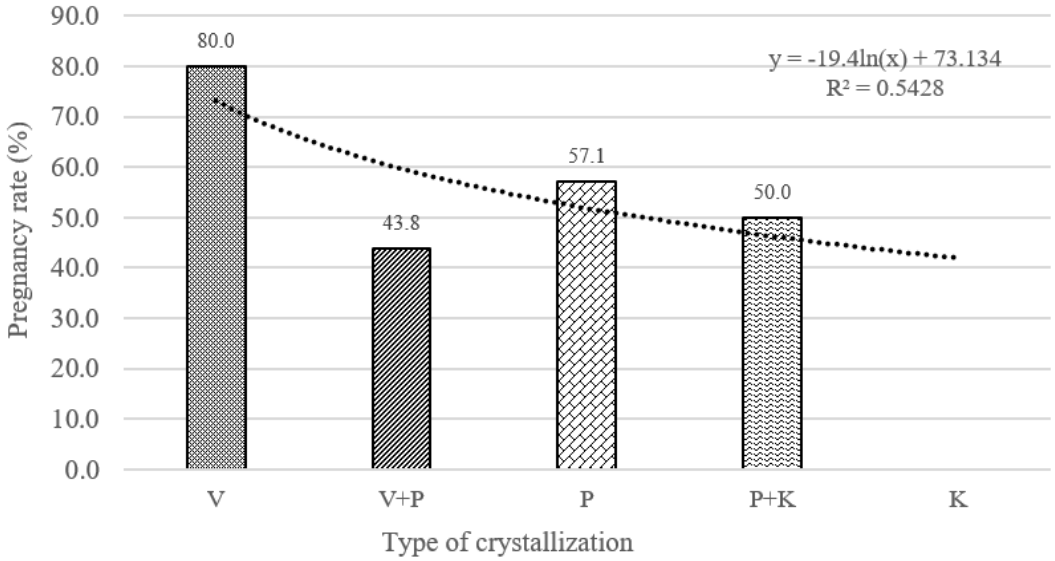

The overall rate of pregnancy rate after insemination was 54.9% (28 pregnancies out of 51 inseminated). This is below average, compared to the average of 60% reported by Kuchtík et al. (2007).

CONCLUSION

In this research, it was found that the type of crystallization of cervical mucus at the time of insemination had a conclusive effect on the subsequent pregnancy values. Animals with type "V" crystallization had the highest values of pregnancy and animals with atypical type "C" crystallization had the lowest values.

The most common types of crystallization in the animals studied were the "V" type and the mixed "V"+"P" form. These forms occur in cattle in the pre-estrus and early estrus. In relation to the temporal sequence of changes in crystallization patterns reported in cattle, these values are opposite, with a decreasing trend in the values of pregnancy.

The resulting values for the different types of crystallisations differ from those reported for cattle. To obtain more accurate results, it is necessary to repeat the experiment on a larger number of animals and to determine at what times during estrus the changes in each type of crystallisation occur and, in particular, whether the sequence of changes in crystallisation structures during estrus is identical to the results reported for cattle.

ACKNOWLEDGEMENTS

The research was financially supported by the grant no. AF-IGA2021-IP093.

REFERENCES

Čunát, L. et al. 2013. Využití inseminace ovcí v chovatelské praxi, 1st ed., Praha: Česká zemědělská univerzita.

Cortés, M.E. et al. 2014. Crystallization of Bovine Cervical Mucus at Oestrus: An Update. Revista de Medicina Veterinaria, 28(28): 103–108.

Eppleston, J., Maxwell, W.M.C 1995. Sources of variation in the reproductive performance of ewes inseminated with frozen-thawed ram semen by laparoscopy. Theriogenology, 43(4): 777–788.

Fonseca, J.F. et al. 2017. Evaluation of cervical mucus and reproductive efficiency of seasonally anovular dairy goats after short-term progestagen-based estrous induction protocols with different gonadotropins. Reproductive Biology, 17(4): 363–369.

Gimenez, D., Rodning, S. 2007. Reproductive Management of Sheep and Goats. Alabama A&M and Auburn Universities [Online]. Available at: https://ssl.acesag.auburn.edu/pubs/docs/A/ANR-1316/ANR-1316-archive.pdf. [2021-08-02].

Gonçalves, A.S. et al. 2020. Saliva Crystallization in Sheep Subjected to Estrus Induction and Synchronization Protocols. Acta Scientiae Veterinariae, 48(1): 1719.

Ježková, A. et al. 2007. Study of cervical mucus crystallization, sperm survival in cervical mucus and reproductive results of Holstein cows. In Proceedings of 58th Annual Meeting of the European Association for Animal Production. Ireland, 26–29 August. Dublin, pp. 235–235.

Ježková, A. et al. 2008. Factors affecting the cervical mucus crystallization, the sperm survival in cervical mucus, and pregnancy rates of Holstein cows. Journal of Central European Agriculture, 9(2): 377–384.

Kuchtík, J. et al. 2007. Chov ovcí. 1st ed., Brno: Mendelova zemědělská a lesnická univerzita v Brně.

Leethongdee, S. 2010. Development of trans-cervical artificial Insemination in sheep with special reference to anatomy of cervix. Suranaree Journal of Science and Technology, 17(1): 57–69.

Maddison, J.W. et al. 2017. Oestrus synchronisation and superovulation alter the cervicovaginal mucus proteome of the ewe. Journal of Proteomics, 155(1): 1–10.

Romano, J.E. 2021. Hormonal Control of Estrus in Goats and Sheep. MSD Manual: Veterinary Manual [Online]. Available at: https://www.msdvetmanual.com/management-and-nutrition/hormonal-control-of-estrus/hormonal-control-of-estrus-in-goats-and-sheep. [2021-08-01].

Stádník, L. et al. 2013. Stanovení vlivu krystalizace a metabolických indikátorů cervikálního hlenu na přežitelnost spermií u skotu, Výzkumný ústav pro chov skotu: Česká zemědělská univerzita v Praze.

Štolc, L. et al. 2007. Základy chovu ovcí. 3st ed., Praha: Ústav zemědělských a potravinářských informací.

Whitley, N.C., Jackson, D.J. 2004. An update on estrus synchronization in goats: A minor species. Journal of Animal Science, 82(13): 270–276.

Effect of storage and preincubation on hatching egg quality and hatchability in meat type chicken

Martina Pesanova Tesarova[1], Martina Lichovnikova[1], Marian Foltyn[2]
[1]Department of Animal Breeding
Mendel University in Brno
Zemedelska 1, 613 00 Brno
[2]Vykrm Trebic, s.r.o.
Karlov 196, 28401 Kutna Hora
CZECH REPUBLIC

martina.tesarova@mendelu.cz

Abstract: The aim of the study was to evaluate the effect of hatching eggs storage and their preincubation on eggs quality, hatchability and one-day old chick weight in young meat-type ROSS 308 parent stock, 31 weeks of age. Total of 1920 hatching eggs were used in this experiment for incubation, for egg quality analysis. Eggs were divided into three groups and stored for 21 days. Group P0 was not treated by preincubation. Group P1 contained hatching eggs which were preincubated once at the fifth of storage. Group P2 contained hatching eggs which were preincubated at days 5 and 10 during storage period. Egg quality was analysed for fresh eggs too. Long storage and repeated preincubation decreased both egg weight and yolk dry matter ($P < 0.05$). After application of preincubation, the degree of embryonic development significantly increased ($P < 0.05$). Preincubation and 21day storage of hatching eggs had no effect on hatchability and embryonic mortality. The weight of day-old chicks significantly decreased in chicks hatched form eggs twice treaded by preincubation.

Key Words: embryonic development, embryonic stage, broiler, quality of hatching eggs

INTRODUCTION

Long term storage has a negative effect on hatchability of chickens, increases embryonic mortality, especially early embryonic mortality (Fasenko et al. 2001), reduces the quality of one day-old chicks and their viability. Negative effects of long-term storage include increased hatching time (Tona et al. 2003), increased mortality after hatching (Yassin et al. 2008), impaired growth after hatching, which is reflected in reduced growth and quality during and at the end of fattening (Tona et al. 2004). The reduction in hatchability is around 0.2% per day up to 7 days of storage, after 7 days of storage the hatchability decreases by 0.5% (Yassin et al. 2008).

Storage temperatures must correspond to the so-called physiological zero, ie the temperature at which the embryo's ability to continue embryonic development is almost stopped (Funk and Biellier 1944). The way, to eliminate these negative consequences of long-term storage at least partially is the application of modern biotechnological methods, such as the method of preincubation hatching eggs. The preincubation of hatching eggs is carried out once or repeatedly during storage, the first preincubation is applied until the 7th storage, most often on the 5th day of storage. The principle of this method is to increase the temperature above physiological zero, preferably with the help of the Re-Store device (Fasenko 2001). Preincubation can also have a negative effect on the hatchability of chickens if the application of elevated temperature is longer than optimum and thus exceeds the stage of embryonic development 13 developmental stage according to the methodology of Eyal-Giladi and Kochav (1976), when the hypoblast is completely formed, in the next phase already forms the basis of the primitive strip (Fasenko et al. 2001, Tesařová 2018). When applying preincubation, it is therefore necessary to determine the stage of embryonic development before and after its application, so that the 13 developmental stage is not exceeded (Fasenko et al. 2001). Although preincubation has a positive effect on the hatchability of chickens with the correct application of preincubation, ie not exceeding 13 degrees of embryonic development according to the methodology of Eyal-Giladi and Kochav (1976), in some cases this positive effect is lost and hatchability is reduced. This negative effect occurred in long-term stored eggs that came from an older parent flock at 45 weeks of age. Hatching eggs which

were not preincubated before and during long-term storage showed 1.1% higher hatchability than eggs treated before and during long-term storage by preheating. The same parental flock at the age of 30 weeks responded to the application of preincubation before and during long-term storage by increasing the hatchability by 3.11% (Tesařová 2018). Reijrink et al. (2009) also reported that a parent flock of the Cobb 500 hybrid combination at 61 weeks of age showed that preincubation had a negative effect on stored eggs for 12 days, reducing hatching by 6.2%. On the contrary, a young parent flock at the age of 28 weeks showed a positive reaction to preincubation and subsequently to hatchability. Eggs stored 11 days after preheating were increased by 5.3% compared to the unpreincubated control.

The reduction in hatchability can be caused by cell death in a few processes, that take place inside the egg during long-term storage. These negative consequences can be caused by a change in the weight of the yolk and protein, thinning of the vitreous membrane of the yolk, weight loss of the egg, enlargement of the air chamber, and a rapid and high increase in pH of the white and yolk (Scott and Silversides 2000). Protein has an average value of 7.6 in fresh eggs, during long-term storage it can reach up to 9 (Lapão et al. 1999). During storage, the pH of the yolk also changes, although not as significantly as in the case of egg white. The pH value after laying in the yolk is approximately 6, it can reach values up to 6.8 pH (Kirunda and McKee 2000). The pH value of the yolk is affected not only by the storage time, but also by the storage temperature, the higher the temperature, the faster the pH rises (Jin et al. 2011). Increasing the weight of the yolk due to the migration of water from the protein further causes a thinning of the yolk vitreous membrane and a loss of elasticity due to which increases its susceptibility to mechanical damage Moran (1936).

MATERIAL AND METHODS

In a total 1920 hatching eggs of meat type hybrid ROSS 308 at the age 31 weeks were used in this study. Thirty fresh eggs (control group) were used for their quality measurements at the day, when they arrived to the hatchery. The rest of these eggs was divided into three groups and these eggs were stored 21 days prior incubation.

Group P0 was not treated by preincubation. Group P1 contained hatching eggs which were preincubated once at the fifth of storage. Group P2 contained hatching eggs which were preincubated at days 5 and 10 during storage period.

Hatching eggs were preincubated according to the standard Petersime program. This program heated hatching eggs to 95 °F and, after reaching this temperature, heated the hatching eggs for one hour. The temperature of the hatching eggs was monitored with Ovoscan. The storage temperature was 14 °C, humidity 70% and during storage the eggs were turned at hourly intervals at an angle of 90 °.

In each group eggs were sat in 11 trays, 60 eggs per 10 trays and one tray with 30 eggs. These thirty eggs in each group were used for egg quality measurements at 21st day of storage.

At day 7 of incubation, all hatching eggs were candled, and clear eggs were opened to macroscopically determine embryonic mortality and fertility; blastoderms and blastodics were differentiated. On hatching day, live hatched chicks were counted per basket. All unhatched eggs were opened to determine the stage of embryo mortality; early stage embryonic mortality to 9d of incubation (black eye visible, embryo without feathers), middle stage embryonic mortality 10-17d of incubation (small embryo with feathers), late stage embryonic mortality 18–21d (full grown embryo with yolk out or full grown embryo dead or alive with yolk subtracted). Because fertility was determined macroscopically, it is possible that an embryo that died during storage was classified as an infertile egg, therefore hatchability and embryonic mortality were calculated as a percentage of set eggs, where egg origin was the same for all treatments. One hundred randomly selected chicks per treatment were weighed.

Under egg quality following parameters were evaluated: egg weight, yolk weight, shell weight, shell thickness, egg shape index, eggshell strength, Haugh units, pH of yolk and white and dry matter of yolk and white. Furthermore, the degree of embryonic development of the eggs was evaluated.

Blastoderm from hatching eggs were isolated and subsequently determined according to the methodology for determining the degree of embryonic development Eyal-Giladi and Kochav (1976).

Observed characteristics were expressed by means and variability by standard error and coefficient of variability. The results for egg quality and incubation variables were analysed by ANOVA with a general linear model procedure (Unistat 5.1 software, UNISTAT Ltd, ENGLAND). Mean differences were tested using the LSD test.

RESULTS AND DISCUSION

The results show (Table1) that during long-term storage, the pH of the albumen increased and the quality of the white expesed by Haugh units decreases ($P < 0.05$). However preincubation did not have effect on white pH.

Table 1 Egg quality in fresh and 21 days stored eggs and stage of embryonic development

Monitored parameters	Experimental groups											
	P0 ($\bar{x}$)	SE	v_x	P1 $\bar{x}$	SE	v_x	P2 $\bar{x}$	SE	v_x	Control $\bar{x}$	SE	v_x
Weight of eggs	56.0^{b}	0.32	0.03	55.3^{ab}	0.48	0.05	54.9^{a}	0.51	0.05	57.8^{c}	0.72	0.05
Weight of yolk	16.5^{a}	0.17	0.05	16.7^{a}	0.20	0.06	16.8^{a}	0.23	0.07	16.4^{a}	0.20	0.05
Yolk dry matter	49.00^{b}	0.21	0.01	48.35^{b}	0.27	0.02	45.32^{a}	0.99	0.07	50.27^{c}	0.12	0.01
White dry matter	13.3^{a}	0.55	0.13	13.2^{a}	0.55	0.13	12.47^{a}	0.62	0.15	12.67^{a}	0.24	0.06
pH of yolk	6.29^{a}	0.03	0.02	6.5^{c}	0.05	0.04	6.38^{b}	0.04	0.03	6.3^{ab}	0.05	0.04
pH of white	9,1^{b}	0.01	0.01	9.1^{b}	0.01	0.01	9.1^{b}	0.02	0.01	9.06^{a}	0.03	0.01
Eggshell strength	35.2^{b}	0.74	0.11	35.2^{b}	0.83	0.12	34.3^{ab}	1.05	0.15	32.5^{a}	1.29	0.17
Eggshell thickness	0.5^{a}	0.01	0.06	0.5^{b}	0.01	0.00	0.5^{b}	0.01	0.05	0.5^{b}	0.01	0.05
Eggshell weight	5.4^{a}	0.19	0.18	5.29^{a}	0.09	0.09	5.1^{a}	0.07	0.07	5.1^{a}	0.09	0.08
Egg shape index	80.2^{a}	0.44	0.03	79.9^{ab}	0.38	0.02	80.1^{b}	0.59	0.04	79.0^{a}	0.68	0.04
HU	80.5^{a}	0.91	0.06	83.18^{b}	1.05	0.07	81.7^{ab}	0.96	0.06	96.8^{c}	0.77	0.03
Stage of embryonic development	10^{a}	0	0	10.3^{b}	0.09	0.05	11.5^{c}	0.19	0.07	10^{a}	0	0

Legend: SE – standard error of the mean, v_x – coefficient of variation, a,b,c – means in the same row designated by different letters are significantly different ($P < 0.05$), P0 is the mean for the group that was stored, P1 is the mean for the group that was stored and preincubated (1x), P2 is the mean for the group that was stored and preincubated (2x)

These data are consistent with the results of Lapão et al. (1999), which state that overall, albumen pH increased from 8.20 to 9.15 in eggs stored between 0 and 8 day, but most of this increase occurred during the first 4 d of storage. These results are confirmed by the results of Tona et al. (2004) who also report a reduction in HU after long-term storage.

Alsobayel et al. (2017) report that long-term storage (15 days) increased the yolk pH from 6.10 to 6.36. The results in this experiment show that the yolk pH of the control group was 6.3 and of P0 6.29, without significant difference. Preincubation significantly increased yolk pH in groups P1 and P2 compared with P0 ($P < 0.05$).

The weight of the eggs decreased after the application of long-term storage and pre-incubation ($P < 0.05$), and these results agree with the results of Khan et al. (2014), who report that the weight of hatching eggs from RIR decreased after 9 days of storage from 44.7 to 43.63 g.

In the yolk, there was a slight increase in weight in groups P0, P1 and P2 compared to the control group. Khan et al. (2014) report an increase in yolk weight after 9 days of storage from 15.90 to 17.27 g.

Due to the migration of water from the white to the yolk during long-term storage, the vitelline membrane is mechanically stretched and its elasticity is reduced (Moran 1936). Due to the increase in water in the yolk, the dry matter content of the yolk decreases and the dry matter in the barrel increases. In this experiment, the dry matter of the white increased from 9.06% to 9.01% and the dry matter of the yolk decreased from 50.27% to 49.0% for group P0, 48.35% for P1 and 45.32% for P2 ($P < 0.05$).

After preincubation, the degree of embryonic development shifted in both groups ($P < 0.05$). Similar data were concluded by Tesařová (2018), who determined stage of embryonic development

in hybrid meat type ROSS 308 at the age of parent flocks 30, 45 and 58 weeks. Most fertilized eggs were stage X, but stage XI eggs were observed in all three groups.

Table 2 Hatchability, embryonic mortality and weight day-old chick

Monitored parameters	Experimental groups								
	P0 $\bar{x}$	SE	v_x	P1 $\bar{x}$	SE	v_x	P2 $\bar{x}$	SE	v_x
Hatchability	88.8[a]	1.91	0.07	87.1[a]	1.12	0.04	87.2[a]	1.08	0.04
Early embryonic mortality	7.3[a]	1.4	0.6	7.7[a]	0.7	0.3	7.4[a]	1.11	0.47
Middle embryonic mortality	1.0[a]	0.37	1.16	1.5[a]	0.46	0.96	1.0[a]	0.45	1.4
Late embryonic mortality	3.2[a]	0.78	0,77	3.7[a]	0.89	0.75	4.4[a]	0.44	0.32
Weight of day-old chick	39.1[b]	0.22	0.06	38.9[ab]	0.24	0.06	38.6[a]	0.24	0.06

Legend: SE – standard error of the mean, v_x – coefficient of variation, a,b – means in the same row designated by different letters are significantly different (P <0.05), (P <0.05), P0 is the mean for the group that was stored, P1 is the mean for the group that was stored and preincubated (1x), P2 is the mean for the group that was stored and preincubated (2x)

Preincubation (Table 2) had no significant effect on the hatchability of chickens compared to the non-preincubated group. The same result was achieved by Tesařová (2018) in chickens at the age of the parent flock of 45 weeks.

The weight of day-old chicks decreased in both groups to which preincubation was applied. These results correspons with Tona et al. (2004), who also reported reduced chicken weight after long-term storage. The weight reduction of day-old chicks is also reported by Khan et al. (2014). In their experiment, the weight was reduced from 30.46 g to 29.89 g after 9d storage hatching eggs from RIR (rhode islands red).

CONCLUSION

Long storage and repeated preincubation decreased both egg weight and yolk dry matter (P <0.05). After application of preincubation, the degree of embryonic development significantly increased (P <0.05). Preincubation and 21day storage of hatching eggs had no effect on hatchability and embryonic mortality. The weight of day-old chicks significantly decreased in chicks hatched form eggs twice treaded by preincubation.

ACKNOWLEDGEMENTS

The research was financially supported by the grant no. AF-IGA2021-IP027.

REFERENCES

Alsobayel, A.A. et al. 2017. Effects of Preincubation Storage Length and Egg Quality of Baladi Hatching Eggs on Hatchability Parameters. International Journal of Agriculture Innovations and Research, 5(5): 877–881.

Eyal-Giladi, H., Kochav, S. 1976. From Cleavage to Primitive Streak Formation: A Complementary Normal Table and a New Look at the First Stages of the Development of the Chick. Developmental Biology, 49(2): 321–337.

Fasenko, G.M. et al. 2001. Prestorage Incubation of Long-Term Stored Broiler Breeder Eggs: 1. Effects on Hatchability. Poultry Science, 80(10): 1406–1411.

Funk, E.M., Biellier, H.V. 1944. The Minimum Temperature for Embryonic Development in the Domestic Fowl (Gallus domesticus). Poulty Science, 23(6): 538–540.

Jin, Y.H. et al. 2011. Effects of Storage Temperature and Time on the Quality of Eggs from Laying Hens at Peak Production. Asian–Australasian Journal of Animal Sciences, 24(2): 279–284.

Khan, M.J.A. et al. 2014. The effect of Storage Time on Egg Quality and Hatchability Characteristics of Rhode Island (RIR) Hens. Veterinarski Archiv, 84(3): 291–303.

Kirunda, D.F.K., Mckee, S.R. 2000. Relating Quality Characteristics of Aged Eggs and Fresh Eggs to Vitelline Membrane Strength as Determined by a Texture Analyzer. Poultry Science, 79(8): 1189–1193.

Lapão, C. et al. 1999. Effects of Broiler Breeder Age and Length of Egg Storage on Albumen Characteristics and Hatchability. Poultry Science, 78(5): 640–645.

Moran, T. 1936. Physics of the Hen's Egg. II. The Bursting Strength of the Vitelline Membrane. Journal of Experimental Biology, 13(1): 41−47.

Reijrink, I.A.M. et al. 2009. Influence of Prestorage Incubation on Embryonic development, Hatchability, and Chick Quality. Poultry Science, 88(12): 2649–2660.

Scott, T.A., Silversides, F.G. 2000. The Effect of Storage and Strain of Hen on Egg Quality. Poultry Science, 79(12): 1725–1729.

Tesařová, M. 2018. Vliv preinkubace vajec během dlouhodobého skladování na líhnivost kuřat masného typu. Diploma thesis (in Czech), Mendel University in Brno.

Tona, K. et al. 2003. Effects of Egg Storage Time on Spread of Hatch, Chick Quality, and Chick Juvenile Growth. Poultry Science, 82(5): 736–741.

Tona, K. et al. 2004. Effect of Age of Broiler Breeders and Egg Storage on Egg Quality, Hatchability, Chick Quality, Chick Weight and Chick Posthatch Growth to Forty-Two Days. Journal of Applied Research, 13(1): 10–18.

Yassin, H. et al. 2008. Field Study on Broiler Eggs Hatchability. Poultry Science, 87(11): 2408–2417.

Evaluation of Holstein cows originated from embryo transfer

Marketa Popelkova, Radek Filipcik, Tomas Kopec, Zuzana Reckova
Department of Animal Breeding
Mendel University in Brno
Zemedelska 1, 613 00 Brno
CZECH REPUBLIC

popelkovamarketa@seznam.cz

Abstract: Embryotransfer (ET) is used in reproduction worldwide. This thesis deals with the evaluation of milk yield at Holstein cows that were from ET. This evaluation was done by performed flushes and transferring the offspring, born and included in the breeding during the years 2015 and 2016. All data for the experiment evaluation was obtained from an agricultural cooperative, which has three farms located in the region Pardubice. For statistical analysis of the data, we used multifactor analysis of variance. In 2015, 14 donor cows were flushed. A total of 212 embryos were obtained from which 113 embryos could be used. In 2016, 19 donor cows were flushed and 241 embryos were obtained, but only 113 embryos met the criteria. In the experiment, we evaluated the performance of daughters from embryo transfer and compared their performance with their peers (not from ET) born in the same stable and the same years. Performance evaluation was obtained during the first and second lactation. From the results, where the production performance is compared, it is evident that there was no statistically significant different production difference between dairy cows from ET and their peers.

Key Words: embryo transfer, Holstein cows, donors, reproduction, milk yield

INTRODUCTION

Embryotransfer (ET) is used worldwide. In the context of dairy cows, it is commonly used as a tool for genetic improvement. In addition, ET can be used to increase the reproductive efficiency of herds, especially among cows that live in specific physiological conditions such as heat stress (Oliveira 2016). Embryotransfer has multifaceted and broad importance. It is still a popular technique in cattle breeding that achieves top performance (Ježková 2020). It interferes with the reproduction and breeding of cattle (Vaněk et al. 2002). For all livestock species, the result of embryo transfer depends mainly on the quality of the recipients and the quality of the embryo. If the embryo meets the morphological criteria, it can be referred to as usable embryo. In terms of dairy breeds, heifers are declared to be better recipients than cows, especially for their easy manipulation or frozen embryos (embryos obtained from cryopreservation process). This statement can be partly explained by the fact that heifers have a higher concentration of progesterone in the blood (Machaty et al. 2012). Biological reproduction procedures that are based on embryo transfer have in particular a significant increase in the number of oocytes that ovulate and can be subsequently fertilized. This makes it possible to obtain a larger number of calves that a cow can produce in one year (Ježková 2019).

Embryotransfer offers the breeder the acquisition of more offspring from a particular cow (Ježková 2020). It enables the production of meat breeds from dairy cows in a relatively short time and the acquisition of a purebred herd of a specific breed (Vaněk et al. 2002). Embryotransfer allows us to produce offspring of the desired sex. It is used to produce calves from genetically valuable parents. Another advantage of ET is also that we can obtain offspring from infertile mothers (Jakubec et al. 2012).

MATERIAL AND METHODS

All data for the experiment evaluation was obtained from an agricultural cooperative, which has three farms located in the region Pardubice. The company manages 3,000 ha of agricultural land in 14 cadastral areas over an altitude of 450 meters above sea level. The evaluation of embryo transfer was performed on data from the years 2015 and 2016. Among donors, the number of usable embryos and the number of transferred and frozen embryos were monitored too. Additionally, we monitored

the attachment of the embryos and the number of born calves. Dairy cows that were selected as donors achieved three lactations. As a result, they produced 12,819 kg of milk. The fat content was around 3.99% and the protein content was around 3.21%. The fat content in kg was 509 kg and the protein content was 410 kg.

In the second part of the experiment, we evaluated the performance of daughters from embryo transfer and compared their performance with their peers born in the same stable and the same years. Performance evaluation was obtained during the first and second lactation. The main utility parameters that were monitored are the efficiency during lactation with the protein and fat content in relative and absolute terms.

For statistical analysis of the data, we used multifactor analysis of variance available in program STATISTICA 12.0.

RESULTS

Table 1 evaluated the effect of embryo transfer on milk yield. The milk content from ET dairy cows averaged 11,445 ± 2,634 kg. For peers cows, the values averaged 11,214 ± 2,311 kg. There was no statistically significant ($p > 0.05$) difference between dairy cows. The fat content from ET dairy cows averaged 3.98 ± 0.41%. For their peers, the values ranged on average 3.98 ± 0.39%. No statistically significant ($p > 0.05$) difference was found in fat content (kg). The values for dairy cows from ET averaged 452 ± 98.81 kg. The values from peers were the same, with a fat content averaging 452 ± 56.88 kg.

There was no statistically significant ($p > 0.05$) difference in milk production between dairy cows derived from ET and their peers (Table 2). It was also proven that there is no significant difference in relative and absolute milk fat content. Dairy cows from ET produced an average of 11,150 ± 2,774 kg of milk, which is on average about 1 066 kg more than the production from their peers. Peers produced an average of 10,084 ± 2,689 kg of milk. Regarding the fat content from ET dairy cows, the values ranged from 3.79 ± 0.33 %. The fat content of their peers was almost comparable to 3.78 ± 0.36%. The absolute fat content from ET dairy cows was 420 ± 99.70 kg. The values of their peers were 41 kg lower (379 ± 100.23 kg). The values in ET dairy cows averaged 3.35 ± 0.19% and their peers had a protein content of 3.35 ± 0.20% in milk. Higher absolute protein content (374 ± 93.38 kg) was demonstrated in ET dairy cows. Their peers produced 337 ± 88.44 kg of proteins during lactation. There was no statistically significant ($p > 0.05$) difference between the monitored protein contents. The amount of protein in ET dairy cows reached a similar average of 3.27 ± 0.17% as in contours on average 3.27 ± 0.21%. The average protein content of dairy cows from ET was 373 ± 80.84 kg, the average protein content of their peers was 374 ± 53.51 kg. The higher absolute protein content (374 ± 93.38 kg) was demonstrated at ET dairy cows. Their peers produced 337 ± 88.44 kg of proteins during lactation.

Table 1 Comparison of performance between dairy cows from ET and their peers born in 2015, 2016

Cows	Number	Milk (kg)	Fat (%)	Fat (kg)	Protein (%)	Protein (kg)
From ET	43	11 445 ± 2 634	3.98 ± 0.41	452 ± 98.81	3.27 ± 0.17	373 ± 80.84
peers	42	11 214 ± 2 311	3.98 ± 0.39	452 ± 56.88	3.27 ± 0.21	374 ± 53.51

Table 2 Comparison of performance between dairy cows from ET and their peers born in 2016, 2017

Cows	Number	Milk (kg)	Fat (%)	Fat (kg)	Protein (%)	Protein (kg)
From ET	38	11 150 ± 2 774	3.79 ± 0.33	420 ± 99.70	3.35 ± 0.19	374 ± 93.38
peers	38	10 084 ± 2 689	3.78 ± 0.36	379 ± 100.23	3.35 ± 020	337 ± 88.44

DISCUSSION

From 1992 to 2009, the author Doormaal (2013) followed the growth trend in the number of embryos obtained from donors. He stated that 10 or more embryos can be obtained from one donor. Doormaal (2017) stated that it was possible to obtain 20 or more embryos per flush from some individuals. The results of this work agree with the author. In our work we obtained around 20 or more embryos from one donor which is comparable to the xpextation. Hasler (2014), in his study, reported that it is possible to obtain 6 embryos by a single flush from only a single donor. The total obtained

number of embryos can affect the age of the donor, which according to the author should be within 8 months.

From the results shown in tables 1 and 2, where the production performance is compared, it is evident that there was no production difference between dairy cows from ET and their peers. Their values in milk, fat, and protein production were similar. A smaller difference was recorded in Table 4, where 11,150 kg of milk was obtained from dairy cows from ET and 10,084 kg of milk were obtained from their peers. The other values of milk components don't differ. The author Szabari (2009) stated in his work that there was a smaller difference in milk production between dairy cows that are from ET and are not from ET. Dairy cows from ET produced an average of 8,762 kg and their peers produced an average of 8,419 kg of milk. Furthermore, in his publication, the author stated that most dairy cows from ET reach a maximum of 2 lactations and then they are excluded for health reasons. Szabari et al. (2008) report that in dairy cows derived from ET, milk, fat, and protein production tended to exceed their contour lines.

CONCLUSION

When evaluating the quality of Holstein cows, which came from ET, we found that it was possible to obtain 25 or more embryos from some donors. A higher number of embryo attachments was recorded in immediately transferred embryos. A lower number of attachments was seen after the transfers of frozen embryos. Heifers predominated in the number of live births and in the sex ratio.

The subsequent evaluation was based on a comparison of the performance of daughters who came from ET with their peers. There was no significant difference in the effect of lactation order on the performance of dairy cows in the first and second lactation. Dairy cows produced slightly more milk on the second lactation than on the first lactation. The fat content in % was higher on the first lactation compared to the second lactation. The protein content in % in dairy cows at the first and second lactation did not differ significantly. It can be stated that dairy cows on both, the first and the second, lactations achieved high production.

When comparing dairy cows that came from ET with their peers, milk yield doesn't differ significantly. Dairy cows from ET were as productive as their peers. A smaller difference was found when dairy cows from ET had slightly higher milk production. The content of milk components of fat and protein was balanced between both dairy cows.

REFERENCES

Doormal, V.B. 2013. Embryo Transfer Activity in Canadian Holsteins [Online]. Available at: https://www.cdn.ca/document.php?id=299. [2021-07-15].

Doormal, V.B. 2017. Embryo Transfer Activity in Canada: A Snapshot Look [Online]. Available at: https://www.cdn.ca/document.php?id=484. [2021-07-15].

Hasler, F.J. 2014. Forty years of embryo transfer in cattle: A review focusing on the journal Theriogenology, the growth of the industry in North America, and personal reminisces. Theriogenology, 81(1): 152–169.

Jakubec, V. et al. 2012. Šlechtění a management genetických zdrojů zvířat. Rapotín: Agrovýzkum.

Ježková, A. 2019. Reprodukční technologie u hospodářských zvířat fungují. Náš chov, 6: 51–52.

Ježková, A. 2020. Inseminace a embryotransfer– běžné biotechnologie v reprodukci. Náš chov, 6: 42–43.

Machaty, Z. et al. 2012. Production and manipulation of bovine embryos: Techniques and Terminology. Theriogenology, 78(5): 937–950.

Oliveira, L.H. et al. 2016. Short communication: Follicle superstimulation before ovum pick-up for in vitro embryo production in Holstein cows. Journal of Dairy Science, 99(11): 9307–9312.

Szabari, M. et al. 2008. Az Embryó – átültetés Hatása a Holstein- Fríz Fajta Tenyésztésére, 4(2): 202–208.

Szabari, M. 2009. Az embrió-átültetés hatása a hazai holstein-fríz tenyésztésében. PhD disertion, Aposvári Egyetem Állattydományi Kar Nagyállattesztés És Termeléstechnologiai Tanszék.

Vaněk, D. et al. 2002. Chov skotu a ovcí. 1. ed., Praha: Česká zemědělská univerzita.

Condition of honeybee colonies overwintered with winter stores enriched by extracts of polypore mycelia

Jan Prouza, Jan Musila, Antonin Pridal
Department of Zoology, Fisheries, Hydrobiology and Apidology
Mendel University in Brno
Zemedelska 1, 613 00 Brno
CZECH REPUBLIC

apridal@mendelu.cz

Abstract: The health of honeybees is current issue namely due to colony collapse disorder. The presence of healthy long-living honeybees is necessary for successful overwintering of the colony. However, vitality of the honeybees is threatened by the synergy of pathogens, pesticides and malnutrition. It was found that mushroom extracts decrease honeybee viral load. We tested a potential of the mycelial extracts (*Fomes fomentarius*, *Ganoderma lucidum*) as additive in winter stores for improving of the overwintering. Treated colonies showed a slight tendency to overwinter in stronger condition. The possible effects of tested mycelial extract are discussed.

Key Words: Fomes fomentarius, *Ganoderma lucidum*, *Apis mellifera,* supplementation, colony growth

INTRODUCTION

Studies about the positive effect of mushroom extracts on honeybees have been published recently. After feeding the mushroom supplement the colonies became stronger (brood rearing, adult population growth) (Pătruică et al. 2017, Stevanovic et al. 2018), the bees lived longer (Parish et al. 2020), the *Nosema ceranae* infection was reduced (Glavinic et al. 2021) and in the case of *Zygosaccharomyces* sp., this yeast is considered to be a source of essential ergosterol important for larval metamorphosis (Paludo et al. 2018). It was found the fungicides can reduce diversity of fungi in bee bread. Following this, there arose suggestion that any substances from fungi can lack in bee bread (Yoder et al. 2013).

In winter, the survival of honeybee colony is particularly dependent on the longevity of bees (Döke et al. 2015) while viral infections are considered to be one of the causes of the colony collapses (McMenamin and Genersch 2015). Evidence that ethanol extracts from mycelia of Polyporales reduce viral load in honeybees and increase their lifespan is therefore particularly interesting (Stamets et al. 2018, Stamets 2020).

The promising effects of mycelial extracts from Polyporales have not been tested in wintering colonies yet because the antiviral effects were tested only in cage experiments and in 12-day summer experiment in the nucleus colonies (Stamets et al. 2018, Stamets 2020) and effects on the longevity were tested only in cage experiments (Stamets 2020).

Towards beekeeping practice, it is desirable to prove the potential benefit of mushroom supplements. The aim of this experiment was to test the effect of the polypore mycelial extract added to the winter colony stores on colony overwintering and early spring growth.

MATERIAL AND METHODS

Preparation of mycelial extract

The mycelial extract was prepared from *Fomes fomentarius* (collected as the basidiocarp in a birch forest Kurimska Nova Ves, Czech Republic 49°20′52″N, 16°17′6″E) and from *Ganoderma lucidum* (purchase as mycelium from Dipl.-Ing. N. Krämer, Hannover, https://shii-take.de). Cultivation and extraction procedure was carried out according the method by Stamets et al. (2018) as described in Prouza et al. (2020).

Field experiment groups of colonies settings

There were six experimental and six control colonies of *Apis mellifera* in comparable condition in the experiment. The condition for the selection of colonies was assessed on a subjective scale of 1–5 grades reflecting a strength of colony (1 = very weak, 2 = weak, 3 = medium, 4 = strong, 5 = very strong colony). This and other subjective evaluations of the experiment were always performer by the same person. Four medium, one weak and one strong colony formed the experimental or control group. All colonies were of the same origin (inseminated queens, Vigor® strain).

In the late summer, winter stores of colonies were supplemented by feeding of sucrose syrup (3:2 sucrose/water, w/w). In total, 16.5 kg of sucrose per colony was fed in three partial doses during the second half of July 2019. In contrast to the control colonies, the doses of sucrose syrup for experimental colonies were enriched by one or two percent (v/v) of the extract from *F. fomentarius* or *G. lucidum* (colonies with ME). Specifically, doses of syrup fed to experimental colonies contained mycelial extract in the following proportions: 1st dose – *F. fomentarius* extract (1%), 2nd dose – 4/5 *F. fomentarius* extract and 1/5 *G. lucidum* extract (1%), 3rd dose – *G. lucidum* extract (2%).

Evaluation of the colony condition during field experiment

The evaluation was performed in as short as possible time interval in the morning as long as the honeybees were predominantly inside the hive to prevent recording of differences caused by increasing of temperatures. The early spring condition was assessed on 18th March 2020. The parameter "condition after winter" reflects the subjective evaluation of colony strength after overwintering on a scale of 1–10 grades (zero is given for dead colony). Colonies can be divided according to this scale as follows: Grade 1–3 (very weak colonies without growth potential and with less than three occupied frames), grade 4 and 5 (weak colonies with substandard growth), grade 6 and 7 (colonies in good condition with standard growth), grade 8–10 (strong colonies with above-standard growth). Besides condition after winter, other partial parameters were evaluated. Namely the rest of winter stores in kilograms, the number of occupied supers and frames (gaps among frames), the number of brood frame, the area of brood in square decimetres and number of extremely weakened colonies which had to be shrunk.

The spring condition was assessed on 22nd April 2020, i.e. at the cherry florescence. Spring growth was evaluated, i.e. the overall subjective impression of the spring growth colony condition that was classified using the same subjective ten-point scale as in the early spring. In addition to the spring growth, other parameters were also evaluated such as the number of occupied frames, the number of brood frames and the area of brood in square decimetres again.

Statistical evaluation

Condition and partial parameters of colonies in early spring and spring were always averaged within a specific parameter, separately for the group of colonies with ME and for the group of control colonies. The deviations given correspond to the standard error of the mean. Student´s t-test (two-sided division, two-sample with equal variance) was always used to compare the experimental and control group of colonies in a specific parameter. Differences with a p-value above 0.05 ($p > 0.05$) were considered statistically insignificant.

RESULTS

All colonies overwintered successfully. Colonies supplemented with the mycelial extract (ME) showed the average value of the condition after winter and the spring growth slightly higher compared to the control colonies wintering without the addition of ME in winter stores (Figure 1, Figure 2). The differences were statistically insignificant ($p_{\text{condition after winter}} = 0.157$ a $p_{\text{spring growth}} = 0.088$). The specific distribution of condition after winter and spring growth values for individual colonies is depicted in Figure 3. Some tendency towards better overwintering is more pronounced for colonies with ME here. The colonies with ME are accumulated more in the left while the control colonies are predominantly in the right part of the figure.

Some of the partial parameters in early spring showed statistically significant differences. Colonies with ME occupied on average more frames ($p = 0.043$) and supers ($p = 0.01$), on the contrary, these colonies had less rest of winter stores after winter ($p = 0.035$). Other parameters were not

statistically significant. The area of the brood was insignificantly larger in colonies with ME in early spring (p = 0.141) and during spring growth (p = 0.467). Colonies with ME also reared insignificantly fewer brood frames in early spring (p = 0.667), but these colonies had already more of it during spring (p = 0.57). In contrast to the control colonies, colonies with ME were not shrunk in early spring (p = 0.145) and during the spring growth occupied insignificantly more frames (p = 0.061).

Figure 1 Condition and partial parameters of colonies in early spring, average values

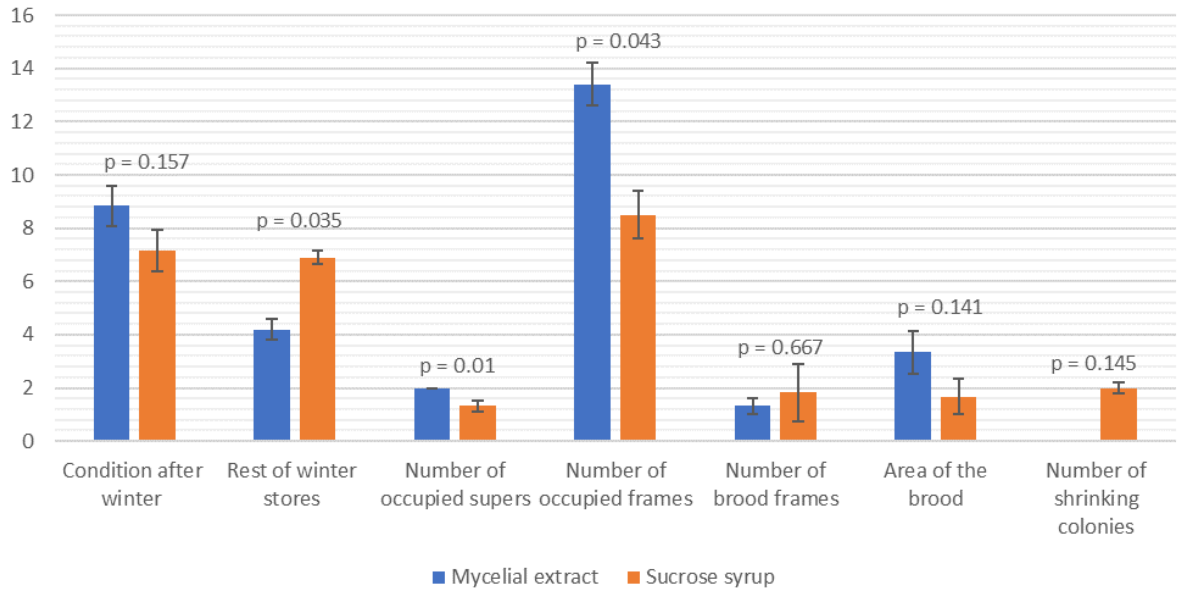

Legend: Blue colour represents colonies with ME, control colonies are in orange.

Figure 2 Condition and partial parameters of colonies in spring, average values

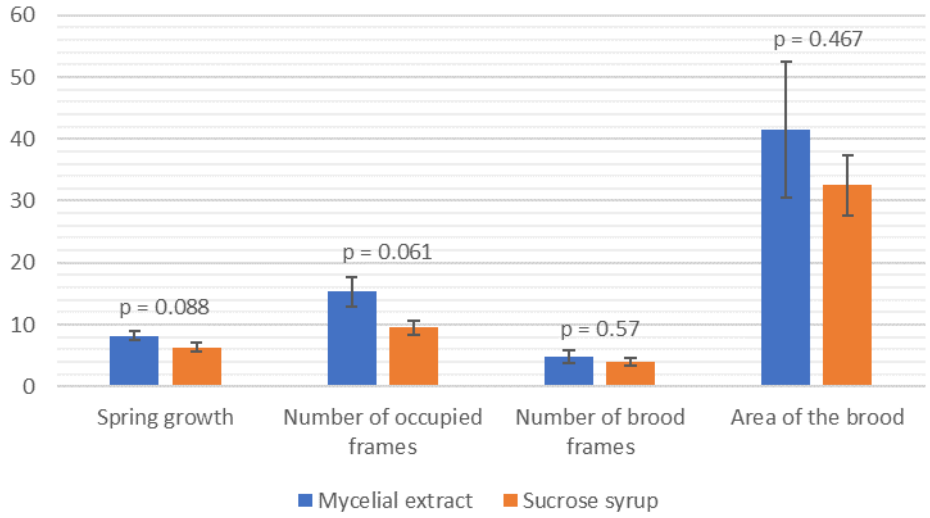

Legend: Blue colour represents colonies with ME, control colonies are in orange.

DISCUSSION

The results suggest that the addition of ME to winter stores of colonies can positively affect colony strength in early spring and spring. It is in agreement with a similar experiment where increased colony strength was observed after *Agaricus brasiliensis* extract treatment (Stevanovic et al. 2018). However, it has to be emphasized that no colony losses were observed at apiary that winter. Therefore, the expected beneficial effect of ME was not countered by other negative factors. Stronger colonies are more likely to overwinter successfully (Döke et al. 2015). Strong colonies resist cold weather better and can be more resistant to viral infections (Di Prisco et al. 2011). There can be no significant differences between colony strength and the prevalence or viral load (Cirkovic et al. 2018). The condition of the colony is not

only about its strength but also about the health of the colony which does not have to affect the number of honeybees in the colony just now. To what extent the tested ME affected the health or the number of honeybees remains a question. Previous studies about the effect of mushroom extracts on honeybees suggest both of these effects (Pătruică et al. 2017, Stamets et al. 2018, Stevanovic et al. 2018, Stamets 2020, Glavinic et al. 2021).

Figure 3 Condition of colonies during the field experiment, values of individual colonies in descending order of wintering

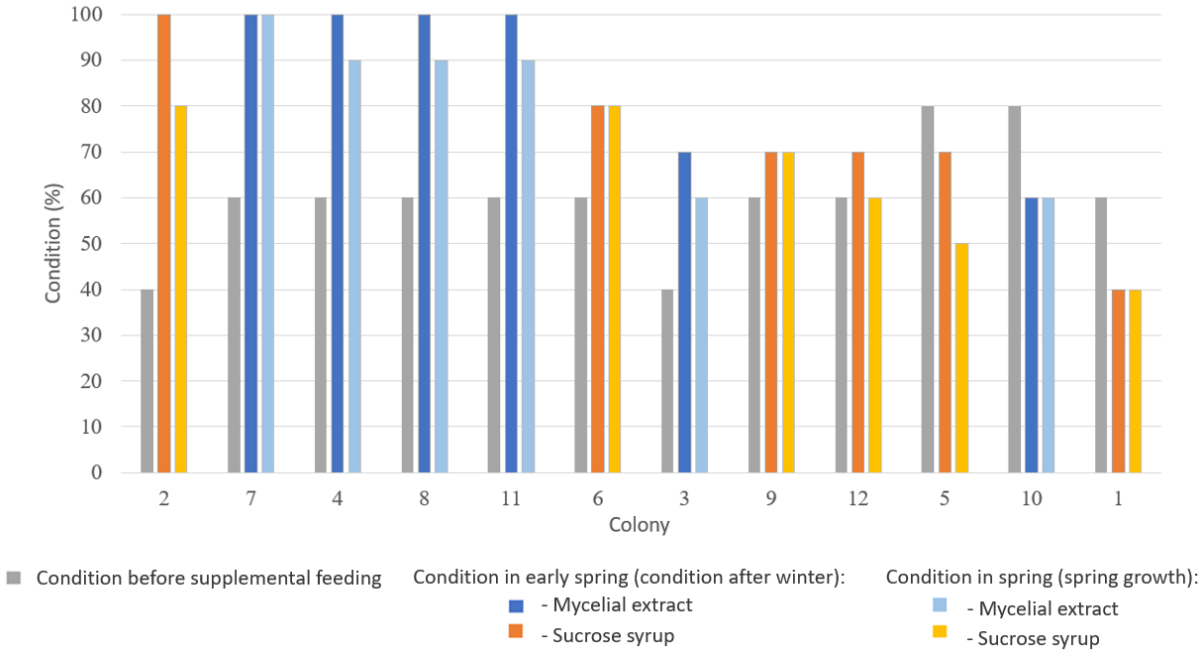

Legend: Shades of blue represent colonies with ME, control colonies are in shades of orange.

Similarly to the experiment by Prouza et al. (2020), Stevanovic et al. (2018) also did not observe any significant effect of their ME on prolongation of the lifespan in worker honeybees in cage experiment. In their experiment the positive effect of the extract on colony strength also was not apparent until the field experiment with colonies was carried out. This supports the hypothesis that the mushroom extracts could have a positive effect on the queen´s egg-laying (Pătruică et al. 2017). In early spring, when honeybee colony is still dependent on winter stores, the increase in brood rearing was more apparent in colonies with ME than in the spring when spring flow replace winter stores, i.e. the supply of ME.

The second point of view considers that ME positively affect honeybee health especially that reducing viruses in honeybees (Stamets et al. 2018) and increases bee´s lifespan at the same time (Stamets 2020). Due to viruses are common in honeybee colonies (Tentcheva et al. 2004, Cirkovic et al. 2018) and that temperature decline could lead to increase severity of the viral infection (Di Prisco et al. 2011), some interaction could have occurred during the winter. The toxicological question can also be considered if honeybees are exposed to pesticides which can have a negative effect on their health including reproduction (Chmiel et al. 2020). At the same time, there is a presumption that the mycelial extract could have a detoxifying effect (Stamets 2020). The mycelial extract could contribute to a re-increase in egg-laying, to return to a standard brood rearing and to increase lifespan of honeybees and thus to make the colonies stronger in general. The experimental colonies with ME showed statistically insignificant tendency to have more brood on fewer frames. Even this more compact structure could be an advantage for these colonies.

The effect of ME on honeybee nutrition is another question. It can be presumed that the lesser rest of the winter stores in early spring could be caused by higher consumption. If due to higher palatability or number of bees in colony is not clear.

CONCLUSION

Results of the field experiment suggest that colonies wintered with stores enriched by the polypore mycelium extracts overwintered in slightly better condition (number of bees and brood) compared with the control colonies. It was followed by better spring colony growth in experimental group too. The differences were with low or without statistical significance, therefore, the expected beneficial impact of polypore mycelial extract on the condition of overwintered honeybee colonies remains unconfirmed.

ACKNOWLEDGEMENTS

The research was financially supported from the donations by company elitbau, Ltd. We are grateful for consultations with Svetlana Gaperova (Dept. of Biology and Ecology, Matej Bel University in Banska Bystrica), Dagmar Palovcikova (Dept. of Forest Protection and Wildlife Management of Mendel University in Brno), and with Jan Mlecka (mushroom grower, Kurimska Nova Ves) about general details on laboratory cultivation of mushrooms and collection of biological material. We are grateful to Marketa Londynova (CEITEC MU Brno) and Ales Vladek (MENDELU) for technical assistance.

REFERENCES

Chmiel, J.A. et al. 2020. Understanding the effects of sublethal pesticide exposure on honey bees: A role for probiotics as mediators of environmental stress. Frontiers Ecology Evolution, 8: 22.

Cirkovic, D. et al. 2018. Honey bee viruses in Serbian colonies of different strength. PeerJ, 6(11): e5887.

Di Prisco, G. et al. 2011. Dynamics of Persistent and Acute Deformed Wing Virus Infections in Honey Bees, *Apis mellifera*. Viruses, 3(12): 2425–2441.

Döke, M.A. et al. 2015. Overwintering honey bees: Biology and management. Current Opinion in Insect Science, 10: 185–193.

Glavinic, U. et al. 2021. Potential of Fumagillin and Agaricus blazei mushroom extract to reduce *Nosema ceranae* in honey bees. Insects, 12(4): 282.

McMenamin, A.J., Genersch, E. 2015. Honey bee colony losses and associated viruses. Current Opinion in Insect Science, 8: 121–129.

Paludo, C.R. et al. 2018. Stingless Bee Larvae Require Fungal Steroid to Pupate. Scientific Reports, 8(1): 1122.

Parish, J.B. et al. 2020. Nutritional benefit of fungal spores for honey bee workers. Scientific Reports, 10(1): 15671.

Pătruică, S. et al. 2017. The effect of using medicinal plant extracts upon the health of bee colonies. Romania Biotechnological Letters, 22(6): 13182–13185.

Prouza, J. et al. 2020. Survival rate in the honeybee workers (Apis mellifera L.) additively fed with polypore mycelial extract. In Proceedings of International PhD Students Conference MendelNet 2020 [Online]. Brno, Czech Republic, 11–12 November, Brno: Mendel University in Brno, Faculty of AgriSciences, pp. 151–154. Available at: https://mnet.mendelu.cz/mendelnet2020/mnet_2020_full.pdf. [2021-09-04].

Stamets, P.E. 2020. Integrative fungal solutions for protecting bees. U.S. Patent 20200376055. Available at: https://patents.justia.com/patent/20200376055. [2021-09-01].

Stamets, P.E. et al. 2018. Extracts of Polypore Mushroom Mycelia Reduce Viruses in Honey Bees. Scientific Reports, 8(1): 1–6.

Stevanovic, J. et al. 2018. The effect of Agaricus brasiliensis extract supplementation on honey bee colonies. Anais da Academia Brasileira de Ciências, 90(1): 219–229.

Tentcheva, D. et al. 2004. Prevalence and seasonal variations of six bee viruses in *Apis mellifera* L. and *Varroa destructor mite* populations in France. Applied and Environmental Microbiology, 70(12): 7185–7191.

Yoder, J.A. et al. 2013. Fungicide contamination reduces beneficial fungi in bee bread based on an area-wide field study in honey bee, *Apis mellifera*, colonies. Journal of Toxicology and Environmental Health, 76(10): 587–600.

The effect of cumin (*Carum carvi* L.) on medium-slow growing chickens performance parameters

Michal Rihacek, Jakub Novotny, Lucie Horakova, Dana Zalesakova, Andrea Roztocilova, Eva Mrkvicova, Ondrej Stastnik, Leos Pavlata
Department of Animal Nutrition and Forage Production
Mendel University in Brno
Zemedelska 1, 613 00 Brno
CZECH REPUBLIC

xrihace2@mendelu.cz

Abstract: The aim of this study was to evaluate the effect of addition of cumin (*Carum carvi*) on broilers performance parameters. The male broiler chickens Hubbard JA 57 were used in the experiment and they were divided into two groups (Control and Cumin group). The control group was fed a diet without addition of *Carum carvi* and the Cumin group was fed a diet containing of 1% of *Carum carvi* in a diet. *Carum carvi* had positive influence on body weight of medium-slow growing chickens. Also, it was confirmed that dietary cumin addition affected the jejunum length and cecum weight of slaughtered chickens.

Key Words: Hubbard JA 57, poultry nutrition, *Carum carvi*, digestive tract

INTRODUCTION

Cumin (*Carum Carvi* L.) is an herb that is grown in West Asia, Europe and North America (Pourmortazavi et al. 2005). Nowadays the main producer of cumin is the Netherlands. It's also grown in Bulgaria, Canada, Germany, Great Britain, India, Morocco, Poland and United States (Weiss 2002).

This plant contains approximately 30 compounds (carvone and limonene represent about 95% of them). Cumin seeds contain trace amount of other compounds such as acetaldehyde, furfural, carveole, pinene, thujone, camphene, phellandrene, etc. The volatile oils are the main constituents of *Carum Carvi* including carvone (40–60%), limonene, carveol, dihydrocarveol and thymol in addition to glycosides and flavanoids. Furthermore, seeds contain 9–13% water, 13–21% fats, 25–36% nitrogen compounds, 5–10% of extractive nitrogen-free compounds, 13–19% of crude fibre, 5–7% of ash, 1.5% of waxes and small amount of tannins and resin (Špaldon et al. 1986). The current research trend is to find natural by-products of feed sources used as feed additives to increase feed efficiency and growth rate of broilers (Lee et al. 2004). According to Seidavi et al. (2020) cumin seed support improved performance (at supplementation levels of 3–5 % in diet) and positively affect (at 2–3 % levels of dietary supplements) the intestinal microflora of broilers. The available literature reports that the effects of cumin could have a positive effect on growth, nutrient digestibility, increased breast and thigh muscle (Khajeali et al. 2012), meat quality (Lee et al. 2004) and serum parameters (Gandkanlo et al. 2011).

MATERIAL AND METHODS

Experimental design

The animal procedures were reviewed and approved by the Animal Care Committee of Mendel University in Brno and by the Ministry of Education, Youth and Sports (MSMT-21593/2020-3). The experiment was performed at the experimental stables of Mendel University in Brno. During the experiment, the microclimatic conditions and the light regime was controlled.). A conventional system of deep litters with wood shavings was used as the bedding material.

Animals and diets

The total of 36 medium-slow growing male chickens (Hubbard JA 57) were used. The trial lasted from one day to 50th day of chicken's age. Broilers were fed experimental starter diets until 21st day

of age. Chickens were fed experimental grower diets until 34th day of age. Broilers were fed experimental finisher diets from 36th day of age until the end of the experiment. At the first day of age broilers were divided by body mass into two equal groups with two replicates per treatment, i.e., there were 18 broilers in one experimental pen. The control group (Control; n=18) was fed a diet without addition of *Carum carvi*. The second experimental group (Cumin; n=18) was fed a diet with addition of 1% *Carum carvi*. Diets were formulated as isoenergic and isonitrogenous.

Chickens had free access to water and feed. Composition of used diets are shown in Table 1, Table 2 and Table 3 for starter, grower and finisher diets, respectively. The chemical compositions of all diets (Table 4) were determined for dry matter, crude protein, crude fat, crude fibre, and ash according to the EC Commission Regulation (Commission Regulation 152/2009).

Table 1 Ingredient composition (g/kg) of starter diets

Component	Control	Cumin
Maize	330.0	354.1
Soybean meal	341.0	339.0
Wheat	252.2	220.0
Rapeseed oil	33.6	33.6
Premix*	30.0	30.0
Limestone milled	0.8	0.8
Monocalcium phosphate	10.0	10.0
Cumin	-	10.0
DL-Methionine	2.4	2.5

*Legend: *Premix contains (per kg): L-lysine 2.34 g; DL-Methionine 2.4 g; Threonine 0.99 g; calcium 5.25 g; phosphorus 1.95 g; sodium 1.44 g; copper 15 mg; iron 84 mg; zinc 99 mg; manganese 99 mg; iodine 0.99 mg; selenium 0.18 mg; retinol 13,500 IU (international units); calciferol 5,001 IU; tocopherol 45 mg; phylloquinone 1.5 mg; thiamine 4.2 mg; ri-boflavin 8.4 mg; pyridoxin 6 mg; cobalamin 30 µg; biotin 0.21 mg; niacinamid 36 mg; folic acid 1.8 mg; calcium pantothenate 13.5 mg; cholin chloride 180 mg.*

Table 2 Ingredient composition (g/kg) of grower diets

Component	Control	Cumin
Maize	357.6	372.0
Soybean meal	295.0	292.0
Wheat	272.0	251.15
Rapeseed oil	37.6	37.0
Premix*	30.0	30.0
Monocalcium phosphate	5.6	5.6
DL-Methionine	2.2	2.25
Cumin	-	10

*Legend: Legend: *Premix contains (per kg): L-lysine 2.58 g; DL-Methionine 2.52 g; Threonine 1.47 g; calcium 5.04 g; phosphorus 1.65 g; sodium 1.38 g; copper 15 mg; iron 75 mg; zinc 99 mg; manganese 99 mg; iodine 0.9 mg; selenium 0.36 mg; retinol 9,900 IU (international units); calciferol 5,001 IU; tocopherol 45 mg; phylloquinone 1.5 mg; thiamine 4.2 mg; ri-boflavin 8.4 mg; pyridoxin 6 mg; cobalamin 28.8 µg; biotin 0.18 mg; niacinamid 36 mg; folic acid 1.71 mg; calcium pantothenate 13.35 mg; cholin chloride 180 mg.*

Table 3 Ingredient composition (g/kg) of finisher diets

Component	Control	Cumin
Maize	399.1	393.0
Soybean meal	252.0	247.8
Wheat	272.5	272.5
Rapeseed oil	40.0	40.25
Premix*	30.0	30.0
Monocalcium phosphate	4.9	4.9
DL-Methionine	1.5	1.55
Cumin	-	10

*Legend: *Premix contains (per kg): L-lysine 2.58 g; DL-Methionine 2.52 g; Threonine 1.47 g; calcium 5.04 g; phosphorus 1.65 g; sodium 1.38 g; copper 15 mg; iron 75 mg; zinc 99 mg; manganese 99 mg; iodine 0.9 mg; selenium 0.36 mg; retinol 9,900 IU (international units); calciferol 5,001 IU; tocopherol 45 mg; phylloquinone 1.5 mg; thiamine 4.2 mg; ri-boflavin 8.4 mg; pyridoxin 6 mg; cobalamin 28.8 µg; biotin 0.18 mg; niacinamid 36 mg; folic acid 1.71 mg; calcium pantothenate 13.35 mg; cholin chloride 180 mg.*

Samples and analysis

During the experiment chickens feed intake and body weight were evaluated. The percentual carcass yield was calculated as the carcass weight / slaughter live weight * 100. Yield of breast meat and leg meat was calculated as their proportion from the slaughter weight. The feed conversion ratio (FCR) was determined as total feed consumption/weight body gain at the end of trial. Some of individual parts of digestive tract, liver and heart were determined.

Statistical analysis

The one-way analysis of variance (ANOVA) was used to evaluate the differences between the groups. Post-hoc testing of differences between groups was performed by the Sheffe's test. $P < 0.05$ was regarded as a statistically significant difference.

RESULTS AND DISCUSSION

Feed consumption

The following table (Table 4) expresses the values of feed consumption per day and whole experiment. FCR values are also included here. As shown in the table the experimental group with Cumin had a higher average feed consumption per day and per whole experiment. According to results of the Ustrasice test station live weight of the group without addition of cumin was 2 405 g in Hubbard JA 57 chickens.

Table 4 Feed consumption and FCR of fattened chickens in relation to the dietary group

Trait	Control	Cumin
Average feed intake per trial/bird (kg)	4.08	4.41
Average feed intake per day/bird (g)	83.17	90.03
FCR (kg/kg)	1.63	1.66

Legend: FCR – Feed Conversion Ratio

Body weight

Table 5 shows the body weights of the chickens during the experiment. Statistically significant differences between dietary groups assessed were found at 8th, 15th, 36th, 43rd and 50th day of age ($P < 0.05$). At the end of the trial the average live weight was 2 502 g in the Control group and 2 654 g in the Cumin group. In an experiment of Khajeali et al. (2012), which lasted 42 days, the live weights were significantly higher ($P < 0.05$) in the group with addition of 1 % cumin compared to the control group. However, the study of Gandkanlo et al. (2011) confirms even better increase in live weights of chickens with the addition of 1 % cumin in feed. In study of Guler et al. (2007) was found out no significant difference in daily feed intake for 42 days in broilers fed a diet containing 1% cumin seeds. However, mean daily weight gains between the treatments were significantly different.

Table 5 Live weight (g) of broilers in relation to the dietary group

Age	Control	Cumin
n	18	18
1st day	37.50 ± 0.83	37.89 ± 0.66
8th day	96.17 ± 3.18^{b}	108.00 ± 3.55^{a}
15th day	246.56 ± 9.35^{b}	274.50 ± 6.43^{a}
22nd day	527.17 ± 15.20	561.22 ± 13.45
28th day	891.78 ± 12.44	920.00 ± 15.46
36th day	1430.61 ± 22.01^{a}	1496.50 ± 22.12^{b}
43rd day	1956.39 ± 32.07^{a}	2057.50 ± 28.15^{b}
50th day	2501.33 ±36.25^{a}	2654.89 ± 32.07^{b}

Legend: ^{a,b} means with different superscript letters differ significantly at $P < 0.05$; n – number of cases

Weight of digestive tract, liver and heart

There were found significant differences ($P > 0.05$) in the jejunum length and cecum weight of chickens between the dietary groups (Table 6).

Carcass characteristics

Table 7 shows the carcass characteristic of slaughtered chickens. There were found no significant differences in values for the carcass weight and yield and yields of main meat parts ($P > 0.05$) between dietary groups of chickens. Based on the results of carcass analysis at 49 days of age Hubbard JA 57 achieved 74.80 % (Machander 2018). The breast meat yield in the control group of the present study was 25.97% and chickens of the cumin group reached this yield at the level of 26.75%. In contrast,

the leg meat yield was 19.54% in the control group and 19.88% in the experimental group. Machander (2018) reports the achieved values of breast yield 19.07% and of leg yield 22.72%.

Table 6 Weights and length of particularparts of digestive tract, and weights of liver and heart in chickens (per kg of BW) in relation to the dietary group

	Control	Cumin
n	6	6
	Mean ± SE	
Crop (g)	2.46 ± 0.29	3.54 ± 0.1.10
Proventriculus (g)	3.69 ± 0.30	3.83 ± 0.05
Gizzard (g)	13.35 ± 0.45	12 ± 0.62
Duodenum (g)	4.49 ± 0.50	4.23 ± 0.01
Duodenum (mm)	120.28 ± 5.48	112.90 ± 6.60
Jejunum (g)	7.60 ± 0.49	9.20 ± 0.45
Jejunum (mm)	**243.39 ± 1.34^{b}**	**274.12 ± 4.64^{a}**
Ileum (g)	6.70 ± 0.99	7.12 ± 0.57
Ileum (mm)	215.49 ± 12.67	206.74 ± 9.77
Colon (g)	1.13 ± 0.19	1.16 ± 0.10
Colon (mm)	39.90 ± 8.46	36.73 ± 5.27
Cecum (g)	**2.75 ± 0.28^{b}**	**3.62 ± 0.20^{a}**
Cecum (mm)	64.97 ± 6.65	75.26 ± 1.85
Liver (g)	15.20 ± 0.62	15.91 ± 0.35
Heart (g)	4.91 ± 0.07	6.06 ± 1.04

Legend: ^{a,b} means different superscript letters differ significantly at $P < 0.05$; n – number of case; SE – standard error

Table 7 Carcass characteristics of chickens in relation to the dietary group

	Control	Cumin
n	6	6
	Mean ± SE	
Carcass weight (g)	1846.89 ± 42.59	1803.18 ± 33.81
Carcass yield (%)	71.84± 0.20	70.68 ± 0.52
Breast meat (%)	25.97 ± 0.29	26.78 ± 0.65
Leg meat (%)	19.54 ± 0.49	19.88 ± 0.16

Legend: There was not found statistically significant differences ($P > 0.05$) between dietary groups; n – number of cases; SE – standard error

CONCLUSION

In the trial the effect of dietary addition of cumin on broilers performance and carcass parameters were evaluated. The diet with addition of 1% cumin (*Carum carvi*) had the positive influence on the body weight of medium-slow growing chickens. Also, it was confirmed that dietary cumin addition affected the jejunum length and cecum weight as individual parts of the digestive tract assessed.

ACKNOWLEDGEMENTS

The research was financially supported by the Internal Grant Agency of Faculty of AgriSciences (Mendel University in Brno) no. AF-IGA2020-TP012.

REFERENCES

Commission regulation (EC) 152/2009. Laying down the methods of sampling and analysis for the official control of feed. Brussels: The commission of the European Communities.

Guler, T. et al. 2007. Effect of dietary supplemental black cumin seeds on antioxidant activity in broilers. Medycyna Weterynaryjna, 63(9): 1060–1063.

Gandkanlo, M. et al. 2011. The effects of different dietary levels of Black Caraway (*Carum carvi* L.) seeds on performance and some blood indices in broiler chickens. Animal Sciences Journal (Pajouhesh & Sazandegi), 93: 26–33.

Khajeali, Y. et al. 2012. Effect of use different levels of caraway (Carum carvi L.) powder on performance, some blood parameters and intestinal morphology on broilers chickens. World Applied Sciences Journal, 19(8): 1202–1207.

Lee, K.W. et al. 2004. Essential oils in broiler nutrition. International Journal of Poultry Science, 3(12): 738–752.

Pourmortazavi, S.M. et al. 2005. Supercritical fluid extraction of volatile components from *Bunium persicum* Boiss. (Black cumin) and *Mespilus germanica* L. (medlar) seeds. Journal of Food Composition and Analysis, 18(5): 439–446.

Seidavi, A.R. et al. 2020. Feeding of black cumin (Nigella sativa L.) and its effects on poultry production and health. World's Poultry Science Journal, 76(2): 346–357.

Špaldon, E. et al. 1986. Rostlinná výroba. Praha: SZN.

Weiss, E.A. 2002. Spice crops. Wallingford, Oxon, UK, New York, USA: Cabi Publishing.

The influence of different variations of selenium sources in diets on blood biochemical parameters in fast growing broiler chickens

Dana Zalesakova, Jakub Novotny, Michal Rihacek, Lucie Horakova, Andrea Roztocilova, Ondrej Stastnik, Eva Mrkvicova, Leos Pavlata
Department of Animal Nutrition and Forage Production
Mendel University in Brno
Zemedelska 1, 613 00 Brno
CZECH REPUBLIC

xzalesa4@mendelu.cz

Abstract: The effect of different forms of selenium on blood biochemical parameters was monitored in 35-day-old broilers of the Ross 308 hybrid combination. A total of 69 one-day-old chickens were divided into 3 groups: Control without selenium supplementation, Organic with organic selenium supplementation (selenomethionine from *Saccharomyces cerevisiae*) and Inorganic with inorganic selenium supplementation (sodium selenite). The total added selenium content was 0.4 mg/kg fo Organic and Inorganic group. No significant differences in feed consumption and conversion ratio were observed between groups during the experiment ($P<0.05$). Statistically significant differences were observed in live weights from 28th–35th day of fattening – the difference was noted between the higher weight control group and the lower weight organic and inorganic group (2203 g vs. 1990 g, resp. 2081 g). In the case of biochemical parameters, significant differences ($P<0.05$) were recorded between the parameters of selenium (Se) and glutathione peroxidase (GSH-Px), which were higher in the organic and inorganic groups (0.18 mg/l, 0.15 mg/l for Se; 216.9 U/g Hb, 181.23 U/g Hb for GSH-Px) compared to the control groups (0.03 mg/l for Se; 33.22 U/g Hb for GSH-Px). In none of the monitored cases the organic and inorganic group significantly differ from each other.

Key Words: broiler nutrition, selenite, selenomethionine, *Saccharomyces cerevisiae*, Ross 308

INTRODUCTION

Selenium is an essential microelement, commonly added to feed rations and mixtures of livestock. It mainly ensures the optimal function of the immune system (Surai 2002), which is related to the activity of the enzyme glutathione peroxidase (GSH-Px). This enzyme was discovered in 1973 and it was subsequently identified as a very effective antioxidant, protecting the body from damage caused by free radical oxidation (Rotruck et al. 1973). The activity of GSH-Px is directly related with the supply of selenium to organism (Watanabe et al. 1997).

Selenium is usually added to poultry feeds in organic form such as selenomethionine or inorganic form, mainly selenate or selenite (Surai and Fisinin 2014). The organic form of selenium obtained from yeast provides higher bioavailability than the inorganic form (Mahan 1999, Mahmoud and Edens 2003). Some experiments have shown that organic selenium from yeast increases the quality of meat and the growth of feathers (Wang and Xu 2008) as well as the oxidative stability of meat and thus its quality (Mahan 1999), which is desirable in fattening chickens. In contrast, Payne and Southern (2005) reported that plasma GSH-Px activity was not affected by the form or concentration of selenium added to feed mixtures. The aim of this experiment is to verify whether and how the different forms of selenium supplied to the feed mixtures will affect the concentrations of selenium and GSH-Px in the blood plasma of fattened chickens and whether they affect other blood biochemical parameters.

MATERIAL AND METHODS

Experimental conditions

Mendel University laboratory was used for the experiment. The microclimatic conditions and light regime in laboratory were controlled via computer and kept in requirements according to actual age of chickens (Aviagen 2018). The Animal Care Committee of Mendel University in Brno

and The Ministry of Education, Youth and Sports (MSMT-21593/2020-3) reviewed and approved animal procedures used in this experiment.

Animals and diets

In this study 69 male Ross 308 broiler chickens were used. Length of experiment was 35 days, starting with 1st day of chicken's age. Feeding was realized by experimental starter diet for first 10 days, after that experimental grower diet was used until the end of the study. At the first day of the study which is also first day of age for examined chickens, they were split according to body mass into three even groups with different diet. First was control group (Control; n=23) which was fed with a diet without addition of selenium (selenium was supplied only with its natural content in the feeds), followed by the first experimental group (Organic; n=23) which was fed with natural Se content in the feeds and organic source of selenium (Sel-Plex – *Saccharomyces cerevisiae* CNCM I-3060) and lastly the second experimental group (Inorganic; n=23) which was fed with natural Se content in the feeds and inorganic source of selenium (Sodium selenite – Na_2SeO_3). The total added selenium content was 0.4 mg/kg for Organic and Inorganic group.

According to the EC Commission Regulation (Commission Regulation 152/2009) fraction of dry matter, crude protein, crude fat, crude fibre, and ash in both diets were determinate as is show in Table 1 together with used diets composition.

Table 1 Composition and chemical analysis of starter and grower diets

	Starter			Grower		
Components (g/kg)	Control	Organic	Inorganic	Control	Organic	Inorganic
Maize	300	300	300	370	370	370
Soybean meal	436	436	436	395.5	395.5	395.5
Wheat	176.7	176.7	176.7	151.7	151.7	151.7
Rapeseed oil	40	40	40	40	40	40
Premix[1]	30	30	30	-	-	-
Premix[2]	-	-	-	30	30	30
Limestone milled	5.5	5.5	5.5	3.3	3.3	3.3
Monocalcium phosphate	8	8	8	8	8	8
DL-Methionine	2	2	2	1.5	1.5	1.5
Wheat gluten	1.8	1.8	1.8	-	-	-
Sodium selenite (mg/kg)	-	-	7.5	-	-	7.8
Saccharomyces cerevisiae (mg/kg)	-	150	-	-	155	-
Dry matter (g/kg)	880	880	880	880	880	880
AME_N (MJ/kg)[3]	12.1	12.1	12.1	12.33	12.33	12.33
Crude protein (g/kg)	233.9	234.7	230.1	222.4	219.6	222.8
Ether extract (g/kg)	58.9	62.4	59.1	61.1	59.8	62.8
Crude fiber (g/kg)	35.7	35.6	37.5	36.4	36.3	38.4
Crude ash (g/kg)	65.9	65.8	65.4	61	61.2	61.5

Legend: [1]Premix contains (per kg): L-lysine 2.34 g; DL-Methionine 2.4 g; Threonine 0.99 g; calcium 5.25 g; phosphorus 1.95 g; sodium 1.44 g; copper 15 mg; iron 84 mg; zinc 99 mg; manganese 99 mg; iodine 0.99 mg; retinol 13,500 IU (international units); calciferol 5,001 IU; tocopherol 45 mg; phylloquinone 1.5 mg; thiamine 4.2 mg; riboflavin 8.4 mg; pyridoxin 6 mg; cobalamin 30 µg; biotin 0.21 mg; niacinamid 36 mg; folic acid 1.8 mg; calcium pantothenate 13.5 mg; cholin chloride 180 mg. [2]Premix contains (per kg): L-lysine 2.58 g; DL-Methionine 2.52 g; Threonine 1.47 g; calcium 5.04 g; phosphorus 1.65 g; sodium 1.38 g; copper 15 mg; iron 75 mg; zinc 99 mg; manganese 99 mg; iodine 0.9 mg; retinol 9,900 IU (international units); calciferol 5,001 IU; tocopherol 45 mg; phylloquinone 1.5 mg; thiamine 4.2 mg; riboflavin 8.4 mg; pyridoxin 6 mg; cobalamin 28.8 µg; biotin 0.18 mg; niacinamid 36 mg; folic acid 1.71 mg; calcium pantothenate 13.35 mg; cholin chloride 180 mg. [3]Apparent metabolize energy – calculated value

There were health status checks on daily basis with weight measurement performed periodically. On the last day of experiment all chickens were weighted and slaughtering by decapitation. Blood samples were collected from 6 chickens from each group. During study only one premature death was registered.

Sample collection and data processing

The feed intake was calculated daily, the weight changes were measured weekly. The blood samples were collected into heparinized tubes after the slaughtering. Plasma was collected after centrifugation (10 minutes, 3,000 rpm) till 2 hours after blood collection and then it was frozen (-20 °C) until biochemical examination. Biochemical parameters were determined using Erba Lachema commercial sets on the Ellipse biochemical analyzer in plasma samples. Following parameters were measured: AST – aspartate aminotransferase, GGT – gamma-glutamyltransferase, ALT – alanine aminotransferases, ALP – alkaline phosphatase, LD – lactate dehydrogenase, TBili – total bilirubin, TG – triglycerides, cholesterol, urea, creatine kinase, creatinine, TP – total protein, albumin, Se – selenium, GSH-Px – glutathione peroxidase. The content of globulins (total protein minus albumin) and albumins to globulins ratio were calculated.

The obtained data were processed in StatSoft Statistica, version 12.0 and Microsoft Excel. Analysis of Variance (ANOVA) with a one-way design using the general linear model was performed and the level of significance was established at $P<0.05$.

RESULTS AND DISCUSSION

Feed consumption and live weight of chickens

A distinct effect of different diets didn't occur in feed consumption and feed conversion ratio of fattening chickens, as shown in Table 2.

Table 2 Average feed consumption and feed conversion ratio per bird

Group	Average feed intake per experiment (g)	Average feed intake per day (g)	Average FCR per experiment
Control	2881.66	84.75	1.31
Organic	2710.88	79.73	1.36
Inorganic	2681.39	78.86	1.29

Legend: FCR – feed conversion ratio; P>0.05

In performance objectives of Aviagen Group (2019), average feed consumption per 35-day-old chicken is 3476 g and feed conversion ratio are 1.463. In our study these values were lower in all groups. Between groups with selenium supplementation and control group was only small difference in feed consumption (control group had slightly higher feed consumption) which wasn't statistically significant ($P>0.05$).

However, significant changes ($P<0.05$) were detected in life weights of chickens during the fattening (n = 22), represented in Figure 1.

Figure 1 Average life weight (g ± SE) of chickens during the experiment

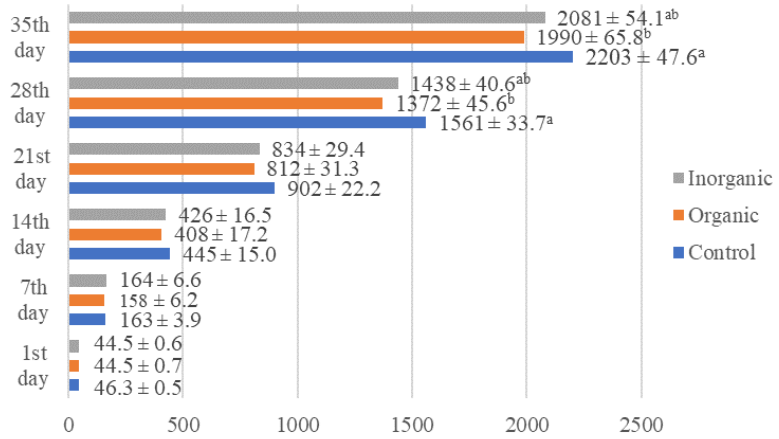

Legend: SE – Standard Error; $^{a:b}$ – different characters show statistically significant difference P<0.05

The differences in weights began to show 21st day of age and from the 28th day of age they became statistically significant. This finding is likely to be related to the slightly higher feed intake of the control

group compared to the selenium-supplementation groups. However, live weight in all groups in the end of the experiment reached less values (Control 2203 g, Organic 1990 g, Inorganic 2081 g) than stated by the performance objectives of Aviagen Group (2019), which is 2376 g. Closest to this value was the control group. Our results do not correspond with the results of other authors who observed a positive effect on live weight after supplementation of selenium into the feed mixture (Skřivan et al. 2008, Ševčíková et al. 2006). In opposite, Wang and Xu (2008) didn't find any significant difference in live weight after adding the organic selenium form to feed mixture.

Blood biochemical parameters of chickens

The results of blood analysis are shown in Table 3.

Table 3 Blood biochemical parameters of 35-day-old chickens

Group	Control			Organic			Inorganic		
n	6			6			6		
	Mean ± SE								
ALT (μkat/l)	0.09	±	0.01	0.12	±	0.01	0.10	±	0.01
AST (μkat/l)	3.80	±	0.23	3.67	±	0.22	3.81	±	0.24
GGT (μkat/l)	0.27	±	0.02	0.26	±	0.02	0.27	±	0.03
ALP (μkat/l)	112.19	±	14.25	74.01	±	20.77	73.35	±	13.23
LD (μkat/l)	69.20	±	7.76	76.32	±	18.98	68.85	±	12.12
CK (μkat/l)	354.30	±	77.22	217.01	±	30.71	287.44	±	94.35
Tbili (μmol/l)	5.60	±	0.25	4.80	±	0.17	5.48	±	0.38
Urea (mmol/l)	1.46	±	0.06	1.49	±	0.04	1.46	±	0.05
Creat (μmol/l)	22.82	±	1.56	20.48	±	1.43	20.32	±	0.52
UA (μmol/l)	248.43	±	30.51	287.95	±	24.23	268.22	±	27.54
TP (g/l)	30.45	±	0.24	30.25	±	0.73	30.05	±	0.53
Alb (g/l)	17.76	±	0.18	17.64	±	0.54	17.62	±	0.44
Glob (g/l)	12.69	±	0.24	12.61	±	0.50	12.43	±	0.29
Alb/Glob	1.40	±	0.03	1.41	±	0.07	1.42	±	0.05
Glu (mmol/l)	7.65	±	0.61	7.96	±	0.43	8.46	±	0.38
Chol (mmol/l)	2.74	±	0.04	2.70	±	0.14	2.62	±	0.08
TG (mmol/l)	0.73	±	0.04	0.83	±	0.07	0.82	±	0.03
Se (mg/l)	0.03	±	0.00^{a}	0.18	±	0.01^{b}	0.15	±	0.01^{b}
GSH-Px (U/g Hb)	33.22	±	3.95^{a}	216.90	±	12.51^{b}	181.23	±	9.55^{b}

Legend: n – number of cases; SE – Standard Error; $^{a:b}$ – different characters show statistically significant differences P<0.05; ALT – alanine aminotransferase; AST – aspartate aminotransferase; GGT – gama-glutamyltransferase; ALP – alkaline phosphatase; LD – lactate dehydrogenase; CK – creatine kinase; Tbili – total bilirubin; Creat – creatinine; UA – uric acid; TP – total protein; Alb – albumin; Glob – globulin; Glu – glucose; Chol – cholesterol; TG – triglycerides; Se – selenium; GSH-Px – glutathione peroxidase

As we can see, there were no differences (P>0.05) between groups in liver enzymes activity or indicators of nitrogen, lipid or energetic metabolism. This could indicate that they were not affected by selenium supplementation. Statistically significant differences (P<0.05) were observed in value of selenium, which was higher in organic (0.18 mg/l) and inorganic group (0.15 mg/l) and lower in control group (0.03 mg/l). Differences were also detected in GSH-Px activity, which corresponds with selenium level of blood plasma: it was lower in control group (33.22 U/g Hb) compared to organic (216.90 U/g Hb) and inorganic group (181.23 U/g Hb). These findings correspond to results of Hu et al. (2012) and Arnaut et al. (2021). Even if the values of selenium and GSH-Px in organic group are slightly higher than in inorganic group, these results are insignificant, which corresponds with trial of Wang and Xu (2008).

CONCLUSION

In presented study, feed consumption, conversion ratio, live weight and blood biochemical parameters of broiler chickens were monitored. The experiment didn't show any significant differentials (P>0.05) in feed consumption during the trial. Significant differences were observed in live weight from 28th till 35th day of age, which was lower in selenium supplemented groups comparing to control

group and in blood indicators of selenium and GSH-Px, which was higher in supplemented groups comparing to control group. The data obtained from this study suggest that the addition of various form of selenium to feed can affect blood biochemical parameters and live weight of fattening chickens. However, no differences between the organic and inorganic groups were noted.

ACKNOWLEDGEMENTS

The research was financially supported by the Internal Grant Agency of Faculty of AgriSciences (Mendel University in Brno) no. AF-IGA2020-TP012.

REFERENCES

Arnaut, P.R. et al. 2021. Selenium source and level on performance, selenium retention and biochemical responses of young broiler chicks. BMC Veterinary Research, 17(1): 1–13.

Aviagen Group 2018: Technological procedure for broiler Ross. Available at: http://eu.aviagen.com/language-mini-site/show/cz. Last modified July 24, 2019. [2021-08-23].

Aviagen Group 2019. Broiler ROSS: Performance Objectives. Available at: http://eu.aviagen.com/tech-center/download/1339/Ross308-308FF-BroilerPO2019-EN.pdf. [2021-08-23].

Hu, C.H. et al. 2012. Comparative effects of nano elemental selenium and sodium selenite on selenium retention in broiler chickens. Animal Feed Science and Technology, 177(3–4): 204–210.

Mahan, D.C. 1999. Organic selenium: using nature's model to redefine selenium supplementation for animals. In Proceedings of the 15th Annual Symposium. Biotechnology in the Feed Industry. Nottingham, UK: Nottingham University Press, 523–535.

Mahmoud, K.Z., Edens, F.W. 2003. Influence of selenium sources on age-related and mild heat stress-related changes of blood and liver glutathione redox cycle in broiler chickens (Gallus domesticus). Comparative Biochemistry and Physiology Part B: Biochemistry and Molecular Biology, 136(4): 921–934.

Payne, R.L., Southern, L.L. 2005. Comparison of inorganic and organic selenium sources for broilers. Poultry Science, 84(6): 898–902.

Rotruck, J.T. et al. 1973. Selenium: biochemical role as a component of glutathione peroxidase. Science, 179(4073): 588–590.

Skřivan, M. et al. 2008: Effect of dietary selenium on lipid oxidation, selenium and vitamin E content in the meat of broiler chickens. Czech Journal of Animal Science, 53(7): 306–311.

Surai, P.F. 2002. Selenium in poultry nutrition 2. Reproduction, egg and meat quality and practical applications. World's Poultry Science Journal, 58(4): 431–450

Surai, P.F., Fisinin, V.I. 2014. Selenium in poultry breeder nutrition: An update. Animal Feed Science and Technology, 191: 1–15.

Ševčíková, S. et al. 2006: The effect of selenium source on the performance and meat quality of broiler chickens. Czech Journal of Animal Science, 51(10): 449–457.

Wang, Y.B., Xu, B.H. 2008. Effect of different selenium source (sodium selenite and selenium yeast) on broiler chickens. Animal Feed Science and Technology, 144(3–4): 306–314.

Watanabe, T. et al. 1997. Trace minerals in fish nutrition. Aquaculture, 151(1–4): 185–207.

Blood biochemical parameters in the evaluation of chicken nutrition during the starter feed period

Dana Zalesakova, Michal Rihacek, Jakub Novotny, Lucie Horakova, Ondrej Stastnik, Eva Mrkvicova, Leos Pavlata
Department of Animal Nutrition and Forage Production
Mendel University in Brno
Zemedelska 1, 613 00 Brno
CZECH REPUBLIC

xzalesa4@mendelu.cz

Abstract: The effect of age and different diets on the blood biochemical parameters of the 1 to 8-day-old Ross 308 broilers during the starter fattening period was evaluated. The chickens were divided into three different groups fed: a standard feed mixture (C – control group), a mixture with a 30% deficiency of crude protein (N group), and a mixture with a 30% deficiency of calcium, phosphorus, zinc, copper and selenium in the mineral premix (M group). Feed consumption and body weight didn't differ between groups ($P>0.05$) during the experiment. Significant differences ($P<0.05$) were demonstrated in biochemical indicators of nitrogen, fat, mineral and energy metabolism between 1st and 8th day of chicken's age. Depending on the different diets, at 8th day of age significant changes were detected mainly in the parameters of total protein, albumin, globulin, triglycerides, cholesterol and glucose. The parameters of mineral substances in blood were not affected by using diets with different nutrients content in present study.

Key Words: poultry nutrition, Ross 308, mineral substance, crude protein

INTRODUCTION

In the assessment of nutritional control through the biochemical parameters of blood, it is important to focus on especially those parameters that we consider to be the basic indicators of metabolism. The existence of the organism depends not only on the received nutrients of the feed, but also on the ability to use them and the subsequent exclusion of the final products of metabolism (Jelínek et al. 2003). In contrast to large livestock, where blood tests are widely used, poultry medicine lacks a large number of reference physiological blood values. Their evaluation enables the identification of metabolic changes and helps to detect possible health problems already in the preclinical phase of the disease (Silva et al. 2007).

Many experiments have shown that with a standard diet, the blood biochemical parameters change with age. Total protein and albumins increase (Filipović et al. 2007, Piotrowska et al. 2011) while the level of the final product of protein metabolism, uric acid, remains higher in younger chickens (Silva et al. 2007). Similar changes were observed in other parameters, some of them raise with increasing age – for example calcium, phosphorus (Ansar et al. 2004) or liver enzyme aspartate aminotransferase (Meluzzi et al. 1992). Others decrease – eg magnesium, iron (Piotrowska et al. 2011) or alkaline phosphatase activity (Silva et al. 2007). The results of individual studies then differ on the possibility of influencing biochemical parameters depending on eventual nutrient deficiency. The aim of this experiment was to determine how the young broilers blood biochemical parameters will change during the starter period of the chickens' nutrition and to assess whether they will be affected by predetermined nutrient deficiencies.

MATERIAL AND METHODS

Animals and experimental diets

A total of 90 1-day-old male broilers of the Ross 308 hybrid combination were included in the experiment. They were divided into 3 groups in 3 replicates. The chickens were placed in a room with a computer-controlled temperature and humidity using an automatic sensor. The set parameters

corresponded to the technological instructions for the selected hybrid combination. Chickens was regularly health checked, had unrestricted access to drinking water and was fed ad libitum.

A total of three non-pelleted starter feed mixtures were used for feeding. The mixture for the control group was formulated according to the recommended nutritional requirements of chosen hybrid combination. Another mixture contained approximately a 30% crude protein deficit (N group) compared to the control group and the third group (M) was fed a mixture with approximately 30% deficiency of selected minerals (calcium, phosphorus, zinc, copper, selenium) in the mineral premix. The composition and nutritional composition of these mixtures is shown in Table 1.

Table 1 Composition and nutrient content of feed mixtures

Components (g/kg)	C	N	M
Wheat	195	382	200.10
Maize	290	352	290
Soybean meal	430	195	430
Limestone milled	6	7	3.5
Rapeseed oil	41	20	41
Vitamin-mineral premix 1	30	30	-
Vitamin-mineral premix 2	-	-	30
Monocalcium phosphate	8	8	4.3
L-Lysine	-	5.8	-
DL-Methionine	-	0.7	-
AME_N (MJ)[3]	12.12	12.39	12.20
Dry matter	860	860	860
Crude protein	231.23	161.12	226.49
Ether extract	6.48	4.69	6.37
Crude fiber	3.03	2.49	3.10
Ash	63.24	51.84	55.49
Ca	17.34	25.88	11.53
P	4.42	4.23	2.93
Cu (mg/kg)	11.22	10.61	6.40
Zn (mg/kg)	120.50	106.60	75.60

Legend: [1]Vitamin-mineral premix for starter contains (per kg): L-lysine 2.34 g; DL-Methionine 2.4 g; Threonine 0.99 g; calcium 5.25 g; phosphorus 1.95 g; sodium 1.44 g; copper 15 mg; iron 84 mg; zinc 99 mg; manganese 99 mg; iodine 0.99 mg; selenium 0.18 mg; retinol 13,500 IU (international units); calciferol 5,001 IU; tocopherol 45 mg; phylloquinone 1.5 mg; thiamine 4.2 mg; riboflavin 8.4 mg; pyridoxin 6 mg; cobalamin 30 µg; biotin 0.21 mg; niacinamid 36 mg; folic acid 1.8 mg; calcium pantothenate 13.5 mg; cholin chloride 180 mg. [2]Vitamin-mineral premix for starter contains (per kg): L-lysine 2.34 g; DL-Methionine 2.4 g; Threonine 0.99 g; calcium 3.675 g; phosphorus 1.365 g; sodium 1.44 g; copper 10.5 mg; iron 60.6 mg; zinc 69.3 mg; manganese 99 mg; iodine 0.99 mg; selenium 0.126 mg; retinol 13,500 IU (international units); calciferol 5,001 IU; tocopherol 45 mg; phylloquinone 1.5 mg; thiamine 4.2 mg; riboflavin 8.4 mg; pyridoxin 6 mg; cobalamin 30 µg; biotin 0.21 mg; niacinamid 36 mg; folic acid 1.8 mg; calcium pantothenate 13.5 mg; cholin chloride 180 mg. [3]Apparent metabolize energy, calculated value. Ca – calcium; P – phosphorus; Cu – copper; Zn – zinc; C – control group; N – group with 30% crude protein deficiency; M – group with 30% deficiency of mineral substances

Sample collection and data processing

The experiment lasted 8 days. On the 1st and 7th day of age all chickens were weighed. The feed was renewed regularly at the same time every day and the unaccepted residues were weighed. Blood was collected on the 1st and the 8th day after slaughtering of selected broilers (2 samples from each replicate, 6 samples from group). Blood samples were taken into heparinized tubes and then placed in a centrifuge where blood elements and plasma were separated. Centrifugation lasted for 15 minutes at 3,000 rpm. The obtained plasma was kept frozen (-20 °C) until biochemical determination was made. For this operation, standardized biochemical methods using commercial Erba Lachema kits were used and performed on an Ellipse automated biochemical analyzer. The following parameters were assessed: enzymes activity AST – aspartate aminotransferase; GGT – gamma-glutamyltransferase; ALT – alanine aminotransferases; ALP – alkaline phosphatase, LD – lactate dehydrogenase and CK – creatine kinase. As other markers of hepatic metabolism, nitrogen and fat metabolism were determined concentrations of the total bilirubin – Bili, TG – triglycerides, cholesterol, urea, creatinine, TP – total protein and albumin. The content of globulins (total protein minus albumin) and albumins to globulins ratio

were calculated. Minerals were also determined, specifically calcium, phosphorus, magnesium, sodium, potassium, chlorine, zinc, copper, iron, selenium, as well as the activity of the enzyme GPx – glutathione peroxidase.

The obtained data were processed by Microsoft Excel and StatSoft Statistica, version 12.0. One-factor and two-factor ANOVA were used to evaluate the results. Differences between groups were tested by Scheffe's test. The level of significance was established at $P<0.05$.

RESULTS AND DISCUSSION

Feed intake and live weight

In our experiment average feed rate of chicken from the control group compared to the chickens of other groups (N, M) showed no significant differences ($P>0.05$) as shown in Table 2.

Table 2 Average feed intake of starter diets

Group	n	Average feed intake per experiment (g)			Average feed intake per day (g)		
		Mean ± SE					
C	3	185.52	±	12.61	28.28	±	1.76
N	3	189.71	±	4.28	28.65	±	0.70
M	3	168.45	±	8.87	25.94	±	1.38

Legend: n – number of cases; SE – Standard Error; C – control group; N – group with 30% crude protein deficiency; M – group with 30% deficiency of mineral substances; P>0.05

Although there were no significant differences in feed intake, the group with the deficiency of selected minerals had a slightly lower feed intake. This does not correspond with the experiment of Khajali et al. (2006), which observed the opposite trend, but concerned the later stages of fattening. However, average consumption for the age categories of all groups approximately corresponded to the performance targets presented by Aviagen (2019).

In the case of comparing live weights (n = 20), significant changes between groups in the 1st and 7th day of life wasn't observed ($P>0.05$) as shown in Figure 1.

Figure 1 Average weight of chickens (g ± SE) in 1st and 7th day of age

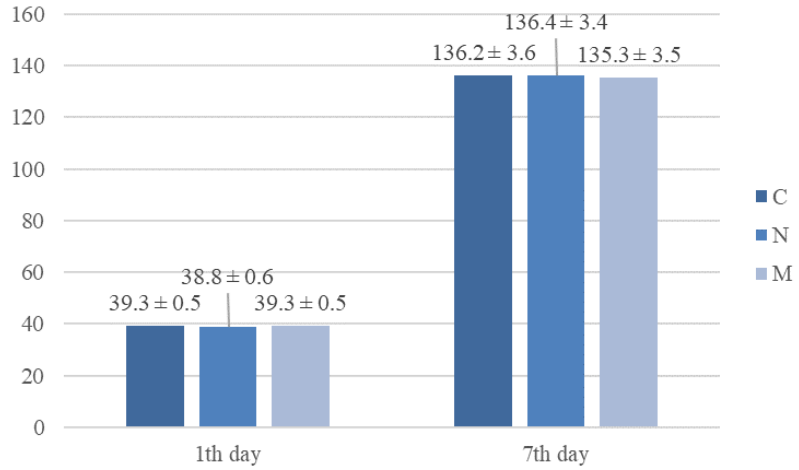

Legend: C – control group; N – group with 30% crude protein deficiency; M – group with 30% deficiency of mineral substances; SE – Standard Error; P>0.05

Although the weight differences between groups in the 1st and 7th days of age were insignificant, it can be assumed that in the next phases of the experiment the groups would start to differ. As Maia et al. (2021) prove, chickens fed with a higher proportion of crude protein weighed more compared to chickens fed with lower proportion of crude protein. The mineral deficiency did not cause any significant weight decrease compared to groups with normal mineral levels. In our experiment the average weight of 1-day-old chicken was approximately 39 g and 7-day-old chicken 136 g in all groups which is less than the performance targets presented by Aviagen (2019), which is 43 g on 1st, respectively 0th day of age (after hatching) and 207 g on 7th day of age.

Blood biochemical parameters

In blood biochemical parameters, differences between sampling in the 1st and 8th days of age were monitored. We also monitored the differences between the individual groups in 8th days of age. Obtained results is shown in Table 3.

Table 3 Blood biochemical parameters in broiler chickens during the starter feeding period

Group	1st day ALL		8th day C		8th day N		8th day M	
n	6		6		6		6	
	Mean ± SE							
ALT (µkat/l)	0.43 ± 0.04	b	0.14 ± 0.04	a	0.17 ± 0.02	a	0.12 ± 0.01	a
AST (µkat/l)	2.63 ± 0.16		3.21 ± 0.53		3.39 ± 0.32		3.18 ± 0.12	
GMT (µkat/l)	0.12 ± 0.01		0.19 ± 0.02		0.16 ± 0.01		0.18 ± 0.04	
ALP (µkat/l)	30.95 ± 1.29	b	360.57 ± 19.77	a	287.00 ± 40.86	a	288.37 ± 55.56	a
LD (µkat/l)	12.08 ± 0.78	a	14.50 ± 1.03	ab	16.09 ± 0.86	b	13.97 ± 0.81	ab
CK (µkat/l)	34.21 ± 6.27	b	135.53 ± 18.57	a	99.51 ± 27.93	ab	120.52 ± 14.87	a
Tbili (µmol/l)	3.93 ± 0.64		2.02 ± 0.59		4.87 ± 1.68		4.50 ± 0.84	
Urea (mmol/l)	6.35 ± 0.53	b	1.85 ± 0.15	a	1.36 ± 0.07	a	1.67 ± 0.08	a
Creat (µmol/l)	33.03 ± 1.99		28.63 ± 1.02		34.45 ± 4.02		31.92 ± 0.89	
UA (µmol/l)	857.18 ± 213.28		623.50 ± 61.05		598.48 ± 65.61		673.82 ± 59.18	
TP (g/l)	21.70 ± 0.57	a	28.17 ± 1.10	b	19.85 ± 1.57	a	27.82 ± 0.92	b
Alb (g/l)	5.19 ± 0.31	b	14.36 ± 1.00	a	10.36 ± 0.90	c	15.04 ± 0.29	a
Glob (g/l)	16.51 ± 0.55	a	13.81 ± 1.60	a	9.49 ± 0.74	b	12.78 ± 0.64	ab
Alb/Glob	0.32 ± 0.02	b	1.13 ± 0.16	a	1.09 ± 0.05	a	1.19 ± 0.04	a
Glu (mmol/l)	12.03 ± 0.26	a	14.62 ± 0.41	ab	22.45 ± 1.64	c	16.44 ± 0.44	b
Chol (mmol/l)	8.56 ± 0.32	b	3.40 ± 0.19	c	3.99 ± 0.37	a	3.74 ± 0.11	ac
TG (mmol/l)	0.71 ± 0.08	a	0.88 ± 0.06	ab	1.60 ± 0.30	c	1.28 ± 0.16	abc
Ca (mmol/l)	2.12 ± 0.09	b	2.67 ± 0.11	a	2.56 ± 0.21	a	2.63 ± 0.07	a
P (mmol/l)	1.21 ± 0.10	b	2.37 ± 0.16	a	2.29 ± 0.21	a	2.07 ± 0.07	a
Mg (mmol/l)	0.79 ± 0.07	b	1.26 ± 0.09	a	1.31 ± 0.06	a	1.29 ± 0.04	a
Na (mmol/l)	141.92 ± 6.71		131.90 ± 1.01		129.85 ± 1.48		132.77 ± 2.01	
K (mmol/l)	4.46 ± 0.11		4.77 ± 0.31		3.88 ± 0.33		4.45 ± 0.14	
Cl (mmol/l)	123.63 ± 5.65	b	106.28 ± 0.88	a	108.12 ± 0.92	a	105.98 ± 0.91	a
Zn (µmol/l)	16.63 ± 0.79	b	25.75 ± 1.95	a	23.55 ± 1.23	a	24.24 ± 1.01	a
Cu (µmol/l)	3.84 ± 0.28		5.60 ± 0.76		5.07 ± 0.44		5.59 ± 0.24	
Fe (µmol/l)	12.10 ± 2.67		15.81 ± 2.56		14.17 ± 2.08		20.18 ± 2.27	
Se (mg/l)	0.17 ± 0.01	b	0.10 ± 0.01	a	0.09 ± 0.01	a	0.10 ± 0.01	a
GPX (µkat/l)	340.98 ± 16.98	b	193.38 ± 12.90	a	176.98 ± 16.48	a	209.10 ± 12.70	a

Legend: $^{a:b:c}$ – the different characters indicate a statistically significant differences P<0.05. ALT – alanine aminotransferases; AST – aspartate aminotransferase; GMT – gama-glutamyltransferase; ALP – alkaline phosphatase; LD – lactate dehydrogenase; CK – creatine kinase; Tbili – total bilirubin; Creat – creatinine; UA – uric acid; TP – total protein; Alb – albumin; Glob – globulin; Glu – glucose; Chol – cholesterol; TG – triglycerides; Ca – calcium; P – phosphorus; Mg – magnesium; Na – sodium; K – potassium; Cl – chlorine; Zn – zinc; Cu – copper; Fe – iron; Se – selenium; GPx – glutathione peroxidase; n – number of cases; SE – Standard Error

A large part of the monitored biochemical parameters between the initial state in the 1st day of age with the 8th day of age is significantly different (P<0.05). Differences occurred in the liver enzyme ALT, whose activity has fallen in all groups, as well as the ALP, where the activity increased. However, this does not match the findings of other researchers, such as Silva et al. (2007). Differences concerning nitrogen metabolism were then captured for CK, Urea, TP, Alb and Glob parameters. Piotrowska et al. (2011) states that TP and Glob increasing during the fattening, which, in our study, is confirmed only by TP in comparison of day 1 with C and M group of day 8. For N group TP decreased. Globulins were significantly higher in the 1st day of life and then decreased. UA is the end product of nitrogen metabolism of poultry. As mentioned by Szabo et al. (2005), its level should be higher for younger chickens compared to the older. Our experiment didn't support this statement with significant difference, but higher value of UA was monitored in 1st day of life in comparison with 8th day of life. Same trend was detected in urea values, which was confirmed in our experiment too (P<0.05). Important differences were also observed in cholesterol, TG and glucose parameters. Cholesterol was highest in the first day of life and then its value dropped, while the representation of TG increased. Peebles et al. (1997) claims that TGA in the initial stages of fattening have a descending tendency, which was not confirmed in our

study. However, similar experience applies to cholesterol (Piotrowska et al. 2011), which our experiment clearly confirmed. The glucose level is then significantly increased in the N group, which indirectly confirms the Hernández et al. (2012), who found that blood glucose concentration decreases in the chickens fed with a higher crude protein proportion. In the assessment of the level of mineral substances, significant changes in the following parameters have occurred: Ca, P, Mg, Cl, Zn and Se. Together with selenium, GPx activity has changed. All mentioned parameters except chlorine and selenium had ascending tendency, chlorine, selenium and GPx activity decreased after a week of life. The increasing tendency of monitored minerals is also confirmed by Ansar et al. (2004) or Silva et al. (2007).

Statistically significant differences ($P<0.05$) in the parameters of individual groups at the 8th day of age were observed for the parameters of nitrogen metabolism in the following values: TP, Alb, Glob. TP was significantly higher in the groups not suffering from crude protein deficiency, which is in accordance with their higher content in the diet. Higher levels of TP, albumins and globulins in the blood have also been observed in chickens fed a higher dose of mineral premix (Islam et al. 2004). Although there were no observed statistically significant difference, uric acid was lower in the N group, which is consistent with the experiment of Hernández et al. (2012). The findings from their experiment also correspond to our results regarding glucose levels, which were significantly higher in the N group. In present study were also observed differences in the parameters of cholesterol and TG, where it was found that the N group had higher level of cholesterol and TG compared to the C and M groups without crude protein deficiency. Other experiments have shown similar results (Jariyahatthakij et al. 2018, Abd-Elsamee et al. 2020). The parameters of blood minerals and liver enzymes in our experiment were not significantly affected using various diets.

CONCLUSION

Feed intake, live weight and blood biochemical parameters were monitored in broiler chickens during the starter period. Our experiment did not show any significant differentials ($P>0.05$) in feed intake and live weights between groups. But almost all monitored blood biochemical parameters (except of several liver enzymes, bilirubin, creatinine, uric acid and several mineral substances) were significantly different ($P<0.05$) between the 1st and 8th day of the age. The value of important indicators of nitrogen, fat and energy metabolism was significantly different between groups on the 8th day of age. For mineral deficiency groups compared to groups without mineral substances deficit, no more significant differences were observed in the representation of mineral substances in the blood. The data obtained from this study suggest that in the initial stages of the fattening, the biochemical parameters are changing, and the early nutrient reduction can affect some of them, which was reflected in the changes of several blood metabolites.

ACKNOWLEDGEMENTS

The research was financially supported by the Internal Grant Agency of Faculty of AgriSciences (Mendel University in Brno) no. AF-IGA-2021-IP064.

REFERENCES

Abd-Elsamee, M.O. et al. 2020. Effect of Different Dietary Crude Protein Levels and Citric Acid on Broiler Chickens' Performance, Carcass Characteristics, Intestinal Morphology, and Blood Components. World's Veterinary Journal, 10(3): 362–374.

Ansar, M. et al. 2004. Effects of high dietary calcium and low phosphorus on urinary system of broiler chicks. Pakistan Veterinary Journal, 24(3): 113–116.

Aviagen Group 2019. Broiler ROSS: Performance Objectives. Available at: http://eu.aviagen.com/tech-center/download/1339/Ross308-308FF-BroilerPO2019-EN.pdf. [2021-09-10]

Bregendahl, K. et al. 2002. Effect of low-protein diets on growth performance and body composition of broiler chicks. Poultry science, 81(8): 1156–1167.

Filipović, N. et al. 2007. Changes in concentration and fractions of blood serum proteins of chickens during fattening. Veterinarski Arhiv, 77(4): 319–326.

Hernández, F. et al. 2012. Effect of low-protein diets and single sex on production performance, plasma metabolites, digestibility, and nitrogen excretion in 1-to 48-day-old broilers. Poultry Science, 91(3): 683–692.

Islam, M.S. et al. 2004. Effects of vitamin-mineral premix supplementation on body weight and certain haemato-bio-chemical values in broiler chickens. Bangladesh Journal of Veterinary Medicine, 2(1): 45–48.

Jariyahatthakij, P. et al. 2018. Effects of adding methionine in low-protein diet and subsequently fed low-energy diet on productive performance, blood chemical profile, and lipid metabolism-related gene expression of broiler chickens. Poultry Science, 97(6): 2021–2033.

Jelínek, P. et al. 2003. Fyziologie hospodářských zvířat. 1. ed., Brno: Mendelova zemědělská a lesnická univerzita v Brně.

Khajali, F. et al. 2006. Effect of vitamin and trace mineral withdrawal from finisher diets on growth performance and immunocompetence of broiler chickens. British Poultry Science, 47(2): 159–162.

Maia, R.C. et al. 2021. Low crude protein diets for broiler chickens aged 8 to 21 days should have a 50% essential-to-total nitrogen ratio. Animal Feed Science and Technology, 271: 114709.

Meluzzi, A. et al. 1992. Determination of blood constituents reference values in broilers. Poultry Science, 71(2): 337–345.

Peebles, E.D. et al. 1997. Effects of added dietary lard on body weight and serum glucose and low density lipoprotein cholesterol in randombred broiler chickens. Poultry Science, 76(1): 29–36.

Piotrowska, A. et al. 2011. Changes in blood chemistry in broiler chickens during the fattening period. Folia Biologica, 59(3–4): 183–187.

Silva, P.R.L. et al. 2007. Blood serum components and serum protein test of Hybro-PG broilers of different ages. Brazilian Journal of Poultry Science, 9(4): 229–232.

Szabo, A. et al. 2005. Developmental dynamics of some blood biochemical parameters in the growing turkey (Meleagris gallopavo). Acta Veterinaria Hungarica, 53(4): 397–409.

The effect of housing technology on the milk performance of Holstein dairy cows in selected breeding

Lenka Zapletalova, Milan Vecera, Gustav Chladek, Marketa Popelkova, Richard Langer
Department of Animal Breeding
Mendel University in Brno
Zemedelska 1, 613 00 Brno
CZECH REPUBLIC

xzaplet7@mendelu.cz

Abstract: The goal of the research was to analyse the effect of the housing technology on the milk performance of Holstein dairy cows. The analysis took place in the Dubicka zemedelska Inc. between January and December in 2020. The analysis was performed on two technologies - the tie stall barn system and the loose-housing system. During the research were used the milk performance data and pooled milk samples data. We obtained and subsequently evaluated the data considering the number of cows, milk performance, fat and protein content of the milk, lactation sequence, lactation stages and the somatic cell count (SCC) in the milk. When comparing the tie stall barn system and the loose-housing system it was found that the housing technology did not have great impact on milk performance. However, it had a major impact on the somatic cell count in the milk. Using the loose-housing system had leaded to better results.

Key Words: housing system, milk performance, Holstein dairy cows, loose-housing system, the tie stall barn system

INTRODUCTION

The cow population in Czech Republic is decreasing as we import cheaper milk from abroad while domestic stockbreeders are facing low farm gate prices. There is an effort in dairy to close the complex: breed - feeding - environment - human, which determines the success of the breeding and the economic efficiency. The choice of the ideal housing system is the essential element for achieving this complex. Long-term breeding efforts have led to improvement in the cow lactation, increased milk performance, nutrient conversion, health, shape and functional properties of the mammary gland, and others (Bouška et al. 2006). The success of stockbreeding can therefore guarantee a better efficiency and an individual production costs reduction (Matoušek et al. 1996). We have to provide the best possible living conditions if we want to achieve these results. The stable for dairy cows should meet the following requirements: adequate ventilation, plenty of light, permanent access to water, easy access to feed ration. It should also provide overall comfort for ensuring the milk performance preservation and improvement, as well as health and well-being of the cows. (Trch 2010). The results of the diseases are worsened milk and reproductive performance and thus endanger the effectiveness of production (Huzzey and Keyserlingk 2013). The current major task is to eliminate heat stress and prevent breeding risks (low reproduction, an increased incidence of mastitis, limb diseases). In dairy farming the loose-housing system is the most preferred, not only because of the animal wellbeing, but also due to lower work intensity and higher possibilities of automation, which saves time and money. Apart from loose-housing systems which can be either in boxes or stalls both with or without litter we also recognize the tie stall barn systems that can be with or without litter aswell. (Bouška et al. 2006).

MATERIAL AND METHODS

Material

The research took place in the Dubicka zemedelska Inc. in Dubicko (Olomouc Region) and follows up the breeding of Holstein cattle. In 2020 Dubicka zemedelska Inc. had 687 Holstein dairy

cows. The company was used two housing technologies. These technologies were named A (the tie stall barn system) and B (the loose-housing system) for the use of the research.

For the technology A, it was a tie stall barn system with the medium stand space with a total capacity for about 200 dairy cows. Cleaning the coat of a dairy cows twice a day was provided the cow keeper during his working hours. Dairy cows in the tie stall were not divided according to production. Cow waterers serve as a source of water, one was used by two cows. The cows were milked twice by tube milking devices.

For the technology B, it was a loose-housing system, which was a reconstructed stall. The production part was divided into sections according to production, according to which was the feed for the cows modified. One section was holder about 60 cows. The capacity of one hall was approximately 228 dairy cows. The vertical drop of the roof ridge was about 3.5 meters. The manure corridor and feeding space were 2.5 metres wide, the grazing table was 3.5 metres wide. The size of the box was 2.5 x 1.25 metres in the production part. The number of boxes was equal to the number of cows – the ratio of 1 : 1 was maintained. There were also scrubbing brushes available for the cows to clean themselves, as well as tempered waterers for drinking. They were milked twice a day in the herringbone milking parlour.

Methods

The data on milk recording scheme and pooled milk samples were collected for both housing technologies throughout the year 2020. Data on the number of cows, milk yield, fat content, protein content, lactation sequence, lactation stages, and SCC were all obtained from the milk recording scheme report. The pooled milk samples were collected from milk tanks once a month contained mixed milk from both evening and morning milking - 24 samples in total were collected and evaluated. The samples were frozen and transported in insulated boxes. The analysis of the samples took place in the research laboratory of the Department of Animal Breeding, Faculty of AgriSciences, Mendel University in Brno. For analysis, the samples were slowly unfrozen in a water bath. Subsequently, their analysis was performed using the Julie C5 Automatic device by Scope Electric. The obtained data were arranged in the MS Excel program and evaluated by one-factor analysis (ANOVA) in the program STATISTICA 12.0.

RESULTS AND DISCUSSION

According to results of the milk analyses, the tie stall barn system had worse values in the somatic cell count when compared to the loose-housing system (Table 1). The average values for fat, protein and lactose content, solids non fat, density, water content, dry mass and freezing point were identical and statistically inconclusive, except for SCC, where the values were statistically significant difference $p < 0.05$.

In the data obtained from the Milk Recording Scheme (Table 2), the tie stall barn system showed better results for fat and protein content but worse results in the amount of obtained milk and the lactation sequence. The obtained values were statistically inconclusive in milk production performance and lactation stage. The values were statistically significant difference $p < 0.01$ for the fat and protein content and lactation sequence.

The average daily milk yield was 29.59 kg of milk while using the tie stall barn system and 29.66 kg of milk while using the loose-housing system. The average amount of collected milk was lower with the tie stall barn system, as the comfort of the animals was reduced and the dairy cows were more exposed to heat stress than with loose-housing system, which leaded to reduction of the milk yield. The results of the "Development of purebred Holstein cows milk performance in Milk Recording Scheme" showed a value of 10 196 kg of milk per lactation (i.e. 33.4 kg of milk per day) in 2019 (Bucek et al. 2020). The breeding goal and the breeding standard of the Holstein breed for 2019 set a value for milk yield in standardized lactation for adult cows of 10 000 kg of milk and more (i.e. 32.8 kg of milk per day) and for first calves 9 000 kg of milk and more (i.e. 29.5 kg of milk per day) in 2019 (Svaz chovatelů holštýnského skotu ČR 2019). The results showed that the dairy cows reach lower values at the average daily milk yield in analyzed company. This could be caused by worse housing conditions (reduced lighting intensity, insufficient air circulation, disturbing the animals by stable work, reduced water intake, higher temperature of the environment) resulting in a decrease in milk yield and poorer

environmental hygiene (especially with the tie stall barn system), as well as worse management of the company, mainly due to inappropriate nutritional arrangements, or even a larger number of first-calf cows included in the herd.

The average content of fat and protein was higher for the tie stall barn system, as the content of milk components correlates negatively with the amount of milk - the content of milk components increased with decreasing yield. The protein and fat then correlated positively.

The average fat content was 3.8% in cow's milk (Štolc et al. 1999). The results of the "Development of purebred Holstein cows milk performance in Milk Recording Scheme" showed a value of 3.84% in 2019 (Bucek et al. 2020), while the breeding goal and breeding standard of the Holstein breed in 2019 set a value only 3.5% for fat content (Svaz chovatelů holštýnského skotu ČR 2019). In Tables 1 and 2, the average annual value of fat content in milk was higher. This can be caused by nutrition, milk yield, individuality of the animals and environmental conditions, including the microclimate of the stall. The difference can also be seen when comparing the fat content in pooled milk analyses and data from Milk Recording Scheme. From analyses of pooled milk samples came out higher percentage of fat comparing to data from Milk Recording Scheme. The higher percentage of fat can also be caused by the fat rising to the surface during milk storage, so it was necessary to mix the milk well before sampling. Although this condition was met, but the milk was mixed only by the ladle not mixing blades and it could have had an effect to a higher fat content.

The average protein content was 3.2% to 3.4% (Frelich et al. 2001). The results of the "Development of purebred Holstein cows milk performance in Milk Recording Scheme" showed a value of 3.37% in 2019 (Bucek et al. 2020). While the breeding goal and breeding standard of the Holstein breed set a value for protein content of 3.4% and more in 2019 (Svaz chovatelů holštýnského skotu ČR 2019). A lower value appeared in pooled milk samples, while a higher value was obtained from data of Milk Recording Scheme. The same factors were affected the protein content as well as the fat content.

The average content of lactose in cow milk was 4.8% (Fox 2003). The lactose content in milk can only be affected to a very small extent by nutrition. The decrease in lactose content occurred with diseases of the mammary gland and the fluctuation also occurred during metabolic disorders (alkalosis, ketosis, acidosis) (Navrátilová et al. 2012). In the analyses of pooled milk samples, the values were rather below the optimum or close to it. This was affected by the presence of mastitis, especially in the period of high temperatures from June to October, and also by metabolic disorder – ketosis, which was associated with poor nutritional arrangements provided by the food supplier.

The optimal somatic cell count was up to 300 000 cells/ml (Štolc et al. 1999). The laboratory set a limit of up to 400 000 cells/ml (Laboratoř pro rozbor mléka 2021). According to the analyses, the count of somatic cell was ideal. It was higher in the tie stall barn system, as their number was significantly affected by housing and milking technology. The higher somatic cell count was further affected by dairy cow diseases and mammary gland inflammation (Frelich et al. 2001). Somatic cell count was associated with the cellular immune response to the inflammatory process (Lindmark-Mänson et al. 2006). More somatic cell count occurred in the spring and autumn months due to changes in the feed doses. In the spring, the feed dose was enriched with green feed, and in the autumn it was switched to winter feed dose (Frelich et al. 2011). The count of somatic cell was therefore affected by the seasons. There was fewer somatic cell count in the colder months, while they increase in the summer months, also due to bad hygiene of the breed (Kadlec 2003). Kadlec's statement about the seasonal factor on the somatic cell count was to a certain extent different from the founded values. The tie stall barn system had the highest average somatic cell count – 509 000 cells/ml - during August. The second largest count was in February, when the value reached 430 000 cells/ml. The highest value for the loose-housing system was 355 000 cells/ml in November. The biggest influence on somatic cell count had higher annual temperatures associated with the heat stress together with the development of microorganisms and consequently even higher incidence of mastitis. Furthermore, there could be the effect of milking technology or poor hygiene in the stall, especially with the tie stall barn system. Another cause of the increased somatic cell count in the second part of the year was secondary contamination and decay of the haylage after heavy rainfall when the water got into the underground channels. Subsequently, a large increase in somatic cell count in milk occurred.

The average achieved lactation sequence was lower for the tie stall system, which was related to lower quality of housing conditions and welfare when dairy cows were more exposed to environmental stress (heat stress, limited movement, etc.). That leaded to a worsened health, reduced longevity and bigger exhaustion of the animals, which results to the reduction of dairy cows. The average achieved lactation sequence was only 2.2 for tie stall barn system, while 2.4 was for loose-housing system. The breeding goal and breeding standard of the Holstein breed in 2019 set a value for the average number of completed lactations of 3.5 (Svaz chovatelů holštýnského skotu ČR 2019). The lower number of lactations indicated poorer cows health on the farm and increased herd replacing.

The Czech and Moravian Society of Breeders (further CMSCH) stated that the ideal content of solids non fat was at least 8.50% (Laboratoř pro rozbor mléka 2021). Pooled milk samples met this value.

The density of milk was in the range from 1.027 to 1.033 g/cm^3. It was affected by a number of factors, such as temperature, milk composition and changes also occurred with diseases or metabolic disorders associated with malnutrition. The content of proteins, lactose and minerals increased the density. The fat content or the addition of water reduced the density (Navrátilová et al. 2012). The values were in the optimal range for milk analyses.

The water content was 0%, which also indicated that in the Czech Republic it is illegal to add and remove anything from the milk or dilute it with water to increase the volume.

The freezing point values for cow's milk were -0.512 °C to -0.550 °C. Its value was influenced by factors such as the breed, lactation stage, the incidence of mastitis, nutrition, heat stress or water intake (Navrátilová et al. 2012). The values of individual pooled milk samples mostly met this range, only in a few cases the values were slightly higher, however, the average annual value fell within the optimal range.

Table 1 Effect of housing technology on milk yield parameters (data from analyses of pooled milk samples)

Technology	n	Average fat content [%]	Average SNF (solids non fat) [%]	Average density [g/cm^3]	Average protein content [%]	Average lactose content [%]	Average added water [%]	Average dry matter [%]	Average freezing point [°C]	Average somatic cell count [cells/ml]
The tie stall barn system	12	4.39	8.53	1.03	3.14	4.69	0.00	0.70	-0.548	196 909 ^{a}
The loose-housing system	12	4.39	8.52	1.03	3.13	4.68	0.00	0.70	-0.548	172 545 ^{b}
The level of evidence	-	NS	NS	NS	NS	NS	NS	NS	NS	*
Total	24	4.39	8.53	1.03	3.13	4.68	0.00	0.70	-0.548	184 727

*Legend: The level of evidence = statistically significant difference/N.S. = non significant. The values in the columns marked with different letters are conclusive at the level of $p < 0.01$ ** (A, B); $p < 0.05$ * (a, b); $p > 0.05$ NS. Total is the sum for the whole data set. n – number of pooled milk samples*

Table 2 Effect of housing technology on milk yield parameters (data from Milk Recording Scheme)

Technology	n	Average milk yield [kg]	Average fat content [%]	Average protein content [%]	Average order of lactation [n]	Average lactation stage [days]
The tie stall barn system	1 862	29.59	4.24 ^{A}	3.57 ^{A}	2.2 ^{A}	177
The loose-housing system	5 028	29.66	4.07 ^{B}	3.53 ^{B}	2.4 ^{B}	174
The level of evidence	-	NS	**	**	**	NS
Total	6 890	29.64	4.12	3.54	2.3	175

*Legend: The level of evidence = statistically significant difference/N.S. = non significant. The values in the columns marked with different letters are conclusive at the level of $p < 0.01$ ** (A, B); $p < 0.05$ * (a, b); $p > 0.05$ NS. Total is the sum for the whole data set. n – number of cows*

CONCLUSION

Compared to the loose-housing system, the tie stall barn system showed lower milk yield, higher fat and protein content, lower average lactation sequence and higher somatic cell count at the average annual values from Milk Recording Scheme. The values from the pooled milk samples only differed in the somatic cell count, when the tie stall barn system showed a higher number, because there was a reduced udder cleanness, poor hygiene during milking and worsened health of the animals. When comparing the tie stall barn system and loose-housing system, it was found that the housing technology did not have much effect on milk yield in terms of the amount of the produced milk, protein content and fat content. However, it had a major effect on the somatic cell count in the milk. When comparing these two technologies, loose-housing system shows better hygiene and health for the cows and better reproductive and production indicators. The loose-housing systems are more perspective when considering wellbeing of the cows and production conditions. Also they give advantages in terms of work and time, which is why they are slowly replacing tie stall barn systems.

REFERENCES

Bouška, J. et al. 2006. Chov dojeného skotu. 1. ed., Praha: Profi Press, s.r.o.

Bucek, P. et al. 2020. Ročenka 2019 - chov skotu v České republice 2020. [Online]. Available at: https://www.cmsch.cz/plemenarska-prace/ku-kontrola-uzitkovosti/chovatelske-rocenky/rocenky-chovu-skotu/. [2021-09-06].

Fox, P.F. 2003. Encyclopedia of Dairy Sciences. 1. ed., New York: Academic Press.

Frelich, J. et al. 2011. Chov hospodářských zvířat I. 1. ed., České Budějovice: JU ZF.

Frelich, J. et al. 2001. Chov skotu. 1. ed., České Budějovice: Jihočeská univerzita.

Huzzey, J., Keyserlingk, M. 2013. Managing the costs of metritis: Using feeding behaviour to facilitate disease detection and improve dairy cattle welfare. 1. ed., Rome, Italy: FAO.

Kadlec, I. 2003. Jakost mléka, vazby a příčinná souvislost mezi výsledky jednotlivých ukazatelů jakosti a jejich vliv na mlékárenskou výrobu. 1. ed., Praha: Mlékařské listy.

Laboratoř pro rozbor mléka (LRM). 2021. Rozbory zpeněžování. ČMSCH, a.s. (Českomoravská společnost chovatelů) [Online]. Available at: https://www.cmsch.cz/laboratore/lrm-laborator-pro-rozbor-mleka/rozbory-mleka/rozbory-zpenezovani/. [2021-09-06].

Lindmark-Mänson, H. et al. 2006. Relatioship between somatic cell count, individual leukocyte populations and milk components in bovine udder quarter milk. International Dairy Journal, 16(7): 717–727.

Matoušek, V. et al. 1996. Speciální zootechnika. 1. ed., České Budějovice: Jihočeská univerzita, Zemědělská fakulta.

Navrátilová, P. et al. 2012. Hygiena produkce mléka. 1. ed., Brno: Veterinární a farmaceutická univerzita Brno.

Svaz chovatelů holštýnského skotu ČR, z. s. 2019. Šlechtitelský program českého holštýnského skotu. [Online]. Available at: https://www.holstein.cz/cz/soubory/soubry-ke-stazeni/slechteni/273-slechtitelsky-program-2019/file. [2021-09-06].

Štolc, L. et al. 1999. Chov hospodářských zvířat I: (chov skotu, ovcí a koní). 2. rework. ed., Praha: Česká zemědělská univerzita, Institut sociálních vztahů.

Trch, J. 2010. Vliv technologie chovu na užitkové vlastnosti dojnic. Bachelor thesis (in Czech), University of South Bohemia in České Budějovice.

FISHERIES AND HYDROBIOLOGY

Is oral application of plastic particles able to provoke the oxidative stress and alter expression of an immunity related genes in rainbow trout?

Aneta Hollerova[1,2], Nikola Hodkovicova[2], Jana Blahova[1], Martin Faldyna[2], Denisa Medkova[1,3], Jan Mares[3], Zdenka Svobodova[1]
[1]Department of Animal Protection and Welfare & Veterinary Public Health
University of Veterinary Sciences
Palackeho tr. 1, 612 42 Brno
[2]Department of Infectious Diseases and Preventive Medicine
Veterinary Research Institute
Hudcova 296/70, 621 00 Brno
[3]Department of Zoology, Fisheries, Hydrobiology and Apiculture
Mendel University in Brno
Zemedelska 1665/1, 613 00 Brno
CZECH REPUBLIC

hollerova@vri.cz

Abstract: In these days aquatic pollution by plastic materials is a worldwide environmental problem and may negatively affect the health of organisms exposed to oral intake of these contaminants. The main task of this study was the evaluation of polystyrene (PS) microparticles effects on selected health parameters of rainbow trout (*Oncorhynchus mykiss*) juveniles. Tested fish were divided into 4 groups – with 0.5%, 2% and 5% concentration of PS microparticles in diet and control group without the addition of microplastics. The experiment was divided into two samplings – after 4 weeks and 6 weeks of exposure. Significant differences were found in liver tissue and gills in the highest PS concentration related to control. In conclusion, PS microparticles can affect health indices of *O. mykiss* and the potential risk for aquatic environment and even human consumption should be considered.

Key Words: microplastics, aquatic environment, *Salmonidae*, qRT-PCR, oxidative stress, toxicology

INTRODUCTION

Plastic production is showing dramatic growth around the world and is rated as a serious threat to aquatic organisms, mainly due to poor recycling of these materials. Moreover, the massive use of face masks due to emergency of covid-19 and the global pandemic disrupted the ongoing regulation of plastic pollution in the environment and, in contrast, caused higher burden for the aquatic environment (Aragaw 2020). In the aquatic environment, the external conditions promote the release of smaller particles from larger plastic objects – these are called as microplastics with defined size < 5 mm (Eerkes Merano et al. 2015). The presence of microplastics has been showed in the digestive tract of most aquatic organisms at various trophic levels, with negative effects on viability, oxidative stress parameters, immune system and others (Hollerova et al. 2021). In addition, microplastic particles are not stored in the gastrointestinal tract and particles < 0.6 mm in size are able to cross the intestinal barriers, enter the blood stream or can be transported to body tissues (Hodkovicova et al. 2021). Polystyrene (PS) is plastic material commonly used in various industries, which highly contributes to water pollution and oral exposure was defined as the main way of microplastic exposure in fish (Vivekanand et al. 2021).

The PS particles with an average size of 52.5 ± 11.5 µm (EPRUI Biotech Co. Ltd, China) were used in our experiment, when have been added to the feed of the tested groups. The main task of the study was to confirm the hypothesis that PS have effects on the expression of selected genes and oxidative stress parameters of rainbow trout's liver tissue and gills.

MATERIAL AND METHODS

Our study was performed with 128 juveniles of *O. mykiss* (average body length 188.7 ± 12.1 mm, average body weight 81.8 ± 16.4 g), which were divided into 8 water tanks of 18 fish each with connection to recirculation system. At first, juveniles were acclimatized for two weeks to laboratory conditions. The experimental phase lasted six weeks and two samplings were performed during the experiment – at 4th and 6th week. The study was conducted in duplicate – two tanks were exposed to 0.5% PS, two tanks to 2% PS and two tanks to 5% PS concentration in feed. Two aquariums served as a control without addition of PS in the diet. Fish were fed three times a day with a total dose of 1.5% of their body weight; this dose was adjusted every two weeks according to the current weight of the fish mass. The water condition was monitored every 12 hours and the average parameters were as follow: temperature 16.2 ± 0.1 °C, oxygen saturation 8.8 ± 0.2 mg/l, pH 7.3 ± 0.2, total ammonia < 0.01 mg/l chlorides 113.6 ± 4.3 mg/l, nitrites < 0.01 mg/l.

At the end of 4th and 6th week, fish were stunned with a blow to the head, killed by spinal transection and each piece was individually measured for basic biometric parameters (body mass, total length, width, height, liver mass) and autopsy. For the subsequent analysis, the samples of liver and gill were immediately frozen at – 80 °C (n = 8 per one PS concentration).

For oxidative stress analysis, the tissue samples were homogenized in phosphate buffer (pH 7.2) in a 1:10 weight: volume ratio. Half of the homogenate was used for lipid peroxidation analysis using malondialdehyde (MDA) measurement by the thiobarbituric acid reactive substances method (TBARS) according to Lushchak et al. (2005). The second part of homogenate was centrifuged (11,000 x g for 20 min at 4 °C) to obtain the supernatant and then used for spectrophotometric analysis of enzyme activities. The glutathione-*S*-transferase (GST) activity was measured according to Habig et al. (1974), glutathione peroxidase (GPx) catalytic activities were measured according to Flohe and Gunzler (1984).

Samples of tissues for gene expression analysis with quantitative real-time polymerase chain reaction (qRT-PCR) method were processed according to Hodkovicova et al. (2021); the primer sequences of selected genes – tumor necrosis factor alpha (*tnfα*), interleukin 1 beta (*il1β*) and reference gene *60S* ribosomal protein were adapted from the same study.

The difference was considered as a statistically significant and highly significant if $p < 0.05$ and $p < 0.01$. Box plot graphs were constructed using medians with whiskers of maximum 1.5 interquartile range and outliers denoted as points.

RESULTS AND DISCUSSION

There was no statistically significant difference in biometric parameters during the study lasting. Regards the oxidative stress indices, a statistically significant increase of TBARS activity in liver ($p < 0.05$) was observed in the highest PS concentration (5%) after six-week exposure. In the gills, the GPx activity ($p < 0.05$) increased in highest PS concentration (5%) after four-week exposure related to the control group.

Oxidative stress is valuable tool in ecotoxicology testing, which is applied for the evaluation of balance between production of reactive oxygen species (ROS) and antioxidant capacity (Velisek et al. 2011). Prokić et al. (2019) referred that the PS microparticles may affect mitochondrial function that led to higher ROS production, altered activity of oxidative stress enzymes which could, in conclusion, cause the tissue damages. The results of our experiment showed that PS microparticles may negatively affect antioxidant system of the rainbow trout due to changes in GPx and TBARS marker. The results are given in Figure 1.

During the experiment lasting, the expression of gene *tnfα* ($p < 0.05$) increased in the group exposed to the highest PS concentration (5%) in the liver tissue after six weeks. Also in the gills, the expression of *il1β* ($p < 0.05$) increased as well in 5% PS after six week exposure. The results are given in Figure 2. The increased expression of the pro-inflammatory cytokines, *il1β* and *tnfα*, may cause severe chronic diseases and could lead to changes in leukocyte migration ability, altered neutrophil activation and phagocytosis (Gionfra et al. 2019). The inflammation discovered in liver and gills by gene expression analysis will be further verified by histopathological examination. Even with these results, the impact of PS on immunological processes in tissues is obvious. As the liver and gills are main detoxifying, metabolic and osmotic organs, their prolonged weakening can cause severe homeostatic

and immunity changes with consequent susceptibility to infectious diseases and increased fish mortality (Hodkovicova et al. 2021).

Figure 1 The results of oxidative stress indices in gills and liver for GPx and TBARS parameters. Results are given as n ± SD (n=8).

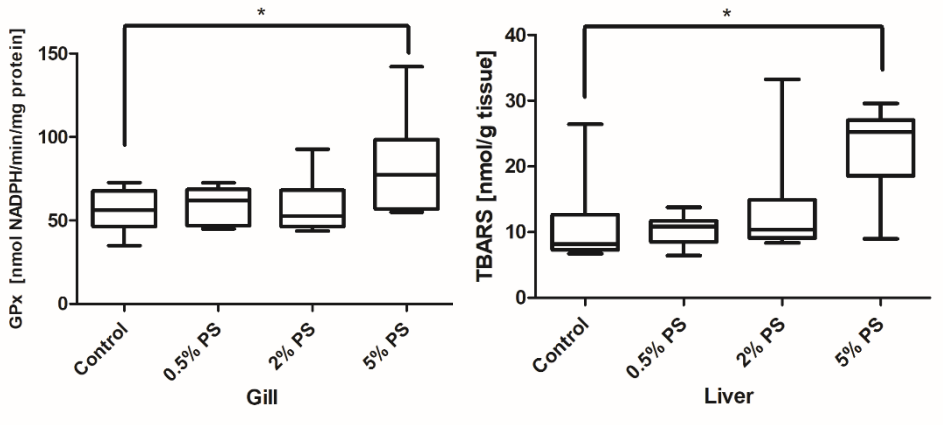

Figure 2 The results of relative gene expression in liver and gills for selected genes (tnfα, il1β) in relation to the reference gene 60S. Results are given as n ± SD (n=8).

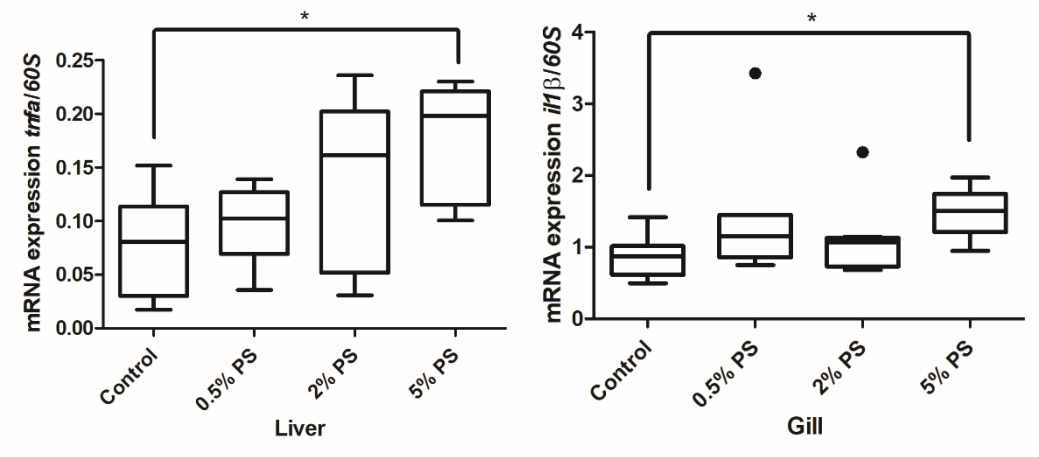

CONCLUSION

Our study confirmed the hypothesis that PS microparticles (in average size 52.5 µm) contained in diet of rainbow trout (*Oncorhynchus mykiss*) have the negative effect on antioxidant and immune system of liver and gill tissue. After four- and six-week exposure to the highest tested PS concentration (5%), differences were observed for *tnfa* and *il1b* gene expression and for GPx and TBARS activity. The prolonged weakening of the liver and gills may cause severe homeostatic and immunity disruption and increased fish mortality.

ACKNOWLEDGEMENT

This research was supported by the Internal Grant Agency of the University of Veterinary and Pharmaceutical Sciences Brno [no. 212/2020/FVHE] and by the ERDF/ESF "Profish" [no. CZ.02.1.01/0.0/0.0/16_019/0000869].

REFERENCES

Aragaw, T.A. 2020. Surgical face masks as a potential source for microplastic pollution in the COVID-19 scenario. Marine Pollution Bulletin, 159: 111517.

Eerkes-Medrano, D. et al. 2015. Microplastics in freshwater systems: A review of the emerging threats, identification of knowledge gaps and prioritisation of research needs. Water Research, 75: 63–82.

Flohe, L., Gunzler, W.A. 1984. Assays of glutathione peroxidase. Methods in Enzymology, 105: 114–1520.

Gionfra, F. et al. 2019. The role of thyroid hormones in hepatocyte proliferation and liver cancer. Frontiers in Endocrinology, 10: 532.

Habig, W.H. et al. 1974. Glutathione S-Transferases: The first enzymatic step in mercapturic acid formation. Journal of Biological Chemistry, 249(22): 7130–7139.

Hodkovicova, N. et al. 2021. Do foodborne polyethylene microparticles affect the health of rainbow trout (*Oncorhynchus mykiss*)? Science of the Total Environment, 793: 148490.

Hollerova, A. et al. 2021. Microplastics as a potential risk for aquatic environment organisms – a review. Acta Veterinaria Brno, 90: 99–107.

Lushchak, V.I. et al. 2005. Hypoxia and recovery perturb free radical processes and antioxidant potential in common carp (*Cyprinus carpio*) tissues. The International Journal of Biochemistry & Cell Biology, 37: 1319–1330.

Prokić, M.D. et al. 2019. Ecotoxicological effects of microplastics: Examination of biomarkers, current state and future perspectives. TrAC Trends in Analytical Chemistry, 111: 37–46.

Velisek, J. et al. 2011. Comparison of the effects of four anaesthetics on blood biochemical profiles and oxidative stress biomarkers in rainbow trout. Aquaculture, 310 (3–4): 369–375.

Vivekanand, A.C. et al. 2021. Microplastics in aquatic environment: Challenges and perspectives. Chemosphere, 282: 131151.

Selected biochemical parameters of two common carp (*Cyprinus carpio*) breeds infected with koi herpesvirus

Radek Machat[1,2], Lenka Leva[1], Lubomir Pojezdal[1], Martin Faldyna[1]
[1]Department of Infectious Diseases and Preventive Medicine
Veterinary Research Institute
Hudcova 70, 621 00 Brno
[2]Department of Experimental Biology
Masaryk University
Kamenice 5, 625 00 Brno
CZECH REPUBLIC

radek.machat@vri.cz

Abstract: Koi herpesvirus (KHV) is infective agent causing one of the most serious diseases of common carp. Koi herpesvirus disease (KHVD) morbidity and mortality might reach 100%. Two common carp breeds with completely different susceptibility to KHV were chosen in this study. Koi carp, which is highly susceptible to KHV and amur wild carp. In this study, levels of chosen biochemical markers at 7 dpi (days post infection) were measured, namely: total protein, albumin, alanine aminotransferase, aspartate aminotransferase, glucose, triglycerids, cholesterol, calcium. Nevertheless, no differences in monitored blood factors were measured at this time point.

Key Words: koi carp, amur wild carp, cyprinid herpesvirus 3, blood plasma, biochemic analysis

INTRODUCTION

Common carp is one of the most economically important freshwater fish in the world. According to FAO (Food and Agriculture Organization of the United Nations) data, both fishery and aquaculture produced more than 4.2 million tons of common carp, which constitute more than 7.5% of global freshwater fish production in 2017 (FAO 2020). Significance of common carp is even higher in Europe, where carp accounts almost one third of freshwater fish production.

Koi herpesvirus, taxonomically called Cyprinid herpesvirus 3 (CyHV-3), causes emerging disease affecting only common carp, its subspecies and some hybrids of common carp with other cyprinids (Bergmann et al. 2020, Hedrick et al. 2006). KHVD is seasonal disease, which manifests itself in water temperatures between 18 °C and 28 °C (Pokorova et al. 2005). KHV causes significant economic losses. As no treatment or vaccine for KHVD has been approved in EU so far, all that remains after KHVD detection is complete eradication of affected fish farm (Bergmann et al. 2020). KHVD mortality influence multiple factors, except of water temperature also for example stress, age, overall physical condition of host fish and belonging to the breed of common carp (Piačková et al. 2013). KHVD is severe disease, because is spread almost all around the world. (Ilouze et al. 2011, Novotny et al. 2010, Toffan et al. 2020, Zrnčić et al. 2020)

KHVD can cause pathological changes in liver (Gotesman et al. 2013). Biochemical parameters for analysis were chosen to describe expected changes in liver functioning as well as changes in overall metabolism of two breeds of common carp with totally different susceptibility to KHV.

MATERIAL AND METHODS

Experimental design

Two breeds of common carp were chosen as experimental organisms, highly KHV resistant breed- Amur wild carp (AS), and KHV susceptible breed- koi. Twenty-six fish from both carp breeds were divided into four groups: two control (five fish in each group) and two infected (eight fish in each group). Carps from control groups were injected intraperitoneally with virus free media. Carps from infected groups were injected intraperitoneally with dosage 10^4 TCID50/mL of KHV suspension.

Both groups were kept in separated water tanks with the same temperature 23 °C for 7 days. The time point was chosen because deaths of KHV infected koi carps were reported repeatedly at approximately 7 dpi (Gilad et al. 2004, Hedrick et al. 2000, Piačková et al. 2013). Further, blood samples were collected at 7 dpi. Blood samples were centrifuged, and plasma samples were removed for further use. However, only blood plasma of two control fish per carp breed and six infected fish per carp breed was used for biochemical analysis, because small amount of blood was acquired from remaining fish.

Biochemical analysis

Total protein, albumin, glucose, alanine aminotransferase (ALT), aspartate aminotransferase (AST), triglycerids, cholesterol, calcium were analysed in blood plasma by enzymatic-colorimetric method using BS-200 chemistry analyser (Mindray, Shenzhen, China) and commercial kits (Greiner DiagnosticGmbH, Bahlingen, Germany). Actual concentration of plasma albumin was calculated by its conversion from total protein concentration in samples.

Statistics

Data acquired from infected groups were statistically evaluated in this study. Obtained data were evaluated using GraphPad Prism 5.03 software. Nonparametric Kruskal-Wallis statistic method was used for analysis.

RESULTS AND DISCUSSION

Biochemical analysis of blood plasma samples

Six plasma samples from infected koi and six from infected AS were compared searching for changes in plasma levels of markers of liver damage (mainly ALT, AST), marker of stress (glucose) etc. influenced by KHV infection between carp breeds. Control samples could not be compared, because their small amount. No mortalities were among fish and only two fish showed symptoms of KHV. One AS showed very high production of mucus and one koi carp had haemorrhages at base of fins. The changes of selected biochemical parameters at 7 dpi were expected as we measured significant differences in levels of expression of some immune system related genes between AS and koi (data not yet published; Gilad et al. 2004, Hedrick et al. 2000, Piačková et al. 2013). However, no changes were measured in biochemical parameters (Table 1).

Until now, only a few published studies, which include biochemical analysis, are available. After oral application of KHV suspension no significant differences were measured in plasma concentration of calcium and total protein at 8 dpi (Negenborn et al. 2015). Further, plasma concentration of albumin, ALT, AST, glucose, and total protein in common carps infected with KHV remained in physiological range in samples acquired during KHV monitoring in 2005 (Pokorova et al. 2008). For this reason, the current results are not entirely surprising. Faint course of the disease may be the reason of insignificant differences in concentrations of selected plasma parameters.

Table 1 Biochemical analysis of blood plasma composition of common carp breeds

Indices	Units	AS control	AS infected	Koi control	Koi infected
Albumin	g/l*total protein	0.59 ± 0.06	0.46 ± 0.19	0.25 ± 0.09	0.56 ± 0.13
ALT	µkat/l	0.72 ± 0.28	1.13 ± 0.98	0.69 ± 0.00	0.97 ± 1.17
AST	µkat/l	10.31 ± 4.28	10.51 ± 2.06	9.60 ± 4.97	6.85 ± 2.90
Glucose	mmol/l	5.98 ± 0.35	5.45 ± 3.01	5.46 ± 0.61	6.43 ± 0.88
Triglycerids	mmol/l	2.24 ± 0.41	2.06 ± 0.73	1.61 ± 0.25	1.87 ± 0.35
Total protein	g/l	39.70 ± 3.13	26.93 ± 7.82	33.54 ± 7.27	31.01 ± 5.17
Cholesterol	mmol/l	5.53 ± 0.79	2.57 ± 0.98	3.60 ± 0.46	3.23 ± 0.63
Calcium	µmol/l	3.08 ± 0.40	2.26 ± 0.52	2.20 ± 0.52	2.40 ± 0.32

Legend: ALT - Alanine aminotransferase, AST - Aspartate aminotransferase, AS – amur wild carp, Koi – koi carp. Data are expressed as mean ± SEM

CONCLUSION

Biochemical analysis of blood plasma samples retrieved from KHV infected amur wild carps and koi carps shows no significant differences in monitored factors at 7 dpi. Nevertheless, this observation is not so unexpected, because no mortalities of fish were there, and one koi carp and one AS had symptoms of KHV.

ACKNOWLEDGEMENTS

This study was supported by European Regional Development Fund in the Operational Programme Research, Development and Education and The Czech Ministry of Education, Youth and Sports, project PROFISH CZ.02.1.01/0.0/0.0/16_019/0000869.

REFERENCES

Bergmann, S.M. et al. 2020. Koi herpesvirus (KHV) and KHV disease (KHVD) – a recently updated overview. Journal of Applied Microbiology, 129: 98–103.

FAO. 2004. Food and Agriculture Organization of the United Nations. Fishery Statistical Collections. Global Production [Online]. Available at: http://www.fao.org/fishery/statistics/global-production/en. [2020-11-7].

Gilad, O. et al. 2004. Concentrations of a Koi herpesvirus (KHV) in tissues of experimentally infected *Cyprinus carpio* koi as assessed by real-time TaqMan PCR. Diseases of Aquatic Organisms, 60: 179–187.

Hedrick, R.P. et al. 2006. Susceptibility of Koi Carp, Common Carp, Goldfish, and Goldfish × Common Carp Hybrids to *Cyprinid Herpesvirus-2* and *Herpesvirus-3*. Journal of Aquatic Animal Health, 18: 26–34.

Hedrick, R.P. et al. 2000. A Herpesvirus Associated with Mass Mortality of Juvenile and Adult Koi, a Strain of Common Carp. Journal of Aquatic Animal Health, 12: 44–57.

Ilouze, M. et al. 2011. The outbreak of carp disease caused by CyHV-3 as a model for new emerging viral diseases in aquaculture: a review. Ecological Research, 26: 885–892.

Negenborn, J. et al. 2015. Cyprinid herpesvirus-3 (CyHV-3) disturbs osmotic balance in carp (*Cyprinus carpio L.*)—A potential cause of mortality. Veterinary Microbiology, 177: 280–288.

Novotny, L. et al. 2010. First clinically apparent koi herpesvirus infection in the Czech Republic. Bulletin- European Association of Fish Pathologists, 30: 85–91.

Piačková, V. et al. 2013. Sensitivity of common carp, *Cyprinus carpio L.*, strains and crossbreeds reared in the Czech Republic to infection by *Cyprinid herpesvirus 3* (CyHV-3; KHV). Journal of Fish Diseases, 36: 75–80.

Pokorova, D. et al. 2005. Current knowledge on koi herpesvirus (KHV) a review. Veterinarni Medicina, 50: 139–148.

Pokorova, D. et al. 2008. Tests for the presence of koi herpesvirus (KHV) in common carp (*Cyprinus carpio carpio*) and koi carp (*Cyprinus carpio koi*) in the Czech Republic. Veterinarni Medicina 52, 562–568.

Toffan, A. et al. 2020. First detection of koi herpesvirus and carp oedema virus in Iraq associated with a mass mortality in common carp (*Cyprinus carpio*). Transboundary and Emerging Diseases, 67: 523–528.

Zrnčić, S. et al. 2020. Koi herpesvirus and carp edema virus threaten common carp aquaculture in Croatia. Journal of Fish Diseases, 00: 1–13.

Effects of pesticides on catfish (*Silurus glanis*) embryos

Denisa Medkova[1,2], Pavla Lakdawala[2], Veronika Doubkova[2], Jana Blahova[2], Aneta Hollerova[2,3], Zuzana Weiserova[2], Nikola Hodkovicova[3], Zdenka Svobodova[2], Jan Mares[1]

[1]Department of Zoology, Fisheries, Hydrobiology and Apiculture
Mendel University in Brno
Zemedelska 1, 613 00 Brno
[2]Department of Animal Protection and Welfare & Veterinary Public Health
University of Veterinary Sciences Brno
Palackeho tr. 1, 612 42 Brno
[3]Department of Infectious Diseases & Preventive Medicine
Veterinary Research Institute
Hudcova 296/70, 621 00 Brno
CZECH REPUBLIC

H19004@vfu.cz

Abstract: Pesticides and many other types of contaminants have been constantly entering the aquatic environment. Pesticides, which are commonly used in agriculture, can have a negative impact on non-target species as well as human health. In the few past decades, water pollution caused by pesticides has become a commonly discussed issue. Residues of pesticides enter water environment, where they persist and have bioaccumulation potential. The aim of this research was to compare the effects of herbicide MCPA (4-chloro-2-methylphenoxyacetic acid), fungicide prochloraz and herbicide metazachlor on catfish (*Silurus glanis*) embryos in 96 hours long acute toxicity test with the five different tested concentrations. In the study, statistically significant changes were observed only at high concentrations that do not occur in nature. The results of the study show that the substances had a negative effect on fish development at some tested concentration. However, this screening study must be followed by studies of sub chronic and chronic toxicity with focus on lower tested concentrations in order to reveal a potential negative impact of long-term exposure to non-target species.

Key Words: development, malformation, mortality, hatching

INTRODUCTION

Surface waters are polluted by residues of various substances, such as industrial chemicals, substances used for plants protection, pharmacological active substances or personal care products. There are many studies that show a negative effect on the development of non-target aquatic organisms. Fish are on the top of the aquatic food chain, therefore, they are a good model organisms for toxicity tests on aquatic organism (Sehonova et al. 2016).

Pesticides are commonly used products in agriculture and in households. Among the most used products belong herbicides and fungicides. Residues of these substances are frequently found in surface and ground waters. Moreover, they are known to be persistent and also to have a bioaccumulation potential. These properties can subsequently result in negative effects on aquatic biota, such as fish and other non-target organisms (Rahman et al. 2021). Gaillard et al. (2016) monitored pesticide concentrations in surface water in the north-east of France, where the concentration of MCPA was 26.5 µg/l. In Australia, herbicides as MCPA, simazine, diuron, and atrazine were detected at five places near Melbourne (Allinson et al. 2017). MCPA, metazachlor, and other pesticides were regularly detected in European surface waters (Sjerps et al. 2019). Metazachlor is one of the most used herbicide in the United Kingdom and in Germany (Mohr et al. 2008). Mohr et al. (2008) reported the concentration of metazachlor in surface waters to be up to 100 µg/l. Pesticides are used widely in agriculture and they can enter to surface water (Sjerps et al. 2019), also Rodriguez Ortega et al. (2019) described

that prochloraz is widely used imidazole fungicide. The aim of study was to evaluate potential negative effect of pesticides (MCPA, prochloraz, metazachlor) on development of catfish embryos in the acute toxicity test.

MATERIALS AND METHODS

Fish embryonic acute toxicity test was performed according to the Guideline for Test No. 236: Fish Embryo Acute Toxicity (FET) Test (OECD 2013) for the period of 96 hours with five different concentrations of each substances and three control groups (explained below). Catfish (*Silurus glanis*) eggs came from commercial farm Rybníkářství Pohořelice a.s. (Czech Republic). The quality of eggs was checked and eggs were selected using binocular microscope. Fertilized eggs were distributed into 24-microwell plates, dead and unfertilised eggs were destroyed. For each concentration and the control, 24 embryos were used. MCPA and metazachlor were tested at concentrations 0.05 µg/l (environmentally relevant), 50 µg/l, 500 µg/l (wastewater relevant), 5 000 µg/l and 100 000 µg/l, prochloraz was tested at the concentrations 0.1 µg/l (environmentally relevant), 1 µg/l, 100 µg/l (wastewater relevant), 1 000 µg/l and 100 000 µg/l. Tested pesticides are insoluble in water, prochloraz and metazachlor are soluble in DMSO, MCPA is soluble in ethanol. Therefore, three control groups had to be created. First control group was exposed to ISO water only prepared according to standard ISO 7346 (ISO 1996), second control group was exposed to ISO water with DMSO and third control group was exposed to ISO water with ethanol. Temperature during the test was 23 °C and photoperiod was 12 hours light/12 hours dark. Tested solutions were changed every day and embryos were observed to record lethal and sublethal endpoint (coagulation, lack of somite formation, malformation rate, and hatching) (OECD 2013).

Statistical analysis was conducted using Unistat 5.6 (Czech Republic). Cumulative mortality, development and hatching data were analyzed using chi-square and contingency tables.

RESULTS AND DISCUSSION

Figure 1 Mortality of catfish during 96hour exposure at the highest tested concentration (100 000 µg/l)

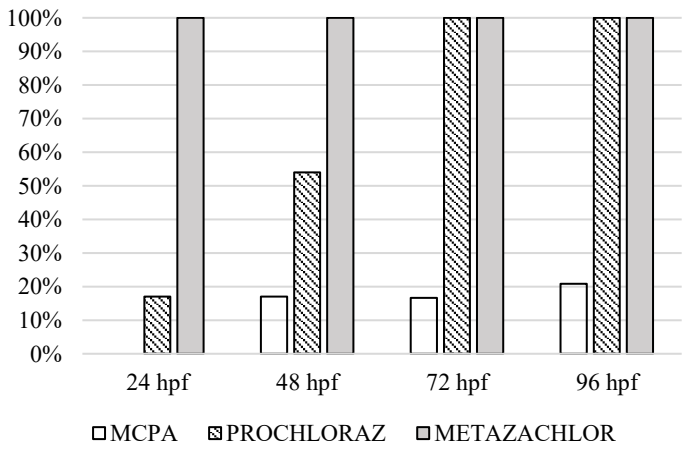

No significant changes were observed in the control group. MCPA exposure did not cause any effect on hatching or mortality. However, MCPA had a negative effect on embryos development at the highest tested concentration, where malformations were observed in 37.5% ($p<0.05$) of catfish embryos. The most common malformation caused by MCPA was heart oedema and blood clot. Johansson et al. (2006) reported LC50 for fish 100 mg/l and for amphibians 3.6 g/l. Prochloraz and metazachlor had a negative effect on catfish mortality, where mortality at the concentration 100 000 µg/l of metazachlor reached 100% ($p<0.01$) after 24 hours post fertilization (hpf). Mortality of catfish exposed to prochloraz at the concentration 100 000 µg/l was 54% after 48 hpf and increased to 100% at 72 hpf. Moreover, embryos exposed to prochloraz and metazachlor showed significantly higher malformation rate compared to control groups. In case of prochloraz, 33% ($p<0.05$) of malformation were observed at the concentration of 1 000 µg/L at 96 hpf. Similarly, at 48 hpf, 33% of specimen coming from the concentration of 100 000 µg/l were also found to have some developmental malformations. At 96 hpf, metazachlor at 5 000 µg/l caused malformations to 29.1% ($p<0.05$) of catfish embryos and at the concentration of 500 µg/l to 33.3% ($p<0.05$) embryos. In the study of Mohr et al. (2008), metazachlor had a strong

effect on the stream and pond mesocosm communities at the concentration higher than 5 µg/l. Prochloraz and metazachlor did not have significant effect on hatching.

CONCLUSION

The results of the study show that prochloraz and metazachlor are more toxic than MCPA. Prochloraz and metazachlor caused a high percentage of mortality at the concentration of 100 000 µg/l and malformation at the concentration 1 000 µg/l and 100 000 µg/l of prochloraz and at the concentration 500 µg/l and 5 000 µg/l of metazachlor. MCPA had significant effect only on malformation rate. LOEC for prochloraz was determined to be 1 000 µg/l and for metazachlor was determined to be 500 µg/l. Pesticides can have a negative effect on development of aquatic organisms, thus it is important monitor the concentrations in surface water.

ACKNOWLEDGEMENTS

This research was supported by project PROFISH – Mendel University in Brno, CZ.02.1.01/0.0/0.0/16_019/0000869 and IGA VETUNI 223/2021/FVHE.

REFERENCES

Allinson, M. et al. 2017. Herbicides and trace metals in urban waters in Melbourne, Australia (2011-12): concentrations and potential impact. Environmental Science and Pollution Research, 24(8): 7274–7284.

Gaillard, J. et al. 2016. Potential of barrage fish ponds for the mitigation of pesticide pollution in stream. Environmental Science and Pollution Research, 23(1): 23–35.

ISO 7346. 1996. Waterquality – Determination of the acute lethal toxicity of substances to a freshwaterfish [*Brachydanio rerio* Hamilton-Buchanan (Teleostei, *Cyprinidae*)] – Part 1: Static method.

Johansson, M. et al. 2006. Toxicity of six pesticides to common frog (*Rana temporaria*) tadpoles. Environmental Toxicology and Chemistry, 25(12): 3164–3170.

Mohr, S. et al. 2008. Response of plankton communities in freshwater pond and stream mesocosms to the herbicide metazachlor. Environmental Pollution, 152(3): 530–542.

OECD. 2013. Test No 236: Fish Embryo acute Toxicity (FET) Test. OECD Guidelines for the Testing of Chemicals, Section 2, OECD Publishing, Paris, France.

Rahman, M. et al. 2021. Monitoring of pesticide residues from fish feed, fish and vegetables in Bangladesh by GC-MS using the QuEChERS method. Heliyon, 7(3): e06390.

Rodriguez Ortega, P.G. et al. 2019. Synthesis and structural characterization of a ubiquitous transformation product (BTS 40348) of fungicide prochloraz. Journal of Agricultural and Food Chemistry, 67(31): 8641–8648.

Sehonova, P. et al. 2016. Embrya ryb jako alternativní modely v toxikologii. Veterinářství, 66(9): 692–696.

Sjerps, R.M.A. et al. 2019. Occurrence of pesticides in Dutch drinking water sources. Chemosphere, 235: 510–518.

Toxicity tests on *Daphnia magna*

Petra Melezinkova, Eva Postulkova, Radovan Kopp
Department of Zoology, Fisheries, Hydrobiology and Apiculture
Mendel University in Brno
Zemedelska 1, 613 00 Brno
CZECH REPUBLIC

xmelezin@mendelu.cz

Abstract: The aim of this study was to determine the toxic effect of chemicals on the tested organism *Daphnia magna*. The following substances were selected for testing: polyaluminium chloride (PAX 18), its aqueous solution (PAX 19) and potassium dichromate ($K_2Cr_2O_7$) as a reference substance. The experimental concentrations for PAX 18 were in the intervals 1–100 mg/l, for PAX 19 10–300 mg/l and for $K_2Cr_2O_7$ 40–150 mg/l. Testing was performed in three replicates with ten specimens. Each test took 48 hours without changing the medium. The test organisms were not fed, and a tap water was used as a medium. The 24hEC50 values were as follows: 45.06 mg/l for PAX 18, 97.82 mg/l for PAX 19 and 1,57 mg/l for potassium dichromate. The 48hEC50 values were as follows: 22.62 mg/l for PAX 18, 37.20 mg/l for PAX 19 and 0.864 mg/l for $K_2Cr_2O_7$. Changes in pH, dissolved oxygen content and number of inhibited individuals were regularly monitored. The pH values for PAX 18 were between 4.56–8.40, for PAX 19 within the range of 5.63–8.40 and for $K_2Cr_2O_7$ did not drop below 7. Low pH values for PAX 18 and PAX 19 can be explained by very low pH value of the test substances, therefore the results can be considered as valid. The oxygen content was sufficient for all three test substances. The concentrations of chemical substances used in toxicity tests were more toxic for daphnids than the concentrations introduced into the aquatic environment.

Key Words: PAX 18, PAX 19, toxicity, *Daphnia magna*, ecotoxicology, inhibitions, biotests, acute tests

INTRODUCTION

The ever-increasing level of the economy and industry brings certain risks of adverse effects on ecosystems. All components of the environment are, to a certain extent, contaminated by a constant supply of substances produced by human activity. They can be past or present substances, which enter the nature in various ways. Due to these events improves monitoring of the movement, intensity and amount of these substances, together with their development and impact on organisms (Melezínková 2019).

One of the possibilities of environmental contamination monitoring are ecotoxicological assays, which can be defined as experiments on organisms to determine if a test substance toxic to organisms occur in a particular ecosystem and to what extent. These assays are provided under the precisely defined conditions. The concentration of the test substance is very important because survey results are based on monitoring of reaction of the test organism. A certain concentration of a toxic substance can cause either mortality or alterations in development or changes in metabolic functions (Kočí and Mocová 2009).

Due to the existence of innumerable toxicants, toxicity tests have to meet the following standards: simplicity, repeatability of results, easy implementation and low costs (Hodgson 2010). And that is why *Daphnia magna* were chosen for biotic toxicity tests as they can meet the above criteria. For example, flexible repeatability of tests is in fact the result for rapid reproduction of *Daphnia*.

Here we evaluated the acute toxicity effect of three chemical substances on *Daphnia magna*: PAX 18, PAX 19 and potassium dichromate. PAX 18 is a concentrated solution of polyaluminium chloride. Its active substance is Al^{3+} in a concentration of 9.0 ± 0.3%. It has a clear yellowish colour, acidic properties, is odourless, non-flammable and soluble in water. It is used in the treatment of drinking water and pool water, wastewater, and industrial water treatment etc. PAX 19 is an aqueous solution of polyaluminium chloride, and its active substance is Al^{3+} in a concentration of 12.5 ± 0.3%. It is a light yellow, colourless solution odourless and non-flammable. It is used in the treatment of drinking water,

industrial water, wastewater treatment and in the cosmetic industry. Potassium dichromate ($K_2Cr_2O_7$) is an orange-red toxic substance, standardly used as a reference substance in toxicity tests.

MATERIAL AND METHODS

We used *Daphnia magna* as the test organism. Concentration series of test substances (PAX 18, PAX 19 and $K_2Cr_2O_7$) were prepared using aged tap water. The tests were performed according to ČSN ISO 6341. A mixture of green algae *Parachlorella kessleri* (80%) and *Tetradesmus obliquus* (20%) as food for breeding individuals. Ten individuals of *Daphnia magna* were pipetted into a 100 ml flask. Then aged tap water and the appropriate concentration of test substance were added, the final volume of medium was 100 ml. Three replicates were prepared for each concentration and the control. Daphnids were not fed during the test. Temperature was set to 23 ± 0.3 °C, light conditions corresponded to 16:8 hours (day:night). The organisms were checked after 24 and 48 hours and immobilised individuals were recorded. Individuals showing no signs of motion – either dead or with no significant motion until 15 seconds after gentle mixing (even if they still moved their antennules) were identified as immobilised. The test was performed with no pH adjustment. The pH value and dissolved oxygen content was measured using a Eutech PD 450 multimeter.

The EC50 value was determined by linear regression in the GraphPad Prism 7 software. A statistically significant difference of the monitored substances as a function of time (24, 48 h) was evaluated by F-test.

RESULTS

The tested substance PAX 18 had different effects on the inhibition of *Daphnia magna* at different concentrations and the results showed lower toxicity after 24 hours than after 48 hours. Toxicity values after 24 hours are highly significantly different from toxicity values after 48 hours ($p < 0.001$).

Concentration ranges of 1–100 mg/l was chosen for the experiments. The pH value at lower concentrations (1–40 mg/l) did not deviate from the range of optimal values for *Daphnia magna* (6–9) throughout the test. At concentrations of 60 mg/l and higher, the pH ranged between 4.60–6.16. The pH increased gradually and was initially outside the requested optimum at higher concentrations of test substance. This condition was caused by the very low pH of PAX 18 (1.0 ± 0.5). The dissolved oxygen content was sufficiently high during the test – it did not fall below 82% saturation. Although the value slightly decreased during the test, all measured values were high without a negative effect on the tested organism. The 24hEC50 value for PAX 18 was determined to be 45.09 mg/l (501 mg/l PAX 18) and the 48hEC50 value to be 22.62 mg/l (251 mg/l PAX 18).

Figure 1 Results of acute toxicity tests with PAX 18 on Daphnia magna. Toxic effect (EC) expressed in Al^{3+} concentrations

	log c EC50	mg/l EC50	R^2
24hIC50	1.654	45.09	0.775
48hIC50	1.354	22.62	0.752

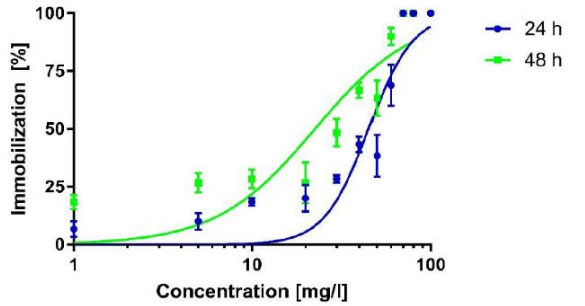

Legend: D. magna – curve of dependence of daphnia immobilization on the test substance PAX 18 (data are logarithmic and present the degree of effect ± SEM). The values of the acute toxicity test after 24 hours are statistically highly significant ($p < 0.001$) from the values after 48 hours.

The test substance PAX 19 had different effects at different concentrations on the inhibition of *Daphnia magna* and the results showed less toxicity after 24 hours than after 48 hours. Toxicity values after 24 hours were significantly different from toxicity values after 48 hours ($p < 0.001$).

The pH value increased gradually, but usually at the beginning of the test at the highest concentration of PAX 19. It slightly decreased below the limit of the optimal range. The lowest pH value obtained was 5.63. The pH value did not decrease so significantly as for PAX 18, mainly due to the higher pH value of PAX 19 (1.5–4.0). The values of dissolved oxygen content decreased but were sufficiently high throughout the test. The value fell below 80% saturation (77.4%) only once for 24 hours but even this value was sufficient for the organism. The 24hEC50 value for PAX 19 was determined to be 97.82 mg/l (783 mg/l PAX 19) and the 48hEC50 value to 37.20 mg/l (298 mg/l PAX 19).

Figure 2 Results of acute toxicity tests with PAX 19 on Daphnia magna. Toxic effect (EC) expressed in Al^3 concentrations

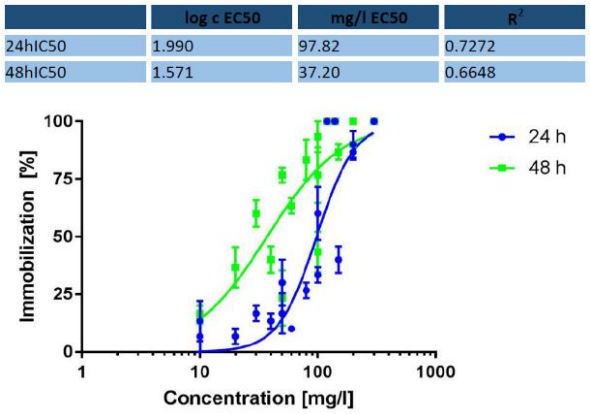

Legend: D. magna – curve of dependence of Daphnia immobilization on the test substance PAX 18 (data are logarithmic and present the degree of effect ± SEM). The values of the acute toxicity test after 24 hours are statistically highly significant ($p < 0.001$) from the values after 48 hours.

The reference substance potassium dichromate also had different effects at different concentrations on the inhibition of *Daphnia magna*. The results showed lower toxicity after 24 hours than after 48 hours. During this test, pH did not fall below 7 and the dissolved oxygen saturation below 80%.

Figure 3 Results of acute toxicity tests with potassium dichromate on Daphnia magna

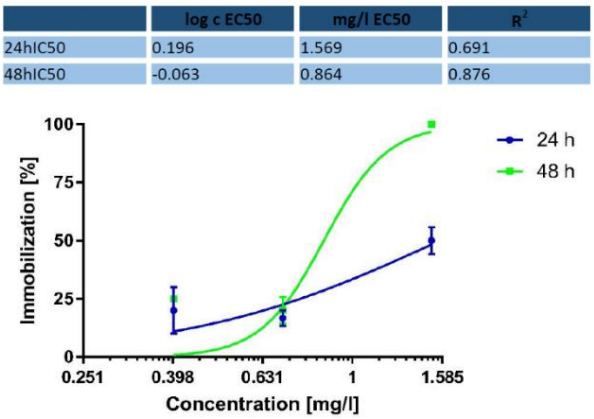

Legend: D. magna – curve dependence of Daphnia immobilization on test substance potassium dichromate (data are logarithmic and present measure of effect ± SEM).

DISCUSSION

The pH value below the optimal range was observed in PAX 18. The decrease of pH was due to the acidic nature of the test substance. The lowest pH values (4.56–4.59) were recorded at a test concentration of 80 mg/l. Veselá (2004) stated the optimal pH range for *Daphnia* within the range of 6 to 9. El-Deeb Ghazy et al. (2011) reported a narrower range of optimal values for *Daphnia magna* within the interval of 7.9 to 8.3. *Daphnia magna* is relatively sensitive to a higher decrease in pH. Values in the range of 5.3–4.5 can be considered as a critical pH. Compared to *Daphnia pulex*, for which pH values within the range of 4.9 to 3.9 is critical, *Daphnia magna* is thus more sensitive to pH (Brehm and Meijering 1982, El-Deeb Ghazy et al. 2011). In combination with the increased aluminium concentration, the low pH value might be the reason for the immobilization of *Daphnia*. The highest pH

values ranged from 8.50–8.52 at an aluminium concentration of 1 mg/l. With the highest tested concentration of 100 mg/l, the highest pH value was 4.75, which is lower than published optimal values for fish (Svobodová et al. 2007) or for Daphnis. (Veselá 2004). Jančula et al. (2011) reports an EC50 for *Daphnia magna* in the range of 9.89–54.29 Al^{3+}. These values were given depending on the quality of the water used in the test. These values also well correspond with EC50 value in this study (22.62 mg/l Al^{3+}).

It is very interesting to compare the toxicity of PAX 18 for *Daphnia magna* with the toxicity of PAX 18 for fish. Macová et al. (2010) reported LC50 for PAX 18 in the juvenile stage of *Danio rerio* fish 67.5 mg/l Al^{3+} (750 mg/l of PAX 18) and 65.8 mg/l Al^{3+} (731 mg/l PAX 18) for the embryonic stages of the same fish. For the early stages of common carp (*Cyprinus carpio*), 96LC50 is very similar to 67.8 mg/l Al^{3+} (753 mg/l of PAX 18) (Macová et al. 2009). Thus, fishes tolerate concentrations of PAX 18 much better than *Daphnia*. On the other hand, at the highest concentrations of PAX 18 in fish tests, the pH was around 4.5. The low pH value could be contributed to the increase in fish mortality even in combination with aluminium.

The concentration of the test substance PAX 18 used in the natural environment and its effectiveness is different according to the type of use (e.g. in eutrophication of water) and according to the composition of the water. According to Macová et. al (2009) it is possible to apply PAX 18 directly into the water, where the usual amount is 5–10 mg/l Al or to sediment (in tens of grams per 1 m^2). For example, Jančula et al. (2011) used four types of freshwaters in their study (standard fresh ISO water, water from the Brno Reservoir, Novoveský Pond and Splavisko Pond) with different concentrations
of PAX 18 in the range of 3.125–500 mg/l Al^{3+}. The resulting EC50 values ranged as follows – 24hEC50 10.71–54.29 mg/l Al^{3+} and 48hEC50 9.89–43.37 mg/l Al^{3+}. Based on the comparison of Jančula et al. (2011) and results obtained in the present study, it can be concluded that the detected effective concentrations are higher than those used in the natural environment. However, the concentrations of chemical substances applied to the natural environment are higher than the detected LOEC value of 1 mg/l Al^{3+}. With a high probability, we can assume a negative effect of applied concentrations of PAX 18 on aquatic organisms.

PAX 19 is more suitable for applications to the natural environment due to lower toxicity to aquatic organisms than PAX 18. Unfortunately, due to lower public awareness and higher price, this product is not as intensively used as PAX 18. Therefore, there is a lack of information in the literature about the toxicity of PAX 19 to aquatic organisms. If we compare PAX 18 and PAX 19, these substances differ from each other primarily in the Al^{3+} content and in the pH value. According to the CLP directive classifying the danger of concentration of substances according to their effects on aquatic organisms, both substances (PAX 18 and PAX 19) are classified with their results in category H412: harmful to aquatic organisms with long-term effects (Regulation (EC) No 1272/2008).

The last tested substance was potassium dichromate which served as a reference substance to verify the correct sensitivity of *Daphnia* in the tests. According to the standard (ČSN 2013), the result value of EC50 was adequate and *Daphnia* responded to this substance according to the expected response. Toxicity tests provided were therefore valid according to the requirements of the standard.

CONCLUSION

Based on the toxicity tests performed, it can be stated that due to the higher pH value and higher Al^{3+} content, the aquatic toxicity of PAX 19 is lower than that of PAX 18. It would therefore be appropriate to use rather PAX 19 than "more toxic" PAX 18 for aluminium application, mainly due to lower risk to non-target organisms, aquatic invertebrates.

ACKNOWLEDGEMENTS

This study was supported by the project PROFISH CZ.02.1.01/0.0/0.0/16_019/0000869. The project is financed by European Regional Development Fund in the Operational Programme Research, Development and Education and The Czech Ministry of Education, Youth and Sports.

REFERENCES

Brehm, J., Meijering, M.P.D. 1982. On the sensitivity of low pH of the some selected freshwater crustaceans (*Daphnia* and *Gammarus*, Crustacea). Archiv für Hydrobiologie, 95(1/4): 17–27.

ČSN EN ISO 6341 2013. Water quality - Mobility inhibition test *Daphnia magna* Straus (Cladocera, Crustacea) - Acute toxicity test. UNMZ.

El-Deeb Ghazy, M.M. et al. 2011. Effects of pH on Survival, Growth and Reproduction Rates of The Crustacean, *Daphnia magna*. Australian Journal of Basic and Applied Sciences, 5(11): 1–10.

Hodgson, E. 2010. A Textbook of Modern Toxicology. 4th ed., North Carolina: John Wiley & Sons, Inc.

Jančula, D. et al. 2011. Effects of polyaluminium chloride on the freshwater invertebrate *Daphnia magna*. Chemistry and Ecology, 27(4): 351–357.

Kočí, V., Mocová, K. 2009. Ecotoxikologie pro chemiky. Praha: VŠCHT Praha.

Mácová, S. et al. 2009. Polyaluminium chloride (PAX 18) – acute toxicity and toxicity for early development stages of common carp (*Cyprinus carpio*). Neuro endocrinology letters, 30(S1): 192–198.

Mácová, S. et al. 2010. Acute Toxicity of the Preparation PAX 18 for Juvenile and Embryonic Stages of Zebrafish (*Danio rerio*). Acta Veterinaria Brno, 79(4): 587–592.

Melezínková, P. 2019. Testy toxicity na perloočce *Daphnia magna*. Diploma thesis (in Czech), Mendel University in Brno.

Regulation (EC) No 1272/2008 on Classification, Labeling and Packaging of substances and mixtures, amending and repealing Directives 67/548 / EEC and 1999/45 / EC and amending Regulation (EC) No 1907/2006

Svobodová, Z. 2007. Nemoci sladkovodních a akvarijních ryb. Praha: Informatorium, spol. s r. o.

Veselá, Š. 2004. Jak úspěšně chovat perloočky (Média pro laboratorní chov perlooček). In Ekotoxikologické biotesty 4: sborník pracovní konference, Chrudim, 15.–17. September. Praha: University of Chemistry and Technology Prague. Department of Environmental Chemistry.

Rotifers and microcrustaceans communities in natural and restored peatlands

Lukas Pfeifer, Michal Sorf
Department of Zoology, Fisheries, Hydrobiology and Apiculture
Mendel University in Brno
Zemedelska 1, 613 00 Brno
CZECH REPUBLIC

lukas.pfeifer@mendelu.cz

Abstract: Peatlands in the Czech Republic were significantly affected by anthropogenic pressure, drainage and the subsequent drying. The reason was mainly the peat extraction. Nowadays, there is the effort to restore peatlands to their natural character and to protect them. The aim of this study was to evaluate the current state of selected peatlands based on species composition of rotifers and microcrustaceans in both the natural and restored peatland localities in the Ore Mountains and the Bohemian Forest. A total of 39 rotifer and microcrustacean taxa were found.

Key Words: peatland, restoration, rotifers, microcrustaceans, cladocerans, copepods

INTRODUCTION

Peatlands are a special type of wetland with high formation of organic matter. Primary production in peatlands is higher than biomass decomposition, resulting in formation of peat (Jeník and Soukupová 1989). The total area of peatlands in the Czech Republic is currently ca 285.4 km^2. Approximately one half of this area is situated in south Bohemia. A similarly large area can be found in western and northern Bohemia. The Ore Mountains and the Bohemian Forest are localities with significant area of peatlands.

Many anthropogenically degraded peatland localities are now being restored. One of the most significant restoration in the Czech Republic and the neighbouring Germany is the huge project of peatland restoration in the Bohemian Forest and in Bavarian Forest. The aim is to restore almost 1672 ha of wetlands and drained peatlands.

Peatland is the mosaic of both the terrestrial and aquatic habitats inhabited by organisms adapted to extreme conditions like low pH level. Rotifers and microcrustaceans inhabiting lakes and bogs of both the natural and restored peatlands are often the target of studies (Hannigan and Kelly-Quinn 2014).

Here we evaluate differences between the natural and restored peatlands based on occurrence of rotifer and microcrustacean taxa. We hypothesise that restored peatland may host the higher number of species than the natural peatland.

MATERIAL AND METHODS

Site description

Three peatland localities were sampled. The Pernink peatland and Oceán are situated in the Ore Mountains, Blatenská slať in the Bohemian Forest. While samples in the Ore Mountains were taken in September 2020, samples from the Bohemian Forest in August 2017.

Natural monument Pernink peatland is situated between municipality of Pernink and Abertamy in altitudes of 863–902 m a.s.l. The total area is 69 ha and covers the northern part of Special Area of Coservation Pernink (99.85 ha). The subject of the protection of a natural monument declared in 2016 are spruce swamp forests, transitional mires, and peat bogs habitats, which were drained in the past due to the logging and planting of spruce monoculture. A restoration took place in 2018. Samples were taken from three small lakes within Pernink peatland, hereafter abbreviated P1, P2 and P3.

Nature reserve Oceán representing natural peatland is situated among municipalities of Pernink, Oldřichov and Nejdek. The total area of the nature reserve declared in 1969 is 38.8 ha. The subject of the protection are almost natural mires and spruce swamp forests. The sample was taken

approximately 400 metres southeast of the northern border of the reserve from the small pool abbreviated O.

Blatenská slať is located southwest of the municipality of Modrava in altitude of 1250 m a.s.l. Locality is a part of the natural monument Modravské slatě in the first zone of protection within the Šumava National Park. The locality represents a complex of mires, transitional mires, and spruce swamp forests.

Thanks to the spring of the Březnický brook, the intact northern part is well supplied with water (hereafter abbreviated Bn). In the past, the southern part (hereafter abbreviated Bs) was heavily drained due to the planting of forest. The restoration of Bs took place between 2005 and 2006 when the outflow from the southern area of Blatenská slať was reduced.

Field sampling and laboratory analysis

Dissolved oxygen concentration and saturation, water temperature and pH were measured using Hach HQ40D (P1, P2, P3, O) or YSI ProDSS multimeter (Bn, Bs). Conductivity was measured using pen tester PCSTEST35 (P1, P2, P3, O) or YSI ProDSS multimeter (Bn, Bs).

Rotifers and microcrustaceans were sampled using plastic vessel (volume of 1 litre) and concentrated through 40 µm plankton net. Altogether 8 l (P1, P2, P3, Bn, Bs) or 4 l of water were sampled, concentrated, and preserved by formaldehyde.

In the laboratory, samples were analysed under light microscope (Labo Profi 3913i-T LED). Determination was done to the most detailed level as possible, often to species level. Semi-quantitative scale was used to estimate representation of each species in the sample. Modified semi-quantitative scale according to Hrbáček et al. (1972) was used: D – dominant taxa, C – common taxa, R – rare taxa. Determined taxa were classified into two groups according to their preferences to peatland localities: peatland species or species with broad ecological valence.

RESULTS

Temperature ranged between 14.9 and 18 °C, overall oxygen saturation was high (Table 1). Peatland is often limited by the low pH value. Studied localities showed relatively high range in pH from 2.9 in natural O to 6.25 in restored P1.

Table 1 Basic physico-chemical parameters of studied peatlands

	P1	P2	P3	O	Bn	Bs
Temperature [°C]	14.9	14.1	17.4	17.6	17	18
Dissolved oxygen concentration [mg/l]	8.02	7.72	7.59	8.51	7	7.7
Dissolved oxygen saturation [%]	88.1	82.9	87.5	98.9	83	95
pH	6.25	4.05	5.23	2.89	4	4.2
Conductivity [µS/cm]	34	39	73	183	40	26

Legend: P1 – Pernink 1, P2 – Pernink 2, P3 – Pernink 3, O – Oceán, Bn – Blatenská slať – north, Bs – Blatenská slať – south

In Pernink, altogether 16 rotifer taxa were determined, 31% out of it constituted of peatland species. Taxa *Cephalodella* sp., *Kellicottia bostoniensis*, *Keratella serrulata*, *Polyarthra remata* and Bdelloidea were found in all three pools (P1–3). Alongside rotifers, seven cladoceran taxa and three cyclopoid species (with the dominance of their copepodite stages) inhabited sampled localities. *Alona guttata*, *Ceriodaphnia quadrangula*, *Chydorus sphaericus* and *Scapholeberis mucronata* were the most common cladoceran taxa. All above mentioned microcrustaceans belong to species with broad ecological valence.

The lowest number of species were found in locality O where only six rotifer taxa was determined. Peatland rotifers accounted for 50%. *Chydorus sphaericus*, a cosmopolitan species found in al localities in both the Ore Mountains and the Bohemian Forest, was the only cladoceran species inhabiting locality O. No copepod was found in O except for their juveniles, copepodites.

Table 2 Checklist of rotifers and microcrustaceans in studied peatlands

	P1	P2	P3	O	Bn	Bs
Rotifera						
Bdelloidea gen. spp.	C	R	C	R	R	R
Cephalodella sp.	R	R	R	R	-	-
Euchlanis dilatata Ehrenberg, 1832	-	R	-	-	R	-
Kellicottia bostoniensis (Rousselet, 1908)	D	R	C	-	-	-
Keratella cochlearis (Gosse, 1851)	-	-	-	-	-	D
Keratella serrulata (Ehrenberg, 1838)*	R	R	R	-	-	-
Keratella valga (Ehrenberg, 1834)	-	C	D	-	-	-
Lecane acus (Harring, 1913)*	-	-	R	C	R	R
Lecane obtusa (Murray, 1913)*	-	-	-	R	-	-
Lecane tryphema Harring & Myers, 1926	-	-	-	-	R	-
Lecane depressa (Bryce, 1891)*	-	-	-	-	-	R
Lecane flexilis (Gosse, 1886)*	-	R	R	R	-	-
Lecane lunaris (Steinecke, 1916)	C	C	-	-	R	-
Lecane mira (Murray, 1913)*	R	-	-	-	R	R
Lecane stichaea Harring, 1913*	-	-	-	-	R	R
Lepadella sp.	-	-	-	R	-	R
Microcodon clavus Ehrenberg, 1830*	-	R	-	-	R	-
Monommata sp.	-	R	-	-	-	-
Ploesoma triacanthum (Bergendal, 1892)	-	-	-	-	R	-
Polyarthra remata Storikov, 1896	C	R	D	-	D	D
Synchaeta sp.	R	-	R	-	-	C
Trichocerca cf. *bicristata* (Gosse, 1887)	C	-	-	-	-	-
Trichocerca simoneae De Smet, 1990	-	R	R	-	R	C
Trichocerca collaris (Rousselet, 1896)	-	-	-	-	R	-
Cladocera						
Acantholeberis curvirostris (O.F.Müller,	-	-	-	-	R	R
Acroperus harpae (Baird, 1835)	-	-	-	-	R	R
Alona affinis (Leydig, 1860)	R	-	-	-	-	-
Alona guttata Sars, 1862	D	R	C	-	-	R
Alonella excisa (Fischer, 1854)	-	-	-	-	R	R
Alonella nana (Baird, 1850)	R	-	-	-	R	-
Ceriodaphnia quadrangula (O.F.Müller, 1785)	R	C	R	-	C	C
Daphnia gr. *pulex* Leydig, 1860	-	-	C	-	-	-
Daphnia sp. (juveniles only)	-	R	-	-	-	-
Chydorus sphaericus (O.F.Müller, 1776)	C	D	R	C	R	C
Polyphemus pediculus (Linnaeus, 1758)*	-	-	-	-	C	-
Scapholeberis mucronata (O.F.Müller, 1776)	C	D	C	-	C	C
Copepoda						
Acanthocyclops americanus (Marsh, 1893)	R	-	C	-	-	-
Eucyclops serrulatus (Fischer, 1851)	C	-	-	-	-	-
Cyclopoida copepodites	C	R	D	R	R	R

* = peatland species

Legend: P1 – Pernink 1, P2 – Pernink 2, P3 – Pernink 3, O – Oceán, Bn – Blatenská slať – north, Bs – Blatenská slať - south; R – rare species, C – common species, D – dominant species

A total of 12 species of rotifers were found in Bn with the dominance of *Polyarthra remata*. Other rotifer species were rarer. Eight cladoceran species including *Acantholeberis curvirostris* and *Polyphemus pediculus* as representatives of peatland species was found in Bn. Like in the Ore mountains, copepods were found only in copepodite stages. Peatland microcrustaceans in Bn accounted for 29%.

Out of ten rotifer taxa found in Bs, the dominant species were *Keratella cochlearis* and *Polyarthra remata*. Cladocerans consisted of ten species including predatory *Polyphemus pediculus*. Like elsewhere, copepods were represented only by copepodite stages. The percentage of peatland species in Bs was 28%. Generally, cladoceran peatland species were found only in the Bohemian Forest localities.

Due to the low abundance of species in Oceán, it was not possible to compare species composition of natural locality O with restored peatland P1, P2 and P3 in the Ore Mountains. Peatland species formed only a minor part of species richness; most species belong to taxa with broad ecological valences.

Figure 1 Comparison of the number of determined taxa among studied peatlands

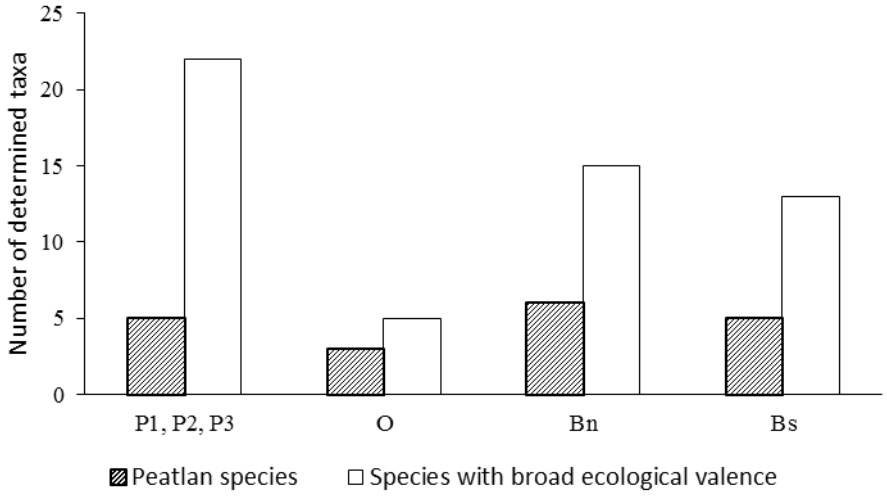

Legend: P1 – Pernink 1, P2 – Pernink 2, P3 – Pernink 3, O – Oceán, Bn – Blatenská slat – north, Bs – Blatenská slat - south

DISCUSSION

One of the most important factors in peatland is the pH value. Localities at the Bohemian Forest (Bs and Bn) were very similar to each other while localities in the Ore Mountains differed significantly in physico-chemical parameters. The most numerous species group of rotifers was family Lecanidae with 8 determined taxa. Moreover, Lecanidae was family with the highest number of peatland species (75%). The most frequent taxa typically inhabiting peatlands was *Lecane acus*. Cladocerans species richness (12 determined species) was higher than copepods (2). *Chydorus sphaericus*, found in every monitored location, occurred also in various degree of semi-quantitative representation and in four monitored natural and restored peat lakes in Ireland. It is a species with broad ecological valence. (Higgins et al. 2007).

Rosenberg and Danks (1987) proposed several features common to peatland species: (i) the smaller body size suitable in conditions of nutrient deficiencies or seasonal water level fluctuations; (ii) tolerance to the extreme environment and/or anoxia; (iii) slow development with dormant stages or, on the contrary, very rapid individual development. Gibbons (1998) explains the relatively high abundance of predators in peatlands by reduced plant production which promotes bacteria utilising humic substances.

The occurrence of particular species inhabiting peatlands is dependent of their dispersion ability. The passive dispersion of permanent eggs (such as hydrochory, anemochory or zoochory) plays an important role. Organisms are often found in various dormant stages which form germ bank (Evans and Dennehy 2005).

CONCLUSION

Besides relatively rare natural peatland, there are many degraded localities due to human impact. There is an effort to restore such localities, especially in terms of natural hydrological regime. In total, 29 taxa of rotifers and microcrustaceans including six peatland species was determined in the Ore Mountains. Altogether 26 taxa including eight peatland species was determined in the Bohemian Forest localities. Although the northern part of Blatenská slať (Bn) represents a natural peatland while the southern part (Bs) underwent restoration, both localities were very similar to each other. The reason may be the successful restoration which took place a long time ago. Unfortunately, the comparison of the natural and restored localities in the Ore Mountains was not possible due to very low observed pH value and low number of determined species (8) in Oceán. On the other hand, Pernink peatland was rather slightly acidic to neutral and hosted 27 taxa. It is worth mentioning the occurrence of *Daphnia*. Because Pernink peatland has been restored recently we recommend further monitoring of this locality. Long term monitoring can answer the question whether Pernink will return to its natural character or specific communities inhabiting new ecosystem would develop.

ACKNOWLEDGEMENTS

This study was supported by the project PROFISH CZ.02.1.01/0.0/0.0/16_019/0000869. The project is financed by the European Regional Development Fund in the Operational Programme Research, Development and Education and The Czech Ministry of Education, Youth and Sports.

REFERENCES

Evans, M.E.K., Dennehy, J.J. 2005. Germ Banking: Bet-Hedging and Variable Release from Egg and Seed Dormancy. The Quarterly Review of Biology, 80(4): 431–451.

Gibbons, D. 1998. From observation to experiment. In: Patterned mires and mire pools. London: The British Ecological Society, pp. 142–146.

Hannigan, E., Kelly-Quinn M. 2014. Aquatic invertebrate communities of ombrotrophic bogs in Ireland with special reference to microcrustaceans. In: Biology and Environment: Proceedings of the Royal Irish Academy. Royal Irish Academy, pp. 249–263.

Higgins, T., Kenny, H., Colleran, E. 2007. Plankton communities of artificial lakes created on Irish cutaway peatlands. In: Biology and Environment: Proceedings of the Royal Irish Academy. Royal Irish Academy, pp. 77–85.

Hrbáček, J. et al. 1972. Limnologické metody. Praha: SPN.

Jeník, J., Soukupová, L. 1989. Evropský význam československých rašelinišť. In Sborn. Rašeliniště a jejich racionální využívání. České Budějovice: ČSVTS, pp. 26–37.

Rosenberg, D.M., Danks, H.V. 1987. Aquatic insects of peatlands and marshes in Canada. Memoirs of the Entomological Society of Canada.

Use of peas in fish nutrition

Filip Zezula, Jan Mares, Ondrej Maly, Michal Sorf, Lukas Pfeifer
Department of Zoology, Fisheries, Hydrobiology and Apiculture
Mendel University in Brno
Zemedelska 1, 613 00 Brno
CZECH REPUBLIC

xzezula1@mendelu.cz

Abstract: The aim of the study was to evaluate the effect of peas as a component in feed mixture for common carp (*Cyprinus carpio*). During 70-day experiment, we especially targeted to production parameters (SGR, FCR, individual increment in %, total increment in %). Standard feed mixture commonly used in fisheries, KP1 containing 18% of nitrogenous substances (Stříbrné Hory) was used as a control diet. Six experimental treatments were as follows: control, 30% peas, 60% peas, 30% peas including citric acid and phytase and 60% peas including citric acid and phytase. The addition of citric acid was 3% and phytase 500 FTU. Fish were fed twice a day with a diet corresponding to 3% of average weight of fish stock. Weighting and adjustment of feed ration took place every 14 days. Fish were measured and weighted at the end of the experiment when samples were also taken. Besides production parameters, a length-weight parameters were also determined. Results were statistically evaluated using Kruskal-Wallis test. Common carp production measured as both the production and length-weight parameters revealed better performance in acidified diets. To conclude, peas addition in suitable ratio especially in combination with citric acid positively influenced common carp production and length-weight parameters.

Key Words: pea, common carp, nutrition, production parameters, citric acid

INTRODUCTION

The breeding of common carp (*Cyprinus carpio*) in fishponds is the basis of fish farming in the Czech Republic (Ženíšková et al. 2017). Fish farming in fishponds is based on natural food sources. Such resources may be limited due to various factors such as temperature, water chemistry, oxygen concentration or competing predators. Higher production can be achieved by feeding with quality feed (Mareš et al. 2015). Peas is classified as protein feed of plant origin. Protein feeds are most often fed during periods of low availability of natural food sources. Due to the high proportion of nitrogenous substances, feeds containing peas can largely replace feeds of animal origin (Krupauer 1985).

A study performed on rainbow trout (*Oncorhynchus mykkis*) and Nile tilapia (*Oreochromis niloticus*) (Magalhães 2017). Ganzon-Naret et al. (2013) showed that pea flour does not cause any negative effect on Asian perch (*Lates calcarifer*) and can generally replace fish meal in fish nutrition. The ban on feeding with animal products after 2000 resulted in necessity of changing the feed composition and finding sources of nitrogenous substances of plant origin. Legumes such as peas appeared to be an ideal replacement of animal feed. Due to its high protein content, the feed mixture based exclusively on peas (without other plant components) would decrease feed costs (Urban 1997). Peas are a versatile component because its high nitrogen content can provide a fast energy supply (Craig et al. 2017). Peas contain approximately 20–25% of nitrogenous substances, which is almost twice the amount in cereals. The content of nitrogenous substances depends on the genetic predisposition and potential of individual pea varieties (Brindza et al. 1998). A direct relationship between protein content and amino acid content throughout pea varieties was also confirmed (Fan and Sauer 1999). The enzyme Phytase was added to some of the experimental diets to increase the digestibility of phytic acid, which is almost indigestible for carp fish. Phytic acid is a complex to which minerals, salts, enzymes, and proteins are bound etc. (Velíšek and Hajšlová 2009). To increase the efficiency of phytase, citric acid was added to feed diets. Vitamin C added to the diet can also positively affect overall health and metabolism (Stefanyshyn et al. 1998).

MATERIAL AND METHODS

Characterization of feeding mixtures

The feed KP1 containing 18% of nitrogenous substances (VKS Stříbrné Hory, Czech Republic) for carp fry was used as a basis of all experimental diet and as the control in the experiment. The addition of peas in various ratio was added to the experimental feed mixtures. The feed was modified by granulation. Phytase Phyzyme XP 10,000 TPT (Danisco Animal Nutrition, DuPont) was added to some diets. The activity of phytase is possible only in acid environment hence citric acid was added to treatments containing phytase. Six treatments differed in feed composition were used in this experiment (cf. Table 1). Besides the control, diets with the addition of 30% (H30) and 60% (H60) of pea scrap, respectively, was used. The last three treatments were enriched with 3% of citric acid and phytase (500 FTU): no peas addition (KC3F), 30% (H30C3F) and 60% (H60C3F) of added peas, respectively.

Experimental design

Experiment was done in 12 tanks (water volume of 180 litres). Altogether 240 common carp individuals were used. Fish were randomly distributed into experimental tanks in abundance of 20 individuals per tank according to the experimental treatments. Fish were allowed to acclimate to experimental conditions for two weeks. Fish were measured and weighted just before the beginning of the experiment. Resulting feed dose corresponding to 3% of average fish biomass was set.

Water temperature, dissolved oxygen concentration, oxygen saturation and pH were measured every day during the experiment. The overall averages were as follows: temperature (24.1 °C), oxygen content (6.9 mg/l), oxygen saturation (84.2%) and pH (7.65).

Figure 1 The design of the experiment

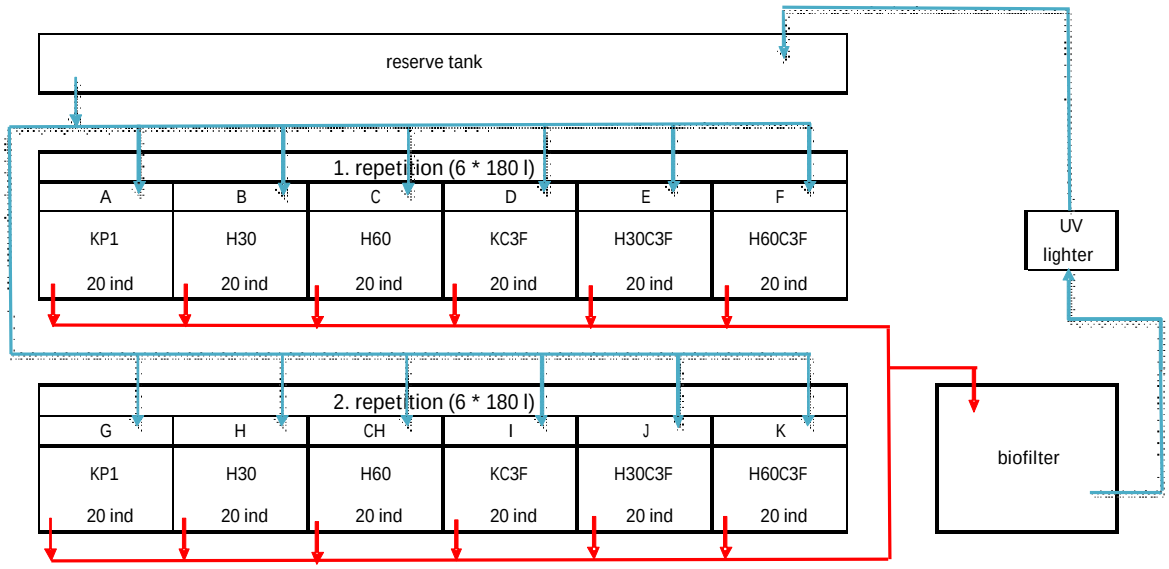

Monitored parameters

Basic production parameters such as the FCR (feed conversion ratio) and the SGR (specific growth ratio) and their mutual ratio (FCR/SGR) were monitored (Mareš et al. 2015).

Statistical analyses

Since the analysed dataset do not followed assumptions of parametric tests, data were evaluated using non-parametric Kruskal-Wallis test with the subsequent multiple comparisons. Statistical analyses were performed in Statistica 13 (TIBCO Software Inc. 2018).

Table 1 Composition of experimental diets (g/kg)

	KP1	PEAS	CITRIC ACID	PHYTASE
CONTROL	1000	-	-	-
H30	667	333	-	-
H60	334	666	-	-
KC3F	1000	-	30	500
H30C3F	667	333	30	500
H60C3F	334	666	30	500

Table 2 Results of main production parameters after 70-day experiment

	CONTROL	H30	H30	KC3F	H30C3F	H60C3F
FCR	3.72	3.03	3.26	2.78	2.82	2.81
SGR	0.79	0.89	0.83	0.96	0.95	0.96
FCR/SGR	4.73	3.40	3.90	2.88	2.96	2.93
Increment (g)	961	1273	1164	1391	1329	1341
Increment (%)	69.12	86.55	79.36	96.26	95.12	95.43

RESULTS AND DISCUSSION

The table show that higer values were reached by acidified values. Experimental diets affected both the FCR and SGR, but not significantly. The highest FCR values (3.72) and the lowest SGR (0.79) values were determined in the control. All acidified treatments including acidified KP1 feed mixture showed highest values and balanced FCR and SGR values.

Production parameters

The diet H30 shows more suitable values of FCR (3.03) and SGR (0.89) for fish production compared to the control (Table 2). In contrast, FCR is higher and SGR lower in H60 compared to H30 and both parameters values were closer to the control diet. Described trend can be observed in other results. The reason of this phenomenon may be the excessive proportion of the basic feed mixture replaced by peas. Kudláček (2019), who performed 57-day study on carp fry, found that the addition of 15% peas only slightly reduced the FCR value. In contrast, Tewari et al. (2019) found that the addition of 20% pea flour significantly lowered FCR values, increased SGR values and, as a result, significant increased the weight of carp fry. Zugárková (2018) who studied the effect of citric acid and phytase on common carp, found that diets with the addition of citric acid decreased FCR and increased SGR. Al-Zayat (2019) experimenally fed Nile tilapia (*Oreochromis niloticus*) with citric acid supplemented diet. Results showed improvement in growth, increase in increment and other monitored parameters. Craig et al. (2017) stated that water soluble vitamins, especially vitamins B and C, are key vitamins in fish nutrition. Øverland et al. (2009) confirmed no negative effects on salmon fed with pea protein up to 20%.

Fitness and exterior indicators

All non-acidified diets revealed higher values of the Fulton coefficient than acidified diets (Table 3). Significant reduction was found in the KC3F and H30C3F diets ($P < 0.01$) compared to the H30 diet, where the highest value of Fc was determined (3.52). Kudláček (2019), who performed similar study, determined Fc being 3.22 in diet containing 15% of added pea. Our Fc values are therefore comparable. The similar trend – lowered Cc in acidified diets – was found in Cc but results were not significant. The H30 showed the highest Cc value (3.09). Gouveia et al. (1998) who studied European sea bass (*Dicentrarchus labrax*) stated that up to 40% of pea flour can serve as an alternative to replacing some components of feed with no effects on growth or fitness indicators.

The values of both the hepatosomatic (HSI) and viscerosomatic (VSI) indices are determined by fat content in intestines and fattening of liver. There was a trend in decreasing of both evaluated

indices with increasing pea content in the diet. Lower values of both indices were again observed in acidified diets, maintaining the same downward trend. The addition of pea component in the diet of common carp lowered the values of both the HSI and VSI indices (Table 3). The highest indices were found in the control, significant reduction of VSI was proved in H60C3F compared to the control. Kudláček (2019) reported rather higher value in HSI (2.77) in diet containing 15% addition of peas than found in this study for the H30 diet.

Table 3 Fitness and exterior indicators (mean ± SD, Fc- n = 40, Cc-n = 20), (mean ± SD, HSI and VSI-n = 20), (mean ± SD, IV and IŠ-n = 40); Fc – Foulton coefficient, Cc – Clarc coefficient, HSI – hepatosomatic index, VSI – viscerosomatic index, HBI - high-back index, BBI - broad-back index)

	CONTROL	H30	H60	KC3F	H30C3F	H60C3F
Fc	**3.44** ± 0.40	**3.52** ± 0.29 *	**3.46** ± 0.30	**3.29** ± 0.25 *	**3.28** ± 0.27 *	**3.34** ± 0.29
Cc	**3.07** ± 0.34	**3.09** ± 0.33	**3.04** ± 0.25	**2.93** ± 0.26	**2.9** ± 0.25	**2.93** ± 0.30
HSI	**2.79** ± 0.51	**2.71** ± 0.55	**2.49** ± 0.31	**2.59** ± 0.41	**2.53** ± 0.38	**2.45** ± 0.37
VSI	**11.95** ± 1.55 *	**10.9** ± 1.58	**10.73** ± 1.50	**11.27**± 2.11	**10.99** ± 1.39	**10.93** ± 1.39 *
HBI	**2.79** ± 0.16	**2.75** ± 0.15	**2.78** ± 0.15	**2.77** ± 0.16	**2.78** ± 0.19	**2.79** ± 0.18
BBI	**18.92** ± 1.03	**18.77** ± 0.81	**18.98** ± 0.87	**18.96**± 0.71	**18.84** ± 0.87	**18.94** ± 0.84

The values of the high-back index and the broad-back index were determined as part of the evaluation of exterior indicators. No significant differences were found among studied diets. Values of both indices are almost the same across treatments. These indices are mainly influenced by the breed of fish.

CONCLUSION

Obtained results showed a positive effect of peas addition on the production parameters of common carp farming, especially when 30% of peas was used. The addition of 60% of pea scrap resulted in deterioration in observed production parameters, e.g., length, weight, length-weight indices, or fitness indicators. Acidified diets revealed even improved results in the above-mentioned parameters compared to unacidified diets. Moreover, differences between 30% and 60% of peas addition lowered in acidified diets. In some parameters all acidified treatments including KC3F revealed similar values.

We can conclude that peas addition into feed mixtures used for common carp, especially when added in optimal proportion of peas, improved selected basic production parameters of fish. In addition, the combination of peas component with citric acid and phytase further enhance observed parameters.

ACKNOWLEDGEMENTS

This study was supported by the project PROFISH CZ.02.1.01/0.0/0.0/16_019/0000869. The project is financed by European Regional Development Fund in the Operational Programme Research, Development and Education and The Czech Ministry of Education, Youth and Sports.

REFERENCES

Al-Zayat, A.H. 2019. Effect of different levels of citric acid as supplementation on growth performance, feed utilization, body composition, water quality, and blood profile of Monosex Male Nile Tilapia (*Oreocheromis niloticus*) fingerlings. Egyptian Journal of Aquatic Biology and Fisheries, 23(3): 611–624.

Brindza, J. et al. 1988. Hodnotenie diverzity rodu Pisum. Učebné texty pre dištančné štúdium ochrana biodiverzity. Nitra: Slovenská polnohospodářská univerzita v Nitre.

Craig, S. et al. 2017. Understanding Fish Nutrition, Feeds, and Feeding. (Publication 420–256), Virginia Cooperation Extension, Yorktown.

Fan, M.Z., Sauer, W.C. 1999. Variability of apparent ileal amino acid digestibility in different pea samples for growing-finishing pigs. Canadian Journal of Animal Science, 79: 467–475.

Ganzon-Naret, E.S. 2013. The use of green pea (*Pisum sativum*) as alternative protein source for fish meal in diets for Asian sea bass, Lates calcarifer. Aquaculture, Aquarium, Conservation and Legislation, International Journal of the Bioflux Society, 6(4): 399–406.

Gouveia, A., Davies, S.J., 1998: Preliminary nutritional evaluation of pea seed meal (*Pisum sativum*) for juvenile European sea bass (Dicentrarchus labrax). Aquaculture, 166(3–4): 311–320.

Krupauer, V., Kubů, F. 1985. Kapr obecný. Praha: Nakladatelství Naše vojsko.

Kudláček, J. 2019. Využití komponentů a krmiv rostlinného původu ve výživě kapra obecného (*Cyprinus carpio* L.). Diploma thesis (in Czech), Mendel University in Brno.

Magalhães, S.C.Q et al. 2017. Apparent digestibility coefficients of European grain legumes in rainbow trout (*Oncorhynchus mykiss*) and Nile tilapia (*Oreochromis niloticus*). Aquaculture Nutrition, 24: 332–340.

Mareš, J. et al. 2015. Akvakultura-základy výživy a krmení ryb. Brno: Mendelova univerzita.

Øverland, M. et al. 2009. Pea protein concentrate substituting fish meal or soybean meal in diets for Atlantic salmon (*Salmo salar*)—Effect on growth performance, nutrient digestibility, carcass composition, gut health, and physical feed quality. Aquaculture, 288(3–4): 305–311.

Stefanyshyn, B. et al. 1998. Research Summaries: Canola and pea in livestock diets. Saskatchewan: University of Saskatchewan.

Tewari, G. et all. 2019. Effect of pea pod as feed ingredient on growth performance of common carp, *Cyprinus carpio*. Journal of experimental zoology India, 22(2): 795–799.

TIBCO Software Inc. 2018. Statistica (data analysis software system), version 13.

Urban, F. 1997. Chov dojeného skotu: [reprodukce, odchov, management, technologie, výživa]. Praha: Apros.

Velíšek, J., Hajšlová, J. 2009. Chemie potravin. 3. ed., Tábor: OSSIS.

Zugárková, I. 2018. Využití krmiv se sníženým zatížením vodního prostředí fosforem v chovu kapra obecného (*Cyprinus carpio* L.). Diploma thesis (in Czech), Mendel University in Brno.

Ženíšková, H. et al. 2017. Situační a výhledová zpráva ryby. Praha: Ministerstvo zemědělství.

WILDLIFE RESEARCH

Contribution to the faunistic research of beetles (Insecta: Coleoptera) in Natural Monument Růžový kopec near Mikulov

David Kopr
Department of Zoology, Fisheries, Hydrobiology and Apiculture
Mendel University in Brno
Zemedelska 1, 613 00 Brno
CZECH REPUBLIC

kopr.d@seznam.cz

Abstract: The research of Natural Monument Růžový kopec took place at 2020. There were made six visits of the site during the vegetation season. During the survey, 183 species of beetles belonging to 26 families were found at the site, of which 5 species are protected pursuant to Section 56 Paragraphs 1 and 2 of Act No. 114/1992 Coll. and 38 species are included in the Red list of threatened species of the Czech Republic (Hejda et al. 2017). The most valuable species caught were *Agrilus roscidus* (Buprestidae), *Licinus cassideus* (Carabidae), *Zabrus spinipes* (Carabidae), *Liparus dirus* (Curculionidae), *Pseudocleonus cinereus* (Curculionidae), *Rhabdorrhynchus echii* (Curculionidae), *Cardiophorus vestigialis* (Elateridae), *Melanotus tenebrosus* (Elateridae) , *Coptocephala chalybaea* (Chrysomelidae), *Cheilotoma musciformis* (Chrysomelidae) and *Tituboea macropus* (Chrysomelidae).

KeyWords: beetles, faunistics, Coleoptera, entomology, Pálava

INTRODUCTION

Natural Monument Růžový kopec is situated in western part of Pálava Landscape Protected Area. It is a steppe lada with scattered shrubs, with preserved rocky outcrop in the top of the area and a combination of rock vegetation and vegetation of narrow-leaved and broad-leaved dry grasslands and high and low shrubs with the occurrence of specially protected thermophilic species of plants and animals typical of the ridge zone of Pavlovské vrchy. At the same time, it is a habitat of bird species and an example of a typical landscape element of the Pálava Landscape Protected Area. It is surrounded by vineyards and fields, somewhat drowned in the surrounding intensively used landscape. It thus represents an important refuge of steppe flora and fauna, which does not find suitable habitats on the surrounding land. The monument itself consists of the top part, terraces and steep slopes of Růžový kopec, the highest peak of which is less than 300 m above sea level (Mackovčin et al. 2007).

The research of Natural Monument Růžový kopec was carried out within the overall extensive survey of Pálava Landscape Protected Area (Rozkošný and Vaňhara 1995, 1996), although no comprehensive data are known from this locality. There was made management plan for the period 2013–2022, where list of protected species is present, including invertebrates (AOPK 2013).

MATERIAL AND METHODS

Material

The material was collected using various methods as sweep net, clap net, individual collecting from flowers, under bark and in dead wood, also under stones and from dung and cadavers. There were also placed pitfall traps at the site for collecting epigeic insect. The traps were installed during the first visit of the site and have been working throughout the research. The total number of traps was 15; they were placed in five series of three pieces and continuously emptied. Propylene glycol was used as a preservative liquid. The collected material was stored in vials with 70% ethanol and part of the material was mounted by gluing on the mounting boards and deposited in the private collection of the author. The material was identified with using relevant literature and identification keys (Hůrka 2017, Hůrka 1996, Mertlík 2011).

Table 1 The list of protected species and species contained in Redlist

Family/Species	PS	Red list	Frequency
Buprestidae			
Agrilus hyperici (Creutzer, 1799)		**NT**	2
Agrilus roscidus (Kiesenwetter, 1857)		**EN**	2
Anthaxia fulgurans (Schrank, 1787)		**EN**	1
Anthaxia podolica Mannerheim, 1837		**VU**	3
Coraebus elatus (Fabricius, 1787)		**VU**	3
Cylindromorphus filum (Gyllenhal, 1817)		**VU**	2
Trachys fragariae (C. Brisout de Barneville, 1874)		**NT**	2
Carabidae			
Cicindela campestris (Linnaeus, 1758)	**III.O**		2
Cylindera germanica (Linnaeus, 1758)	**III.O**	**NT**	1
Licinus cassideus (Fabricius, 1792)		**EN**	2
Poecilus sericeus Fischer von Waldheim, 1824		**VU**	3
Zabrus spinipes (Fabricius, 1798)		**VU**	2
Curculionidae			
Cyphocleonus dealbatus (Gmelin, 1790)		**VU**	3
Foucartia ptochioides (Bach, 1856)		**VU**	1
Liparus coronatus (Goeze, 1777)		**NT**	2
Liparus dirus (Herbst, 1795)		**VU**	2
Pseudocleonus cinereus (Schrank, 1781)		**EN**	3
Rhabdorrhynchus echii (Brahm, 1790)		**EN**	3
Stomodes gyrosicollis (Boheman, 1843)		**NT**	2
Dermestidae			
Dermestes fuliginosus Rossi, 1792		**EN**	2
Elateridae			
Cardiophorus vestigialis Erichson, 1840		**EN**	1
Dicronychus rubripes (Germar, 1824)		**VU**	2
Melanotus tenebrosus (Erichson, 1841)		**CR**	3
Pheletes quercus (Olivier, 1790)		**NT**	2
Chrysomelidae			
Coptocephala chalybaea (Germar, 1824)		**CR**	3
Coptocephala rubicunda (Laicharting, 1781)		**VU**	2
Cryptocephalus pygmaeus vittula Suffrian, 1848		**EN**	1
Cheilotoma musciformis (Goeze, 1777)		**CR**	1
Pachybrachis fimbriolatus Suffrian, 1848		**VU**	2
Tituboea macropus (Illiger, 1800)		**CR**	3
Nitidulidae			
Urophorus rubripennis (Heer, 1841)		**VU**	1
Scarabaeidae			
Holochelus aequinoctialis (Herbst, 1790)		**NT**	3
Chaetopteroplia segetum (Herbst, 1783)		**NT**	2
Onthophagus semicornis (Panzer, 1798)		**NT**	1
Oxythyrea funesta (Poda, 1761)	**III.O**		1
Pleurophorus caesus (Creutzer in Panzer, 1796)		**NT**	3
Sisyphus schaefferi (Linnaeus, 1758)	**III.O**	**VU**	1
Tropinota hirta (Poda, 1761)	**II.SO**	**VU**	1
Tenebrionidae			
Omophlus proteus Kirsch, 1869		**VU**	1
Podonta nigrita (Fabricius, 1794)		**VU**	1

Legend: PS - protected species, categories I. KO, II. SO and III.O; Red list - categories according to IUCN (CR - critically endangered, EN - endangered, VU - vulnerable, NT - near threatened); frequency - 1(highest) - 3(lowest)

RESULTS AND DISCUSSION

During the research there were found 183 species of beetles belonging to 26 families at the site, of which 5 species are protected pursuant to Section 56 Paragraphs 1 and 2 of Act No. 114/1992 Coll. and 38 species are included in the Red List of Invertebrates of the Czech Republic (Hejda et al. 2017). There has been reported abundance in beetles, three categories has been established – 1 (highest),

2 (medium) and 3 (lowest). Within the research, there was recorded one species not present in the previous management plan (AOPK 2013), it is a species of *Cylindera germanica* (III.O) from Carabidae family. This species has recently spread throughout the country. Individuals of this species were found in pit fall traps in quite large numbers. Among the beetles captured at the site, there is a large number of steppe species that occur locally in southern Moravia. The locality is extremely rich in species of short-stemmed grasslands and xerothermic steppe species, occurring on loess substrates. The most numerous family was Chrysomelidae family, which included 33 found species. The family Curculionidae – weevils was rich in protected species, out of the total number of 18 recorded species, 7 species are included in the Red List of the Czech Republic. The spectrum of scarabaeid beetles is also interesting. Out of a total of 17 recorded species, 6 of them are included in the Red List of the Czech Republic and three species are included among the protected ones.

Figure 1 Photographies of the locality Růžový kopec (A in May, B in June, C in July and D in August)

Notes to most interesting species

Agrilus roscidus (Kiesenwetter, 1857) (EN) is widespread in warm areas of Europe, especially in the Mediterranean and sub-Mediterranean. South Moravia probably runs through the northern border of its distribution and the findings are rare (Škorpík et al. 2011). Found in the northern part of the site in several pieces sitting on *Prunus* spp branches.

Licinus cassideus (Fabricius, 1792) (EN) is a rare and declining species found at the best preserved steppe localities in central and northern Bohemia and in southern Moravia (Hůrka 1996). Several specimens were found at the site in pit fall traps.

Zabrus spinipes (Fabricius, 1798) (VU) is a large, black, flightless species of ground beetle, locally occurring in steppe unshaded habitats, vineyards and field edges. In the Czech Republic, it occurs locally in southern Moravia at a few localities (Hůrka 1996). There were several individuals found in pit fall traps at the site.

Liparus dirus (Herbst, 1795) (VU) adults occur since March in xerothermic habitats, mainly on steppes with short-stemmed grasslands. Adults occur nearby the trampled paths or penetrate the grass. The larvae develop on *Laserpitium latifolium*. It occurs rarely and locally in the Czech

Republic, especially in southern Moravia (Stejskal and Krátký 2007). There were found great numbers of individuals at the site, crawling through the grass or in pit fall traps.

Pseudocleonus cinereus (Schrank, 1781) (EN) is scattered and very locally occurring rare species in the Czech Republic, which inhabits xerothermic habitats such as steppes, pastures and road edges, especially in southern Moravia. Adults are active from March to June and from August to October. Mating usually takes place in May and June. It is oligophagus on *Asteraceae*, found on cornflowers (*Centaurea* spp.) and *Leontodon* spp. (Stejskal and Krátký 2007). There were several individuals found near the northern part of the site at the edge of the field.

Rhabdorrhynchus echii (Brahm, 1790) (EN) adults occur from late May to August with a maximum in June and July. They inhabit xerothermic open habitats with sandy, loess or limestone substrate with disturbed, free places and sparse vegetation. Quarries, sand pits and ruderals are also secondary habitats. In these habitats, it searches for early disturbed places with bare soil. It is oligophagous species feeding plants of family *Boraginaceae*. In the Czech Republic, the preferred food plant is *Echium vulgare*, the species is rarely found on *Cynoglossum* spp. Adults live hidden under leaf roses, but in sunny weather they sometimes climb on the leaves and flowers of food plants. The larvae feed in the roots and root necks and form a relatively large swell, there are also pupae. It is a rare species of the warmest areas in the Czech Republic. It has been spreading lately. It is endangered by succession and poor care for open sandy and steppe habitats. Appropriate management is the disturbance of these habitats by grazing, trampling, vehicle movement and removing bushes. There were found several individuals in pit fall traps at the site.

Cardiophorus vestigialis (Erichson, 1840) (EN) In the Czech Republic, it is a widespread species in loess steppe habitats, especially in southern Moravia. Larvae develop in the soil.

Melanotus tenebrosus (Erichson, 1841) (CR) is a sub-Mediterranean species of click beetle, adults occur in sunny open localities of forest-steppe character, often persisting on flowering trees and shrubs. This species is very local and rare in the Czech Republic, there is poor data known about its occurrence, the records are mainly from South Moravia (Laibner 2000). Several individuals sitting on hawthorn flowers (*Crataegus* spp.) were found at the site.

Coptocephala chalybaea (Germar, 1824) (CR) is a rare thermophilic species, occurring only locally in southern Moravia, adults are found since the end of May on herbs and shrubs in xerothermic habitats. Several individuals were caught using sweep net.

Cheilotoma musciformis (Goeze, 1777) (CR) is a rare species of preserved steppe habitats with the occurrence of its food plants, which in our country are mainly *Anthyllis vulneraria* and *Onobrychis viciifolia* (Warchałowski 1991). Adults were found in large numbers at the site.

Tituboea macropus (Illiger, 1800) (CR) is a very rare and locally occurring thermophilic species. The larvae develop on *Anthyllis vulneraria* (Warchałowski 1991). In the Czech Republic, it occurs only in the southernmost Moravia in the Pálava region, in xerothermic habitats of steppe character. There was found only one individual on vegetation at the site.

CONCLUSION

Růžový kopec locality is very valuable, it provides a refuge for many rare, local and endangered species of beetles, which in today's intensively managed cultural landscape we can find little where. It is therefore necessary to protect it from tree infestations and overgrowth with lush herbaceous vegetation. A suitable type of management would be partial grazing of vegetation by sheep.

ACKNOWLEDGEMENTS

This research was financially supported by the Nature and landscape agency (AOPK) of Czech Republic. I would also like to thank to Jaroslav Bašta for help with identification of Carabid beetles and Jan Bezděk for help with identification beetles of Chrysomelidae family.

REFERENCES

AOPK-Agentura ochrany přírody a krajiny. 2013. Plán péče o Přírodní památku Růžový kopec na období 2013–2022. Mikulov: Správa Chráněné krajinné oblasti Pálava.

Hejda, R. et al. 2017. Červený seznam ohrožených druhů České republiky. Bezobratlí [Red list of threatened species in the Czech Republic. Invertebrates]. Příroda, Praha, 36.

Hůrka, K. 2017. Brouci České a Slovenské republiky. 2. ed. Zlín: Kabourek.

Hůrka, K. 1996. Carabidae of the Czech and Slovak Republics. 1. ed., Zlín: Kabourek.

Laibner, S. 2000. Elateridae of the Czech and Slovak Republics. Zlín: Kabourek.

Mackovčin, P. et al. 2007. Chráněná území ČR IX. Brněnsko. Agentura ochrany přírody a krajiny ČR, Brno: EkoCentrum Brno.

Mertlík, J. 2011. The species of the subfamily Cardiophorinae (Coleoptera: Elateridae) of the Czech Republic and Slovakia. Elateridarium [Online], 5: 59–204. Available at: http://www.elateridae.com/elateridarium. [2021-09-02].

Rozkošný, R., Vaňhara, J. 1996. Terrestrial Invertebrates of the Pálava Biosphere Reserve of UNESCO, III. Folia Facultatis Scientiarium Naturalium Universitatis Masarykianae Brunensis, Biologia, 94: 409–630.

Stejskal, R., Krátký J. 2007. Notes to host plants of the weevils *Liparus dirus* (Herbst, 1795) and *Aphytobius sphaerion* (Boheman, 1845) (Coleoptera, Curculionidae). Curculio-Institute [Online], 36: 5 pp. Available at: https://curci.de/data/wnarchives/36/index.html. [2021-09-02].

Škorpík, M. et al. 2011. Faunistika krascovitých (Coleoptera: Buprestidae) Znojemska, poznámky k jejich rozšíření, biologii a ochraně. Thayensia, 8: 109−291.

Warchałowski, A. 1991. Fauna Poloniae 13. Chrysomelidae. Part II. (subfamilies *Clythrinae* i *Cryptocephalinae*). Warszawa: Wydawnictwo naukowe PWN.

Importance of cereals for population dynamics of common voles (*Microtus arvalis*) – a case study from Moravia (Czech Republic)

Gabriela Skopalova, Jan Sipos, Josef Suchomel
Department of Zoology, Fisheries, Hydrobiology and Apiculture
Mendel University in Brno
Zemedelska 1, 613 00 Brno
CZECH REPUBLIC

xskopal3@mendelu.cz

Abstract: The case study evaluates the importance of cereals for population dynamics and the occurrence of common voles. A time series data (2011–2020), obtained from the Phytosanitary Portal, was used, concerning repeated monitoring of the number of active burrows in different districts of the country. The data were then evaluated using a linear mixed-effects model. The results showed that the abundance of common vole in cereals was conclusively lower than in the other monitored crops and thus represents one of the least suitable habitats for common voles in agrocenoses, despite the considerable damage caused by voles in these crops. Across the Czech Republic, the numbers of active vole burrows in cereals were significantly lower than in perennial forage crops and winter rape. In Moravia, similar results were found in the South Moravian, Olomouc and Zlín regions.

Key Words: vole, cereals, rape, perennial forage, population dynamics

INTRODUCTION

The common vole (*Microtus arvalis*) is an important pest of field crops with a large economic impact on agricultural production (Jacob and Tkadlec 2010, Jacob et al. 2014). This is due to its food preferences and population dynamics (Jacob et al. 2014, Baláž et al. 2019). Common vole population dynamics are characterized by multi-year cyclical fluctuations, with population peaks occurring every 2–5 years. These are when the highest damage occurs (Tkadlec and Stenseth 2001, Lambin et al. 2006). In our conditions, the most damaged crops are perennial forage crops, rape and cereals, which are among the most important economic crops (Heroldová et al. 2020, Suchomel et al. 2021) Cereals are the dominant traditional crops in agricultural production in the Czech Republic and represent approximately 32% of the sown area. In recent decades, the cultivation of winter rape (*Brasica napus L.*) has also become increasingly widespread (ČSÚ 2020). The level of vole damage is compounded by the significant size of soil blocks, which in the Czech Republic is on average 27 ha, ranging from 1–200 ha (Heroldová et al. 2020).

The study was carried out in Moravia (Czech Republic) because it is the most agriculturally important area in terms of cereal, winter rape and perennial forage crops. The total sown area here is more than 317 000 ha. Cereals are grown on 194 000 ha (the second largest sown area in the Czech Republic), of which winter wheat (*Triticum aestivum* L.) on over 113 000 ha and winter barley (*Hordeum vulgare* L.) on over 35 000 ha. The area sown to winter oilseed rape is then in third place with around 43 000 ha and is thus the closest behind forage crops with just under 45 000 ha (ČSÚ 2020). As cereal crops are not among the primary habitats of the common vole (Jacob et al. 2014), they are neglected in terms of studying their importance for vole population dynamics. Yet, their numbers here can be high in years of gradation and damage to crops can then be significant (Suchomel et al. 2021). The aim of this study is therefore to assess the long-term importance of cereals for common vole population dynamics in intensive agricultural landscapes.

MATERIAL AND METHODS

Used data

The analysis was focussed on common vole abundances measured as counts of active entrances to burrow systems (BI – burrow index) in fields, and we examined vole abundances in the crops

attractive to voles in the agricultural landscape. These were perennial crops (alfalfa and clover), winter crops (winter wheat, winter barley and winter rape) and annual crops (spring barley). These crops served as comparative samples to evaluate the importance of cereals.

Data on voles were taken from the database of the State Phytosanitary Administration (Phytosanitary Portal), which contains records of the number of active burrows in a specific time and space. Data for the whole Czech Republic were used for the overall evaluation of the importance of cereals, and data for Moravia were used for regional comparison. These were data for the years 2011 to 2020, ie in the range of 10 years.

Used statistical methods

The analysed data had a hierarchical structure, individual fields were clustered within districts and within each district the number of active burrows were repeatedly sampled over 10 years. Therefore, to analyse burrow index (active burrows per hectare) patterns for different crop types during ten years, the linear mixed-effects model (LMM) was fitted with Gaussian error distribution by using "lme" function (Pinheiro et al. 2020). For all models burrow index was used as dependent variable, crop types as fixed effect factor, and crop types nested within district was set as a random effect. The serial correlation between samples within particular district was specified by a first-order autoregressive covariance structure. Before LMM analysis was done burrow index was transformed by decimal logarithm to meet the assumptions of normality and homogeneity of variance. Significance of the explanatory variables was then tested by type II analysis of deviance with Kenward-Roger approximations for degrees of freedom. To compare means among particular crop types the Tukey multiple comparison test with Bonferroni adjustment of p-values was used. Data were analysed in the R program (R Development Core Team 2020).

RESULTS

The abundance of the common vole significantly differed between the studied crops across the Czech Republic (lmmANOVA: $F_{3,225} = 172.22$, $p < 0.0001$). We did not revealed significant difference.

In the number of active burrows between Moravian regions. There was a significant relationship between crop type and Moravian regions (lmmANOVA: $F_{39,225} = 2.15$, $p < 0.001$), i.e. the difference in the number of burrows between crops was influenced by the region in which the crop was grown. The average number of burrows was also significantly different between years.

Across the Czech Republic, alfalfa + ryegrass differed significantly from all other crops in the number of burrows and rape differed from winter barley (Table 1). Thus, the results of the importance of cereals over the 10-year monitoring period show that the numbers of active voles were significantly lower in cereals than in perennial forage crops. Numbers were significantly lower in winter wheat compared to alfalfa and clover (Table 1) and in winter barley compared to alfalfa and clover (Table 1). There were also lower numbers in cereals compared to winter rape, although the results were only significant in winter barley (Table 1). The difference in abundance of active burrows between rape and winter wheat was not significant (Table 1).

Table 1 Results of a post-hoc Tukey test for an LMM with correction for multiple comparisons. The random effect was specified as crop types nested within district. Using this analysis, we tested the zero hypotheses – there is no difference in common vole's abundance between different crop types across the Czech Republic.

Contrast	Estimate	SE	Df	t.ratio	p.value
Alfalfa + clover – winter barley	0.4421	0.0287	234	15.412	<.0001
Alfalfa + clover – winter rape	0.3453	0.0229	234	15.048	<.0001
Alfalfa + clover – winter wheat	0.3851	0.0234	234	16.484	<.0001
Winter barley – winter rape	-0.0967	0.0286	234	-3.378	0.0047
Winter barley – winter wheat	-0.0570	0.0289	234	-1.971	0.2019
Winter rape – winter wheat	0.0397	0.0231	234	1.719	0.3164

In all the regions monitored in Moravia, cereals appeared to host relatively low numbers of voles in the long term compared to the other crops monitored (Figure 1). In the South Moravian region, the number of active burrows was lower in cereals than in perennial forage crops during the 10-year monitoring period. The numbers were significantly lower in winter wheat compared to alfalfa and clover (Tukey HSD test: $t = 4.51$, $df = 25$, $p<0.001$) and in winter barley compared to alfalfa and clover (Tukey HSD test: $t = 4.11$, $df = 25$, $p<0.01$) (Figure 1A). Lower numbers were also found in cereals compared to winter rape.

In the Moravian-Silesian region, the number of active burrows was not significantly different among any crops over the 10-year follow-up period (Figure 1B).

In the Olomouc region, the numbers were significantly lower in winter barley compared to alfalfa and clover (Tukey HSD test: $t = 5.31$, $df = 15$, $p<0.001$), winter wheat compared to alfalfa and clover (Tukey HSD test: $t = 3.50$, $df = 15$, $p<=0.0152$) and winter rape compared to alfalfa and clover (Tukey HSD test: $t = 2.91$, $df = 15$, $p<=0.0479$) (Figure 1C). Lower numbers were also found in cereals compared to winter rape, although results were only significant for winter barley (Tukey HSD test: $t = -3.35$, $df = 15$, $p<=0.0204$).

In the Zlín region, there were significantly lower numbers in stands of winter wheat compared to alfalfa and clover (Tukey HSD test: $t = 4.54$, $df = 9$, $p<0.01$) and winter rape compared to alfalfa and clover (Tukey HSD test: $t = 5.58$, $df = 9$, $p<0.01$) (Figure 1D).

Figure 1 Shows the dependence of the active burrow index of voles in relation to individual crops over 10 years. The graph curves then show oscillations and fluctuations, i.e. population density cycles of vole for individual crops over a period of 10 years. Changes in the number of burrows over 10 years vary significantly between crops. The average number of burrows also varies significantly between years. Error bars represents 95% confidence intervals.

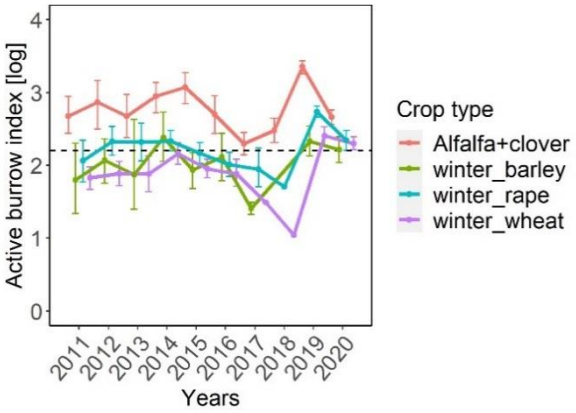

A) South-Moravian region

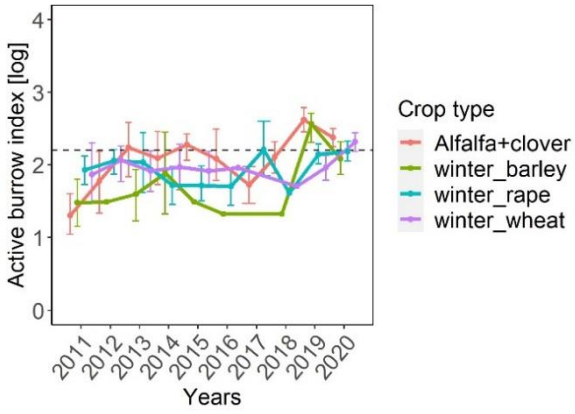

B) Moravian-Silesian region

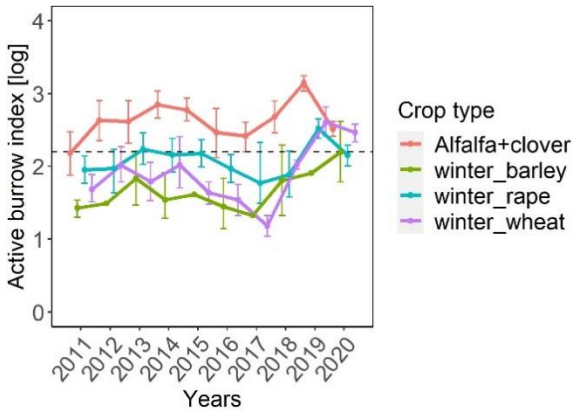

C) Olomouc region

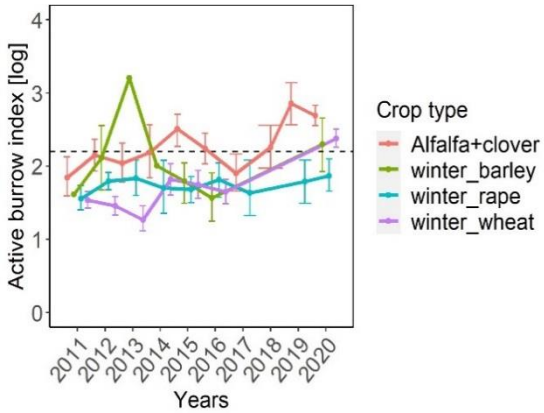

D) Zlín region

DISCUSSION

From the point of view of survival and stabilization of populations on the site, cereals represent a less optimal habitat than winter rape and perennial forages (Heroldová et al. 2020). Unlike winter rape, cereals do not provide as suitable a food base and shelter options from autumn to late spring. The biomass of cereals is not as high quality as that of rape, therefore voles in cereals have a harder time overwintering compared to rape and reach lower population densities in spring. Thus, common voles prefer winter rape to winter wheat in autumn, winter and spring, which has been confirmed by a number of studies (Truszkowski 1982, Heroldová et al. 2020). However, higher vole numbers in cereal crops may also be related to changes in the quality of rape stands. This occurs when the two crops are adjacent to each other (Suchomel et al. 2021). As flowering and seed ripening occurs, around the end of June, food availability in rape decreases and voles move on to other crops where they cause further significant damage. This particularly threatens cereal crops. It is therefore fair to say that the reduction in food quality can trigger a shift of voles from winter rape to neighbouring crops. The movement of voles between different crops is an important process that affects the population dynamics and community structure of common voles in agricultural landscapes (Landis et al. 2000, Blitzer et al. 2012, Tscharntke et al. 2012). Thus, winter rape, like forage crops or semi-natural vegetation, is a much more suitable habitat for common voles than cereals, and voles remain there for nine months, from September to May (Jacob et al. 2014, Heroldová et al. 2004, 2020). And even though canola acts as a major habitat for only part of the year, voles can cause significant damage to adjacent cereal crops during peak population periods. The migration of voles between different crop species is also influenced by the different maturation times of agricultural crops. Mature crops prior to harvest can thus act as a source of individuals moving to neighbouring fields (Suchomel et al. 2021). Cereals are then, compared to perennial crops and rape, the least stable habitat for common voles of the above crops. This is due to regular tillage, which leads to an annual decline in vole populations. However, there is a stronger edge effect in cereal crops than, for example, in alfalfa stands or in primary habitats. Thus, field margins tend to be 8-9 times more colonized in spring than in summer, resulting in a large movement of voles into cereal fields at a time when population densities are increasing (Rodríguez-Pastor et al. 2016).

Thus, it can be said that even in cereal fields, vole populations fluctuate in more or less regular cycles over the long term. However, vole abundance here is also significantly influenced by the nature of the surrounding cultivated crops (especially rape and perennial crops), which can serve as source habitats from which voles colonize cereal crops depending on the phase of the population cycle.

CONCLUSION

The results showed that the abundance of the common vole in cereals is significantly lower than in the other monitored crops and thus represents one of the least stable habitats for the common vole. Within the Czech Republic, the numbers of active vole burrows in cereals were significantly lower than in perennial forage crops. Lower numbers in cereals were also recorded compared to winter rape. The same was also found in the South Moravia and Olomouc regions. In the Zlín region, only winter wheat had significantly lower numbers than alfalfa and clover. In the Moravian-Silesian region, the number of active burrows did not significantly differ among all crops over the 10-year monitoring period.

Cereals do not provide as good living conditions for voles in terms of food base, shelter and crop density in spring as, for example, winter rape and forage crops. It is only when the quality of food decreases that voles move into adjacent cereal fields, which then affects the population dynamics and population structure of common voles in the agricultural landscape and can cause significant damage to cereal crops at peak population times.

ACKNOWLEDGEMENTS

We thank the State Phytosanitary Report (Phytosanitary portal) for permission to use data.

REFERENCES

Baláž, I. et al. 2019. Fluktuácia početnosti hraboša poľného na západnom Slovensku a možnosti jeho monitoringu. Ekologické štúdie, 10: 25–40.

Blitzer, E.J. et al. 2012. Spillover of functionally important organisms between managed and natural habitats. Agriculture Ecosystems and Environment [Online], 146(1): 34–43. Available at: https://doi.org/10.1016/j.agee.2011.09.005. [2021-08-01].

ČSÚ. 2020. Srovnání krajů v České republice 2019 [Online]. Available at: https://www.czso.cz/csu/czso/srovnani-kraju-v-ceske-republice-2019. [2021-07-31].

Heroldová, M. et al. 2004. Importance of winter rape for small rodents. Plant Soil Environment [Online], 50(4): 175–181. Available at: https://www.agriculturejournals.cz/publicFiles/52813.pdf. [2021-08-01].

Heroldová, M. et al. 2020. Interactions between common vole and winter rape. Pest Management Science [Online], 77(2): 599–603. Available at: https://doi.org/10.1002/ps.6050. [2021-07-31].

Jacob, J., Tkadlec, E. 2010. Rodent outbreaks in Europe: dynamics and damage. In Rodent outbreaks: ecology and impacts. Los Baños: International Rice Research Institute, pp. 207–223.

Jacob, J. et al. 2014. Common vole (Microtus arvalis) ecology and management: implications for risk assessment of plant protection products. Pest Management Science [Online], 70(6): 869–878. Available at: https://doi.org/10.1002/ps.3695. [2021-07-29].

Lambin, X. et al. 2006. Vole population cycles in northern and southern Europe: is there a need for different explanations for single pattern? Journal of Animal Ecology [Online], 75(2): 340–349. Available at: https://besjournals.onlinelibrary.wiley.com/doi/10.1111/j.1365-2656.2006.01051.x. [2021-07-30].

Landis, D.A. et al. 2000. Habitat management to conserve natural enemies of arthropod pests in agriculture. Annual of Review Entomology [Online], 45: 175–201. Available at: https://doi.org/10.1146/annurev.ento.45.1.175. [2021-08-01].

Pinheiro, J. et al. 2020. nlme: Linear and Nonlinear Mixed Effects Models. R package version 3.1–148. [Online]. Available at: https://cran.r-project.org/web/packages/nlme/index.html. [2021-09-01].

R Development Core Team. 2020. R: A Language and Environment for Statistical Computing. R Foundation for Statistical Computing Vienna [Online]. Available at: https://www.r-project.org/. [2021-09-01].

Rodríguez-Pastor, R. et al. 2016. "Living on the edge": the role of field margins for common vole (*Microtus arvalis*) populations in recently colonised Mediterranean farmland. Agriculture Ecosystems and Environment [Online], 231: 206–217. Available at: https://doi.org/10.1016/j.agee.2016.06.041. [2021-08-01].

Suchomel, J. et al. 2021. Spill over of the common voles from rape fields to adjacent crops. Biologia [Online], 76: 1747–1752. Available at: https://doi.org/10.2478/s11756-020-00675-9. [2021-08-07].

Tkadlec, E., Stenseth, N.C. 2001. A new geographical gradient in vole population dynamics. Proceedings of the Royal Society B-Biological Sciences [Online], 268(1476): 1547–1552. Available at: https://doi.org/10.1098/rspb.2001.1694. [2021-07-30].

Truszkowski, J. 1982. The impact of the common vole on the vegetation of agroecosystems. Acta Theriologica [Online], 27(23): 305–345. Available at: https://rcin.org.pl/dlibra/doccontent?id=10959. [2021-08-01].

Tscharntke, T. et al. 2012. Landscape moderation of biodiversity patterns and processes – eight hypotheses. Biological Reviews [Online], 87(3): 661–685. Available at: https://doi.org/10.1111/j.1469-185X.2011.00216.x. [2021-08-01].

Influence of different forage mixtures treated selenium and zinc on pollinators

Karolina Sodomova, Marian Hybl, Jan Sipos
Department of Zoology, Fisheries, Hydrobiology and Apiculture
Mendel University in Brno
Zemedelska 1, 613 00 Brno
CZECH REPUBLIC

xsodomov@mendelu.cz

Abstract: Biodiversity and pollinator abundance are still declining. Due to many environmental influences, the health of pollinators is also endangered. This harms the environment and crop production, as pollinators are an irreplaceable component of our ecosystems. The constant deterioration of this situation is due to several factors. These are oxidative stress, pesticides, low resistance to diseases, habitat loss, and, last but not least, the quality and availability of their diet. In this study, we focused on two elements that are very important for the proper function of metabolism and contribute to the overall defence of the body, namely selenium and zinc. Both elements should increase the quality of pollen and nectar produced by the treated plants. Based on our results pollinators was not affected by the application of microelements, but rather by the botanical composition of flowering meadow mixtures. Thus, pollinators responded to differences in species composition and abundance of flowering plants rather than to treatment. The richness of pollinators was higher on meadow mixtures containing more flowering plants, which produce more pollen and nectar and have a higher nutritional value than others.

Key Words: biodiversity, abundance, pollinators, meadow mixture, selenium, zinc

INTRODUCTION

In recent years, the decline in the diversity and abundance of wild pollinators (Bommarco et al. 2011) same as massive collapses of honeybee colonies are observed globally (Biesmeijer et al. 2006). In addition to landscape fragmentation and the use of pesticides, the loss of natural and semi-natural habitats is a major contributing factor to declining pollinator populations (Cane and Tepedino 2001). As a result of the loss of these habitats, the spatial and temporal distribution of food resources changes, thus significantly negatively affecting pollinator communities (Westrich 1996).

The survival ability and healthy development of pollinators can depend to a large extent on the quality and the availability of nutrients in the environment (Brodschneider et al. 2010). Nevertheless, the diversity and availability of pollinators' food resources continually declining because of increasing agricultural intensification (Naug 2009). As a result, the diversity and abundance of flowering plants have decreased and the low species diversity of entomophilic plants means reduced diversity and availability of macro and microelements in pollinator nutrition (Di Pasquale et al. 2013; Johnson et al., 2010), which negatively affects pollinator populations (Naug 2009). Inadequate nutrition may cause more vulnerability to diseases (Alaux et al. 2010), greater susceptibility to pesticides (Wahl and Ulm 1983), in the end, causes the decrease of diversity and abundance of pollinators (Keller et al. 2005).

Plant condition and pollinator nutrition can be improved by optimizing certain elements, such as zinc, which can be deficient in the environment. Zinc is a very important element for all organisms including pollinators because it increases the activity of antioxidant chains (Zhang et al. 2015). It is a component of more than 200 metalloenzymes and other metabolic compounds. These modulate biochemical processes and essential functions such as cellular respiration and reproduction, maintenance of cell membrane integrity, and many others (Eisler 1993). Moreover, zinc affects antioxidant enzymes which eliminate many of the reactive oxygen species (ROS) that can damage macromolecules produced during oxidative metabolism (Sohal and Weindruch 1996). Except it, adding zinc nutrient to plants significantly increased flower nectar secretion (Sawidis et al. 2014).

The next element competent to affect the quality of nectar, same as organism vitality is selenium. Since nectar contains almost all essential amino acids, including methionine and cysteine, which are the amino acids to which selenium binds to form selenomethionine and selenocysteine, selenium concentrations in the nectar should be increased after foliar application (Terrab et al. 2007). In an organism, selenium has catalytic, structural, and regulatory functions. It starts the action of many hormones, vitamins, and enzymes, thus ensure the implementation of many biochemical and physiological reactions in the body and helps to keep a normal function of biological systems (Sobolev et al. 2018).

According to mentioned information, we assume, adding these elements can improve the health and fitness of treated plants, improve the quality and quantity parameters of nectar and pollen as resources of pollinators' nutrition. As a result, pollinators' nutritional stress may be decreased, and their overall fitness may be increased. This can positively affect pollinator populations and increase their richness and abundance.

The first goal of this study was to verify the suitability of 3 different types of flower meadows with different botanical compositions for pollinators.

The second goal was to test the impact of foliar application of Se and Zn in amounts corresponding to a safe dose for the environment on the richness of the main pollinators.

MATERIAL AND METHODS

Locations

The experiment testing the effect of treatment was carried out in spring and summer 2021 at two different localities. Troubsko (southern Moravia, Czech Republic) is represented typically by a dry and warm habitat. The flat surface with an average altitude of 285m and average precipitation of 506.5 mm and average year temperature over 9.5 °C dominate in this area. Vatín (western Moravia, Czech Republic) is represented by humid and cold conditions. The hilly surface with an average altitude of 560 m and average precipitation of 617 mm and average year temperature over 6.9 °C dominate in this area.

Three varieties of meadow mixture were created for this experiment. Their composition is shown in the table below (Table 1).

Table 1 Overview of the composition of mixtures

	Meadow mixtures		
Plant families	a	b	c
Poaceae	0%	70%	90%
Fabaceae	40%	10%	3%
Other blossom plants	60%	20%	7%

Design of experiment

For treatments testing plots measuring 1.25 x 8 m have been created. Therefore, four treatments were founded:

a) Foliar application of Se

b) Foliar application of Zn

c) Foliar application of Se and Zn

d) Control (without application of Zn and Se)

Each variety (meadow mixture) and each treatment (foliar application) consist of three repetitions – triplets (n=3). Every plot was monitored once per week, from the beginning of flowering until mowing. Species foraged on the plot's mixture were identified by line transect. Pollinators' visits to the blossom of the observed plot were assessed visually in three transects throughout each plot.

Attendance of pollinators of blossoming mixed meadows was recorded. The visits suggesting pollination were observed visually in three repetitions on each plot once a week for four consecutive

weeks, from the beginning of flowering until mowing. Visits by pollinators were observed for a total of 10 minutes each by slowly walking around flowering plots at 10:00, 12:00, 14:00, and 16:00 for each locality. The recorded pollinators were divided into 5 taxonomic groups: *A. mellifera*, *Bombus* spp., solitary bees, Lepidoptera and Diptera. Only the presence / absence of individual taxonomic groups was recorded. Based on the insect observations we calculated taxon richness (i.e. number of taxa from five studied taxonomic groups) for each replication. One replication was represented by samples collected during particular date, from the single site in the plot with particular combination of treatment and meadow mixture.

Statistical analysis

To analyse the relationship between observed taxon richness and variety of meadow mixtures or application of microelements we used a mixed-effect model with Poisson error distribution. Meadow mixtures, application of microelements, and their interaction were used as fixed effect variables in the model. Based on the experimental design (each site consists of several plots which were sampled repeatedly through the year) a mixed model was designed as a random intercept model in which study plots nested into locality was included as a variable with random effect. Finally, the marginal effect of each explanatory variable in the model was tested by F-test in the analysis of variance with Kenward-Roger approximations of the degrees of freedom. In addition, significance testing between each variety of meadow mixture was analysed by Tukey HSD post-hoc test of multiple comparisons. Data were analysed in the R statistical software (R Core Team 2020).

RESULTS

Differences in the observed taxon richness independence of the meadow mixture and treatment of foliar fertilizer are depicted in Figure 1. The differences were highly significant among meadow mixtures ($P < 0.05$). Differences in pollinators' richness independence of treatment were not significant, same as interaction meadow and treatment.

Table 2 Results of the analysis of variance with Kenward-Roger approximations of the degrees of freedom testing the relationship between observed taxon richness, explanatory variables (i.e. meadow mixtures and microelements application), and its interaction.

	Sum Sq	Mean Sq	NumDF	DenDF	F-value	p-value
Meadows	85.386	42.693	2	8	11.6728	0.004243
Treatment	18.671	6.224	3	3	1.7016	0.336544
Meadows:Treatment	32.061	5.344	6	8	1.4610	0.301961

Figure 1 Differences of observed taxon richness according to types of the meadow mixture and treatment. Error bars represent 95% confidence intervals.

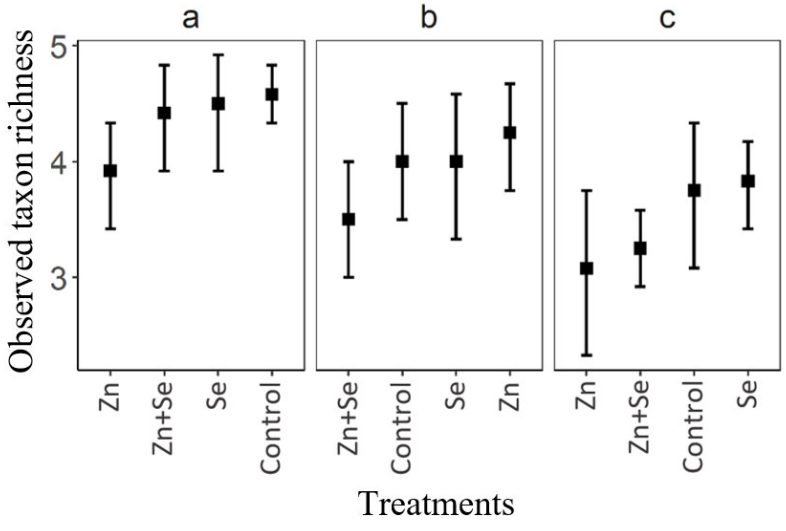

Figure 2 Differences of observed taxon richness according to types of meadow mixture. Error bars represent 95% confidence intervals.

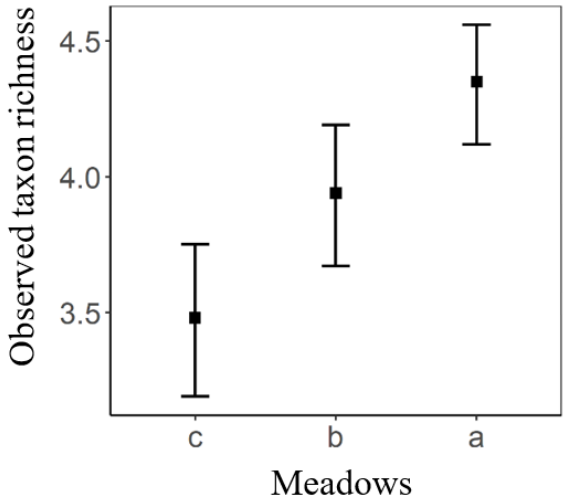

Taxon richness varied considerably between all the tested meadow mixtures. The significantly highest taxon richness was observed at the meadow mixture **a**. On the opposite, the lower level of richness was evaluated in meadow mixture **c**. Meadow mixture **b** had a lower richness value than mixture **a**, but a higher value of richness than mixture **c**.

Table 3 Results of Tukey HSD post-hoc test of multiple comparisons testing the differences among varieties of meadow mixture.

Contrasts	Estimate	SE	Df.	t.ratio	p-value
a–b	1.07	0.403	126	2.654	0.0242
a–c	2.15	0.403	126	5.343	<0.0001
b–c	1.08	0.403	126	2.689	0.0220

DISCUSSION

The differences in observed taxon richness of pollinators among treatments (i.e., microelements applications) were not significant (Figure 1), probably because most pollinators species do not respond to low doses of applied microelements. This property is assumed in evolutionarily more advanced species such as eusocial species. This includes the highly social honeybee (*A. mellifera)* and eusocial species of bumblebees (*Bombus* spp.) (Hendriksma et al. 2019).

When comparing the results of plots measurements with different meadow mixtures (Figure 2), high differences in the results are seen. Pollinators visited the meadow mixture the most, as it contained the most flowering plants (40% Fabaceae and 60% other blossom plants), which produce nectar and nutritionally valuable pollen compared to Poaceae (Mader et al. 2010), which were not present in the mixture a. Conversely, the least pollinators richness was observed on mixture c, which contained the highest proportion of Poaceae and represented the least suitable nutrition conditions.

From the above information, we can conclude that the biodiversity of pollinators is closely related to flowering plants, which is in agreement with the literature (Fleury et al. 2015), where are “meadow flowers,” seen as a symbol of biodiversity. But in our meadows, managed in conventional agriculture, mostly grasses (Poaceae) are grown. These do not produce enough nectar and pollen, because grass species are generally regarded as anemophilous (Hawkeswood 2011). For these reasons, malnutrition of pollinators occurs, affects their health, resistance to oxidative stress and diseases, and in the end, the diversity of pollinators decreases.

Due to the generality of the results, it is necessary to focus in further measurements on the preferences of individual monitored taxa and their abundance, which will help to reveal the real impact of the application of microelements more deeply on pollinators.

CONCLUSION

The observed taxon richness of pollinators was not significantly affected by the application of microelements, but by the botanical composition of meadow mixtures as food sources.

Pollinators have been shown to prefer flowering plants that produce more nectar and pollen than sources that have low pollen and nectar production and lower nutritional values.

The relationship between the number of flowering plants and the diversity and number of pollinators was confirmed.

ACKNOWLEDGEMENTS

This manuscript was financially supported by the Technology Agency of the Czech Republic grant number TJ04000048: "Foliar nutrition of forage plants with selenium and zinc and its impact on their qualitative and quantitative characteristics and the environment of the organisms occurring within these ecosystems".

REFERENCES

Alaux, C. et al. 2010. Diet Effects on Honeybee Immunocompetence. Biology Letters, 6(4): 562–565.

Biesmeijer, J.C. et al. 2006. Parallel declines in pollinators and insect-pollinated plants in Britain and the Netherlands. Science, 313: 351–354.

Bommarco, R. et al. 2011. Drastic historic shifts in bumble-bee community composition in Sweden. Proceedings. Biological sciences The Royal Society, 279: 309–15.

Brodschneider, R., Crailsheim, K. 2010. Nutrition and Health in Honey Bees. Apidologie, 41: 278–294.

Cane, J.H., Tepedino, V.J. 2001. Causes and extent of declines among native North American invertebrate pollinators: detection, evidence, and consequences. Conservation Ecology 5: 1.

Di Pasquale, G. et al. 2013. Influence of Pollen Nutrition on Honey Bee Health: Do Pollen Quality and Diversity Matter? PLoS ONE, 8: e72016.

Eisler, R. 1993. Zinc Hazards to Fish, Wildlife, and Invertebrates: A Synoptic Review. U.S. Washington D.C., USA: Department of the Interior Fish and Wildlife Service.

Fleury, P. et al. 2015. “Flowering Meadows”, a result-oriented agri-environmental measure: Technical and value changes in favour of biodiversity. Land Use Policy, 46: 103–114.

Hawkeswood, T.J. 2011. First record of Micraspis frenata (Erichson, 1842) (Coleoptera: Coccinellidae) feeding on pollen from Carex appressa R.Br. (Cyperaceae) in New South Wales, Australia. Calodema, 144: 1–3.

Hendriksma, H.P. et al. 2019. Individual and Colony Level Foraging Decisions of Bumble Bees and Honey Bees in Relation to Balancing of Nutrient Needs. Frontiers is Ecology and Evolution, 7: 177.

Johnson, R.M. et al. 2010. Pesticides and Honey Bee Toxicity–USA. Apidologie, 41: 312–331.

Keller, I. et al. 2005. Pollen Nutrition and Colony Development in Honey Bees–Part II. Bee World, 86: 27–34.

Naug, D. 2009. Nutritional Stress Due to Habitat Loss May Explain Recent Honeybee Colony Collapses. Biological Conservation, 142: 2369–2372.

Sawidis, T. et al. 2014. Effect of zinc on nectar secretion of Hibiscus rosa-sinensis L. Protoplasma, 251: 575–589.

Sobolev, O. et al. 2018. Biological role of selenium in the organism of animals and humans. Ukrainian Journal of Ecology, 8: 654–665.

Terrab, A. et. al. 2007. Analysis of amino acids in nectar from Silene colorata Poiret (Caryophyllaceae). Botanical Journal of the Linnean Society, 155(1): 49–56.

Wahl, O., Ulm, K. 1983. Influence of Pollen Feeding and Physiological Condition on Pesticide Sensitivity of the Honey Bee Apis mellifera Carnica. Oecologia, 59: 106–128.

Westrich, P. 1996. Habitat Requirements of Central European Bees and the Problems of Partial Habitats. London, UK: Academic Press.

Zhang, G. et al. 2015. Zinc nutrition increases the antioxidant defenses of honey bees. Entomologia Experimentalis et Applicata, 7: 17.

AGROECOLOGY AND RURAL DEVELOPMENT

Integrated national-scale assessment of climate change impacts on agriculture: the case of the Czech Republic

Juliana Arbelaez Gaviria[1,2,3], Esther Boere[3], Petr Havlik[3], Miroslav Trnka[1,2]
[1]Department of Agrosystems and Bioclimatology
Mendel University in Brno
Zemedelska 1, 613 00 Brno
[2]Global Change Research Institute AS CR v.v.i.
Belidla 986/4b, 603 00 Brno
CZECH REPUBLIC
[3]Biodiversity and Natural Resources Program
International Institute for Applied System Analysis (IIASA)
Schlossplatz 1 - A-2361 Laxenburg
AUSTRIA

xarbelae@mendelu.cz

Abstract: In recent years, investigating climate change impacts in the agricultural sector at the national level has become a priority for adaptation decision-making. Most of these studies quantify the impacts of biophysical effects and often ignore the cross-sectoral interactions and economic effects on relative competitiveness, international trade, global food supply, and food prices for the Czech Republic. Ignoring future productivity changes globally under climate change scenarios can underestimate or overestimate climate change impacts at the national level. Here, we use GLOBIOM-CZE, a global economic model, as part of a climate change impact assessment framework to evaluate the impacts on the Czech agricultural sector in terms of environmental and economic indicators. By comparing with the baseline, the ensemble of scenarios suggests a decrease in crop area and production while increasing grassland, positively affecting livestock production by mid-century. Corn and barley show the most adverse response in production and area, while rapeseed increases under scenario RCP 8.5 with CO_2 fertilization effect. Livestock products production is projected to increase, especially bovine meat and milk, as within RCP 8.5, no constraints are placed on growing greenhouse gas emissions.

Key Words: climate change impacts, Czech agriculture, global assessment model

INTRODUCTION

Climate change is considered a global driver that impacts the global supply and demand of land-based commodities and, along with population dynamics and economic development, impose challenges for the agricultural sector and food security worldwide. However, the effects of these global changes are restrained in the national context by environmental and socioeconomic conditions. In return, the biophysical impacts on agricultural productivity and their adaptation alter the resulting economic effects on relative competitiveness, international trade, global food supply, and food prices. Hence, ignoring future productivity changes globally under climate change scenarios can underestimate or overestimate climate change impacts at the national level (Zhang et al. 2014).

Climate change impacts assessments of the Czech agricultural sector have relied on the country or regional scale modelling approaches that do not explicitly account for global market interactions and feedback and often focus on single commodities analysis. Nevertheless, several studies evaluated the impacts of climate change on the potential productivity of Czech agriculture (Duffková et al. 2019), main Czech commodities such as maize, spring barley, winter wheat (Trnka et al. 2014), Saaz hops, and livestock sector (Malý et al. 2017).

National impact assessment studies must consider the linkages between global drivers and local responses and feedback at national and global scales. Contributing to previous climate change impacts assessment in Czech agriculture, the main goal of this contribution is to quantify the impacts in terms of economic indicators of the foremost Czech commodities accounting for global climate impacts when

projecting domestic implications at the national level. It explores the changes in production, area, yield, and trade of key agricultural commodities.

MATERIAL AND METHODS

GLOBIOM-CZE

In this study, we used GLOBIOM-CZE, a global economic model (GEM) based on the European version of The Global Biosphere Management Model (GLOBIOM-EU) (Frank et al. 2015) and adapted to the Czech agricultural context. GLOBIOM-CZE is a partial equilibrium model that integrates land-use-based sectors: agriculture, forest, and bioenergy (Havlík et al. 2014). Crops, forestry, livestock products, and subproducts are optimized by allocating land across production activities. Using a market equilibrium approach in a 10-year time step from 2000 to 2050, GLOBIOM-CZE maximizes the sum of producer and consumer surplus conditioned to resources, technological, demand, and policy constraints (McCarl and Spreen 1980). The demand for final products and the international trade is represented at 57 aggregated economic regions, where 28 corresponds to EU member states and UK and 29 regions outside Europe. The supply side of the model follows a bottom-up approach based on detailed spatial units' information, including land cover, land use, management system, and other biophysical and technical cost information. The representation of crops, livestock, and forest production activities relies on detailed biophysical models. The primary forest productivity and harvesting costs are estimated by The Global Forest Model (G4M) (Kindermann et al. 2008). The biophysical process-based model Environmental Policy Integrated Climate (EPIC) computes productivity, fertilizer rates, and irrigation management (Williams 1995). The European crop sector is represented by crop rotations of 18 crops derived from crop shares calculated from EUROSTAT statistics based on crop areas at NUTS2 level using the crop rotation model CropRota (Schönhart et al. 2011). The livestock sector and its production system parameterization is based on the RUMINANT model (Herrero et al. 2013). Additional information and model descriptions can be found in (Havlík et al. 2014) for the global version and (Frank et al. 2015) for the European version.

The Czech Republic is represented by its demand and trade flow functions. Every European country can trade with other countries in the EU and with regions outside the EU through a common EU hub market. Hence, the Czech Republic trades from/to single EU countries and to/from an EU hub and subsequently to another a world region outside the European Union. GLOBIOM-CZE has been validated against the 2010-2020 Czech National Statics and FAOSTAT dataset for production, consumption, and yields. Additionally, the traded quantities and trade flows were also adjusted and validated for 2010 and 2020.

Modelling framework

The impact modelling chain used in this study combines General Circulation Models (GCM), EPIC model as global gridded crop model (GGCM), and GLOBIOM-CZE as the global economic model (GEM) of the agricultural sector (Leclère et al. 2014). First, GCMs are used to study the response of the climate system to different trajectories of greenhouse gases emission defined by the representative concentration pathways (RCPs), then changes on atmospheric variables such as precipitation, temperature, wind speed, and CO_2 concentration are used as input in the biophysical models. Next, EPIC simulates yields keeping consistent the scenario combinations between GCMs and RCPs. Finally, simulated yields impacts are included in GLOBIOM-CZE as spatially explicit yield shifters for each climate scenario, crop, grassland, and management system. This analysis was conducted using six indicators across demand, supply, and trade. The supply is described by the attainable yield in tonnes per hectare, defined as the exogenous productivity due to changes in climatic conditions. The yield in tonnes per hectare is the endogenous response of the productivity, which includes consequential changes in the management system and the effect of crop relocations. The area represents the total harvested area in hectares, and production is defined as the total production for the Czech Republic in tonnes. The total consumption characterizes the demand in tonnes of the commodities for food, feed, biofuels, and other uses. And the net trade is defined as the difference between net exports and imports in tonnes.

Scenarios

Socioeconomic development is one of the main drivers of GLOBIOM-CZE. Therefore, the Shared Socioeconomic Pathway 2 (SSP2) was used as a baseline scenario. SSP2 narrative described a future where medium challenges to mitigation and adaptation are assumed, and current trends for society and natural systems are expected (O'Neill et al. 2014). The Czech population reaches 11,704 million, and GDP is considered to be 396,167 billion US$2005/year by 2050.

The ISI-MIP Fast Track Protocol determined climate change scenarios; the EPIC model used them to estimate the crops and y grass yield impact projections. Four RCPs were used covering the increasing radiative forcing levels by (the 2.6 W m^{-2}, 4.5 W m^{-2}, 6 W m^{-2}, and 8.5 W m^{-2} scenarios) as projected by HadGEM2–ES. In addition, four GCM were implemented using RCP 8.5 for studying the uncertainty across climate models: GFDL–ESM2M, IPSL–CM5A–LR, MIROC–ESM–CHEM, and NorESM1–M. Yield impacts were projected assuming CO_2 fertilization effects for all the GCM x RCP combinations. Additionally, RCP 8.5 x HadGEM2–ES was also simulated without this effect to analyze the CO_2 fertilization effect. In total, 13 scenarios were used and analyzed in this contribution.

RESULTS AND DISCUSSION

The EPIC model determines climate change biophysical impacts on crop yields and accounts for crop productivities due to changes in temperature and precipitation and correspond to averaging the yields across years and do not consider different cultivars. Therefore, these impacts can be understood as potential changes compared to the baseline scenario, thereby providing adaptation opportunities. By mid-century, the biophysical impacts on Czech key crops increase attainable productivity across RCP x GCM combinations equivalent to - 3% and + 9% change compared to the baseline for all the crops (see Figure 1). However, the magnitude varies across crops from - 29% for corn to + 29% for barley being HadGEM2–ES under RCP 8.5 without CO_2 fertilization effect the scenario that shows the more significant impacts for corn and potatoes and HadGEM2–ES under RCP 8.5 with CO_2 fertilization effect for the rest of the crops (see the first column in Table 1), which suggest an adaptation potential through changes in specialization, area reallocation, and management of agricultural systems. Assuming no CO_2 effects (RCP 8.5 x HadGEM2–ES) worsen the biophysical impacts on attainable yields about 10% for the Czech Republic and specifically for C4 crops such as corn by 8% (see Table 1).

Figure 1 Percentage (%) of change to the baseline scenario in attainable yields and total area for cropland (left) and grassland (right) by 2050 in the Czech Republic

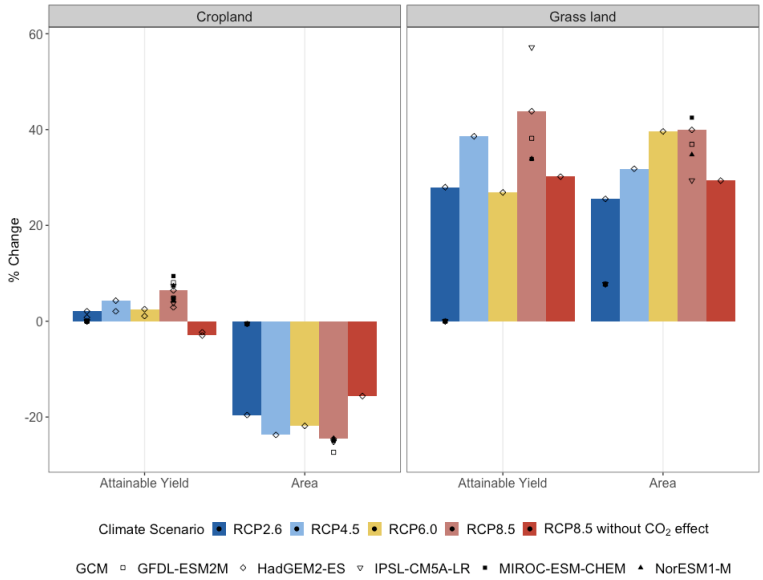

Impacts on agricultural output

The impacts of climate change on Czech agriculture are quantified in changes in endogenous yield, area, production, consumption, and net trade compared to the baseline scenario assumed to have

no climate change conditions. The percentage of change of these indicators is defined as the relative difference between the baseline scenario and the climate scenario (GCM x RCP). The attainable yield changes by 2050 projected by EPIC for crops and grass are depicted in the first column in Figure 1. Overall, climate change's biophysical effect on attainable yield is positive across GCM x RCP in the Czech Republic. On the other hand, negative impacts are expected under RCP 8.5 x HadGEM2–ES without CO_2 effect.

Figure 2 Percentage (%) of change to the baseline scenario for wheat indicators in the Czech Republic by 2050

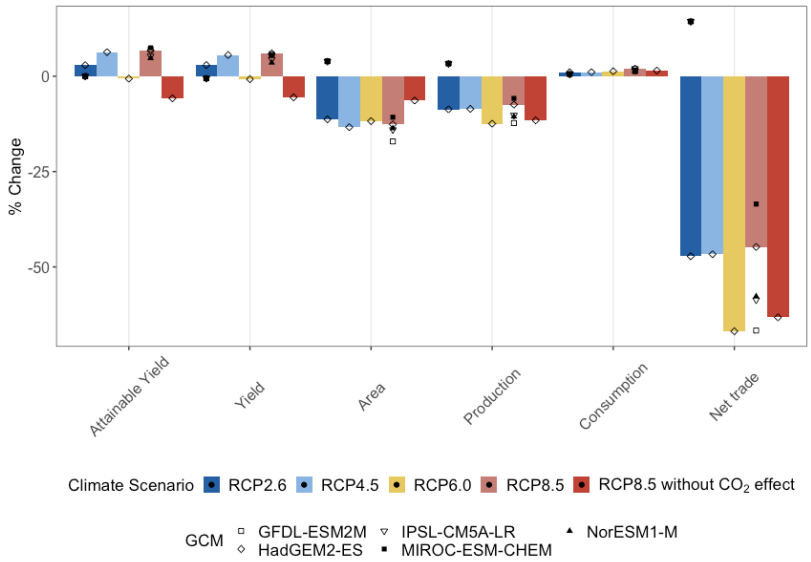

Consequently, the changes in cropland and grassland projected by GLOBIOM-CZE are outlined in the second column in Figure 1. The attainable grassland productivity is expected to increase up to 57% under the scenario RCP 8.5 x IPSL-CM5A-LR. Nevertheless, the total area for crops in the Czech Republic is expected to decrease while the grassland will increase across all scenarios by mid-century. The impacts on grassland yields affect the livestock sector due to losses in productivity, and reduced production of crops used a livestock feed.

Figure 3 Percentage (%) of change to the baseline scenario for corn indicators in the Czech Republic by 2050

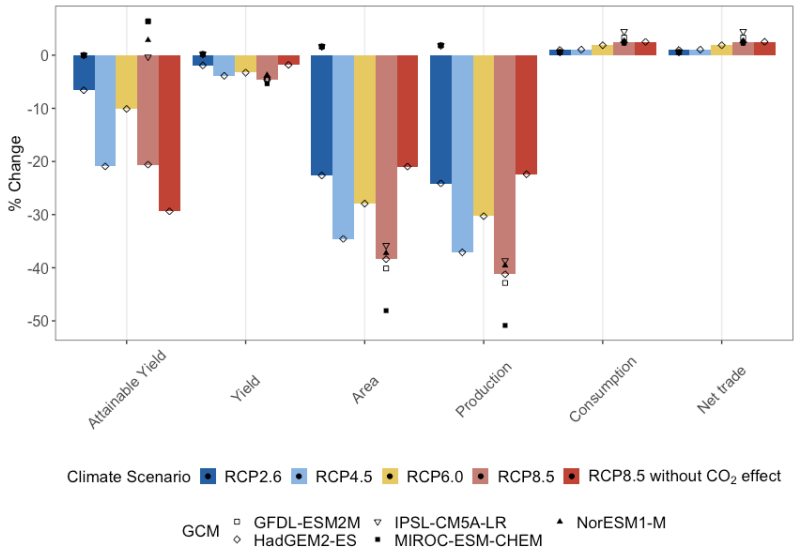

By 2050, The Czech production of barley shows potential for adaptation of 7% under RCP 8.5 x HadGEM2–ES, yet it will not be enough to hold the domestic demand causing an increase in imports

(see Table 1). Furthermore, as expected from Figure 1, the arable land in the Czech Republic is expected to decrease for all the key crops.

On the other hand, corn production shows an adaptation potential of more than 25% in 2050 under RCP 8.5 x HadGEM2–ES with CO_2 fertilization effect (see Figure 3). Notwithstanding, the drop in production of this product leads to an increase in the quantity of Czech Republic imports to span the domestic use, primarily feed for livestock. The indirect climate effect can explain the negative change in corn yields modelled by EPIC (Table 1). As corn is a C4 crop with already high water use efficiency, the positive so-called fertilization effect caused by the increase of ambient CO_2 is smaller than in C3 crops (e.g., wheat, rapeseed, barley). At the same time, relatively low daily solar irradiance of the Czech Republic higher latitudes toward the start and end of growing season does not allow corn to capitalize fully on the longer growing season, while the corn sensitivity to water stress during warmer and drier summer months also contributes to lower yield projections. However, it should be noted that temperature and water stress are more critical for summer crops than for winter or spring crops, leading to a higher adaptation potential through management systems and area reallocation. In contrast, wheat's adaptation potential is limited, and yields are expected to slightly increase in the Czech Republic.

As the attainable yield in grassland and area are expected to increase across all RCP X GCM combinations, the production of the primary livestock commodities in the Czech Republic also shows a positive response. Bovine meat production is projected to increase +2% - 17% by mid-century, yet the country will still rely on imports from neighboring countries for domestic consumption. That is not the case with eggs, sheep, and goat meat (see Table 1).

Table 1 Summary of percentage % change the main indicators for key commodities for the Czech agricultural sector under HadGEM2–ES RCP 8.5 with and without CO_2 fertilization effect

	Attainable yield		Yield		Area		Production		Net trade		Consumption	
	yes*	no**	yes	no	yes	no	yes	no	yes	no	yes	no
Wheat	6.7	-5.8	5.9	-5.5	-13	-6.4	-7.4	-12	-45	-63	2	1.4
Corn	-21	-29	-4	-1.8	-38	-21	-41	-22	2.5	2.5	2.4	2.5
Barley	24	1.4	17	-1.6	-38	-24	-27	-26	-113	-105	2.5	1.7
Rapeseed	12	1.5	13	2.8	-8.9	-4.7	3.4	-2	3.3	-5.1	8.8	7.4
Potatoes	-5	-19	-5	-19	-1.7	0.3	0.4	2.1	2.7	6.1	-2.8	-3.8
Crops	6.4	-3	9.6	1.5	-24	-15	-26	-19	-28	-26	-12	-7.5
Bovine meat	-	-	-	-	-	-	17	12	-20	-13	6.2	5
Pig meat	-	-	-	-	-	-	0.4	0.3	6.4	2.9	3.9	1.8
Poultry meat	-	-	-	-	-	-	0.1	0.1	8.4	6.6	5	4
Sheep/goat meat	-	-	-	-	-	-	51	21	-126	-49	21	8.6
Eggs	-	-	-	-	-	-	-0.4	-2.1	9.9	8.3	-2.5	-4.2
Milk	-	-	-	-	-	-	9	11	-80	-7.5	4.8	3.6
Livestock	-	-	-	-	40	29	7.2	8.7	0.5	-4.2	4.6	3.2

*Legend: *yes: with CO_2 fertilization effect, **no: without CO_2 fertilization effect*

CONCLUSION

We provide an economical and environmental assessment of climate change impacts on Czech agriculture. We use the GLOBIOM-CZE model to investigate the adaptation potential in the key agricultural outputs in production, area, consumption, and net trade under climate change conditions. Additionally, we study the impacts on cropland and grassland to understand the potential state of Czech agriculture by mid-century. The scenarios ensemble used in this contribution also explores the uncertainties across representation concentration pathway (RCPs), global circulation models (GCMs), and CO_2 fertilization effect. GLOBIOM-CZE constitutes a framework to evaluate the trade-offs between biophysical climate change impacts, economic adaptations, land-use competition,

and feedbacks into the global market, adding an economic scope to the previous physical-based models used for climate change impact assessments.

As per the knowledge of the authors, this is one of the first attempts to assess the climate change impacts on the Czech agricultural sector by understanding the complexity between the biophysical conditions, the land opportunities by reallocation, the changes in comparative advantages, and the economic competitiveness of the Czech Republic in the region.

ACKNOWLEDGEMENTS

The main author´s research was financially supported by Zhodnocení vlivu klimatických změn na zemědělství ve Střední a Východní Evropě v kontextu globálních podmínek (SP2210041 - AF-IGA2021-IP015). Access to GLOBIOM source code, consultation time of IIASA experts (P.H. and E.B), computing and data facilities as well as contribution by M.T. was made possible thanks to the project SustES - Adaptation strategies for sustainable ecosystem services and food security under adverse environmental conditions (CZ.02.1.01/0.0/0.0/16_019/0000797).

REFERENCES

Duffková, R. et al. 2019. Long-Term Water Balance of Selected Field Crops in Different Agricultural Regions of the Czech Republic Using Fao-56 and Soil Hydrological Approaches. Sustainability, 11(19): 5243.

Frank, S. et al. 2015. The dynamic soil organic carbon mitigation potential of European cropland. Global Environmental Change, 35: 269–278.

Havlík, P. et al. 2014. Climate change mitigation through livestock system transitions. Proceedings of the National Academy of Sciences, 111(10): 3709–3714.

Herrero, M. et al. 2013. Biomass use, production, feed efficiencies, and greenhouse gas emissions from global livestock systems. Proceedings of the National Academy of Sciences, 110(52): 20888–20893.

Kindermann, G. et al. 2008. A global forest growing stock, biomass and carbon map based on FAO statistics. Silva Fennica [online], 42(3). Available at: http://www.silvafennica.fi/article/244. [2021-09-08].

Leclère, D. et al. 2014. Climate change induced transformations of agricultural systems: insights from a global model. Environmental Research Letters, 9(12): 124018.

Malý, M. et al. 2017. Valuation of Public Goods: The Case of Emissions from Livestock Holdings in the Czech Republic. Agris on-line Papers in Economics and Informatics, 09(01): 99–111.

McCarl, B.A., Spreen, T.H. 1980. Price Endogenous Mathematical Programming As a Tool for Sector Analysis. American Journal of Agricultural Economics, 62(1): 87–102.

O'Neill, B.C., et al. 2014. A new scenario framework for climate change research: the concept of shared socioeconomic pathways. Climatic Change, 122(3): 387–400.

Schönhart, M. et al. 2011. CropRota – A crop rotation model to support integrated land use assessments. European Journal of Agronomy, 34(4): 263–277.

Thaler, S. et al. 2012. Impacts of climate change and alternative adaptation options on winter wheat yield and water productivity in a dry climate in Central Europe. The Journal of Agricultural Science, 150(5): 537–555.

Trnka, M. et al. 2014. Adverse weather conditions for European wheat production will become more frequent with climate change. Nature Climate Change, 4: 637–643.

Trnka, M. et al. 2004. Projections of uncertainties in climate change scenarios into expected winter wheat yields. Theoretical and Applied Climatology, 77: 229–249.

Williams, J.R. 1995. The EPIC model. In Computer Models of Watershed Hydrology. Highlands Ranch: Water Resources Publications, pp. 909–1000.

Zhang, Y. et al. 2014. Modeling Climate Change Impacts on the US Agricultural Exports. Journal of Integrative Agriculture, 13(4): 666–676.

Analysis of small forest catchments evapotranspiration determined by precipitation/runoff measurements, remote sensing model DisALEXI and water balance model SoilClim

Tomas Ghisi[1], Milan Fischer[1], Filip Oulehle[2], Zdenek Zalud[1], Miroslav Trnka[1]
[1]Department of Agrosystems and Bioclimatology
Mendel University in Brno
Zemedelska 1, 613 00 Brno
[2]Department of Biogeochemistry
Czech Geological Survey
Klarov 131, 118 00 Praha
CZECH REPUBLIC

tomas.ghisi@mendelu.cz

Abstract: The below-average precipitation combined with above-average temperature during the period 2015–2019 showed high susceptibility of the Czech landscape to drought stress. This particular drought caused significant economics losses in the forestry, agcicultural and water management sectors. Because the climate models predict recurrence of drought period with increasing intensity and frequency, accurate knowledge of individual ecosystems evapotranspiration is needed to develop suitable adaptation to climate change. This contribution detects the evapotranspiration determined by precipitation/runoff measurements, diagnostic remote sensing model DisALEXI and semi–empirical model SoilClim in small forest (mostly Norway spruce) catchments areas (GEOMON network). Based on altitudinal gradient analysis (470–942 m), two of the three applied methods (DisALEXI and SoilClim models) confirm the previously accepted hypothesis, that at low elevation the evapotranspiration is limited by precipitation while at higher altitudes by available energy. Moreover, these two models identify the break point where evapotranspiration reaches maximum values and the altitude where evapotranspiration begins to be limited by a lack of available energy (DisALEXI at 758 m, SoilClim at 685 m). However, the DisALEXI model as the only one that best captures the relationship between evapotranspiration, precipitation and altitude. This analysis can by useful for detection suitable conditions for sustainable spruce forest management.

Key Words: evapotranspiration, climate changes, remote sensing, water balance, catchment

INTRODUCTION

Current change in climate and model projections for the future indicate a trend towards more extreme events including changes in precipitation and runoff in individual river catchments (Štěpánek et al. 2016). The network GEOMON consists of 13 small forest catchments in mountains and sub–mountains areas of the Czech Republic, where hydrochemical and hydrological conditions are primarily observed. The network is managed by the Czech Geological Survey. The network of small forest catchments was established in 1994 and is therefore suitable for long–term observations of ecosystem changes of Norway spruce and European beech ecosystem (Oulehle et al. 2017). Small forest catchments, except (Lesní potok, Jezeří and Polomka), are located in spruce stands. Therefore, it is relatively easy to capture changes in spruce forests caused by anthropogenic or naturogenic degradation effects, such as acid rain (Oulehle et al. 2021).

In the context of changing climatic conditions, it is also necessary to recall the recent significant collapse of spruce stands in the middle and lower altitudes of the Czech landscape, mainly due to the dry period 2015–2019 and the action of bark beetles. According to the forecast of climate scenarios (Štěpánek et al. 2016) and future predictions of heat waves (Lhotka et al. 2018) and current climatic trends the existence of Norway spruce in the lower and middle positions of the Czech Republic is significantly endangered and it is likely that it will probably not be the main commercial forest species at these altitudes. At lower altitudes, the climate–growth relationship of Norway spruce indicates strong

dependence of spruce and beech growth on water availability in summer period (June–August). Moreover, the significant temporal shifts and prolongation of growing season indicate the increasing drought sensitivity of spruce and beech forest ecosystem (Kolář et al. 2017). One of the main challenges of current forestry management is therefore to determine suitable conditions and altitude for the cultivation of Norway spruce in the Czech Republic with regard to climate changes. Krejza et al. (2021) reported the altitude of 900 m as the critical altitude below which the Norway spruce is at risk in for the conditions of the Czech Republic.

Based on previously accepted hypotheses, we assume that the amount of actual evapotranspiration (ET_a) varies with altitude, depending on the availability of precipitation and energy. While in lower positions the amount of ET_a is limited by precipitation, in mountainous locations ET_a is limited by available energy. The main aim of study is to analyze the ET_a over the altitudinal gradient (470–942 m) in small forest catchments using the GEOMON precipitation and runoff method, remote sensing model DisALEXI and water balance model SoilClim. In addition, use these methods to detect the break point where ET_a reaches a maximum value and the point where ET_a begins to be limited by lack of available energy. ET_a is tightly related to biomass productivity and hence plays a significant role in the occurrence of Norway spruce.

MATERIAL AND METHODS

The small forest catchments – GEOMON network

The 13 small forest catchments used in this study are located in the mountains and sub-mountains areas of the Czech Republic. The elevation gradient of these catchments is from around 400 to 950 m. The sizes of these catchments range between 21 to 260 ha. All these catchments are dominated by Norway spruce, except for the Jezeří, Lesní potok and Polomka catchments, where beech forests dominate. The forestry management ongoing in all small forest catchments. The characteristics of the selected catchments are shown in the Table 1. In this contribution the mean annual ET determined by i) precipitation/runoff measurements, ii) diagnostic remote sensing model DisALEXI, and iii) water balance model SoilClim are analysed across the altitudinal gradient at small forest catchments of GEOMON network over the period (2001–2018).

Precipitation/runoff measurement - P/Q method

The evapotranspiration is estimated based on the precipitation/run off measurement (P/Q method) method and calculating of hydrological balance equations. The runoff fluxes from all catchment is computed through V-notch weirs with established rating curves and all measuring stations were equipped with infrared or pressure types of water level recorders. In this study, the precipitation values measured by Czech Geological Survey was replaced by the precipitation values measured by the CHMI (Czech Hydrometeorological Institute), which are interpolated to the spatial by GCRI (Global Change Research Institute of the Czech Academy of Sciences)**.** The ET_a is computed based on the hydrological balance equations, assuming no groundwater recharge, according to:

$$ET_a = P - Q$$

where P is precipitation in an open area (mm) and Q is water runoff from catchment (mm). Evapotranspiration includes interception loses, evaporation from bare soil and transpiration of vegetation.

ALEXI/DisALEXI model

The Atmosphere Land Exchange Inverse (ALEXI) surface-energy balance model uses the remotely sensed surface temperature data to estimate ET_a in landscape (Norman et al. 2003, Anderson et al. 1997). The model is based on the two-source energy balance algorithm (Norman et al. 1995) where the available surface energy is partitioned between bare soil and vegetation cover. The model can be applied from polar or geostationary satellites, which allows sensing in thermal infrared bands (Anderson et al. 2003).

Model ALEXI is constrained to operate on spatial scale more than 5km, whereas the model DisALEXI (Normal et al. 2003) is the disaggregation form of this model, which allows to operate

in finer resolution up to 30 m. In this study, the remotely sensed data available for the model DisALEXI was acquired for the period 2001–2018 by MODIS sensor in 500 m resolution.

SoilClim model

The semi-empirical SoilClim model represent a tool for simulating water balance in soil, vegetation and atmosphere system (Hlavinka et al. 2011, Řehoř et al. 2021). The ET_a data estimated by SoilClim model was acquired in spatial resolution of 500 m according to methods described in details by Řehoř et al. (2021). The input data and meteorological data was acquired from meteorological station CHMI which are spatially interpolated to 500 m grids by GCRI.

Reference evapotranspiration

The reference evapotranspiration (ET_o) was calculated by Penman-Monteith method specified in FAO (Allen et al. 1998). The input meteorological data was acquired from meteorological station CHMI which are spatially interpolated to 500 m grids by GCRI. In this case, the ET_o is represents ET the values of a hypothetical reference grass surface which has ideal conditions for growth and that is not limited by lack of water. The input meteorological data was acquired from meteorological station CHMI which are spatially interpolated to 500 m grids by GCRI.

Table 1 The summary of the selected small forest catchments within GEOMON network

Name of the forest catchment	Area (ha)	Average altitude (m)	Location	Main tree species
Anenské povodí	28	520	Českomoravská vrchovina	Spruce *(Picea abies)*
Červík	181	802	Moravskoslezské Beskydy	Spruce *(Picea abies)*
Jezeří	260	758	Krušné hory	Beech *(Fagus sylvatica)*
Lesní potok	63	471	Středočeská pahorkatina	Beech *(Fagus sylvatica)*
Litavka	179	774	Brdy	Spruce *(Picea abies)*
Liz	94	942	Šumava	Spruce *(Picea abies)*
Loukov	54	577	Českomoravská vrchovina	Spruce *(Picea abies)*
Lysina	25	881	Slavkovský les	Spruce *(Picea abies)*
Pluhův bor	21	764	Slavkovský les	Spruce *(Picea abies)*
Polomka	64	614	Železné hory	Beech *(Fagus sylvatica)*
Salačova lhota	200	640	Českomoravská vrchovina	Spruce *(Picea abies)*
Spálenec	53	826	Šumava	Spruce *(Picea abies)*
Uhlířská	180	818	Jizerské hory	Spruce *(Picea abies)*

RESULTS AND DISCUSSION

The Figure 1 shows the annual average precipitation and ET_o values of the small forest catchments in the period (2001–2018). The points represent data from the 13 small forest catchments and linear regression was used to fit the linear trends. The plot shows the precipitation increases with increasing

altitude of catchments, while ET_o decreases with increasing altitude due to decreasing amount of available energy.

Figure 1 The trends of the annually averaged precipitation and ET_o of small forest catchments in period (2001–2018). The red line depicts the line regression trend.

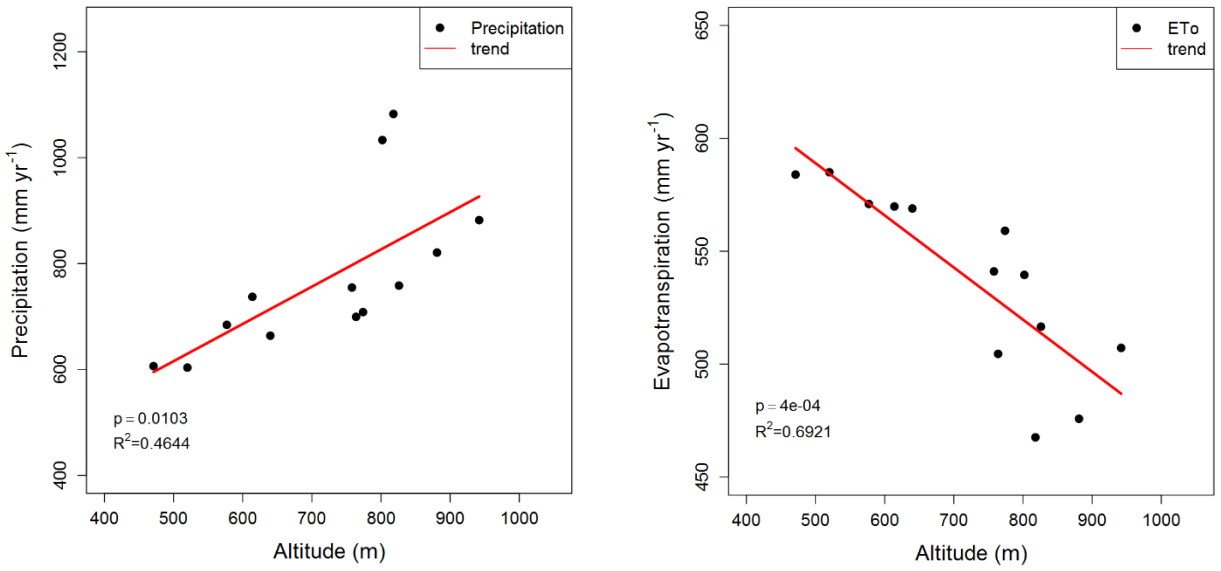

Figure 2 The annual average ET_a values of the small forest catchments in the period (2001–2018) estimated by the DisALEXI, SoilClim model and calculated by P/Q method. The ET_a values are related to the altitudes (left) and to the average annual precipitation (right). The peaks of the polynomial curves (break points) are showed by triangle.

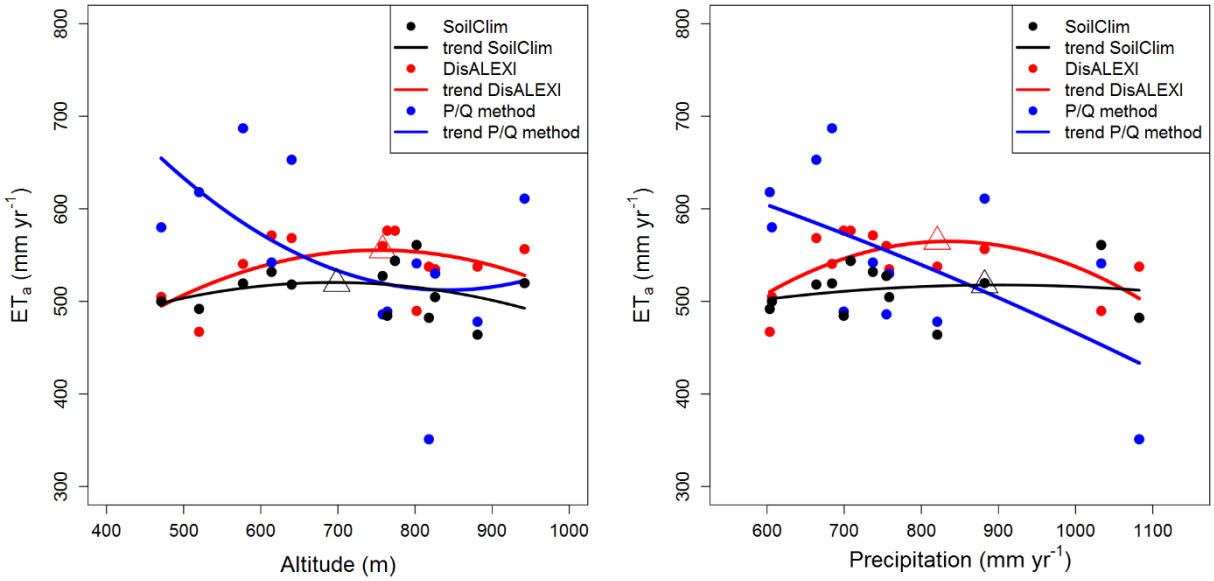

In the Figure 2, the fitted curves of models DisALEXI and SoilClim shows the different trend then P/Q method. The values of the average ET_a of P/Q method are relatively inconsistent. In the left graph, the curve of the DisALEXI and SoilClim models detect the ET_a peaks (break points) at an altitude of 758 m DisALEXI and SoilClim at 685 m. The increasing tendencies of ET_a with the altitude can be explained by sufficient available energy at the catchments but limiting precipitation. At the altitudes lower than the break point ET_a thus increases according to the amount of precipitation. The decreasing trend of ET_a after the break point can be explained by lack of available energy for ET_a. At these altitudes, the amount of ET_a decreases according to decreasing amount of the available energy.

The right plot shows the average annual ET_a depending on average annual precipitation in the catchments. Assuming that the ET_a is limited by precipitation at lower altitudes and available energy at higher altitudes, this plot would identify the precipitation break point where ET_a reaches the maximal values and the point where ET_a begins to be limited by lack of available energy. The break point of ET_a is easily detected by model DisALEXI 820 mm of precipitation, model SoilClim 882 mm. The P/Q method does not identify this point.

The results of Figures 1 and Figures 2 can be explained as follows. The DisALEXI model best captures the relationship between ET_a, precipitation and altitude. The model detects the break point ET_a at an altitude of 758 meters. This altitude roughly corresponds to the breaking point from the relationship between evapotranspiration and precipitations (Figure 2 right). The DisALEXI model therefore determines that the break point between the limitation of evapotranspiration by precipitation and available energy is detected at altitude of 758 m at a precipitation value of 820 mm. The Soil Clim model detects the ET_a break point at an altitude of 685 m. This altitude does not correspond to the peak (break point) of evapotranspiration depending on precipitation (882 mm). The P/Q method does not detect the break point of ET_a depending on altitude and precipitation.

Because the positive growth response of Norway spruce is related to climatic conditions with enough precipitation in the Czech Republic (Kolář et al. 2017), the results of the DisALEXI model may support the independent findings of Krejza et al. (2021), suggesting that 900 m above sea level may be the current lower limit of the positive growth response of Norway spruce.

The results detect the differences of estimating of trends ET_a between DisALEXI, SoilClim models and the P/Q method. The spatial detection of ET_a in mountain areas is a challenge for available methods, because amount of the energy and water on the surface areas, is strongly dependent on the local weather and surface conditions, that may not sometimes be fully captured by the selected methods or models: For example, the disadvantage of P/Q method is uncertainties in groundwater flow and thus undetected losses in the catchments. The DisALEXI model has a large potential for application in mountains and sub-mountains areas, however the disadvantage is that the model is relatively limited by cloudy days and in temporal resolution by the overpass frequency of the polar satellites and thus the scarcity of high resolution thermal data (Castelli et al. 2018).

CONCLUSION

As we expected, the average annual precipitation increases with increasing altitude of catchments, while the average annual ET_o decreases with increasing altitude due to decreasing amount of available energy in the catchments. The three methods or models for estimating ET_a were analysed at small forest catchments areas and compared to average altitudes of catchments in the period (2001–2018). The indirect development of ET_a depending on altitudes, where ET_a is limited by precipitation in lower or mid-lower elevations, while ET_a is limited by lack of available energy in mid-mountains or mountains areas. This previously accepted hypothesis can be confirmed by DisALEXI model and SoilClim model. Moreover, these models identified the break point, that detects the point, below which ET_a is limited by precipitation and above which ET_a is limited by available energy. The DisALEXI model best captures the relationship between ET_a, precipitation and altitude. According to the DisALEXI model, the altitude breaking point is detected at a height of 758 m. The ET_a results of SoilClim model does not correspond to the precipitation. Given the climatic conditions of Norway spruce growth, this analysis can be useful in identifying suitable conditions for sustainable spruce management.

ACKNOWLEDGEMENTS

The research was financially supported by the SustES - Adaptation strategies for sustainable ecosystem services and food security under adverse environmental conditions (CZ.02.1.01/0.0/0.0/16_019/0000797).

REFERENCES

Allen, R.G. et al. 1998. Crop evapotranspiration-Guidelines for computing crop water requirements-FAO Irrigation and drainage paper 56 [Online]. FAO, Rome, 300(9): D05109.

Anderson, M.C. et al. 2003. Upscaling and downscaling - A regional view of the soil–plant–atmosphere continuum. Agronomy Journal [Online], 95(6): 1408–1423. Available at: https://doi.org/10.2134/agronj2003.1408. [2021-09-18].

Anderson, M.C. et al. 1997. A two-source time-integrated model for estimating surface fluxes using thermal infrared remote sensing. Remote sensing of environment [Online], 60(2): 195-216. Available at: https://doi.org/10.1016/S0034-4257(96)00215-5. [2021-09-18].

Castelli, M. et al. 2018. Two-source energy balance modeling of evapotranspiration in Alpine grasslands. Remote Sensing of Environment [Online], 209: 327–342. Available at: https://doi.org/10.1016/j.rse.2018.02.062. [2021-09-18].

Hlavinka, P. et al. 2011. Development and evaluation of the SoilClim model for water balance and soil climate estimates. Agricultural Water Management [Online], 98(8): 1249–1261. Available at: https://doi.org/10.1016/j.agwat.2011.03.011. [2021-09-18].

Kolář, T. et al. 2017. Temporal changes in the climate sensitivity of Norway spruce and European beech along an elevation gradient in Central Europe. Agricultural and Forest Meteorology [Online], 239: 24–33. Available at: https://doi.org/10.1016/j.agrformet.2017.02.028. [2021-09-18].

Krejza, J. et al. 2021. Evidence of climate-induced stress of Norway spruce along elevation gradient preceding the current dieback in Central Europe. Trees [Online], 35(1): 103–119. Available at: https://doi.org/10.1007/s00468-020-02022-6. [2021-09-18].

Lhotka, O. et al. 2018. Climate change scenarios of heat waves in Central Europe and their uncertainties. Theoretical and applied climatology [Online], 131(3): 1043–1054. https://doi.org/10.1007/s00704-016-2031-3. [2021-09-18].

Norman, J.M. et al. 2003. Remote sensing of surface energy fluxes at 101-m pixel resolutions. Water Resources Research [Online], 39(8). Available at: https://doi.org/10.1029/2002WR001775. [2021-09-18].

Norman, J.M. et al. 1995. Source approach for estimating soil and vegetation energy fluxes in observations of directional radiometric surface temperature. Agricultural and Forest Meteorology [Online], 77(3–4): 263–293. Available at: https://doi.org/10.1016/0168-1923(95)02265-Y. [2021-09-18].

Oulehle, F. et al. 2017. Recovery from acidification alters concentrations and fluxes of solutes from Czech catchments. Biogeochemistry [Online], 132.3: 251–272. Available at: https://doi.org/10.1007/s10533-017-0298-9. [2021-09-18].

Oulehle, F. et al. 2021. The GEOMON network of Czech catchments provides long-term insights into altered forest biogeochemistry: From acid atmospheric deposition to climate change. Hydrological Processes [Online], 35(5): e14204. Available at: https://doi.org/10.1002/hyp.14204. [2021-09-18].

Řehoř, J. et al. 2021. Effects of Climatic and Soil Data on Soil Drought Monitoring Based on Different Modelling Schemes. Atmosphere [Online], 12(7): 913. Available at: https://doi.org/10.3390/atmos12070913. [2021-09-18].

Štěpánek, P. et al. 2016. Projection of drought-inducing climate conditions in the Czech Republic according to Euro-CORDEX models. Climate Research [Online], 70(2–3): 179–193. Available at: https://doi.org/10.3354/cr01424. [2021-09-18].

Analysis of awareness of the implementation of agricultural production in Czech Republic

Richard Langer[1], Tamara Dryslova[2]
[1]Department of Animal Breeding
[2]Department of Agrosystems and Bioclimatology
Mendel University in Brno
Zemedelska 1, 613 00 Brno
CZECH REPUBLIC

richard.langer@mendelu.cz

Abstract: The aim of the work was to monitor the awareness of specific age groups in the implementation of agricultural production in the Czech Republic. The main topics were issues related to land, farming methods, primary crop production, animal production and economic aspects of the agricultural sector in relation to the awareness of respondents. For the intergenerational comparison of the monitored aspects, four age groups were created, whose answers were compared and evaluated with each other. Based on the respondents' answers, it was found that awareness of less complex questions that do not require prior knowledge is relatively good among respondents. Ignorance of agricultural production has manifested itself mainly in questions concerning farming methods, control bodies, the impact of cultivated crops on the soil or in connection with the cultivation of GMO crops. For these issues, the intergenerational impact was also relatively negligible. In the overall comparison, we can say that the younger group of respondents is more demanding when choosing food, especially the origin and quality of the product. Answers to questions about organic farming were also often far removed from the legislative requirements for the sector. This is especially true for the older group of respondents.

Key Words: agriculture, farming methods, problem aspects

INTRODUCTION

From time immemorial, man has looked at the origin of the food he consumes. In the past, he managed to procure a large part himself. Today, however, it is different, we buy food most often in retail chains and the origin of food can only be read on the packaging (Sedláková 2011). We can also find many articles on topics that interest us and may not be about food. However, many articles contain false information to make it attractive to readers (Albright 2017). The level of agriculture is such that it can provide us with enough safe food for all the inhabitants of our country (Nárt 2006). Like others, this area is subject to a number of controls. These are important not only for consumer or producer protection, but also for the environment. With the growing consumption of food, the volume of agricultural production also increased. Growing consumption along with the economy of threads produce more and more food from a smaller unit area. We need to realize that every system has its limits, which we must respect (Šarapatka et al. 2010). Today, we have a considerable amount of information about food that comes to us from various places. It is necessary to pay attention to the credibility of these sources, because it often happens that they are not based on empirical principles (Kopecký and Szotkowski 2019).

MATERIAL AND METHODS

The research part of the work was based on a questionnaire survey. The questionnaire, which was created for this purpose, aimed to collect information on public awareness of the soil, farming practices, crop and animal production and the overall economic situation in the agricultural sector with a focus on consumer information in the Czech Republic. The questionnaires were disseminated mainly through social networks, and in older age categories in printed form into the hands of the respondent. The questionnaire read a total of 34 questions related to agricultural production. A total of 304 responses were recorded from individual respondents, whose answers were considered complete to the mentioned

questionnaire. Respondents were divided into groups so that there was a noticeable intergenerational difference. They were groups up to 25 years, from 25 to 40 years, from 40 to 65 years and from 65 years onwards. The recorded answers were evaluated with regard to the valid legal regulations of the Czech Republic.

RESULTS AND DISCUSSION

In the section dealing with land, respondents mentioned, for example, the problems that farmers perceive in land use. The youngest age categories most often perceived water erosion, the older ones mostly the species composition of cultivated field crops. The problem of pesticide residues was perceived at least by the age group of 65 years. On the contrary, this group of respondents perceived the problems most significantly with fertilization and method of soil treatment. The most distinctive disproportion within the answers of individual age categories of respondents was monitored between the youngest group under 25 and the oldest group over 65. So, we can say that the generational influence is evident in this question.

Figure 1 Answers to question 3 What problems associated with the use of land by farmers for agricultural production, do you perceive as the main?

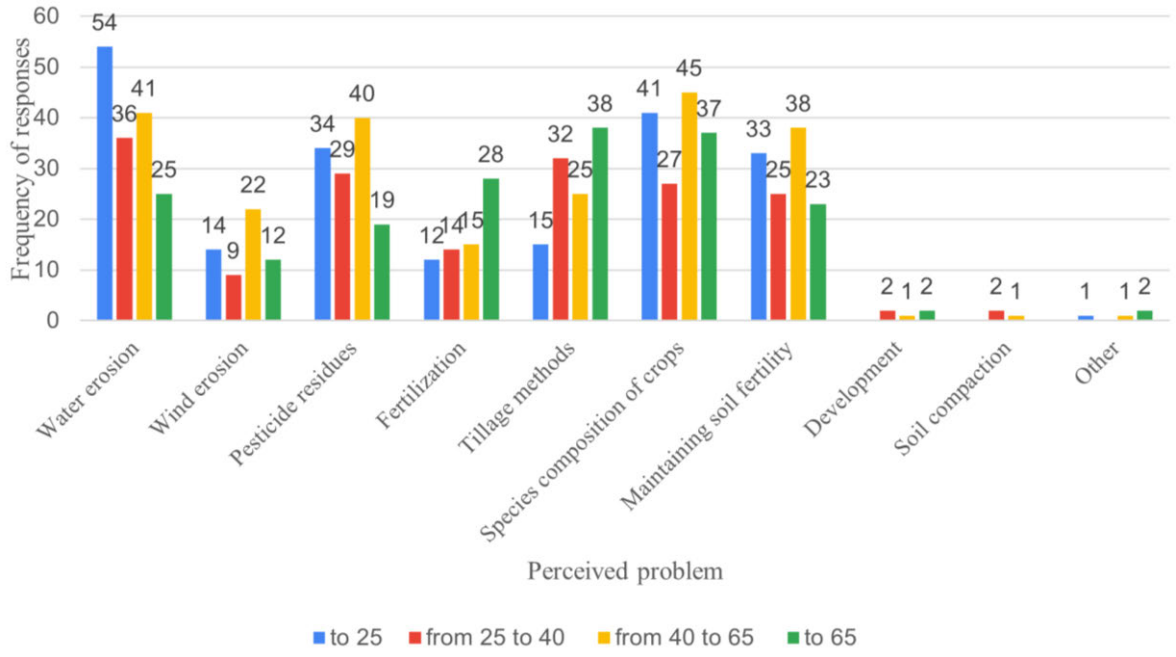

For questions about crop production, respondents rated oilseed rape for its effect on soil. They also dealt with the legislative requirements of erosively endangered soils or access to and availability of information regulating the application of pesticides. The question concerning the amount of genetically modified organisms in agriculture led to the finding that the vast majority of respondents believed that the percentage of cultivated GMO crops in our country ranges from 5 to 30% of total production. This answer was given by most respondents, regardless of age. As there was a representation of groups respondents across the answers relatively balanced, we can say that age does not affect the estimated percentage of GMO crops grown in the Czech Republic. This finding is completely at odds with (Trnková et al. 2019), which states that since 2017 it has not been in the Czech Republic no registered entity that would grow GMO crops. The largest share of GMO crops in the Czech Republic was in 2008. The total area on which GMO crops were grown was 8300 ha, is it 0.2% of arable land in the Czech Republic.

The block on livestock production revealed that respondents perceived the impact of declining livestock numbers after 1990, mainly in meat prices and the lack of self-sufficiency of these commodities on the domestic market. The perception of animal welfare has been shown to be good in all age groups. The question on the subject of cage farming, and in particular their ban with an impact on breeders, has made it clear that conditions for breeders should be set evenly throughout the EU.

Figure 2 Answers to question no. 18 Could you estimate whether GMO crops are grown in the Czech Republic and in what amount? (GMO = genetically modified organisms)

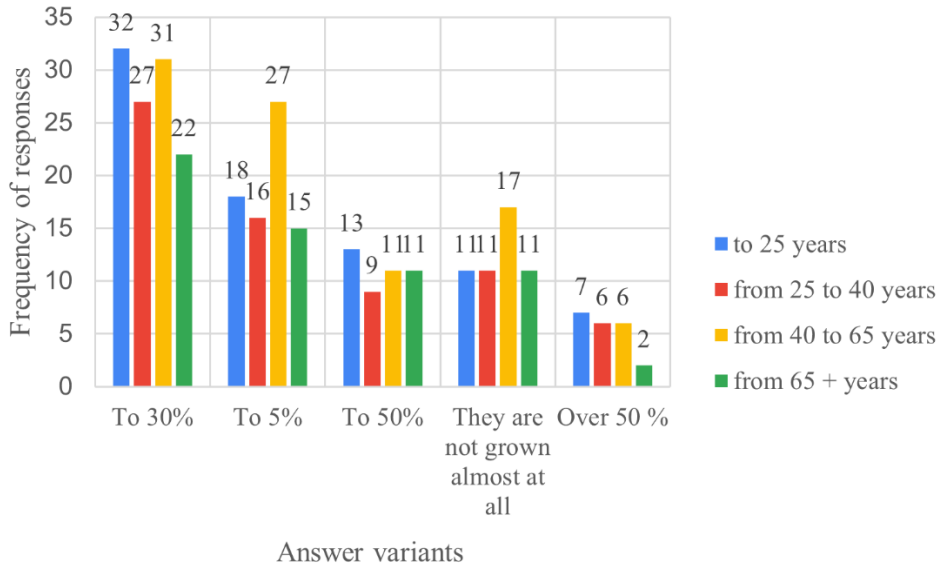

The most frequently chosen answer to the question Are you aware that according to the currently set rules, the ban on caged laying hens is disadvantageous for Czech breeders? Across the age range of respondents, the answer was "Yes, conditions should be set equally across the EU", which accounted for 56.1% of the total number of responses. From this conclusion we can conclude that the addressed group of respondents is aware of the problem and agrees with the setting of equivalent conditions for the whole EU.

Figure 3 Answers to question no. 24 Are you aware that according to the currently set rules, the ban on cage laying hens is disadvantageous for Czech breeders?

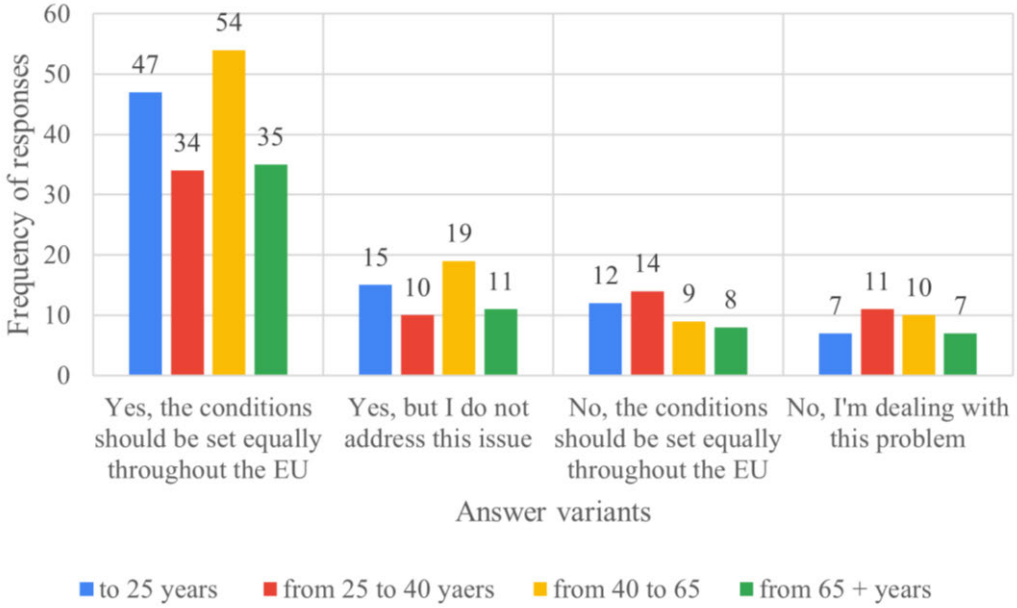

The last part of the work focused on the economy, consumers and information showed what preferences of individual age groups when buying and how they perceive organic farming. When buying food, the younger age categories follow the origin and composition more, while the older age categories follow the price of the product more. In the question of organic farming, it turned out that especially the older age groups perceived organic farming without distinction compared to the convention or even

as meaningless. Across all groups, it turned out that respondents did not perceive the current situation agriculture as sustainable. Today's agriculture is considered the most sustainable by the oldest age group.

Figure 4 Answers to question 31 The concept of agricultural sustainability is defined as: it does not limit the needs of the current generation and at the same time does not endanger the next generation. Do you think that is current agriculture sustainable by this definition?

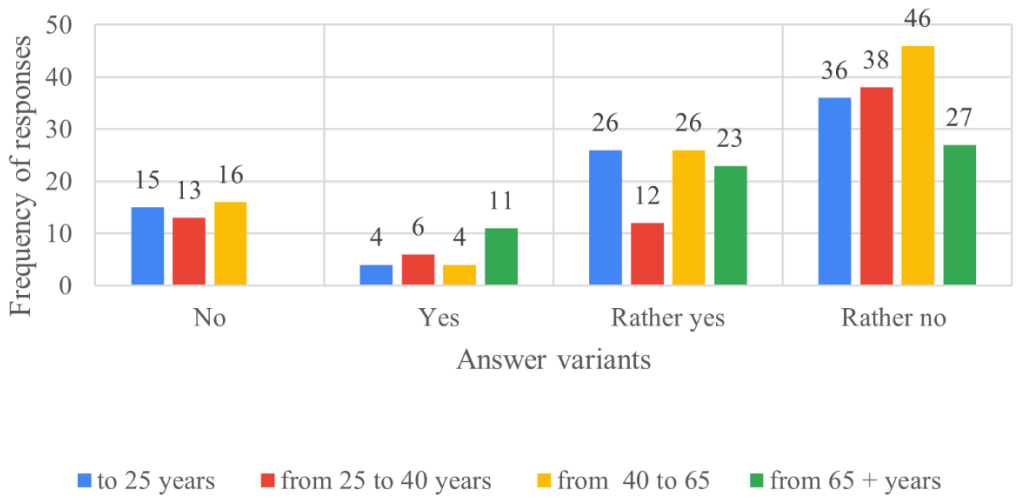

CONCLUSION

It follows from the above finding that the respondents answered the questions of the basic issues that do not require deeper knowledge in accordance with the professional literature. However, for more complex issues, they differed more and more from practice and professional literature. Regarding the issue of soil protection, the respondents perceived water erosion, pesticide residues and species composition of crops as the most fundamental problems. Regarding the question concerning the occurrence of GMO crops in the Czech Republic, most respondents, regardless of age, believed that they are grown in our country to a much greater extent than is actually the case. The planned ban on cage laying hens is perceived by respondents as a problem and they believe that conditions should be set equally throughout the EU. 56.1% answered this way respondents by age categories. The results also show that respondents perceived the current state of agriculture as poorly sustainable, considered the older age group to be the most sustainable. The age groups of the respondents played a relatively crucial role in some questions from the point of view of the issue. It was recommended for all age groups work in an acceptable way in education for the category.

REFERENCES

Albright, J. 2017. Welcome to the Era of Fake News. Media and Communication [Online], 5(2): 87–89. Available at: doi:10.17645/mac.v5i2.977. [2021-03-21].

Kopecký, K., Szotkowski, R. 2019. Dezinformace a Fake News. Olomouc: Univerzita Palackého v Olomouci.

Nárt, L. 2006. Rozvoj trvale neudržitelný. Praha Karolinum: Univerzita Krlova v Praze.

Sedláková, G. 2011. Charakteristika zemědělství. Adoc.pub. [Online]. Available at: https://adoc.pub/queue/charakteristika-zemdlstvi.html. [2020-03-15].

Šarapatka, B. et al. 2010. Agroekologie: východiska pro udržitelné zemědělské hospodaření. Olomouc: Bioinstitut.

Trnková, J. et al. 2019. Organizace a kontrola pěstování GM plodin v ČR. B.m.: Ministerstvo zemědělství.

Historical and contemporary endangered wetland species of the southeastern part of the Bohemian-Moravian Highlands

Jan Oulehla[1], Martin Jirousek[2,3], Milada Stastna[1]
[1]Department of Applied and Landscape Ecology
[2]Department of Plant Biology
Mendel University in Brno
Zemedelska 1, 613 00 Brno
[3]Department of Botany and Zoology
Masaryk University
Kotlarska 2, 611 37 Brno

jan.oulehla@mendelu.cz

Abstract: Wetlands are among the most endangered ecosystems in Central Europe. Therefore, large number of wetland organisms are endangered at the same time. Frequency of 94 red-list species were evaluated in the studied area of the south-eastern part of the Bohemian-Moravian Highlands. Historical data were taken from literature, botanical surveys, and databases. Recent occurrences are the result of the own field survey. Almost half of the evaluated species are recently considered as disappeared, or extinct in the area. *Carex lasiocarpa* and *Pedicularis palustris* are plants of high conservancy importance and at the same time belongs to recently missing species, with high probability of extinction, in the studied region. *Drosera rotundifolia* survives only at one locality. Prevailing decreasing number of species localities is associated mainly with the loss of suitable low-productive aquatic and wetland habitats. The study points to the continuing negative trend of reducing the occurrence of most of the evaluated endangered species and the related degradation of natural habitats in the selected area.

Key Words: degradation of habitats, nature protection, plant survey, species extinction

INTRODUCTION

The decrease of wetland species occurrence, in some cases also extinction of species, fully corresponds to the degradation and decrease in the number of wetland localities. Most endangered wetlands are included in the red list of endangered habitats of the Czech Republic. The main threats to endangered wetland habitats are abandonment of traditional management, nutrients inputs from surrounding agricultural land, invasion of non-native species and atmospheric deposition (Chytrý et al. 2019). Thanks to human activity, the processes of succession have been facilitated and accelerated, which leads to a significant transformation of wetland ecosystems towards terrestrial (Szabó et al. 2017).

The biggest problem in comparing the historical occurrence of endangered species (Grulich and Chobot 2017) with the current one is the lack of available historical data. Many current endangered species have been relatively abundant in the past, so they have not received much attention. In study area, there is availability of comparisons with historical data due to the extensive surveys of Filip Lysák in 1990–2010s (Lysák 2000). Therefore, assessment of the development of the number of localities with occurrences of endangered plant species is possible, contrary to the other areas. The main goal of this study is to compare the lists of endangered species associated with wetland habitats that have occurred in the past and in the present.

MATERIAL AND METHODS

South-eastern part of the Bohemian-Moravian Highlands is located in the middle of the Czech Republic, north of the town of Velké Meziříčí and is delimited by four mapping quadrates of the Central European Basic Area (CEBA): 6561,6562,6661,6662.

Occurrence data of endangered wetland species were obtained from Lysák's diploma thesis (Lysák 2000), available botanical literature and databases (Kaplan et al. 2015–2021, Čech et al. 2017, Wild 2019, AOPK 2021) and from our own field surveys. For each species, the number of localities

in which it occurs was counted separately for four time periods: historical records until 1995, records from 1996–2005, records from 2006–2015 and records from 2016 to the present. The possible extinction of the species is supplemented by the year of the last record of occurrence. For non-found species, we distinguish between *disappeared* and *extinct* depending on the probability whether the species can survive secretly in the locality or not.

An overview table was created for all endangered species. Species nomenclature is unified according to Kubát et al. (2002), the category of threat follow the red list of vascular plants of the Czech Republic (Grulich and Chobot 2017) and regional red list of vascular plants of the Vysočina (Čech et al. 2017). Czech red list categories as well as red list categories created for Vysočina region correspond approximately to the IUCN red list categories as follows: C1 = CR (critically endangered); C2 = EN (endangered); C3 = VU (vulnerable); C4 = NT (near threatened). The table also contains the numbers of species localities and various notes concerning occurrence or extinction of the species. The optimal habitat for each species was determined based on data from the PLADIAS database (Sádlo et al. 2007). In the case of a larger number of optimal habits, the one that best corresponds to the occurrence in the studied area was selected. Habitat names were taken from the habitat catalogue of the Czech Republic (Chytrý et al. 2010).

RESULTS AND DISCUSSION

Based on our study, a total of 94 wetland vascular plants are included in the list of endangered species (Table 1). Of this number, a total of 15 species are in the critically endangered category (C1), a total of 22 species are in the category of endangered species (C2), 28 species are in the category of vulnerable species (C3) and 29 species are in the category of species near threatened (C4).

The disappearance and probably extinction was found for 29 vascular plants. Only a part of the species evaluated as disappeared have higher probability to survive and next field resurveys are highly recommended, eg. *Hypericum humifusum*. The mentioned species was considered as extinct until 2010, after which it was not verified at all in the following years. Similarly, *Scirpus radicans, Potamogeton alpinus* or *Lysimachia thyrsiflora* were found even though they were considered extinct (Table 1). The extinction of species itself corresponds to the categories of endangerment. Figure 1 shows the preferential extinction of critically endangered species until 1995. In the last 25 years, relatively less endangered species of the Czech Republic have disappeared.

Figure 1 Extinct species by Red List threat category and period of negative finding

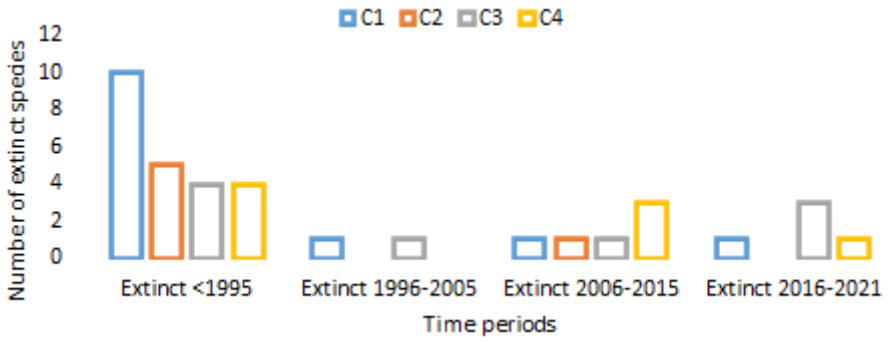

The decrease in the number of localities is evident in 31 species. On the other hand, the increase in the number of localities was also found. *Tephroseris crispa, Carex flava* and *Trientalis europaea* were recorded on higher number localities contrary to the historical periods. However, these data may be also affected by less attention given to the overall plant inventarisations in the history contrary to the recent.

For some species reduction of abundance in the last few decades is significant, which can be illustrated in the case of *Drosera rotundifolia*. Occurrence in history was common at majority of fen meadows. At nowadays there is only one last isolated locality. This phenomenon is similar for several species, which are very sensitive to changes in the habitat environment and become extinct in the event of a significant negative intervention, eg. abandonment of traditional management. For some species, survival in the locality is typical despite the negative intervention, which significantly changed

the natural conditions of the locality and for the species the locality became unsuitable. For example, *Dactylorhiza majalis, Menyanthes trifoliata* or *Comarum palustre* have been surviving for many years at degraded localities, then finally disappeared.

Table 1 List of endangered wetland plant species with number of localities of occurrence in time periods

Species	RLCZ	RLV	Number of sites				Condition
			<1995	1996–2005	2006–2015	2016–2021	
Arnoseris minima	C1	A	4	0	0	0	extinct (1905)
Carex dioica	C1	C1	1	0	0	0	uncertain, extinct (1911)
Centunculus minimus	C1	A	2	0	0	0	extinct (1905)
Dactylorhiza incarnata	C1	C1	1	0	0	0	extinct (1887)
Eleocharis quinqueflora	C1	C1	4	0	0	0	extinct (1935)
Juncus capitatus	C1	A	1	0	0	0	extinct (1947)
Nymphaea alba	C1	C1	2	0	0	0	extinct (1996)
Nymphaea candida	C1	C2	1	0	0	0	uncertain, extinct (1911)
Pedicularis palustris	C1	C1	2	2	1	0	disappeared (2014)
Pseudognaphalium luteoalbum	C1	A	3	0	0	0	extinct (1968)
Radiola linoides	C1	A	3	1	0	0	extinct (1997)
Sedum villosum	C1	A	7	0	0	0	extinct (1991)
Taraxacum paucilobum	C1	not	1	0	0	0	extinct (1898)
Taraxacum vindobonense	C1	not	-	8	3	3	decrease
Tillaea aquatica	C1	C2	2	10	4	2	fluctuations
Blysmus compressus	C2	C1	4	2	2	2	decrease
Bolboschoenus maritimus	C2	C3	5	3	3	2	decrease
Carex diandra	C2	C3	19	9	8	5	decrease
Carex elata	C2	C3	4	4	6	5	without change
Cnidium dubium	C2	C1	-	1	0	0	extinct (1999)
Elatine hexandra	C2	C2	2	0	0	0	uncertain, extinct (1935)
Eleocharis uniglumis	C2	C1	2	0	0	0	uncertain, extinct (1935)
Eriophorum latifolium	C2	C2	7	4	3	2	decrease
Gratiola officinalis	C2	C2	1	0	0	0	uncertain, extinct (1930)
Montia hallii	C2	C2	10	3	3	1	decrease
Myosotis discolor	C2	C4	-	-	3	3	without change
Ophioglossum vulgatum	C2	C1	-	4	4	3	decrease
Parnassia palustris	C2	C2	11	15	8	6	decrease
Pedicularis sylvatica	C2	C3	23	12	5	1	decrease
Pilosella lactucella	C2	C3	-	4	2	1	decrease
Pinus uncinata subsp.uliginosa	C2	C1	1	0	0	0	uncertain, extinct (1947)
Potamogeton alpinus	C2	C2	5	0	0	1	decrease
Spergularia echinosperma	C2	C2	3	3	10	5	increase
Thalictrum flavum	C2	C1	-	2	2	2	non native, without change
Trifolium spadiceum	C2	C3	15	4	4	1	decrease
Triglochin palustre	C2	C2	5	2	1	1	decrease
Utricularia minor	C2	C2	3	1	0	0	uncertain, extinct (1947)
Potamogeton acutifolius	C3	C1	11	0	0	0	uncertain, extinct (1935)

Calla palustris	C3	C3	-	1	2	2	increase
Carex curvata	C3	C2	-	-	-	1	uncertain
Carex distans	C3	C1	-	2	1	1	decrease
Carex lasiocarpa	C3	C3	-	1	1	0	extinct (2006)
Coleanthus subtilis	C3	C3	15	33	27	6	fluctuations
Dactylorhiza majalis	C3	C3	ab.	49	31	24	decrease
Drosera rotundifolia	C3	C3	17	1	1	1	decrease
Elatine hydropiper	C3	C3	6	2	1	0	extinct (1997)
Elatine triandra	C3	C3	7	37	14	8	fluctuations
Hypericum humifusum	C3	C3	3	0	1	0	disappeared (2010)
Iris sibirica	C3	C1	-	-	-	1	unoriginal
Isolepis setacea	C3	C3	8	4	6	4	fluctuations
Juncus alpinoarticulatus	C3	C1	2	1	1	0	disappeared (2007)
Laserpitium prutenicum	C3	C2	1	0	0	0	extinct (1910)
Leersia oryzoides	C3	C3	4	3	4	4	without change
Leucojum vernum	C3	C3	1	0	0	0	extinct (1932)
Lysimachia thyrsiflora	C3	C2	2	5	3	3	decrease
Menyanthes trifoliata	C3	C3	28	13	9	7	decrease
Platanthera bifolia	C3	C3	-	10	3	3	decrease
Poa remota	C3	C4	1	4	4	4	without change
Potamogeton lucens	C3	C2	5	1	0	0	extinct (1935)
Potamogeton obtusifolius	C3	C3	-	4	4	1	decrease
Potamogeton trichoides	C3	C3	7	0	4	3	decrease
Salix rosmarinifolia	C3	C3	6	8	5	4	decrease
Scirpus radicans	C3	C3	7	1	3	1	decrease
Soldanella montana	C3	C3	2	3	3	3	without change
Thelypteris palustris	C3	C1	1	0	0	0	extinct (1924)
Carex bohemica	C4	C4	11	45	48	42	fluctuations, increase
Carex buekii	C4	C3	-	1	0	0	disappeared (2000)
Carex cespitosa	C4	C3	3	2	1	0	disappeared (2011)
Carex disticha	C4	C3	1	0	0	0	extinct (1907)
Carex flava	C4	not	1	2	4	5	increase
Carex hartmanii	C4	C4	-	2	2	0	disappeared (2010)
Carex paniculata	C4	C2	-	1	0	1	disappeared (2004)
Carex pseudocyperus	C4	C3	-	1	2	1	little fluctuations
Comarum palustre	C4	C4	ab.	49	34	18	decrease
Eleocharis mamillata	C4	C4	1	9	6	3	fluctuations
Eleocharis ovata	C4	C4	11	44	27	16	decrease
Epilobium palustre	C4	C4	21	14	29	12	fluctuations or decrease
Galium boreale	C4	C3	1	0	0	0	extinct (1910)
Limosella aquatica	C4	C3	10	8	26	9	fluctuations
Listera ovata	C4	C3	-	5	3	3	decrease
Myosotis caespitosa	C4	C4	-	6	16	8	fluctuations
Salix pentandra	C4	C4	-	10	6	6	decrease
Scorzonera humilis	C4	C4	2	0	0	0	extinct (1911)
Scrophularia umbrosa	C4	C2	ab.	0	0	0	extinct (1892)
Schoenoplectus lacustris	C4	C3	ab.	5	3	1	decrease

Taraxacum nordstedtii	C4	C3	5	14	6	4	fluctuations
Tephroseris crispa	C4	C4	1	29	33	22	increase
Trientalis europaea	C4	C3	2	7	15	13	increase
Utricularia australis	C4	C3	4	9	9	5	decrease
Valeriana dioica	C4	C4	ab.	63	38	31	decrease
Valeriana excelsa	C4	not	-	1	7	5	decrease
Veronica scutellata	C4	C4	3	28	29	28	increase
Cirsium heterophyllum	not	C4	2	5	3	2	decrease
Cirsium rivulare	not	C4	2	6	3	3	little fluctuations

Explanatory notes: "RL CZ" threat category from Red List of vascular plants of Czech republic, "RL V" threat category from Red List of vascular plants of Vysočina region, "extinct" certain extinction, long-term missing and recent survival very unlikely, "disappeared" missing, recent extinction with high probability, but contrary to the previous point the plant species is less conspicuous and few individuals can survive hidden in vegetation or seed bank and yet can be found again in case of more suitable conditions or after restoration activity, "uncertain" species with problematic determination and uncertain historical occurrence, "non-native" planted or unintentional dispersion from near culture, "ab." abundant, "-"no record, "0" no historical record, or no confirmation during field survey

The largest disappearance or extinction of species is evident in the aquatic macrophyte vegetation of oligotrophic waters and from fens and fen meadows. As the area is struggling with the supply of nutrients from agricultural activities and intensive fish production, the habitat is being lost together with the related specific flora. Fens in the area are rare and degraded due to drainage. In the case of alluvial meadows and transitional mires, no threatened plant species occurred here due to the significant degradation of these habitats.

Figure 2 Habitats of occurrence of recorded species. Color-coded are species that have become extinct in a particular habitat. Recent occurrences of species are shown in grey.

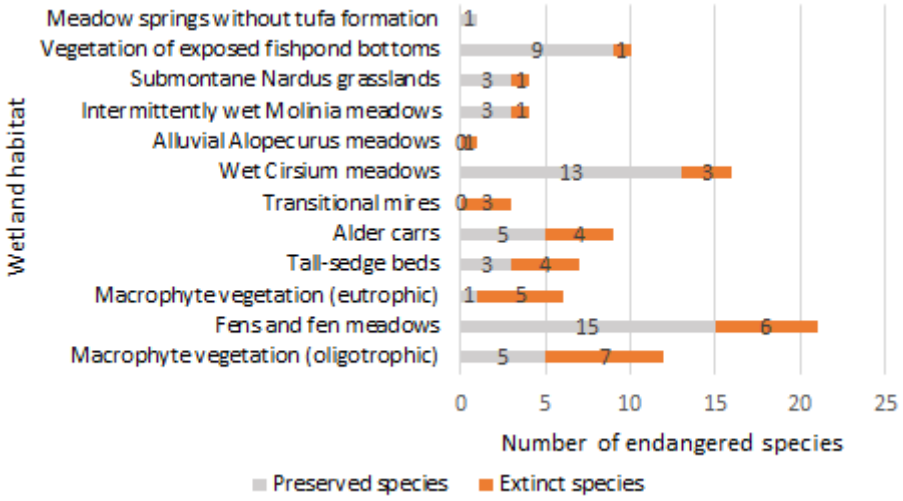

In long-term studies of wetland habitats, changes of vegetation have been recorded, characterized mainly by a decrease in the abundance of many species. Today's species composition is not in balance with environmental conditions and therefore the extinction of some species can be expected (Koch and Jurasinski 2014). Current surveys show extinction preferentially in small populations or small localities, while larger ones remain (Deane et al. 2017). In our studied area there are mostly smaller localities of wetland habitats.

For most species, the main reason for extinction is the loss of habitat, or environmental condition change. Global influences such as climate change may be the reason for population decline of some sensitive species. For example, we recorded a significant decrease in the population of *Pedicularis sylvatica* after the dry period between years 2014–2019. The related species *Pedicularis longiflora* is expected to decline in China due to climate change (Cao et al. 2020).

The data contained in the PLADIAS database are less numerous than the data in the nature protection finding database of the Czech Republic (AOPK 2021). Without own field research, these

databases would be unusable due to an abundance of less studied species. As a result, it is recommended to implement the identified data more into these databases.

CONCLUSION

A total of 94 endangered species were recorded from the territory during last century. Of this number, a total of 36 are recently extinct with high probability. Due to the ongoing degradation of wetland habitats, extinction is expected in other species that will either be directly affected or become extinct based on extinction debt. In the studied area, there are only several species that are not classified as endangered, but there is a threat of their occurrence. To prevent the extinction of species, it is necessary to maintain well-care management, which should be restored in neglected localities. At the same time, it is appropriate to reduce intensive agricultural production and intensive fish production. Suitable variants for the restoration of quality natural habitats include, topsoil removal, the removal of drainage and the elimination of fertilizer input.

ACKNOWLEDGEMENTS

We would like to thank Filip Lysák who provided us useful information on selected localities and plant species. Participation of M.J. was partly supported by the Czech Science Foundation (project GJ19-20530Y).

REFERENCES

AOPK ČR. 2021. Nature Conservancy Species Occurrence Finding Data Database. [Online]. Praha. Agentura ochrany přírody a krajiny ČR. Available at: http://www.portal.nature.cz. [2021-9-6].

Cao, B. et al. 2020. Wetlands rise and fall: Six endangered wetland species showed different patterns of habitat shift under future climate change. Science of the Total Environment 731, 138518.

Chytrý, M. et al. 2010. Habitat Catalogue of the Czech Republic. 2nd ed., Praha: Agentura ochrany přírody a krajiny ČR.

Chytrý, M. et al. 2019. Red list of habitats of the Czech Republic. Ecological Indicators 106, 105446.

Čech, L. et al. 2017. Vascular plants of Vysočina region. [Online]. Available at: http://www.prirodavysociny.cz/. [2021-09-06].

Deane, D.C. et al. 2017. Future extinction risk of wetland plants is higher from individual patch loss than total area reduction. Biological Conservation, 209: 27–33.

Grulich, V., Chobot, K. 2017. Red List of vascular plants of the Czech Republic. Příroda, 35: 75–132.

Kaplan, Z. et al. 2015–2021. Distributions of vascular plants in the Czech Republic. Part 1–10. Preslia, electronic appendices. [Online]. Available at: http://www.preslia.cz/maps.html. [2021-09-06].

Koch, M., Jurasinski, G. 2014. Four decades of vegetation development in a percolation mire complex following intensive drainage and abandonment. Plant Ecology and Diversity, 8: 49–60.

Kubát, K. et al. 2002. Klíč ke květeně České republiky. Academia, Praha.

Lysák, F. 2000. Ohrožená mokřadní květena Velkomeziříčska a její ochrana. Diploma thesis, Univerzita Palackého v Olomouci.

PLADIAS. 2018. Database of the Czech flora and vegetation. [Online]. Available at: http://www.pladias.cz/. [2020-09-17].

Sádlo, J. et al. 2007. Regional species pools of vascular plants in habitats of the Czech Republic. Preslia 79: 303–321.

Szabó, P. et al. 2017. Trends and events through seven centuries: the history of a wetland landscape in the Czech Republic, Regional Environmental Change, 17 (2): 501–514

Wild, J. et al. 2019. Plant distribution data for the Czech Republic integrated in the Pladias database. Preslia, 91: 1–24

Variation of glomalin content in the Czech soils and the relationships to the chemical soil characteristics and climatic regions

Vojtech Polach[1,2], Sneha Patra[1], Karel Klem[1,2]
[1]CzechGlobe – Global Change Research Institute
Czech Academy of Sciences
Belidla 986/4a, 603 00 Brno
[2]Department of Agrochemistry, Soil Science, Microbiology and Plant Nutrition
Mendel University in Brno
Zemedelska 1665/1, 613 00 Brno
CZECH REPUBLIC

vojta.polach@seznam.cz

Abstract: Glomalin is being investigated as a substance that improves soil quality, the resistance of soil aggregates and play a role in carbon sequestration. This study is the first nationwide survey of the glomalin content in the soil. Soil samples were collected from 181 locations in the Czech Republic to describe the variability of glomalin content in the soils of the Czech Republic and its dependence on soil chemical properties and climatic area. Sodium citrate buffer was used to extract easily extractable glomalin (EEG), and the glomalin concentration was determined spectrophotometrically. The soil glomalin content correlates most with the ratio of humic and fulvic acids. Moreover, the interrelation between glomalin content and climatic regions was also observed. The content of glomalin decreases from the warmest regions to the coldest. We also compared the glomalin content among different soil types groups and found out that the lowest glomalin content was found in Entic Podzols and Gleysols. On the contrary, the highest glomalin content was found in Vertisols, Phaeozems and Luvisols.

Keywords: glomalin, humic and hulvic acids, climatic regions, soil types

INTRODUCTION

With the coming of global change, it is necessary to understand better the processes that take place in nature, including the processes in the soil. One of the substances affecting soil properties is glomalin. Sara Wright and colleagues first described glomalin as a highly thermostable glycoprotein, probably produced by arbuscular mycorrhizal fungi (Wright et al. 1996, Wright and Upadhyaya 1996). The glomalin content in the soil also has a positive correlation with the stability of aggregates (Singh et al. 2018), and it contributes to carbon sequestration in soil (Wang et al. 2020).

This present research was carried out to describe the variability of the glomalin content in different regions of the Czech Republic and to find out whether it has codependency on soil chemical properties, soil type, and climatic area.

MATERIAL AND METHODS

Sampling spots were selected to cover high diversity of soil types and climatic regions (according to BPEJ classification). Soil samples for research were sampled at 181 locations in the Czech Republic. At sites with high topographic variability we sampled two contrasting spots (mostly from upper and bottom part of the field) to include also the effect of soil erosion. Figure 1 shows a map of sampling locations. A spade was used for soil sampling of topsoil in the field.

The “easily extractable glomalin” method – EEG according to (Wright and Upadhyaya 1998) later adapted (Knorr et al. 2003, Steinberg and Rillig 2003) was used to extract glomalin. For extraction of each soil sample, 1 gram of air-dried, homogenized soil was mixed thoroughly with 8 ml of freshly prepared 20 mM sodium citrate extraction buffer pH 7.0. Samples were autoclaved in Tuttnauer 2840 EL at 121 °C for 30 minutes and centrifuged immediately in Eppendorf centrifuge 5810R at RCF 2683

for 20 minutes. The supernatant was stored separately at 4 °C, and this procedure was repeated until the supernatant became straw in color (Nichols and Wright 2006, Wright et al. 2006). To achieve this color, we performed seven to ten extraction cycles depending on the soil samples. The glomalin content of collected supernatant was determined in Specord 250 PLUS spectrophotometer using the commercially available Bradford assay (Bio-Rad protein assay) where the Bovine serum albumin (Protein Standard II #5000007, Bio-Rad.com) was used as the standard protein.

Redundancy analysis (RDA) and the corresponding ordination diagram of RDA were conducted in the software CANOCO 5 (Šmilauer and Lepš 2014).

Figure 1 Map of sampling points

RESULTS

The glomalin content

The glomalin content extracted from 181 soil samples varies to a large extent. Low glomalin content (1–4.99 mg/g soil) was found in 54 soil samples, moderate amount (5–9.99 mg/g soil) was found in 103 soil samples, high content (10–14.99 mg/g soil) in 21 samples and very high glomalin content (15≤ mg/g soil) was found in 3 soil samples.

Relation of the glomalin content to other soil properties

We tested the association of the glomalin content in soil with the chemical soil properties by using multivariate redundancy analysis (RDA). According to this, the glomalin content is associated with other chemical soil properties (Figure 2). The highest association of the glomalin content was found with the ratio between humic and fulvic acids (HA/FA) and the total nitrogen content in soil (Nt). The rectangular position of glomalin content to Cox, CEC, Ca and P content means that these parameters are not affecting glomalin content at all. It is also evident that between P content on one side and CEC, Cox and Ca content exists strong negative relationships.

The highest correlation was found for HA/FA ratio (Figure 3). The significant ($p<0.01$) correlation coefficient for the relationship between the glomalin content and the HA/FA ratio means that HA/FA is a potentially good indicator of glomalin content even when evaluated within the set of soil samples with a high diversity of soil types.

The correlation analysis shows that besides a relatively high correlation coefficient to HA/FA and Nt, there is also a positive correlation to Mg and H+ (Table 1).

Table 1 Correlation coefficients of the glomalin content and other soil properties

	Glomalin	Nt	Cox	Ca	K	Mg	P	H+	CEC	HA/FA
Glomalin	1	0.351	-0.02	-0.217	0.105	0.262	-0.026	0.283	-0.174	0.515

As the soil was sampled to cover high diversity of soil types and climatic regions (according to BPEJ classification), the effect of both factors on the glomalin content was also tested. The impact

of climatic regions is evident, indicating a general trend in the decline of the glomalin content with decreasing mean annual temperature (glomalin decline from warm to the cold area) (Figure 4).

Figure 2 RDA analysis of the glomalin content and other soil properties

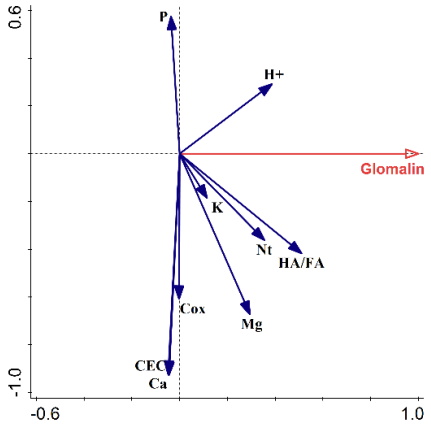

Figure 3 Relation of the glomalin content and humic to fulvic acids ratio

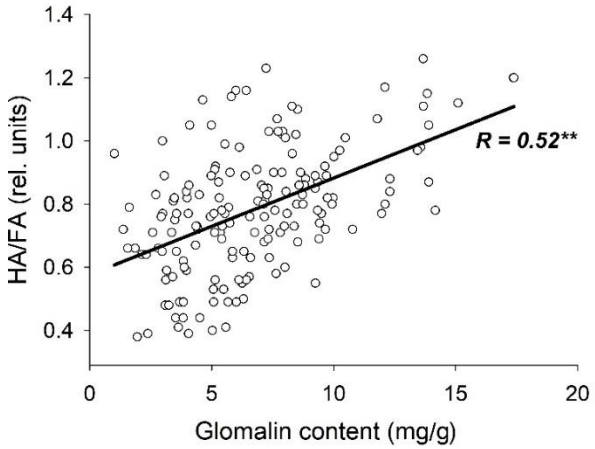

Figure 4 Relation of the glomalin content to climatic regions

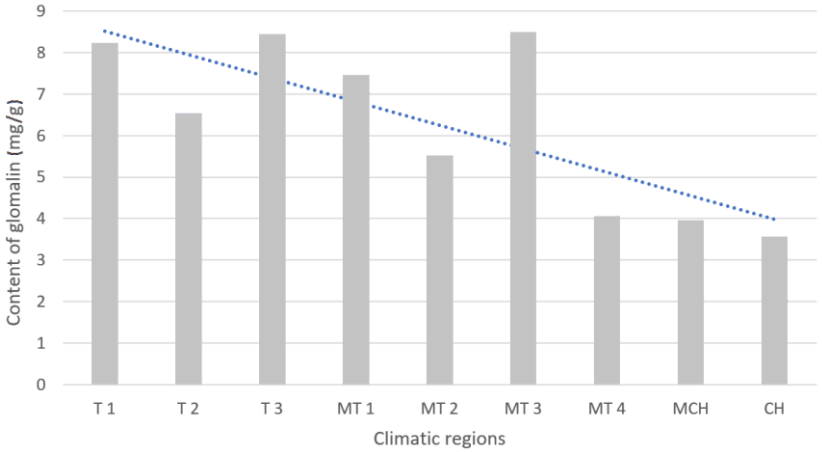

Legend: T 1 – Warm region 1, T 2 – warm region 2, T 3 – warm region 3, MT 1 – moderate warm region 1, MT 2 – moderate warm region 2, MT 3 – moderate warm region 3, MT 4 – moderate warm region 4, MCH – Moderate cold region, CH – Cold region

Figure 5 The glomalin content in different soil types groups

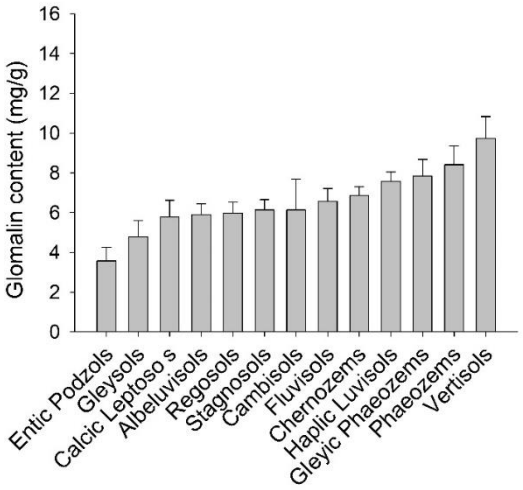

Since we sampled soils of various diversity, we were able to identify different soil types from BPEJ code. Figure 5 compares soil types groups and the glomalin content where the lowest glomalin content was found in Entic Podzols and Gleysols. On the contrary, the highest glomalin content was found in Vertisols, Phaeozems and Luvisols.

DISSCUSION

Soil aggregation and the related aggregate stability are based on complex processes largely dependent on soil microorganisms producing glue glycoprotein complexes that hold soil particles together. Such functions are mainly found in arbuscular mycorrhizal fungi (AMF), which produce glomalin, and carbon-containing glycoprotein that protects AMF from drying out. Soil aggregation and aggregate stability, which are strongly dependent on glomalin accumulation, have significant consequences for soil carbon sequestration (Six et al. 2000). AMF represent an essential component of soil fungal communities in agricultural soils, accounting for about 30% of whole microbial biomass (Olsson et al. 1999). The occurrence of AMF is strongly affected by management practices, such as soil cultivation, fertilizer use and pesticide application (Helgason et al. 1998). Recently the effect of soil type on glomalin accumulation in soil was studied by Gałązka et al. (2020). They found that the highest glomalin content was found in soil types belonging to the group of very good and good soil physical quality also characterized by high biological activity. Such groups were represented by Gleyic Phaeozem Rendzic Leptosol and Fluvic Cambisol. Similarly, in our study, the highest glomalin contents were found generally in vertisols, phaeozems and luvisols.

Humic substances, such as humic acids and fulvic acids play a vital role in soil fertility and plant nutrition. Plants grown on soils that contain adequate humin, humic acids, and fulvic acids are less subject to stress, are healthier and produce higher yields. The humification index, HA/FA for composts and soils ranges from >1.0 to 5.0. The higher HA/FA ratio of compost amended soils the more accumulation of slowly decomposable organic substances in soils (Stevenson 1982, Inbar et al. 1990) and hence soil organic carbon would deplete at a slower rate and be maintained over a longer period (Zinati et al. 2001).

As the glomalin content is correlated to the ratio of humic and fulvic acid, we can conclude that glomalin plays its role in the soil fertility.

Wang et al. (2017) found a reduction of the glomalin content with increasing temperature, which is contrary to our results.

CONCLUSION

Analyzes of 181 soil samples across the Czech Republic show that the glomalin content in the soil correlates most with the ratio of humic and fulvic acids. A relationship between glomalin content in soil and climatic regions was also found. The glomalin content decreases from the warmest regions to the coldest. Comparison of the content of glomalin among different soil types groups showed that the lowest glomalin content was found in Entic Podzols and Gleysols. On the contrary, the highest glomalin content was found in Vertisols, Phaeozems and Luvisols.

ACKNOWLEDGEMENTS

We acknowledge the support by SustES – Adaptation strategies for sustainable ecosystem services and food security under adverse environmental conditions (CZ.02.1.01/0.0/0.0/16_019/0000797).

The research was supported by the Department of Agrochemistry, Soil Science, Microbiology and Plant Nutrition, Mendel University in Brno.

REFERENCES

Gałązka, A. et al. 2020. Fungal Community, Metabolic Diversity, and Glomalin-Related Soil Proteins (GRSP) Content in Soil Contaminated With Crude Oil After Long-Term Natural Bioremediation. Frontiers in Microbioly, 11: 1–17.

Helgason, T. et al. 1998. Ploughing up the wood-wide web. Nature, 394(6692): 431–431.

Inbar, Y. et al. 1990. Humic substances formed during the composting of organic matter. Soil Science Society of America Journal, 54(5): 1316–1323.

Knorr, M.A. et al. 2003. Glomalin content of forest soils in relation to fire frequency and landscape position. Mycorrhiza, 13(4): 205–210.

Nichols, K.A., Wright, S.F. 2006. Carbon and nitrogen in operationally defined soil organic matter pools. Biology and Fertility of Soils, 43: 215–220.

Olsson, P. A. et al. 1999. Estimation of the biomass of arbuscular mycorrhizal fungi in a linseed field. Soil Biology and Biochemistry, 31(13): 1879–1887.

Singh, G. et al. 2018. Crop rotation and residue management effects on soil enzyme activities, glomalin and aggregate stability under zero tillage in the Indo-Gangetic Plains. Soil and Tillage Research, 184: 291–300.

Six, J. et al. 2000. Soil macroaggregate turnover and microaggregate formation: a mechanism for C sequestration under no-tillage agriculture. Soil Biology and Biochemistry, 32(14): 2099–2103.

Steinberg, P.D., Rillig, M.C. 2003. Differential decomposition of arbuscular mycorrhizal fungal hyphae and glomalin. Soil Biology & Biochemistry, 35(1): 191–194.

Stevenson, F.J. 1982. Humus chemistry: Genesis, composition, reactions. 1. ed., New York: John Wiley & Sons.

Šmilauer, P. Lepš, J. 2014. Multivariate Analysis of Ecological Data using CANOCO 5. 2nd ed., Cambridge: University Press.

Wang, W. et al. 2017. Glomalin contributed more to carbon, nutrients in deeper soils, and differently associated with climates and soil properties in vertical profiles. Scientific Reports, 7(1): 1–13.

Wang, Q. et al. 2020. Urbanization led to a decline in glomalin-soil-carbon sequestration and responsible factors examination in Changchun, Northeastern China. Urban Forestry & Urban Greening, 48: 126506.

Wright, S.F., Upadhyaya, A. 1996. Extraction of an abundant and unusual protein from soil and comparison with hyphal protein of arbuscular mycorrhizal fungi. Soil Science, 161(9): 575–586.

Wright, S.F., Upadhyahya, A. 1998. A survey of soils for aggregate stability and glomalin, a glycoprotein produced by hyphae of arbuscular mycorrhizal fungi. Plant and Soil, 198: 97–107.

Wright, S.F. et al. 1996. Time-course study and partial characterization of a protein on hyphae of arbuscular mycorrhizal fungi during active colonization of roots. Plant and Soil, 181: 193–203.

Wright, S.F. et al. 2006. Comparison of efficacy of three extractants to solubilize glomalin on hyphae and in soil. Chemosphere, 64(7): 1219–1224.

Zinati, G.M. et al. 2001. Utilization of Compost Increases Organic Carbon And Its Humin, Humic and Fulvic Acid Fractions In Calcareous Soil. Compost Science & Utilization, 9(2): 156–162.

Determining the phytotoxicity of rubber granulate from waste tires

Marketa Sourkova, Dana Adamcova
Department of Applied and Landscape Ecology
Mendel University in Brno
Zemedelska 1, 613 00 Brno
CZECH REPUBLIC

xsourkov@mendelu.cz

Abstract: The annually increasing global production of tires ranges around 1 billion and the number of waste tires is growing too. A question comes to the fore how to handle the waste to prevent environmental risks. The most advanced recycling facilities can process waste tires by sophisticated methods leading to their further use. One of products is a so-called rubber granulate which enjoys great interest of gardeners who use it instead organic mulch. In relation with this research, phytotoxicity of rubber granulate made from waste tires was studied in laboratory conditions using a test kit (Phytotoxkit^{TM}) for the determination of inhibitory/stimulating effect. The testing was made on the reference soil and tested seeds were the seeds of white mustard (*Sinapis alba* L). The granulate was applied onto the soil at rates of 5%, 10%, 25%, 50% and 75%. Research results demonstrated the inhibition of *Sinapis alba* L. seeds already from the rate of 5%, i.e. 6.50%. In the other rates, the inhibition ranged between 26.37% and 62.36%. The granulate is therefore considered phytotoxic and should not be used on the soil.

Key Words: white mustard, reference mixture soil, Phytotoxkit^{TM}, mulch, environmental risks

INTRODUCTION

At the moment when a tire is at the end of its service life, it becomes waste which has to be handled appropriately (Llompart et al. 2013, Birkholz et al. 2012). In the past, waste tires were disposed in landfills without any use. However, they captured methane due to their large volume, which caused upward pressure and subsequent damage to the sealing of landfills that was to prevent substances from leaking into the environment (Price and Smith 2006). Waste tires are valorized for energy, namely in cement works as a replacement fuel for brown coal which has a calorific value three times lower than tires (Kizlink 2014, Kuraš 2014). Apart from that, tires can be converted into valuable products (active coal, fuel) and energy source by means of pyrolysis (Sathiskumar and Karthikeyan 2019, Ramos et al. 2011). Waste tires can be also used as gravel or as admixture to asphalt roadbeds where they improve adhesion and considerably reduce traffic noisiness (Kuraš 2014, Kumaran et al. 2008, Cao 2007).

Waste tires are currently increasingly used for recycling. The produced granulate is most frequently utilized as rubber mulch in gardens, non-slip material of filling for artificial turfs. Its use is still popular for the floor surface of fitness centers, sports grounds and children's playgrounds (Llompart et al. 2013, Birkholz et al. 2012, Li et al. 2010). Although some studies claim the tires to be inert and non-toxic (Kizlink 2014, Nelson et al. 1994, Schnick et al. 1982), it is already known today that they contain heavy metals (arsenic, cadmium, chromium, lead and zinc), polycyclic aromatic hydrocarbons and other toxic additives (Šourková et al. 2021, Wink and Dave 2005). Tire consists of three basic components: rubber polymers (ca 50%), soot (ca 28%) and softeners (ca 18%). Other additives are anti-degrading agents, activators, accelerators and vulcanizing agents (Šourková et al. 2021, Wink and Dave 2005). In this sense, it is important to monitor impacts of rubber granulate on the environment and human health.

Tests of phytotoxicity were conducted to determine the effect of rubber granulate made from waste tires. Contaminants in the rubber granulate represent environmental risks and the assessment of their impact on the environment is therefore very important.

The goal of this study was to determine the phytotoxicity rate of rubber granulate from waste tires in laboratory conditions using the Phytotoxkit™ testing kit.

MATERIAL AND METHODS

Phytotoxicity of rubber granulate from waste tires with the use of micro-biotests

The fraction of rubber granulate tested in our study was 1–3 mm and the granulate was produced of rubber for general use (SBR) by the technology of crushing and sowing. Rubber granulate has been recently ever more used as a replacement of organic mulch as it does not attract insects and is almost indecomposable. Nevertheless, harmful substances can gradually be released from the granulate into the soil and plants despite all these advantages. The goal of this study was to determine the rate of its phytotoxicity.

In accordance with the Phytotoxkit™ methodology, the phytotoxicity of rubber granulate was tested in combination with the seeds of white mustard (*Sinapis alba* L.) at rates 5%, 10%, 25%, 50% and 75%. A mixture of reference (OECD) soil certified for the tests of phytotoxicity was applied on the testing Phytotoxkit in combination with distilled water and the determined rate of rubber granulate from waste tires. A control sample was OECD soil (85% of silica sand, 10% of kaolin clay, 5% of peat and $CaCO_3$) prepared with distilled water. Ten seeds of *Sinapis alba* L. were placed in a row on the filter paper. Each rate of rubber granulate was given three repetitions. A summary of phytotoxicity tests is presented in Table 1. The prepared sample container was sealed, installed in a holder in vertical position and incubated for 72 hours in the Ecocell dryer without light access at a controlled temperature of 23±1 °C. After the lapse of the set-up time, partial lengths of individual roots of *Sinapis alba* L. were measured by means of Image Tool 3.0 for Windows, and the percentage of plant growth inhibition/stimulation (IR) was calculated from the following equation (Šourková et al. 2021, Vaverková et al. 2019) (1):

$$IR\ (\%) = \frac{(L_C - L_S)}{L_C} \times 100 \qquad (1)$$

where L_C is an average value of plant root length in the sample without the rubber granulate (mm) and L_S is an average value of plant root length in the sample with the rubber granulate (mm).

The resulting value is considered growth inhibiting when IR is >0 or growth stimulating when IR is <0. A scheme of the experiment is presented in Figure 1.

Figure 1 Phytotoxicity of rubber granulate, Brno, Czech Republic, 2021

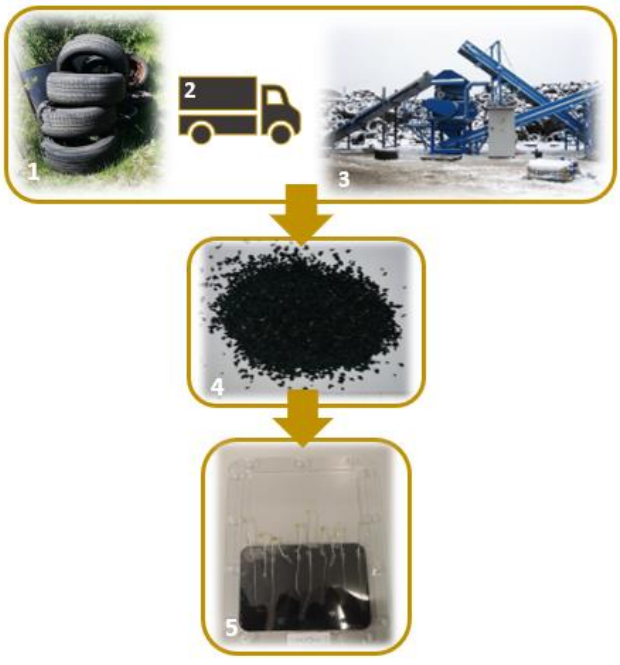

Legend: 1 – Waste tires; 2 – Transport to the recycling line; 3 – Tire recycling line; 4 – Granulate from waste tires; 5 – Phytotoxicity test

Table 1 Phytotoxicity tests and their labelling

Designation	Addition of granulate from tires	Number of repetition
Control	-	3×
1	5%	3×
2	10%	3×
3	25%	3×
4	50%	3×
5	75%	3×

Legend: Control – control sample, tests without granulate, 3 replicates; 1 – tests with 5% granulate, 3 replicates; 2 – tests with 10% granulate, 3 replicates; 3 – tests with 25% granulate, 3 replicates; 3 – tests with 50% granulate, 3 replicates; 4 – tests with 75% granulate, 3 replicates

RESULTS AND DISCUSSION

Results of the growth inhibition of *Sinapis alba* L. for the tested rates of rubber granulate were determined using the equation of percentage inhibition/stimulation of plant growth (IR) and are presented in Table 2.

The average value of plant root length in the sample without the rubber granulate (Control) was 92.40 mm (L_C). Average values of root length (mm) in the sample with the rubber granulate (L_S) were calculated for each percentage rate separately.

Table 2 Results of Sinapis alba L. growth inhibition in the phytotoxicity tests of rubber granulate

Designation	Addition of granulate from tires	L_S (mm)	IR (%)
1	5%	86.39	6.50
2	10%	68.03	26.37
3	25%	57.53	37.73
4	50%	47.37	48.73
5	75%	34.78	62.36

Legend: 1 – tests with 5% granulate; 2 – tests with 10% granulate; 3 – tests with 25% granulate; 3 – tests with 50% granulate; 4 – tests with 75% granulate; L_S – average values of root length in the sample with rubber granulate (mm); IR – results of percentage inhibition/stimulation of plant growth (%)

The lowest inhibition values were recorded at testing the 5% rubber granulate (6.50%). In contrast, the highest inhibition values were recorded at testing the 75% rubber granulate (62.36%). In the other rates of rubber granulate, the values of inhibition ranged from 26.37% to 48.73%. The values were related to the control sample and were also used to plot the diagram in Figure 2. The use of higher rates of rubber granulate on the OECD soil significantly inhibited the growth of *Sinapis alba* L. An error analysis of the experimental procedure in the following graph was plotted by the application of error lines in the Microsoft Excel application. The analysis helps evaluate the measurement accuracy and reliability despite the random nature of the measurement.

The results demonstrate that in terms of phytotoxicity, rubber granulate from waste tires with the size of fractions 1–3 mm has an environmental impact. Residues of chemical substances (most frequently excess zinc) from the original tires remain also in the rubber granulate which may impair the quality of soil and plants if applied on the soil in the form of mulch. In addition, rubber granulate has a very long decomposition time and does not provide nutrients to plants unlike organic mulch.

Chalker-Scott (2018) and Jared (2001) say that rubber mulch is offered by the manufacturer as a durable, safe and non-toxic plant material that retains irrigation (Chalker-Scott 2018, Jared 2001). But the opposite is true. People do not realize the risks associated with their use. Toxic substances (mentioned in the Introduction) contained in rubber leach out during decomposition and contaminate soil and plants. However, some substances bioaccumulate and act gradually over time (Chalker-Scott 2018). This is confirmed in their study by William and Shenker (2016), who performed a hydroponic experiment with cucumbers, to which rubber granulate was added. They tested at 0%, 5% and 10% granulate concentration. The soil to which the granulate was applied showed a significant reduction

in plant growth (toxicity) compared to the control sample. This condition was mainly caused by the leachability of heavy metals in granulate (especially zinc), which accumulated both in plants and in the soil itself (William and Shenker 2016).

Figure 2 Graphical illustration of the results of Sinapis alba L. root growth inhibition in the tests of rubber granulate phytotoxicity, Brno, Czech Republic, 2021

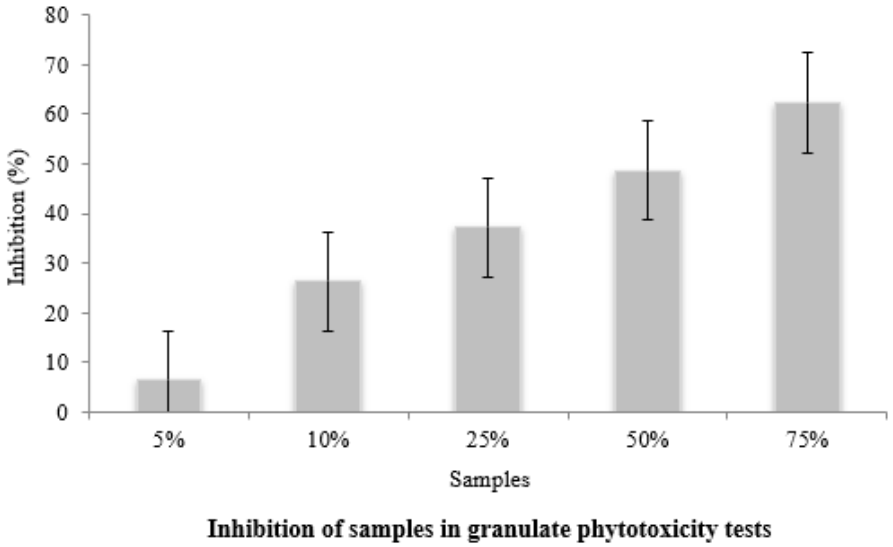

Legend: 5% – 75% samples with the given rates of granulate

In spite of its advantages mentioned in the chapter of Material and Methods, rubber granulate should not be therefore used as a substitute for organic mulch. As to the disposal of waste tires, the most appropriate option of its valorization is its energy use as fuel in cement works instead of brown coal.

CONCLUSION

Rubber granulate which arises from recycling waste tires represents a potential environmental risk in terms of phytotoxicity. In the production of tires, no technologies exist so far that would be able to reduce the toxicity of rubber and maintain at the same time all singular functions of tires (resistance, direction guidance, permanence irrespective of climatic conditions, shock absorption etc.). Tire manufacturers currently try to make tires that would be more sustainable for the environment and to reduce the consumption of natural resources for their production.

The phytotoxicity of rubber granulate from waste tires was determined in laboratory conditions according to the methodology of Phytotoxkit™. All tested rates of the rubber granulate (5%, 10%, 25%, 50% and 75%) exhibited the growth inhibition of *Sinapis alba* L. Being phytotoxic already at low rates, rubber granulate should not be used as a substitute for organic mulch.

REFERENCES

Birkholz, D.A. et al. 2003. Toxicological Evaluation for the Hazard Assessment of Tire Crumb for Use in Public Playgrounds. Journal of the Air & Waste Management Association [Online], 53(7): 903–907. Available at: https://pubmed.ncbi.nlm.nih.gov/12880077. [2021-08-08].

Cao, W. 2007. Study on properties of recycled tire rubber modified asphalt mixtures using dry process. Construction and Building Materials [Online], 21(5): 110–116. Available at: https://www.sciencedirect.com/science/article/pii/S095006180600016X?via%3Dihub. [2021-08-08].

Chalker-Scott, L. 2018. Is Rubber Mulch Safe for My Garden? [Online], Available at: https://www.motherearthnews.com/nature-and-environment/is-rubber-mulch-safe-zm0z14onzsor. [2021-10-23].

Jared, D.M. 2001. Evaluation of Recycled Rubber Mulch Products. Georgia DOT, Office of materials and research [Online], 1–38. Available at:

http://g92018.eos-intl.net/ELIBSQL14_G92018_Documents/9808.PDF. [2021-10-23].

Kizlink, K. 2014. Waste: collection, processing, recovery, disposal, legislation. 3rd ed., Brno: Academic Publishing house CERM, pp. 183–204.

Kumaran, G.S. et al. 2008. A Review on Construction Technologies that Enables Environmental Protection: Rubberized Concrete. American Journal of Engineering and Applied Sciences [Online], 1(1): 40–44. Available at: https://thescipub.com/abstract/ajeassp.2008.40.44. [2021-08-08].

Kuraš, M. 2014. Odpady a jejich zpracování. 1st ed., Chrudim: Vodní zdroje Ekomonitor.

Li, X. et al. 2010. Characterization of substances released from crumb rubber material used on artificial turf fields. Chemosphere. [Online], 80(3): 279–285. Available at: https://www.sciencedirect.com/science/article/pii/S0045653510004285?via%3Dihub. [2021-08-07].

Llompart, M. et al. 2013. Hazardous organic chemicals in rubber recycled tire playgrounds and pavers. Chemosphere [Online], 90(2): 423–431. Available at: https://www.sciencedirect.com/science/article/pii/S0045653512009848. [2021-08-07].

Nelson, S.M. 1994. Identification of tire leachate toxicants and a risk assessment of water quality effects using tire reefs in canals. Bulletin of Environmental Contamination and Toxicology [Online], 52: 574–581. Available at: https://link.springer.com/article/10.1007%2FBF00194146#citeas. [2021-08-10].

Ramos, G. et al. 2011. The recycling of end-of-life tyres. Technological review. Revista De Metalurgia [Online], 47(3): 273–284. Available at: https://revistademetalurgia.revistas.csic.es/index.php/revistademetalurgia/article/view/1197/1208. [2021-08-07].

Price, W. et al. 2006. Waste tire recycling: environmental benefits and commercial challenges. International Journal of Environmental Technology and Management [Online], 6: 362–374. Available at: http://www.inderscience.com/offer.php?id=9001. [2021-08-05].

Sathiskumar, C. et al. 2019. Recycling of waste tires and its energy storage application of by-products–a review. Sustainable Materials and Technologies [Online], 22. Available at: https://www.sciencedirect.com/science/article/pii/S2214993719300636. [2021-08-06].

Schnick, R.A. et al. 1982. Mitigation and enhancement techniques for the Upper Mississippi River system and other large river systems. Resource publication. Washington, DC: U.S. Department of the Interior, Fish and Wildlife Service, pp. 102.

Šourková, M. et al. 2021. Phytotoxicity of Tires Evaluated in Simulated Conditions. Environments [Online], 8(6): 49. Available at: https://www.mdpi.com/2076-3298/8/6/49#cite. [2021-08-03].

Vaverková, M.D. et al. 2019. Landfill leachate effects on germination and seedling growth of hemp cultivars (*Cannabis Sativa* L.). Waste and Biomass Valorization [Online], 10: 369–376. Available at: https://link.springer.com/article/10.1007/s12649-017-0058-z. [2021-08-11].

Wik, A., Dave, G. 2005. Environmental labeling of car tires—toxicity to Daphnia magna can be used as a screening method. Chemosphere [Online], 58(5): 645–651. Available at: https://www.sciencedirect.com/science/article/pii/S004565350400760X. [2021-08-10].

William, M., Shenker, M. 2016. Pulverized Tires as Soil Amendment for Plant Growth. International Journal of Scientific & Engineering Research [Online], 7(6): 161–167. Available at: https://www.ijser.org/researchpaper/Pulverized-Tires-as-Soil-Amendment-for-Plant-Growth.pdf. [2021-10-23].

Optimization of ATS system for pollutants removing

Vladimira Tarbajova[1], Pavel Chaloupsky[1], Dalibor Huska[1,2,3]
[1]Department of Chemistry and Biochemistry
[2]Central European Institute of Technology (CEITEC)
Mendel University in Brno
Zemedelska 1, 613 00 Brno
[2]Central Institute of Technology (CEITEC)
Brno University of Technology
Purkynova 123, 612 00 Brno
CZECH REPUBLIC

xtarbajo@mendelu.cz

Abstract: Industrialization increases use of emerging contaminants which contribute significantly to water pollution. This critical problem attract considerable public attention, hence appropriate technology is needed. Various microorganisms such as algae, cyanobacteria, fungi, yeast and bacteria can be used under certain conditions as ecological and low cost alternative method. One of the options, typically with dominance of some algal taxa, that can improve natural wastewater treatment processes is an algal turf scrubber (ATS) technology. It is an ecologically algae-based system characterized by a broad and dynamic non-specific consorcia with various advantages compared to conventional ones. This work focused on optimazing the initiation, formation and maintaining of microbial consortia. Amaranth (azo dye) was chosen as the test pollutant. Results indicate the potential of the ATS system for removal of azo dye amaranth in concentration 20 mg/l.

Key Words: algal turf scrubber, azo dye, amaranth, non-specific consortia

INTRODUCTION

There is still a technical challenge to develop innovative and cost-effective technologies that can facilitate different types of pollutants. Several methods such as adsorption, precipitation, chemical oxidation, photodegradation, or membrane filtration are available for removing emerging contaminants from industrial effluents, but most of them are energy and cost intensive and with large amount of sludge production (Robinson et al. 2001). Comparatively, the biological methods are attracted alternative with great potential to convert these contaminants and biodegrade them to less hazardous compounds. Various microorganisms such as algae, bacteria, fungi and yeast can be used for pollutant removal under certain environmental conditions. This techniques are more efficient and eco friendly as well as allows complete mineralization of organic pollutants (Bhatia et al. 2017).

Ecologically engineered system algal turf scrubber (ATS) is a biological method designed to treat a range of contaminated water. This system is based on natural mixed assemblage of microorganisms dominated by benthic, filamentous algal taxa (Craggs et al. 1996). The concept of technology was introduced by Dr. Walter Adey of the Smithsonian Institution in the early 1980s for effectiveness of water quality improvement, so there is a long-term and well-known backround which allow to develope sustainable technology with possitive impact on environment (Siville and Boeing 2020). ATS is relatively simple in design with undemanding construction which makes it a suitable low-cost system (Adey et al. 2013). The ATS system consists of non-specific microbial consortia growing on solid surface trough which polluted water is pumped. As water flows onto the surface with attached algae, they provide uptake of inorganic compounds and release dissolved oxygen through photosynthesis. The nutrients removal is realized by biological uptake and stored in the biomass (Ray et al. 2015).

Moreover, for the sustainable wastewater treatment using ATS system several significant factors such as water depth, flow rate, light sources and intensity and frequency of harvest can be adjust to maximaze microbial metabolism which lead to improvement in water treatment capacity (Pizzaro et al. 2006). Accordingly, the advantage of attached filamentous algae is simplicity in harvesting with

low energy consuption which is crucial as it rejuvenates the community facilitate high growth rates. The algae are harvested periodically, approximately once per week, to remove the assimilated nutrients (Ray et al. 2015).

The microbial community present at system is a high in diversity which is desirable in pollutant removing. These contaminants are complex and mostly formed of many different compounds so that the cooperative biotic interactions between species are commonly require. Furthermore, the majority of microbial approaches are specific to certain chemical constituents and cannot be simply up-scaled for industrial wastewater treatment (Newby et al. 2016). Individual microorganisms are able to metabolize a limited range of substrates, hence mixed populations with overall enzymatic capacities allow for the further rate and extent of azo dye biodegradation. Therefore using microbial communities instead of individual culture can be preferable in the remediation procceses (Liu et al. 2017).

This work focused on optimazing of ATS system in lab scale condition with ephasis on azo dye removal which comprise the largest class of synthetic dyes used in commercial applications. More than 70 thousand tons of these dyes are produced yearly while a certain part of them are released into the environment. Furthermore, some azo dyes have been reported as carcinogenic and toxic in nature so their decrease in water effluent by inovative technology would be beneficial (Pandey et al. 2007).

MATERIAL AND METHODS

ATS System

The ATS system consisted of two parts, the upper one with surface area 60x40x7.5 cm which were equipped with common fiberglass for easy microalgae attachment (Figure 1). In the second bottom part, a circulation pump EHEIM CompactON 1000 was placed to allow the system recirculate 20 l of BG-11 media (UTEX, 2009) over the ATS. The system had a flow rate of 500 ml at one draining of the water tank and light intensity was maintained at 500 µmol m^2/s with photoperiod 16/8 (light/dark) at temperature 28 °C. We replaced BG-11 media every seven days for ensurement of sufficient nutrients.

Figure 1 Schematic drawing of the Algal Turf Scrubber used in this study

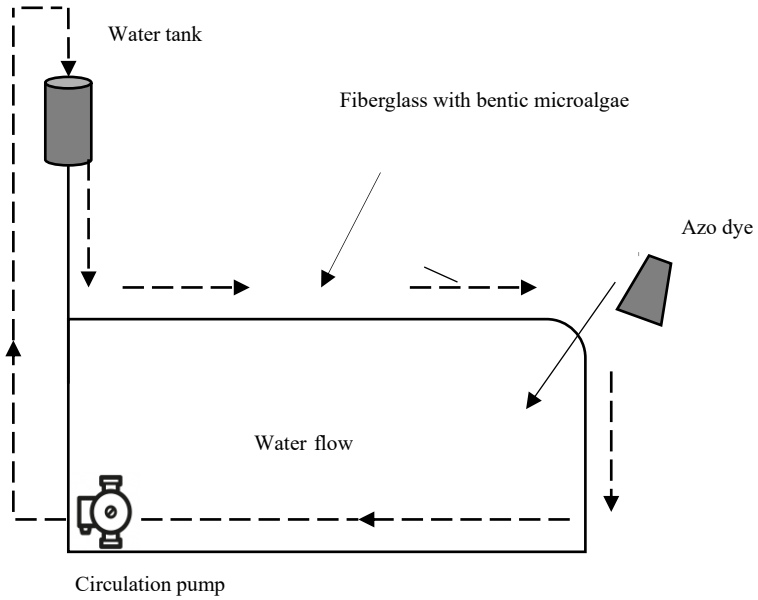

Sample collection and cultivation

Samples of non-specific consortia was collected by standard methods directly from the field with focus on locations where the environment is presumed to be contaminated or extreme in physicochemical conditions and then inoculated to the ATS system. Based on that we selected for the pilot experiment the small lake near by reclaimed landfill in Přerov as we assumed more resistant and adapted species.

Characterization of non-specific consortia

Characterization of external species morphology was performed using scanning electron microscopy (SEM) on a Tescan MAIA 3 equipped with a field emission gun (Tescan Ltd., Brno, Czech Republic).

Azo dye concentration and decolorization

Amaranth (C.I. Acid Red 27) was purchased from Sigma–Aldrich (USA) and was used for decolorization experiments using ATS system at a final concentration of 20 mg/l. Decolorization of amaranth were monitored by spectrophotometric methods. The quantification of azo dye decolorization was assessed spectrophotometrically at 520 nm, which is adsorption maximum of used azo dye. Decolorization efficiency (%) was calculated according to the absorbance decrease of supernatant of samples collected every 24 hours for 5 days.

Amarant decolorization efficiency (DE, %) was calculated with following formula:

$$\text{DE (\%)} \frac{A_0 - A_t}{A_0} \times 100$$

where A_0 is the initial absorbance of supernatant and A_t is the absorbance at time t (h).

Statistical analysis

The results were expressed as the mean ± the standard error deviation of the mean. Significant difference was determined using one-way ANOVA with subsequent post hoc Tukey comparisons tests.

RESULTS AND DISCUSSION

Experimental set-up

The primary focus of this research was to successfully construct ATS system and subsequently optimize its efficiency for pollutant removal. This system was developed with the purpose of wastewater treatment and thus obtaining innovative and ecological technology (Liu et al. 2020). Although, our system is in lab scale conditions, it is an open type of bioreactor with a simple biomass harvest.

The non-specific consortia from the field with emphasis on species from contaminated environment was inoculated to the system and allowed to grow (Figure 1). Based on the experiments we found that optimal harvest time of biomass was around seven days. Siville and Boeing (2020) also observed harvest rate between one to two weeks. Exceeding this time could result in lower biomass production and growth rates.

The consortia was scraped from the surface and studied by scanning electron microscopy (Figure 2). It shows that non-specific consortia was dominated by filamentous *Cyanobacteria*, but specific species and the rest of the community present in the consortia cannot be confirmed with certainty, with further analysis via MiSeq sequencing we will obtain a complete microbial profile.

Figure 2 Detail image of unknown microalgae growing on the fiberglass

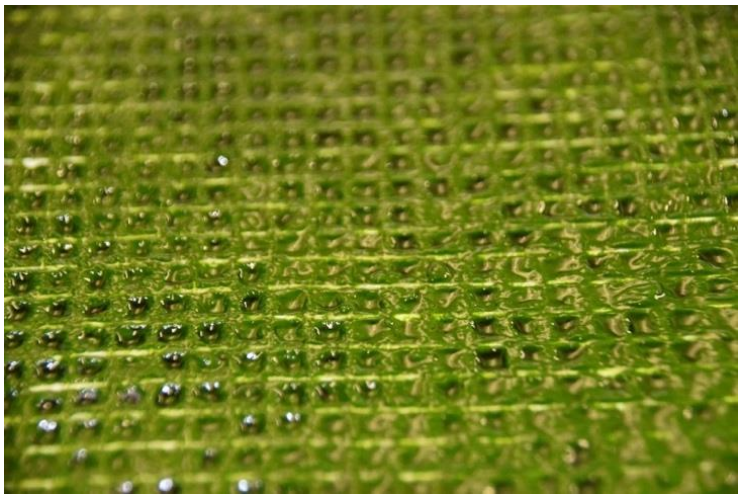

Figure 3 SEM images of non-specific consortia from the lake near by reclaimed landfill in Přerov

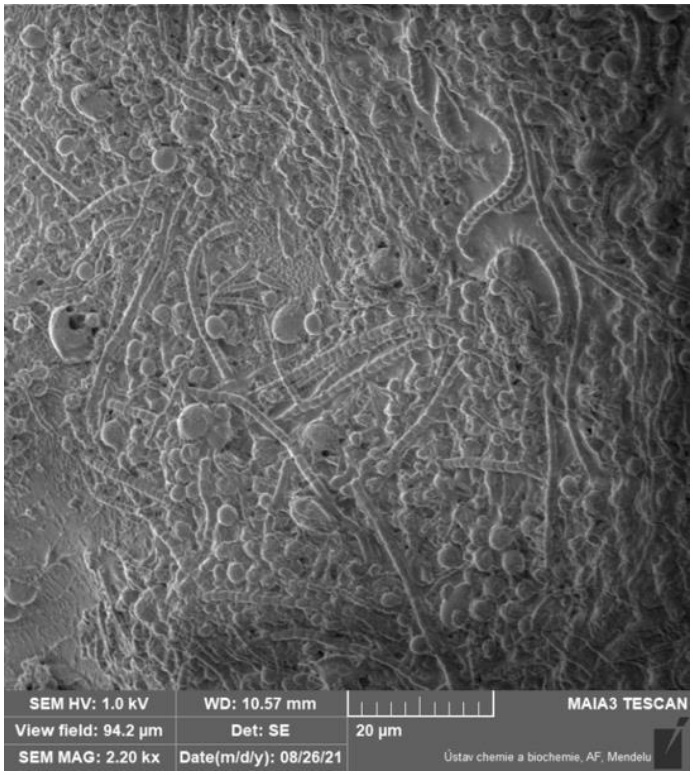

Decolorization of azo dye amaranth

The ATS system was design to promote azo dye removal treatment (Figure 4). The capability of a non-specific consortia growing in the ATS system to bioremediate contaminants was evaluated by using azo dye amaranth. Amaranth is an acidic monosulfonated azo dye widely used in the textile industry. Moreover, amaranth, like other types of azo dyes, is recalcitrant which have considerable and dangerous impact on an environment (Chan et al. 2012). Accordingly, efficient and innovative methods for their degradation are needed.

Figure 4 ATS system with amaranth application

Decrease in concentration of amaranth is shown in Figure 5 and we observed it at absorbance 520 nm. The highest decolorization rate was exhibit after 5 days and it was around 70%, which is also shown visibly in the Figure 5. Shabbir et al. (2017) studied bioremediations capabilitites of periphyton, which is complex mixture of microbial organisms attached to surface, immobilized although in a different type of bioreactor, but on a similar principle. Likewise, they observed as a dominant phyla in consortia *Cyanobacteria*, along with *Proteobacteria* and *Bacteroidetes* and achieved complete decolorization of amaranth within 20 hours. These results suggest that there is a possibility of complete decolorization of amaranth through consortia using our system, but further optimization will be needed to obtain such a results. A high concentration of amaranth, 200 mg/l, was also tested, but we observed a very low percentage of decolorization, not even 10%. Based on this finding, we assume that the concentration was highly toxic to the consortia, as there was no visible growth of biomass either.

However, the studies associated with ATS system are mostly focused on wastewater treatment with analysis of nutrient, especially to nitrogen and phosphorus decrease, not specifically on azo dyes removal. The technology was used for treatment of dairy manure effluent in outdoor ATS raceways with nitrogen and phosphorus decreased to 50–80% (Mulbry et al. 2008) and Salvi et al. (2021) demonstrated complete removal of $P\text{-}PO_4^{3-}$ and $N\text{-}NH_4^+$ in 24 h at all concentrations. So, there is a great potential of this technology in wastewater treatment processes.

Figure 5 Decolorization of azo dye amaranth (A) Percentage of amaranth decrease during 5 days (B) Image of visible decolorization of amaranth on day 0 compared to day 5. Data are presented as mean ± standard deviation of the mean (n = 3). (*) indicates a significant difference compared to the control group (p <0.05). (**) indicates a significant difference compared to the control group (p <0.01) and according to the Tukey post hoc test

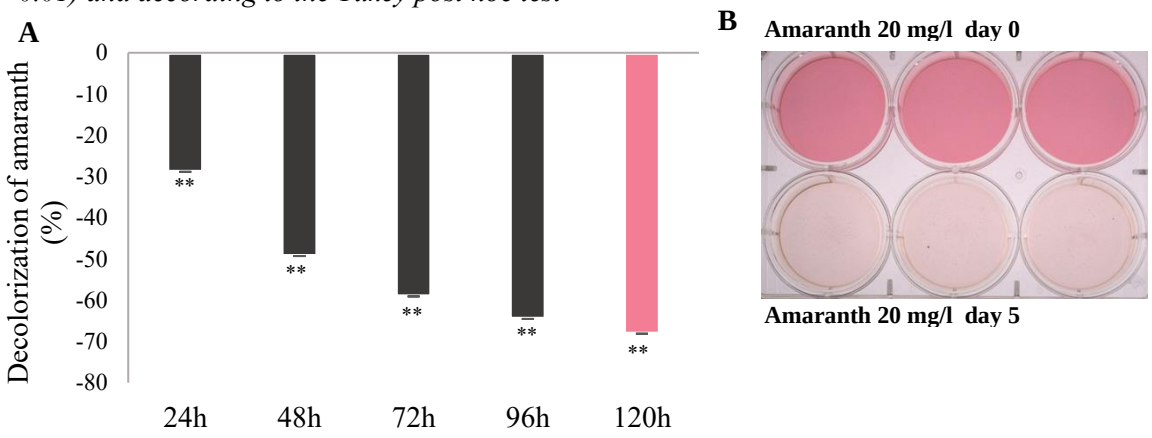

CONCLUSION

Bioremediation, biodegradation are currently becoming important again. The number of pollutants is increasing both quantitatively and qualitatively. Our work demonstrates the potential utilisation of ATS bioreactors based on unknown microbial consortia collected directly from problematic parts of contaminated waters. Subsequently, such a consortium may be transferred to *in-vitro* experimental settings and its growth can be controlled under adverse conditions. In this study, we used azo dye Amaranth as a pollutant. The system provided a reduction of the pollutant in solution. It remains a question whether uptake, translocation or biodegradation has occurred, and future research will focus on this issue. However, according to spectrophotometric measurements, there was a rapid decolorization of the original contaminated medium by a naturally occurring consortium of microorganisms.

ACKNOWLEDGEMENTS

The research was financially supported by the Internal Grant Agency of Mendel University in Brno (AF-IGA2021-IP055).

REFERENCES

Adey, W.H. et al. 2013. Algal turf scrubber (ATS) floways on the Great Wicomico River, Chesapeake Bay: productivity, algal community structure, substrate and chemistry1. Journal of Phycology, 49(3): 489–501.

Bhatia, D. et al. 2017. Biological methods for textile dye removal from wastewater: A review. Critical Reviews in Environmental Science and Technology, 47(19): 1836–1876.

Chan, G.F. et al. 2012. Communal microaerophilic–aerobic biodegradation of Amaranth by novel NAR-2 bacterial consortium. Bioresource Technology, 105: 48–59.

Craggs, R.J. et al. 1996. Phosphorus removal from wastewater using an algal turf scrubber. Water Science and Technology, 33(7): 191–198.

Liu, J. et al. 2017. Advanced nutrient removal from surface water by a consortium of attached microalgae and bacteria: a review. Bioresource Technology, 241: 1127–1137.

Liu, J. et al. 2020. Wastewater treatment using filamentous algae–a review. Bioresource Technology, 298: 122556.

Mulbry, W. et al. 2008. Treatment of dairy manure effluent using freshwater algae: algal productivity and recovery of manure nutrients using pilot-scale algal turf scrubbers. Bioresource Technology, 99(17): 8137–8142.

Newby, D.T. et al. 2016. Assessing the potential of polyculture to accelerate algal biofuel production. Algal Research, 19: 264–277.

Pandey, A. et al. 2007. Bacterial decolorization and degradation of azo dyes. International Biodeterioration & Biodegradation, 59(2): 73–84.

Pizarro, C. et al. 2006. An economic assessment of algal turf scrubber technology for treatment of dairy manure effluent. Ecological Engineering, 26(4): 321–327.

Ray, N.E. et al. 2015. Nitrogen and phosphorus removal by the Algal Turf Scrubber at an oyster aquaculture facility. Ecological Engineering, 78: 27–32.

Robinson, T. et al. 2001. Remediation of dyes in textile effluent: a critical review on current treatment technologies with a proposed alternative. Bioresource Technology, 77(3): 247–255.

Salvi, K.P. et al. 2021. A new model of Algal Turf Scrubber for bioremediation and biomass production using seaweed aquaculture principles. Journal of Applied Phycology, 1–10.

Shabbir, S. et al. 2017. Evaluating role of immobilized periphyton in bioremediation of azo dye amaranth. Bioresource Technology, 225: 395–401.

Siville, B., Boeing W.J. 2020. Optimization of algal turf scrubber (ATS) technology through targeted harvest rate. Bioresource Technology Reports, 9: 100360.

FOOD TECHNOLOGY

Development of 3D printing in food processing

Josef Bauer, Stepan Janoud, Filip Beno, Rudolf Sevcik
Department of Food Preservation
University of Chemistry and Technology, Prague
Technicka 5, 166 28 Prague 6
CZECH REPUBLIC

bauerj@vscht.cz

Abstract: The aim of this work was to convert a 3D printer for plastic to a printer for printing food materials with a piston extruder and 200 ml storage container (maximum dimensions of the printed object: X = 232 mm, Y = 232 mm, Z = 250 mm). Using Sharp3D graphics software, a final model of a pasty extruder was built after several prototypes, using the original stepper motor along with two gears, a housing, and a piston. The models that were printed corresponded to the original computer model, including dimensions. The main parameters were to determine the height of the layer of the printed samples, the number of solid layers to ensure the homogeneity of the printed samples, and the infill density, as it ensures the correct filling of the model. For sample 1 (vegan pate), the optimal filling value is 60% and layer height is 1 mm.

Key Words: three-dimensional printing, extrusion, 3D structures, food products, vegan pate

INTRODUCTION

Evolving technology for the food industry, which represents a great opportunity to take advantage of the diversity of shapes produced, the possibility of replacing certain types of food, can help in culinary, for food preparation at home and in the future in production processes, is three-dimensional printing (3DP). 3D printing as an additive manufacturing process (AM process) uses the application of material layer by layer with predetermined parameters to create 3D structures. 3D printing uses computer aided design (CAD) technology to help a digital device create 3D objects without the added tool (Dick et al. 2019, Gross et al. 2014). The application of 3D printing (associated with the development of stem cells) includes several advantages in food processing. For example, creativity in the production of new types of products, full nutritional composition of manufactured foods, and waste reduction. Disadvantages are, for example, longer printing time, more complex software work, and sanitation of these devices. However, to produce a food product by 3D printing, it is necessary to assess the rheological properties of the printed material with a suitable sensory and nutritional profile and further set the parameters of the 3D printer (Dick et al. 2019).

Based on printability, we can divide food into three categories. Native food materials are characterized by sufficient flow capacity (cheese, chocolate, confectionery, dough). Furthermore, food products, which are of more viscous forms and require a properly controlled flow rate of this material (meat and vegan products). The last category are alternative ingredients, which we could generally include functional foods, and these are mainly proteins, polysaccharides (fiber) obtained from algae, fungi, bacteria, or insects (Sun et al. 2018, Wang et al. 2018).

There are several techniques used in 3D printing. For food products where the basic material is liquid or low viscosity mass, the most used 3D printing technique is extrusion, for example, extrusion of soft materials (melted cheese, dough), extrusion at increased temperature (chocolate, confectionery). Furthermore, these materials use a technique called inkjet printing (chocolate, cheese, jam). For powder mixtures, the most used 3D printing technique is selective laser sintering (SLS) (sugar, cocoa powder). And the rapidly developing method of 3D bioprinting worldwide (used for cultured meat), which will certainly have practical applicability in larger volumes in the future than just the extrusion method (Godoi et al. 2016). In this work, an extrusion technique was used, which is based on the principle of extruding polymer (food material) from a moving nozzle layer by layer to create the desired shape on a heated or cooled pad. Thus, in the extrusion process, the food material is inserted into the extruder,

and the material is extruded from the extruder by the action of a hydraulic piston. Following deposition of the layers is performed by orienting the extruder along the XYZ axis according to the selected object in the program (Godoi et al. 2016, Murphy and Atala 2014).

Cultured meat, also called as clean meat, cell-based meat, and cultivated meat is often associated with 3D bioprinting technology. The principle of cultured meat production could be summarized in the following points: suitable selection of stem cells, correct selection of growth medium, setting of bioreactor parameters, tissue growth, and selection of 3D printing parameters (Gu et al. 2012, Handral et al. 2020). Collection of stem cells is very difficult due to the possible contamination of these cells by other cells depending on the substrate, for example, from the blood, and the possibility of a defect in their multiplication (inability to reproduce). Another point is the appropriate choice of growing medium. A suitable growing medium can be fetal bovine serum (FBS) based on mainly globular proteins. The third point is the scaffolding. The most suitable materials for myoblast formation are cellulose, alginate, chitosan, collagen, soy protein, or gelatin. And finally, the use of 3D bioprinting, thanks to which the resulting material will have acceptable organoleptic properties and nutritional values, and involvement of the following production and culinary processes (pasteurization, sterilization, baking, smoking, freezing storage, and more) (Handral et al. 2020, Zhang et al. 2017).

MATERIALS AND METHODS

Sample preparation

For this experiment were made 3 samples of different food materials: sample 1 (vegan pate), sample 2 (pate), and sample 3 (dough):

Sample 1 (1 kg): 630 g water, 160 g oil, 160 g mixture of additives (pea protein, citrus fiber, coconut fat, carrageenan, sodium alginate, sodium diphosphate, sodium triphosphate), 35 g spice mixture (sugar, yeast extract, onion, garlic, beetroot, black pepper, ginger, coriander, nutmeg), and 15 g salt. For sample 1 water was added to thermomixer (Vorwerk, Germany), followed by salt, spice mixture, mixture of additives, and oil was gradually added to form an emulsion.

Sample 2 (1 kg): 400 g chicken liver, 250 g pork fat, 130 g butter, 100 g cream, 53 g water, 50 g spice mixture (onion, sugar, garlic, black pepper, thyme), 17 g curing salt. For sample 2 chicken liver was minced to 5 mm and was added to thermomixer with salt, and mixed. Then were added all other ingredients and mixed to form homogenous mixture.

Sample 3 (1 kg): 600 g wheat flour, 300 g whole milk, 90 g fresh eggs, and 10 g salt. Sample 3 was prepared in a food processor (Sencor, Czech Republic) in which the ingredients were mixed.

Construction of 3D printer for food material

For the purposes of this experiment, a three-dimensional system with a piston extruder was assembled, which was made using a standard 3D printer Ender 3 (maximum dimensions of the printed object: X = 232 mm, Y = 232 mm, Z = 250 mm). Figure 1A shows a modified 3D printer Ender for printing of food material and Figure 1B shows a record of the printing of sample 1. First, the original construction of the plastic extruder was removed along with the cabling (only the X-axis on the original aluminium support was left on printer). Furthermore, the source code of the original printer's firmware was modified so that the original extruder did not heat up, which caused errors in the system, as the extruder was no longer connected. The firmware is also needed to change the direction of rotation of the extruder stepper motor to achieve the required direction of rotation, as well as thermal protection for printing below 170 °C (preventing the stepper motor from rotating below the temperature). Using Sharp3D graphics software, a final model of a pasty extruder was built after several prototypes, using the original stepper motor along with two gears, a housing, a piston and a storage container made of a 200 ml syringe. All parts of the model were printed on a 3D printer Ender 3 made of PLA (polylactic acid) material and subsequently constructed using standard connecting materials (screws, threaded rod, nuts). The next step was to move the Z-axis stop to the required height to avoid a collision of the pasty extruder with the heated bed. Finally, the extruder was attached to the original aluminium carrier on the X-axis and all necessary cablings were connected.

3D food printer and printing parameters

The model for printing was created using the graphics software Sharp3D and then prepared for printing using the slicing program PrusaSlicer. The print parameters were tested sequentially until the optimal values for correct printing were reached. The temperature of the heated bed was chosen to the maximum value (110 °C) to denature the proteins of the printed material as quickly as possible. For the selected model, a filling density of 10% and a layer height of 1 mm were chosen. The nozzle diameter can be changed, and a diameter of 1 mm has been selected. The material flow must be varied depending on the density of the material. For the purposes of this experiment, a value of 20% of the default value was chosen. The print parameters have been changed many times and the most optimal are listed in Table 1.

Physico-chemical analyses

For all samples were analyzed water content, fat content, ash, protein, water activity and pH value. The water content of the samples was determined by drying at 103 ± 2 °C in an oven HS 32 A (ZPA, Czech Republic) to a constant weight loss. The fat content was determined by the Soxhlet method using a Soxtec 2043 extraction unit (Foss, Sweden). Protein was determined by the Kjeldahl method. The ash was determined in the laboratory furnace (Nabertherm, Germany) in four stages: in the first phase, heating the furnace to 200 °C for 8 hours. Next, heat the furnace to 300 °C (6 hours), in the third phase, heat the furnace to 400 °C for 8 hours, and in the last phase of heating the furnace to a temperature of 500 °C (28 hours). Water activity was measured with an a_w meter Aqualab 4 TEV (Decagon Devices, USA) at a temperature of 25 °C. The pH determination was measured using pH meter Portavo 904 X (KNICK, Germany) with needle probe SE 104 N (KNICK, Germany).

RESULTS AND DISCUSSION

Construction of 3D printer for food material

As a part of our experiment, we converted a 3D printer for plastic to a printer for printing food materials using a pneumatic extruder. The printer worked very precisely, and the models that were printed corresponded to the original computer model, including dimensions. The heated pad was used to denature the food material and worked perfectly. The extruder itself reacted very sensitively to the engine and gear rotation, which generated pressure inside tank. Compared to the printing of plastic, the printing of food materials is many times faster, and the errors caused by air bubbles in the sample do not affect the final product. The disadvantage of our equipment is the time required for the preparation of the print, this problem could be eliminated on a production scale if it runs continuously. Therefore, the next step is replace pneumatic extruder with a peristaltic pump which can dose food materials continuously. During the experiment, we found a problem where the pressure in the tank increased and the gears began to slip, but this was solved by reducing the pressure in the tank. In general, for samples of pate and meat products, a homogeneous material is necessary to avoid blocking of nozzle, as has been tested for the printing of sample 2. For sample 3, it is easy to form a 2D pattern of any shape (in our case, the symbol of Batman, Spiderman, or star), but due to the slow denaturation of dough on the heated bed, there is a problem during applying higher layers, so additional heat treatment is required. Sample 1 is discussed in the following chapters.

3D food printer and printing parameters

Due to the range of this work, the data are presented only for sample 1. After several experiments and reconfigurations, the optimal print parameters for sample 1 are listed in Table 1.

The main parameter was to determine the height of the layer of the printed object to apply the material uniformly and adhere to the heated bed. This parameter was also important to avoid scattering and destruction of already printed material. Another important parameter was the number of solid layers to ensure the homogeneity of the printed object. Infill density was a very variable value as it ensures the correct filling of the model. If the value was too low (10%), gaps were formed, which is evident from the Figure 3A. However, if the value was too high (80% and more), there was an overdone supply of printed material flowing out of the printed object. For sample 1, the optimal filling value is 60%. In figure 3A is shown the printing of the model with infill density set to 10% where is possible to see gaps. In Figure 3B is shown printed model with 60% infill density, which we found

as optimal and in Figure 3C is the same sample in Figure 2B which was head treated for 30 minutes at 70 °C. The printed materials show better structural properties in comparison to the literature (Liu et al. 2018).

Figure 1 3D printer with our custom modification for printing of food material

A) Construction of 3D printer

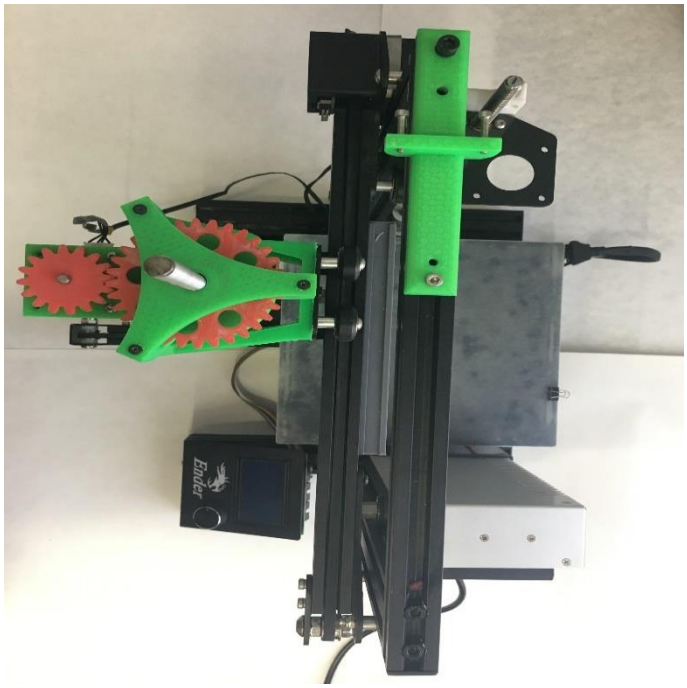

B) During of printing of sample 1

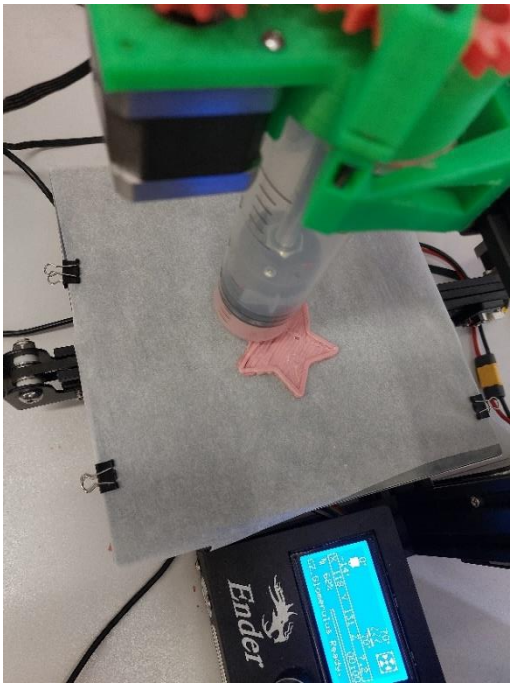

Figure 2 System operation process flow diagram

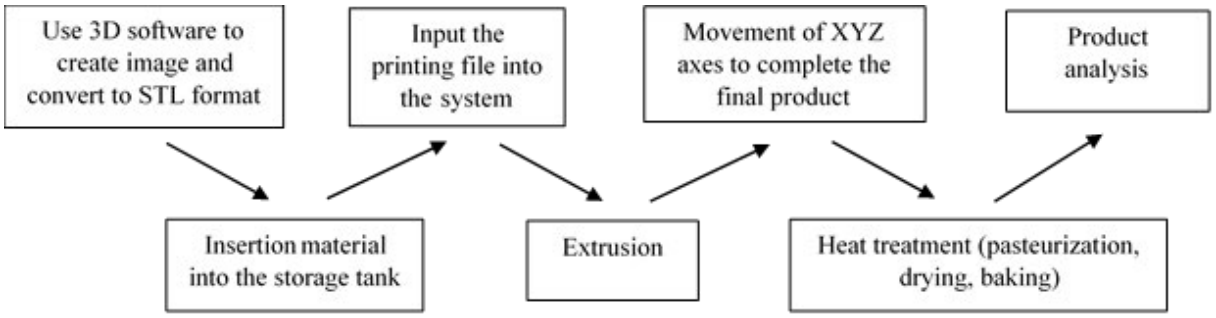

Table 1 Printing parameters

Setting	Value	Setting	Value
Layer height	1 mm	Auto cooling	On
First layer height	0.2 mm	Bed temperature	110 °C
Top solid layers	3	Extrusion multiplier	2
Infill density	60%	Retraction length	5 mm
Fill pattern	Grid	Retraction speed	60 mm/s
Perimeters	60 mm/s	Detraction speed	40 mm/s
Small perimeters	15 mm/s	Lift Z	0 mm
External perimeters	50 mm/s	Travel	130 mm/s
Infill	80 mm/s	First layer	30 mm/s
Top solid infill	15 mm/s	Perimeters	1

Figure 3 Sample 1

A) Infill density set to 10% *B) Infill density set to 60%* *C) Infill density set to 60% after drying process*

Physico-chemical analyses

Each sample was measured three times in a parallel determination from which the average values and standard deviation were calculated. Chemical composition of sample 1 is shown in Table 2.

Table 2 Chemical composition of sample 1

Water content (%)	Fat (%)	Protein (%)	Ash (%)	pH	Water activity
67.31 ± 2.09	16.80 ± 0.84	6.64 ± 0,39	2.81 ± 0.08	5.82 ± 0.12	0.955 ± 0.007

CONCLUSION

In this work, the Ender 3 printer was converted into a printer able to print low viscous and middle viscous food material with 200 ml storage container (maximum dimensions of the printed object: X = 232 mm, Y = 232 mm, Z = 250 mm). All parts of the model were printed on a 3D printer Ender 3 made of PLA (polylactic acid) material and subsequently constructed using standard connecting materials (screws, threaded rod, nuts). We mainly focused on printing of vegan pate (sample 1), due to the suitable chemical composition of this product for our printer. The most important parameters for printing this material are the infill density (60%) and layer height (1 mm). Thanks to the heated bed, it was possible to manipulate with printed sample and the possibility of subsequent heat treatment immediately after the printing of the model. For all samples were analyzed water content, fat content, ash, protein, water activity, and pH value. In future research we would like to use continuous process instead of discontinuous and use our involved technology for cultured meat.

ACKNOWLEDGEMENTS

This work was supported from the grant of Specific university research - grant No A2_FPBT_2021_046.

REFERENCES

Dick, A. et al. 2019. 3D printing of meat. Meat Science, 153: 35–44.

Godoi, F.C. et al. 2016. 3d printing technologies applied for food design: Status and prospects. Journal of Food Engineering, 179: 44–54.

Gross, B.C. et al. 2014. Evaluation of 3D printing and its potential impact on biotechnology and the chemical sciences. Analytical Chemistry, 86(7): 3240–3253.

Gu, D.D. et al. 2012. Laser additive manufacturing of metallic components: Materials, processes and mechanisms. International Materials Reviews, 57(3): 133–164.

Handral, K.H. et al. 2020. 3D Printing of cultured meat products. Critical Reviews in Food Science and Nutrition, 0(0): 1–10.

Liu, C. et al. 2018. The development of 3D food printer for printing fibrous meat materials. IOP Conference Series: Materials Science and Engineering, 284(1): 1201–1209.

Murphy, S.V., Atala, A. 2014. 3D bioprinting of tissues and organs. Nature Biotechnology, 32(8): 773–785.

Sun, J. et al. 2018. Extrusion-based food printing for digitalized food design and nutrition control. Journal of Food Engineering, 220: 1–11.

Wang, L. et al. 2018. Investigation on fish surimi gel as promising food material for 3D printing. Journal of Food Engineering, 220: 101–108.

Zhang, Y.S.K. et al. 2017. 3D Bioprinting for tissue and organ fabrication. Annals of Biomedical Engineering, 45(1):148–63.

Use of leftover bread for beer production

Alan Dymchenko[1], Milan Gersl[1], Tomas Gregor[2]
[1]Department of Agricultural, Food and Environmental Engineering
[2]Department of Food Technology
Mendel University in Brno
Zemedelska 1, 613 00 Brno
CZECH REPUBLIC

xdymchen@mendelu.cz

Abstract: This research is aimed at the sustainable use of bakery leftovers with the help of beer production technology, thus preventing an increase in the number of unused bakery products by returning them to commodity circulation by introducing the postulate of the circular economy. Conducting research includes two investigations: First, brewing beer by partly using a malt substitute (bakery leftovers); and second, condition optimisation of brewing beer with bread. In the first part of our research, we were challenged by sensorial problems (weak saturation and fullness; undesirable taste) that was connected to the chemical composition of the final beer and the chemical composition of the bread that was used for the beer production, respectively. We changed some conditions in the different stages of brewing (we added glucose, α-amylase, used double and triple decoction, applied higher and lower temperatures during fermentation and boiled for a longer period). To conclude, the best option for brewing beer with bread is to boil for a longer period (65 °C for 60 min and 75 °C for 60 min), which will help extract more elements from bread and malt. The best first fermentation temperature to achieve the most fullness and saturation is 4 °C. Two samples were contaminated by *Leuconostoc mesenteroides*, which caused a viscous taste and a bad evaluation in the total rating. To prevent an undesirable taste, the brewer must prevent contamination of the beer during all stages of brewing, especially during fermentation, and must know the composition of the bread being used.

Key Words: beer production, bakery leftovers, food waste

INTRODUCTION

Beer is one of the most-consumed alcoholic beverages in the world. In 2019, 1.91 billion hectolitres of beer were produced worldwide (Statista 2021). One of the key ingredients in brewing is barley. In the 2020/2021 crop year, 159.74 million metric tons of barley were produced worldwide (Statista 2021). Barley contains approximately 80% starch, which is converted to sugars by enzyme diastase during brewing, a process called malting (Lavilla 2010). These sugars are later used by yeasts to provide fermentation, which is the process of making alcohol and carbon dioxide (Rodman et al. 2016). Barley is the one ingredient in beer production that has a big environmental impact due to its energy and water loss during maturing and the carbon dioxide production during its transportation to the place of use (Hedal et al. 2009, Salazar et al. 2021). Each hectare of barley uses approximately 1,200,000 litres of water per crop in Australia (Callow et al. 2006).

However, there is a large amount of bread waste worldwide. At the consumers' level, the loss is 18% of the produced bread (Sarlee 2015). Bread production uses large amounts of water, energy and fuel. The craft brewery Toast Ale in Great Britain has made it a goal to utilise approximately 5 million slices of surplus bread every year to partially replace barley in brewing. According to its estimation, approximately 24 million bread slices are wasted annually in Great Britain.

In other European countries, small breweries also understand the importance of eliminating the wasting of leftover bread and have started brewing beer with bread as a malt substitute, such as Crumbs Brewing (UK), Instock (NL), Brussels Beer Project (BE) and Troggeling (BE). They use no more than 30% of bread in their recipes.

Brancoli et al. (2020) performed a study that examined 16 impact categories of environmental savings associated with the brewing of beer with the use of bread. It shows that the utilisation of surplus bread in the brewing process is one of the most environment-saving options, along with source

reduction, donations, production of ethanol, and animal feed. The higher savings of brewing bread beer are observed in the global warming category.

The aim of the presented research was to find out whether it is possible to replace malt with old bread. The produced beer should be economically interesting and at the same time the sensory properties should not be negatively affected. This research is focused on the sustainable use of bakery leftovers through beer production technology so as to decrease food waste.

MATERIAL AND METHODS

Seven batches of beer (25 liters each) were prepared (Table 1). The products were chemically and sensory evaluated.

Material

The following raw materials were used to prepare the beer:

Water from the tap, its quality in accordance with the parameters for drinking water in Decree No. 252/2004 Coll. of the Czech Republic. The chemical composition of the tap water is presented in Table 2.

Czech malt.

Bread (wheat, wheat-rye). For the experiments we used fresh bread.

Granulated hops: Sladek (α-bitter acids = 4.5–7.0% w.) and Saaz (ŽPČ) (α-bitter acids = 2.5–4.0% w.).

Dry bottom-fermentation yeast: Saflager W 34/70 at 11.5 g per 10 to 15 litres. Temperature range: 9–22 °C, ideal temperature 12–15 °C

Analyses

Chemical analysis of the pilot experiment:

Chlorides and sulphates were measured by HPLC method using the Dionex ICS-2000 Ion Chromatography System (ICS-2000, Thermo Fisher Scientific, U.S.) with IonPac® AS 18 analytical (2 x 250 mm) column.

Acid Neutralization Capacity to pH 4.5 (ANC4.5) were determined by titration with 0.1 N hydrochloric acid.

Hydrocarbonates (HCO3–) and carbonates (CO3–) concentrations were calculated based on the results of (ANC4.5) and alkalinity.

Calcium (Ca), magnesium (Mg), sodium (Na), potassium (K), were detected by inductively coupled plasma mass spectrometry (ICP-MS) using ICP-MS Agilent Technologies 7700 (Agilent Technologies Inc., U.S.).

Sensory evaluation of the beer:

The sensory properties of beer were evaluated according to ČSN ISO 6658 by five examiners (one woman and four men, range = 25–46 years). The beer-tasting session was performed in a tasting room at a temperature of 18 degrees. Before tasting, the beer was cooled to 7 °C. The amount of drink to be evaluated was 150 ml. The sample was poured into half a glass. Colourless clear glasses were used. Cheese and pastries were used as flavour neutralizers.

Conditions for preparing the batch

The ratio of bread to malt were calculated by the following formula:

The total amount of malt is 3,124 g

3,124 x 50% = 1,562 g (malt)

3,124 x 50% = 1,562 g (dry bread)

Fresh bread contains 40% of water and 60% of dry matter

dry bread / 60% of dry matter in fresh bread = fresh bread

1,562 / 60% = 2,603 g (fresh bread)

Table 1 Preparation parameters used for individual batches

Preparation step	Pilot	1st test	2nd test	3rd test	4th test	5th test	6th test	7th test
Boiling	11 l of water + malt + bread, 40 °C, 10 min							
Boiling	52 °C, 10 min							
Boiling	62 °C, 30 min	65 °C, 60 min	65 °C, 60 min	Double decoc-tion	Triple decoc-tion	62 °C, 30 min	62 °C, 30 min	62 °C, 30 min
Boiling	72 °C, 30 min	75 °C, 60 min	75 °C, 60 min			72 °C, 30 min + 120 g of glucose	72 °C, 30 min + 120 g of glucose	72 °C, 30 min + 3.5 g of α-amylase
Boiling	85 °C, 5 min							
Filtration	filtrated matter + 5 l of 85 °C water left to filtrate for 15 minutes + 11 l of 85 °C water							
Boiling + Hopping	100 °C, 90 min Sladek: 9 g at 0 min and 11 g at 45:00 min; Saaz (ŽPČ):30 g at 90:00 min + 20 min standing under cover							
Filtration	Filtration from the granulated hops through the small sieve							
Cooling	to 12–16 °C							
Add yeast + Aeration	2–3 minutes of aeration							
Fermentation	11 °C, from 7 to 14 days	11 °C, 14 days	4 °C, 14 days	11 °C, 14 days	11 °C, 14 days	11 °C, 14 days	4 °C, 14 days	11 °C, 14 days
Second fermentation in the bottles with 0.5 g of glucose on 1l of beer	11 °C, 20 days	4 °C, up to 60 days						

RESULTS AND DISCUSSION

Chemical analysis of the pilot experiment

We did a chemical analysis of the beer, and the following deviations were found:

We observed that beers that were produced with bread have a high sodium content (see Table 2). A sodium (Na) content of more than 150 mg/l is undesirable. In another study, which analysed 30 different beer samples without bread, sodium content was not more than 93 mg/l (Michalski et al. 2021).

Likewise, chlorides (Cl-) and sulphates (SO_4^{2}-) in the samples made with bread have increased chemical indicators (see Table 2). In the study by Michalski et al. (2021), we can see that the content of chlorides in 30 samples of different beers ranges from 8 to 235 mg/L. In our experiment, beer made with bread has a much higher chloride content (821–1,200 mg/L).

Mineral elements like K, Mg and Ca in the water influence the taste, colour and durability of beer (Rajkowska 2009). There is currently no law that regulates the amount of those elements in beer.

In the study by Michalski et al. (2021), we can see that the content of K was much lower (87–329 mg/L) in 30 samples of different beers than in our control sample and samples with bread (326–631 mg/L).

Table 2 Chemical composition of beers and the water used for brewing in the pilot experiment

Parameter	water	0:100	20:80	40:60	50:50
pH	7.3	4.6	4.5	4.5	4.4
Cl-	19.9	141	821	1.200	985
SO_4^{2}-	< 0.5	72.4	73.6	55.6	52.6
Ca	98.5	95.5	98.2	152	136
K	1.44	514	631	326	389
Mg	3.46	114	150	107	113
Na	2.73	14.9	450	727	586

Sensorial analysis of the beer after optimisation

The beer's sensory properties are the most evaluated (see Table 3). The increasing amount of bread had a significant effect on the beer rating. Samples 3 and 7 were contaminated by *Leuconostoc mesenteroides*, which is why they had a viscous taste. *Leuconostoc mesenteroides* is a species of lactic acid bacteria associated with fermentation, under conditions of salinity and low temperatures (Özcan et al. 2019).

Table 3 Average values of sensorial parameters after optimisation

Sample	Clearness	Aroma	Fullness	Saturation	Total rating	Defects in taste and aroma
1	faint opal	medium	medium	weak	good	salty
2	faint opal	medium	medium	medium	good	hazel
3	strong opal	medium	medium	medium	very bad	esters
4	turbid	medium	medium	medium	medium	phenolic, diacetyl
5	faint opal	medium	medium	medium	medium	salty, phenolic, diacetyl
6	strong opal	medium	strong	strong	bad	hazel
7	strong opal	medium	medium	weak	bad	esters

CONCLUSION

In the presented research we found out that the increasing the proportion of bread instead of malt above 40% causes poor taste properties of beer.

In the pilot experiment, we were challenged by the weakness in saturation and fullness in the samples of beer that contained bread. We tried to optimise the conditions for brewing to make the beer fuller and saturated with good taste. We provided seven different optimisations, which led to the following results. Samples 1 and 2 were boiled for a longer period than other samples, and they received the best results in the total rating. Also, sample 2 had more saturation than sample 1. The possible reason is that the second sample was fermenting at a low temperature (4 °C). We can see the same in sample 6, which was also fermented at 4 °C: the fullness and saturation were stronger than in sample 5, which fermented at a higher temperature (11 °C). Samples 3 and 7 were contaminated by *Leuconostoc mesenteroides*, which is why they had a viscous taste and received a poor evaluation in the total rating. To conclude, the best option for brewing beer with bread is to boil for a longer period and higher temperatures (65 °C for 60 min + 75 °C for 60 min), as this will help extract more elements from bread and malt. The best first fermentation temperature to achieve robust fullness and saturation is 4 °C.

ACKNOWLEDGEMENTS

The research was financially supported by the internal grant project, 'The perspective of the circular economy of gastronomic waste with regard to the production of beer-based beverages', AF-IGA2021-IP029.

REFERENCES

Brancoli, P. et al. 2020. Environmental impacts of waste management and valorisation pathways for surplus bread in Sweden. Waste Management, 117: 136–145. Available at: https://doi.org/10.1016/j.wasman.2020.07.043. [2021-09-16].

Callow, M. et al. 2006. Estimating Annual Irrigation Water Requirements. Queensland Government Department of Primary Industries and Fisheries.

Hedal, J. et al. 2009. Comparative Life Cycle Assessment of Malt-based Beer and 100% Barley Beer. Novozymes A/S, Denmark. Available at: https://www.novozymes.com/en/about-us/sustainability/lca. [2021-09-16].

Lavilla, J. 2010. The wine, beer & spirits handbook: a guide to styles and service. New Jersey: John Wiley.

Michalski, R. et al. 2021. Major Inorganic Ions in Polish Beers. Bulletin of University of Agricultural Sciences and Veterinary Medicine Cluj-Napoca Food Science and Technology, 78(1): 48. Available at: https://doi.org/10.15835/buasvmcn-fst:2021.0001. [2021-09-16].

Özcan E. et al. 2019. A genome-scale metabolic network of the aroma bacterium *Leuconostoc mesenteroides subsp. cremoris*. Applied Microbiology and Biotechnology, 103(7): 3153–3165. Available at: doi:10.1007/s00253-019-09630-4. [2021-09-16].

Rajkowska, M. et al. 2009. Macro- and microelements in various beers. Zywnosc Nauka Technologia Jakosc (Poland), 2(63): 112–118.

Rodman, A.D., Gerogiorgis, D.I. 2016. Dynamic Simulation and Visualisation of Fermentation: Effect of Process Conditions on Beer Quality. IFAC-PapersOnLine, 49(7): 615–620. Available at: https://doi.org/10.1016/j.ifacol.2016.07.236. [2021-09-16].

Salazar, M.B.T. et al. 2021. Economic and environmental performance of instantaneous water heating system for craft beer production. Food and Bioproducts Processing, 127: 472–481. Available at: https://doi.org/10.1016/j.fbp.2021.04.006. [2021-09-16].

Sarlee, W. et al. 2015. Voedselverlies en verpakkingen. 53–55. Retrieved from OVAM.

Statista. 2021. World barley production from 2008/2009 to 2020/2021. Available at: https://www.statista.com/statistics/271973/world-barley-production-since-2008/. [2021-09-16].

Statista. 2021. Beer production worldwide from 1998 to 2019. Available at: https://www.statista.com/statistics/270275/worldwide-beer-production/. [2021-09-16].

ČSN ISO 6658 (560050) Senzorická analýza - Metodologie - Všeobecné pokyny.

Vyhláška č. 252/2004 Sb., kterou se stanoví hygienické požadavky na pitnou a teplou vodu a četnost a rozsah kontroly pitné vody. In Sbírka zákonů České Republiky. Available at: https://www.zakonyprolidi.cz/cs/2004-252. [2021-09-16].

Reduction of weight loss after defrosting of meat using a gelatin-based coating

Jakub Martinek[1], Robert Gal[2], Pavel Mokrejs[1], Kristyna Suchackova[2]
[1]Department of Polymer Engineering
[2]Department of Food Technology
Tomas Bata University in Zlin
Vavreckova 275, 760 01 Zlin
CZECH REPUBLIC

j_martinek@utb.cz

Abstract: Freezing is one of the methods to extend the storage time of meat. However, the negative phenomenon is the weight loss that occurs after its thawing. The main goal of this paper is to reduce these losses by using gelatine coatings. Poultry processing by-products, such as paws, have prepared gelatine with a proteolytic enzyme (Protamex). The meat was immersed in gelatine solution (8% gelatine, 10% glycerol and 1% glutaraldehyde). Losses in uncoated samples ranged from 0.42 to 3.84%, depending on the freezing rate and defrosting method. From the obtained weight loss results, for all tested combinations of freezing and thawing, it was found that the application of a gelatine coating had a positive effect on the reduction of weight losses after thawing of meat. The most significant losses occurred at -18 °C and defrosting in the microwave, with an average of more than 2% lower when the coating was applied. According to the results, freezing at -80 °C and defrosting in a refrigerator appeared to be the most considerate way of storing and processing meat. The uncoated sample weighed 0.42% less after defrosting, while the coated samples had an average weight loss of 0.33%. Due to the above results, the gelatine-based coating is suitable for eliminating meat juice losses.

Key Words: coatings, poultry by-products, gelatine, weight loss, beef

INTRODUCTION

Freezing meat is one of the possible technological steps that can be used to extend its shelf life. Unfortunately, this process is accompanied by side effects such as ice crystals in the meat structure. Depending on the freezing temperature, either a more significant number of smaller ice crystals or a smaller number of but larger crystals may be formed. With the increasing size of the crystals comes a more significant disruption of the fibrous structure of the meat and thus the ability to keep water inside (Devine et al. 2014). After defrosting, the damaged structure cannot keep the meat juice inside the meat and water, and extractives are lost. This work deals with the possibility of applying edible packaging based on gelatine, which could help keep the juice in the meat and reduce water loss during defrosting. (Lovatt 2014).

The raw material for producing the edible coating is gelatine obtained by enzymatic hydrolysis from collagen contained in chicken paws. Consumption of poultry meat has been growing steadily since 2013 when it was around 25 kg per capita in the Czech Republic per year. In 2019 it was already 30 kg (Czech Statistical Office 2020). However, by-products such as bones, tendons, paws or heads have no significant use because they cannot be processed in the food industry (Seong et al. 2015). Despite the high content of valuable proteins, by-products were traditionally added to feed mixtures or burned without much benefit (Míková 2013). However, companies producing meat products are increasingly aware that these by-products have potential economic benefits. Therefore, processes (adsorption, membrane technology) are being used to separate other valuable substances from the by-products for further processing (Zhang et al. 2020, Przybylski et al. 2020).

Gelatine can be prepared by partial hydrolysis of collagen. Traditional methods of making gelatine are using acids and bases. However, an enzymatic production method has been used in this paper, which is more environmentally friendly but not more environmentally friendly.

Our department has long been dedicated to processing poultry by-products into collagen and its subsequent enzymatic hydrolysis to gelatine. This contribution offers the possibility of using the obtained gelatine as a protective coating in freezing meat. The paper aimed to test the effect of gelatine obtained from chicken paws in the form of a coating on the size of the weight loss of meat after defrosting.

MATERIAL AND METHODS

Chicken paws (2 kg) were provided by Raciola s.r.o. Uherský Brod and beef sirloin (5 kg) by Steinhauser, s.r.o.

Appliances, tools and chemicals

WTB Binder dryer, shaker LT2 and 3, pH meter WTW 526, Kern 770 electronic analytical laboratory scale, Kern 440–47 electronic laboratory scale, Schott Garate GMBH heating plate with a magnetic stirrer, Schott cooker, muffle furnace Nabertherm, refrigerator, mixer Eta, stopwatch, gas burner, desiccator, Sevens - LFRA analyzer, thermostat Thermo Hauke, Thermo Spectronic Helios ε; vacuum machine Henkelman vacuum systems, freezer Arctiko, microwave Whirlpool, bags for vacuum packaging, laboratory and kitchen equipment.

0.2M NaCl, 0.03M NaOH, petrol ether, ethanol, enzyme Protamex (Bacillus protease complex developed by Novozymes for hydrolysis of food proteins; declared activity 1.5 AU/g), glycerol, glutaraldehyde.

Processing of chicken paws into gelatine

Separation of soluble proteins (albumins, globulins and glutelins) was performed according to the procedure from a previously published work, only with minor modifications (Du 2013). The material was defatted in a 1 : 1 mixture of ethanol and petroleum ether. The raw material was shaken with the above mixture in a ratio of 1 : 6 for three days, with the solvent being changed every 24 hours.

The remaining material was dried for four days at 35–40 °C. The tissue was then spread on a plate and left in a fume hood to evaporate the remaining solvent. The raw material was mixed with distilled water in a ratio of 1 : 10, and the pH was adjusted to 6.5–7.0. Then the proteolytic enzyme Protamex was added in an amount of 0.4% to the collagen dry matter, and the mixture was shaken for 15 hours. The washed material was mixed with distilled water in a ratio of 1 : 8, and gelatine was extracted from the mixture after heating at 65 °C for 4 hours. The gelatine solution of the first fraction separated from the solid tissue residue was brought to a boil for 5 minutes and dried at 45 °C for about two days. After extraction of the first fraction of gelatine, the solid tissue residue was poured mixed with distilled water in a ratio of 1 : 7. The second fraction was extracted from the mixture after heating at 85 °C for 4 hours. The gelatine solution of the second fraction was boiled, boiled for 5 minutes and dried at 45 °C for two days.

Film preparation

The coating was prepared by dissolving 8% gelatine in water with stirring and heating. Glycerol (10% by weight of gelatine) and glutaraldehyde (1% by weight of gelatine) were added to the solution.

Samples preparation

Slices approximately 2.5 cm wide and 200 g in weight were cut from a nineteen-month-old beef. For the whole experiment, 20 slices of meat were used, immersed in a solution of gelatine, glycerol and glutaraldehyde.

The meat samples prepared in this way were weighed, packaged and, with the help of a vacuum device, they were partially sucked out of the air (-0.6 bar). The packaged samples were frozen at two temperatures (-18 ± 2 °C, -80 ± 2 °C) and stored at this temperature for two weeks. Part of the samples was thawed in the refrigerator (R) at a temperature of 4 ± 2 °C and the other half of the samples in a microwave oven (MW), where the defrosting process lasted 15–20 min.

Thawed meat was found to lose weight, which is often most affected by freezing and subsequent thawing temperatures.

Measurement of weight losses

Defrosting of the samples was followed by transport, and the values were re-recorded. The weight losses were therefore determined from the weights of the meat before freezing and after thawing according to the equation:

$$WL = \frac{m_F - m_D}{m_F} \cdot 100$$

WL is the weight loss (%), m_F is weight before freezing, m_D is weight after defrosting.

RESULTS AND DISCUSSION

The values obtained are given in Table 1–4 and divided according to the type of coating used, the freezing temperature, and the defrosting method. For comparison to the effect of the gelatine coating, slices of meat without coating were subjected to the same experiment and loss values are listed on the last row of each table.

Table 1 Weight loss of meat frozen at -18 °C and defrosted in the refrigerator

Sample	Weight before freezing (g)	Weight after defrosting (g)	Weight loss (%)
1	198.82	195.70	1.57
2	210.27	207.17	1.47
3	159.07	157.80	0.80
4	168.06	167.35	0.42
5	284.50	275.92	3.02

The first group of samples presented is shown in Table 1. The average weight loss of samples frozen at -18 °C and thawed in a coated refrigerator was 1.07%, while the uncoated sample showed a loss of almost 2% higher. Of the selected freezing temperatures, this is lower, i.e. the freezing was slower. Of the selected freezing temperatures, this is lower, i.e. the freezing was slower.

Thus, the water in the samples formed larger crystals inside the meat, which disrupted the structure of the meat. On the other hand, slow thawing and application of coatings were able to reduce weight loss significantly.

Table 2 Weight loss of meat frozen at -80 °C and defrosted in the refrigerator

Sample	Weight before freezing (g)	Weight after defrosting (g)	Weight loss (%)
1	220.05	219.51	0.25
2	219.40	218.82	0.26
3	209.49	208.69	0.38
4	209.01	208.08	0.44
5	204.84	203.98	0.42

The results of the combination of freezing at -80 °C and thawing the refrigerator are shown in Table 2. In terms of weight loss, this method is the gentlest to the meat. At the same time, the effect of the coating was the least noticeable in this case. The uncoated sample lost only 0.42% of its original weight after thawing in the refrigerator, while the coated samples had an average loss of 0.33%. In this case, there was faster freezing so that the individual flight crystals were smaller and did not disturb the structure of the meat so much. Moreover, in combination with slow thawing, the most negligible losses between the remaining groups were achieved. The disadvantage, however, is the time-consuming nature of such storage and subsequent preparation of meat and the economic side of things when using more powerful freezers.

The results shown in Table 3 showed the highest loss compared to the other samples. Coated samples had an average weight loss of 1.66%. In comparison, the uncoated sample of 3.84% had a positive effect and eliminated the effect of slow freezing (large ice crystals and disruption of meat structure) and rapid defrosting (meat structure did not gradually adapt to melting crystals). By applying the coating, the samples approached the values of the samples thawed in the refrigerator.

Table 3 Weight loss of meat frozen at -18 °C and defrosted in the microwave

Sample	Weight before freezing (g)	Weight after defrosting (g)	Weight loss (%)
1	162.53	160.37	1.33
2	191.17	187.03	2.17
3	219.23	217.37	0.84
4	169.51	165.59	2.31
5	171.29	164.71	3.84

Table 4 Weight loss of meat frozen at -80 °C and defrosted in the microwave

Sample	Weight before freezing (g)	Weight after defrosting (g)	Weight loss (%)
1	214.58	212.73	0.86
2	202.14	201.04	0.54
3	162.00	160.91	0.67
4	166.29	165.52	0.46
5	158.15	155.39	1.75

The weight losses from the last set of samples, which were frozen at -80 °C and thawed in the microwave, are shown in Table 4. The coating application eliminated the loss of water from the meat by almost onethird of the weight loss in uncoated meat. The freezing temperature alone had a positive effect, but after rapid thawing in the microwave, the untreated sample lost 1.75% of its original weight. In contrast, for coated samples, this loss dropped to 0.63% on average. Although the values are not as low as defrosting in the refrigerator, the coating still significantly affects weight loss.

Figure 1 Weight loss of meat after defrosting depending on freezing temperature and method of defrosting

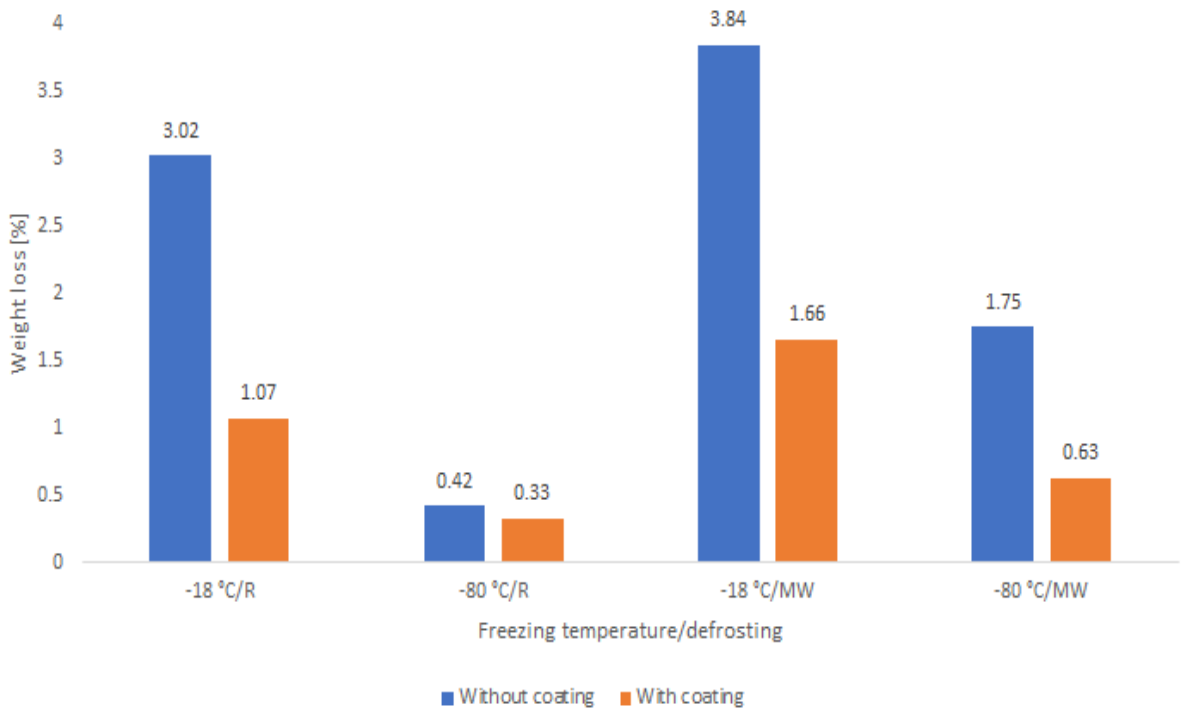

The second most suitable method of storing meat is again at -80 °C and defrosting in the microwave, then freezing at -18 °C and defrosting in the refrigerator. Figure 1 shows the average weight losses depending on the freezing and defrosting method for comparison; in addition to the combination of lower temperature and slow defrosting in the refrigerator, half of the lower weight losses were achieved with the remaining sets of gelatine-coated samples.

It can also be seen from Figure 1 that the freezing temperature has the most significant effect on weight loss. The defrosting method also affects the number of losses, but the effect of the factor is smaller than in the case of the freezing rate.

The minor weight losses occurred with rapid freezing at -80 °C and thawing in the refrigerator at four ± 2 °C. Higher weight losses occurred when frozen at -18 °C and thawed in the refrigerator. At such a temperature, ice crystals are formed, which are larger and disrupt the structure of the meat fibre so that a more significant amount of meat juice is washed out. The second environment in which the meat was thawed was a microwave oven. More minor weight losses occurred in meat frozen at -80 °C, but the weight losses were more significant than when thawed in the refrigerator. The reason is the rapid melting of ice crystals.

The most significant losses occurred in slowly frozen meat at -18 °C and thawed in a microwave oven. The rapid melting of large ice crystals brought with it the enormous amount of washed-out meat juice, and therefore this method was evaluated as the worst possible method of freezing and thawing meat.

According to Rahman, H. et al. 2014, meat thawed in the refrigerator should have a maximum weight loss of up to 3.49% and Oliveira, M. R., et al. 2015 state that 3.30% weight loss of meat is acceptable. The values of this experiment were still lower than in these articles. This may be due to the higher freezing temperature. Oliveira, M. R., et al. 2015 also indicate the limit value for meat thawed using a microwave oven. Their set value reaches up to 7.29% (Oliveira et al. 2015, Rahman et al. 2014).

Şahin, A. et al. 2021 in their study, compared the effect of slaughter weight on the composition of fatty acids and other qualitative parameters of meat. One of them was weight loss after thawing, which was observed in two groups. In meat from animals heavier than 504 kg, the loss was 4.35% greater than in the group up to 503 kg. The loss values were generally higher than in this study due to differences in methodology and meat used. (Şahin et al. 2021).

Cheng, A. et al. 2019 examined how repeated freezing and thawing affects the quality of meat in terms of quantity and distribution of water. After the first cycle, the weight losses were about 4%, which corresponds to the results of the uncoated samples of this research (Cheng et al. 2019).

Sales, L.A. et al. 2020 compared the technological parameters of beef (including losses after thawing) in chilled, thawed and radiation-treated meat. Beef in this experiment had a loss of about 7% after thawing, which is 3% higher than in this study (Sales et al. 2020).

CONCLUSION

Samples to which a protective coating was applied before freezing showed the most negligible weight loss after thawing. Uncoated samples were used for verification, whose weight after thawing was higher than for coated samples. The results show that the most suitable freezing method is temperatures below -18 °C, and the best environment for thawing is a refrigerator. Defrosting in a microwave oven is not very suitable and entails weight losses of up to 2%.

The above combination of freezing at -80 °C and defrosting in a refrigerator, in which the effect of the coating also manifested itself, but to a lesser extent, can be disadvantageous in practice in time and energy. By using coatings, the loss values for the other freezing and defrosting combinations were very close to the values obtained by this method. Thanks to the application of this coating, it is thus possible to change the freezing temperature or the method of defrosting without this modification of the conditions being associated with a sharp increase in weight losses.

ACKNOWLEDGEMENTS

The research was financially supported by the Internal Grant Agency of the Faculty of Technology, Tomas Bata University in Zlin, ref. IGA/UTB/FT/2021/007.

REFERENCES

Cheng, S. et al. 2019. Influence of multiple freeze-thaw cycles on quality characteristics of beef semimembranous muscle: With emphasis on water status and distribution by LF-NMR and MRI. Meat Science [Online], 147(2019): 44–52. Available at: doi:10.1016/j.meatsci.2018.08.020. [2021-10-29].

Czech Statistical Office. ©2020 Food consumption - 2019 [Online]. Available at: https://www.czso.cz/csu/czso/spotreba-potravin-2019. [2021-07-14].

Devine, C.E. et al. 2014. Red Meats. In Encyclopedia of Meat Science, New Zeeland: Meat Industry Research Institute of New Zealand, pp. 51–82.

Du, L. et al. 2013. Physicochemical and functional properties of gelatins extracted from turkey and chicken heads. Poultry Science, 92(9): 2463–2474.

Lovatt, S.J. 2014. Refrigeration and freezing technology. In Encyclopedia of Meat Science, New Zeeland: Meat Industry Research Institute of New Zealand, pp. 178–234.

Míková, K. 2013. Strojně oddělené drůbeží maso. Výživa a potraviny [Online], 68(3): 42–43. Available at: https://www.bezpecnostpotravin.cz/strojne-oddelene-drubezi-maso.aspx. [2021-07-21].

Oliveira, M.R. et al. 2015. Meat Quality of Chicken Breast Subjected to Different Thawing Methods. Brazilian Journal of Poultry Science, 17(2): 165–172.

Przybylski, R. et al. 2020. Electroseparation of Slaughterhouse By-Product: Antimicrobial Peptide Enrichment by pH Modification. Membranes [Online], 10(5): 1–14. Available at: https://doi.org/10.3390/membranes10050090. [2021-10-28].

Rahman, M.H. et al. 2014. Effect of Repeated Freeze-Thaw Cycles on Beef Quality and Safety. Korean Society for Food Science of Animal Recources, 34(4): 482–494

Şahin, A. et al. 2021. Fatty acid profilies and some meat quality traits at different slaughter weights of Brown Swiss bulls. Tropical Animal Health and Production [Online], 53(3): 1–10. Available at: doi:10.1007/s11250-021-02817-w. [2021-10-29]

Sales, L.A. et al. 2020. Effect of freezing/irradiation/thawing processes and subsequent aging on tenderness, color, and oxidative properties of beef. Meat Science [Online], 163(2020): 1–9. Available at: doi:10.1016/j.meatsci.2020.108078. [2021-10-29].

Seong, P.N. et al. 2015. Characterization of Chicken By-products by Mean of Proximate and Nutritional Compositions. Korean Journal for Food Science of Animal Resources, 35(2): 179–188.

Zhang, W. et al. 2020. Enhanced adsorption/extraction of five typical polycyclic aromatic hydrocarbons from meat samples using magnetic effervescent tablets composed of dicationic ionic liquids and $NiFe_2O_4$ nanoparticles. Journal of Molecular Liquids [Online], 315(2020): 1–10. Available at: doi:10.1016/j.molliq.2020.113682. [2021-10-28].

Quality of malt made from current and historical malting barley varieties

Michaela Nemethova[1], Vratislav Psota[2], Tomas Gregor[1]
[1]Department of Food Technology
Mendel University in Brno
Zemedelska 1, 613 00 Brno
[2]Research Institute of Brewing and Malting
Mostecka 971/7, 614 00 Brno
CZECH REPUBLIC

xnemeth1@mendelu.cz

Abstract: Breeding changed quality of malting barley. Historical barley varieties and malt made from them have not been sufficiently researched. The aim of this study was to measure the parameters related to cytolytic (friability, β–glucans in wort), proteolytic (relative extract at 45 °C, Kolbach Index) and amylolytic modification of grain (final attenuation, diastatic power, malt extract). The historical varieties showed lower values of friability, relative extract, Kolbach Index, diastatic power, and malt extract and they contained more nitrogenous substances compared to the current varieties. Based on the values of malt parameters, the Malting Quality Index was determined: for the Chlumecky variety–1; Stupicky starocesky–2; Bojos–3; Sebastian–3.

Key Words: barley, malt, malting quality index, historical varieties of barley, barley grain modification

INTRODUCTION

Barley (*Hordeum vulgare* L.) is the fourth most cultivated cereal in the world (Carvalho et al. 2021). Spring barley is one of the oldest cultivated plants and has remained an important crop since its domestication (Hoyle et al. 2020).

The quality of barley grain affects its processing and the resulting quality of the final product. In the case of malting barley, the quality of the grain influences the sensory characteristics of beer (taste, colour, foam, colloidal stability, drinkability, fullness), which subsequently determine the success of the final product on the market, and the economic aspects of the individual stages of beer production.

In malting barley, several characteristics are evaluated: subjective, mechanical and physical properties, physiological properties, chemical composition of barley and varietal purity (Basařová 2015).

The quality of malt is evaluated according to the level of cell wall modification, content of soluble nitrogenous substances, activity of the individual groups of enzymes and wort composition. Even and complete cytolytic modification and the required degree of proteolytic modification are essential features in terms of the needs of large-scale production technology. The high extract, the homogeneity of the malt and the effect of malt on the sensory and colloidal stability of the final product are considered to be the basic economic properties of the malt (Psota et al. 2008).

MATERIAL AND METHODS

Characterization of samples

Four samples of Pilsner malt were analyzed. Two samples were made from historical varieties of malting barley – Chlumecky (registered in 1902) and Stupicky starocesky (registered in 1927) and two samples from the current varieties Bojos (registered in 2005) and Sebastian (registered in 2005). All four varieties were grown under the same conditions. The analyses were performed at the Research Institute of Brewing and Malting.

International methods were used to evaluate the quality of malting barley and malt made from it (EBC Analysis Committee 2010, MEBAK 2011).

Recently, the Malting Quality Index (MQI) has been used to assess the quality of malting barley varieties. MQI evaluates the following characteristics: extract, relative extract at 45 °C, the Kolbach Index, diastatic power, final attenuation, friability, β-glucans in wort. Each value of the above given parameters is assigned a number on a 1–9 scale where 9 indicates the optimal values (Psota and Kosař 2002).

RESULTS AND DISCUSSION

Content of nitrogenous substances in unmalted barley

The content of nitrogenous substances in unmalted barley grain was higher in the historical varieties 12.3–12.6%; in the current varieties Bojos and Sebastian it was in the range of 11.1–11.8%. Most historical varieties tend to accumulate more nitrogen in the grain (Marečková et al. 2010). The high content of nitrogenous substances in the samples of unmalted grain significantly affected other technological parameters (namely the extract content and the Kolbach Index).

Malting barley parameters related to cytolytic modification

During the malting process, the cell walls of the grain are modified. Optimal cytolytic modification allows easier enzymatic breakdown of starch during mashing. Insufficient cytolytic modification leads to losses during wort preparation and to the conversion of high molecular weight β–glucans to a soluble form, which can lead to problems in wort drainage (Psota et al. 2008).

Table 1 Cytolytic modification

Parameter	Unit	Chlumecky	Stupicky starocesky	Bojos	Sebastian
Friability	%	65.4	61.0	82.2	78.4
β–glucans in wort	mg/l	170	239	123	213

Table 1 shows that the degradation of cell walls was significantly lower in the historical varieties (friability 61–65%). Degradation of cell walls in modern varieties was significantly faster and was at the level of 78–82 %. The low level of cell wall degradation in the studied historical varieties indicated a higher content of β–glucans in wort, this, however, was not confirmed. β–glucans in wort in the current and historical varieties was at similar levels (Psota and Kosař 2002).

Malting barley parameters related to proteolytic modification

The activity of proteolytic enzymes leads to the breakdown of insoluble nitrogenous substances into soluble products. The nitrogen content of the wort affects the multiplication of the yeast during fermentation. The yeast deficiency in wort results in the formation of undesirable compounds (e.g. diacetyl). Too high content of nitrogenous substances leads to excessive degradation of these substances, which together with an excess of some amino acids (e.g. lysine, arginine, histidine) can have a negative effect on the foam quality and stability. Beers with higher amino acid contents are more prone to microbial spoilage and may have odour defects. Nitrogenous substances with medium and higher molecular weight in wort affect foaming and fullness of beer and can have a negative effect on the beer colloidal stability (Kosař et al. 2000).

Table 2 Proteolytic modification

Parameter	Unit	Chlumecky	Stupicky starocesky	Bojos	Sebastian
Relative extract at 45 °C	%	29.1	26.3	32.8	35.9
Kolbach Index	%	33.1	29.3	38.3	43.8

The relative extract at 45 °C contains information on the cytolytic and proteolytic activity available in wort. The Kolbach Index indicates the amount of nitrogenous substances which migrated

to the wort. Significantly higher and lower values of all the features mentioned are not desirable and can cause technological problems (Psota et al. 2008).

Proteolytic modification was also lower in the historical varieties compared to the representatives of the current varieties (Table 2). The optimal values of the Kolbach Index are 42–48%. Only Sebastian met the criteria. Bojos was included among the varieties recommended for the production of beer with the protected geographical indication "České pivo". A lower level of proteolytic modification is required for this group of varieties (European Union 2008). For relative extract at 45 °C, the optimal value is 40–48%, this value was met only by Sebastian (Psota and Kosař 2002). Other studied varieties showed low values.

Malting barley parameters related to amylolytic modification

Amylolytic modification is characterised by diastatic power, final attenuation and malt extract. Final attenuation gives information on how much sugar can be fermented by brewer's yeast. Too high values are not suitable as they cause an empty taste of the beer. Diastatic power expresses the activity of the amylolytic enzymes, mainly beta-amylase. The current varieties did not have any problem with this parameter. Extract reflects the total amount of carbohydrates in the wort. This is the most important economical feature. Low values of the extract can lead to economic losses as low values of the extract content can again cause an empty taste of the produced beer (Psota et al. 2008, Basařová 2015).

Table 3 Amylolytic modification

Parameter	Unit	Chlumecky	Stupicky starocesky	Bojos	Sebastian
Final attenuation	%	76.8	81.1	80.1	80.0
Diastatic power	WK	193	256	361	321
Extract	%	76.8	77.0	82.1	81.4

The acceptable values for the final attenuation are 79–82%. All varieties except Chlumecky met this value (Table 3). Chlumecky had lower final attenuation of 76.8%. In the case of diastatic power, higher values are more appropriate. Chlumecky also exhibited very low values of diastatic power – 193 WK (Windisch-Kolbach). The optimal values for malt extract range from 81.5 to 83%. All the varieties tested had a lower extract (Psota and Kosař 2002).

Malting Quality Index (MQI)

Based on the data above, the individual characters were assigned values and the MQI (Psota, Kosař 2002) was calculated from them: for for the Chlumecky variety–1; Stupicky starocesky–2; Bojos–3; Sebastian–3.

CONCLUSION

In our contribution, the changes in the quality of malting barley caused by breeding were described. We assessed the quality of Pilsner malt made from two historical (Chlumecky, Stupicky starocesky) and two currently bred malting varieties (Bojos, Sebasian).

We examined the parameters related to cytolytic (friability, β-glucans in wort), proteolytic (content of nitrogenous substances, relative extract at 45 °C, Kolbach Index), and amylolytic modification of barley grain (final attenuation, diastatic power, malt extract).

Significant differences between the historical and current varieties were detected. The historical varieties exhibited lower values of friability, relative extract, the Kolbach Index, diastatic power and malt extract and a higher content of nitrogenous substances. From a practical point of view, the most significant feature is the higher extract in the current varieties. The higher content of nitrogenous substances influenced other technological parameters (mainly the extract content and the Kolbach Index).

Based on the obtained values, the Malting Quality Index was determined: for the Chlumecky variety–1; Stupicky starocesky–2; Bojos–3; Sebastian–3. The presented data showed that better quality of malting barley varieties was achieved by breeding and thus, better malt and better beer can be produced.

ACKNOWLEDGEMENTS
This research was financially supported by the grant agency of the Ministry of Agriculture of the Czech Republic (NAZV), project number QK1910197 and by the operation programme INTERREG V-A Slovenská republika – Česká republika, project number 304011P506.

REFERENCES
Basařová, G. 2015. Vlastnosti sladovnického ječmene. In Sladařství – Teorie a praxe výroby sladu. Praha: Havlíček Brain Team, pp. 97–144.

Carvalho, G.R. et al. 2021. Physical properties of barley grains at hydration and drying conditions of malt production. Journal of Food Process Engineering [Online], 44(4): 1–4. Available at: https://doi.org/10.1111/jfpe.13644. [2021-09-01].

EBC Analysis committee. 2010. Analytica – EBC. Germany, Fachverlag Hans Carl.

European Union. 2008. Council Regulation (EC) No 510/2006 'České Pivo'. In Official Journal of the European Union. L 276/27. Available at: https://eur-lex.europa.eu/legal-content/EN/TXT/HTML/?uri=CELEX:32008R1014&from=en. [2021-09-10].

Hoyle, A. et al. 2020. Relation between specific weight of spring barley and malt quality. Journal of Cereal Science [Online], 95: 1–8. Available at: https://doi.org/10.1016/j.jcs.2020.103006. [2021-09-05].

Kosař, K. et al. 2000. Sladovnický ječmen. In Technologie výroby sladu a piva. Brno: VÚPS, pp. 30–63.

Marečková, J. et al. 2010. Agronomical parameters and characteristics of barley genetic resources under the conditions of the forage production area, crop 2010. Kvasny Prumysl [Online], 57(6): 155–160. Available at: https://doi.org/10.18832/kp2009013. [2021-09-10].

MEBAK. 2011. Raw materials: Collection of Brewing Analysis Methods of the Mitteleuropäische Brautechnische Analysenkommission (MEBAK), Germany, Freising-Weihenstephan.

Psota, V., Kosař, K. 2002. Malting quality index. Kvasny Prumysl [Online], 48(6): 142–148. Available at: https://doi.org/10.18832/kp2002011. [2021-09-10].

Psota, V. et al. 2008. Ječmen. In Kvalita rostlinných produktů na prahu 3. tisíciletí. Praha: VÚPS, pp. 116–132.

Encapsulation of fortifying ingredients in colloidal emulsions of lecithin

Kristyna Ondrouskova[1], Barbora Lapcikova[1,2], Lubomir Lapcik[1,2], Lilianna Szyk Warszynska[3], Romana Buresova[1]
[1]Department of Food technology
Tomas Bata University in Zlin
nam. T.G. Masaryka 5555, 760 01 Zlin,
[2]Department of Physical Chemistry
Palacky University Olomouc
tr. 17. listopadu 1192/12 771 46 Olomouc
CZECH REPUBLIC
[2]Jerzy Haber Institute of Catalysis and Surface Chemistry
Polish Academy of Sciences
Niezapominajek 8, 30239 Krakow
POLAND

k1_ondrouskova@utb.cz

Abstract: The present contribution focuses on the study of the encapsulation of enrichment components in colloidal dispersions. The research focuses on curcumin and vitamin C as active ingredients that have potential applications in the food industry or pharmaceuticals. Another part is devoted to liposomal encapsulation of active ingredients in colloidal dispersions. Furthermore, the contribution focuses on the study of the stability of liposomal dispersions containing soy lecithin and carboxymethylcellulose as suitable encapsulants for curcumin and vitamin C. The zeta potential values for the vitamin C dispersions ranged from -24 to -27 mV. The zeta potential values for the dispersions with curcumin ranged from -64 to -79mV. The data showed that the dispersion with encapsulated curcumin was approximately 2 times more stable than the dispersion with encapsulated vitamin C.

Key Words: encapsulation, emulsion, curcumin, vitamin C

INTRODUCTION

Vitamin C is a water-soluble vitamin exists in two forms. In a reduced form (ascorbic acid) it is a crystalline powder - and in an oxidized form (dehydroascorbic acid) that allows the release of electrons and explains its intervention in various redox mechanisms. Both forms are in equilibrium with the intermediate, unstable form, the ascorbyl radical. Vitamin C is the most fragile of all vitamins. In contact with water, air and light, it is easily oxidized. It is gradually destroyed by cooking food (Buxeraud and Faure 2021).

Curcumin (1,7-bis(4-hydroxy-3-methoxyphenyl)-1,6-heptadiene-3,5-dione) is a polyphenolic compound that is obtained from the rhizome of the Curcuma longa plant. Many studies have demonstrated the potent antioxidant effects of curcumin. It also exhibits anti-inflammatory, antimicrobial and anticancer effects (Scartezzini and Speroni 2000).Curcumin is characterized by low solubility and stability (very susceptible to oxidation under UV light) (Guo et al. 2020).

Encapsulation methods are used to improve the stability and preserve the bioactivity of these compounds. This contribution focuses on encapsulation into liposome, then the effect of the addition of a stabilizer, specifically a carboxymethylcellulose derivative, on the stability of the formed emulsions will be investigated (Nedovic et al. 2011).

Liposomes are formations composed of phospholipid molecules. The success of liposomes as carriers for vitamin C and curcumin are based on the interaction between vitamin C or curcumin and phospholipid molecules (Hudiyanti et al. 2019).

MATERIAL AND METHODS

Chemicals

Vitamin C (Sigma Aldrich, USA), Potassium hydrogen carbonate (Ing. Petr Lukeš, Uherský Brod), carboxymethylcellulose derivative (CMC) (Hercules, USA) Curcumin (50 g, 95% total curcuminoid content, turmeric rhizome, manufacturer Alfa Aesar, LOT 10228603), Lecithin natural (soy granulate 250 g, producer Mogador s.r.o.), Sunflower oil Aro (1liter, Czech trade network), producer Compagnia Alimentare Italiana S.p.A. Ethanol (absolute p.a. 1 liter, producer Ing. Petr Švec PENTA s.r.o.), redistilled water

Encapsulation of vitamin C

Lecithin was dissolved in redistilled water at a defined concentration ratio, mechanically stirred to achieve a smooth dispersion. Potassium ascorbate was formed by mixing ascorbic acid (vitamin C) with potassium hydrogen carbonate and redistilled water. The resulting mixtures were stirred and then placed in the ultrasonic bath. Preparation of carboxymethyl cellulose solution (2% w/w). Five samples were prepared containing a mixture of lecithin and potassium ascorbate, 2% w/w CMC solution and redistilled water in different proportions. The compositions of the samples with encapsulated vitamin C are described in Table 1.

Table 1 Composition of the sample with encapsulated vitamin C

Volume (ml)	Sample				
	1A	2A	3A	4A	5A
Lecithin + potassium ascorbate	9	9	9	9	9
CMC 2% (w/w)	1	2	2.5	3	4.5
Redistilled water	4	3	2.5	2	0.5

Encapsulation of Curcumin

The lecithin solution was prepared in the same manner as for vitamin C encapsulation. For the encapsulation of curcumin, a 1% (w/w) carboxymethylcellulose derivative was chosen as the stabilizer. Curcumin solution was prepared by dissolving 1 g of curcumin in 100 ml of sunflower oil. Six samples of liposomal dispersion were prepared. All samples had the same composition. The differences were only related to the CMC appendage. The compositions of the samples with encapsulated curcumin are described in Table 2.

Table 2 Composition of samples with encapsulated curcumin

Volume (ml)	Sample					
	1B	2B	3B	4B	5B	6B
Lecithin	10.3	10.3	10.3	10.3	10.3	10.3
Curcumin	0.5	0.5	0.5	0.5	0.5	0.5
1% CMC(w/w)	0	0.2	0.4	0.6	0.8	1
Redistilled water	23	23	23	23	23	23

Determination of liposome particle size by dynamic light scattering

The effective diameter of liposomal particles was determined by dynamic light scattering (DLS) using Zeta Plus (Brookhaven Instruments. USA). Samples were diluted with redistilled water at a ratio of 1:10. All experiments were performed 60 minutes after their preparation. Measurements were performed at room temperature of 25 °C. The measurement parameters were set as follows: refractive index 1.330, wavelength 658 nm, detection angle 90°. Each measurement was repeated four times.

Determination of the Zeta potential (ζ-potential)

Zeta potential was measured using the Zeta Plus instrument (Brookhaven Instruments, USA). Individual samples were diluted 1:10 with redistilled water. The pH of the measured samples was 5.5. The measurements were carried out at room temperature. The measurements were converted to zeta potential by applying the Smoluchowski mathematical model and are presented as the average of five replicate cycles, each of samples were measured five times. Zeta potential was measured by electrophoresis in a capillary cuvette.

Thermal analysis

The thermal behavior of the samples was characterized by differential scanning calorimetry (DSC, Mettler Toledo, Switzerland). The instrument was calibrated using indium as a standard. Approximately (17.0 ± 0.2) mg of the studied samples was placed in aluminum pan, 40 µl. The pans were then hermetically sealed to maintain constant humidity and air conditions during the measurements. The empty pan was used as a reference. Thermal behavior was investigated by heating/cooling temperature program: 1. cycle 25 to -50 °C and 2. cycle range from -40 to 210 °C. Results were represented as peak temperature T_o – onset temperature. T_p – peak temperature. T_e – endset temperature and fusion enthalpy ΔH (J/g).

Measurement of rheological properties

The rheological properties were determined on a Haake Viscometer (Viscometer 6L/R state) in a cylinder-cylinder configuration at a speed of 0.3–200 rpm. The rotational viscometer works on the principle of measuring the force required to rotate a rotating cylinder-shaped body immersed in a liquid. The body is attached to a shaft rotating at a defined speed.

Confocal laser microscopy

The visualization of the encapsulated liposomal micelles was conducted using a Zeiss LSM780 confocal microscope (Germany) equipped with a Plan-Apochromat 63 × /1.4 Oil DIC M27 objective. The image size was set to 134.95 µm × 134.95 µm, and the scanning on the Z-axis was every 0.7 µm. Recorded images were analysed using ZEN software.

Statistical analysis

The obtained results of the experimental measurements were subjected to statistical analysis significance of individual data by ANOVA (α = 0.05 level of significance).

RESULT AND DISCUSSION

Particle size of liposome by dynamic light scattering

Results of the particle size measurements are shown in Figure 1. There are shown changes of the effective diameter obtained from dynamic light scattering measurements as a function of the storage temperature and addition of the CMC solution for vitamin C liposomal micelles dispersions. There was observed an effective particle size diameter (310 ± 30) nm for the room temperature stored samples. With increasing storage temperature, the steady increase of the effective diameter was found. Addition of the CMC did not affect the observed micelles diameter at 25 °C, however for higher temperatures of 40, 50 and 60 °C the exponential increase of the particle size was found. With higher temperature the higher effective diameter was triggered due to the excessive Brownian movement and CMC macromolecular chain expansion and disentanglement. From the latter DLS data there was suggested that the higher CMC addition have a positive influence on stability of the prepared liposomal dispersions (stable for 6 moths). Samples without CMC exhibited phase separation. For the comparison, the blank experiment measurements gave (265 ± 35) nm effective particle size diameter at 25°C. By the particle size of liposomes with encapsulated curcumin as shown in Figure 2, the critical micellar concentration (which is the lowest surfactant concentration at which micelles were formed) was determined. Measurements were carried out only at 25 °C temperature. The critical micellar concentration was determined at an addition of 0.4 ml of CMC corresponding to the concentration of 0.04 g/l (1% CMC). Particle size data presented in the Figure 2 are given as the median surface average diameters.

Zeta potential (ζ-potential)

Magnitude of the zeta-potential affects the colloidal stability of the emulsions. A system with a zeta potential value of ± 30 mV can be considered as being stable. Samples with encapsulated vitamin C (Figure 3) and with the highest addition of CMC (samples 5A) showed the highest zeta-potential (in absolute value), indicating the highest colloidal stability when stored at room temperature (25 °C), but conversely the lowest zeta-potential (in absolute value) and therefore the least stable dispersion system when stored at 60 °C. The figure below shows the higher electrokinetic zeta potential

of the prepared liposomal dispersions stored at 25 °C, with the sample with the highest CMC addition appearing to be the most stable. Since the differences between the measured zeta potentials of the dispersions at different temperatures were only minor, the curves appear to be only slightly skewed from the horizontal x-axis direction. However, neither emulsion exceeded ± 30 mV, indicating that neither emulsion is electrostatically stable. The zeta potential for samples with encapsulated curcumin (Figure 4) increased (in absolute value) with the amount of added CMC. This ranged from a value of -64 mV for the sample that contained no CMC to -79 mV for the sample with 1 mL of CMC. The data shows that the greater the surfactant addition, the higher the zeta potential value (in absolute value) and the higher the dispersion stability. Considering the zeta potential values, we can say that the dispersions with encapsulated curcumin are electrostatically stable.

Figure 1 Particle size of vitamin C dispersion

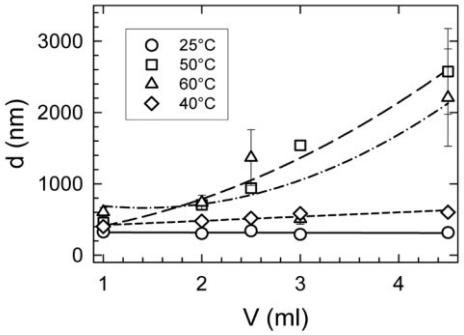

Figure 2 Particle size of curcumin dispersion

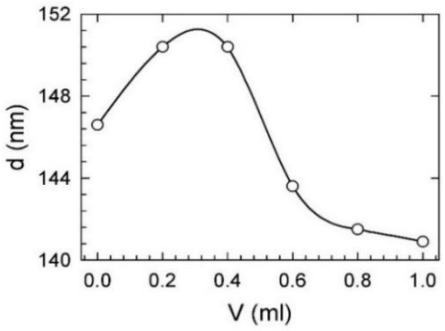

Figure 3 ζ-potential of vitamin C dispersion

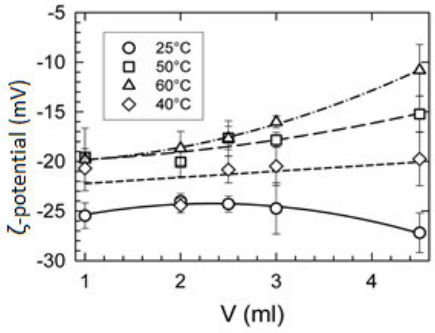

Figure 4 ζ-potential of curcumin dispersion

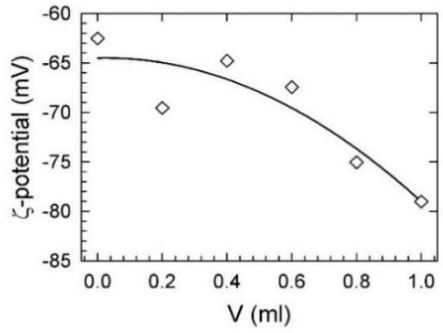

Thermal analysis

DSC method was used for characterisation of thermal behaviour of liposomal dispersions with vitamin C to highlight the state of water and evaluate the strength of interactions between surfactant molecules and the water. Samples represented complex system characterized by the occurrence of the peaks during a cooling cycle (Table 3) and heating cycles (Table 4). The first exothermic peak occurred at cooling cycle in range temperature from -11.345 °C to -16.087 °C which was ascribed to the liposome encapsulated water with vitamin C exhibiting enthalpy of fusion of 177.85 J/g to 187.37 J/g (Table 3). Onset of melting freezing point was decreasing with increasing CMC content.

First endothermic peak occurred at heating cycle ranging from the temperature of -40 °C to + 210 °C was detected at the peak temperatures of 0.674 °C to -0.187 °C with the corresponding fusion enthalpies of 262.43 J/g to 265.9 J/g. This peak was associated with the melting of freezing water present in the dispersion. The freezing temperature of water can therefore be dependent on water and surfactant content, and consequently the strength of their mutual interactions (Gosenca et al. 2013) such as ones present in the internal volume of the micelles or liquid crystalline phases created in the system. Similar effects were found e.g., in the case of the alkyl derivatives of the hyaluronic acid modified with the pendant alkyl chains (Lapcik et al. 2010). As the amount of surfactant was increased, the peak temperature of the frozen water was decreased as well (Table 3), what was supporting our hypothesis of the entrapment of the bound water in the internal volume of the liposomal micelles. It means that the water was strongly bound by polar groups of the surfactant. Second endothermic peak corresponded to the water vaporization. The same trend was observed also during heating cycles

by the appearance of the melting peak. Water vaporization temperature was decreasing with increasing amount of polymer surfactant.

Rheology

Rheological behavior of the studied liposomal dispersions was characterized by the decrease of the relatively high values of the initial apparent viscosity with increasing shear rate, typical for the pseudoplastic dispersions (Lapcikova et al. 2017).

In Figure 5 are shown flow patterns of the studied liposomal dispersions with the encapsulated vitamin C at 25 °C. Here the viscosity was increased with increasing surfactant content. For liposomal dispersion with encapsulated curcumin at 25 °C (Figure 6), the flow curve showed pseudoplastic viscosity pattern at added 0.4 ml (1%) of polymeric surfactant. This phenomenon occurs in more concentrated lyophilic colloids and in some micellar systems with anisometric particles. It is explained by the existence of continuous structures, which represent a transition to entangled network forming gels or higher order liquid crystalline systems (Valenta et al. 2018).

Table 3 DSC of samples with vitamin C – cooling cycle

Samples	Cooling (+25 to -50 °C)			
	Exothermic peak (°C)			ΔH (J/g)
	T_o	T_{p1}	T_e	
1A	-20.317	-11.345	-15.306	177.85
2A	-24.687	-15.395	-20.314	180.51
3A	-24.036	-14.331	-19.650	188.54
4A	-20.633	-11.799	-18.811	186.24
5A	-24.918	-16.087	-20.975	177.37

Table 4 DSC sample with vitamin C – heating cycle

Samples	Heating (-40 to +210 °C)				Heating (-40 to +210 °C)	
	1. endo peak (°C)			ΔH (J/g)	2. endo peak T_{p3} (°C)	ΔH (J/g)
	T_o	T_{p2}	T_e			
1A	-10.204	0.674	7.104	262.43	108.395	1740.64
2A	-10.513	0.231	7.430	262.09	104.937	1736.39
3A	-10.518	0.535	8.095	268.06	104.539	1778.99
4A	-11.122	0.248	7.296	261.51	105.114	1758.55
5A	-10.957	-0.187	6.476	265.90	104.976	1745.51

Figure 5 Flow curve of vitamin C dispersion

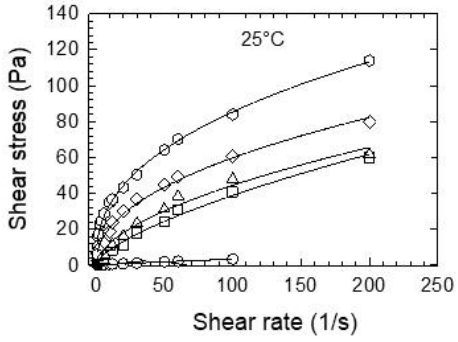

Legend (Figure 5): ○ sample 1A, □ sample 2A, Δ sample 3A, ◊ sample 4A, ⌂ sample 5A

Figure 6 Flow curve of curcumin dispersion

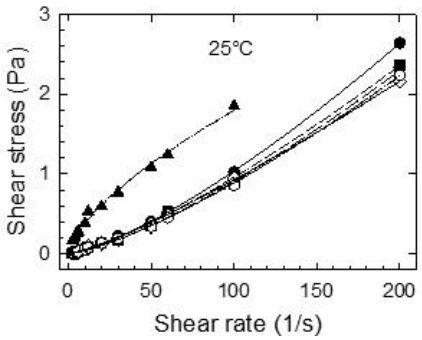

Legend (Figure 6): ●sample 1B, ○ sample 2B, ▼sample 3B, Δ sample 4B, ■ sample 5B, □ sample 6B

Confocal laser scan microscopy

Results of the confocal microcopy (CM) are shown in Figure 7. Here the micelles of encapsulates vitamin C (Figure 7A) and of the curcumin (Figure 7B) were visualized. Samples were stored 48 hours

at 25 °C prior to the analysis. Measured vitamin C dispersions were stored for the period of 4 months at the temperature of 6 °C prior to the CM experiments, curcumin dispersions were stored for the period of 1 months only. That is why the particle size measured by DLS experiments were different in comparison with the CM due to the partial flocculation patterns observed. This result confirmed better dispersion of micelles after sonication used prior to the DLS measurements.

Figure 7 Confocal microscopy images of the encapsulated liposomal vitamin C (A) and of the liposomal curcumin (B)

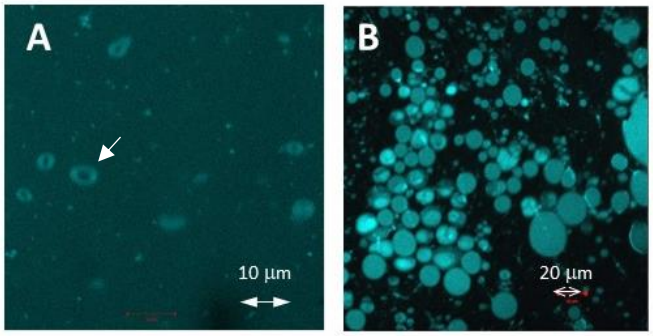

CONCLUSION

It was found in this contribution that the preparation of the encapsulated active ingredients such as vitamin C and curcumin by the proposed method was successfully realized. Prepared colloidal emulsions were of non-Newtonian rheological behaviour at the whole concentration range of the added surfactant. Results of the thermal analysis confirmed existence of the freezing encapsulated water molecules as reflected on the cooling DSC patterns by the appearance of the supercooled water crystallization peak in the temperature range of -11 °C to -16 °C depending on the colloidal system composition. Confocal fluorescence imagining confirmed existence of the prepared micelles encapsulated with the active ingredients studied (vitamin C and curcumin).

ACKNOWLEDGEMENTS

Financial support from the internal grants of Palacky University in Olomouc (project number IGA_PrF_2021_031) and of Tomas Bata University in Zlin (project numbers IGA/FT/2021/004 and IGA/FT/2021/005) are gratefully acknowledged.

REFERENCE

Buxeraud, J., Faure, S. 2021. La Vitamine C. Actualités Pharmaceutiques, 60(604): 24–26.

Guo, Q. et al. 2020. Curcumin-loaded pea protein isolate-high methoxyl pectin complexes induced by calcium ions: Characterization, stability and in vitro digestibility. Food Hydrocolloids, 98: 105284.

Hudiyanti, D. et al. 2019. Encapsulation of Vitamin C in Sesame Liposomes: Computational and Experimental Studies. Open Chemistry, 17(1): 537–543.

Lapčík, L. et al. 2010. Chemical Modification of Hyaluronic Acid: Alkylation. International Journal of Polymer Analysis and Characterization, 15(8): 486–496.

Lapčíková, B. et al. 2017. Rheological Properties of Food Hydrocolloids based on Polysaccharides. Journal of Polymer Materials, 34(3): 621–635.

Nedovic, V. et al. 2011. An overview of encapsulation technologies for food applications. Procedia Food Science, 1: 1806–1815.

Scartezzini, P., Speroni, E. 2000. Review on some plants of Indian traditional medicine with antioxidant activity. Journal of Ethnopharmacology, 71(1–2): 23–43.

Valenta, T. et al. 2018. Determination of kinetic and thermodynamic parameters of food hydrocolloids/water interactions by means of thermal analysis and viscometry. Colloids and Surfaces A: Physicochemical and Engineering Aspects, 555: 270–279.

Quality of superworm (*Zophobas morio*) fats determined by Raman spectroscopy

Martina Pecova, Boris Pleva, Matej Pospiech
Department of Plant Origin Food Sciences
University of Veterinary Sciences Brno
Palackeho tr. 1948/1, 612 42 Brno
CZECH REPUBLIC

pecovam@vfu.cz

Abstract: Insects with their high content of proteins and fats are among the good-quality sources that can be used for food industry and feed purposes. Fat for use in food or feed industries can be of various origins. To use a new source of fat in food and feed industries, it is necessary to analyse its composition. An important parameter of fat quality is the representation of fatty acids which are a significant element of nutrition. Various representations of fatty acids can be found in conventional sources, such as olive oil, canola oil or lard, as well as in the fat of superworms (*Zophobas morio*). This paper evaluates the composition of fats of animal and vegetable origin from a qualitative point of view and assesses the vibration characteristics of fatty acids of the compared fats. Namely, fatty acids of domestic pig, wild boar, domestic goose, river nutria, domestic sheep, rice, linseed, canola, olive, plant based fat – Hera, sunflower, and superworm were compared. Superworm differs in the following regions of wavenumbers: 599.27 cm/1 from domestic sheep, 720.4 cm/1 from domestic sheep and coconut fat, 796.32 cm/1 from sunflower, coconut, and pig fat, 1022.8 cm/1 from coconut and pig fat.

Key Words: superfood, fatty acids, animal fat, plant oil, edible insect

INTRODUCTION

In recent years, insects have gained a lot of attention in both, feed and foodstuffs areas. They contain high quality proteins, fats and they are an excellent source of micronutrients. Insects, as a quality source of nutrients, can enrich human diet and contribute to animal nutrition. High quality and highly digestible protein has been studied in several publications (DeFoliart 1992, Schlüter et al. 2017). The high energy value is mainly influenced by the fat content. It was found that a higher proportion of fat is present in the larval stages than in adults (Kouřimská and Adámková 2016).

Zophobas morio (Z. morio) contains about 40% fat in 100g dry matter (Rumpold and Schi 2013). In addition, some studies have observed specific formulations. It was demonstrated that it contains 14.4% DM total saturated fatty acids, 10.8% DM monounsaturated fatty acids, and 8.6% DM polyunsaturated fatty acids (Benzertiha et al. 2019). The composition of insects as such has great potential for animal and human nutrition. Qualitative and quantitative profile not only of *Z. morio*, but also other species, supports their application. According to the FAO recommendations, dietary fats should account for 15% of total energy, with polyunsaturated fatty acids (PUFA) accounting for 6–11%. Saturated fatty acids (SFA) should not exceed 10% in human nutrition and should be replaced by monounsaturated fatty acids (MUFA) and PUFA. Trans fatty acids (TFA) should account for <1% in human diet.

Polyunsaturated fatty acids include two important groups also called ω 6 (n–6) and ω 3 (n–3). N– 3 PUFA include α-linolenic acid, decosahexaenoic acid (EPA), and eicosapentaenoic acid (EPA). The main one is α-linolenic acid which is one of the essential fatty acids. N-6 PUFAs include linoleic acid and arachidonic acid, both of which are also essential. The main sources of intake of these essential acids are generally nuts, seeds, vegetable oils and some fish. Linoleic acid is significantly present, for example, in sunflower oil or safflower (*Carthamus tinctorius*). EPA and DHA are found primarily in fish and α-linolenic acid in seeds such as lineseed or a hemp (Kaur et al. 2014). Their intake, generally the intake of essential fatty acids, affects the proper functioning of the body, so they should be consumed in the diet in adequate amounts.

The classic method for determining the fat content in biological matrices is the Soxhlet extraction. Gas and liquid chromatography with various types of detectors, which require the use of capillary columns, are then used for qualitative determination. The quality of fats is reflected in the amount and proportion of fatty acids in the sample. Spectroscopy is another analytical method capable of identifying qualitative composition. The big advantage is its low price and easy sample preparation. These techniques include NIR and Raman spectroscopy.

Raman spectroscopy is also a suitable method for detecting adulteration of vegetable and animal fats, based on the different composition of fatty acids. Each lipid has a specific amount of fatty acids that are well detectable by Raman spectroscopy. Proper sample preparation is important for the correct detection of animal fats; in the case of vegetable oils, detection is performed directly from the sample without any modification (Farhad et al. 2009).

Raman spectroscopy is a fast non–destructive method that is able to determine the content of individual components very accurately (Yang and Ying 2011). This method is based on the principle of energy exchange of monochromatic light in interaction with the electron beam of molecules. This monochromatic radiation that the sample scatters can come from the near ultraviolet, infrared, or visible spectrum. In principle, when irradiating a sample with monochromatic radiation, light is scattered, which can be flexible or inelastic. Elastically scattered light has the same frequency and energy as incident light. This phenomenon is called Rayleigh scattering. For inelastic scattering, there are two processes that depend on the energy of the radiation. If the incident radiation has a lower energy, it is Stokes scattering, but if the incident radiation has a higher energy than the energy of the scattered radiation, the so–called anti–Stokes scattering occurs.

Raman process occurs when there is a disproportionate scattering of incident light, which causes a vibrational shift of the wavenumber (Zhu et al. 2015). The so-called Raman spectrum is achieved by irradiating the sample with a laser beam. The resulting spectrum is obtained after filtering out the scattered radiation, which is composed of several weaker bands at a lower frequency level. This filtered spectrum is called Stokes bands. The shift to individual frequencies does not depend on the original radiation, but corresponds to the vibrational frequency of the molecules in the examined sample (Stephanie 2006).

MATERIAL AND METHODS

The samples were divided into two groups according to their nature. One group of samples included biological matrices from which the fat was extracted. These were mainly fats of animal origin. The second group did not require extraction and could therefore be measured directly with Raman spectroscope.

Table 1 Sources of fats and oils for analysis

	Sample	Binomial nomenclature	Extraction
Animal	Domestic pig	*Sus domesticus*	✓
	Wild boar	*Sus scrofa*	✓
	Domestic goose	*Anser anser domesticus*	✓
	Superworms	*Zophobas morio*	✓
	River nutria	*Myocastor coypus*	✓
	Domestic sheep	*Ovis aries*	✓
Plant	Canola	*Brassica napus*	
	Rice	*Oryza*	
	Linseed	*Linum usitatissimum*	
	Coconut tree	*Cocos nucifera*	
	Plant based product Hera	-	✓
	Olive	*Olea europaea*	
	Sunflower	*Helianthus annuus*	

Fats of animal origin, see Table 1, were subjected to extraction. The solvent used was cyclohexane. 15 g of fat was homogenized together with the solvent in a beaker. A weight of 30 g was used to obtain fat from the larvae of superworms. The samples were filtered to remove undesirable substances. The filtrate in a round bottom flask was connected to a condenser assembly. The solvent was constantly evaporated in vacuum at 45 °C. The extracted fat was poured into vials and left in a cool place until the measurement to prevent oxidation and undesired changes. Prior to measurement, the samples were warmed to room temperature. All samples were analysed in duplicate. The prepared samples were measured using Raman spectroscope of HR-TEC-X2-785 (StellarNet, USA). The measuring range of the wavenumber was from 300 to 2000 cm/1. A laser (Ondax, DE) with a wavelength of 785 nm and a power of 91 mW was used for the measurement. The Raman spectroscope was further set to the following parameters, namely

integration time 2000 ms, scan averaging was set to eight times, from which the average measurement value of each sample was obtained and base line correction was chosen as MPLS.

Statistical analysis was performed in 2014.5.03 XLSTAT software (Addinsoft, USA), samples did not have a normal distribution (Shapiro Wilk Normality Test). The non-parametric Kruskal-Wallis test was applied.

RESULTS AND DISCUSSION

Spectral bands caused by vibrations of hydrocarbon chains were recorded within the range from 300 to 2000 cm/1. The data collected show differences between the carbonyl groups and the hydrocarbon chains of the individual samples. Table 2 presents the regions of vibration formation important for the determination of fatty acids (Abbas 2009, Farhad 2009). The region from 700 to 1200 captures the spectral bands of the Raman spectra. These bands are characteristic for the primary structure of C-C bonds and C-O bonds (Baeten et al. 1998). The performed Kruskal-Wallis test showed a high difference of superworm fat from some samples in the regions of 599.27 cm/1, 720.4 cm/1, 796.32 cm/1, and 1022.8 cm/1. In the region of 599.27 cm/1 the superworm differs from sheep, 720.4 cm/1 from sheep and coconut, 796.32 cm/1 from sunflower, pig and coconut, and finally 1022.8 cm/1 from pig and coconut ($p < 0.05$). Bands in this region are not only characteristic for fats. The vibration of molecules provides information about carbon chains and is also caused by non-fatty substances (Baeten et al. 1998).

Table 2 Typical vibrational spectra of Raman spectroscopy of fatty acids

Wavenumber (cm^{-1})	Vibrations
3020	=C-H asymetric stretching
3015	C-H of olefinic simetric stretching vibrations of =C-H groups
2970	C-H stretching vibrations of methyl groups
2855	C-H simetric stretching vibrations of CH_2
1750	C=O stretching in a ester
1670	C=C stretching made of the trans unsaturrated fatty acids
1660	C=C stretching made of the cis unsaturatedfatty acid part
1440	CH_2 scisoring made of the saturated fatty acid part
1295	=CH_2 deformation
1270	=C-H deformation of unconjugated cis C=C

Among other areas, there are significant vibrations arising at 1440 cm/1 corresponding to saturated fatty acids, and 1660 cm/1 and 1670 cm/1 which correspond to unsaturated fatty acids. The Kruskal-Wallis test confirmed the difference between superworm fat and sunflower in saturated fatty acids. The content of unsaturated fatty acids differs from lineseed for both regions of wavenumbers ($p < 0.05$).

Figure 1–3 compare the wavenumbers of 1440 cm/1, 1660 cm/1, and 1670 cm/1 depending on the absorbance measured by Raman spectroscopy. These figures show the similarity of the superworm fatty acid composition with other samples of both animal and vegetable origin. The superworm is located in the middle of the chart for these important regions. Superworm contains the second highest amount of saturated fatty acids from the analysed fats of animal species. It has the highest content of animal fats for cis and trans unsaturated fatty acids. It is surpassed only by the fat of domestic goose. In general, animal fats contain more saturated fatty acids. These acids increase the cholesterol content when consumed and are therefore not very appropriate from the nutritional perspective.

Figure 1–3 Fat samples in different wavenumbers

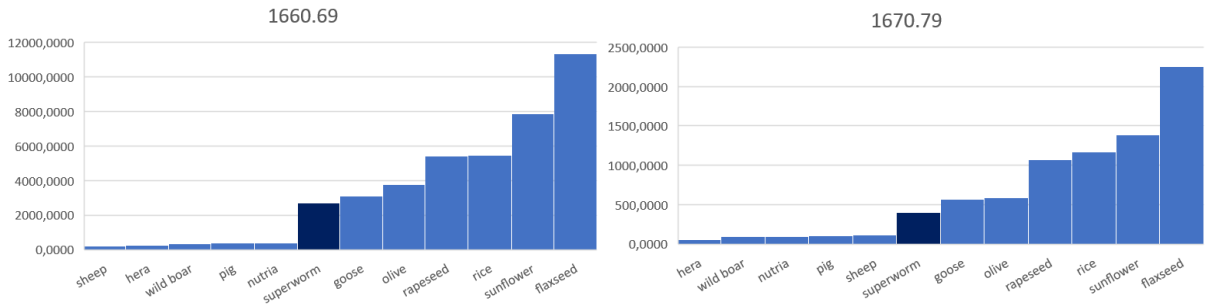

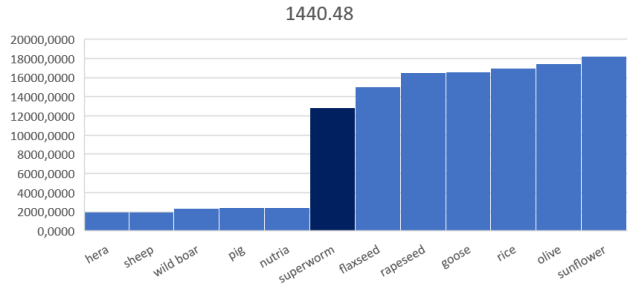

The resulting Raman spectrum appears at different positions for different samples (Gao et al. 2018, Boyaci et al. 2014). The resulting spectra and individual peaks very well characterize the quality of fats. However, it is necessary to take into account the water content of the individual samples and the excess cyclohexane which remains in the extract. Evaluate the quality of fats and identify possible food adulteration, finding out that the product contains a different than the declared fat is possible. Fats can also be assessed by other statistical methods, such as in the study by Kwofie et al. (2020), where the difference in fats of plant origin is very well evaluated using Raman spectroscopy and PCA analysis.

Data based on standards will need to be obtained for final evaluation. The fat of superworms and other insect species will need to be assessed in more detail, which may be the subject of further studies.

CONCLUSION

Based on the analysis of the Raman spectrum, in the fat of *Z. morio* was confirmed a higher content of unsaturated and saturated fatty acids than in some other fats of animal origin. In addition, the Kruskal– Wallis test showed significant differences from sunflower in the area of the resulting vibrations important for saturated fatty acids. Different content was also confirmed for lineseed in the areas for cis and trans orientation of unsaturated fatty acids.

ACKNOWLEDGMENTS

This research was supported by an internal project of the University of Veterinary Sciences Brno 224/2021/FVHE.

REFERENCES

Abbas, O. et al. 2009. Assessment of the discrimination of animal fat by FT-Raman spectroscopy. Journal of Molecular Structure, 924: 294–300.

Baeten, V. et al. 1998. Oil and Fat Classification by FT-Raman Spectroscopy. Journal of Agricultural and Food Chemistry, 46(7): 2638–2646.

Benzertiha, A. et al. 2020. Tenebrio molitor and Zophobas morio full-fat meals as functional feed additives affect broiler chickens growth performance and immune system traits. Poultry Science, 99(1): 196–206.

Boyaci, I. H. et al. 2014. A novel method for discrimination of beef and horsemeat using Raman spectroscopy. Food Chemistry, 148: 37–41.

DeFoliart, G.R. 1992. Insects as human food. Gene DeFoliart discusses some nutritional and economic aspects. Crop Protection, 11(5): 395–399.

Farhad, S.F.U. et al. 2009. Determination of Ratio of Unsaturated to Total Fatty Acids in Edible Oils by Laser Raman Spectroscopy. Journal of Applied Sciences, 9(8): 1538–1543.

Gao, F. et al. 2018. Analytical Raman spectroscopic study for discriminant analysis of different animal-derived feedstuff: Understanding the high correlation between Raman spectroscopy and lipid characteristics. Food Chemistry, 240: 989–996.

Kaur, N. et al. 2014. Essential fatty acids as functional components of foods- a review. Journal of Food Science and Technology, 2289–2303.

Kouřimská, L., Adámková, A. 2016. Nutritional and sensory quality of edible insects. NFS Journal, 4: 22–26.

Kwofie, F. et al. 2020. Differentiation of Edible Oils by Type Using Raman Spectroscopy and Pattern Recognition Methods. Applied Spectroscopy, 74(6): 645–654.

Rumpold, B.A., Schï, O.K. 2013. Nutritional composition and safety aspects of edible insects. Molecular Nutritional Food Research, 57: 802–823.

Schlüter, O. et al. 2017. Safety aspects of the production of foods and food ingredients from insects. Molecular Nutrition and Food Research, 61(6): 1–14.

Stephanie, J.R. et al. 2006. The application of Raman and anti-stokes Raman spectroscopy for in situ monitoring of structural changes in laser irradiated titanium dioxide materials. Applied Surface Science, 252: 7948–7952.

Yang, D., Ying, Y. 2011. Applications of Raman spectroscopy in agricultural products and food analysis: a review. Applied Spectroscopy Reviews, 46: 539–560.

Zhu, H. et al. 2015. Femtosecond coherent anti-Stokes Raman scattering spectroscopy of hydrogen bonded structure in water and aqueous solutions. Spectrochimica Acta Part A: Molecular and Biomolecular Spectroscopy, 151: 262–273.

Effects of a preparation based on a functional collagen polymer on the skin in the periorbital area

Aneta Prokopova[1], Jana Pavlackova[2], Robert Gal[3], Pavel Mokrejs[1]
[1]Department of Polymer Engineering
[2]Department of Fat, Surfactant and Cosmetics Technology
[3]Department of Food Technology
Tomas Bata University in Zlin
Vavreckova 275, 760 01 Zlin
CZECH REPUBLIC

a_polastikova@ft.utb.cz

Abstract: Aging is an inevitable process that manifests itself in the body through a number of physiological changes. They also include the formation of wrinkles and a decrease in collagen in the skin. Poultry protein-rich by-products can be used as a source of collagen. For the cosmetic industry, collagen hydrolyzate is used for its potential. The study tested the effect of a 1% hydrolyzate prepared from chicken stomachs mixed in a gel formulation on the condition of the skin (elasticity, change in skin relief and reduction in the amount of wrinkles). The aim was to determine, using non-invasive *in vivo* testing, whether collagen-based preparations incorporated into a carbopol gel applied topically for 8 weeks could have a positive effect on the biophysical properties of the skin in the periorbital area. For skin elasticity, the resonance times decreased on average from 257 ± 48 A.U. at 218 ± 58 A.U. to the right and from 258 ± 46 A.U. at 219 ± 57 A.U. on the left area. According to the values found, all roughness parameters R1 to R5 also decreased. For parameter R1 there was an average decrease of 38 ± 3%, for parameter R2 there was a decrease of 43 ± 4%, roughness parameter R3 decreased by 39 ± 3%, roughness parameter R4 decreased by 34 ± 5% and finally roughness parameter R5 decreased by 39 ± 5%. Visualization of the area showed a decrease in the amount of wrinkles by 16 ± 2% on the right and by 15 ± 3% on the left. The results of regular application of the formulation with the addition of 1% collagen hydrolyzate confirmed the assumption of increased elasticity, reduced skin roughness and reduced amount of wrinkles in the periorbital area. Chicken collagen could thus find application in the production of antiaging agents.

Key Words: cosmetic formulation, chicken collagen hydrolyzate, skin elasticity, skin relief, wrinkle reduction

INTRODUCTION

Collagen is a natural resource that can be used in the cosmetic field. This scleroprotein is able to reduce the amount of wrinkles and thus slow down the negative effects of aging due to both external and internal influences during human life. Substances based on natural polymers are sought-after components for the development of effective cosmetic products. A significant effect on the treated skin occurs with long-term application of such preparations. Biopolymers are an attractive raw material due to their biocompatibility to the skin and biodegradability in relation to the environment (Peng et al. 2004, Sahana and Rekha 2018).

The skin is the largest organ of the human body, occupies 16% of the body's weight and its surface covers about 1.8 m^2. The skin acts as a protective barrier against mechanical shocks, ultraviolet radiation, toxic substances and has a thermoregulatory, sensory, metabolic and regulatory function (Bensouilah and Buck 2006). The skin consists of three layers; these are the *epidermis*, *dermis* and *subcutis*. The *epidermis* or epithelial tissue represents the uppermost layer of the skin and protects the skin primarily against the penetration of foreign substances. The *epidermis* layer can be divided into four sublayers; namely *stratum basale*, *stratum spinosum*, *stratum granulosum* and *stratum corneum*. In the lowest basal layer of the skin or *stratum basale*, cell division and the formation of new skin cells occur. This is a very important property of the skin. The basal layer produces keratinocytes

and desmosomal proteins that form the skin cytoskeleton (Feather et al. 2020). Keratinocytes are the cornering cells that have the largest presence in the skin and are capable of so-called keratinization, as well as differentiation and migration of cells towards the surface, where they form the outer corner layer of the skin or *stratum corneum* (Caterina 2014). The *dermis* or fibrous joint is the middle part of the skin and is made up mainly of collagen and elastin, which give the skin strength and elasticity. The *subcutis* or subcutaneous ligament consists mainly of the fat part and contains a different number of fat cells in different places (Mallat and Marieb 2005). Aging can be defined as the progressive inability of an organism to maintain its internal environment in a constant, non-declining quality. Aging affects the whole organism, including the skin, where the rate of aging is individual for each individual and is influenced by many factors. The main trigger of the skin's aging process is the lack of nutrients and moisture that enter the skin through the bloodstream, from which the skin takes important nutrients and oxygen. This negative phenomenon reduces skin thickness, slows the rate of keratinocyte renewal, and decreases blood flow through the skin (Kittnar et al. 2020).

Worldwide poultry production is growing year by year. According to the Czech Statistical Office, the consumption of poultry meat in 2020 was around 29 kg/person/year (Czech Statistical Office 2021). With the ever-increasing production of poultry meat, there is also an increasing amount of by-products, which account for up to 30% of total production. As these wastes contain significant amounts of protein, the study seeks to improve procedures for obtaining quality raw material from unused by-products that are not normally edible, thus enabling the raw material to be refined for further applications (Jayathilakan et al. 2012). When wet collagen is heated to a temperature of around 60 °C, significant structural changes occur. This is a first-order transformation, ie the conversion of crystalline biopolymer modification (ordered structure) to amorphous modification (disordered structure) (Slezák and Ryška 2006). Functional polymers, so-called collagen hydrolysates, are formed. Thanks to their properties, they can be used, for example, in the cosmetic industry in the development of formulations with an antiaging effect.

MATERIALS AND METHODS

The process of production of chicken collagen hydrolyzate, the process of preparation of cosmetic gel formulation, and also the selection of volunteers were already published in last year's paper (Polastikova et al. 2020).

Appliances, tools and chemicals

Shaker LT2 (Kavalier, Czech Republic), Schott Gerate GMBH heating plate with stirrer (Schott, Czech Republic), RZR 2020 stirrer (Ika, Germany), analytical laboratory balances (Kern & Sohn, Germany), WTB Binder E-28 dryer-TB1 (Binder, Germany), Braher P22/82 meat cutter (Braher, Spain), MPA 10 station with individual probes, Reviskometr® RV 600, Skin Visiometer® SV 700 USB, vacuum pump VP 45, Visioskop® PC 35 (Courage & Khazaka, Germany), ordinary laboratory glassware, metal sieve, mortar, plastic utensils, PA fabric, scissors, pulp, double-sided adhesive paper rings, plastic sticks and cups, transparent cover foil, paper frames, tweezers.

Protamex 6.0 T enzyme (*Bacillus* protease complex developed for protein hydrolysis in the food industry, meets strict hygiene requirements for collagen extraction; declared activity 1.5 AU/g), carbopol gel, 10% and 0.03 M NaOH solution, water, ice CH_3COOH, make-up remover Bioderma Sensibio H_2O, petroleum ether and ethanol, Jarisch's solution, 0.2 M NaCl, two-component silicone.

The objectives of this work

The study verified the effect of a cosmetic formulation based on collagen on selected biophysical parameters of the skin (skin elasticity, change of skin relief and reduction of wrinkles) using bioengineering non-invasive methods *in vivo*. Collagen was obtained by processing chicken stomachs. It was then incorporated into a gel to treat the periorbital area of the face of a group of volunteers for 8 weeks each morning and evening. The study builds on a previous study (Polastikova et al. 2020), in which the positive effects of chicken collagen on hydration and transepidermal water loss were found. Scientific hypothesis: application of a cosmetic gel formulation in the periorbital area with 1% chicken collagen hydrolyzate can be expected to increase skin elasticity and reduce eye wrinkles.

Statistical analysis

The obtained data were processed and statistically evaluated in Microsoft Excel (2010). From all the results, the arithmetic mean $\bar{x}$ was first calculated and then the standard deviation s was determined according to the following equations (1) and (2).

$$\bar{x} = \frac{1}{N}\sum_{i=1}^{N} x_i \qquad s = \sqrt{\frac{1}{N}\sum_{i=1}^{N}(x_i - \bar{x})^2} \qquad (1)\ and\ (2)$$

Where: $\bar{x}$ – arithmetic mean, N – number of measurements, x_i – measurement value, s – standard deviation

Organization and principle of measurement

The study group consisted of 10 volunteers aged 50 ± 9 years. Wrinkle reduction and skin elasticity in the periorbital area were monitored in February, March and April 2020, always in the same laboratory, under the same conditions (air temperature 21 ± 2 °C and relative humidity 38 ± 2%). The volunteers were acquainted with the organization of the work before the first measurement, and since the measurement was based on international ethical principles of biomedical research with human participants, the volunteers had to sign an individual informed consent and then complete a health questionnaire; at the same time, they could terminate the study at any time and without giving a reason. Prior to the measurement, the participants' skin was cleansed with Bioderma make-up water and Jarisch's solution and then left to stand for 20 minutes. The collagen gel was applied in a thin layer in the morning and evening to the periorbital area for eight weeks. After four weeks, the volunteers came for a control measurement and then after another four weeks for the final measurement.

The principle of measuring the elasticity of the skin with the Reviscometer® RV 600. The device evaluates the elasticity, or elasticity of the skin, using the speed of propagation of the acoustic wave. The measurement is focused on measuring the skin at different angles and the results depend on the anisotropy and isotropy of the skin. The Reviscometer® RV 600 is a device used to measure the elasticity of the skin using two sensors, one sensor emitting a shock wave and the other sensor receiving a wave; it all depends on the speed at which the wool spreads through the skin fibers. An adhesive paper ring is glued to the measuring point on both sides and then a probe is attached, which allows measurements in 30° steps, and the data are immediately displayed on a computer monitor, which is connected to the MPA station. For each volunteer, 13 skin elasticity values were measured for each angle of rotation (0° to 360°) (The Reviscometer® RV 600: Technical charges 2013).

The principle of measuring the change in the relief of wrinkles using Visiometer® SV 700. It is a device that is used to analyze the microrelief of the skin, where light passes through a very thin blue silica replica and is displayed on a CCD camera. The amount of light transmitted depends on the thickness of the silicone casting. The procedure for measuring skin relief was as follows; first it was necessary to glue a double-sided adhesive paper ring to define the measured area and then to prepare a two-component silicone, which consisted of a base and a catalyst. While mixing, the substances were applied in a ratio of 1 : 1 to a plastic cup and the excess air was sucked off by means of a vacuum pump, mixing time 20 s. After solidification, about 5 minutes, the replica was glued to a paper stencil, which was inserted into a Skin Visiometer® SV meter. Roughness parameters R1 to R5 were determined for each replica obtained (Courage & Khazaka: Technical charges 2016).

The principle of measuring wrinkle reduction using Visioscope® PC 35. It is a USB camera equipped with polarizing filters, which is able to take images with a magnification of thirty times, which can then be analyzed. The camera was applied to the periorbital area, then an image was taken, which was immediately evaluated. Using this method, we visually used the photo to determine the smoothing of the skin after eight weeks of application of the collagen formulation and also the percentage of wrinkles in the area. The change in skin relief and the reduction of eye wrinkles were recorded using the CSI-Complete Skin Investigatio program (Courage & Khazaka: Technical charges 2016).

RESULTS AND DISCUSSION

Evaluation of the effect of collagen gel on skin elasticity

The study verified the effect of a cosmetic product with collagen on the elasticity of the skin. Resonance time (RRT) values were obtained at different angles of rotation (0° to 360°) and are reported in reviscometric units [A.U.]. Due to the circular shape of the probe, ray graphs were constructed for better clarity, which show the RRT results for individual angles in the right and left areas of the face; we can see the graphs in Figure 1. It is true that the higher the RRT values, the higher the stiffness or lower elasticity of the volunteers' skin. The data obtained show that the cosmetic formulation had an effect on increasing elasticity, as RRT values decreased in more than 85% of cases during the eight-week application. On average, there was a decrease in RRT from 257 ± 48 A.U. at 218 ± 58 A.U. on the right temple and from 258 ± 46 A.U. at 219 ± 57 A.U. on the left temple. Thus, it has been shown that collagen hydrolyzate in a cosmetic formulation has a positive effect on the skin and also improves its elasticity, as it directly promotes the formation of type I collagen and fibroblasts in the *dermis* layer.

Similarly, in 25 Japanese women taking 7 g of collagen hydrolyzate orally, a significant improvement in forearm elasticity was found. In another innovative study involving 60 women, topical and oral administration of collagen hydrolyzate were combined. After only one month, the condition of the skin improved, specifically the hydration increased. After ninety days, the elasticity of the skin improved and even the wrinkles on the forehead were reduced (Aguirre-Cruz et al. 2020).

Figure 1 Comparison of average RRT values for individual angles of rotation of the probe in the periorbital region

A) Right sleeping area *B) Left sleeping area*

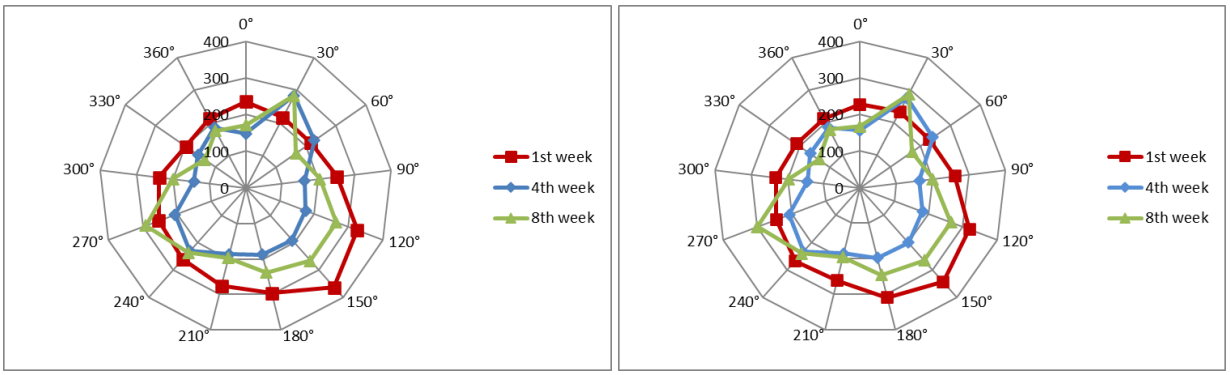

Evaluation of the effect of collagen gel on skin roughness

Skin roughness was evaluated using roughness parameters R1 to R5 obtained by processing replicas removed from the periorbital area using a Visiometer® SV 700. The definition of roughness parameters is based on DIN 4762-4768. The roughness parameter R1 (Rt) defines the distance between the highest peak and the deepest depression; the roughness parameter R2 (Rmax) represents the maximum local roughness from the roughness values of the different segments; the roughness parameter R3 (Rz) calculates the average roughness from the five highest and at the same time from the five lowest segments; the roughness parameter R4 (Rp) indicates the maximum height of the profile and its value is related to the length of the wrinkle, and finally the roughness parameter R5 (Ra) determines the average deviation of the actual profile from the average. The relationship between the individual parameters is: R1≥R2≥R3≥R4≥R5 (DIN 4762–4768: Determination of water content in Honig. Deutsche Industrie Norm). From the average values of the roughness parameters R1 to R5, bar graphs were constructed in individual weeks of measurement for both the left and right areas. It is evident from the graphs that wrinkles were gradually smoothed out due to the cosmetic formulation, as all roughness parameters decreased during the eight-week application. According to the calculated values, there was an average decrease of the parameter R1 by 35 ± 3% (right area) and by 41 ± 2% (left area); roughness parameter R2 decrease by 41 ± 5% (right area) and by 44 ± 3% (left area); roughness parameter R3 decrease by 37 ± 4% (right area) and by 40 ± 2% (left area); roughness parameter R4 decrease by 32 ± 5% (right area) and by 36 ± 4% (left area) and finally roughness parameter R5 decrease

by 32 ± 6% (right area) and by 45 ± 4% (left area). Thus, the results shown in Figure 2 show that collagen has a significant effect on reducing the depth of wrinkles in the periorbital area when applied for a long time.

Proksch et al. tested the effect of collagen hydrolyzate administered orally on the reduction of wrinkles in the periorbital area in women aged 45–65 years. One group received placebo and the other group collagen hydrolyzate. After eight weeks, wrinkles were reduced by 20.1% compared to the placebo-only group (Proksch et al. 2014).

Figure 2 Average values of roughness parameters R1 to R5 in individual weeks of measurement in the periorbital area

A) Right sleeping area

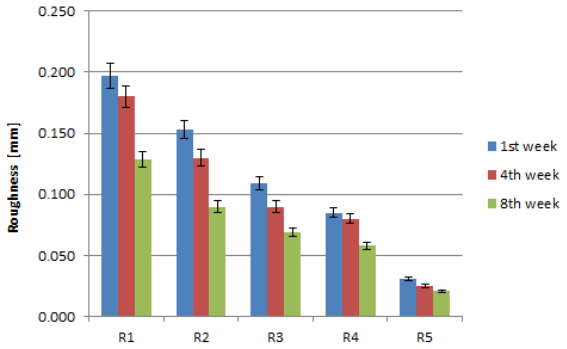

B) Left sleeping area

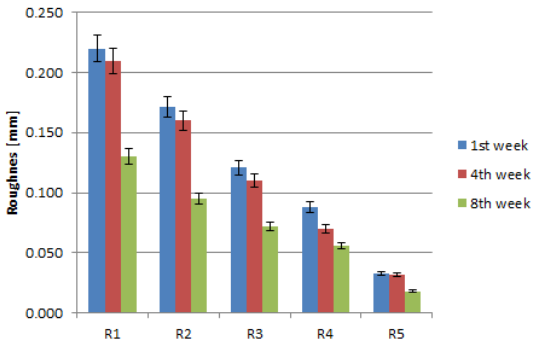

Evaluation of the effect of collagen gel on wrinkle reduction

The amount of wrinkles found after the end of the study correlated with the evaluation of the previous annotated parameters. In volunteers, the mean amount of wrinkles on the right side of the study was 16 ± 2% on the right side and 15 ± 3% on the left side. During the eight-week application, it decreased to 13 ± 1% (right side) and to 12 ± 2% (left side). In Figure 3, we can observe the change in skin relief before and after the eight-week application of the gel formulation in volunteers, in which there was an average reduction in wrinkles from 12.2 ± 0.6% to 10.6 ± 0.4%.

Figure 3 Change in skin relief in the periorbital area before and after application of the gel cosmetic formulation (age of the volunteer 45 years)

A) Before application of the formulation

B) After application of the formulation

CONCLUSION

The study tested the effect of a gel cosmetic formulation enriched with 1% addition of chicken collagen hydrolyzate. During eight weeks of regular two-day application in the periorbital area, skin parameters such as elasticity, skin roughness and wrinkle reduction were monitored. The change of parameters before the application of the model formulation and after the eight-week application was monitored. It was expected to increase skin elasticity, reduce skin relief, and reduce wrinkles.

The obtained results show that all studied parameters improved the condition of the skin in the periorbital area. The improvement in skin elasticity was manifested by a reduction in the values of resonance times in individual directions and thus to an increase in elasticity in more than 85% of volunteers. The decrease in the roughness parameters R1 to R5 showed a reduction in the depth of the wrinkles present, which resulted in a smoother texture of the skin surface. Visualization of the periorbital area revealed a decrease in wrinkles.

The experiments confirmed that the effect of chicken collagen hydrolyzate and due to regular two-day application (morning and evening) will improve the condition of the skin in the periorbital area. The prepared collagen hydrolyzate from chicken stomachs in a gel formulation has demonstrably contributed to alleviating the signs of skin aging by reducing skin irregularities and can be recommended as a suitable preparation for skin regeneration into antiaging cosmetics without health risks.

ACKNOWLEDGEMENTS

This research was financially supported by the Internal Grant Agency of the Faculty of Technology, Tomas Bata University in Zlín, ref. IGA/UTB/FT/2021/007.

REFERENCES

Aguirre-Cruz, G. et al. 2020. Collagen hydrolysates for skin protection: Oral administration and topical formulation. Antioxidants, 9(2): 181.

Bensouilah, J., Buck, P. 2006. Aromadermatology: Aromatherapy in the treatment and care of common skin conditions. 1st ed., London, UK: Routledge.

Caterina, M.J. 2014. TRP channel cannabinoid receptors in skin sensation, homeostasis, and inflammation. ACS Chemical Neuroscience, 5(11): 1107–1116.

Courage & Khazaka: Technical charges. 2016. [Online]. Available at: https://www.courage-khazaka.de/de/. [21-07-21].

Český statistický úřad. 2021. [Online]. Available at: https://www.czso.cz/csu/czso/spotreba-potravin-byla-nejvyssi-od-vzniku-ceska. [21-07-21].

DIN 4762–4768: Bestimmung des Wassergehalts in Honig. Deutsche Industrie Norm.

Feather, A. et al. 2020. Kumar and Clark´s clinical medicine. 10th ed,. Elsevier, UK: © Elsevier 2020.

Jayathilakan, K. et al. 2012. Utilization of byproducts and waste materials from meat, poultry and fish processing industries: a review. Journal of Foof Science and Technology, 49(3): 278–293.

Kittnar, O. et al. 2020. Lékařská fyziologie. 2nd ed., Praha: Grada.

Mallat, J., Marieb, E.N. 2005. Anatomie lidského těla. 1st ed., Praha: Computer Press CP Book.

Peng, Y. et al. 2004. Evaluation for collagen products for cosmetic application. International Journal of Cosmetic Science, 55: 327–341.

Polastikova, A. et al. 2020. The use of chicken collagen hydrolyzate as a functional polymer in cosmetics. In Proceedings of International PhD Students Conference MendelNet 2020 [Online]. Brno, Czech Republic, 11–12 November, Brno: Mendel University in Brno, Faculty of AgriSciences, pp. 371–376. Available at: https://mnet.mendelu.cz/mendelnet2020/mnet_2020_full.pdf. [21-07-21].

Proksch, E. et al. 2014. Oral supplementation of specific collagen peptides has beneficial effects on human skin physiology: a double-blind, placebo-controlled study. Skin Pharmacology and Physiology, 27(1): 47–55.

Sahana, T.G., Rekha, P.D. 2018. Biopolymers: Applications in wound healing and skin tissue engineering. Molecular Biology Reports, 45(6): 2857–2867.

Slezák, R., Ryška A. 2006. Kouření a dutina ústní. 1st ed., Praha: Havlíček Brain Team.

The Reviskometer® RV 600: Technical charges. 2013.

A comparative study on the selected quality properties of frankfurters with using chicken breast meat

Jan Slovacek[1], Lucie Grossova[1], Nikol Snupikova[1], Marketa Piechowiczova[1], Ondrej Stastnik[2], Miroslav Juzl[1]
[1]Department of Food Technology
[2]Department of Animal Nutrition and Forage Production
Mendel University in Brno
Zemedelska 1, 613 00 Brno
CZECH REPUBLIC

xslovac2@mendelu.cz

Abstract: The use of chicken meat could be strategies for high quality meat processing and sausage production. It could have advantages for consumers and producers in nutritional and specific consumer-based conditions and their specific requirements. Chicken meat is a lean and economically very expensive recipe item that can be compared to pork lean meat. Currently, mechanically separated chicken meat is most often used. However, this is reflected on the quality parameters and reduces the value of such sausages for consumers who require quality. The aim of the study was to compare a control frankfurters (PLF) with frankfurters with added 33% chicken breast meat (CBF) instead of pork lean meat. Most of basic chemical, colour and microbiological parameters after storage were not different between groups ($P > 0.05$). Contrary to expectations, few differences ($P < 0.05$) were found in sensory analysis with trained panellists. The difference in the juiciness of the sausages between groups was found ($P < 0.05$), further in evaluating their odour and taste intensity. No differences ($P > 0.05$) in descriptors were found for 30 untrained assessors who represented a group of common consumers. Despite the economic cost, the use of high-quality sausage recipes items is essential for the vast majority of consumers. However, consumers are unable to find significant differences in the quality of meat products. They are therefore dependent on the data on the food label.

Key Words: sausage, colour, sensory analysis, consumer

INTRODUCTION

At a global level, the dominant livestock types are poultry, cattle (includes beef and buffalo meat), pig, and sheep and goat to a lesser extent. Pigmeat is the most popular meat globally, but the production of poultry is increasing most rapidly. In Czech Republic was an increase in the consumption of chicken meat and a decrease in beef consumption, with pork stagnating in the trend (Kameník 2019). Consumer evaluation has been used extensively over the past decades to evaluate acceptability and quality of food products (Kameník 2017).

Pork together with beef forms the basis of meat products. Poultry meat, on the other hand, is limited in the recipe to mechanically separated meat, which is not meat in the technical and legislative sense. In addition, from a qualitative point of view, the consumer is perceived as a substitute that reduces the price of a meat product (Baéza et al. 2021).

Nevertheless, chicken meat is missing from recipes for minced meat products such as sausages and salamis on the market in the Czech Republic. The basic composition of each type of sausage is the basis given by the type of meat, the basis given by the type of meat, towards the expected sensory quality parameters represented by the descriptors (Čuboň 2021). Chicken meat is commercially finalized by the sale of chilled or frozen chickens. In products other than cooked ham, it is included as a recipe item minimally. Typical gastronomic features of pork breast muscle are lower juiciness and pale colour, to some extent it is related to post-mortem factors and the processes of transforming muscle into meat (Ovchynnikova 2020).

The aims of the study were to compare frankfurter based on chicken breast meat with control variant with pork and to evaluate any differences in the quality parameters of such products in relation to sensory evaluation and to the consumer.

MATERIAL AND METHODS

Material

The animal procedures were reviewed and approved by the Animal Care Committee of Mendel University in Brno and by the Ministry of Education, Youth and Sports (MSMT- 22771/2019-3). The trial was performed with one group of poultry. Commercial male broilers Ross 308 in age of 50 days were slaughtered by decapitation, chilled at 2 °C and the next day processed into a meat product together with pork meat (lean and/or fat meat, from local slaughterhouse, Ivančice) in the meat facility (Mendel University, CZ 22067) according to the common procedure (Komprda et al. 2021). Recipes: control variant (PLF, frankfurters with pork lean meat) contain lean pork with fat content up to 10% 33.4 kg, experimental variant (CBF, frankfurters with chicken breast meat) contain chicken *pectoralis major* in same amount 33.4 kg/100 kg. Both recipes (PLF and CBF) further contained fat pork with fat content up to 50% 40.0 kg, water (ice) 23.85 kg, nitrite salt mix 1.8 kg, and commercial spice mixture 0.95 kg (MASOPROFIT, EAN: 859 235 561 1106) with pepper, ginger, coriander, nutmeg, stabilizer E451, flavour enhancer E621, antioxidant E300, paprika extract E120c.

Meat processing and frankfurters production

The main physical traits of *pectoralis major* and pork lean, and fat meat were collected in special room and next day processed. For making frankfurters were used cutter, filler, and smoker. Meat emulsion was prepared in two steps in cutter (Seydelmann, Germany). Sausages were filled (HTS 150, Germany) in ovine intestines (calibre 20/22 mm) and heated (70 °C, 10 min) in smoker (Bastramat, Germany).

Chemical analysis

Dry matter, protein, fat, and salt content (g/100 g), and the (g/100 g) were analysed. Samples (aprox. 250 g) were homogenized in mixer and were analysed twice. Dry matter content was analysed gravimetrically, for total amount of protein was used the Kjeldahl method, the total fat content was analysed by Soxhlet extraction, and the salt content was determined by Mohr method according to the methodology described in the article of Komprda et al. (2021).

Microbiology analysis

Samples were taken in three weeks after processing, it is the end of the shelf life. Samples were homogenized and was prepared ten-fold dilution series. One ml of the original solution or a dilution of it was inoculated in a Petri dish. Appropriate substrate (total count of microorganisms and psychrotrophic microorganisms – PCA, coliform bacteria – VRBL, yeasts and moulds – Chloramphenicol Glucose Agar) was suffused to Petri dish and then was Petri dish incubated (total count of microorganisms 30 °C after 72 hours, psychrotrophic microorganisms – 6.5 °C after 10 days, coliform bacteria – 37 °C after 24 hours, yeasts and moulds – 25 °C after 120 hours). Finally, the numbers of characteristic colonies were summed.

Colour measurement

Colour CIE parameters L*, a* and b* were measured by CM 3500d spectrophotometer (Konica Minolta, Japan) on the sausage surface and on the sausage cutting surface with SCE (Specular Component Excluded) and 8 mm slot (D 65, 6500 °K). Also, there were analysed heated sausages prepared in standard convection oven (Rational SCC WE 61, Germany) by 80 °C, 100% humidity, 10 minutes, the same process for sensory analysis. Each sample was measured in triplicate (3 pairs and in 2 batches).

Sensory analysis

Sensory analysis was assessed by a 10-member trained panel of academic staff (5 men, 5 women) in special room (Department of Food Technology) under ČSN ISO 6658 (560050) condition and according to current practice and training, which the Department of Food Technology carries

out at least once a month. For this sensory analysis was selected 100 mm line scale with a description of outer points. For consumer´s test we used 30 untrained assessors who represented commonly consumers of meat products (sausages, frankfurters). There were 15 men and 15 women.

Descriptors expressed as the quantitative or hedonic scores, where 0 is the sign minimum and 100 is maximum of pleasure or intensity. There were analysed heated sausages prepared in standard convection oven (Rational SCC WE 61, Germany) by 80 °C, 100% humidity, 10 minutes. Samples were identified by a four-digit code. The sample groups were offered randomly to the assessors.

Statistical analysis

The measured data were statistically evaluated and by analysis of variance (one-way ANOVA), including Tukey´s test ($p < 0.05$) for multiple comparisons, significant difference was determined with using probability test (Tukey's HSD test) on level $P \leq 0.05$ in STATISTICA 12 (StatSoft, Prague, Czech Republic).

RESULTS AND DISCUSSION

The production of frankfurters with chicken meat was without complications like a common production. There were no statistical differences ($P > 0.05$) between groups in basic chemical composition of frankfurters. The low differences in values are surprising (Table 1) but indicate that replacing chicken breast meat with pork lean meat is possible and does not affect the composition.

Table 1 Chemical analysis of frankfurters according to different recipe

Content (g/100 g)	Group of samples	
	PLF ($\overline{x} \pm$ SD)	CBF 1.5% ($\overline{x} \pm$ SD)
Dry matter	35.55 ± 0.87	36.02 ± 0.95
Proteins	16.56 ± 0.98	17.21 ± 0.68
Fat	15.88 ± 0.49	16.56 ± 0.98
NaCl	2.30 ± 0.07	2.29 ± 0.09

Legend: PLF, frankfurters with pork lean meat, CBF, frankfurters with chicken breast meat; Values with different superscripts in the same rows means there are significant differences ($p < 0.05$).

The hygienic effects of the experiment were also not changed. Microbiological analysis was performed three weeks after processing (21 days), the total count of microorganisms was low, with CFU up to 10^2, and therefore frankfurters were microbiologically acceptable. No differences ($P > 0.05$) were found in any other microbiological analysis (or not detected). The results of the chemical and microbiological analysis do not differ from the data from similar studies where the same recipes are used (Komprda et al. 2021). In the Table 2 are results of colour measurement of frankfurters. Sausages with chicken meat were brighter with higher L* ($P < 0.05$) on the surface and on cross-section than control group with pork.

Table 2 Colour measurement of frankfurters colour according to different recipe

Colour parameter (CIE)		Unheated		Heated	
		PLF ($\overline{x} \pm$ SD)	CBF ($\overline{x} \pm$ SD)	PLF ($\overline{x} \pm$ SD)	CBF ($\overline{x} \pm$ SD)
Surface	L*	53.49 ± 1.93 ^{a}	58.27 ± 2.61 ^{b}	48.23 ± 4.13 ^{a}	52.92 ± 1.68 ^{a}
	a*	18.10 ± 0.49 ^{a}	17.07 ± 0.72 ^{a}	17.48 ± 0.81 ^{a}	19.15 ± 0.51 ^{b}
	b*	28.44 ± 0.59 ^{a}	28.34 ± 2.56 ^{a}	26.58 ± 1.68	28.10 ± 1.86
Cross-section	L*	63.64 ± 1.68 ^{a}	67.01 ± 1.43 ^{b}	60.46 ± 1.59 ^{a}	65.55 ± 1.56 ^{b}
	a*	11.82 ± 0.31 ^{a}	12.70 ± 0.27 ^{a}	12.37 ± 0.22 ^{a}	12.77 ± 0.36 ^{a}
	b*	14.12 ± 0.09 ^{a}	11.73 ± 0.45 ^{b}	15.66 ± 0.36 ^{a}	11.36 ± 0.31 ^{b}

Legend: PLF, frankfurters with pork lean meat, CBF, frankfurters with chicken breast meat; Values with different superscripts in the same rows means there are significant differences ($p < 0.05$).

The results by Kim et al. (2014) are similar to our results, L* value was increased gradually with the addition of chicken meat, when reducing the values parameters, a* and b* for unheated sausages.

We confirmed these results, as in this study the decrease for the parameter b* was also not confirmed after the addition of chicken meat after heating. Thus, the addition of chicken meat has the effect of maintaining the parameter b* (yellow colour) after sausage heat treatment.

Table 3 Sensory analysis of frankfurters according to different recipe

Traits/descriptors	Trained panellists (n = 10)		Untrained panellists (n = 30)	
	PLF ($\overline{x} \pm$ SD)	CBF ($\overline{x} \pm$ SD)	PLF ($\overline{x} \pm$ SD)	CBF ($\overline{x} \pm$ SD)
Odour intensity	85.1 ± 9.5 ^{b}	72.1 ± 8.5 ^{a}	82.1 ± 15.5 ^{bc}	80.3 ± 13.2 ^{bc}
Odour acceptance	82.4 ± 9.8 ^{a}	83.7 ± 6.1 ^{a}	80.1 ± 15.2 ^{a}	85.7 ± 10.3 ^{a}
Colour	80.7 ± 8.4 ^{a}	75.7 ± 7.2 ^{a}	83.7 ± 12.1 ^{a}	80.5 ± 11.2 ^{a}
Cohesiveness	76.6 ± 9.5 ^{a}	79.7 ± 9.1 ^{a}	70.8 ± 17.6 ^{b}	71.4 ± 16.3 ^{b}
Gumminess	80.0 ± 11.1 ^{a}	76.2 ± 10.3 ^{a}	81.3 ± 14.5 ^{a}	77.7 ± 14.5 ^{a}
Tenderness	78.2 ± 8.4 ^{a}	79.3 ± 8.8 ^{a}	81.7 ± 14.1 ^{a}	78.2 ± 13.1 ^{a}
Juiciness	75.9 ± 9.4 ^{b}	55.9 ± 9.0 ^{a}	73.6 ± 19.8 ^{b}	70.4 ± 18.6 ^{b}
Flavour acceptance	76.1 ± 12.6 ^{a}	72.3 ± 14.2 ^{a}	84.1 ± 15.2 ^{a}	87.7 ± 10.3 ^{a}
Spices intensity	72.4 ± 8.8 ^{a}	85.2 ± 7.6 ^{b}	80.2 ± 18.6 ^{ab}	82.4 ± 17.5 ^{ab}
Bitter taste	5.3 ± 2.1 ^{a}	9.4 ± 4.7 ^{a}	11.6 ± 11.2 ^{a}	10.8 ± 8.5 ^{a}
Salt intensity	51.1 ± 12.8 ^{a}	55.3 ± 10.9 ^{a}	45.1 ± 18.1 ^{a}	49.1 ± 16.0 ^{a}
Overall acceptance	85.2 ± 7.5 ^{a}	87.3 ± 9.1 ^{a}	83.5 ± 17.3 ^{a}	85.7 ± 10.6 ^{a}

Legend: PLF, frankfurters with pork lean meat, CBF, frankfurters with chicken breast meat; Values with different superscripts in the same rows means there are significant differences ($p < 0.05$).

The results in Table 3 show more sensitive senses and perceptions in the trained evaluators, while satisfaction of all panellists with both recipes of frankfurters. The difference in the juiciness of the sausages between groups was found ($P < 0.05$), further in evaluating their odour and taste intensity. The addition of chicken did not have a significant effect ($P > 0.05$) on the peremptory quality parameters of frankfurters. Kim et al. (2014) produced sausages with pork loin and chicken breast, the addition of chicken breast above 50% may contributed to a softer and more flexible texture of emulsion sausages. They also found that for sensory evaluations, an increase in the added amount of chicken breast contributes to a rich umami taste and deeper flavour within the emulsion sausages. Torrico et al. (2018) described the importance of using the test and at the same time the experience of the panellists. Testing with meat is challenging due to the high variability of the meat samples. Untrained panellists evaluated with greater variance of values in the sensory questionnaire. This shows and confirms Torrico et al. (2018), it very much depends on the choice of method and type of evaluators for the experiment.

CONCLUSION

Chicken meat belongs to meat products recipes, not only for ham production, but also to minced meat products such as frankfurters. Despite the economic cost, the use of high-quality sausage recipes items is essential for the vast majority of consumers. We confirmed that consumers are unable to find significant differences in the quality of meat products. They are therefore dependent on the data on the food label. In this study, we also confirmed the usefulness of chicken meat, trained evaluators found the experimental frankfurters to be less juicy, but this was not confirmed in a consumer test in untrained evaluators. It therefore depends on the producer which strategy he chooses when producing high-quality meat products. For this purpose, the use of chicken meat is certainly desirable.

ACKNOWLEDGEMENTS

The research was financially supported by the Internal Grant Agency of Faculty of AgriSciences Mendel University in Brno No. AF-IGA2020-TP012.

REFERENCES

Baéza, E. et al. 2021. Review: Production factors affecting poultry carcass and meat quality attributes. Animal [Online], 100331. Available at: https://doi.org/10.1016/j.animal.2021.100331. [2021-09-10].

Čuboň, J. et al. 2021. The use of mutton in sausage production. Potravinarstvo Slovak Journal of Food Sciences [Online], 15: 506–512. Available at: https://doi.org/10.5219/1602. [2021-09-01].

Kameník, J. 2017. Meat Industry in Central and Eastern Europe: changes, trends and challenges. In Proceedings of the 43rd food quality and safety conference. Brno, Czech Republic, 1–2 March. Mendel University in Brno, pp. 22–28. Available at: https://www.ingrovydny.af.mendelu.cz/historie. [2021-09-01].

Kameník, J. 2019. Current meat production in selected countries of the world a in the EU. In Book of the 45th food quality and safety conference. Brno, Czech Republic, 4–7 March. Mendel University in Brno, pp. 24–28. Available at: https:// https://www.ingrovydny.af.mendelu.cz/historie. [2021-09-01].

Kim, H.W. et al. 2014. Effect of Mixing Ratio between Pork Loin and Chicken Breast on Textural and Sensory Properties of Emulsion Sausages. Korean Journal for Food Science of Animal Resources [Online], 24(2): 133–140. Available at: https://doi.org/10.5851/kosfa.2014.34.2.133. [2021-09-01].

Komprda, T. et al. 2021. Fatty acid composition, oxidative stability, and sensory evaluation of the sausages produced from the meat of pigs fed a diet enriched with 8% of fish oil. Journal of Food Science, 86(6): 2312–2326. Available at: https://onlinelibrary.wiley.com/doi/10.1111/1750-3841.15749. [2021-09-01].

Ovchynnikova, O. 2020. Relationship between pH values and electrical conductivity, their usability in chicken breast meat evaluation as marker post mortal quality. In Proceedings of International PhD Students Conference MendelNet 2020 [Online]. Brno, Czech Republic, 11–12 November, Brno: Mendel University in Brno, Faculty of AgriSciences, pp. 359–364. Available at: https://mnet.mendelu.cz/mendelnet2020/mnet_2020_full.pdf. [2021-09-01].

Torrico, D.D. et al. 2018. Novel techniques to understand consumer responses towards food products: A review with a focus on meat. Meat Science [Online], 144: 30–42, Available at: https://doi.org/10.1016/j.meatsci.2018.06.006. [2021-09-01].

Possibilities of use and quality parameters of beaver canned meat (*Castor fiber* L.)

Jan Slovacek[1], Miroslav Juzl[1], Vendula Popelkova[1], Marketa Piechowiczova[1], Jakub Drimaj[2], Ondrej Mikulka[2]
[1]Department of Food Technology
[2]Department of Forest protection and Wildlife Management
Mendel University in Brno
Zemedelska 1, 613 00 Brno
CZECH REPUBLIC

xslovac2@mendelu.cz

Abstract: The aim of this study was to determine the sensory properties of canned beaver meat. The study also included determination of chemical composition and instrumental colour measurement of the canned meat. Two samples with different amounts of beaver meat were made (36%, 51% of beaver meat) and compared with samples which contain the beef meat instead of beaver meat (36%, 51% beef meat) other ingredients in the recipe was pork meat, boiled pork skin, salt, and spices. There were not considerable differences in chemical composition between products ($p > 0.05$). Instrumental colour measurement displayed that samples with beaver meat were significantly lighter than those with beef meat ($p < 0.05$). Sensory analysis did not prove significant differences between individual samples, but preferential test showed that the sample with 36% of beaver meat was rated the best. The study confirm that beaver meat can be used in canned meat and offer a fine quality product. There is not enormous difference between the product properties if you replace beef meat with beaver meat. The beaver meat can be used in heat treated meat products and enhance the meat product market.

Key Words: beaver, game, canned meat, colour, sensory analysis

INTRODUCTION

Beaver meat was a common part of the diet in European countries until its extinction (Halley et al. 2012). In the 18th century, only a few reservoirs remained in Europe (1,200 individuals; Vorel et al. 2008). Currently, the beaver is widespread in most European countries (Wróbel 2020) and with growing conflicts comes areas where it is hunted again in a controlled manner, including the Czech Republic, and the possibility of using beaver game is offered.

Consumer interest in non-traditional types of meat has been growing in recent years (Florek et al. 2017a). Game meat, which also includes beaver meat, is characterized by its high nutritional value and specific organoleptic properties (Jankowska et al. 2005). It is a good source of B vitamins, micro and macro nutrients, meat is high in iron, and it is also free of drug residues and growth hormones (Serratosa et al. 2006). The game also contains a lower amount of fat and cholesterol compared to a pork meat. This is also reflected in the lower energy value of the raw material (Berrisch-Hempen 1995).

The objective of this study is to make a meat product which contain higher amount of beaver meat and is also safe for consumers. Then evaluate the manufactured product in terms of chemical composition and sensory analyses and compare the beaver product with classic product with meat of common slaughter animals. For this case we have chosen canned meat. It is one of the durable food thanks its long-term sustainability and very high nutrition value (Barrett and Cardello 2012).

MATERIAL AND METHODS

Meat and sample production

Three young beaver individuals (age under 3 years) were used. The animals were shot, and carcasses were cooled to 2 °C. The lean meat from beaver's thighs and shoulders was obtained.

Lean beef or beaver meat (depends on product) and pork fat meat were manually cut into smaller pieces, mechanically minced (8 mm pieces) and mixed with NaCl (2%), crushed cumin (0.3%) and crushed pepper (0.1%). Thereafter mechanically minced again and then the meat batters were stuffed into cleaned jars (120 ml). All meat jars were heat treated (85 ºC for 2.5 hours) after that they were cooled down fast. After 24 hours jars were heated again (85 ºC for 2 hours) and cooled down below 4 ºC.

Proximate composition

Water, fat, and salt content (g/100 g), and the (g/100 g) were analysed. 2 samples of each can (aprox. 250 g) were homogenized in mixer and were analysed twice. Dry matter content was analysed gravimetrically, the total fat content was analysed by Soxhlet extraction, and the salt content was determined by Mohr method according to the methodology described in the article of Komprda et al. (2021).

Colour measurement

Colour space L*, a* and b* was determined by CM 3500d spectrophotometer (Konica Minolta, Japan). The samples were measured (D 65, 6500 °K) on the surface with SCE (Specular Component Excluded) and 8 mm slot in triplicate (Jůzl et al. 2018). Canned meat was left to heat up to 20–25 °C and measured.

Microbiological analysis

Samples were homogenized and 90 ml physiological saline solution were added to 10 g from each. This mixture was homogenized for 1 min. Samples were insert into water bath (85 °C, 10 min) to determine thermoresistant microorganism. 1 ml of each sample was pipette to Petri dish and covered with hot agar. After solidification were the dishes put into thermostat with ideal temperature conditions and there were cultivate (Table 1).

Table 1 Microorganisms and conditions of cultivation

Group of Microorganisms	Soil	Temperature (ºC)	Time of cultivation (hours)
Total plate count	PCAM agar	30	72
Thermoresistant bacteria	PCAM agar	30	48

Statistical analysis

Data collected from experiments were analysed by analysis of variance (one-way ANOVA) and Tukey´s test ($p < 0.05$) to compare used meat by programme STATISTICA 12. Samples were considered significant at 95% confidence level ($p < 0.05$) and data were tested for normality by Shapiro–Wilk test.

Sensory analysis

Sensory analysis was assessed by a 10-member trained panel of academic staff (5 men, 5 women) in special room (Department of Food Technology) under ČSN ISO 6658 (560050) condition and according to current practice and training, which the Department of Food Technology carries out at least once a month. All panel´s members consume canned meat regularly and do know the aroma and flavour of the beaver meat. All analyses were performed at the same time of the day, at 11 am.

Samples were left in room temperature for 2 hours. Every evaluator got a jar from each sample and did not know the meat composition of it. Water, pure distillate, and non-salted bread were provided as neutralizers.

For each canned meat sample, assessors were asked to indicate their score on a 100 mm line scale ranging from 0 at the left to 100 at the right. Descriptors are described in Table 2.

The preferential test was based on the Friedman method.

RESULTS AND DISCUSSION

Proximate composition

The approximate composition of our canned meat products is shown in Table 2. There are small differences in fat content between samples. The difference between samples in fat content could be caused by different amounts of fat in used pork meat. The distinction between beaver lean meat and beef lean meat in fat content is not that meaningful to create such differences (Razmaitė 2011). The addition of salt was the same in all samples, diversity could occur during mixing process.

Table 1 List of attributes and reference frame

Attributes		Definition	Intensity/acceptability	
			Low	High
Appearance	Acceptability	Acceptability of overall appearance, adequate amount of fat and aspic, acceptable colour, clarity of aspic.	dislike extremely	like extremely
	Colour intensity (lightness)	Intensity of the characteristic red colour (light-dark).	very light pink, beige	very dark red, brown, purple
Odour	Acceptability	Acceptability of overall odour.	unpleasant, atypical, foreign	pleasant, typical, pure
	Off-odour	Odour that is not natural or up to standard owing to deterioration or contamination.	none	prominent
Texture	Juiciness	Perception of the amount of water released by the product during first bites.	dry	juicy
	Tenderness	Time and numbers of chewings required to masticate the sample ready for swallowing.	tough	tender
	Cohesiveness	The extent to which a material can be deformed before it ruptures.	incoherent	cohesive
Flavour	Acceptability	Acceptability of overall flavour.	unpleasant, atypical, foreign	pleasant, typical, pure
	Intensity	Intensity of sum of all flavours.	none	prominent
	Saltiness	Intensity of salt flavour.	unsalted	extremely salted
	Off-flavour	Flavour that is not natural or up to standard owing to deterioration or contamination.	none	prominent
Overall appreciation		Total quality of sample.	dislike extremely	like extremely

Table 2 Chemical composition of canned meat

Component	Group of samples			
	36% of beaver meat ($\bar{x} \pm SD$)	36% of beef meat ($\bar{x} \pm SD$)	51% of beaver meat ($\bar{x} \pm SD$)	51% of beef meat ($\bar{x} \pm SD$)
Water (%)	65.11 ± 1.58	63.76 ± 1.78	64.74 ± 1.98	66.92 ± 1.67
NaCl (%)	1.80 ± 0.05	1.64 ± 0.05	1.75 ± 0,7	1.69 ± 0.08
Fat (%)	16.03± 0.40	17.22 ± 0.43	15.41 ± 0.50	13.45 ± 0.35

Colour measurement

According to colour measurements (Table 3) there is variance between the beaver and beef canned meat. Both beaver canned meat samples are significantly lighter ($p < 0.05$) than their beef analogues. This fact is interesting because lightness (L*) values of lean beef meat are higher than values of lean beaver meat (Florek et al. 2017b, Hernández et al. 2016). This colour change had to happen during

the heat treatment. The beaver meat had to become lighter after that procedure. There was also a significant difference in yellowness (coordinate b*) between the 51% beaver meat sample and the others ($p < 0.05$). Statistical analysis did not find any difference ($p > 0.05$) in redness (coordinate a*).

Table 3 Instrumental colour measurement

Attribute	Group of samples			
	36% of beaver meat ($\bar{x} \pm SD$)	36% of beef meat ($\bar{x} \pm SD$)	51% of beaver meat ($\bar{x} \pm SD$)	51% of beef meat ($\bar{x} \pm SD$)
L*	47.24 ± 1.41^{a}	44.57 ± 0.92^{bc}	46.03 ± 0.55^{ab}	43.84 ± 1.39^{c}
a*	6.28 ± 0.72	5.86 ± 0.47	6.29 ± 0.06	5.50 ± 0.60
b*	13.87 ± 0.16^{a}	13.69 ± 1.04^{a}	12.31 ± 0.19^{b}	14.24 ± 1.27^{a}

Legend: Values with different superscripts in the same rows means there are significant differences ($p < 0.05$).

Sensory analysis

The analysis of sensory properties showed that there are not significant differences ($p > 0.05$) between canned meat samples (Figure 1). In fact, there was not sensory detectable difference ($p > 0.05$) between 51% and 36% used lean meat. There was visually higher fat content in 36% jars but in rated properties evaluators did not find any difference ($p > 0.05$). Sensory analysis also did not prove any divergence between the beaver and beef products ($p > 0.05$). This fact shows that beaver meat is comparable to beef meat in canned meat. However preferential test evaluated the 36% beaver canned meat as the best and 36% beef canned meat as the worst product of all. The results show that beaver meat can be used very well in a canned meat production with good influence on product itself. All the beaver products were evaluated undoubtedly high in key sensory attributes. Żochowska-Kujawska et al. (2016) published that addition of 20–40% of beaver meat has positive effect on palatability. We can state that the addition even 51% of beaver meat has pleasant effect on canned meat sensory properties and no off-odour or off-flavour is present.

Figure 1 Sensory analysis results

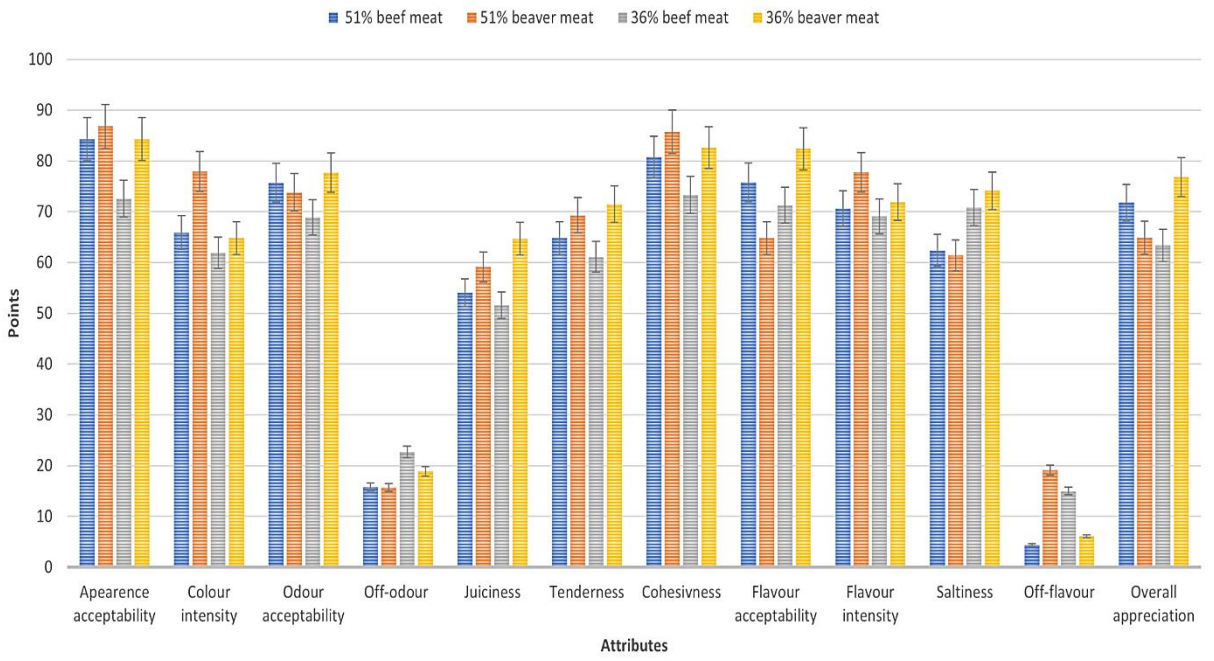

At last canned beaver meat is microbiologically safe and meets the EU law conditions (Commission Regulation (EC) No 2073/2005 of 15 November 2005 on microbiological criteria for foodstuffs).

CONCLUSION

The beaver meat can replace the beef meat in canned products and create an interesting game delicacy. All beaver products were evaluated very well in essential sensory attributes. Despite the smell of beaver meat, the sensory analysis did not find any off odour or off flavour in canned products. It is a very safe meat product according to microbiological analysis. Canned beaver meat is microbiologically safe, easy to manufacture and sensory interesting product which can be recommended to every meat-eating customer.

ACKNOWLEDGEMENTS

We would like to thank Marián Šutovský for his cooperation in providing samples and valuable information. The research was financially supported by the internal grant IGA FA MENDELU No. AF-IGA2021-IP076 The nutritional, hygienic and sensory quality properties of European beaver´s meat (*Castor fiber* L.) and its technological evaluation in meat products.

REFERENCES

Barrett, A.H. et al. 2012. Military food engineering and ration technology. 1. ed., Lacaster, Pennsylvania: DEStech Publications Inc.

Berrisch-Hempen, D. 1995. Fettsäurenzusammensetzung von Wildfleisch – Vergleich zum Fleischschlachtbarer Haustiere. Fleischwirtschaft [Online], 75: 809–813. Available at: https://doi.org/10.17221/350/2015-CJFS. [2021-09-01].

Florek, M. et al. 2017a. Proximate composition and physicochemical properties of European beaver (Castor fiber L.) meat. Meat Science [Online], 123: 8–12. Available at: https://doi.org/10.1016/j.meatsci.2016.08.008. [2021-09-01].

Florek, M. et al. 2017b. Chemical composition, amino acid and fatty acid contents, and mineral concentrations of European beaver (Castor fiber L.) meat. Journal of Food Measurement and Characterization [Online], 11: 1035–1044. Available at: https://doi.org/10.1007/s11694-017-9479-4. [2021-09-01].

Halley, D. et al. 2012. Population and distribution of Eurasian beaver (Castor fiber). Baltic Forestry [Online], 18: 168–175. Available at: https://www.researchgate.net/publication/234077944_Population_and_distribution_of_Eurasian_beaver_Castor_fiber. [2021-09-01].

Hernández, B. et al. 2016. CIELAB color coordinates versus relative proportions of myoglobin redox forms in the description of fresh meat appearance. Journal of Food Science and Technology [Online], 53(12): 4159–4167. Available at: https://doi.org/10.1007/s13197-016-2394-6. [2021-09-01].

Jankowska, B. et al. 2005. The composition and properties of beaver (Castor fiber) meat. European Journal of Wildlife Research [Online], 51: 283–286. Available at: https://doi.org/10.1007/s10344-005-0102-3. [2021-09-01].

Jůzl, M. et al. 2018. Evaluation of selected quality parameters of reduced salt frankfurters. Potravinarstvo Slovak Journal of Food Sciences [Online], 12(1): 279–284. Available at: https://doi.org/10.5219/908. [2021-09-01].

Komprda, T. et al. 2021. Fatty acid composition, oxidative stability, and sensory evaluation of the sausages produced from the meat of pigs fed a diet enriched with 8% of fish oil. Journal of Food Science. 86(6): 2312–2326. Available at: https://onlinelibrary.wiley.com/doi/10.1111/1750-3841.15749. [2021-09-01].

Razmaitė, V. et al. 2011. Compositional Characteristics and Nutritional Quality of Eurasian Beaver (Castor fiber) Meat. Czech Journal of Food Sciences [Online], 29: 480–486. Available at: https://doi.org/10.17221/313/2010-CJFS. [2021-09-01].

Serratosa, J. et al. 2006. Residues from veterinary medicinal products, growth promoters and performance enhancers in food-producing animals: a European Union perspective. Revue scientifique et technique [Online], 25(2): 637–653. Available at: https://pubmed.ncbi.nlm.nih.gov/17094703. [2021-09-01].

Vorel, A. et al. 2008. The Eurasian beaver population monitoring status in the Czech Republic. Natura Croatica: Periodicum Musei Historiae Naturalis Croatici [Online], 17(4): 217–232. Available at: https://hrcak.srce.hr/33968. [2021-09-01].

Wróbel, M. 2020. Population of Eurasian beaver (Castor fiber) in Europe. Global Ecology and Conservation [Online], 23: e01046. Available at: https://doi.org/10.1016/j.gecco.2020.e01046. [2021-09-01].

Żochowska-Kujawska, J. et al. 2016. Compositional characteristics and nutritional quality of European beaver (Castor fiber L.) meat and its utility for sausage production. Czech Journal of Food Sciences [Online], 34: 87–92. Available at: https://doi.org/10.17221/350/2015-CJFS. [2021-09-01].

Quality of beer made from bakery leftovers

Nikol Snupikova, Lucie Grossova, Ludek Hrivna, Tomas Gregor, Veronika Kourilova, Renata Dufkova, Miroslav Juzl
Department of Food Technology
Mendel University in Brno
Zemedelska 1, 613 00 Brno
CZECH REPUBLIC

xsnupiko@node.mendelu.cz

Abstract: The project solved the issue of beer production using bakery leftovers. A regular pastry was prepared in the recipe with a different amount of fat. Breadcrumbs were then made from the prepared dried pastry. Microsamples of beer from water, hops, brewer's yeast and malt were produced. Partial replacement of barley malt was carried out using bakery leftovers in different proportions (up to 0%, 10%, 20%, 30%). The colour of individual laboratory samples was determined on a Konica Minolta CM 3500d device and the basic parameters of beer were determined on a FermentoFlash device.

Key Words: beer, bakery leftovers, malt, quality of beer, colour

INTRODUCTION

Beer is an alcoholic beverage formed by a dispersion system containing more than a thousand different compounds such as proteins, nucleic acids, carbohydrates and lipids (Škoda et al. 2016).

The basic raw materials needed for beer production include water, cereal malts, European hops and brewer's yeast. In some countries, malt and sugar malt substitutes are used to reduce the production costs (Basařová et al. 2010). Global consumption and beer production are constantly growing because of the interest in beers prepared from non-traditional ingredients. Therefore, new suitable raw materials are constantly being sought for beer production (Panda et al. 2015). The use of new raw materials also helps to eliminate food waste. One way to reduce the losses of the bakery industry is to use unsold and unconsumed bread (Brancoli et al. 2020). Unused bread can be used as a partial substitute for malt in the form of breadcrumbs.

Malts supply beer with the largest share of the extractive substances. They thus influence the basic properties of beer and the entire production process (Cejpek 2014). During malting, the enzymes contained in barley grains, which are necessary for the degradation of storage substances, must be activated (Benešová et al. 2017). Similarly, with the addition of bakery leftovers to the process, a considerable amount of storage substances must be supplied to be decomposed using specific enzymes.

The beer production with the addition of bakery leftovers takes place in several steps. The first step is the crushing of malt, wiping, in which breadcrumbs are added, mashing, in which the storage substances are decomposed by the enzymes present in the malt and the enzymes that are added during mashing (Kosař and Procházka 2000, Basařová et al. 2010). This is followed by draining and hopping (Kosař and Procházka 2000). The wort is then filtered and cooled. After cooling, brewer's yeast is added to the process followed by fermentation, final fermentation, maturation, filtration and stabilization of the beer (Basařová et al. 2010).

It is well known that about one third of total world food production is not used each year. Bakery waste makes up about 7–10% of the original production. These are not only unsold products but also wastes generated during the production (Adessi et al. 2018, Eriksson et al. 2017). Most bakery waste is currently processed mainly into breadcrumbs (Samray et al. 2019).

MATERIALS AND METHODS

Ordinary pastries (rolls) were made different in various fat content (up to 0.85, 3.55, 6.65%) for the experiment. The pastry was dried followed by crumb for which the granulation was determined (Table 1) prepared in a Romill MS 100 shredder (Designed by Romill Czech Rep.).

At the same time, chemical analysis was performed such as Soxhlet fat content, sugar content before and after Luff-Schoorl inversion, sodium chloride content argentometrically (Mohr's method), Ewer starch content and Kjeldahl nitrogen content on a Tecator Kjeltec 8200 (Tecator company). The results of the analyses are presented in Table 2.

Table 1 Fat content and granulation crumbs (%)

Fat content (%)	Fraction-share in %					
	> 2 mm	> 1 mm	> 0.485 mm	> 0.257 mm	> 0.162 mm	Fall over < 0.162 mm
0.85	21.9	29.6	24.3	14.4	5.8	4.0
3.55	9.0	21.0	36.5	21.0	7.3	5.2
6.65	7.8	21.6	38.0	20.6	10.0	2.0

Table 2 Chemical analysis of breadcrumbs (%)

Fat (%)	Dry matter	Carbohydrates	NaCl	Starch	Nitrogenous substances
0.85	88.34	0.92	2.86	74.48	12.19
3.55	90.09	0.92	2.75	70.70	11.74
6.65	89.71	0.95	2.72	69.40	11.39

Water and malt of the Pilsen type Malz variety (Rajhrad malting plant) were also used for the production of beer microsamples. The enzymes were used in the mashing process: thermostable alpha amylase, glucoamylase and a mixture of lipase, protease and amylase in Panzynorm Forte-N and Pangrol tablets. Sládek and Žatecký semi-early Červeňák hop varieties were used for hopping. The fermentation was performed using Brew Master Lager Yeast that is a bottom fermentation yeast of *Saccharomyces cerevisiae* of the Lager type.

Up to11 micro samples of beers were prepared according to different recipes (Table 3). The recipes with different proportions of breadcrumbs in the sprinkling were used and breadcrumbs with low (the sample no. 1–3), medium (the sample no. 4–6) and high (the sample no. 7–9) fat was used within the project. The samples without the addition of breadcrumbs (the samples no. 10 and 11) were also prepared for the comparison.

The wort was prepared in mashing vessels. Both malt and breadcrumbs were wiped into 2.5 l of water at 37 °C. This was followed by the addition of alpha-amylase and up to 0.3 ml of glucoamylase. An increase in temperature and mashing was carried out at 72 °C for 40 minutes. The process was then cooled to 55 °C and up to 0.2 ml of glucoamylase, one tablet of Pangrol enzyme mixture and one tablet of Panzynorm Forte-N were added to the mash. The addition of enzymes was followed by a delay of 30 minutes. Subsequently, the temperature of the mash was raised to 72 °C and heated to 83 °C for 5 minutes after 15 minutes of stirring.

Subsequently, the sieving and sweetening was carried out with hot water at a temperature of 80 °C to a final volume of 4 l of wort. The wort was cooked with hops. The first hopping was carried out at the beginning of boiling (the dose of Sládek hop up to 3.8 g) followed after 45 minutes by the second dose of Sládek hop (up to 2.5 g) and Žatecký semi-early Červeňák (up to 7.2 g) was given after 30 minutes. After 15 minutes, the hop machine was terminated. After 20 minutes, the wort was pumped into fermentation vessels and the wort was cooled to a fermentation temperature of 10 °C. Up to 3 g of yeast were added to the wort followed by the main fermentation for 5 days at 12 °C. After 5 days, the beer was pumped into ripening jars and matured at 4 °C for 21 days.

The mashing of samples no. 10 and 11 took place according to the scheme given in the Table 4. Alpha amylase and glucoamylase in the sample no. 10 were added in a full dose at 52 °C.

The basic characteristics of the finished beer such as the alcohol content by weight and volume percentage, the actual and apparent extract and the original wort extract were determined using a FermentoFlash machine (Funke Gerber, Germany). The samples were dehydrated and filtered before the analysis. Prior to each determination, the machine was calibrated with distilled water.

Table 3 Malt to crumb ratio and a dose of enzymes

Sample	Barley malt (g)	Breadcrumbs (g)	The ratio of crumbs and malt	α- amylase (ml)	Glucoamylase (ml)	Panzynorm (tablet)	Pangrol (tablet)
1	453.0	50.4	10/90	0.5	0.5	1	1
2	403.2	100.8	20/80	0.5	0.5	1	1
3	352.8	151.2	30/70	0.5	0.5	1	1
4	453.6	50.4	10/90	0.5	0.5	1	1
5	403.2	100.8	20/80	0.5	0.5	1	1
6	352.8	151.2	30/70	0.5	0.5	1	1
7	453.6	50.4	10/90	0.5	0.5	1	1
8	403.2	100.8	20/80	0.5	0.5	1	1
9	352.8	151.2	30/70	0.5	0.5	1	1
10	504.0	0	0/100	0.5	0.5	0	0
11	504.0	0	0/100	0	0	0	0

Table 4 Temperature and time mashing

Temperature (°C)	Time (min)
37	10
45	10
52	15
62	30
72	30

The beer samples were instrumentally evaluated for colour using a Konica Minolta CM - 3500d benchtop spectrophotometer with a d/8 ° geometry that means the measurement of the reflected light at an angle of 8 °. Depending on the used material, the measurement of reflectance or transmittance was chosen to be used in the measurement of beer samples. The spectrophotometer was connected to a computer with the CMs-100w Spectramagic NX program. With this software, L* (lightness) values ranging from 0 (black) to 100 (white) can be measured. Colour coordinates a* and b*, in which the value a* defines the colour green (–a*) to red (+a*) and the value b* defines the colour blue (–b*) to yellow (+b*). Negative and positive values depend on the location in the three-dimensional CIELAB system. Using the deviation ΔE (ab*), the difference between two measurements can be described for beer.

Statistical Evaluation of Data

The measured data were statistically evaluated in the Statistica 12 program (StatSoft, USA). The Shapiro-Wilk test was used to calculate normality and the homogeneity was calculated by the Levene test. The data were further evaluated by the analysis of variance (one-dimensional ANOVA) and Scheffé's multiple comparison method at a significance level of $p < 0.05$. The tables were created in Microsoft Excel 2013.

RESULTS AND DISCUSSION

Analysis of the Main Parameters of Beer

As follows from the Table 1, the quality, especially the fat content, significantly affecting the proportion of the individual size fractions, must be taken into account in the use of bakery leftovers. The higher fat content increases the brittleness of the bread and the proportion of fractions with smaller dimensions. On average, the added breadcrumbs rather reduced the alcohol content. The highest content was determined in a sample of beer from the recipe no. 11 (Table 5) using only barley malt as a source

of the extractives. The higher alcohol content of this variant corresponded to a higher proportion of fermentable sugars (Johansson et al. 2021). The lowest alcohol content was determined for the samples 1 and 3 using the crumb with the lowest fat content. In general, the fat content had a positive effect on the alcohol content of beer. While low-fat breadcrumbs were used in the variants 1–3, the alcohol content was on average up to 1.76% by weight but the beer made from high-fat breadcrumbs (var. 7–9) reached up to 2.16% by weight of alcohol. The level of crumb granulation probably manifested itself here. The higher proportion of the finer fractions proved a positive effect on the yield of alcohol.

The highest values of the real and the apparent extract indicating the concentration of the assimilable carbohydrates such as glucose, maltose and maltotriose (Shioya et al. 2004) were measured in the sample 10 using additionally the food enzymes in the recipe in the mashing process.

The extract of the original wort was detected lower in all beers produced with a share of bakery leftovers in the sprinkling.

Table 5 Determination of the basic parameters of beer

Sample	Alcohol weight (%)	Alcohol volume (%)	True extract (%)	Virtual extract (%)	Original wort extract (%)
1	1.23	1.72	7.72	11.59	10.65
2	2.81	3.51	6.05	8.18	11.64
3	1.25	1.77	8.76	13.23	11.82
4	2.08	2.72	7.73	11.19	12.17
5	1.78	2.37	8.01	11.79	11.95
6	1.96	2.60	8.44	12.37	12.74
7	2.32	2.94	6.21	8.67	10.93
8	2.33	2.95	6.21	8.67	10.96
9	1.83	2.42	7.53	11.00	11.51
10	1.92	2.58	9.20	13.60	13.50
11	2.93	3.71	7.51	10.42	13.46

Instrumental Colour Measurement

In the case of instrumental colour measurement, we focused on determining the brightness (L*) in which it is the rule that the higher L* value causes the lighter colour. The values of the coordinates a* and b* range between –100 and +100, which for the coordinate a* means the transition from green (–a*) to red (+a*) and for the coordinates b* is from blue (–b*) to yellow (+b*) (Koren et al. 2020). The results of our measurements are presented in Table 6.

Table 6 Colour parameters

Colour parameter	Group of samples				
	C	CEN	BRE 10%	BRE 20%	BRE 30%
L* (D65) on average	70.88667	64.33667	65.93222	66.84778	66.61556
a* (D65) on average	2.20000	3.860000	2.477778	1.737778	1.884444
b* (D65) on average	30.18000	34.10000	31.26000	27.08556	28.73556

Legend: C – control group without crumbs and enzymes, CEN – the group without crumbs with enzyme content, BRE 10% – the group containing up to 10% of crumbs, BRE 20% – the group containing up to 20% of crumbs, BRE 30% – the group containing 30% of crumbs

Figure 1 Effects of recipe on the lightness of beer colour L(D65)*

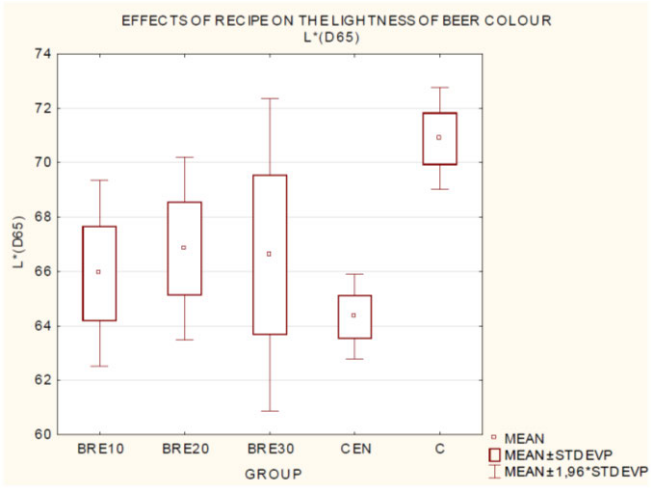

Legend: BRE 10% – the group containing up to 10% of crumbs, BRE 20% – the group containing up to 20% of crumbs, BRE 30% – the group containing 30% of crumbs, CEN – the group without crumbs with enzyme content, C – control group without crumbs and enzymes

The highest L* value was evaluated the lightest in the beer of the control sample without using crumb or enzymes in the production (Figure 1). The lowest value L* means the darkest beer was detected in the beer made without breadcrumbs but with the addition of enzymes. The addition of enzymes in the control variant conclusive increased the colour of the beer ($p > 0.95$). It can be assumed that the darker colour of beers was caused by the addition of enzymes that led to better decomposition of storage substances, increased the content of reducing sugars supporting the Maillard reactions subsequently reflected in the darker colour of beer.

Figure 2 Effects of recipe on the lightness of beer colour a(D65)*

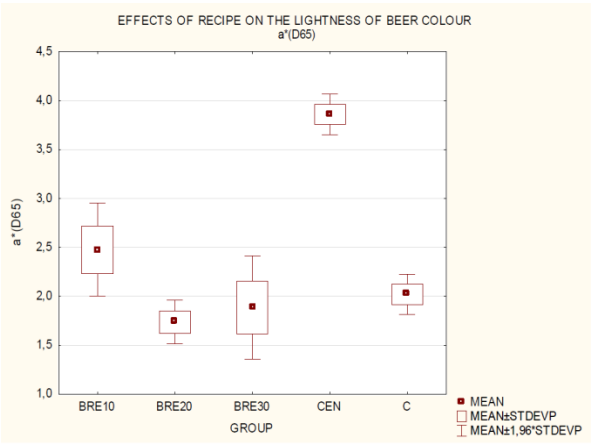

Figure 3 Effects of recipe on the lightness of beer colour b(D65)*

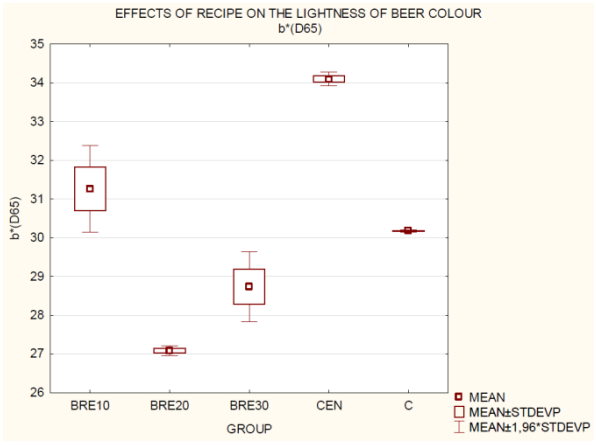

Legend: BRE 10% – the group containing up to 10% of crumbs, BRE 20% – the group containing up to 20% of crumbs, BRE 30% – the group containing 30% of crumbs, CEN – the group without crumbs with enzyme content, C – control group without crumbs and enzymes

The use of enzymes during the mashing process caused a conclusive increase in a* (red) and b* (yellow) in the control variant ($p > 0.95$). Compared to the other samples, the beers with a high value of a* and b* were characterized by darker and yellower colours (Figure 2 and 3). The use of breadcrumbs in the beer production also affected the values of a* (red) and the conclusive values of b* (yellow) ($p > 0.95$). The highest values of a* and b* were observed in the samples with the addition of 10% breadcrumbs. Higher crumb additions reduced the values of a* and b*.

CONCLUSION

Total 11 recipes were prepared for beer production. In nine of them, breadcrumbs were used in the range of 10–30% of the total proportion of sprinkles. The addition of breadcrumbs reduced the alcohol content compared to the classic recipe. The fat content of the used breadcrumbs was reflected in the level of its granulation. It increased the proportion of finer fractions of the grist and this was

positively reflected in the growth of the alcohol content in beer. The addition of enzymes in the classic recipe without the addition of breadcrumbs increased the extractivity of wort and thus beer.

On the other hand, its brightness (L*) was decreased and influenced by significantly higher values of a* and b*.

ACKNOWLEDGEMENTS
This work was supported by a grant entitled IGA AF MENDELU 2021-IP013.

REFERENCES

Adessi, A. et al. 2018. Bread wastes to energy: Sequential lactic and photo-fermentation for hydrogen production. International Journal of Hydrogen Energy [Online], 43(20): 9569–9576. Available at: https://www.sciencedirect.com/science/article/pii/S0360319918311789. [2021-08-14].

Basařová, G. et al. 2010. Pivovarství: Teorie a praxe výroby piva. 1st ed., Praha: VŠCHT Praha.

Benešová, K. et al. 2017. Aktivita proteolytických enzymů v průběhu sladování a výroby piva. Kvasný průmysl [Online], 63(1): 2–7. Available at: https://kvasnyprumysl.cz/artkey/kpr-201701-0001_Aktivita_proteolytickych_enzymu_v_prubehu_sladovani_a_vyroby_piva.php. [2021-08-12].

Brancoli, P. et al. 2020. Environmental impacts of waste management and valorisation pathways for surplus bread in Sweden. Waste Management [Online], 117: 136–145. Available at: https://www.sciencedirect.com/science/article/pii/S0956053X20304219. [2021-08-12].

Cejpek, K. 2014. Vonné a chuťové složky sladů. Chemické listy [Online], 180(5): 426–435. Available at: ww-w.chemicke-listy.cz/ojs3/index.php/chemicke-listy/article/view/498. [2021-08-14].

Eriksson, M. et al. 2017. Take-back agreements in the perspective of food waste generation at the supplier-retailer interface. Resources, Conservation and Recicling [Online], 122: 83–93. Available at: https://www.sciencedirect.com/science/article/pii/S0921344917300411. [2021-08-14].

Johansson, L. et al. 2021. Sourdough cultures as reservoirs of maltose-negative yeasts for low-alcohol beer brewing. Food Microbiology [Online], 94: 1–11. Available at: https://www.sciencedirect.com/science/article/pii/S0740002020302185. [2021-08-14].

Koren, D. et al. 2020. How to objectively determine the color of beer? Journal of Food Science and Technology [Online], 57(4): 1183–1189. Available at: https://link.springer.com/article/10.1007%2Fs13197-020-04237-4. [2021-08-23].

Kosař, K., Procházka, S. 2000. Technologie výroby sladu a piva. 1. vyd. Praha: Výzkumný ústav pivovarský a sladařský.

Panda, S.K. et al. 2015. Anthocyanin-rich sweet potato beer: Technology, biochemical and sensory evaluation. Journal of Food Processing and Preservation [Online], 39(6): 3040–3049. Available at: https://ifst.onlinelibrary.wiley.com/doi/full/10.1111/jfpp.12569. [2021-08-15].

Samray, N.M. et al. 2019. Bread crumbs extrudates: A new approach for reducing bread waste. Journal of Cereal Science [Online], 85: 130–136. Available at: https://www.sciencedirect.com/science/article/pii/S0733521018306349. [2021-08-17].

Shioya, S. et al. 2004. Simultaneous control of apparent extract and volatile compounds concentrations in beer fermentation. IFAC Proceedings Volumes [Online], 37(3): 451–456. Available at: https://www.sciencedirect.com/science/article/pii/S147466701732623X. [2021-08-15].

Škoda, J. et al. 2016. Světelná degradace piva a tvorba letinkové příchuti. Chemické listy [Online], 110(2): 112–117. Available at: www.chemicke-listy.cz/ojs3/index.php/chemicke-listy/article/view/231. [2021-08-15].

PLANT BIOLOGY

Effects of intermittent-direct-electric-current (IDC) on growth and content on photosynthetic pigments in hemp (*Cannabis sativa* L.)

Nikolas Balog, Tomas Vyhnanek, Petr Kalousek, Patrik Schreiber
Department of Plant Biology
Mendel University in Brno
Zemedelska 1, 613 00 Brno
CZECH REPUBLIC

xbalog@mendelu.cz

Abstract: Influence of electricity was studied in hemp plants. Impact on plant growth and physiological and yield parameters was investigated. Two different intensities (1500 mA and 2000 mA) was applied for 1 hour a day for total duration of 11 weeks. Height of the plant, stem diameter, biomass production and also yield of flowers was affected by treatment. Treatment had positive effect on content of photosynthetic pigments as chlorophylls and carotenoids.

Key Words: hemp, electricity, chlorophyll, carotenoids, yield

INTRODUCTION

The effect of electricity on plant have been studied for many years (Blakman 1924). Electricity act as elicitor that can induce plant defence mechanisms, for example accumulation of secondary metabolites (Dannehl et al. 2012). Further effects as increasing plant growth and final yield were described. However influence can be positive or negative depending on plant species and magnitude of stress induction (Dannehl 2018). Hemp plants produce relatively high amount of secondary metabolites with plenty of uses in cosmetics, food supplements or also in medicine. For purposes of this study was chosen CBG (cannabigerol) genotype because of their low content of THC (tetrahydrocannabinol, <0.2%) make this research applicable in commercial sphere. Also for reason that CBG as a substance is still not so well known as THC or CBD (cannabidiol), and some researchers suggest that have many positive effects on human body, but is needed more investigation (Borrelli 2013, Lah 2021). Aim of this study is to investigate the effect of IDC on hemp plant morphology, physiology and yield characteristics, and also identify acceptable rate of electric treatment with positive effect yield outcome.

MATERIAL AND METHODS

Characterization of genetic material

The total 9 plants were propagated from one mother plant using vegetative technique of propagation. Mother plant was selected during past phenotype testing. From legislative point of view it is technical hemp because of low content of THC in flowers (<0.2%). From taxonomic aspect this genotype is more close to *indica* because of low habit and short flowering cycle (9 weeks). According the profiling based on cannabinoid profile it is chemotype IV (CBG dominant). Cuttings were incubated in mini-greenhouse for 12 days and afterwards transplanted to the rockwool cubes (10.0 x 10.0 x 6.5 cm). Plants were decapitated and another week were cultivated as mother plants in greenhouse, thereafter were plants positioned on rockwool slabs 100 x 15 x 7.5 cm (Grodan, NL). Three plants per one slab, each slab represented one treatment group.

Growing facility and equipment

Hemp was cultivated in growing tent 100 x 100 x 200 cm. As light source was used 600W HPS with dual spectrum bulb, light intensity was in the range of 400–500 $\mu mol/m^2/s^1$. First 3 weeks long photoperiod (18/6) and another 9 weeks short photoperiod (12/12). During experiment the temperature was kept from 18–27 °C and relative humidity in range of 40–80%. Two 15 W fans hanged up to top

of the plants were circulating air in space. On the top of the tent was installed exhaust fan which provided exchange of air and temperature regulation. Electricity was inducted with laboratory source KA3303P from company (Shenzen Korad Technology, CH). Electric current was from source with cables and connected to the slab via stainless steel electrodes. Electrodes were positioned on shorter side of rockwool slab.

Plant nutrition used was Dutch Formula procured from company Advanced Hydroponics of Holland B.V. Nutrient schedule was followed by company recommendation. Values of electric conductivity of nutrient solution during the experiment was in range of 0.6–2.3 mS/cm. Drip were used as irrigation system and was automatized with timer.

Experimental design and methodology

The experiment was performed with 2 treatments of different intensities of IDC (1500 mA and 2000 mA) and one control group. Electricity treatment began 1 week after transplanting hemp on rockwool slab. Treatment was cycled daily for duration of 1 hour per day after the irrigation. Total length of experiment was 11 weeks. In total 9 plants were cultivated divided in by 3 plants in 3 groups. Any repetition was not performed.

Growth parameters monitored during the experiment were height of the plant and main stem diameter. Height of the plant was measured from base of the stem till highest part. Stem diameter was measured in height of 2 cm from base of the stem. Data collection was performed weekly.

Physiological measurements were done by measuring activity of photosystem PSII with FluorPen FP100 (Photon Systems Instruments, CZ) in second week of experiment. Observed parameters were non-photochemical quenching (NPQ), index of vitality (Rfd) and maximum quantum yield (QY). Investigated leaves were selected in the same height in top part of plants and were obscured for 15 minutes.

Plant pigments were analysed from leaves of 4th week of experiment. Samples were taken from 3rd node from the top of each plant. Leaves have been lyophilized for 3 days and subsequently grinded and homogenized. Weight 50 mg was placed in mortar and mixed with small amount quartz sand and magnesium carbonate, homogenized thoroughly and extracted with acetone, extraction step was repeated 4 times. Filtration of acetone extract was done with morton filtration apparatus (Merci, CZ). Water pump was used for speed up the filtration process. Filtered extract was placed in volumetric bank and filled up till 50 ml with acetone. This method was applied for preparation all 9 samples. Measuring Absorbance of extracts was measured at 662, 645 and 470 nm using spectrophotometer (Spectronic 20 Genesys, Spectrum Chemical Mfg., USA). Chlorophyll *a* was measured at 662 nm, chlorophyll *b* at 645 nm, and carotenoids at 470 nm. Content of individual pigments was calculated according to the methodology (Lichtenhaler 1987). Used formulas for calculation:

$c_a(\mu g/ml) = 11.24\ A_{662} - 2.04\ A_{645}$

$c_b(\mu g/ml) = 20.13\ A_{645} - 4.19\ A_{662}$

$c_a(\mu g/ml) = (1000\ A_{470} - 1.90\ c_a - 63.14\ c_b)/214$

After 11 weeks of experiment was hemp harvested and measured total fresh weight with accuracy on 0.1g. Whole plants were dried hanged upside down. For preservation bioactive components in hemp flowers was applied slow drying at temperature levels in range 18–22 °C with 50–65%.

Statistical processing was performed in the program MS Excel. Columns in figures are created from average values. Error bars represent standard errors calculated from standard deviations.

RESULTS AND DISCUSSION

Morphological parameters

Final heights of plants are shown on (Figure 1). The tallest plants were in 2nd group (1500 mA) and also the most consistent. An increase of 11.1% compared to the control group was observed at 2nd (1500 mA). At 3rd group (2000 mA) was observed almost 3% increase in height. In another study on IDC was treated African nightshade with IDC of voltage 8 V and 16 V, 10 hours a day. The electrical circuit

was connected from the substrate to the top of the plant, the entire duration of the experiment was 12 days, there was not reported any influence on plant growth and morphological parameters (Gogo et al. 2016). However, the higher voltages have been shown to have an influence such as 110 V to 220 V at varying time from 10 to 30 s was able to improve leaf length, leaf width and stem length of cowpea, guinea corn and ground nut (Kareem 1999).

Figure 1 Average final height of the plant by group (cm), the intervals in the columns represent the mean error – before harvest

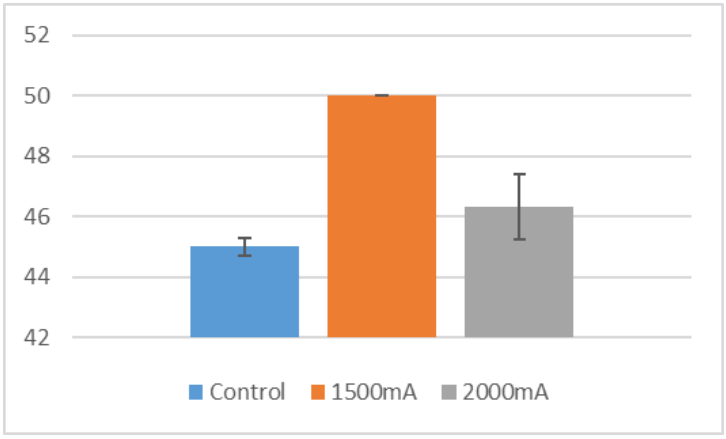

Stem diameter probably was influenced by electric treatment. Up to 11.4% increase of stem diameter was observed compared to the control group at 3rd group. See Figure 2.

Figure 2 Average stem diameter by group (mm), the intervals in the columns represent the mean error – before harvest

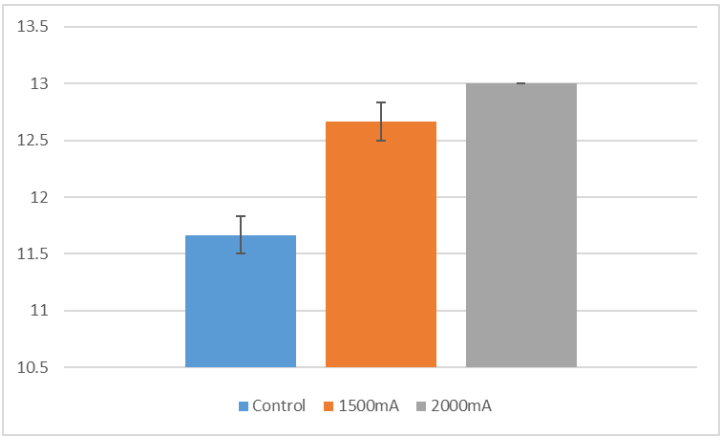

Photosynthetic pigments

Biosynthesis of plant pigments was significantly influenced by IDC. Content of chlorophyll *a* in 2nd group was increased by 32.5% and in 3rd group 30.9% increase compared to control group, see (Figure 3). Similar results occurred at chlorophyll *b* but increase at 2nd group was 34% against control. Alike effect on content of chlorophyll *a* and *b* was observed in garden cress (*Lepidium sativum* L.) with treatment 1400 mA with promoted growth by 15.9% and 19.1% (Dannehl et al. 2012). Carotenoid content also significantly increased by 33.1% and 28.0%. Promotion of biosynthesis of photosynthetic pigments had been observed in african nightshade (*Solanum nigrum* L.) where the increase in content of chlorophyll *a* by 4.0% and carotenoids by 4.5% with treatment 16 V. In the same experiment was detected opposite result with treatment of 8 V, content chlorophyll *a* decreased by 15.5% and carotenoids by 16.0% (Gogo et al. 2016). Among others, results indicate positive influence of IDC mediated-stress on the carotenoid content. In one study was investigated effect of DC 100, 300, 500 mA in different durations 15, 30, 60 minutes as post-harvest treatment on tomato (*Solanum lycopersicum* L.) fruits, the increase of ß- carotene by 45.5% was reported with treatment of 100 mA for 30 minutes.

Figure 3 Average content of chlorophyll a in leaves, the intervals in the columns represent the mean error – 4th week of experiment by group

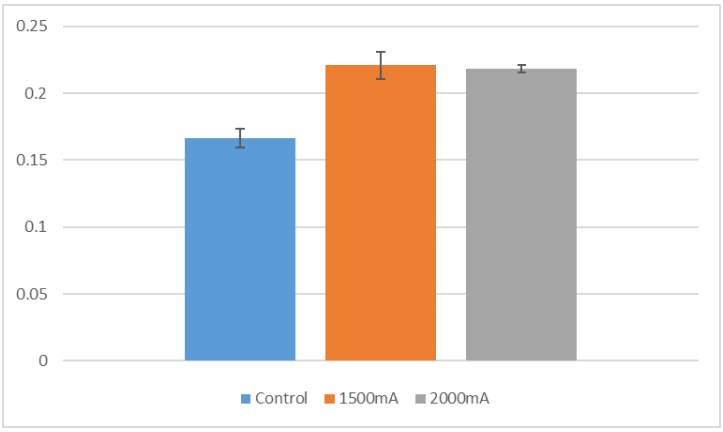

Figure 4 Average content of chlorophyll b in leaves, the intervals in the columns represent the mean error – 4th week of experiment by group

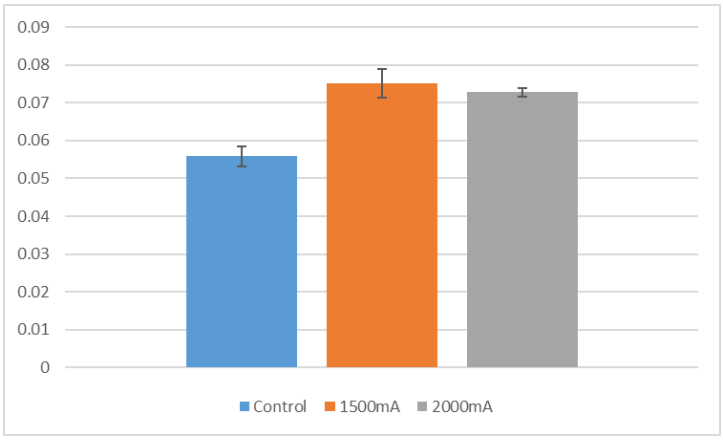

Figure 5 Average content of carotenoids in leaves, the intervals in the columns represent the mean error – 4th week of experiment by group

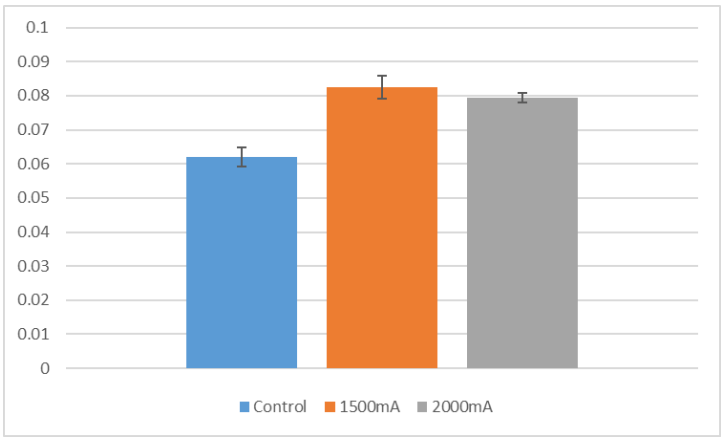

Yield characteristics

Yield characteristics as fresh biomass, flowers and leaves production was significantly influenced by IDC. In general 3rd group (2000 mA) was more affected by IDC. Fresh biomass was increased by 5.9% and 16% see (Figure 6). Flower yield at 2nd group (1500 mA) was negatively affected by 0.5% but at 3rd group (2000 mA) was flower yield increased by 13.6% see (Figure 7). Increasing yield with electricity was investigated by Blackman (1924) on barley (*Hordeum vulgare* L.), oat (*Avena sativa* L.) and wheat (*Triticum aestivum* L.). Where was plants exposed to high tension discharge with high voltage insulated wires in 2 meter height above the crop. Treatment increased the yield for oat up to 30% and 57% for wheat plants. The most affected parameter of yield characteristic was yield of dry leaves.

Yield of leaves was increased by 14.6% and 25.7% see in (Figure 8). Similar effect on yield of leaves was observed in african nightshade (*Solanum nigrum* L.) with treatment 127 µA caused increase by 24.4% (Gogo et al. 2016). Another study with conformable experiment design noticed 17.3% increase in dry matter with treatment 1800 mA in garden cress (*Lepidium sativum* L.) (Dannehl et al. 2012).

Figure 6 Average weight of fresh biomass of 1 plant by group (g)

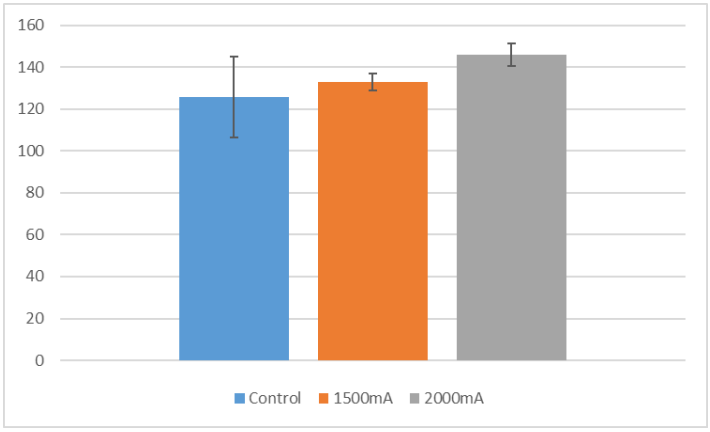

Figure 7 Average flower yield of 1 plant by group(g) the intervals in the columns represent the mean error

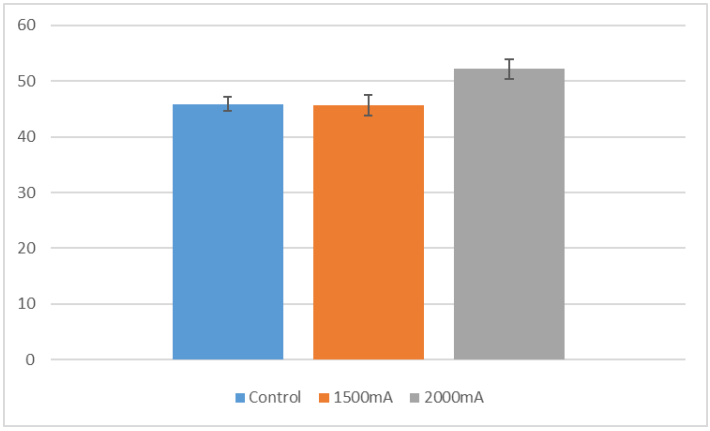

Figure 8 Average leaves yield of plant by group (g) the intervals in the columns represent the mean error

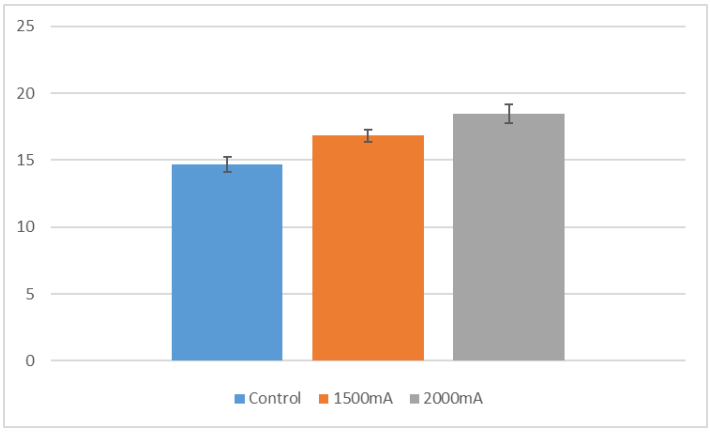

CONCLUSION

Results of this study showed, that IDC could be used as effective plant growth enhancer in hemp flower production. The effect can be various depending on intensity of treatment. From production point of view the most interesting treatment was in 3rd group (2000 mA), because there was the most significant increase of yield characteristics. But interesting fact was that treatment 1500 mA could

be more effective in increasing of content of photosynthetic pigments, and also the plant height. This study is the first to describe impact of IDC on hemp plants. Further investigation on plant secondary metabolites accumulation in hemp plants needed.

ACKNOWLEDGEMENTS
This way I would like to thank to Kamila Lonova with help and support with this research and also to my father Robert Balog which helped me a lot with his knowledge about the electricity.

REFERENCES

Blackman, V.H. 1924. Field experiments in electroculture. Journal of Agricultural Science, 14: 240–276.

Borrelli, F. et al. 2013. Beneficial effect of the non-psychotropic plant cannabinoid cannabigerol on experimental inflammatory bowel disease. Biochemical Pharmacology, 85: 1306–1316.

Dannehl, D. 2018. Effect of electricity on plant responses. Scienta Horticulturae, 234, 382–392.

Dannehl, D. et al. 2011. Effects of direct-electric-current on secondary plant compounds and antioxidant activity in harvested tomato fruits (*Solanum lycopersicon* L.). Food Chemistry, 126: 157–165.

Dannehl, D. et al. 2012. Influence of intermittent-direct-electric-current (IDC) on phytochemical compounds in garden cress during growth. Food Chemistry, 131: 239–246.

Gogo, E.O. et al. 2016. Impact of direct-electric-current on growth and bioactive compounds of African nightshade (*Solanum scabrum* Mill.). Plants Journal of Applied Botany and Food Quality, 89: 60–67.

Kareem, S.A. 1999. Stimulation of plant growth by means of electric shock application. Nigerian Journal of Pure and Applied Science, 4: 855–860.

Lah, T.T. et al. 2021. Cannabigerol is a Potential Therapeutic Agent in a Novel Combined Therapy for Glioblastoma. Cells, 10: 340.

Lichtenthaler, H.K. 1987. Chlorophylls and carotenoids: pigments of photosynthetic biomembranes. Methods in Enzymology, 148: 350–382.

Method for simultaneous detection of *Phytophthora infestans* proteins and DNA in *Solanum tuberosum* samples

Miroslav Berka[1], Veronika Berkova[1], Romana Kopecka[1], Marie Greplova[2]
[1]Department of Molecular Biology and Radiobiology
Mendel University in Brno
Zemedelska 1, 613 00 Brno
[2]Potato Research Institute, Ltd.
Dobrovskeho 2366, 580 01 Havlickuv Brod
CZECH REPUBLIC

miroslav.berka@mendelu.cz

Abstract: Phytophthora infestans is a model organism for the oomycetes, a distinct lineage of fungus-like eukaryotes. However, *P. infestans* is primarily known as a pathogen that causes the serious potato and tomato disease known as late blight. The means of controlling late blight are limited and require early detection of the pathogen. One of the most reliable method for targeted quantitation is based on qPCR. The amount of sample is often limited, which does not allow the use of other analyses such as proteome analysis by LC-MS. Here, we describe the optimized extraction method for simultaneously extracting the DNA and proteins from an infected leaf of *Solanum tuberosum*. Simultaneous analysis of the amount of *P. infestans* DNA and the proteome composition from the infected leaf opens possibilities for a better understanding of the interaction between *P. infestans* and the plant.

Key Words: qPCR, proteomics, *Phytophthora infestans*, quantitation

INTRODUCTION

One of the most destructive plant pathogens is *Phytophthora infestans* belonging to the Oomycota phylum. *P. infestans* is a well-known oomycete that causes the major worldwide disease of potatoes (*Solanum tuberosum*) (Goss et al. 2014). Potatoes are one of the five crops with the largest seasonal production in the Czech Republic. Globally, *P. infestans* is estimated to cause economic losses of up to 7 billion euros (Haverkort et al. 2016) and increases agriculture's dependence on synthetic pesticides. Recent research has expanded our knowledge of *P. infestans* infection, and the findings have been used for resistant breeding. However, *P. infestans* can adapt very quickly and overcome plant resistance (Andrivon et al. 2007). Thus, a better understanding of the interaction between *P. infestans* and the host plant is necessary to suppress *P. infestans* infection.

In the last decades, methods based on mass spectrometry have encountered impressive progress and are a very suitable tool for studying *P. infestans* infection. However, early detection of the pathogen is necessary for the correct interpretation of the data. *Phytophthora* can be detected by plating diseased tissue onto selective culture media containing a cocktail of antibacterial and antifungal chemicals and observing the morphological characters of the resulting mycelial growth (Cooke et al. 2007). However, this is a labour-intensive process and is prone to false negatives (O'Brien et al. 2009). Molecular methods can overcome these disadvantages. The methods such as enzyme immunoassays are sensitive but not species-specific, and thus the most reliable approaches are based on PCR techniques (Jung et al., 2016, Yang and Hong 2018). Therefore, qPCR represents a suitable and simple method for targeted quantification of *Phytophthora* (Llorente et al. 2010).

MATERIAL AND METHODS

Plant and *P. infestans* material

S. tuberosum cv. Keřkovské rohlíčky plants were cultivated on Murashige-Skoog medium (Murashige and Skoog 1962) supplemented with 30 g of sucrose per litre and 7 g agar per litre in culture chamber at 22 °C and 16/8 h light/dark cycles with 60 µmol/m^2/s photon flux density.

P. infestans (isolate U4) was grown on rye agar medium supplemented with 20 g/l sucrose (Caten and Jinks 1968) and incubated for one week in the dark at 18 °C. Part of the mycelium was harvested for DNA isolation and quantitation.

S. tuberosum Leaf Inoculation

Sterile, cold (4 °C) water was added to the sporulating mycelium. After 10 minutes, the sporangiophore suspension was pipette off and incubated at 4 °C for 2 hours to release the zoospores. The spore suspension was then filtered through a nylon sieve (50 µm), and the concentration of zoospores for inoculation was subsequently adjusted to 5×10^4 zoospore/ml.

Fully developed leaves were detached, rapidly submerged in sterilized water (control) or water suspension of *P. infestans* (5×10^3 zoospores/ml) and transferred onto wet cotton wool in a Petri dish. Leaf samples were collected 72 and 96 h after inoculation in three biological replicates and were immediately frozen in liquid nitrogen.

Protein extraction and LC-MS analysis

Frozen samples (leaves and mycelium) were homogenized using RETSCH Mixer Mill MM 400 (Retsch). Proteins were extracted as described previously (Saiz-Fernández et al. 2020). Briefly, proteins and nucleic acid were precipitated with a 1 ml mixture of methanol/methyl tert-butyl ether (1:3) overnight (app. 100 mg of ground tissue was used for precipitation). Pellets were washed with 0.5 ml of 100% methanol, and proteins and nucleic acid were solubilized in 500 µl of solubilizing buffer (8M urea and 100mM AMBIC), aliquots corresponding to 100 µg of proteins were digested in solution with Trypsin Gold, Mass Spectrometry Grade (Promega) overnight. The peptides mixtures were then desalted by C18 SPE (Agilent) and partially dried (Speed-vac system, Thermo). The samples were analysed by nanoflow C18 reverse-phase liquid chromatography (160 min gradient) using a 15 cm column (Zorbax, Agilent), a Dionex Ultimate 3000 RSLC nano-UPLC system (Thermo) and an Orbitrap Fusion Lumos (Thermo) as described previously (Berka et al. 2020a, Berková et al. 2020).

DNA extraction

Aliquots of 200 µl of each sample were transferred to the new tubes. Additional 200 µl solubilizing buffer were added to samples. The samples were mixed with the equal volume of phenol:chloroform:isoamyl alcohol (25:24:1) mixture and vortexed for 30 s. Samples were then centrifuge (10 000 × g, 10 min, 20 °C). The aqueous phase was transferred to the new tube and precipitated with 200 µl of 5M ammonium acetate and 400 µl of isopropyl alcohol. The resulting pellet was washed with 70% (v/v) ethanol, dried on a vacuum evaporator, and resuspended in 50 µl of DNase-free water. The concentrations of DNA were measured using NanoDrop™ 2000/2000c spectrophotometer (Thermo), and samples were diluted to a concentration of 50 ng/µl.

qPCR

P. infestans was detected according to Llorente et al. (2010) by amplifying PiO8, a highly repetitive sequence from its genome, and normalization to *S. tuberosum* gene Ef-1α (LOC102577640). The composition of the reaction mixture (10 µl) for quantitative PCR is given in Table 1. qPCR was performed using a Roche Light Cycler 480 Instrument II thermocycler with a standard protocol (Roche; see Table 1). UPL (Universal Probe Library) probes were used for fluorescence detection of the amplicon. A standard curve was generated to determine the amount of DNA by preparing a DNA concentration series of isolated control leaves and mycelium. The efficiency of the primers was also determined according to the standard curve. The Ct value was determined for individual genes and samples by the second derivative maximum of the fluorescence curve. The amount of *P. infestans* DNA was normalized to the amount of *S. tuberosum* DNA.

RESULTS AND DISCUSSION

Protein yield and LC-MS analysis

A sufficient amount of protein was extracted using the protocol described in materials and methods. The protein concentration in the samples ranged from 1.2 to 2.1 µg/µl. The extraction method is based on the precipitation of proteins and nucleic acids with methanol (Salem et al. 2020). In addition, the combination of methanol and methyl tert-butyl ether disrupts the membrane and removes

substances of a lipophilic nature. The protocol facilitates simple and fast extraction of proteins compared to other classically used methods (precipitation by acetone and trichloroacetic acid and/or phenolic extraction; Černý et al. 2019, Berka et al. 2020b). The results of LC-MS analysis (Figure 1) confirmed that the amount and purity of the extracted proteins are sufficient for proteomic analysis by mass spectrometry.

Table 1 Primer sequences and qPCR conditions

Primers					
Gene	Organism	Forward primer (5'→3')	Reverse primer (5'→3')	UPL sond	Sond sequence
Ef-1α PiO8	*S. tuberosum* *P. infestans*	cttgacgctcttgaccagatt gctcgtacggccaatgtagt	gaagacggagggtttgtct tttgcacagtatcacgcaagt	117 4	agcccaag gcaggaag
Starting concentration and volume of qPCR components					
2× qPCR Master Mix (Roche)	Forward primer (10 µM)	Reverse primer (10 µM)	Probe (10 µM)	Water	Template DNA (50 ng/µl)
5 µl	0.25 µl	0.25 µl	0.2 µl	2.3 µl	2 µl
qPCR conditions					
Initial denaturation	Denaturation	Annealing	Elongation	No. cycles	
95 ˚C (10 min)	95 ˚C (15 s)	60 ˚C (30 s)	72 ˚C (1 s)	45	

DNA extraction and qPCR

Three samples per treatment were used for DNA extraction. DNA with a concentration higher than 250 ng/µl was obtained from all samples. Measurements on nanodrop showed that the method could achieve contamination-free DNA with the ratios of 260/280 and 260/230 ranging between 1.7–2.0. The method is based on the principle that chaotropic agent urea solubilizes nucleic acids. The DNA is purified with a chloroform-phenol-isoamyl alcohol mixture and then precipitated from the aqueous phase. Using material between 50-100 mg gives a visible DNA pellet at the bottom of the tube. Final drying of the pellet removes residual ethanol, resulting in pure DNA.

Figure 1 Total ion chromatogram from LC-MS measurements. (A) Control leaf; (B) Infected leaf.

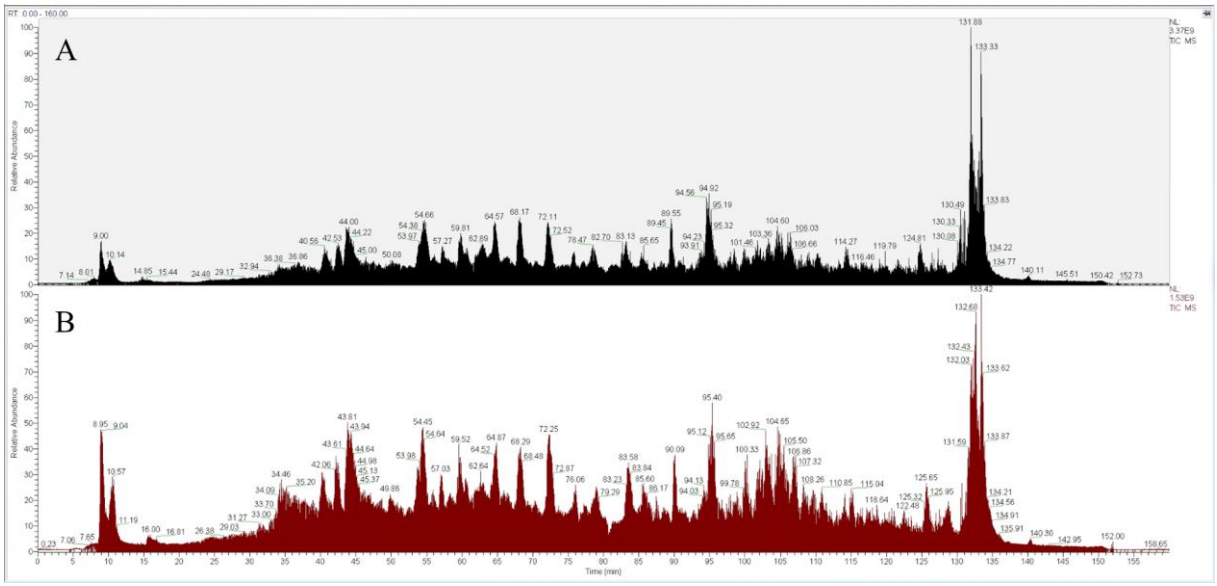

Subsequent qPCR revealed that the isolated DNA was suitable for qPCR and did not contain any inhibiting substances. The efficiency of both reactions was 97%. Based on a study by Llorente et al. (2010), PiO8 was used to detect *P. infestans*, and EF-1α (*S. tuberosum)* were used for normalization. In addition, new primers were designed to use fluorescent probes and increase the reaction specificity.

The optimized method for the simultaneous extraction of protein and DNA is fast, relatively simple, and cheap. The method can be used for subsequent analysis of metabolites, compared to commercially available chemicals for combined extractions (e.g. Trizol or TRIreagent; Chomczynski et al. 1993). Several similar methods of parallel extraction have been published in recent years, including Valledor et al. (2014). However, the main disadvantage of the Valledor et al. (2014) method is that the pellet (proteins and nucleic acids) is firstly solubilized in guanidine-HCl buffer, which prevents direct digestion with trypsin because guanidine-HCl significantly reduces trypsin activity at higher concentrations (Poulson et al. 2013). This fact complicates and prolongs the extraction.

Figure 2 Standard curves for calculating the amount of DNA in samples and primer efficiency

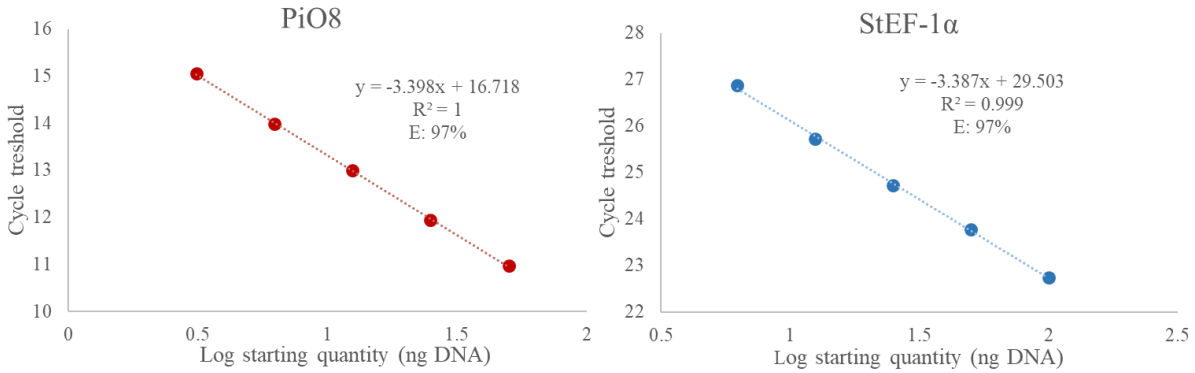

The development of *P. infestans* infection over time

Subsequently, the method was used on samples that were infected with *P. infestans* (Figure 3). The obtained results showed that after 96 hpi, there was a significant spread of infection in potato leaves. Previous studies have also observed a high incidence of infection after 96 hpi (Lees et al. 2012). These results confirmed that this optimized method could be used in practice to quantify the amount of *P. infestans* in potato samples together with proteomics analysis.

Figure 3 The large increase in the amount of P. infestans DNA indicating rapid development of the infection after 96 hpi

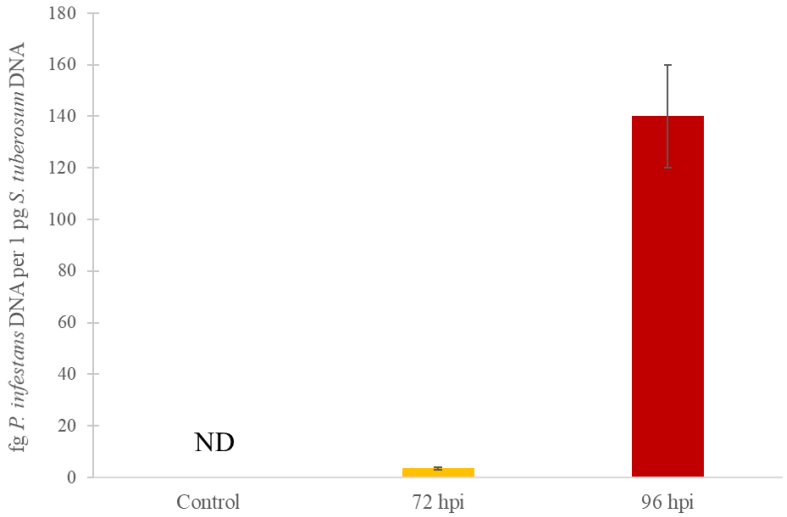

CONCLUSION

This study extends and optimizes the method for extracting proteins and DNA from a single sample, which can be used to very accurately and sensitively detection the presence of *P. infestans*. The study results allow us to monitor the number of proteins and the spread of *P. infestans* in specific samples and directly correlate the observed changes. Using this approach, we can obtain a comprehensive view of the interaction between *P. infestans* and *S. tuberosum*.

ACKNOWLEDGEMENTS

The research was financially supported by the project NAZV QK1910045 Identification of metabolites correlating with quantitative resistance to *Phytophthora infestans*, and internal grant project AF-IGA2021-IP075.

REFERENCES

Andrivon, D. et al. 2007. Adaptation of *Phytophthora infestans* to partial resistance in potato: evidence from French and Moroccan populations. Phytopathology, 97(3): 338–343.

Berka, M. et al. 2020a. Peptide-Based Identification of *Phytophthora* Isolates and *Phytophthora* Detection in Planta. International Journal of Molecular Sciences, 21(24): 9463.

Berka, M. et al. 2020b. Barley root proteome and metabolome in response to cytokinin and abiotic stimuli. Frontiers in Plant Science, 11: 1647.

Berková, V. et al. 2020. *Arabidopsis* response to Inhibitor of Cytokinin Degradation INCYDE: Modulations of cytokinin signaling and plant proteome. Plants, 9(11): 1563.

Caten, C.E., Jinks, J.L. 1968. Spontaneous variability of single isolates of *Phytophthora infestans*. I. Cultural variation. Canadian Journal of Botany, 46(4): 329–348.

Cooke, D. E. L. et al. 2007. Tools to detect, identify and monitor Phytophthora species in natural ecosystems. Journal of Plant Pathology, 89: 13–28.

Chomczynski, P. 1993. A reagent for the single-step simultaneous isolation of RNA, DNA and proteins from cell and tissue samples. Biotechniques, 15(3): 532–4.

Černý, M. et al. 2019. Fractionation Techniques to Increase Plant Proteome Coverage: Combining Separation in Parallel at the Protein and the Peptide Level. In Functional Proteomics. New York: Humana Press, pp. 93–105.

Goss, E.M. et al. 2014. The Irish potato famine pathogen *Phytophthora infestans* originated in central Mexico rather than the Andes. Proceedings of the National Academy of Sciences, 111(24): 8791–8796.

Haverkort, A.J. et al. 2016. Durable late blight resistance in potato through dynamic varieties obtained by cisgenesis: scientific and societal advances in the DuRPh project. Potato Research, 59(1): 35–66.

Jung, T. et al. 2016. Widespread Phytophthora infestations in European nurseries put forest, semi-natural and horticultural ecosystems at high risk of Phytophthora diseases. Forest Pathology, 46: 134–163.

Lees, A.K. et al. 2012. Development of a quantitative real-time PCR assay for Phytophthora infestans and its applicability to leaf, tuber and soil samples. Plant Pathology, 61(5): 867–876.

Llorente, B. et al. 2010. A quantitative real-time PCR method for in planta monitoring of Phytophthora infestans growth. Letters in Applied Microbiology, 51(6): 603–610.

Murashige, T., Skoog, F. 1962. A revised medium for rapid growth and bioassays with tobacco tissue cultures. Physiologia Plantarum, 15(3): 473–497.

O'Brien, P. A. et al. 2009. Detecting phytophthora. Critical Reviews in Microbiology, 35(3): 169–181.

Poulsen, J.W. et al. 2013. Using guanidine-hydrochloride for fast and efficient protein digestion and single-step affinity-purification mass spectrometry. Journal of Proteome Research, 12(2): 1020–1030.

Saiz-Fernández, I. et al. 2020. Integrated proteomic and metabolomic profiling of *Phytophthora cinnamomi* attack on sweet chestnut (*Castanea sativa*) reveals distinct molecular reprogramming proximal to the infection site and away from it. International Journal of Molecular Sciences, 21(22): 8525.

Salem, M.A. et al. 2020. An improved extraction method enables the comprehensive analysis of lipids, proteins, metabolites and phytohormones from a single sample of leaf tissue under water-deficit stress. Plant Journal, 103(4): 1614–1632.

Valledor, L. et al. 2014. A universal protocol for the combined isolation of metabolites, DNA, long RNAs, small RNAs, and proteins from plants and microorganisms. Plant Journal, 79(1):173–180

Yang, X., Hong, C. 2018. Differential usefulness of nine commonly used genetic markers for identifying Phytophthora species. Frontiers in Microbiology, 9: 2334.

Characterization of the potential biological control *Acremonium alternatum* using omics approaches

Veronika Berkova[1], Simona Mensikova[1], Susann Auer[2]
[1]Department of Molecular Biology and Radiobiology
Mendel University in Brno
Zemedelska 1, 613 00 Brno
CZECH REPUBLIC
[2]Chair of Plant Physiology, Institute of Botany, Faculty of Biology
Technische Universität Dresden
Zellescher Weg 20 b, 01217 Dresden
GERMANY

veronikamalych@gmail.com

Abstract: The excessive use of agrochemicals adversely affects the environment and is not sustainable for the long term. Developing alternative pest and weed control strategies that do not burden the environment and stimulate plants' fitness is inevitable. Endophytic fungi naturally colonize plants and promote growth by facilitating biogenic elements (iron, nitrogen, or phosphorus). It has been described that endophytes can also modulate plant hormone levels. The interaction of *A. alternatum* and potential host plants has previously been studied, but the omics characterization of this promising endophyte is missing. Proteins and metabolites were extracted simultaneously from the Petri dishes cultures. A total of 951 proteins were identified in three biological replicates based on more than 3600 unique peptides. Detailed analysis revealed that more than half of the identified proteins were involved in energy metabolism, translation, and protein folding. Metabolites from the polar fraction were derivatized and analyzed by GC-MS. The most abundant metabolites included sugars and amino acids. Analysis revealed minimal changes in the composition of the metabolites between the older and the younger part of the mycelium. In summary, this work provides a first insight into the molecular composition of *A. alternatum.*

Key Words: proteome, metabolome, biocontrol, *Acremonium alternatum*, endophytic fungus

INTRODUCTION

Many endophytic microbes live inside host-plant tissues as mutualists and do not cause any visible disease symptoms (Petrini 1991). Endophytes can be isolated from any plant tissue (leaf, root, stem, flower, seeds, fruits) and can be bacteria or fungi. Generally, most endophytes are fungi (Strobel 2018). Previous studies of cool-season grasses have shown that the inoculation with fungal endophytes increases plant growth, including root growth, root hairs elongation, and enhances total plant biomass (Malinowski and Belesky 2000).

Acremonium alternatum is an unspecialized, widespread, soil-borne endophytic fungus (Gams 1971). Some studies have shown that *A. alternatum* may play a role as biological control for some biotic and abiotic stresses. For instance, Raps et al. (1998) report that colonization of plants with *A. alternatum* had negative effects on development and nutrition status of the herbivore diamondback moth larvae *Plutella xylostella*. Additionally, this endophytic fungus can control mildew fungi and other pathogens (Romero et al. 2003). In *Arabidopsis thaliana* and *Brassica* roots, this fungus inhibits the development of the clubroot disease and reduces symptoms caused by the clubroot pathogen *Plasmodiophora brassicae* (Ludwig-Müller and Auer 2015).

Unfortunately, the *A. alternatum* genome sequence is unavailable, and molecular studies of this fungus thus present a challenge. Here, for the first-time, proteome and metabolome analysis of an agar plate culture of *A. alternatum* was performed to identify putative protein and metabolite candidates that could play a role in biological control.

MATERIAL AND METHODS

Cultivation of *Acremonium alternatum* cultures

Acremonium alternatum was grown in liquid culture with Potato dextrose broth (Sigma-Aldrich, Germany) on a rotary shaker for two weeks in the dark at 27 °C and 150 rpm to propagate fungal material. From this culture, 50 µl of conidia (10^7 conidia/ml) were put on petri dishes with yeast extract medium (YES, Giraldo et al. 2014) and cultivated at 25 °C in the dark. Fungal material from solid medium was harvested ten days after inoculation, flash frozen in liquid nitrogen, homogenized to a fine powder on a Retsch Mill MM400 and stored at -80 °C.

Protein extraction and LC-MS analysis

Proteomic analyses were performed using a gel-free shotgun protocol as described previously (Berka et al. 2020a, Berková et al. 2020). Briefly, proteins were precipitated with 1 ml mixture methanol/methyl tert-butyl ether/water (1:3:1) overnight (app. 100 mg of ground tissue was used for precipitation. Pellets were washed with 80% acetone and proteins were purified by phenol extraction. The resulting protein pellets were solubilized and then digested in solution with Trypsin Gold, Mass Spectrometry Grade (Promega) overnight. The tryptic digests were then desalted by C18 SPE (Agilent), and partially dried (Speed-vac system, Thermo). The samples were analysed by nanoflow C18 reverse-phase liquid chromatography (90 min gradient) using a 15 cm column (Zorbax, Agilent), a Dionex Ultimate 3000 RSLC nano-UPLC system (Thermo) and an Orbitrap Fusion Lumos (Thermo). The mass spectrometer was operated in positive-ionization mode. The instrument was operated with full MS scans over a mass range of m/z 375–1500 with detection in the Orbitrap (resolution 60 000) and with auto gain control (AGC) set to 400 000. The intensity threshold for the most intense ions was set to 50 000. These ions were selected for fragmentation at normalized collision energy of 30% (HCD). Fragment ion spectra were acquired in the Orbitrap (Orbitrap MS2 detection, resolution 15 000) with an AGC of 50 000 and a maximum injection time of 30 ms.

Protein identification

The measured spectra were processed as described previously (e.g. Berka et al. 2020b) with minor modifications. Spectra were recalibrated and searched against the *Acremonium chrysogenum* protein sequence database (Ensembl) by MS Amanda 2.0 with the following parameters: Enzyme - trypsin, max two missed cleavage sites; Mass tolerance - 5 ppm (MS) and 0.02 Da (MS/MS) and Sequest HT with the following parameters: Enzyme - trypsin, max two missed cleavage sites; Mass tolerance – 5 ppm (MS) and 0.1 Da (MS/MS); Dynamic modifications - Met oxidation, Asn/Gln deamidation; Static modification - Carbamidomethylation. Data were processed by ProteomeDiscoverer 2.3 (Thermo).

Protein annotation

Protein interaction map was created using String database (https://string-db.org; source for interaction – experiments databases, co‑expression).

Metabolite extraction and GC-MS analysis

Polar metabolites were extracted as previously described with few modifications from the centre and the edge of the mycelium, representing old and young mycelium, respectively (Berka et al. 2020b, Saiz-Fernández et al. 2020). Briefly, the samples were derivatized with 20 µl of methoxymation reagent (40 mg of methoxamine hydrochloride in 1 ml of pyridine) and then incubated for 90 minutes at 30 °C with continuous stirring at 800 rpm (Thermomixer comfort, Eppendorf). Then, 80 µl of silylation solution (N-Methyl-N-(trimethylsilyl)trifluoroacetamide, MSTFA) was added and the samples were incubated for 30 minutes at 37 °C and 800 rpm. After incubation, samples were transferred to GC-MS inserts and put in GC vials for analysis. The samples were measured using a Q Exactive™ GC Orbitrap™ GC-MS/MS and Trace 1300 Gas chromatograph (Thermo Fisher) with the following settings: split mode (1:10, total volume 0,5 µl) at 250 °C, the separation was performed on a TG-5SILMS column (30 m; 0.25 mm; 0.25 µm; Thermo Fisher) at a 38 min temperature gradient (70 °C for 5 min followed by 9 °C per min gradient to 320 °C and finally 5 min hold time) with following ionization. The mass spectrometer was set to a resolution of 60 000, a mass range of 50–600 m/z, an ion trap filling of 1e6 and an automatic control of the maximum IT. The obtained data were processed by TraceFinder 4.1 with Deconvolution Plugin 1.4 (Thermo) using the default workflow for GC-MS analysis

and a combination of NIST2014, GC-Orbitrap Metabolomics Library and in-house library. Skyline 4.2 (MacCoss Lab Software) was used for targeted quantification. More than a two-fold increase or decrease was considered a significant change in a given metabolite (t-test; $p<0.05$).

RESULTS AND DISCUSSION

Growth of *A. alternatum*

The growth conditions were chosen according to Giraldo et al. (2014). The *A. alternatum* grew very homogeneously and quickly colonized the plate space, which indicate appropriate conditions for the growth. *A. alternatum* created white fluffy mycelium after few days in the chosen condition (Figure 1). White colour corresponds to the cultivation in dark, because this fungus creates orange-pink mycelium under light conditions (Malathrakis 1985).

Identification and quantification of *A. alternatum* proteins

A. alternatum belongs to the order *Hypocreale*s within the phylum *Ascomycota*. As the reference genome for protein identification, *Acremonium chrysogenum* (Terfehr et al. 2014), a species used for the commercial production of antibiotics. *A. alternatum* belongs the *fusidioides*-clade that is closely related to the *chrysogenum*-clade (Summerbell et al. 2011), and the resulting proteomics data indicate that the proteome coverage is sufficient. In total we identified more than 950 protein families represented by more than 3600 unique peptides. Next, the most abundant proteins were selected for functional analysis. The threshold was set at 500 PSMs (peptide spectral matches) and the resulting list contained 50 that represented more than 49% of the estimated protein content.

Figure 1 A. alternatum mycelium after 10 days of cultivation on yeast extract medium in the dark

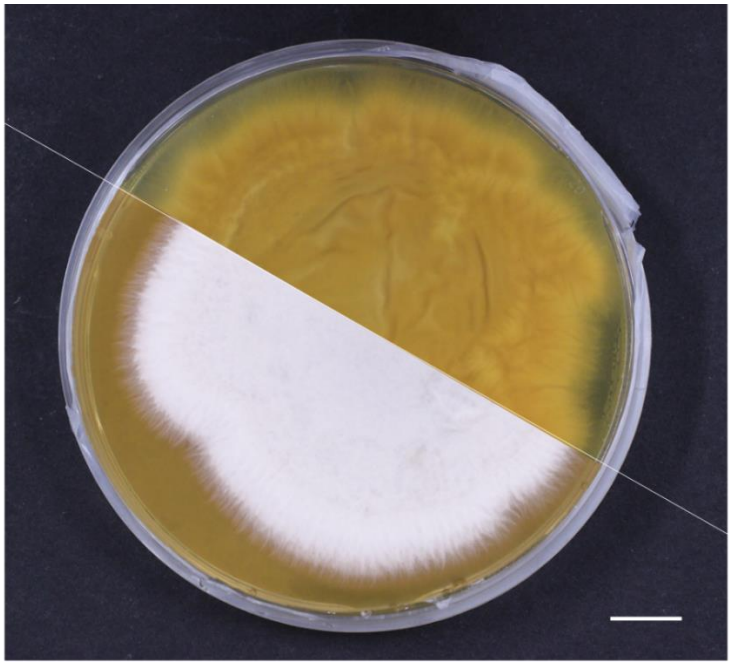

Legend: Bar represents 1 cm.

According to the ProteomeDiscoverer, 25% of the identified proteins are involved in energy metabolism and another 25% in translation (Figure 2a). These findings correlate with the extensive *A. alternatum* growth. The interaction map showed close links between heat-shock proteins, metabolic pathway and ribosome (Figure 2b).

The three most abundant proteins in our samples were identified as elongation factor 1-α-like protein, heat shock 70 kDa protein-like protein and Actin-like protein (Figure 3). Similar results were gained in previous research focused on proteomic analysis of the endophytic fungus *Undifilum oxytropis* (Li et al. 2012). *U. oxytropis* is also member of the phylum Ascomycota. The mentioned study identified actin-like proteins, heat shock 70 kDa protein and other proteins such as tubulins, histones as well ribosomal proteins. These proteins belong to the ubiquitous proteins, which are necessary for the living cells.

Figure 2 A) Functions groups of the 50 most abundant proteins identified from a petri dish culture of A. alternatum. B) Interaction map of the most abundant proteins.

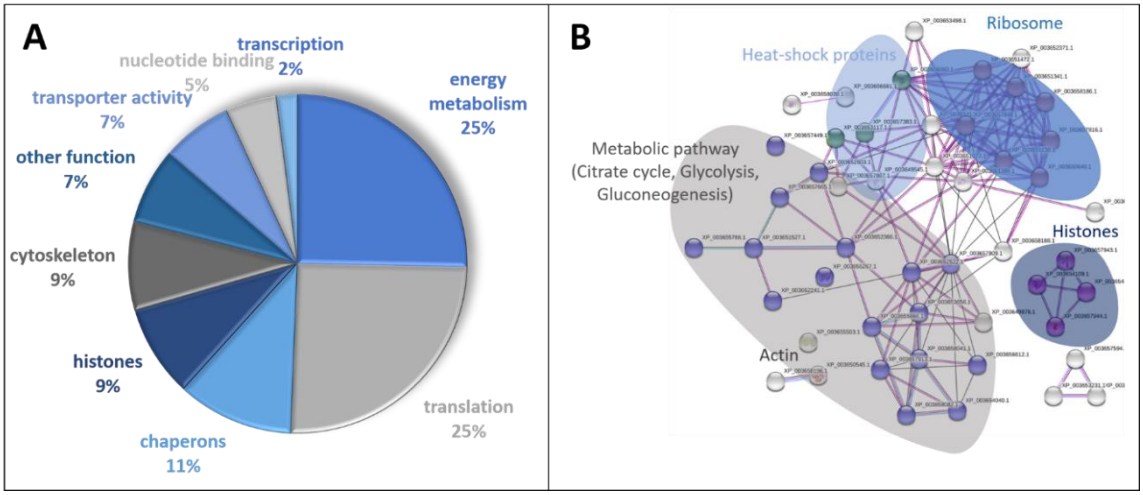

Figure 3 Estimated relative abundances of the most abundant proteins in A. alternatum mycelium

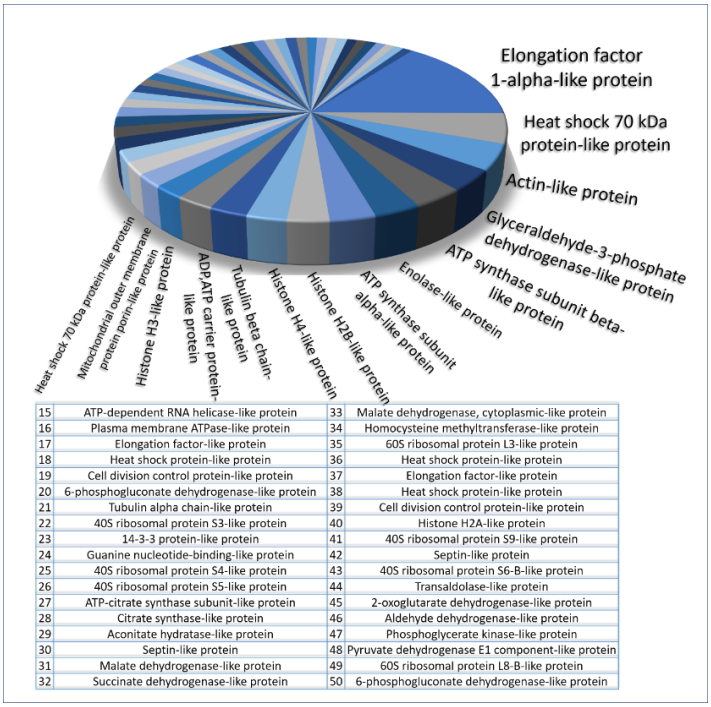

15	ATP-dependent RNA helicase-like protein	33	Malate dehydrogenase, cytoplasmic-like protein
16	Plasma membrane ATPase-like protein	34	Homocysteine methyltransferase-like protein
17	Elongation factor-like protein	35	60S ribosomal protein L3-like protein
18	Heat shock protein-like protein	36	Heat shock protein-like protein
19	Cell division control protein-like protein	37	Elongation factor-like protein
20	6-phosphogluconate dehydrogenase-like protein	38	Heat shock protein-like protein
21	Tubulin alpha chain-like protein	39	Cell division control protein-like protein
22	40S ribosomal protein S3-like protein	40	Histone H2A-like protein
23	14-3-3 protein-like protein	41	40S ribosomal protein S9-like protein
24	Guanine nucleotide-binding-like protein	42	Septin-like protein
25	40S ribosomal protein S4-like protein	43	40S ribosomal protein S6-B-like protein
26	40S ribosomal protein S5-like protein	44	Transaldolase-like protein
27	ATP-citrate synthase subunit-like protein	45	2-oxoglutarate dehydrogenase-like protein
28	Citrate synthase-like protein	46	Aldehyde dehydrogenase-like protein
29	Aconitate hydratase-like protein	47	Phosphoglycerate kinase-like protein
30	Septin-like protein	48	Pyruvate dehydrogenase E1 component-like protein
31	Malate dehydrogenase-like protein	49	60S ribosomal protein L8-B-like protein
32	Succinate dehydrogenase-like protein	50	6-phosphogluconate dehydrogenase-like protein

Metabolome *A. alternatum*

Proteomic analysis points out that large part of proteome consists of proteins involved in energy metabolism. For this reason, we employed GC-MS analysis to monitor changes during mycelial growth. In total, more than 300 substances were detected by GC-MS analysis. The most abundant metabolites included sugars (trehalose, glucose or sucrose), amino acids (lysine, asparagine, aspartic acid and glutamic acid), and e.g. stearic, malic and citric acids.

Analysis revealed minimal changes in the composition of the most abundant metabolites between the centre and the edge of the mycelium, as illustrated in the total ion chromatograms (Figure 4), where are no significant changes in the most abundant metabolites. A significant change was found in the abundance of only five metabolites. It can be concluded that the edges and the centre of the mycelium do not differ significantly in the composition of the identified metabolites. The changed metabolites include succinic acid, fructose, D-mannitol, sugar alcohol and sugar alcohol disaccharide. Interestingly, mannitol is a highly abundant metabolite in filamentous fungi and is stored in hyphae as a carbon source (Landi et al. 2017).

Figure 4 A comparison of the total ion chromatogram of the centre (old) and the outer (young) part of the mycelium.

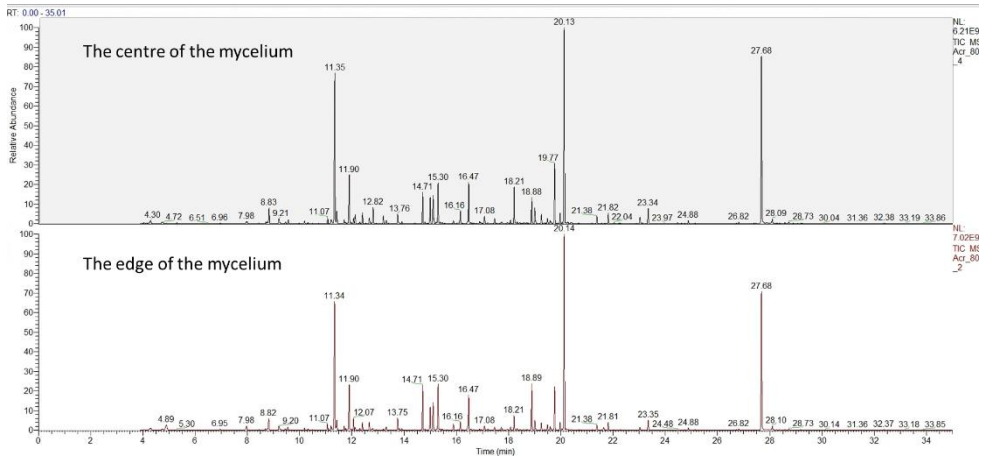

CONCLUSION

Our analysis identified 951 proteins based on 3600 unique peptides. The first 50 identified proteins are mainly involved in energy metabolism and translation, and the available annotations do not imply that these proteins could be involved in biotic interaction. Nevertheless, these results can provide insight into plant-*A. alternatum* interaction once the subset of mycelium proteins is compared with *A. alternatum* proteome in its plant host.

ACKNOWLEDGEMENTS

The research was financially supported by internal grant project AF-IGA2021-IP053.

REFERENCES

Berka, M. et al. 2020a. Peptide-Based Identification of *Phytophthora* Isolates and *Phytophthora* Detection in Planta. International Journal of Molecular Sciences, 21(24): 9463.

Berka, M. et al. 2020b. Barley root proteome and metabolome in response to cytokinin and abiotic stimuli. Frontiers in Plant Science, 11: 1647.

Berková, V. et al. 2020. *Arabidopsis* response to Inhibitor of Cytokinin Degradation INCYDE: Modulations of cytokinin signaling and plant proteome. Plants, 9(11): 1563.

Gams, W. 1971. Cephalosporium-artige Schimmelpilze (*Hyphomycetes*). 1. ed., Stuttgart, Germany: Gustav Fischer Verlag.

Giraldo, A. et al. 2014. *Acremonium* with catenate elongate conidia: phylogeny of *Acremonium fusidioides* and related species. Mycologia, 106(2): 328–338.

Landi, N. et al. 2017. Pioppino mushroom in southern Italy: an undervalued source of nutrients and bioactive compounds. Journal of the Science of Food and Agriculture, 97(15): 5388–5397.

Li, H. et al. 2012. Proteomic analysis of the endophytic fungus *Undifilum oxytropis*. African Journal of Biotechnology, 11(46): 10484–10493.

Ludwig-Müller, J., Auer, S. 2015. Biological control of clubroot (*Plasmodiophora brassicae*) by the endophytic fungus *Acremonium alternatum*. Journal of Endocytobiosis and Cell Research, 26: 43–49.

Malathrakis, N.E. 1985. The fungus *Acremonium alternatum* Line: Fr., a hyperparasite of the cucurbits powdery mildew pathogen *Sphaerotheca fuliginea*. Zeitschrift für Pflanzenkrankheiten und Pflanzenschutz, 92(5): 509–515.

Malinowski, D.P., Belesky, D.P. 2000. Adaptations of Endophyte-Infected Cool-Season Grasses to Environmental Stresses: Mechanisms of Drought and Mineral Stress Tolerance. Crop Science, 40(4): 923–939.

Petrini, O. 1991. Fungal endophytes of tree leaves. In Microbial Ecology of Leaves. New York: Springer-Verlag New York Inc., pp. 179–197.

Raps, A., Vidal, S. 1998. Indirect effects of an unspecialized endophytic fungus on specialized plant–herbivorous insect interactions. Oecologia, 114(4): 541–547.

Romero, D. et al. 2003. Effect of mycoparasitic fungi on the development of *Sphaerotheca fusca* in melon leaves. Mycological Research, 107(1): 64–71.

Saiz-Fernández, I. et al. 2020. Integrated proteomic and metabolomic profiling of *Phytophthora cinnamomi* attack on sweet chestnut (*Castanea sativa*) reveals distinct molecular reprogramming proximal to the infection site and away from it. International Journal of Molecular Sciences, 21(22): 8525.

Strobel, G. 2018. The Emergence of Endophytic Microbes and Their Biological Promise. Journal of Fungi, 4(2): 57.

Summerbell, R.C. et al. 2011. *Acremonium* phylogenetic overview and revision of *Gliomastix*, *Sarocladium*, and *Trichothecium*. Studies in Mycology, 68: 139–162.

Terfehr, D. et al. 2014. Genome sequence and annotation of *Acremonium chrysogenum*, producer of the β-lactam antibiotic cephalosporin C. Genome Announcements, 2(5): e00948–14.

Atmospheric CO_2 concentration, light intensity, and nitrogen nutrition affect spring barley response to drought and heat stress

Hana Findurova[1,2], Barbora Vesela[1], Emmanuel Opoku[1,2], Karel Klem[1,2]
[1]Laboratory of Ecological Plant Physiology
Global Change Research Institute of the Czech Academy of Sciences
Belidla 986/4a, 603 00 Brno
[2]Department of Agrosystems and Bioclimatology
Mendel University in Brno
Zemedelska 1, 613 00 Brno
CZECH REPUBLIC

findurova.h@gmail.com

Abstract: The aim of this study was to compare physiological responses of two spring barley varieties, differing in their oxidative stress tolerance, to drought and heat stress after pre-treatment under different irradiation regimes, CO_2 concentrations, and nitrogen fertilisation levels. High light intensity, elevated CO_2, and additional UV radiation increased flavonoid accumulation. Moreover, more flavonoids were induced in oxidative stress-sensitive variety Barke. Combined drought and heat stress caused a large decline in CO_2 assimilation, whereas heat stress alone caused only minor changes. Under combined stress, plants grown under low light intensity and no UV irradiation performed the best despite their higher initial water use efficiency and lower flavonoids content.

Key Words: flavonoids, CO_2 assimilation, water use-efficiency, Barke, Bojos

INTRODUCTION

The ongoing climate change brings many challenges for agriculture. It is predicted that the frequency of climate extremes will become higher and that they will last longer. These climate extremes, especially drought and high temperatures, represent a serious threat to crop production. Environmental signals interact with these abiotic stresses and highly affect the final response of a plant. Complex multiple treatments are therefore necessary to simulate future climate and evaluate plant responses.

It was shown that elevated CO_2 can partially alleviate the negative impact of drought and heat stress (Avila et al. 2020). Among the known effects of elevated CO_2 concentration on gas exchange are increased photosynthetic rate and decreased stomatal conductance and transpiration rate. Water use efficiency is therefore improved (Ainsworth and Long 2005). Moreover, increased CO_2 assimilation under elevated CO_2 concentration leads to increased biomass. While that can be beneficial under non-limiting conditions, it can lead to faster nitrogen depletion due to the dilution effect in N-limiting soils (Stitt and Krapp 1999).

Light together with CO_2 concentration is one of the most important factors influencing photosynthesis. Light is furthermore an important signal for plant development. Its quality and intensity further influence the production of secondary metabolites such as flavonoids (Klem et al. 2015, Holub et al. 2019). Flavonoids possess UV screening and antioxidative properties (Buer et al. 2010). Their induction can therefore be expected to improve plant performance under environmental stresses such as drought and heat. Considering known interactive effects of CO_2 concentration, light intensity, and quality, and also nitrogen availability on water use efficiency and antioxidative capacity, we also expected significant alleviation of drought and heat stress responses depending on these mutual interactions.

Spring barley is a traditional crop in the Czech Republic. Especially Czech malting barley is well-known for its quality. The yields and the malting quality are, however, jeopardised by climate change. Understanding the interactions of environmental factors can help us to maintain barley production under changing climate.

MATERIAL AND METHODS

Experimental design and growth conditions

Two spring barley (*Hordeum vulgare* L.) varieties differing in their sensitivity to oxidative stress were chosen for this experiment – variety Bojos, which is considered to be relatively tolerant (Klem et al. 2019), and variety Barke that is known for its sensitivity to oxidative stress. Seeds were germinated on wet filter paper and only germinated seeds of uniform size were used for the experiment. Germinated seeds were planted into pots (9x9x14 cm), 4 seeds/ 1 pot, filled with Seedling substrate (Klasmann-Dielmann, Germany). Plants were cultivated in growth chambers with a photoperiod of 15 h light, 9 h dark. Temperature was 25/15 °C (day/night) and relative humidity (RH) 60/90% (day/night). The ambient concentration of CO_2 (AC) was set to 400 ppm, elevated concentration (EC) of CO_2 to 800 ppm. Low light (LL) conditions: daily maxima 400 µmol/m^{2}s PAR, high light (HL) conditions: daily maxima 1300 µmol/m^{2}s PAR, UV+: UV light intensity 4 W/m^2 for UVA and 0.5 W/m^2 for UVB. The sources of UV-B radiation were TL 20 W/12 RS SLV fluorescent lamps (Philips), controlled by digital dimmable ballasts and intensity monitored by SKU 430 sensor (Skye Instruments Ltd, UK). To avoid transmission of UV-C radiation (< 280 nm), the UV-B fluorescent lamps were wrapped in a pre-solarized (8 h) 0.13 mm thick cellulose diacetate film. Fluorescent lamps LT 30W T8/010UV (Narva, DE) were used as the source of UV-A radiation. The UV-A lamps are an integral part of the growth chambers and are controlled by the PLC of the growth chamber. The intensity was monitored using the SKU 420 UV-A sensor (Skye Instruments Ltd, UK). Three days after planting half of the pots (N+) was fertilised with a solution of calcium nitrate with a dosage of 100 kg/ha N. All the plants were regularly watered until the beginning of the stress period.

Drought and high temperature treatment

On the 19th day after sowing (DAS) the drought stress started by withholding irrigation from half of the plants (dry) while the other half was supplied with regular irrigation (wet). At the same time, all the plants were exposed to high-temperature stress - the growing conditions were changed to temperature 39/32 °C (day/night). The stress treatment continued for 5 days.

Timing of the physiological measurements

Physiological measurements were performed at two time points. The first one was done at the beginning of the tillering stage (17 DAS) to monitor the influence of growing conditions, and it is further referred to as “after acclimation”. The second measurement date was at the end of stress treatment (24 DAS), further referred to as “after stress”.

Gas exchange

Gas exchange parameters (light-saturated CO_2 assimilation rate, A_{max}; transpiration rate, E) were measured by LI-6800 (LI-COR, Nebraska, USA) on the first fully developed leaf. The following parameters were set in the leaf chamber: T of the heat exchanger: 25/39 °C (after acclimation/after stress), RH 60/40% (after acclimation/after stress), 1200 µmol/m^{2}s PAR, CO_2 concentration 400 or 800 ppm according to growing conditions. Instantaneous water use efficiency after acclimation was calculated as:

$WUE_{instantaneous} = A_{max}/E$.

Flavonoid index

The relative content of flavonoids was measured *in-vivo* on the basis of epidermal UV screening of chlorophyll fluorescence using the instrument Multiplex (FORCE-A, France) as thoroughly described in Ben Abdallah et al. (2018).

Statistics and data analysis

The data were analysed using three-way analysis of variance (ANOVA) using Statistica 13 software (StatSoft, Tulsa, US). Tukey’s *post hoc* test ($p = 0.05$) was used to identify significant differences between the means.

All plots were created in R software version 4.0.2 using the *ggplot2* package (Wickham 2016).

RESULTS AND DISCUSSION

Instantaneous water use efficiency

$WUE_{instantaneous}$ after acclimation ranged from 4.2 to 10 mmol/mol (Figure 1). It was markedly affected by growth conditions, especially by CO_2 concentration. Plants grown in EC displayed higher $WUE_{instantaneous}$ than AC grown plants, in accordance with our expectations. This effect is a well-known consequence of increased photosynthetic rate and decreased stomatal conductance followed by reduced transpiration rate in elevated CO_2. Such effect was reported before in wheat (Jensen and Christensen 2004). The effect of EC was enhanced in HL conditions. Plants grown in EC HL tended to have higher $WUE_{instantaneous}$ than corresponding treatment in LL. Esmaili et al. (2020) reported a similar response in lettuce. They observed increasing $WUE_{instantaneous}$ with increasing light intensity and CO_2 concentration. In HL conditions UV- plants had higher $WUE_{instantaneous}$ than UV+ treatment except for Barke EC N+. Contrarily, Gitz et al. (2005) reported the opposite effect for soybean. Nitrogen fertilisation effect on $WUE_{instantaneous}$ did not show any uniform trend. On the contrary, increased $WUE_{instantaneous}$ by nitrogen fertilisation was reported for spring wheat (Zhang et al. 2016).

Figure 1 Instantaneous water use efficiency ($WUE_{instantaneous}$) of barley plants after acclimation. Data for oxidative-stress sensitive variety Barke (left) and oxidative stress-tolerant variety Bojos (right); dark grey – nitrogen fertilised plants in ambient CO_2 concentration (AC N+), grey – nitrogen fertilised plants grown in elevated CO_2 concentration (EC N+), light grey – non-fertilised plants grown in ambient CO_2 concentration (AC N-), pale grey – non-fertilised plants grown in elevated CO_2 concentration (EC N-). Columns represent means (n = 5), error bars represent SD. One repetition of the experiment. Different letters indicate significant differences ($p \leq 0.05$) between means within one variety based on Tukey's ANOVA post hoc test.

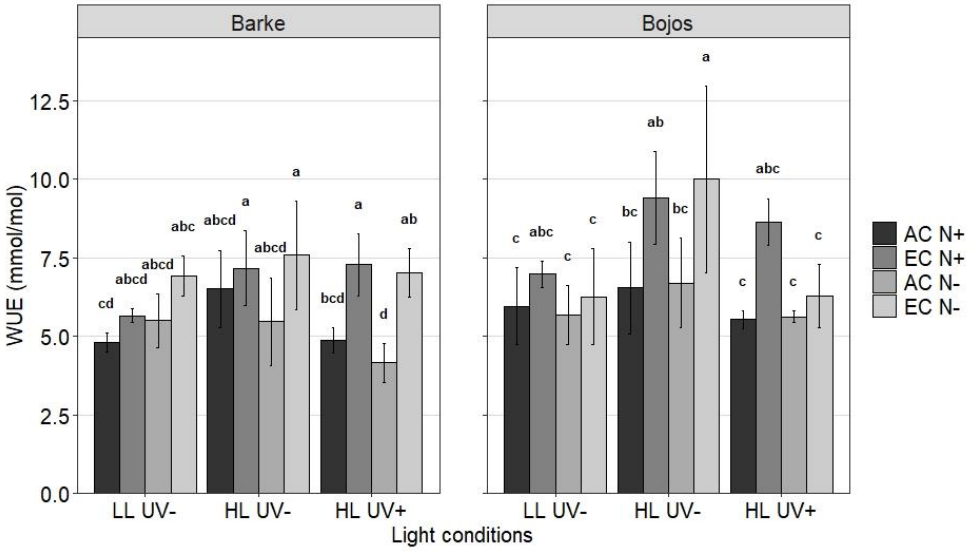

Flavonoid index

Flavonoids are secondary metabolites participating in UV protection, antioxidative processes, hormonal signalling, allelopathy, and many other processes in plants (Buer et al. 2010). It was shown that their content is increasing following high intensity irradiation and UV light treatment (Klem et al. 2015). In this experiment, the flavonoid index differed between light conditions, treatments, and varieties (Figure 2). Variety Bojos had lower content of flavonoids than sensitive variety Barke. Among the light conditions, the lowest content of flavonoids was found in LL treatment similarly to Klem et al. (2015).

In the LL treatment, a tendency for higher flavonoid content in EC grown plants was noted except for well-watered Barke after stress in correspondence with Pérez-López et al. (2018). In accordance with expectations, plants grown in HL had a higher content of flavonoids. For both varieties, an increase in flavonoid content was found after heat stress treatment and even higher increase for the combination of heat stress and drought. In comparison to LL plants, higher flavonoid content was recorded for HL UV- plants and the highest for HL UV+. Similarly to LL in both HL treatments, an increase in flavonoid content after stress treatments was noted. Again, in the case of combined stress, the increase was higher

except for Bojos EC N- HL UV+. In HL conditions, plants displayed a tendency for increased flavonoids content in N- plants, except for combined stress in Barke HL UV+ AC and heat-stressed Bojos HL UV- AC. In HL UV+ after combined stress, there was an opposite trend in contrast to LL regarding CO_2 concentration – EC grown plants had lower content of flavonoids than AC grown.

Figure 2 Flavonoid content index in barley leaves. Data for oxidative-stress sensitive variety Barke (top row) and oxidative stress-tolerant variety Bojos (bottom row) measured at the end of acclimation phase (17 DAS, left column), after 5 days of heat stress (24 DAS, middle column) and after 5 days of combined heat and drought stress (24 DAS, right column); dark grey - nitrogen fertilised plants in ambient CO_2 concentration (AC N+), grey – nitrogen fertilised plants grown in elevated CO_2 concentration (EC N+), light grey – non-fertilised plants grown in ambient CO_2 concentration (AC N-), pale grey – non-fertilised plants grown in elevated CO_2 concentration (EC N-). Columns represent means (n = 5), error bars represent SD. One repetition of the experiment. Different letters indicate significant differences ($p \leq 0.05$) between means within one variety, timepoint, and irrigation regime based on Tukey's ANOVA post hoc test.

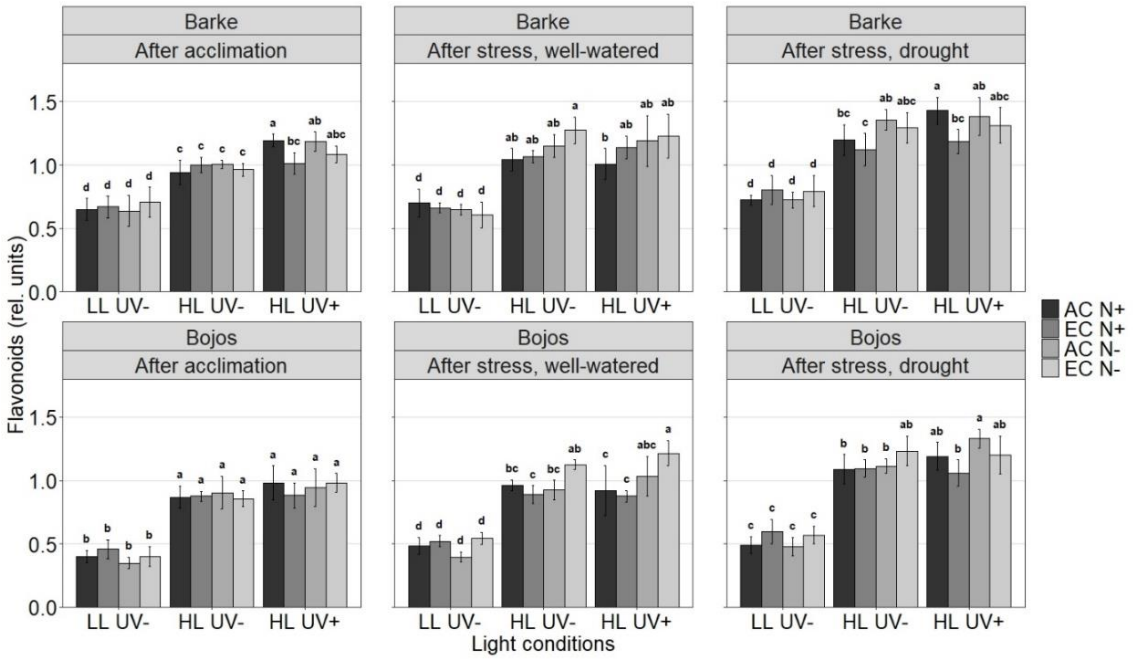

Gas exchange

After the acclimation, the A_{max} was affected the most by CO_2 concentration. Whereas in plants grown in AC it ranged from 16.5–25.5 μmol/m^{2}s, in plants grown in EC it was 21.0–32.0 μmol/m^{2}s (Figure 3). The effect of nitrogen nutrition after acclimation was more apparent in the variety Bojos, where N+ plants tended to have higher A_{max} while in Barke, both fertilised and N- plants showed similar values and no uniform trend.

Similarly to Dikšaitytė et al. (2019), the combination of drought stress and high temperatures caused serious changes in A_{max} and all the drought-stressed plants were wilted. After the stress treatment, all the drought-stressed HL UV- plants were heavily affected, with the A_{max} around zero. The dry HL UV+ were also strongly affected, but low photosynthetic rates were still retained in N- Barke from EC and in Bojos with higher A in the EC environment. The least affected were plants grown in LL UV-. Their A_{max} ranged for Barke 6.9–11.6 (decrease by 62% in comparison to acclimation phase) and for Bojos 13.7–18.3 μmol/m^{2}s (decrease by 16% in comparison to acclimation phase). The high temperatures alone did not show such a strong effect on gas exchange as drought stress. While HL plants were affected very little and mostly negatively, the LL plants showed an increase in A_{max}. After the drought stress, the difference in A_{max} between N+ and N- plants in Barke appeared, with N+ having higher A_{max}.

Figure 3 Light-saturated CO_2 assimilation of barley plants. Data for oxidative-stress sensitive variety Barke (top row) and oxidative stress-tolerant variety Bojos (bottom row) measured at the end of acclimation phase (17 DAS, left column), after 5 days of heat stress (24 DAS, middle column) and after 5 days of combined heat and drought stress (24 DAS, right column); dark grey - nitrogen fertilised plants in ambient CO_2 concentration (AC N+), grey – nitrogen fertilised plants grown in elevated CO_2 concentration (EC N+), light grey – non-fertilised plants grown in ambient CO_2 concentration (AC N-), pale grey – non-fertilised plants grown in elevated CO_2 concentration (EC N-). Columns represent means (n = 5), error bars represent SD. One repetition of the experiment. Different letters indicate significant differences ($p \leq 0.05$) between means within one variety, timepoint, and irrigation regime based on Tukey's ANOVA post hoc test.

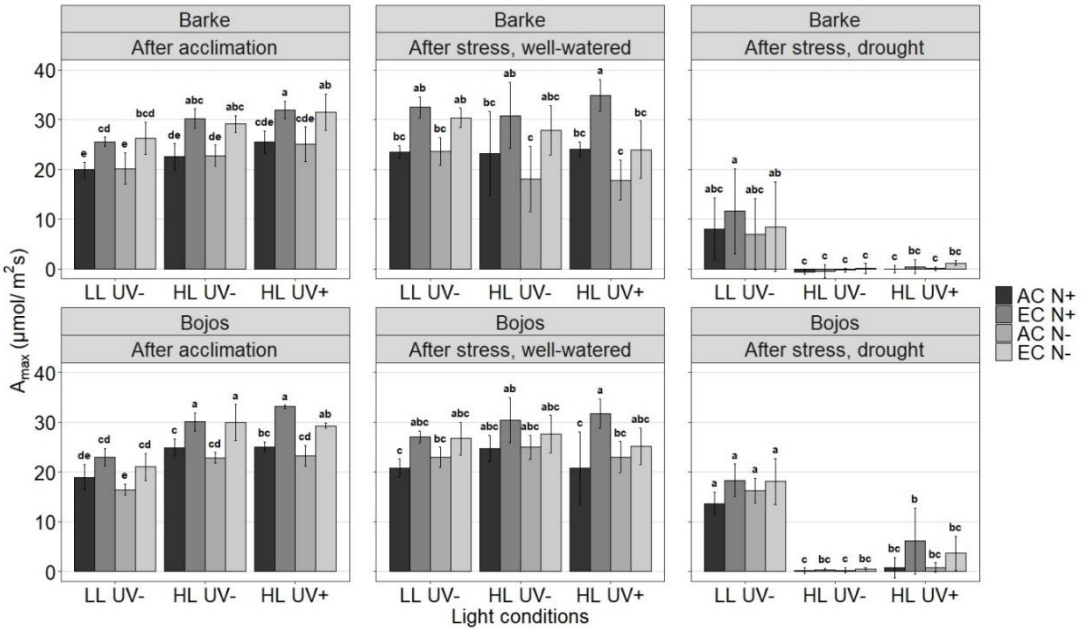

CONCLUSIONS

Within this study, we have shown that growth light quality and intensity substantially affect barley response to subsequent drought and heat stress. LL plants, despite their lower $WUE_{instantaneous}$ during acclimation, overcame the stress treatment better than HL grown plants. Exposure to HL, UV, and EC increased the flavonoid index in leaves. This increase, however, did not provide sufficient stress protection in the means of photosynthetic activity maintenance. Similarly nitrogen nutrition, which has rather a negative effect on flavonoid accumulation, did not significantly modulate the photosynthetic response to heat and drought stress.

ACKNOWLEDGEMENTS

The research was financially supported by grant no. AF-IGA2021-IP019. KK and BV were supported by the project SustES - Adaptation strategies for sustainable ecosystem services and food security under adverse environmental conditions (CZ.02.1.01/0.0/0.0/16_019/0000797).

REFERENCES

Ainsworth, E.A., Long, S.P. 2005. What have we learned from 15 years of free-air CO_2 enrichment (FACE)? A meta-analytic review of the responses of photosynthesis, canopy properties and plant production to rising CO_2. New Phytologist, 165(2): 351–372.

Avila, R.T. et al. 2020. Elevated air [CO_2] improves photosynthetic performance and alters biomass accumulation and partitioning in drought-stressed coffee plants. Environmental and Experimental Botany [Online], 177: 104137. Available at: https://doi.org/10.1016/j.envexpbot.2020.104137. [2021-08-03].

Ben Abdallah, F. et al. 2018. Comparison of optical indicators for potato crop nitrogen status assessment including novel approaches based on leaf fluorescence and flavonoid content. Journal of Plant Nutrition, 41(20): 2705–2728.

Buer, C.S. et al. 2010. Flavonoids: New Roles for Old Molecules. Journal of Integrative Plant Biology, 52(1): 98–111.

Dikšaitytė, A. et al. 2019. Growth and photosynthetic responses in *Brassica napus* differ during stress and recovery periods when exposed to combined heat, drought and elevated CO_2. Plant Physiology and Biochemistry, 142: 59–72.

Esmaili, M. et al. 2020. CO_2 enrichment and increasing light intensity till a threshold level, enhance growth and water use efficiency of lettuce plants in controlled environment. Notulae Botanicae Horti Agrobotanici Cluj-Napoca, 48(4): 2244–2262.

Gitz, D.C. et al. 2005. Ultraviolet-B effects on stomatal density, water-use efficiency, and stable carbon isotope discrimination in four glasshouse-grown soybean (*Glyicine max*) cultivars. Environmental and Experimental Botany, 53(3): 343–355.

Holub, P. et al. 2019. Induction of phenolic compounds by UV and PAR is modulated by leaf ontogeny and barley genotype. Plant Physiology and Biochemistry, 134: 81–93.

Jensen, B., Christensen, B.T. 2004. Interactions between elevated CO_2 and added N: Effects on water use, biomass, and soil ^{15}N uptake in wheat. Acta Agriculturae Scandinavica, Section B: Soil and Plant Science, 54(3): 175–184.

Klem, K. et al. 2019. Distinct Morphological, Physiological, and Biochemical Responses to Light Quality in Barley Leaves and Roots. Frontiers in Plant Science [Online], 10: 1026. Available at: https://www.frontiersin.org/article/10.3389/fpls.2019.01026/full. [2021-07-09].

Klem, K. et al. 2015. Ultraviolet and photosynthetically active radiation can both induce photoprotective capacity allowing barley to overcome high radiation stress. Plant Physiology and Biochemistry, 93: 74-83.

Pérez-López, U. et al. 2018. Concentration of phenolic compounds is increased in lettuce grown under high light intensity and elevated CO_2. Plant Physiology and Biochemistry, 123: 233–241.

Stitt, M., Krapp, A. 1999. The interaction between elevated carbon dioxide and nitrogen nutrition: The physiological and molecular background. Plant, Cell and Environment, 22(6): 583–621.

Wickham H. 2016. ggplot2: Elegant Graphics for Data Analysis [Online]. 1. ed., Springer-Verlag New York. Available at: https://ggplot2.tidyverse.org. [2020-01-19].

Zhang, B. et al. 2016. Mycorrhizal inoculation and nitrogen fertilization affect the physiology and growth of spring wheat under two contrasting water regimes. Plant and Soil, 398: 47–57.

Determination of chlorophyll content, RWC and LDMC in leaves of sorghum and maize during two different phenological stages in the field conditions

Nicole Frantova[1], Michal Rabek[2], Petr Elzner[1], Vladimir Smutny[2]
[1]Department of Crop Science, Breeding and Plant Medicine
[2]Department of Agrosystems and Bioclimatology
Mendel University in Brno
Zemedelska 1, 613 00 Brno
CZECH REPUBLIC

nicole.frantova@mendelu.cz

Abstract: The chlorophyll content, relative water and leaf dry matter content of sorghum varieties and maize varieties were observed and analysed. The chosen varieties of sorghum differed in earliness and type. The maize varieties had a different FAO number. The data from the analyse of the samples taken in the field during two different phenological stages of the sorghum and maize showed differences among types of sorghum in RWC, LDMC and chlorophyll content; differences were also found among maize varieties with different FAO number in chlorophyll content, and among sorghum and maize varieties in LDMC and chlorophyll content. The results of sorghum varieties differed more in type than in earliness. The results of maize varieties differed in FAO number in chlorophyll content. There was not found a statistically significant difference between sorghum varieties and maize varieties in the content of water in the leaves, but maize plants were sown earlier and probably had the optimal conditions under which they could compete with sorghum plants.

Key Words: variety, FAO number, grain, silage, phenology

INTRODUCTION

Sorghum (*Sorghum bicolor*) is a multipurpose crop being cultivated mostly in the semiarid tropic areas of Africa and Asia. In these places, the sorghum is a staple food for poor people, but it is used as fodder and material for the production of biofuel too (Hariprasanna and Patil 2015). It is well adapted to a water-limited environment with the drought-tolerance mechanism such as deep root system, thick leaf wax layer, osmotic adjustment etc. (Tari et al. 2012).

Maize (*Zea mays*) is a crop grown in diverse environments, from the North (Russia and Canada) to the South (Chile) including tropical regions and distinct sea levels being cultivated up to 3 800 m.a.s.l. with the range of growing seasons between 42 up to 400 days. Due to this wide range of environments, the high morphological and physiological diversity among cultivars was evolved (AGDH 2008). A major part of the world maize production is used as animal feed (48.7%); proximately 30% is used for ethanol production and an only minor part is used for fructose syrup, as a sweetener and for cereals (USDA 2015).

Chlorophyll is the most essential plant pigment due to its importance in photosynthesis, it is an indicator of greenness in leaves, and it is frequently used for the detection of nutrient deficiencies (Ali et al. 2017).

RWC (relative water content) is an applicable indicator of plant water balance state expressing the absolute water amount, which the plant needs to reach artificial full saturation. There is a relationship between water potential and RWC, this relationship differs during the age of plant material. Water makes the most of plant cells mass and in every cell, cytoplasm makes about 5–10% of the volume of cell and the remaining volume is taken by a massive vacuole filled with water. There was found a strong correlation between leaf protoplast volume alterations and changes in the photosynthesis activity in leaves (González and González-Vila 2001).

LDMC (leaf dry matter content) is the ratio of dry mass to the fresh mass of the leaf (Yang et al. 2020). Leaves with higher LDMC are usually tougher and may be more tolerant to physical harm (e. g. wind, herbivore insect) in comparison with leaves of lower LDMC (Cornelissen et al. 2003). LDMC increases in summer, and at some species, it is affected by shoot elongation phenology and non-structural carbohydrates sink–source relationship between growing and old plant organs (Palacio et al. 2008).

This experiment aimed to compare differences between two species of C4 crops, sorghum and maize and differences among varieties of each species in chlorophyll content, relative water content and leaf dry matter content in the leaves during two different phenological stages in the field conditions.

MATERIAL AND METHODS

Site description and field sampling

Details about precipitation and sum of average temperature can be found in Figure 1 and Figure 2; the sum of average daily temperatures and the amount of precipitation was calculated from the date of sowing till the date of sampling and for the growing degree day calculation; 10 °C was used as a base temperature. The sampling locality was in Žabčice, South Moravia (49°00'50.3"N, 16°36'03.6"E) where the Field Research Station is situated. The six sorghum and six maize varieties of Syngenta, Seed service and KWS companies were selected (Table 1 and the photos of some varieties in the field conditions can be found in Figure 3–5). The sorghum varieties differed in earliness and the type of variety (for grain or silage production). The maize varieties varied in the FAO number. The sampling took place on 28 July and 12 August at 1 pm, the samples were taken from the sorghum and maize fields. The sorghum plants were sown on 2 June and the maize plants were sown on 12 May. The sorghum plots were the size of 9 m^2 per variety and the maize plots were the size 10.5 m^2. The samples were represented as a cut part of the middle part of the second youngest leaf in the size of 1 x 6 cm, one leaf per plant, two plants per variety for both species.

Table 1 Basic information about tested varieties in our experiment

Sorghum variety	Type	Earliness	Maize variety	FAO (for silage production)
Ruby	grain	early	SY Fregat	260
KWS Nemesis	grain	semi-early	SY Impulse	270
Pampa Centurion BMR	grain-silage	very early	SY Torino	290
KWS Freya	silage	early	unregistered	360
KWS Hannibal	silage	semi-late	SY Infinite	380
KWS Bulldozer	silage	late	SY Minerva	380

Figure 1 Measured values of average temperature sum and growing degree days for both species

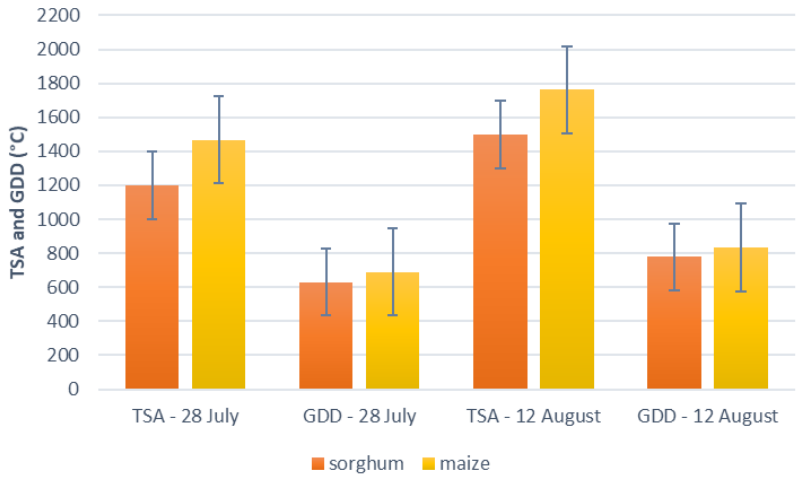

Legend: Abbreviations: TSA – temperature sum of average, GDD – growing degree days, error bars represent standard deviation values.

Figure 2 The amount of precipitation from the day of sowing till the sampling days

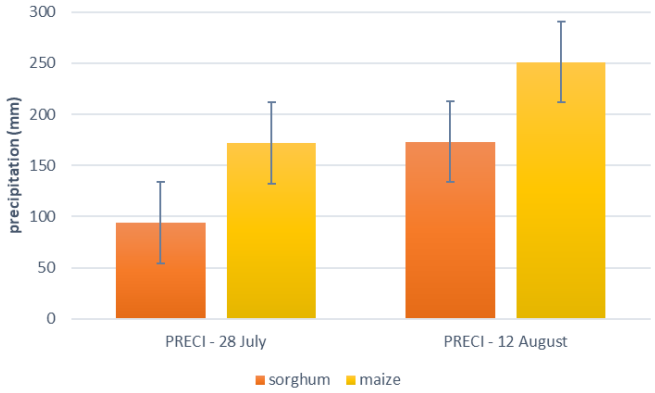

Legend: PRECI – precipitation, error bars represent standard deviation values.

Phenological stage determination and chlorophyll measurement

For the sorghum phenological stage determination was used the growth scale according to Rao et al. (2007), with numbers from 0 to 9; where 0 means emergence and 9 means physiological maturity. For the maize phenological determination was used the BBCH scale (Meier 2018) with numbers from 0 to 99, where 0 means dry seeds and 99 means harvested product.

The chlorophyll content was measured on the third youngest leaf in the middle of the blade by the N-tester (Yara, Norway). For both species, 15 plants per variety were measured with two replications.

Relative water content and dry matter in the leaves

The cut-out parts of leaves were immediately weighed after being cut (fresh weight). Then the leaf samples were cut into 1 x 1 cm squares and put into the tubes with water for 3 hours, all parts were underneath the water level. After 3 hours, the samples were dried with tissue paper and weighed again (saturated weight). The next step was drying the samples in the drying oven at 102 °C for 2 hours. After that, the samples were weighed again (dry weight). The relative water content was calculated according to Gonzáles and Gonzáles–Vivar (2001):

$$\text{RWC} = \frac{\text{fresh weight} - \text{dry weight}}{\text{saturated weight} - \text{dry weight}} \text{ x } 100$$

$$\text{LDMC} = \frac{\text{dry weight}}{\text{fresh weight}} \text{ x } 100$$

Statistical data analysis

Shapiro-Wilk test was used to test the data's normality. Consequently, Kruskal–Wallis test was performed to find differences among varieties and species in chlorophyll content, RWC and LDMC; Dwass–Steel–Critchlow–Fligner test was used to analyse pairwise comparison. Pearson's rank correlation was used to analyse factors affecting chlorophyll content, RWC and LDMC. The $p>0.05$ was used as the level of statistical significance and $n = 30$. The most of statistical analyses were performed in Statistica 12.0 software (Tibco Software, USA), only Dwass–Steel–Critchlow–Fligner test was performed by Jamovi software (The jamovi project, Australia).

RESULTS AND DISCUSSION

Sorghum

There was found a positive significant correlation ($r = 0.4$) between the chlorophyll content and the RWC in sorghum leaves; with the higher content of relative water in leaves, the chlorophyll content increases. The relationship between water and chlorophyll synthesis is known, the lower level of water in leaves negatively affects the chlorophyll synthesis leading to the chlorophyll decomposition, making changes in colours of leaves from green to yellow. The chlorophyll content may be controlled

by soil and climate; therefore, it may be an indicator of plants responses to the changing climate (Li et al. 2018). There was found a significant difference between the RWC of grain and silage type of sorghum, and between grain-silage and silage type. Grain-silage type had the highest percentage of the RWC, then silage and subsequently grain type followed. These results correspond with the fact, that the grain type of sorghum has a lower water level than silage type which is important for fermentation. The relationship between the phenological stage and LDMC (r = 0.5) and the phenological stage and chlorophyll content (r = 0.6) was also found with statistical significance. With the progressed phenology of plants, the chlorophyll content rises, the younger leaves had a light green colour meaning lower content of chlorophyll in comparison with the older leaves having darker green colour, this is related to the earliness of varieties. The highest LDMC was observed in silage type, the lowest in grain type. The silage type may need more LDMC for the higher content of biomass for fermentation than grain type of which is more important grain yield than its total biomass. A statistically significant difference in the chlorophyll content was found between grain and silage type, the variety with the highest chlorophyll content was KWS Nemesis (grain type) and the lowest chlorophyll content was found in KWS Buldozer (silage type). The grain type of sorghum may contain a higher content of leaf chlorophyll because of its shorter height (height data are not included) in comparison with silage or grain-silage type of sorghum which are taller plants.

Figure 3 Ruby (sorghum) *Figure 4 SY Fregat (maize)* *Figure 5 Freya (sorghum)*

Legend: The photos were taken on 12 August (2021) in Žabčice by the authors

Maize

A positive significant moderate correlation was observed between chlorophyll content and LDMC (r = 0.6). These results correspond to the experiment conducted by Bokari (1983), where a close correlation was found between chlorophyll and dry matter content in the leaves of C4 grasses. With increased chlorophyll content, the dry matter increased in leaves too. The correlation between the phenological stage and LDMC were also significant (r = 0.5). With the progressed phenological development, the LDMC in leaves rises, older leaves have a higher LDMC than younger leaves, but the LDMC is strongly affected by environmental factors such as temperature and precipitation. A very strong positive significant correlation was found between the chlorophyll content and the phenological stage (r = 0.8). As mentioned above, the younger leaves contain the lower chlorophyll and the older leaves contain a higher level of chlorophyll, but chlorophyll content is also affected by many external factors e. g. pathogens, temperature, a dose of nitrogen fertilizer, the inappropriate use of pesticides. The statistical difference of the chlorophyll content was found between varieties with FAO number 270 and 380; and 290 and 380. This confirms the theory, the chlorophyll content rises with the progressed development of the plant.

Sorghum and maize

The differences between sorghum and maize LDMC and chlorophyll were found statistically significant but the subsequent analyses which compared all the sorghum varieties, and all the maize

varieties did not find differences between the individuals. The mean numbers of RWC, LDMC and the chlorophyll content for both species can be found in Figure 6 and Figure 7. Sorghum is more tolerant to drought than maize (Schittenhelm and Schroetter 2014). So, to explain smaller differences of the water content in the leaves between sorghum and maize varieties can be caused by the date of sowing. The maize varieties were sown on 12 May and the sorghum varieties on 2 June. The maize varieties were sown earlier, the number of growing degree days was higher than in sorghum, this meant more days with optimal temperature for growing, and the sum of average precipitation from the sowing day till the sampling day was higher too, thus maize could progress in development, protect its sensitive organs (flowers) during the critical days with lower or no precipitation by being in post-anthesis stage and to compete to sorghum under optimal field conditions, but prove this theory, the data of weather conditions should be analysed in more details.

Figure 6 Mean numbers of RWC and LDMC

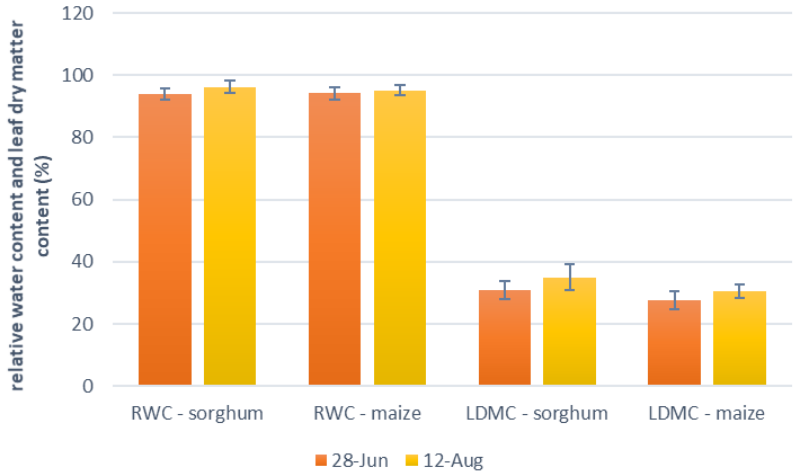

Legend: Error bars represent standard deviation values.

Figure 7 Mean numbers of chlorophyll content in sorghum and maize

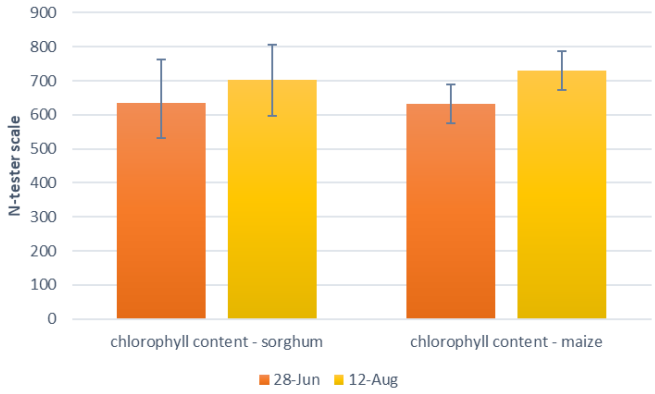

Legend: Error bars represent standard deviation values.

CONCLUSION

The obtained data from the analyse of the samples taken in the field during two different phenological stages of the sorghum varieties and maize varieties showed differences among types of sorghum in RWC, LDMC and chlorophyll content; differences were also found among maize varieties with different FAO number in chlorophyll content, and among sorghum and maize varieties in LDMC and chlorophyll content. The sorghum varieties had a statistically significant higher average LDMC for both sampling dates, but maize varieties had a statistically significant higher average content of the chlorophyll at the second sampling date. The results of sorghum varieties differed more in type than in earliness. The results of maize varieties differed in FAO number from chlorophyll content. There was not found a statistically significant difference between sorghum varieties and maize varieties in the content of water in the leaves, but maize plants were sown earlier and probably had the optimal

conditions under which they could compete with sorghum plants. To study competition to the same field conditions at a given time between sorghum and maize, a higher number of samplings and times of sampling is needy to study changes of chlorophyll content, RWC and LDMC in time.

ACKNOWLEDGEMENTS

This experiment was financially supported by the project MendelFarm – Integrated plant protection in a farm operating in dry conditions as part of the 9.F.m: Demonstration Farm call provided by the Ministry of Agriculture. I would like to express my very great appreciation to the workers at the Field Research Station in Žabčice where the samplings took place, for allowing me to perform this experiment and use their instruments. Special thanks to Assoc. Prof. Ing Petr Škarpa, Ph. D. for lending the N-tester.

REFERENCES

Ali, M.M. et al. 2017. Leaf nitrogen determination using non-destructive techniques–A review. Journal of Plant Nutrition [Online], 40(7): 928–953. Available at: https://www.tandfonline.com/doi/full/10.1080/01904167.2016.1143954. [2021-08-23].

Australian Government. Department of Health (AGDH). 2008. The Biology of Zea mays L. ssp mays (maize or corn) [Online]. Available at: https://biosafety.icar.gov.in/the-biology-of-zea-mays-l-spp-mays-maize-or-corn/. [2021-08-23].

Bokari, U.G. 1983. Chlorophyll, Dry Matter, and Photosynthetic Conversion-Efficiency Relationships in Warm-season Grasses. Journal of Range Management, 36(4): 431–434.

Cornelissen, J.H.C. et al. 2003. A handbook of protocols for standardised and easy measurement of plant functional traits worldwide. Australian Journal of Botany [Online], 51(4): 335–380. Available at: https://experts.umn.edu/en/publications/a-handbook-of-protocols-for-standardised-and-easy-measurement-of-. [2021-8-24].

González, L., González-Vilar, M. 2001. Determination of relative water content. In Handbook of Plant Ecophysiology Techniques. Netherlands: Springer, pp. 207–212.

Hariprasanna, K., Patil, J.V. 2015. Sorghum: Origin, Classification, Biology and Improvement. In Sorghum Molecular Breeding. India: Springer, pp. 3–20.

Meier, U. 2018. Growth stages of mono-and dicotyledonous plants. In BBCH Monograph. Quedlinburg: Open Agrar Repositorium, pp. 28–31.

Schittenhelm, S., Schroetter, S. 2014. Comparison of Drought Tolerance of Maize, Sweet Sorghum and Sorghum-Sudangrass Hybrids. Journal of Agronomy and Crop Science [Online], 200(1): 46–53. Available at: https://onlinelibrary.wiley.com/doi/abs/10.1111/jac.12039. [2021-09-06].

Tari, I. et al. 2012. Response of Sorghum to Abiotic Stresses: A Review. Journal of Agronomy and Crop Science [Online], 199(4): 264–274. Available at: https://onlinelibrary.wiley.com/doi/abs/10.1111/jac.12017. [2021-08-28].

Palacio, S. et al. 2008. Seasonal variability of dry matter content and its relationship with shoot growth and nonstructural carbohydrates. New Phytologist [Online], 180: 133–142. Available at: https://www.jstor.org/stable/25150558. [2021-08-24].

Rao, S.S. et al. 2007. Characterizing phenology of sorghum hybrids in relation to production management for high yields. In NRCS-ICRISAT Learning Program on Sorghum Hybrids Parents and Hybrids Research and Development [Online]. Hyderabad, 6–17 February. India, NRCS and ICRISAT, pp. 1–5. Available at: https://www.millets.res.in/books/chapter/Charcaterizing_phenology_of_sorghum_hybrids_in_relation_to_production_management_for_high_yields.pdf. [2021-8-24].

United States Department of Agriculture (USDA). 2015. USDA Coexistence Fact Sheets Corn – https://www.usda.gov/sites/default/files/documents/coexistence-corn-factsheet.pdf

Yang, B. et al. 2020. A simple method for estimation of leaf dry matter content in fresh leaves using leaf scattering albedo. Global Ecology and Conservation [Online], 23: e01201. Available at: https://www.sciencedirect.com/science/article/pii/S2351989420307423#bib19. [2021-08-24].

Transcript levels of *VRN1*, *PPD-D1*, *PPD-B1* and *PPD-A1* genes during different developmental stages of winter wheat

Nicole Frantova, Pavlina Smutna, Ludmila Holkova
Department of Crop Science, Breeding and Plant Medicine
Mendel University in Brno
Zemedelska 1, 613 00 Brno
CZECH REPUBLIC

nicole.frantova@mendelu.cz

Abstract: The phenology of winter wheat is largely affected by the expression of the vernalization gene *VRN1* and the *PPD-D1*, *PPD-B1* and *PPD-A1* genes responsible for sensitivity to photoperiod. The transcript levels of these genes were studied in six winter and one facultative wheat variety during growing season 2020. During the development of the shoot apex, the activity of *VRN1* and *PPD-D1* is gradually increased, although some transcript level of the *VRN1* gene was found also in the leaves during the cold weather. In the spring, after vernalization fulfilment and during prolonged daylight, the increased expression of VRN1 and PPD-D1 was related to the change of the developmental stage. From a certain developmental stage, an increase in expression was observed, which corresponds to a change in development. However, the activity of the *PPD-B1* decreases when the development of the shoot apex increases. It is possible that certain combinations of *PPD1* loci alleles can alter head timing by acceleration which can protect sensitive floral meristem during unfavourable weather conditions and therefore, the information about allele combination and regulation conditions of these genes can be used for breeding of new varieties suitable for specific environmental conditions.

Key Words: wheat, gene, phenology, vernalization, photoperiod

INTRODUCTION

A transition from the vegetative to the reproductive stage is essential for the formation of the yield component in plants that are grown for their seeds. This transition is represented by the development of the shoot apex, when new leaf primordia are formed, and spikelet starts to take form. Flowering is a subsequent stage to spikelet formation; at this stage, the final leaf number is determined (Waddington et al. 1983).

Plant phenology studies events of the plant life cycle that are activated by environmental changes. Phenological events can be seen as an indicator of local changes in weather and as a touchstone of global changes because of changing climate. During the past decades, many authors published scales of plant development stages for individual species. For the description of microphenological stages of barley and wheat shoot apex is mostly used Waddington's scale (Waddington et al. 1983), which is a quantitative scale classifying spike initial and pistil development in numbers from 1 to 10 (flowering), also using the decimal places.

Winter wheat phenology is mainly affected by genes responsible for vernalization requirement, sensitivity to photoperiod and earliness per se. Winter wheat requires a long period of low temperatures to switch into the reproductive stage and to flower in spring. Vernalization is necessary for flowering meristem protection, it prevents flowering during cold temperatures that would harm this meristem. The pivotal role in the growth habit has a gene *VRN1* (Vernalization1), of which winter wheat carries three homoeologous copies *vrn-A1*, *vrn-B1* and *vrn-D1*, these genes encode MADS-box transcription factors (Yan et al. 2003). There are several other genes in the regulation of *vrn1* during *the* period of vernalization. *Vrn2* (Vernalization2) is one of them, this gene encodes encode proteins with a zinc-finger motive and a CCT domain, it is a flowering repressor that is downregulated by vernalization. The loss of *vrn2* function gives spring wheat habit that does not require vernalization for flowering (Yan et al. 2004). Winter wheat possesses recessive alleles of the *vrn1* gene at all loci, *vrn-A1*; *vrn-B1* and *vrn-D1*; spring wheat needs to have at least one dominant allele of *Vrn1*.

Photoperiod insensitivity is the ability of a plant to flower during the short and long day, for response to photoperiod are associated *PPD1* (Photoperiod1) genes: *PPD-A1*, *PPD-B1* and *PPD-D1* which are pseudo-regulators (Beales et al. 2007). The recessive alleles of *Ppd1* provide photoperiod sensitivity. The key role has *Ppd-D1* gene which has the greatest effect on photoperiod sensitivity, the effect of other *PPD1* genes is followed by *Ppd-B1* and then *Ppd-A1* (Arjona et al. 2018).

The aim of this work was to evaluate the relationships between the expression of the selected genes and the development of shoot apexes of winter wheat varieties with different sensitivity to the photoperiod growing in the field conditions, where plants were exposed to natural forms of different types of abiotic stress.

MATERIAL AND METHODS

Field location and plant material

The six winter and one facultative variety were selected for this experiment. The winter varieties differed in their earliness and photoperiod sensitivity: Bohemia (the earliest), Balitus, IS Conditor, RGT Sacramento, Tobak, Tonnage (the latest) and facultative Tybalt. The plant material for molecular analyses was taken from the small field plots (10.3 m^2) at the locality Obora, at the Field Research Station in Žabčice, South Moravia (49°00'50.3"N, 16°36'03.6"E). The locality is situated at 179 m.a.s.l., with average precipitation proximately 480 mm and an average annual temperature of about 9 °C. Daily average values for above-ground temperatures can be found in Table 1.

Table 1 Daily average values for above-ground temperatures in Žabčice

Date	Above-ground temperature (daily average)
8 January	1.7 °C
12 February	2.8 °C
10 March	6.7 °C
18 March	7.5 °C
1 April	1.1 °C
15 April	6.4 °C
28 April	15 °C

Phenological stage determination

The plant material as whole plants with roots was dug from the field, and at the station shoot apexes and leaves preparation took place, the sampling was performed seven times between January and May (2020). The specific dates of samplings were: 8 January, 12 February, 10 March, 18 March, 1 April, 15 April and 28 April. For the phenological stage, the determination was used Waddington's scale for microphenology of the shoot apex.

RNA isolation and subsequent analyses

The plant material was transported from the field in the liquid nitrogen and the laboratory, the isolation of total RNAs from the leaves and apexes was performed with the use of RNeasy Plant Mini Kit (Qiagen, Germany), the RNA purification was conducted with DNA-free™ DNA Removal Kit (Invitrogen, Thermo Fisher Scientific, USA), the reverse transcription was accomplished with RevertAid RT Reverse Transcription Kit (Thermo Fisher Scientific, USA) and qPCR was carried out with the use of Xceed qPCR SG 2x Mix Lo-ROX (Institute of Applied Biotechnologies, Czech Republic). As a reference gene for qPCR was used Actin, the studied genes were: *VRN1* (regardless of the genome), the transcript level of this gene was analysed in shoot apexes and leaves; activity of *PPD-D1*, *PPD-B1* and *PPD-A1* were analysed only in the leaves. The sequences of primers for qPCR can be found in Table 2.

Before this experiment, the analysis of the *PPD-D1* was performed by the authors at the selected varieties. The insensitive allele was detected at varieties Balitus, Bohemia and RGT Sacramento

(marked as Ppd-D1a allele). The sensitive allele was detected at IS Conditor, Tobak, Tonnage and Tybalt (marked as ppd-D1b allele).

Table 2 Primers used for qPCR

Gene	Primer sequence 5' - 3'	Annealing temperature	References
Actin	ACC TTC AGT TGC CCA GCA AT CAG AGT CGA GCA CAA TAC CAG TTG	60	Gil-Humanes et al. 2009
VRN1	GAA CAA GAT CAA CCG GCA GGT GAC GGA GAA GAT GAT GAC GCC GAC CTC	60	Boldizsár et al. 2016
PPD-D1	AAG ACA AGG CTG ATG AAA TGA G GAA GGA TTG ACC ACA TTG GA	60	Shaw et al. 2012
PPD-B1	AAG ACA AGG TTG ATG ACG TGA GAG GGA TTG ATC ACG TTG G		
PPD-A1	AGA CAA GGC TGA TGA AAC GA CGA TGG ATT GAC CAA ACT G		

Statistical data analysis

Data obtained from qPCR reactions were normalised with the reference gene to correct sample to sample variations and errors in sample quantification (Bustin 2000). The statistical analyse was performed in Statistica 12.0 software (Tibco Software, USA). First, the normality of obtained data was tested by Shapiro–Wilk test, the dependence of transcript levels among the selected genes was tested by Spearman's rank correlation and differences among transcript levels of the chosen varieties and different developmental stages were tested by Kruskal–Wallis test, where the $p>0.05$ was chosen as the statistical significance level.

RESULTS AND DISCUSSION

Total RNAs from apexes and leaves of six winter and one facultative wheat varieties were isolated from samples taken in seven terms during different developmental stages in 2020. The qPCR was performed to detect transcript levels of the genes *VRN-1, PPD-D1, PPD-B1 and PPD-A1*. Descriptive statistics for the transcript levels of the genes can be found in Table 3.

VRN1 expression in apex and leaves

There was found a significant positive correlation between transcript level of the gene *VRN1* expressed in apexes and phenological stage (Table 4 and Figure 1). The *VRN1* gene is a transcription factor that regulates the identity of shoot apex meristem, after vernalization, the *VRN1* gene's activity is induced, and floral meristem begins to initiate. In the selected varieties of winter and facultative wheat in our experiment, the *VRN1* was active at a low level during cold weather and after vernalization, its level increased. These results correspond with the work of Deng et al. (2015). Furthermore, with higher activity of *VRN1* in the leaves which is up-regulated by *PPD-D1*, the activity of *VRN1* in the shoot apexes increased. Vernalization fulfilment in winter wheat results in a gradual induction of VRN1 gene expression which is associated with alterations in VRN1 – associated chromatin epigenetic modifications and subsequently expression of VRN2 gene is reduced. Decreasing VRN2 gene expression allows for increased CO (Constans) gene expression followed by increased VRN3 gene expression. Other genes involved in the photoperiod-activated pathway are also involved in the regulation of CO genes regulation. When *VRN3* (*FT1*) activity increases, the protein product of this gene transports from leaves through the phloem to the shoot apex meristem where the *VRN1* gene is activated (Chen and Dubcovsky 2012).

PPD1 expression in leaves

A very strong significant negative correlation was found between the activity of the *PPD-B1* gene and the phenological stage (Table 4). The activity of the *PPD-B1* throughout apex development was gradually decreased, this explains a detection of some transcript levels of this gene from the samples

taken in January during the short-day conditions. The higher activity of the *PPD-B1* can be given by the higher number of copies which cause expression even during the nighttime (Kiseleva et al 2017). Kiss et al. (2014) suggest, the effect of intercopy junction in the *PPD-B1* on the phenotype. Other obtained data showed a weak relationship between the activity of the *PPD-D1* and the *PPD-A1* genes but a stronger relationship between the *PPD-B1* and the *PPD-A1* genes. In the conducted experiment made by Whittal et al. (2018), the phenology variation of winter wheat varieties from the higher latitudes was explained mainly by the interaction between *PPD-D1* and *PPD-A1* loci and their allelic variation, but the importance of the *PPD-B1* gene is mentioned by Arjona et al. (2018), in their experiment, the presence of sensitive allele of the *PPD-B1* had a positive effect on grain number per unit area. However, it is known that dominant photoperiod insensitive alleles are ranked *Ppd-D1*> *Ppd-B1*> *Ppd-A1* according to their ability to influence the phenotype in European wheat (Worland et al. 1998). Not proven relationship between PPD-D1 gene expression and the phenological stage may be related to the dissimilar dynamics of expression of the insensitive and sensitive alleles of PPD-D1 during the day. As opposed to PPD-A1 (ppd-A1 and Ppd-A1), PPD-B1 (ppd-B1 and Ppd-B1) and ppd-D1, the Ppd-D1 gene had the highest levels of expression at night under short-day (Beales et al 2007). The varieties with both alleles of PPD-D1 (ppd-D1 and Ppd-D1) were included in our experiment and sampling for evaluation of gene expression was always performed in the morning.

No statistically significant differences were found among transcript levels of the chosen genes in the selected varieties (Table 5).

Table 3 Descriptive statistics for the transcript levels of the genes

Variable	N	Average	Variance	Standard Deviation	Coefficient of Variation
VRN1 leaves	49	0.78	0.26	0.52	65.90
VRN1 apexes	49	1.53	1.63	1.28	83.34
PPD-D1 leaves	49	0.47	1.24	1.11	235.45
PPD-B1 leaves	49	1.65	1.68	1.30	78.51
PPD-A1 leaves	42	2.53	5.09	2.26	89.01

Table 4 Spearman's rank correlation for the transcript levels of the genes

Variable	Vrn1 leaves	Vrn1 apexes	Ppd-D1 leaves	Ppd-B1 leaves	Ppd-A1 leaves	Phenological stage
VRN1 leaves		0.32	0.37	0.20	0.15	0.03
VRN1 apexes	0.32		0.13	-0.56	-0.47	0.69
PPD-D1 leaves	0.37	0.13		0.16	0.35	0.08
PPD-B1 leaves	0.21	-0.56	0.16		0.61	-0.80
PPD-A1 leaves	0.15	-0.47	0.35	0.61		-0.32

Legend: p>0.05

Table 5 ANOVA (Non-parametric) for the transcript levels of genes – grouping variable: variety

	χ^2	Degrees of Freedom	p
VRN1 leaves	3.73	6	0.71
VRN1 apexes	3.85	6	0.70
PPD-D1 leaves	3.57	6	0.73
PPD-B1 leaves	2.37	6	0.88
PPD-A1 leaves	8.67	5	0.12
Phenological stage	0.155	6	1.00

Figure 1 Scatterplot of visualized correlation between phenological stage and Vrn1 in apexes

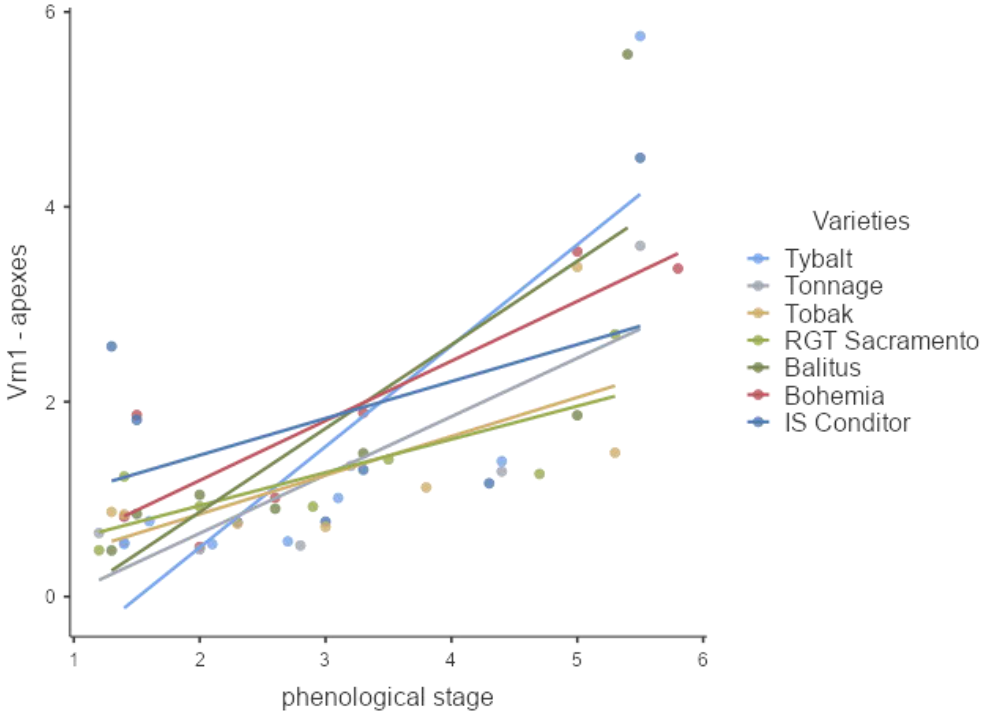

Legend: The numbers on y axe represent RNE - relative normalized expression

CONCLUSION

The transcript levels of the *VRN1*, *PPD-D1*, *PPD-B1* and *PPD-A1* genes were analysed in six winter and one facultative wheat during different developmental stages. We found a significant positive correlation between the activity of the *VRN1* gene in the shoot apexes and the phenological stage. We detected a low level of the *VRN1* gene in the leaves during the cold weather with the increases with warm weather arrives, which was reported in the previous studies. The negative correlation between the activity of *PPD-B1* and phenological stage was observed, which signifies that there is a certain activity of this gene that is gradually decreased during the development of the shoot apex. To understand more to effects of these genes on the flowering pathway of wheat is crucial to also detect specific alleles and observe the time of heading. A certain combination of *PPD1* loci alleles could affect grain yield by the altered head timing which can be one of the major events protecting sensitive floral meristem during unfavourable weather conditions. A more detailed study is needy for the determination of these allele combinations that could be used for the description of genotypes of wheat breeding materials.

ACKNOWLEDGEMENTS

This research was financially supported by the project QK1910269 - Adaptation potential of common wheat in response to drought and extreme temperatures of the National Agency for Agricultural Research.

REFERENCES

Arjona, J. M. 2018. Effect of Ppd-A1 and Ppd-B1 Allelic Variants on Grain Number and Thousand Kernel Weight of Durum Wheat and Their Impact on Final Grain Yield. Frontiers in Plant Science [Online], 9: 888. Available at: https://www.frontiersin.org/articles/10.3389/fpls.2018.00888/full. [2021-08-10].

Beales, J. et al. 2007. A pseudo-response regulator is misexpressed in the photoperiod insensitive Ppd-D1a mutant of wheat (Triticum aestivum L.). Theoretical and Applied Genetics [Online], 115(5): 721–733. Available at: https://pubmed.ncbi.nlm.nih.gov/17634915/. [2021-08-10].

Bustin, S.A. 2000. Absolute quantification of mRNA using real-time reverse transcription polymerase chain reaction assays. Journal of Molecular Endocrinology, 25(2): 169–193.

Boldizsár, Á. et al. 2016. The mvp2 mutation affects the generative transition through the modification of transcriptome pattern, salicylic acid and cytokinin metabolism in Triticum monococcum. Journal of Plant Physiology [Online], 202: 21–33. Available at: http://www.sciencedirect.com/science/article/pii/S0176161716301250?via%3Dihub. [2021-09-16].

Chen, A., Dubcovsky, J. 2012. Wheat TILLING Mutants Show That the Vernalization Gene VRN1 Down-Regulates the Flowering Repressor VRN2 in Leaves but Is Not Essential for Flowering. PloS Genetics [Online], 8(12): e1003134. Available at: https://journals.plos.org/plosgenetics/article?id=10.1371/journal.pgen.1003134. [2021-08-19].

Deng, W. et al. 2015. Direct links between the vernalization response and other key traits of cereal crops. Nature communications [Online], 6: 5882. Available at: https://www.nature.com/articles/ncomms6882. [2021-08-19].

Gil-Humanes, J. et al. 2009. Comparative genomic analysis and expression of the APETALA2-like genes from barley, wheat, and barley-wheat amphiploids. BMC Plant Biology [Online], 9: 66. Available at: https://www.ncbi.nlm.nih.gov/pmc/articles/PMC2700811/pdf/1471-2229-9-66.pdf. [2021-08-17].

Kiseleva, A.A. et al. 2017. Features of Ppd-B1 expression regulation and their impact on the flowering time of wheat near-isogenic lines. BMC Plant Biology [Online], 17(Suppl 1): 172. Available at: https://bmcplantbiol.biomedcentral.com/articles/10.1186/s12870-017-1126-z. [2021-08-19].

Kiss, T. et al. 2014. Effect of different sowing times on the plant developmental parameters of wheat (Triticum aestivum L.). Cereal research communications [Online], 42(2): 239–251. Available at: https://agris.fao.org/agris-search/search.do?recordID=US201600187206. [2021-08-19].

Shaw, L.M. et al. 2012. The impact of photoperiod insensitive Ppd-1a mutations on the photoperiod pathway across the three genomes of hexaploid wheat (Triticum aestivum). The Plant Journal [Online], 71(1): 71–84. Available at: https://onlinelibrary.wiley.com/doi/full/10.1111/j.1365-313X.2012.04971.x. [2021-08-16].

Waddington, S.R. et al. 1983. A quantitative scale of spike initial and pistil development in barley and wheat. Annals of Botany, 51: 119–130.

Whittal, A. et al. 2018. Allelic variation of vernalization and photoperiod response genes in a diverse set of North American high latitude winter wheat genotypes. PloS One [Online], 13(12): e0209543. Available at: https://journals.plos.org/plosone/article?id=10.1371/journal.pone.0203068. [2021-08-20].

Worland, A.J. et al. 1998. The influence of photoperiod genes on the adaptability of European winter wheats. Euphytica [Online], 100: 385–394. Available at: https://link.springer.com/article/10.1023/A:1018327700985. [2021-09-11].

Yan, L. et al. 2004. The wheat VRN2 gene is a flowering repressor down-regulated by vernalization. Science [Online], 303(5664): 1640–4. Available at: https://pubmed.ncbi.nlm.nih.gov/15016992/. [2021-08-10].

Yan, L. et al. 2003. Positional cloning of the wheat vernalization gene VRN1. PNAS [Online], 100(10): 6263–6268. Available at: https://www.pnas.org/content/100/10/6263 [2021-08-09].

Auxin or sugar? Which has higher impact on bud outgrowth regulation?

Attila Kucsera[1], Jozef Balla[1,2], Stanislav Prochazka[1]
[1]CEITEC MENDELU
[2]Department of Plant Biology
Mendel University in Brno
Zemedelska 1, 613 00 Brno
CZECH REPUBLIC
xkucsera@mendelu.cz

Abstract: Apical dominance remains important phenomenon in plant physiology with a lot of questions to be answered. In this work we tried to find an answer, whether we should return to the nutrient hypothesis and ascribe a lesser role to auxin in regulation of apical dominance. 7-Day-old decapitated pea plantlets were used as a model system. The effect of sugar and auxin on bud outgrowth was studied by replacing the cotyledon with auxin or sucrose containing paste. Auxin flow was manipulated by wounding or auxin transport inhibitor (2,3,5-triiodobenzoic acid) application. The obtained results indicating that in young plantlets auxin and/or its flow had more pronounced effect on cotyledonary bud outgrowth regulation than the sucrose availability.

Key Words: apical dominance, phytohormones, auxin, sucrose

INTRODUCTION

One of the mechanisms that ensure that plants can survive and adapt to environmental challenges is apical dominance (AD). Generally, it is a phenomenon where apical shoot dominates over formation of lateral shoots. In case of apical shoot injury, the lateral meristems start to grow out and form new branches trying to assert a new dominance (Barbier et al. 2017). However, AD is abundant widely in plant kingdom, different plant species respond with different shoot branching intensity to internal (e.g. nutrients, added plant regulators) or external influences (e.g. deficiency of light, damaged stem) (Dun et al. in 2006).

With decades of research in this field it seems that auxin takes an indispensable role in regulation of AD. Auxin – indole-3-acetic acid (IAA) – as a signal molecule is primarily synthesized in immature leaves of plant apices and then transferred basipetally in the stem and further acropetally towards a root tip. Among auxin also other plant hormones, mainly cytokinins and strigolactones take place in a complex regulatory mechanism of AD (Müller and Leyser 2011, Gomez-Roldan et al. 2008, Umehara et al. 2008).

For many years it was discussed how is AD maintained and what main forces are behind it. Before the discovery of plant hormones, the prevalent theories focused on nutrient availability and distribution. However, some indications pointed to the fact, that other inhibitory substances can be involved in shoot branching control (Dostál 1908). After discovery of auxin it was demonstrated that IAA can replace the shot apex in its inhibitory effect in axillary bud outgrowth. The role of auxin in growing shoots was explained as a protective role from other inhibitory substances, where axillary buds lacking in auxin are not protected and disable to growth (Snow 1929). In contrary, Thimann and Skoog, (1933) concluded that auxin flow from the plant apex through the stem is responsible for growth inhibition of cotyledonary buds (direct auxin inhibition). The importance of stem auxin flow was also highlighted by Bennett et al. (2006). Auxin mainly produced in young leaves is transported to main stem and effectively filling auxin transport capacity which then blocks auxin from axillary buds and inhibiting their growth. The competitive canalisation assumed that sources of auxin, which are plant apices (primary source) and axillary buds (secondary sources) compete with each other for filling the transport capacity (Balla et al. 2011, Balla et al. 2016).

Nevertheless, plant hormones are not the only substances that affect plant life and processes of growth and development. Another type of important substances are sugars – as they serve not only

as nutritional but also signalling molecules. In some experimental setups it was shown that sucrose – that has much higher mobility in plants than auxin – correlates better in relation to bud release and can trigger bud outgrowth (Barbier et al. 2015). Based on recent studies it seems that sugars take up a major role in the initial part of axillary bud outgrowth most likely via interactions with plant hormones – cytokinins, auxins and maybe strigolactones (Barbier et al. 2019). Another recent study assumed that AD is weakened not only when there is not enough auxin but also in deficiency of sugars (resp. sucrose). There is also a possibility that sucrose can antagonize effect of auxin on bud outgrowth (Bertheloot et al. 2020).

In this work we tried to find an answer, whether we should return to the nutrient hypothesis and ascribe a lesser role to auxin in regulation of AD.

MATERIAL AND METHODS

For all experiments 7-day-old pea (*Pisum sativum* L.) plantlets, variety Vladan (Semo a.s., Smržice, Czech Republic) grown in soaked perlite were used. For every experimental variety 40 plantlets were used in at least one repetition. In all variants the plantlets were decapitated before further treatment.

The base of the pastes was lanolin paste with ratio of 25% water and 75% lanolin. First, we prepared the solutions of the required chemicals (auxin – indole-3-acetic acid, sucrose and TIBA – 2,3,5-triiodobenzoic acid). For the auxin paste the auxin was dissolved in DMSO (dimethyl sulfoxide). The paste was heated in ceramic bowl by steam with temperature not raising above 40 °C and the solution of auxin was added and well incorporated. The still warm paste was transferred to syringe and instead of needle was used modified micropipette tip. The same procedure was used for TIBA paste (dissolved in DMSO) and sucrose (dissolved in distilled water) and then added to lanolin paste and well incorporated.

The treatments in experimental variants were as following:

Plantlets with both cotyledons removed and treatments on right and left cotyledonary petiole stumps

a) 0.5% IAA-lanolin paste and 0,4 mol/l sucrose-lanolin paste; **b)** 0,4 mol/l sucrose-lanolin paste and plain lanolin paste; **c)** 1% TIBA-lanolin paste and 0.5% IAA-lanolin paste

Plantlets with both cotyledons halved vertically, vertical cut was made also into the stem stump and plastic was inserted to this wound and 0.5% auxin-lanolin paste was applied on right side of the wounded stem stump

d) no other treatment; **e)** in addition 0.5% auxin-lanolin paste applied to the halved cotyledons on the left side

Plantlets with both intact cotyledons

f) 0.5% IAA-lanolin paste to the stem stump; **g)** lanolin paste to the stem stump; **h)** in addition, cut was made between the cotyledonary bud and cotyledonary petiole, deep enough to disrupt auxin flow but not to cut the petiole; **i)** in addition on cotyledonary petioles 1% TIBA-lanolin paste was applied

After the treatment plants were grown for 7 days in cultivation cell at temperature 20 °C/18 °C under a 16 h day/8 h night photoperiod and light intensity 150 µmol/m^2/s.

Sucrose concentration used in experiments was based on concentrations used in work of Mason et al. 2014

RESULTS AND DISCUSSION

In the recent years some research data suggest that not only plant hormones but sugar has a role in regulation of AD, whereas some results indicate that sucrose is the main force behind bud release and outgrowth (Mason et al. 2014, Barbier et al. 2019). In this work we addressed the involvement of cotyledons – as nutrient sources, sucrose and auxin and its flow in processes of pea cotyledonary bud outgrowth. In all variants decapitated plants were used.

Plantlets with both cotyledons removed and treatments on right and left cotyledonary petiole stumps

In variant **a)** where sucrose and IAA pastes were applied, the outgrowing shoot was formed predominantly (87%) on the side where sucrose was applied. It is a similar result that was obtained by application of sucrose or IAA agarose gel containing microtubes mounted instead of cotyledons, where the combination of sucrose and IAA on one side and sucrose on the opposite side showed that auxin had stronger impact on bud inhibition than sucrose on bud release (Kucsera et al. 2019). In variant **b)** where sucrose or lanolin was applied, outgrowing shoot was formed in 43% cases on the side with lanolin and in 37% on the side with sucrose added. (In the remaining 20% no bud outgrowth was observed). The outgrowing ratio is similar to the ratio in decapitated plants with intact cotyledons, where it was around 50:50 (Kucsera 2017, Kucsera 2020). In variant **c)** where TIBA or auxin was applied, 33% of buds were formed outgrowing shoot on the side of auxin treatment and 67% where TIBA was applied. Even TIBA is a very effective auxin transport inhibitor (Thomson et al. 1973) and can be transported for short distances and penetrate into the buds, IAA flow through cotyledonary petiole stump showed stronger impact in terms of bud outgrowth inhibition. Results obtained on different model system using 21-day-old pea plants suggested that initiation of bud growth after shoot tip loss cannot be dependent on apical auxin supply whilst sugars are rapidly redistributed over large distances and accumulate in axillary buds before changes in auxin level (Mason et al. 2014). In the same 21-day-old pea plants there was find auxin gradient in the main stem below the shoot tip or outgrowing bud that diminished within some centimetres (Brewer et al. 2015). It should be highlighted that pea plants used in this work were 7-day-old plantlets with much less distances from the treatment sites to the buds, therefore, manipulation with the auxin level could have more pronounced impact. Moreover, 7-day-old plantlets in opposite to mature plants are supplied with nutrients predominantly from cotyledons as their leaves are not developed. Last but not least, this work was focused on cotyledonary buds having a special position in vicinity of two auxin flows, from the main stem and from the cotyledons.

Plantlets with removed half part of both cotyledons, vertical cut was made into the stem stump and plastic was inserted to this wound and IAA was applied on right side of the wounded stem stump

In variant **d)** the plantlets did not form any outgrowing shoots, they remained dormant. However, in longer time scale there was possible to observe some outgrowth in a ratio of 50:50 on the right or the left side. However, IAA was applied only on one side of the stem stump, it seems that the applied amount of IAA was able to fill the stem polar auxin transport capacity and cause bud outgrowth inhibition on both sides. In variant **e)** in addition IAA paste was applied to the halved cotyledons on the left side. The outgrowing shoot was formed in 67% on the side where no auxin was applied to the halved cotyledons. (33% of plants did not release any buds from dormancy). In this case IAA flow was directed not only basipetally but also from the cotyledons. It is known that cotyledons are sources of IAA (DeMason and Polowick 2009). Removing of one of the cotyledons of decapitated plants in dark resulted bud outgrowth on the side of removed cotyledon, as auxin source was removed (Dostál 1908).

Plantlets with both intact cotyledons

In variant **f)** IAA application to stem stumps for 100% inhibited cotyledonary bud outgrowth. This is in accordance to capability of IAA to substitute apex in its inhibitory role on bud outgrowth (Snow 1929, Thimann and Skoog 1933). In a control variant **g)** plane lanolin application to stem stumps allowed bud outgrowth in approx. 50:50 ratio on the right or the left side. In variant **h)** in addition the right side cotyledonary petioles were wounded. Most of the outgrowing shoots were formed on this side – 79%. In variant **i)** in addition on the right side cotyledonary petioles TIBA was applied. 92% of the outgrowing buds were observed on this side. As cotyledons are sources of auxin (DeMason and Polowick 2009) there could exist auxin flow towards the main stem that can keep the cotyledonary buds in inhibition. Indeed, in the cotyledons and their petioles polarized PIN1 auxin efflux protein files were observed indicating auxin flow (Kucsera 2020). Interrupting or weakening this auxin flow (by wounding or auxin transport inhibitor application) it was possible to release the buds from inhibition.

CONCLUSION

The experiments realised in this work were dedicated to enlighten the involvement of nutrients (from cotyledons or applied sucrose) and auxin flow in regulation of bud outgrowth. With series of experimental setup performed on 7-day-old pea plantlets, including auxin flow weakening by wounding or auxin transport inhibitor (2,3,5-triiodobenzoic acid) application the obtained results showed that the impact of auxin and its flow is more pronounced on bud outgrowth regulation than the sucrose availability. It could be interesting in the future to apply the used treatments also on older plants.

ACKNOWLEDGEMENTS

This research was carried out under the project CEITEC 2020 (LQ1601) from the Ministry of Education, Youth and Sports of the Czech Republic under the National Sustainability Programme II, and by the project "CEITEC – Central European Institute of Technology" (CZ.1.05/1.1.00/02.0068).

REFERENCES

Balla, J. et al. 2011. Competitive canalization of PIN-dependent auxin flow from axillary buds controls pea bud out-growth. The Plant Journal, 65(4): 571–577.

Balla, J. et al. 2016. Auxin flow-mediated competition between axillary buds to restore apical dominance. Scientific Reports, 6(1): 1–11.

Barbier, F.F. et al. 2015. Ready, steady, go! A sugar hit starts the race to shoot branching. Current Opinion in Plant Biology, 25: 39–45.

Barbier, F.F. et al. 2017. Apical dominance. Current Biology, 27(17): R864–R865.

Barbier, F.F. et al. 2019. An update on the signals controlling shoot branching. Trends in Plant Science, 24(3): 220–236.

Bennett, T. et al 2006. The Arabidopsis MAX pathway controls shoot branching by regulating auxin transport. Current Biology, 16(6): 553–563.

Bertheloot, J. et al. 2020. Sugar availability suppresses the auxin-induced strigolactone pathway to promote bud outgrowth. New Phytologist, 225(2): 866–879.

Brewer, P.B. et al. 2015. Strigolactone inhibition of branching independent of polar auxin transport. Plant physiology, 168(4): 1820–1829.

Dostál, R. 1908: Correlation relationships in germinating plants of Papilionaceae. Rozpravy České Akademie II, 17: 1–44.

DeMason, D.A., Polowick, P.L. 2009. Patterns of DR5: GUS expression in organs of pea (Pisum sativum). International Journal of Plant Sciences, 170(1): 1–11.

Dun, E.A. et al. 2006. Apical dominance and shoot branching. Divergent opinions or divergent mechanisms? Plant physiology, 142(3): 812–819.

Gomez-Roldan, V. et al. 2008. Strigolactone inhibition of shoot branching. Nature, 455(7210): 189–194.

Kucsera, A. 2020. Vplyv vonkajších a vnútorných faktorov na vyrastanie kotylárnych pupencov hrachu. Master thesis (in Slovak), Mendel University in Brno.

Kucsera, A. et al. 2019. Regulation of cotyledonary bud outgrowth in pea (Pisum sativum L.). In Proceedings of 26th International PhD Students Conference MendelNet 2019. [Online]. Brno, Czech Republic, 6–7 November, Brno: Mendel University in Brno, Faculty of AgriSciences, pp. 443–446. Available at: https://mnet.mendelu.cz/mendelnet2019/mnet_2019_full.pdf [2021–9–10]

Kucsera, A. 2017. Regulácia vyrastania kotylárnych pupeňov hrachu, Bachelor thesis (in Slovak), Mendel University in Brno.

Mason, M.G. et al. 2014. Sugar demand, not auxin, is the initial regulator of apical dominance. Proceedings of the National Academy of Sciences, 111(16): 6092–6097.

Müller, D., Leyser, O. 2011. Auxin, cytokinin and the control of shoot branching. Annals of Botany, 107(7): 1203–1212.

Snow, R. 1929. The young leaf as the inhibiting organ. New Phytologist, 28: 345–358.

Thimann, K., Skoog, F. 1933. Studies on the growth hormone of plants III. The inhibitory action of the growth substance on bud development. Proceedings of the National Academy of Sciences of USA, 19: 714–716.

Thomson, K.S. et al. 1973. 1-N-naphthylphthalamic acid and 2, 3, 5-triiodobenzoic acid. Planta, 109(4), 337–352.

Umehara, M., et al. 2008. Inhibition of shoot branching by new terpenoid plant hormones. Nature, 455(7210): 195–200.

Identification of powdery mildew (Erysiphales) species on ornamental perennial plants (*Asteraceae*) in the gardens of Mendel University in Brno

Marketa Michutova, Radovan Pokorny, Ivana Safrankova
Department of Crop Science, Breeding and Plant Medicine
Mendel University in Brno
Zemedelska 1, 613 00 Brno
CZECH REPUBLIC

xmichuto@mendelu.cz

Abstract: This study is focused on mapping the species representation of powdery mildew (Erysiphales) on ornamental perennial plants of the family *Asteraceae*. During the growing season 2021, the collection of samples was proven in several terms in the Botanical Garden of Mendel University in Brno, in the Academic Garden Horticultural Faculty in Lednice and in the Labyrinth of Nature and Paradise of the Gardens of the Horticultural Faculty of Mendel University in Lednice. A total of 23 plants were collected, which showed signs of powdery mildew infection, of which a specific type of powdery mildew was determined in 15 cases. The samples were subsequently described, processed and specific species of powdery mildew occurring on members of the *Asteraceae* family were identified using microscopic techniques and compared mainly with the Monograph of Erysiphales (Braun and Cook 2012). Subsequently, an inventory of individual species of powdery mildew occurring in the gardens of Mendel University was created and macroscopic and microscopic photographs of these pathogens were taken on the infected plants.

Key words: powdery mildew, *Asteraceae*, ornamental perennials

INTRODUCTION

Plants of the *Asteraceae* family belong to the most important group of ornamental plants. One of the most common pathogens that attacks these plants are powdery mildews (Šafránková 2014). Powdery mildew (Erysiphales) is an order of obligately parasitic fungi belonging to the phylum of Ascomycota. Today, over 820 species (Braun and Cook 2012) parasitizing on more than 10,000 species of vascular plants have been described (Glawe 2008). Macroscopically, the powdery mildew appears as a white to gray layer, formed by mycelium, which most often covers the leaves, but also other green parts of the plant (Lebeda et al. 2017). Powdery mildews are characterized by a relatively complex life cycle involving the alternation of the sexual phase, which is characterized by the formation of chasmothecia and the asexual phase, in which a white layer of mycelium with conidiophores forms (Braun and Cook 2012).

The taxonomy of powdery mildew is very complex and is constantly being refined and updated. While earlier taxonomic systems were built on the morphological properties of the pathogen (Braun 1987), today the system is based solely on molecular analysis of rDNA (Lebeda et al. 2017). Molecular data showed the need to rework previous system. Based on these data, a new taxonomic system was created consisting of 5 basic tribes (Braun et al. 2002). Today, the system is updated mainly at the genus and species level. An example is the original genus Erysiphe, which was divided into three separate genera *Erysiphe*, *Golovinomyces* and *Neoërysiphe* (Takamatsu 2018).

Powdery mildews occurring in the family *Asteraceae* has received much attention in recent years. The taxonomic system is updated mainly at the species level (Mieslerová et al. 2020a, Qui et al. 2020, Braun et al. 2019, Takamatsu et al. 2013).

MATRIAL AND METODS

Sample collection

During the 2021 growing season, twenty three plants from the *Asteraceae* family with visible symptoms of infection were collected. Collections were made in the Botanical Gardens of the Mendel

University in Brno, the Academic Garden Horticultural Faculty in Lednice and in the Labyrinth of Nature and Paradise Gardens in Lednice. Macroscopic photographs of plants with visible (Figure 1) were taken using a Samsung Galaxy A50 mobile phone camera. The samples of host plants were herbarized, each with a serial number date and place of collection. All samples are stored in the Department of Crop Science, Breeding and Plant Medicine Mendel University in Brno.

Microscopic analysis of samples

Conidiophores with conidia (asexual stage) were laboratory-processed by the Shin method, which consists of reherbarization of dried plant material with acid fuchsin (1% fuchsin and 80% lactic acid – 1:1) (Mieslerová 2020b). After dripping the herbarized plant material with the dye, the sample was annealed above the burner to the vapour outlet. After rinsing with distilled water, the sample appears pink were red (Shin 2000). The chasmothecia (sexual phase) is naturally dark, so there was no need to stain these samples. Chasmothecia (sexual phase) were naturally dark, so there was no need to dye these specimens.

Samples were microscoped (Olympus BX41), and 30 measurements (Mieslerová 2020b) of conidial and conidiophore size were taken for each sample. The measured data were processed in MS Excel, where the mean, range of values and statistical deviation were calculated. Quick Photo Pro 3.1 was used to take microscopic photographs (Canon EOS 1000D) (Figure 2) and measurements.

Taxonomic Determination

The host plant species were determined using the Key to the Flora of the Czech Republic (Kubát et al. 2002) and the accuracy was verified using the Index Seminum of the individual gardens. Specific species of mildew were determined on the samples based on a comparison of measured and statistically processed structures with data presented in the Braun and Cook (2012) and Qui et al. (2020).

RESULTS

Of the 23 plant samples, powdery mildew was confirmed in 15 samples (Figure 1). Two representatives of the genus *Centaurea* (*C. dealbata* 'Steenbergii', *C. montana* 'Rosea'), one representative of the genus *Echinops* (*E. sphaerocephalus*), six representatives of the genus *Helianthus* (*H. decapetalus* 'Lemon Queen', *H. grosseserratus*, *H. microcephalus* 'Lemon Queen', *H. tuberosus*., *H* × *laetiflorus* Pers., *H.* × *multiflorus* 'Capenoch Star'), three representative of the genus *Rudbeckia* (*R. hirta* 'Amarillo Gold', *R. laciniata* 'Goldquelle', *R. nitida*) one representative of the genus *Solidago* (*S. virgaurea*), two representatives of the genus *Symphyotrichum* (*S. lateriflorum* 'Chloe', *S. novi-belgii* (Table 1).

The anamorphic phase was present on all 15 samples (Figure 2). The sexual phase was only present on the species *Centaurea dealbata* 'Steenbergii' (Figure 3).

Table 1 List of plants from the family Asteraceae infected by powdery mildew in 2021 in the gardens of Mendel University

Host Plant	Date of collection	Location	Type of Powdery Mildew	Sexual phase/Conidiophore type
Centaurea dealbata 'Steenbergii'	21.07.2021	Brno	*Golovinomyces montagnei*	A,T/E
Centaurea montana 'Rosea'	03.06.2021	Lednice	*Golovinomyces depressus*	A/E
Echinops sphaerocephalus	21.07.2021	Brno	*Golovinomyces echinopis*	A/E
Helianthus decapetalus 'Lemon Queen'	30.08.2021	Lednice	*Golovinomyces latisporus*	A/E
Helianthus grosseserratus	30.08.2021	Lednice	*Golovinomyces latisporus*	A/E
Helianthus microcephalus 'Lemon Queen'	30.08.2021	Lednice	*Golovinomyces latisporus*	A/E
Helianthus tuberosus	25.08.2021	Brno	*Golovinomyces latisporus*	A/E
Helianthus × *laetiflorus* Pers.	21.07.2021	Brno	*Golovinomyces latisporus*	A/E
Helianthus × *multiflorus* 'Capenoch Star'	30.08.2021	Lednice	*Golovinomyces latisporus*	A/E
Rudbeckia hirta 'Amarillo Gold'	25.08.2021	Brno	*Golovinomyces ambrosiae*	A/E
Rudbeckia laciniata 'Goldquelle'	11.07.2021	Lednice	*Golovinomyces ambrosiae*	A/E
Rudbeckia nitida	30.08.2021	Lednice	*Golovinomyces ambrosiae*	A/E
Solidago virgaurea	25.08.2021	Brno	*Golovinomyces asterum* var. *solidaginis*	A/E
Symphyotrichum lateriflorum 'Chloe'	30.08.2021	Lednice	*Golovinomyces asterum* var. *moroczkowskii*	A/E
Symphyotrichum novi-belgii	11.07.2021	Lednice	*Golovinomyces asterum* var. *moroczkowskii*	A/E

A = anamofra, T = telomorfa, E = *Euoidium*,

Based on the comparison of the measured morphological characteristics (Table 2) with the data given in Braun and Cook (2012) and in the case of *Golovinomyces latisporus* with Qui et al. (2020) seven species of powdery mildew were determined on 15 samples of plants of the family *Asteraceae*. *G. montagnei* was determined on *Centaurea dealbata* and *G. depressus* was determined on *Centaurea montana*. *G. echinopis* was determined on the genus *Echinops*. *G. latisporus* has been identified in species of the genus *Helianthus*. *G. ambrosiae* has been identified in species of the genus *Rudbeckia*. The species *G. asterum* var. *solidaginis* was determined on the species *Solidago*. *G. asterum* var. *moroczkowskii* has been identified in *Symphyotrichum* species.

Figure 1 Visible signs of powdery mildew infection on members of the Asteraceae family

Legend: A) *Centaurea dealbata* 'Steenbergii', B) *Centaurea montana* 'Rosea', C) *Echinops sphaerocephalus*, D) *Helianthus decapetalus* 'Lemon Queen', E) *Helianthus grosseserratus,* F) *Helianthus microcephalus* 'Lemon Queen', G) *Helianthus tuberosus,* H) *Helianthus* × *laetiflorus* Pers., I) *Helianthus* × *multiflorus* 'Capenoch Star', J) *Rudbeckia hirta* 'Amarillo Gold', K) *Rudbeckia laciniata* 'Goldquelle', L) *Rudbeckia nitida,* M) *Solidago virgaurea,* N) *Symphyotrichum lateriflorum* 'Chloe', O) *Symphyotrichum novi-belgii*

Table 1 Comparison of morphological characteristics of powdery mildew on species of the family Asteraceae with Braun and Cook (2012) and Qui et al., (2020). [(mean ± SD (max – min)]

Species of Powdery Mildew	Host Plant	Conidia length (µm)	Conidia width (µm)	L/W	Conidiophore length (µm)	Foot cell length (µm)	Number of distal cells	Chasmothecium diameter (µm)	No. of appendages	Length of appendages
Golovinomyces montagnei (Braun and Cook 2012)		(25–)30–45	15–23	–	–	(25–)30–60(–80)	1–3	(70–)80–150(–170)	numerous	0.25–1.5 × diam. chasm
Golovinomyces depressus (Braun and Cook 2012)		25–50	18–30	–	–	80–180	(0–)1–3	80–145	numerous	0.5–2 × diam. chasm.
	Centaurea dealbata 'Steenbergii'	23.7 ± 1.67 (26–10)	15.3 ± 2.71 (20–13)	1.6 ± 0.28 (2.1–1.2)	106.50 ± 26.2 (130–61)	54.7 ± 16.21 (85–34)	1.4 ± 0.7 (0–2)	121 ± 8.1 (129–106)	>10	97.8 ± 16.3 (120–80)
	Centaurea montana 'Rosea'	29.1 ± 3.5 (36–22)	18.4 ± 2.16 (21–13)	1.6 ± 0.22 (2.1–1.2)	275.3 ± 72.4 (450–189)	151.5 ± 28.8 (206–107)	2.7 ± 0.8 (3–1)	–	–	–
Golovinomyces echinopis (Braun and Cook 2012)		25-50	19-30	-	250	40-100(-150)	1-2	100-180	numerous	0.25–2 × diam. chasm.
	Echinops sphaerocephalus L.	24.9 ± 3.1 (30–18)	17.2 ± 2.5 (21–11)	1.4 ± 2.49 (2.3–1.2)	151.38 ± 50.7 (308–102)	78.6 ± 18.6 (115–49)	2.15 ± 1.0 (4–1)	–	–	–
Golovinomyces latisporus (Qui et al. 2020)		25–45	15–27	<2		35–80	1–3	(65–)85–130 (–145)	numerous	0.5–2 × diam. chasm.
	Helianthus decapetalus 'Lemon Queen'	24.6 ± 2.8 (28–20)	15.6 ± 1.1 (18–14)	1.6 ± 0.15 (1.8–1.4)	132.22 ± 7.6 (168–99)	49.2 ± 7.6 (60–34)	1.33 ± 0.24 (2–1)	–	–	–
	Helianthus grosseserratus	23.6 ± 1.9 (26–21)	14.8 ± 1.1 (16–13)	1.6 ± 0.2 (1.9–1.3)	108.5 ± 21.3 (154–90)	41.8 ± 8.3 (55–33)	1.5 ± 0.5 (2–1)	–	–	–
	Helianthus microcephalus 'Lemon Queen'	25.8 ± 2.9 (30–22)	15.7 ± 1.8 (19–14)	1.67 ± 0.3 (2.0–1.2)	155.0 ± 22.3 (181–127)	67.5 ± 15.3 (97–51)	2.3 ± 0,47 (3–2)	–	–	–
	Helianthus tuberosus L.	28.7 ± 2.9 (34–24)	17 ± 1.53 (20–14)	1.7 ± 0.3 (2.3–1.3)	176.3 ± 17.49 (216–151)	71.3 ± 15.6 (101–41)	2.3 ± 0,47 (3–2)	–	–	–
	Helianthus x laetiflorus Pers.	25.1 ± 2.8 (30–21)	15 ± 1.8 (18–11)	1.7 ± 0.3 (2.5–1.4)	118.9 ± 15.17 (167–87)	57.2 ± 15.1 (100–39)	2.2± 0,9 (4–1)	–	–	–
	Helianthus x multiflorus 'Capenoch Star'	26.5 ± 3.1 (31–21)	17.2 ± 1.4 (20–15)	1.55 ± 0.2 (1.8–2.1)	126.3 ± 13.9 (148–91)	54.5 ± 10.4 (74–34)	1.1 ± 0.3 (2–1)	–	–	–
Golovinomyces ambrosiae (Braun and Cook 2012)		25–45	15–27	<2 (1.3–1.9)	–	35–80	1–3	(65–)85–130 (–145)	numerous	0.5–2 × diam. chasm.
	Rudbeckia hirta 'Amarillo Gold'	20.75 ± 3.4 (26–15)	15.7 ± 1.5 (17–12)	1.35 ± 0.3 (2.1–0.9)	86.9 ± 13.3 (107–66)	39.1 ± 7.8 (53–28)	2 ± 0.7 (3–1)	–	–	–
	Rudbeckia laciniata L. 'Goldquelle'	22.9 ± 3.1 (27–17)	14.5 ± 1.8 (18–11)	1.6 ± 0.3 (2.1–1,1)	129.7 ± 21.58 (160–83)	53.4 ± 11.5 (78–35)	2.5 ± 1.1 (4–1)	–	–	–
	Rudbeckia nitida	27.8 ± 2.7 (32–20)	15.3 ± 1.6 (17–12)	1.8 ± 0.1 (2.1–1.5)	149.6 ± 19.89 (178–116)	55.1 ± 16.8 (89–27)	2.2 ± 0.5 (3–1)	–	–	–
Golovinomyces asterum var. *solidaginis* (Braun and Cook 2012)		25–40(–45)	(12–)14–20	–	–	(25–)30–80 (–100)	1–3	85–140	numerous	0.25–1.5 × diam. chasm.
	Solidago virgaurea L.	25 ± 1.8 (27-22)	13.8 ± 1.7 (16-11)	1.8 ± 0.3 (2.4-1,5)	118.0 ± 32.6 (173-73)	61.8 ± 20.2 (100-47)	0.8 ± 0.4 (1-0)	–	–	–
Golovinomyces asterum var. *moroczkowskii* (Braun and Cook, 2012)		(20–)25–40 (–45)	(8–)–12–20 (–22)	–	–	30–80	1–3	85–140	numerous	0.25–1.5 × diam. Chasm
Golovinomyces asterum var. *asterum* (Braun and Cook 2012)		25-40(-45)	(12-)14-20	–	–	(25–)30–80–(–100)	1–3	85–140	numerous	0.25–1.5 × diam. Chasm
	Symphyotrichum lateriflorum 'Chloe'	29.7 ± 2.3 (34–25)	14.9 ± 1.2 (16–13)	2 ± 0.2 (2.5–1,8)	123.3 ± 12.5 (145–101)	55.1 ± 12.12 (88–44)	1.3 ± 0.5 (2–1)	–	–	–
	Symphyotrichum novi-belgii	29.4 ± 2.8 (32–24)	15.4 ± 1.2 (16–13)	1.9 ± 0.1 (2.0–1,8)	144.4 ± 28.8 (185–110)	59.4 ± 2.9 (63–56)	1.9 ± 0.1 (2–1,8)	–	–	–

10 November 2021, Brno, Czech Republic

MendelNet

Figure 2 Conidiophores of powdery mildew isolated from leaves of perennials (Asteraceae)

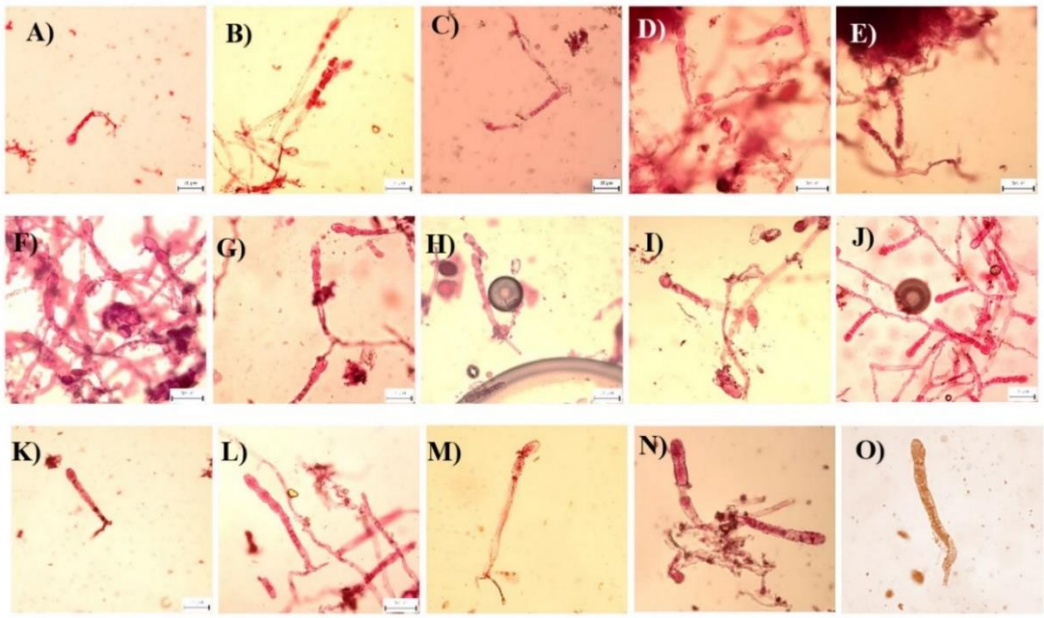

Legend: A) *Golovinomyces montagnei* on *Centaurea dealbata* 'Steenbergii', B) *Golovinomyces depressus* on *Centaurea montana* 'Rosea', C) *Golovinomyces echinopis* on *Echinops sphaerocephalus*, D) *Golovinomyces latisporus* on *Helianthus decapetalus* 'Lemon Queen', E) *Golovinomyces latisporus* on *Helianthus grosseserratus,* F) *Golovinomyces latisporus* on *Helianthus microcephalus* 'Lemon Queen', G) *Golovinomyces latisporus* on *Helianthus tuberosus*, H) *Golovinomyces latisporus* on *Helianthus* × *laetiflorus* Pers., I) *Golovinomyces latisporus* on *Helianthus* × *multiflorus* 'Capenoch Star', J) *Golovinomyces ambrosiae* on *Rudbeckia hirta* 'Amarillo Gold', K) *Golovinomyces ambrosiae* on *Rudbeckia laciniata* 'Goldquelle', L) *Golovinomyces ambrosiae* on *Rudbeckia nitida,* M) *Golovinomyces asterum* var. *Solidaginis* on *Solidago virgaurea,* N) *Golovinomyces asterum* on *Symphyotrichum lateriflorum* 'Chloe', O) *Golovinomyces asterum* on *Symphyotrichum novi-belgii*

Figure 3 Golovinomyces depressus on Centaurea dealbata 'Steenbergii'

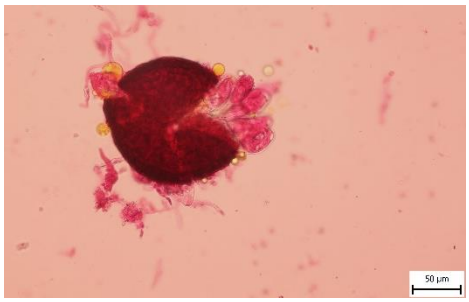

DISCUSSION

Based on morphological characteristics, seven species of powdery mildew were identified on the above-mentioned species of the family *Asteraceae*. Measured values of representatives of *Centaurea* sp. were slightly different and therefore *Golovinomyces montagnei* was identified on *C. dealbata* 'Steenbergii' and *G. depresus* was identified on *C. montana* 'Rosea'. Both of those species are widespread in Europe. *G. echinopis* was identified on the species *Echinops sphaerocephalus* L. This powdery mildew corresponds to the data in Braun and Cook (2012) and geographical distribution.

Six species of *Helianthus* sp. (Table 1) were collected during the 2021 season. *Golovinomyces latisporus* was determined in all species based on a study by Qui et al. (2020), which on *Helianthus* sp. separated this powdery mildew from the original species *G. ambrosiae*. On *Rubdeckia* sp. Braun and Cook (2012) mention the species *G. ambrosiae*, which is very widespread throughout Europe. All three of the above-mentioned *Rudbeckia* sp. correspond to this powdery mildew. However, it should be noted that Qui et al. (2020) mentions the species *G. latisporus*, which is not mentioned in the study in the Czech Republic, but was recorded in neighboring countries (DEU, PL). The measured values are slightly different from this powdery mildew. However, exclusion would be possible only by molecular analysis.

Nowadays, three variants of the species *Golovinomyces asterum* are described. All three are already recorded in the Czech Republic. *G. asterum* var. *solidaginis* is described in the Czech Republic on the species *Solidago* sp. The measured data are the same as those in Braun and Cook (2012), so it is very likely that this will be this powdery mildow. On the species *G. asterum* var. *moroczkowskii* occurs in *Symphyotrichum* sp. in the Czech Republic. However, Mieslerová et al. (2020a) reports on *S. novi-belgi* the first report of *G. asterum* var. *asterum*. Both of those variants of powdery mildew are morphologically very similar in the sexual and asexual phase of the life cycle and therefore a closer determination would be possible only by molecular analysis.

CONCLUSION

In the 2021 season, 23 ornamental perennial plants of family *Asteraceae* occurring in the gardens of Mendel University showed signs of powdery mildew infection. After laboratory and statistical processing of the samples, the powdery mildew was confirmed on 15 species. The asexual stage was present on all 15 sample. The sexual stage was present on one sample. Seven species of powdery mildew were identified on the samples. All species of powdery mildew were of the genus *Golovinomyces*: *G. montagnei, G. depressus*, *G. echinopis*, *G. latisporus*, *G. ambrosiae*, *G. asterum* var. *solidaginis*, *G. asterum* var. *moroczkovskii* (var. *asterum*).

The main task of this work was to the map powdery mildew on perennial ornamental plants. It has been shown that the determination of mildew only based on morphological characteristics is possible. However, because the taxonomic system is still evolving, in many cases, a specific determination is only possible with the help of molecular analysis.

REFERENCES

Braun, U. 1987. A Monograph of the Erysiphales (Powdery Mildews). 1. ed. Stuttgart, Germany: E. Schweizerbart: Beiheft zur Nova Hedwigi.

Braun, U., Cook, R.T.A. 2012. Taxonomic Manual of the Erysiphales (Powdery Mildews). 1. ed. CBS Biodiversity Series.

Braun, U. et al. 2002. The taxonomy of the powdery mildew fungi. In The Powdery Mildews. A Comprehensive Treatise. Saint Paul, MN, USA: APS Press.

Braun, U. et al. 2019. Phylogeny and taxonomy of Golovinomyces orontii revisited. Mycological Progress 18: 335–357.

Glawe, D.A. 2008. The powdery mildews: A review of the world's most familiar (yet poorly known) plant pathogens. Annual Review of Phytopathology 46: 27–51.

Kubát, K. 2002. Klíč ke květeně České republiky. 1. ed., Praha: Academia.

Lebeda, V. et al. 2017. Padlí kulturních a planě rostoucích rostlin. 1. ed, Olomouc: Agriprint.

Mieslerová, B. et al. 2020a. Golovinomyces powdery mildews on *Asteraceae* in the Czech Republic. Plant Protection Science, 56(3): 163–179.

Mieslerová, B. et al. 2020b. Powdery Mildews on Trees and Shrubs in Botanical Gardens, Parks and Urban Green Areas in the Czech Republic. Forest 11(9): 967.

Qui, P-L. et al. 2020. Multi-locus phylogeny and taxonomy of an unresolved, heterogeneous species complex within the genus *Golovinomyces* (Ascomycota, Erysiphales), including *G. ambrosiae*, *G. circumfusus* and *G. spadiceus*. BMC Microbiology, 20: 51.

Šafránková, I. 2014. Choroby okrasných rostlin. 1. ed. Brno: Mendelova univerzita v Brně, Agronomická fakulta.

Shin, H.D. 2000. Erysiphaceae of Korea. 1. ed. Suwon, Korea: National Institute Agriculture Science and Technology.

Takamatsu, S. 2018. Studies on the evolution and systematics of powdery mildew fungi. Journal of General Plant Pathology, 84: 422–426.

Takamatsu, S. et al. 2013. Comprehensive phylogenetic analysis of the genus *Golovinomyces* (Ascomycota: Erysiphales) reveals close evolutionary relationships with its host plants. Mycologia, 105(5): 1135–1152.

Short-term application of elevated temperature and drought influences the isotopic composition of winter wheat grains

Natalie Pernicova[1,2], Otmar Urban[2], Josef Caslavsky[2], Karel Klem[1,2], Miroslav Trnka[1,2]
[1]Department of Agrosystems and Bioclimatology
Mendel University in Brno
Zemedelska 1, 613 00 Brno
[2]Global Change Research Institute Czech Academy of Sciences
Belidla 986/4a, 603 00 Brno
CZECH REPUBLIC

pernicova.n@czechglobe.cz

Abstract: The study aimed to determine the differences in carbon ($\delta^{13}C$) and nitrogen ($\delta^{15}N$) stable isotope ratios in grains of three winter wheat varieties grown under optimal and stress conditions. We found that the wheat variety has a significant effect on both $\delta^{13}C$ and $\delta^{15}N$ isotope ratios. Short-term (nine days) exposure to drought and high temperature during the heading or stem extension development phase significantly enhanced $\delta^{13}C$ values, but only high temperature affected $\delta^{15}N$ values. Enhanced $\delta^{15}N$ values support the assumption that global warming causes a higher representation of the ^{15}N isotope in plants. Moreover, significant interactive effects of temperature and water availability on the values of both isotopes were found implying that C and N metabolisms have been altered under the investigated stress conditions. We conclude that $\delta^{13}C$ and $\delta^{15}N$ isotope ratios of cereal grains are sensitive indicators of stress conditions, even short-term ones.

Key Words: wheat, grain, ^{13}C, ^{15}N, drought, high temperature

INTRODUCTION

Isotopes of biogenic elements represent a powerful approach providing a lot of information about ecosystems, their parts and spatio-temporal changes. The isotopic composition of plants reflects, for example, growth conditions including climatic extremes, anthropogenic pollution, availability of water sources, and/or the type of photosynthesis that plants use (C3, C4 or CAM) (Fiorentino et al. 2015).

Stable isotopes enable to track changes in plant physiological processes, including changes in water use efficiency – the process suitable for the selection of crop varieties resistant to upcoming conditions of climate change (Fiorentino et al. 2015).

Carbon has two stable isotopes, ^{12}C and ^{13}C. Plants prefer to assimilate ^{12}C instead of ^{13}C in photosynthesis leading to discrimination of heavy isotope ^{13}C. Plants thus have lower ^{13}C abundance compared to the atmosphere (Fiorentino et al. 2015). The main reasons for isotope discrimination are carboxylation reaction and diffusion of CO_2 into the leaf intercellular space. Fractionation associated with Rubisco and other enzymes during photosynthetic carbon fixation is 27‰, but it is only 4.4‰ for gaseous diffusion through stomata (Farquhar et al. 1982).

Stomata remain closed under adverse conditions of limited water availability, high vapour pressure deficit in air, and/or insufficient solar radiation. Insufficient stomatal conductance thus leads to a reduced intercellular CO_2 concentration and consequently lower discrimination of the ^{13}C isotope (Farquhar et al. 1989).

Accordingly, drought-stressed plants and well-watered plants have different carbon isotope ratios $\delta^{13}C$ ($^{13}C/^{12}C$). Well-watered plants discriminate ^{13}C more ($\delta^{13}C$ is lower), while drought-stressed plants discriminate ^{13}C to a smaller extent ($\delta^{13}C$ is higher). Under the conditions of high air humidity and sufficient water availability in soil, the stomata are open (i.e., resistance to diffusion of CO_2 is negligible) and CO_2 concentrations outside the leaf and inside the chloroplast are similar. In this case, the fractionation due to carboxylation processes dominates (Urban et al. 2018). On the other hand, closed stomata of drought-stressed plants lead to a substantially higher ambient CO_2 concentration compared

to chloroplastic CO_2 concentration. Gaseous diffusion of CO_2 through the stomata thus contributes dominantly to ^{13}C fractionation (Fiorentino et al. 2015). Similarly to water deficiency, $\delta^{13}C$ values become higher when temperature increases (Van Klinken et al. 1994).

Based on the convention, the $\delta^{15}N$ value of atmospheric nitrogen equals 0‰ (Van Klinken et al. 1994). The value of $\delta^{15}N$ increases with soil age and depth (Högberg 1997), and elevation (Oulehle et al. 2021). In plants, the $\delta^{15}N$ value depends on the nitrogen fixation pathway. Plants fixing atmospheric nitrogen via symbiotic nitrogen-fixing bacteria tend to have values of $\delta^{15}N$ close to zero. On the contrary, plants assimilating nitrogen from other sources, e.g. soil nitrates, have values of $\delta^{15}N$ between 3–5‰ (Bogaard et al. 2007).

$\delta^{15}N$ are also influenced by climate having higher values in warm than in moderate climate (Van Klinken et al. 1994). $\delta^{15}N$ values are further influenced by human activities, especially fertilization. Fertilization increases the $\delta^{15}N$ value by about 2.6–8‰ depending on the amount of applied fertilizer (Bogaard et al. 2007). The major discrimination occurs in the processes of nitrification and denitrification. Products of these processes, NO_3^- and nitrogen oxides, have less representation of ^{15}N compared to the initial nitrogen forms (Högberg 1997).

The fractionation of nitrogen isotopes is also modulated by certain environmental conditions. In particular, high temperature accelerates the volatility of ammonia nitrogen oxides from soils and plants into the atmosphere (Högberg 1997) and leads to an enhancement of $\delta^{15}N$ value in soils and plants (Peñuelas and Filella 2001).

Investigating $\delta^{13}C$ and $\delta^{15}N$ values in grains of three widely grown winter wheat varieties, we aimed to test the following hypotheses: (1) grains of wheat varieties differing in sensitivity to climate conditions have distinct values of $\delta^{13}C$ and $\delta^{15}N$ isotope ratios; (2) short-term application of elevated temperature, drought, and their combination alters $\delta^{13}C$ and $\delta^{15}N$ isotope ratios in wheat grains.

MATERIAL AND METHODS

Plant material

Three winter wheat (*Triticum aestivum* L.) varieties (Pannonia, Pankratz, Elan) were selected for this study. Pannonia is regarded as potentially drought and temperature tolerant, while Pankratz and Elan achieve the highest yields under moderate climate conditions of Central Europe.

In October 2018, two seeds per pot (0.1 × 0.1 × 0.2 m) were sown. The plants were cultivated in the vegetation hall at Mendel University in Brno, the Czech Republic, under ambient weather conditions. The plants were regularly irrigated and fertilized. The temperature ranged between 0 and 13 °C (from October 2018 to May 2019) in the vegetation hall. Plants in the heading (Pannonia) and stem extension (Pankratz, Elan) growth stages were transported to growth chambers (FS-SI 3400; Photon Systems Instruments, Brno, Czech Republic) at the Global Change Research Institute Brno, Czech Republic, where they were exposed to stress conditions for nine days.

All plants were exposed to an ambient CO_2 concentration (400 µmol/mol), the maximum daily intensity of photosynthetically active radiation of 1000 µmol/m^2/s, and night/day vapour pressure deficit of 0.21/1.85 kPa. Ten pots were exposed to a night/day temperature regime of 18/26 °C (control plants; hereafter referred to as 26), while ten pots had the temperature regime of 18/38 °C (temperature stressed plants; hereafter referred to as 38). Under each temperature treatment, half of the pots were daily irrigated to keep soil moisture at 30% (well-watered plants; hereafter referred to as W), while the second half was left without water (drought-treated plants; hereafter referred to as D). Limited water availability resulted in the decrease of soil moisture below approximately 15%. After nine days, the plants were transferred back to the vegetation hall until the ripening stage.

Isotopic analysis

Harvested grains were dried at 60 °C and homogenised in the agate grinding jar of ball mill MM200 (Retsch, Haan, Germany). The samples (approximately 1.5–2.0 mg) were weighed into tin boats (Elementar Analysensysteme, Langenselbold, Germany) for the measurement of $\delta^{13}C$ and $\delta^{15}N$ isotopes.

Stable isotopes were measured using the elemental analyser vario PYRO cube (Elementar Analysen systeme, Germany) coupled to a continual flow isotope ratio mass spectrometer (IRMS).

In the first step, the samples were burnt in the combustion tube of the elemental analyser at a temperature of 960 °C in an oxygen atmosphere, resulting in the formation of N_2 and CO_2. These gases are transported by carrier helium gas into IRMS ISOPRIME100 (Isoprime, Manchester, UK) using Faraday detectors to detect ions containing different stable isotopes of C and N.

Before the analysis, the ion source of the IRMS was tuned and tested for stability (standard deviation ≤ 0.04‰ on 10 pulses over 3 consecutive runs) over the entire range of expected ion currents. The system was calibrated using certified reference materials with known carbon ($\delta^{13}C$; $^{13}C/^{12}C$) and nitrogen ($\delta^{15}N$; $^{15}N/^{14}N$) isotopic ratios from the International Atomic Energy Agency (IAEA) and United States Geological Survey (USGS). $\delta^{13}C$ values were referenced to caffeine (IAEA-600; -27.771‰) and graphite (USGS24; -16.049‰), whereas $\delta^{15}N$ values were referenced to potassium nitrate (USGS-32; 180‰) and caffeine (IAEA-600; 1‰). The values of $\delta^{13}C$ and $\delta^{15}N$ (‰) were calculated as the deviation from Vienna Pee Dee Belemnite (VPDB) and Atmospheric N_2 (AIR) standard, respectively using the formula $R = (R_{sample}/R_{standard} - 1)*1000$, where R is the ratio of the heavy to light isotope.

Statistical analysis

Data were statistically processed using Statistica 12 software (StatSoft, Tulsa, OK, USA). Three-way analysis of variance (ANOVA) was used to determine the effect of wheat variety (Var), water availability (WA), air temperature (Temp), and their interactions (×) on the values of the isotope ratios in wheat grains. To evaluate the differences between the mean values, Fisher's LSD post-hoc test was applied at a significance level of $p = 0.05$.

RESULTS AND DISCUSSION

Impact of wheat variety on $\delta^{13}C$ and $\delta^{15}N$ values

A significant effect of wheat variety was found on both $\delta^{13}C$ and $\delta^{15}N$ (Table 1). Under the control conditions (26-W), Pannonia variety had significantly lower values of $\delta^{13}C$ than Pankratz and Elan varieties (Figure 1A). This result implies lower intrinsic water use efficiency (iWUE) of Pannonia variety. $\delta^{13}C$ values increased with increasing temperature and limited water availability in all wheat variants, but these changes were less pronounced in Elan variety. Higher values of $\delta^{13}C$ indicate an increase of iWUE under the conditions of temperature and drought stress. The significant increase by 5% of $\delta^{13}C$ in grains of Pannonia variety under the combined treatment of high temperature and drought (38-D) compared to control treatment (26-W) demonstrates a great acclimation potential of this variety to stress conditions. Generally, spelt wheat varieties (*T. spelta*) and intermediate forms of bread wheat landraces (*T. aestivum*) have the highest $\delta^{13}C$ values indicating their inclination to drought tolerance, while the lowest $\delta^{13}C$ values were found in einkorn wheat varieties (*T. monococcum*) grown under the natural conditions of the Czech Republic (Konvalina et al. 2014).

Table 1 The effect of wheat variety, temperature, water availability, and their interactions on the composition of carbon and nitrogen stable isotopes in wheat grains

	$\delta^{13}C$		**$\delta^{15}N$**	
	F	*p*	*F*	*p*
Var	27.14	**<0.001**	6.22	**0.003**
Temp	28.38	**<0.001**	11.70	**0.001**
WA	7.39	**0.008**	2.53	0.115
Var × Temp	1.17	0.313	4.60	**0.012**
Var × WA	2.95	0.057	1.42	0.246
Temp × WA	5.30	**0.023**	5.74	**0.018**
Var × Temp × WA	1.26	0.288	0.08	0.925

Legend: Var – variety, Temp – temperature, WA – water availability, × - interactions. F – the value of F test statistic, p – probability value. Bold p-values indicate statistically significant effects at p < 0.05.

Three-way ANOVA analysis revealed a significant interactive effect of wheat variety and temperature on $\delta^{15}N$ (Table 1). Under the control conditions, no statistically significant differences were found in $\delta^{15}N$ values among the investigated varieties. However, significantly higher $\delta^{15}N$ values

(by 7.6–15.3%) were observed in the variety Elan compared to Pannonia and Pankratz varieties under the conditions of higher temperature (38-W, and 38-D). Such finding indicates an improved nitrogen uptake in Elan variety under stress conditions.

Values of $\delta^{13}C$ and $\delta^{15}N$ observed in our study correspond to those reported by Serret et al. (2008). Evaluating a set of 24 wheat genotypes they reported $\delta^{13}C$ and $\delta^{15}N$ values in mature grains ranging between -26 and -26.4‰ and between 4 and 5.8‰, respectively. Noticeably, landraces of durum wheat varieties, often tolerant to local stress factors (Reynolds et al. 2007), were reported to have higher $\delta^{13}C$ values than modern cultivars (Araus et al. 2013). Such findings suggest that modern varieties can sustain higher water use efficiency.

Figure 1 Effect of temperature and water availability on carbon ($\delta^{13}C$; A) and nitrogen ($\delta^{15}N$; B) stable isotopes in grains of three wheat varieties: Pannonia, Pankratz, and Elan

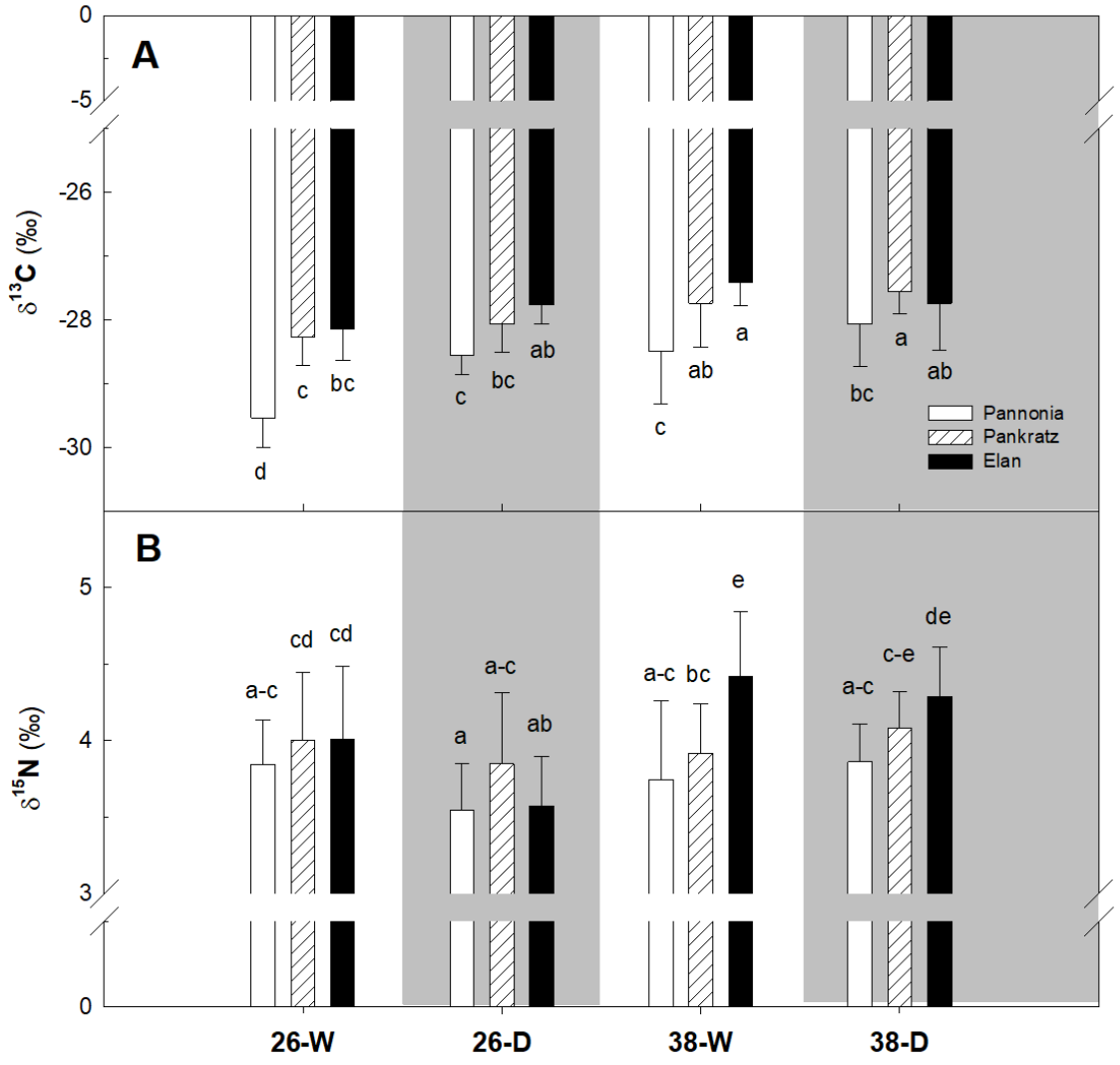

Legend: Means (columns) and standard deviations (error bars) are presented (n = 8). Different letters indicate significant differences ($p \leq 0.05$) between means. 26 – control air temperature (daily maximum of 26 °C), 38 – elevated air temperature (daily maximum of 38 °C), W – well-watered plants, D drought-treated plants.

Impact of drought on $\delta^{13}C$ and $\delta^{15}N$ values

Drought leads to a closure of stomata, a decrease of intercellular CO_2 concentration, and a reduction of photosynthetic CO_2 fixation by the Rubisco enzyme. It is well known that ^{13}C discrimination is reduced at a low intercellular-to-ambient CO_2 concentration ratio (Farquhar et al. 1982). Accordingly, we tested the hypothesis that even short-term drought increases the value of $\delta^{13}C$ in wheat grains. Indeed, analysis of variance (Table 1) revealed a significant effect of limited water availability on $\delta^{13}C$ values. In particular, this effect was markedly pronounced at the growth

temperature of 26 °C (Figure 1A). In accordance with our study, Araus et al. (2013) concluded that water limitation has the main effect on $\delta^{13}C$ and $\delta^{18}O$, whereas $\delta^{15}N$ is influenced particularly by nitrogen fertilization.

In our study, Pannonia variety had the highest ability to increase $\delta^{13}C$ values (less ^{13}C discrimination) under drought conditions, particularly at the control temperature treatment of 26 °C (significant increase by 3.4%). At the temperature treatment of 38 °C, the increase of $\delta^{13}C$ values compared to well-watered (W) plants was only 1.5% and was not statistically significant. Similarly, drought-induced increases in $\delta^{13}C$ values in Pankratz and Elan varieties (up to 1.4%) were not statistically significant ($p > 0.05$; Figure 1A).

Carbon isotope discrimination enables to determine the integrating values of iWUE for biomass production in plants. Higher ^{13}C discrimination indicates low WUE during growth. In general, plants grown under long-term drought have higher values of iWUE and their discrimination is lower compared to well-watered plants (Canavar et al. 2014). The lowest discrimination (highest $\delta^{13}C$ values) was found in Elan and Pankratz varieties amounting up to -27.4‰ (Figure 1A). However, long-term dry Mediterranean conditions may even lead to $\delta^{13}C$ values higher than -24‰ (Araus et al. 2013).

Contrary to $\delta^{13}C$, the analysis of variance (Table 1) did not reveal any effect of insufficient water availability on $\delta^{15}N$ values. At control temperature treatment (26 °C), drought reduced the values of $\delta^{15}N$ in Pannonia and Elan varieties by 7.7 and 10.9%, respectively, but it was significant ($p < 0.05$) only for Elan variety (Figure 1B). Moreover Araus et al. (2013) reported no effect of water limitation on $\delta^{15}N$ values in ten durum wheat varieties. Several studies have shown that the value of $\delta^{15}N$ is primarily influenced by nitrogen availability in soil (Serret et al. 2008). The high availability of mineral nitrogen leads to increased discrimination of heavy isotope ^{15}N in plants and a decrease of $\delta^{15}N$ isotope ratio. This is usually explained by increased discrimination against ^{15}N at the level of the primary assimilation enzyme – nitrate reductase (Peñuelas and Filella 2001). Noticeably, nitrogen fertilization influences also the abundance of ^{13}C in wheat straw (Jenkinson et al. 1995). Particularly in the dry years, when dry matter response to N fertilizer is relatively small, straw grown without fertilizer contains less ^{13}C than straw grown with fertilizer.

Impact of temperature on $\delta^{13}C$ and $\delta^{15}N$ values

High temperatures are usually associated with low vapour pressure deficit leading to stomata closure and decrease of CO_2 concentration in chloroplasts (Urban et al. 2018). In addition, ^{13}C is discriminated during the photorespiration (11.6‰; Lanigan et al. 2008) – process exponentially increasing with increasing temperature. Accordingly, high growth temperature leads to lower discrimination of heavier carbon isotope during assimilation by Rubisco enzyme (Farquhar et al. 1989) and higher $\delta^{13}C$ values. Here we tested the hypothesis that even short-term exposure to high temperature regime will influence the isotopic composition of wheat grains. Our data (Table 1) confirmed the significant effect of temperature on the values of both $\delta^{13}C$ and $\delta^{15}N$.

As expected, short-term cultivation of winter wheat at high temperature (38 °C) decreases the discrimination of ^{13}C compared to control temperature (26 °C) and increases the $\delta^{13}C$ value in all wheat varieties investigated. It is particularly obvious and significant ($p < 0.05$) in well-watered plants. Generally, the lowest $\delta^{13}C$ value was found in grains of wheat plants cultivated under the combined conditions of high temperature and drought (Figure 1A).

The $\delta^{15}N$ value increased after short-term exposure to high temperatures. Plants cultivated in 38 °C have higher values of $\delta^{15}N$ than plants cultivated in 26 °C (Figure 1B). It is particularly true for Elan variety and drought-treated plants. These findings are supported by significant interactive effects between wheat variety and temperature (Var × Temp) and water availability and temperature (WA × Temp) on the $\delta^{15}N$ value (Table 1). Also previous studies reported higher $\delta^{15}N$ values in plants from the warmer climate compared to mild climate plants (Van Klinken et al. 1994). Several hypotheses were proposed to explain this phenomenon. Most importantly, temperature stimulates the volatilization of NH_3 during the plant development and the remaining NH_3 becomes enriched in ^{15}N resulting in an enhanced value of $\delta^{15}N$ (Högberg 1997). Some authors hypothesize that increasing values of $\delta^{15}N$ are caused by decreasing discrimination of ^{15}N nitrogen fixation catalysed by nitrate reductase enzyme (Peñuelas and Filella 2001). Nevertheless, our data indicate that even short-term heat stress may induce substantial changes in nitrogen metabolism.

CONCLUSION

Our data support the hypothesis that grains of different wheat varieties have distinct values of $\delta^{13}C$ and $\delta^{15}N$. Low $\delta^{13}C$ values of Pannonia under control conditions indicate poor water use efficiency compared to Pankratz and Elan varieties. However, a substantial increase in $\delta^{13}C$ after the application of short-term stress implies the great potential of this variety to cope with adverse conditions.

We also confirmed that even short-term (nine days) application of high temperature, drought and their combination during heading/stem extension growth stages influence the $\delta^{13}C$ and $\delta^{15}N$ values of wheat grains. While temperature has a significant effect on both $\delta^{13}C$ and $\delta^{15}N$, limited water availability increases $\delta^{13}C$ values, but does not affect $\delta^{15}N$ value. Our data thus suggest that even short stress periods modify carbon and nitrogen metabolism in plants.

ACKNOWLEDGEMENTS

The research was financially supported by the projects SustES (CZ.02.1.01/0.0/0.0/16_019/0000797) and Internal Grant Agency of MENDELU (AF-IGA2021-IP008).

REFERENCES

Araus, J.L. et al. 2013. Comparative performance of $\delta^{13}C$, $\delta^{18}O$ and $\delta^{15}N$ for phenotyping durum wheat adaptation to a dryland environment. Functional Plant Biology, 40(6): 595–608.

Bogaard, A. et al. 2007. The impact of manuring on nitrogen isotope ratios in cereals: archaeological implications for reconstruction of diet and crop management practices. Journal of Archaeological Science, 34(3): 335–343.

Canavar, O. et al. 2014. Determination of the relationship between water use efficiency, carbon isotope discrimination and proline in sunflower genotypes under drought stress. Australian Journal of Crop Science, 8(2): 232.

Farquhar, G.D. et al. 1989. Carbon isotope discrimination and photosynthesis. Annual Review of Plant Biology, 40(1): 503–537.

Farquhar, G.D. et al. 1982. On the relationship between carbon isotope discrimination and the intercellular carbon dioxide concentration in leaves. Functional Plant Biology, 9(2): 121–137.

Fiorentino, G. et al. 2015. Stable isotopes in archaeobotanical research. Vegetation History and Archaeobotany, 24(1): 215–227.

Högberg, P. 1997. Tansley review no. 95 ^{15}N natural abundance in soil–plant systems. The New Phytologist, 137(2): 179–203.

Jenkinson, D.S. et al. 1995. The influence of fertilizer nitrogen and season on the carbon-13 abundance of wheat straw. Plant and Soil, 171(2): 365–367.

Konvalina, P. et al. 2014. Diversity of carbon isotope discrimination in genetic resources of wheat. Cereal Research Communications, 42(4): 687–699.

Lanigan, G.J. et al. 2008. Carbon isotope fractionation during photorespiration and carboxylation in Senecio. Plant Physiology, 148(4): 2013–2020.

Oulehle, F. et al. 2021. Dissolved and gaseous nitrogen losses in forests controlled by soil nutrient stoichiometry. Environmental Research Letters, 16(6): 064025.

Peñuelas, J., Filella, I. 2001. Herbaria century record of increasing eutrophication in Spanish terrestrial ecosystems. Global Change Biology, 7(4): 427–433.

Reynolds, M. et al. 2007. Drought-adaptive traits derived from wheat wild relatives and landraces. Journal of Experimental Botany, 58(2): 177–186.

Serret, M.D. et al. 2008. The effects of urea fertilisation and genotype on yield, nitrogen use efficiency, $\delta^{15}N$ and $\delta^{13}C$ in wheat. Annals of Applied Biology, 153(2): 243–257.

Urban, O. et al. 2018. Combined effects of drought and high temperature on photosynthetic characteristics in four winter wheat genotypes. Field Crops Research, 223: 137–149.

Van Klinken, G.J. et al. 1994. Bond $^{13}C/^{12}C$ ratios reflect (palaeo-) climatic variations. Geophysical Research Letters, 21(6): 445–448.

Methodology of phenotypes selection of hemp (*Cannabis sativa* L.) for secondary metabolite production

Patrik Schreiber, Nikolas Balog
Department of Plant Biology
Mendel University in Brno
Zemedelska 1, 613 00 Brno
CZECH REPUBLIC

xschrei2@mendelu.cz

Abstract: Hemp is a multipurpose plant which can be used in industry, food production and as a medicine. In medicinal *Cannabis* production, most important factor is content of cannabinoids such as THC (tetrahydrocannabinol), CBD (cannabidiol), CBG (cannabigerol), CBC (cannabichromene), CBL (cannabicyclol) and others. Because medicinal *Cannabis* production is production of pharmaceuticals it is very important to have very standardised product in terms of active compound content. Because of this reason most of medicinal *Cannabis* nowadays is produced from clones of stable selected phenotypes with certain levels of active compounds, mostly cannabinoids. Because it is industry such as any other there are also lots of parameters important for economic model of production facility such as yield, resistance against pests and diseases and many others. During this study we were able to successfully select phenotype dominant in CBG which will be further used for upcoming biological and biotechnological studies under code name G13. Selected phenotype shows unique content of Cannabinoids and was reaching content of CBG 13.57% and THC 0.16%. This selected phenotype may be also used as base material for breeding of hemp variety for Common European Catalogue of agricultural hemp cultivars registered for trading between different European Union countries.

Key Words: Cannabis, variety, cannabinoids, breeding

INTRODUCTION

Cannabis was historically used for spiritual, medicinal and industrial purposes for centuries. Phytocannabinoids as active compounds are known since the end of 19th century. First isolated phytocannabinoid was Cannabinol, known as CBN, which was isolated and identified in year 1899 (Wood 1899).

Since that time scientist were able to identify more than 120 unique phytocannabinoids from which dominant chemotypes are THC, CBD, CBG and their combinations. All cannabinoids isolated from *Cannabis sativa* L. share same C21 terpenophenolic skeleton in their structure. It was thought that phytocannabinoids are exclusive for species of *Cannabis sativa* L. but research has shown that some of them may be discovered also in *Rhododendron* species, legumes, liverwort genus *Radula* and also in some species of fungi (Kinghorn et al. 2017).

In species of *Cannabis sativa* L. phytocannabinoids are accumulated in stalked glandular trichomes developed from sessile trichomes. Most of cannabinoids are located in ball shaped cavity located in glandular part of trichomes which contains secretory vesicles (Gulck 2020).

Phytocannabinoid pathway biosynthesis is occurring between different types of cells and organelles. Biosynthesis of phytocannabinoids is occurring in cytosol of trichome gland cells, plastids and extracellular storage cavity of trichome. Process is starting in cytosol where precursor molecule of hexanoic acid is made through oxidative cleavage of fatty acids. In cytosol is hexanoic acid transformed into olivetolic acid by olivetolic acid cyclase. Further is olivetolic acid transported into plastids. In plastids is olivetolic acid prenylated with geranyl diphosphate into cannabigerolic acid (CBGA) which is further transformed in apoplast into acidic forms of other cannabinoids such as tetrahydrocannabinolic acid (THC-A) or cannabidiolic acid (CBD-A) by enzymes such

as cannabigerolic acid synthase (CBGAS) and Δ^9-tetrahydrocannabinolic acid synthase (Δ^9-THCAS) (Gulck 2020).

Breeding *Cannabis sativa* L. can have many purposes, cannabis may be bred for secondary metabolites, seeds or stalk. In case of breeding of hemp for fibre production there are two main factors which are important and it is content of THC under 0.3% in dry material a secondly it is necessary that variety has very strong apical dominance so auxiliary shoots are not developing and plant than produce very quality fibre (Elma et al. 2014).

In case of breeding for seeds production we are looking mainly of maximalization of production of seeds and its quality. Important in this case is ratio of oils and proteins in seeds, in most of the world it is also necessary to reach level of content of THC under 0.3% (Kriese et al. 2004).

In case of breeding cannabis for secondary metabolites or medicinal market we are looking mostly on factors of such as production of secondary metabolites, yield of dry flower biomass and disease resistence (Naim-Feil et al. 2021).

We have decided to make selection of phenotype dominant in CBG because it is cannabinoid which is not well studied yet. One of the goals is to find out what is the inheritance pattern if we cross variety rich in this cannabinoid with another dominant chemotypes such as CBD, THC and THCV (tetrahydrocannabivarin). Another goal is our effort to stabilise this phenotype through breeding and possibly come out with enough stable variety for its testing as common European hemp variety, because currently there are no CBG rich varieties available in this catalogue.

MATERIAL AND METHODS

Characterization of cultivation

Seeds of two unregistered unfeminized CBG varieties are cultivated in grow tents of 1 meter square equipped with light source HID (High intensity discharge bulb) which is reaching light intensity reaching 600 μmol/m^2/s at canopy level. Each tent is equipped with air circulation fans and exhaust fan connected to thermostat which is controlling air temperature in tent. Temperatures in tent are fluctuating between optimal 18-25 degrees Celsius and air humidity in range between 50-80%. Plants are grown in Plagron light mix (Bertels BV., Netherlands) which is combination of coconut fibre, peat and perlite which is lightly fertilised to electrical conductivity of 0.6 mS/cm. Volume of cultivation pots is 2l and plants are irrigated with fertilised water with EC (electrical conductivity) reaching from 1 up to 1.9 mS/cm and pH 6.2. After full ripeness are plants harvested, dried and seeds collected.

Seeds of crossed variety are sown into the small pots and irrigated. After sprouting we waited until from each variety at least 2 clones of plant could be done via classic cutting. After successful rooting clone which is rooted better can be transplanted into 1 litre pot and transported into grow tent with 12 hours light period for initiation of flowering. Plants are grown until full ripeness between 8–12 weeks under same conditions as parental lines.

Data collection

For selection of desired phenotypes, it is necessary to quantify many different growth parameters which determine patterns important for this industry. In this methodology it is suggested collecting data from following parameters: initial plant height, harvest height, total dry mass, total dry mass of buds, number of main stem internodes, content of cannabinoids, evolution of content of cannabinoids, growth rate, length of maturation, total cannabinoid content.

Initial plant height is height of plants at moment of transplantation of rooted clone into grow container. This parameter is supposed to be measured from base of stem to apex in centimetres.

Harvest height is measured just before harvest of the plants at stage of full maturation. It is measured in centimetres from base of stem to the top of apical flower in centimetres. From this parameter and initial height, we are able to calculate intensity of flowering stretch. Flowering stretch stage of very vigorous growth of cannabis to the height after initiation of reproductive stage, it is key factor to know for producents who are using very low grow space such as multilevel regal systems.

Growth rate is periodically measured parameter which determines how fast is height of plant changing in certain weeks of plant maturation. It is measured weekly from the base of plant to apex.

Number of main stem internodes is measured by counting number of internodes from base of plant to the apex after harvest when all the flowers are collected. This parameter may play very important role in growing techniques relying on pruning for disruption of apical dominance.

Length of maturation is parameter which determines how fast is plant ready for harvest after initiation of generative stage. It is measured in days from time of transition of plant to 12-hour light period up to full maturity of flowers. This factor is very important in intensive cannabis production because it's very important for operation costs of production on energies, fertilisers and wages. It is also important factor for varieties which are grown outdoors because in latitudes with more humid autumns are plants susceptible to fungal diseases and therefore varieties with faster maturation are more suitable for this kind of environment.

Total dry mass is measured after harvest and drying of plants in grams. Total dry weight of flowers is measured after separation of flowers from stems and leaves from dried plant material. Material is ideally dried at temperatures not exceeding 25 degrees Celsius for preservation of most of cannabinoids and terpenoids. According to these two numbers we can calculate index which tell us how successful is certain phenotype in production of final product.

Content of cannabinoids is measured as total content of cannabinoids in percentage to the dry mass. After maturation of plants is flower material dried and cleaned of leaves and stems. From each plant are taken three samples from different parts of plant. Flowers should be taken from lowest branches, middle part of the plant and from apical flower. Material is afterwards analysed for content of specific cannabinoids of interest such as THC, CBD, CBG, CBN (Cannabinol) etc. Data collected can give us average cannabinoid content in plant and also differences in content of cannabinoids in apical and axial branches. For analysis of cannabinoids we used gas chromatography coupled to mass spectrometry in the laboratory of the research group of phytochemistry in the Research Center of the Haná Region for Biotechnological and Agricultural Research under the leadership of Assoc. Prof. Tarkowski.

Evolution of development of cannabinoids is evaluated by taking samples of flowers from same height in different weeks of flower maturation. Flowers are dried and evaluated with same method as content of cannabinoids. This parameter may give us ideal time of harvest.

Total cannabinoid content is calculated on base of multiplication of average percentual content of cannabinoids and total dry mass of harvested flower. It is factor on the basis of which we can select phenotype which is the best in overall production of cannabinoids.

RESULTS AND DISCUSSION

Experiment was set up with 12 seeds from which we obtained only 5 purely female phenotypes, 4 of plants were males and three were showing traits of both sexes.

Final plant height

Initial height of plants was nearly same, but we could see significant differences in final plant height among phenotypes. Lowest of all selected phenotypes was G13 which was reaching height of 51 cm, highest was phenotype D21 which had 83 cm (Figure 1). Height of plants usually has positive correlation with overall biomass and flower production, this hypothesis was proven in study from Naim-Feil et al. (2021).

Plant dry mass

Biggest total dry mass was found in phenotype D21 which had 54.8 g from which there was 43.1 g of flower dry mass (Figure 2). Lowest total dry mas had phenotype G13 which was 20.7 g from which was 12.7 g dry mass of flower. All the phenotypes excluding G13 had percentage of mass of dry flowers to totally dry mass reaching around 75%. Percentage of dry mass of flower in G13 phenotype was compared to that only 60%, highest had G12 with 81% (Figure 3). From this we can assume that plants which have more dry flower material produce more waste material to dry flower mass.

Figure 1 Final height of cultivated plants

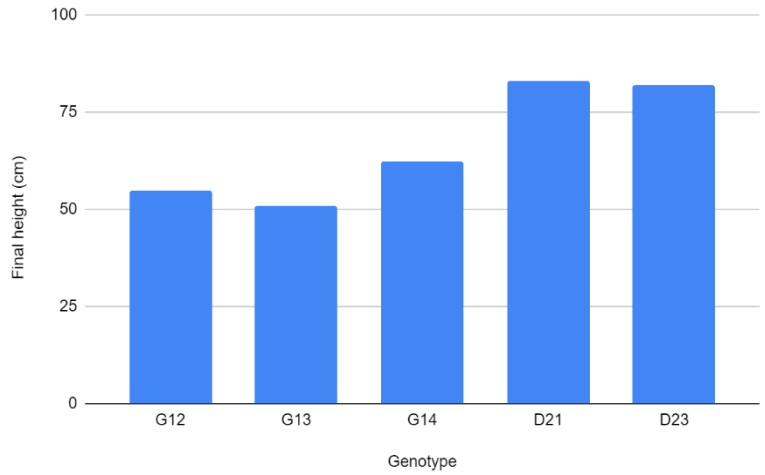

Figure 2 Dry mass of flowers

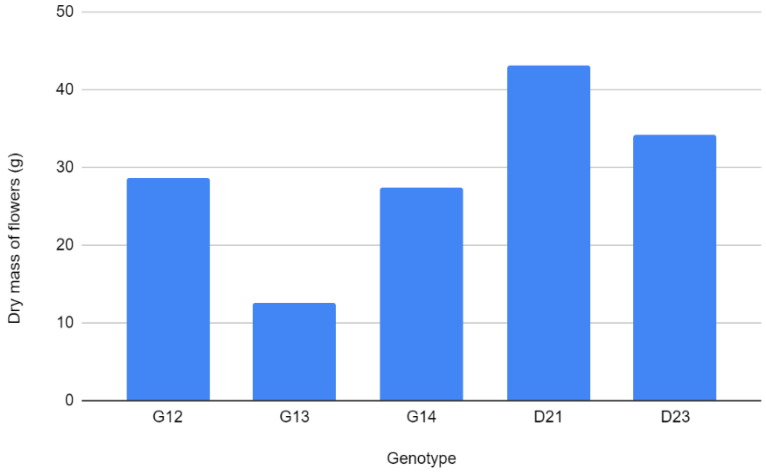

Figure 3 Percentage of final flower material in total dry mass

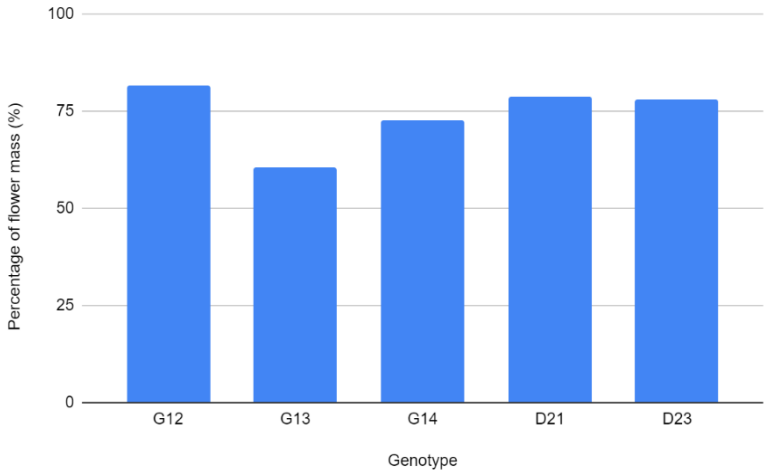

Length of maturation

Tested phenotypes were showing high differences in time of maturation from initiation of flowering to full ripeness of flowers (Figure 4). Fastest maturating phenotype was G13 which was ready to harvest after 47 days. Slowest maturating phenotypes were D21 and D23 which were ready

to harvest after 68 days. This may have been because one of parental varieties was showing traits significant for *Cannabis sativa* spp. *sativa* which is usually slower in maturation (Stack et al. 2021).

Data also showed positive correlation between maturation time and biomass production Naim-Feil et al. (2021).

In controlled environment this disadvantage can be overcomed by enlengthening of vegetative stage via longer light cycle 18 hours of light per day if the variety isn't showing signs of autoflowering typical for *Cannabis sativa* spp. *ruderalis* (Dowling et al. 2021).

Figure 4 Flowering time representing days necessary for full maturation of plants from initiation of flowering

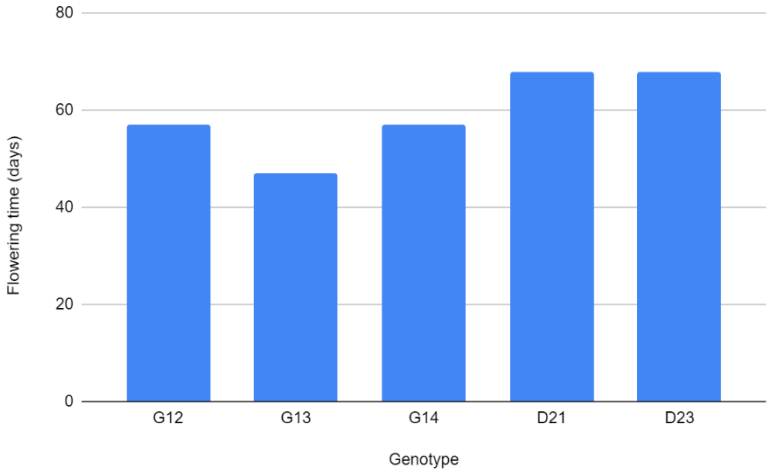

Cannabinoid content

From all selected phenotypes was highest content of cannabinoids present in G13 which reached total cannabinoids content 15%, this variety also showed highest content of CBG 13.57% (Figure 5). Lowest total cannabinoids content was in phenotype D23 which was only 3.98%, this phenotype was not detected on any detectable content of CBG but had 3.7% of CBD. Phenotypes G12, G13 and G14 contained some amount of CBD but phenotypes D21 and D23 contained CBD which other genotypes didn't. All tested phenotypes had levels of THC under 0.3% which is currently limit in most European countries for hemp varieties.

Figure 5 Content of cannabinoids in dry flower mass

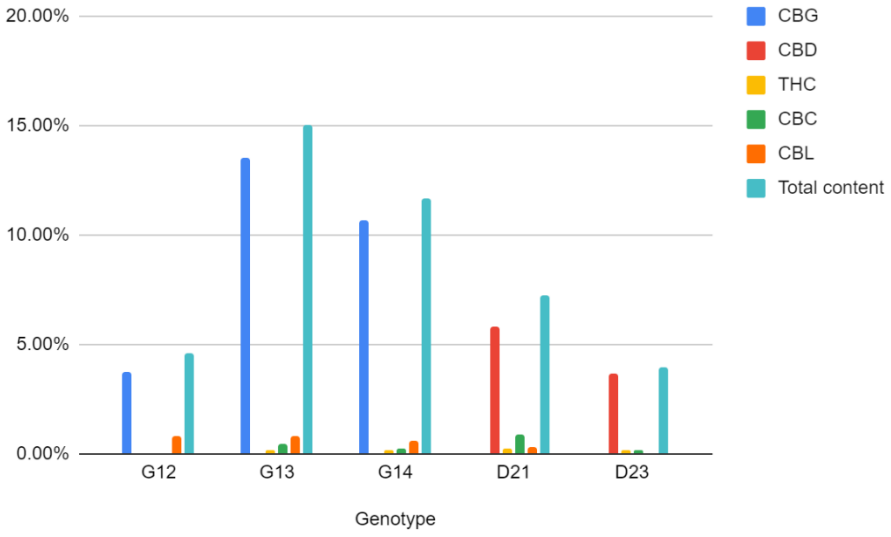

CONCLUSION

In industry of medicinal *Cannabis* production is very important to choose phenotypes which shows the traits of most cost-effective production of secondary metabolites. According to data collected during variety testing we can choose phenotype which shows the traits most sufficient for our growing techniques and plan production schedule very well. Cost-effectiveness in this industry plays very important role because technologies and standards under which can be medicinal cannabis cultivated are very strict and therefore are production costs very high. Although quite small sample of tested phenotypes we were able to select one with very interesting cannabinoid complex. This phenotype was reaching content of non-psychoactive cannabinoids reaching 14.87% of dry flower mass with CBG content of 13.57%. This phenotype will be used for further research focusing on inheritance of cannabinoids and another biological and biotechnological studies.

REFERENCES

Dowling, C.A. et al. 2021. Timing is everything: the genetics of flowering time in *Cannabis sativa*. Biochemist, 43(3): 34–38.

Elma, M.J.S. et al. 2014. New developments in fiber hemp (*Cannabis sativa* L.) breeding. Industrial Crops and Products, 65(1): 32–41.

Gulck, T., Moller, B.L. 2020. Phytocannabinoids: Origins and Biosynthesis. Trends in Plant Sciences, 25(10): 985–1004.

Kinghorn, A.D. et al. 2017. Phytocannabinoids (Progress in the Chemistry of Organic Natural Products). Cham, Switzerland: Springer nature.

Kriese, U. et al. 2004. Oil content, tocopherol composition and fatty acid patterns of the seeds of 51 *Cannabis sativa* L. genotypes. Euphytica, 137(1): 339–351.

Naim-Feil, E. et al. 2021. The characterization of key physiological traits of medicinal cannabis (*Cannabis sativa* L.) as a tool for precision breeding. BMC Plant Biology, 21(1): 294–301.

Stack, G.M. et al. 2021. Season-long characterization of high-cannabinoid hemp (*Cannabis sativa* L.) reveals variation in cannabinoid accumulation, flowering time and disease resistance. OCG-Bioenergy, 13(4): 546–561.

Wood, J. 1899. An oxycannabin from Indian hemp. Proceedings of the Chemical Society, 14(1): 44–45.

ANIMAL BIOLOGY

DNA barcoding and metabarcoding in forensic entomology: casuistic and future challenges

Tereza Oleksakova[1, 2], Vanda Klimesova[1, 2], Hana Sulakova[2]
[1]Department of Ecology
Czech University of Life Sciences Prague
Kamycka 129, 165 00 Prague 6
[2]Institute of Criminalistics in Prague
P.O. BOX 62, Strojnicka 27, 170 89 Prague 7
CZECH REPUBLIC

tereza.oleksakova@pcr.cz

Abstract: Forensic entomology is based on knowledge of species involved in forensic cases. If neither the rearing of early developmental stages nor the determination of species by traditional methods is possible, genetic identification is the only option. The paper describes the case of a dead young child found in a lake with dead insect egg on its body. DNA barcoding was chosen for eggs species identification. The method is based on a segment of approximately 650 bp of a mitochondrial gene encoding cytochrome oxidase subunit I. Sequences were compared to the GenBank BLASTn and BOLD (Barcoding of Life Database) module. Based on the knowledge of the insect species, and the fact that these were only unhatched eggs, it was possible to estimate the colonization interval. The period of colonisation of the dead body by insects was determined to be approximately 8–14 hours. However, if it was a mixture of eggs of several species, DNA barcoding would not have given the necessary results. For this type of sample, DNA metabarcoding and massive parallel sequencing (MPS) can be used. This method would capture the full range of species present in the sample. For example, cases involving illegitimate Traditional Chinese Medicine (TCM) products, containing mixtures and powders of various protected species, could be analysed by this method.

Key Words: DNA Barcoding, DNA Metabarcoding, forensic entomology, species identification, massive parallel sequencing

INTRODUCTION

The most frequent use of forensic entomology is the estimation of the colonization interval, which leads to post mortem interval estimation. The method uses insects collected from dead bodies (Tomberlin et al. 2011). The method is based on determining entomological traces to the species and then calculating the colonization time using temperatures from the body site. This implies that identification of the species is absolutely essential for a correct calculation (Byrd and Castner 2009). In the situation when adults or live larvae are present, species identification is relatively straightforward. Identification of adults is done using expert determination keys. Live larvae are reared to the adult stage. Problematic identification occurs when only killed eggs or first instar larvae are collected. Even some adult flies could be problematic, such as Sarcophaga species females (Jordaens et al. 2013).

If neither the rearing of early developmental stages nor the determination of species by traditional methods is possible, genetic identification is the only option. In previous research, DNA barcoding was chosen as the method for this type of sample (Olekšáková et al. 2018). The method itself is based on a segment of approximately 650 bp of a mitochondrial gene encoding cytochrome oxidase subunit I. DNA barcoding has been shown to be useful as a species identification tool (Hebert et al. 2003). This method has been applied to practice in the Institute of Criminalistics in Prague and is successfully applied in criminal cases and it is compatible with other species identification methods using DNA analysis (Pereira et al. 2019). The following paper describes the case of a dead young child found in a lake with a cluster of dead insect eggs on its body. In this case, genetic analysis was the only way to estimate the time of insect colonization of the body. When the eggs were taxonomically identified to species, it was possible to estimate the amount of time that passed between a child's death and its displacement into the lake.

After the successful application of DNA barcoding, efforts are being made to take this method a little further by applying DNA metabarcoding. The method is suitable for mixed and/or degraded samples and it uses massive parallel sequencing (MPS) instead of Sanger sequencing (Liu at al. 2020).

Regardless of the sequencing method used, bioinformatics analyses can be challenging. The entire dataset generated by NGS analysis typically contains thousands of records, and it is not technically possible to compare each of these records against a sequence database. A solution to this situation is to define operational taxonomic units (OTUs) by grouping reads by similarity and comparing one representative sequence from each OTU against the database. For bioinformatics analysis, the mBRAVE (Multiplex Barcode Research and Visualisation Environment) program can be used, which is directly linked to the BOLD (Barcoding of Life Database) module. This database is used to compare data generated by the DNA barcoding method.

MATERIAL AND METHODS

Sampling and preservation

Egg samples were collected from the dead body of a young child found in the lake in South Bohemia. The body was in the early stages of fresh decomposition with the beginning of soft tissue degradation. In the autopsy room, a single egg cluster was sampled. No first instar larvae were found. Samples were stored in 98% ethanol at -20 °C. Prior to analysis, the egg cluster was rinsed with distilled water, divided into five samples, and placed in a 1.5 ml Eppendorf tube.

DNA isolation and quantification

A Blood & Tissue kit (QIAGEN) was used for DNA isolation. The amount of proteinase K recommended in the instructions was used, and the length of incubation was 3 hours.

DNA quantification was performed on a Qubit fluorimeter (Thermo Fisher). All three samples showed the amount of DNA in the range suitable for further analysis.

PCR amplification

PCR amplification of the standard DNA barcoding marker of each of the DNA extractions was conducted with a set of two universal primers LCO1490: 5'-GGTCAACAAATCATAAAGATA TTGG-3' and HC02198: 5'-TAAACTTCAGGGTGACCAAAAAATCA-3' (Folmer et al. 1994). For the PCR reaction, a protocol for degraded DNA was used because of the fact that samples spend an unknown amount of time underwater, which may cause degradation of the organic material. The PCR reaction mix for one sample contained 10.94 µl ddH_20, 2 µl 10x coralload buffer, 0.8 µl dNTP mix, and 0.32 µl of each 10 µM primer, as well as 0.12 µl Taq DNA polymerase (QIAGEN). The mixture was vortexed and then 2 µl of the extracted DNA was added, after which the samples were loaded into a Biometra Trio cycler (Analytik Jena GmbH). The following protocol was used: 94 °C for 2 minutes; 30 cycles of 94 °C for 30 seconds, 47 °C for 35 seconds, and 72 °C for 45 seconds; 72 °C for 2 minutes; at 4 °C to finish. The PCR products were enzymatically purified using the Illustra EXOProStar 1-STEP kit (GE Healthcare).

Sequencing

In sequence reaction, purified PCR products and BigDye® Terminator v1.1 Cycle sequencing kit (Applied Biosystems) were combined with the forward (LCO) and reverse (HCO) primers. This step was followed by post-sequence reaction purification using the Dye Ex 2.0 Spin kit (QIAGEN).

Samples were run on the ABI 3130xl sequencer (Applied Biosystems) according to the manufacturer's instructions. Negative control (ddH_20) was used as a part of standard procedures. The chromatograms were manually edited with Bioedit v.7 (Hall 1999) and confirmed as being dipteran DNA, using the GenBank BLASTn search and species identification BOLD (Barcoding of Life Database) module.

RESULTS AND DISCUSSION

All samples analysed by BLASTn showed ≥98% identity to the reference sequences. The percent identity for the individual samples ranged between 99.86% and 100%. The range of similarity

for the BOLD database was 1. Based on those results was revealed that all three egg samples collected from the body of the dead child contained eggs of the same species, namely *Lucilia ampullacea* (Calliphoridae, Diptera).

Based on the knowledge of the insect species and the fact that these were only unhatched eggs (without first instar larvae) that were dead when the body was found, it was possible to estimate the colonization interval. Due to the low water temperature in the lake, it can be assumed that the eggs were in the developmental stage before being immersed in the water, but in cold water they immediately stopped their development and died. The period of colonisation of the dead body by insects was determined to be approximately 8–14 hours. Specifically, this is the length of time the child's body was freely exposed before it was disposed into the lake. How long the body was submerged in water cannot be determined from the insects found on the body.

It has been shown through an example from criminalistics practice that DNA barcoding is a useful tool in criminalistics cases solved by the Institute of Criminalistics in Prague. In the above case, only one species of insect was found. However, if it was a mixture of eggs from several species, the Sanger sequencing analysis would not have given the necessary results. For this type of sample, DNA Metabarcoding and massive parallel sequencing (MPS) can be used (Young et al. 2017). This method would capture the full range of species present in the sample. In addition, various mixtures and powders containing protected species could be analysed by this method, for example cases involving Traditional Chinese Medicine (TCM) products (Staats 2016), such as crabs or corals. Protected species may also be present in these mixtures and it is not possible to distinguish the species from each other by conventional morphological methods. Finally, DNA metabarcoding can also be used in research where bulk collections of insects are carried out and it is very time consuming to determine these collections morphologically as hundreds to thousands of individuals are involved.

DNA metabarcoding is usually used to simply detect the presence of species in mixed samples rather than their abundance. Several studies have shown positive relationships between biomass of input species and output sequence reads. It was found to have a strong positive correlation between biomass input and read frequency in certain coleopteran species (Bista et al. 2018). On the other hand, only weak correlations have been found in other arthropod species, and the recent study found limited quantitative DNA metabarcoding ability (Lamb et al. 2018). This fact represents a limitation for the use of DNA metabarcoding in forensic entomology as an equivalent replacement for traditional techniques (for example, the rearing of early developmental stages of insects). Even in the case of a dead sample, it is also necessary to know the length of individual larvae and the abundance ratios of each species, which represents valuable information for estimating the colonization interval, and provides more precise information for further investigation.

CONCLUSIONS

DNA barcoding and DNA metabarcoding are suitable methods for forensic cases solved by the Institute of Criminalistics in Prague. Those methods are using mitochondrial gene encoding cytochrome oxidase subunit I. For mixed samples was chosen DNA metabarcoding, using mitochondrial marker in massive parallel sequencing (MPS). Institute of Criminalistics in Prague currently replaced previously used immunology methods by genetic methods of animal species identification.

ACKNOWLEDGEMENTS

The research was financially supported by the by the project SOFTGEN I., reference number KU-1818/ČJ-2021-230502 (Institute of Criminalistics in Prague).

REFERENCES

Bista, I. et al. 2018. Performance of amplicon and shotgun sequencing for accurate biomass estimation in invertebrate community samples. Molecular Ecology Resources, 18: 1020–1034.

Byrd, J.H. and Castner, J.L. 2009. Forensic Entomology: The Utility of Arthropods in Legal Investigations. 2. ed., Boca Raton, USA: CRC Press.

Folmer, O. et al. 1994. DNA primers for amplification of mitochondrial cytochrome c oxidase subunit I from diverse metazoan invertebrates. Molecular Marine Biology Biotechnology, 3: 294–299.

Hall, T.A. 1999. BioEdit: a user-friendly biological sequence alignment editor and analysis program for windows 95/98/NT. Nucleic Acids Symposium Series, 41: 95–98.

Hebert P.D. et al. 2003. Biological identifications through DNA barcodes. Proceedings of the Royal Society B, 270: 313–321.

Jordaens, K. et al. 2013. Identification of forensically important Sarcophaga species (Diptera: Sarcophagidae) using the mitochondrial COI gene. International Journal of Legal Medicine, 127: 491–504.

Lamb, P.D. et al. 2018. How quantitative is metabarcoding: a meta-analytical approach. Molecular Ecology, 28: 420–430.

Liu, M. et al. 2020. A practical guide to DNA metabarcoding for entomological ecologists. Ecological Entomology, 45(3): 373–385.

Olekšáková, T. et al. 2018. DNA extraction and barcode identification of development stages of forensically important flies in the Czech Republic. Mitochondrial DNA Part A, 29(3): 1–4.

Pereira, F. et al. 2019. Species identification in routine casework samples using the SPInDel kit. Forensic Science International: Genetics Supplement Series, 7(1): 180–181.

Staats, M. et al. 2016. Advances in DNA metabarcoding for food and wildlife forensic species identification. Analytical and Bioanalytical Chemistry, 408(17): 4615–4630.

Tomberlin, J.K. et al. 2011. Basic research in evolution and ecology enhances forensics. Trends in Ecology & Evolution, 26: 53–55.

Young, J.M. et al. 2017. Soil DNA metabarcoding and high-throughput sequencing as a forensic tool: considerations, potential limitations and recommendations. FEMS Microbiology Ecology, 93(2): 207.

Stallion semen cooling using different types of extenders

Katarina Souskova, Zuzana Reckova, Tomas Kopec, Michaela Brudnakova, Radek Filipcik
Department of Animal Breeding
Mendel University in Brno
Zemedelska 1, 613 00 Brno
CZECH REPUBLIC

katarina.souskova@mendelu.cz

Abstract: Due to the advantages it offers, artificial insemination is an important part of current horse breeding. One of the limiting factors influencing the use of cooled insemination doses is the decrease in sperm survival over time, which can be influenced by selected extender. In our work, we focused on samples of insemination doses of Warmblood stallions diluted with a skimmed milk-based extender, INRA 96 and BotuSemen Gold extender stored at a temperature of 4 °C for up to 72 hours. Of the selected diluents, the skimmed milk-based extender reached the lowest values of total and progressive motility for all stallions and the lowest values of morphology for two of them ($p < 0.05$). Differences between INRA 96 and BotuSemen Gold were in sperm motility for one of the stallions, with INRA 96 reaching total motility of 53.66% and progressive motility of 17.13%, and BotuSemen Gold reaching 63.71% and 23.01% ($p < 0.05$). For two of the stallions, INRA 96 reached the highest values of sperm viability ($p < 0.05$). The skimmed milk-based extender, the advantages of which lie in its practicality and affordability, achieved lower values of the quality parameters of equine ejaculate than diluents with a chemically defined composition INRA 96 and BotuSemen Gold. There were differences between stallions in used extender. To maintain the best semen parameters, this should be taken into consideration and extenders should be tested for each stallion before the actual distribution of insemination doses to breeders.

Key Words: stallion, sperm, ejaculate, extender, insemination dose

INTRODUCTION

Equine artificial insemination has become an internationally widespread biotechnical method, thanks to which breeders have access to the world top stallions (Aurich 2012). This advantage also includes removing geographical restrictions, minimizing the transmission of venereological and systemic diseases, reducing the risk of injury, increasing the number of mares that can be inseminated by one ejaculate, possibility of evaluating ejaculate parameters before insemination, improvement of the domestic population by imported stallions, the possibility of breeding on individuals whose mental or physical conditions does not allow natural breeding and reduction of breeding cost (Morel 2008, Brinsko et al. 2011, Lane 2015). Currently there is also possibility of sperm sexing, intrauterine insemination with small doses and intracytoplasmic sperm injection (Aurich 2012).

In contrast with cattle, frozen insemination doses in the equine industry did not replace cooled ones (Aurich 2012), which is caused by the lower parameters of the fertilization ability (Nikitkina 2020) and larger differences between individual stallions in frozen ejaculate (Aurich 2020). Cooled insemination doses are preferred among breeders (Nikitkina 2020). One of the limiting factors in the use of cooled insemination doses is the time-dependent survival of sperm. The insemination success is influenced by numerous factors such as diluent composition, storage temperature, the number of sperm and number of insemination (Batellier et al. 2001).

The role of the diluent and its components is to protect the plasma membrane of sperm against external factors (Aurich 2005). Over the years, several extenders have been developed allowing semen cooling (Batellier et al. 2001, LeFrapper et al. 2010). Some of the most common are milk-based extenders, which are practical, effective (Aurich 2008) and affordable (Frietas et al. 2014). One of its disadvantages is the composition of the milk, containing substances that are beneficial but also harmful for sperm (Batellier et al. 1997). Because of that, extenders with the precisely defined

composition have been developed guaranteeing its stable and reliable quality (Aurich 2008). Such extenders are INRA 96 and BotuSemen Gold, which are considered one of the best on the market (Novello et al. 2020).

In our study we focused on the evaluation of semen parameters of equine ejaculate, such as motility, viability and sperm morphology using different extenders at regular time intervals up to 72 hours of storage.

MATERIAL AND METHODS

Animals

In our study we used 5 Warmblood stallions of Hannoverian, Oldenburger and Zangersheide breed aged from 16 to 19 years old. The stallions were stabled in Provincial Stud Farm Tlumačov. Stallions were active shires used for commercial breeding in 2020.

Semen collections

Collections of ejaculates took place in the Reproduction Centre of the Provincial Stud Farm Tlumačov. The ejaculates were collected from July to August 2020 at regular weekly intervals. A total of 6 ejaculates were taken from each stallion. Ejaculates were collected using Missouri-type artificial vagina.

Semen samples analysis

The gel fraction was removed from the native ejaculate by filtration through the sterile gauze. Subsequently, three samples were taken from the ejaculate and were diluted in a ratio of 1:2 with a skimmed milk-based extender, INRA 96 and BotuSemen Gold extender. Ejaculates were gradually cooled to 4 °C.

Total motility, progressive motility, viability and sperm morphology were monitored at 24, 48 and 72 hours.

Total and progressive motility was assessed using a computer-assisted sperm analysis system (Sperm Class Analyzer, Microptic SL) at 37 °C. At least, 500 sperms were evaluated in five fields of view.

Sperm viability was assessed using a fluorescence microscope (Olympus BX51, Olympus) and Hoechst 33258 dye at 400x magnification. At least, 200 sperms were evaluated.

Smears of ejaculates were fixed and stained using Farelly method. Sperm morphology was evaluated at 1000x magnification using immersion oil. At least 200 sperms were evaluated.

Statistical analysis

The data were statistically processed using the Statistica 12 program (StatSoft CR). Significance of factors and differences between means were tested using the Analysis of Variance (ANOVA). Values are expressed as means ± SEM. Statistical differences are significant for $p < 0.05$.

RESULTS AND DISCUSSION

The results of the study show that in all stallions the total and progressive motility had the lowest values in samples using the skimmed milk-based extender ($p < 0.05$, see Table 1). The total motility of this diluent ranged from 38.79 to 73.75% and the progressive motility from 8.27 to 39.41%. In comparison, the total motility of INRA 96 ranged from 53.66 to 90.32% and the progressive motility from 17.13 to 61.23%. For BotuSemen Gold, it was from 63.71 to 92.54% and from 23.01 to 66.24%. In all stallions except stallion III, no statistically significant differences of sperm motility were observed between INRA 96 and BotuSemen Gold extender. Total and progressive motility of stallion III ejaculate using BotuSemen Gold extender (63.71%, 23.01%) was higher than in INRA 96 (53.66%, 17.13%) ($p < 0.05$). On average, the BotuSemen Gold diluent reached the highest values of motility for stallion I and II and INRA 96 diluent for stallions IV and V.

Sperm viability of stallions I (65.06%) and IV (64.61%) was highest using INRA 96 extender ($p < 0.05$). In stallion III, sperm viability was statistically significantly higher using INRA 96 (69.33%) than with skimmed milk-based extender (64.31%) ($p < 0.05$). In stallions II and V, no statistically

significant differences in sperm viability were observed between diluents. On average, the highest proportion of viable sperm was achieved by INRA 96 extender.

The proportion of sperm with normal morphology was in stallions III (73.08%) and IV (65.11%) lowest using SM extender ($p < 0.05$). No statistically significant differences of sperm morphology between extenders were observed in the other stallions. On average, the BotuSemen Gold diluent reached the highest values for this parameter.

Table 1 Semen parameters of stallion ejaculate (means ± SEM) diluted with skimmed milk-based extender (SM), INRA 96 and BotuSemen Gold extenders

Stallion	Extender	Total Motility (%)	Progressive Motility (%)	Viability (%)	Sperm of Normal Morphology (%)
I	SM	44.19 ± 6.90 b	15.44 ± 4.47 b	60.67 ± 1.87 a	72.53 ± 2.84 a
	INRA 96	65.31 ± 6.26 a	29.14 ± 5.50 a	65.06 ± 1.29 b	76.17 ±2.88 a
	BotuSemen Gold	68.19 ± 5.18 a	32.19 ± 4.97 a	60.72 ± 1.45 a	78.86 ±2.14 a
II	SM	73.75 ± 5.38 b	39.41 ± 6.58 b	66.56 ± 1.56 a	62.89 ± 3.5 a
	INRA 96	90.32 ± 2.60 a	61.23 ± 5.69 a	69.58 ± 1.31 a	67.22 ± 2.6 a
	BotuSemen Gold	92.54 ± 2.17 a	66.24 ± 4.66 a	65.69 ± 2.15 a	68.08 ± 2.04 a
III	SM	38.79 ± 5.53 c	8.27 ± 2.25 c	64.31 ± 2.18 b	73.08 ± 2.71 b
	INRA 96	53.66 ± 5.78 b	17.13 ± 4.54 b	69.33 ± 1.47 a	79.53 ± 1.58 a
	BotuSemen Gold	63.71 ± 5.36 a	23.01 ± 4.38 a	66.42 ± 1.83 a,b	80.19 ± 1.60 a
IV	SM	55.61 ± 4.26 b	17.33 ± 2.74 b	57.97 ± 2.19 a	65.11 ± 3.10 b
	INRA 96	81.13 ± 3.07 a	39.33 ± 3.53 a	64.61 ± 1.82 b	72.33 ± 1.90 a
	BotuSemen Gold	79.83 ± 3.71 a	40.08 ± 3.99 a	59.86 ± 2.04 a	74.83 ± 1.31 a
V	SM	64.54 ± 5.02 b	25.56 ± 3.88 b	67.39 ± 1.11 a	57.47 ± 2.35 a
	INRA 96	81.29 ± 3.52 a	40.79 ± 4.05 a	70.31 ± 1.09 a	59.22 ± 3.24 a
	BotuSemen Gold	78.93 ± 3.78 a	41.69 ± 4.87 a	68.81 ± 1.40 a	62.92 ± 2.06 a

Legend: a, b, c – differences are significant for $p < 0.05$

From the results of our study, there are certain differences between the individual stallions in the semen parameters using different extenders (see Figure 1). These differences were most significant in the parameters of stallion III ejaculate.

In all stallions, the values of motility parameters using the skimmed milk-based extender were statistically demonstrably lower than using commercially available extenders INRA 96 and BotuSemen Gold. Similar results were obtained by LeFrapper et al. (2010). He reported that diluents with defined caseinate components maintained progressive motility after 24 hours of storage better than non-fat dry milk-based ones. This may be due to the fact, that milk is a biological product composed of large number of substances that cannot be standardized (Pagl et al. 2006). Of its fractions, some such as ß-lactoglobulin and native phosphocaseinate have a beneficial effect on sperm, while ultrafiltrate, microfiltrate and α-lactoglobulin have a detrimental effect (Batellier et al. 1997).

Stallion III has the only statistically significant differences in sperm motility between INRA 96 and BotuSemen Gold. In this case, BotuSemen Gold achieved demonstrably higher values of total and progressive motility. This diluent contains cholesterol-loaded cyclodextrin (Novello et al. 2020), which is mainly beneficial for stallions whose ejaculate reacts poorly to cooling (Hartwig et al. 2014). This may have been the reason for the difference between the INRA 96 and BotuSemen Gold extender in stallion III, which had the lowest sperm motility values among the shires.

In sperm viability, differences between extenders were significant for stallions I, III and IV. In stallions I and IV, INRA 96 was statistically the best diluent, and in stallion III, this extender was demonstrably better than the skim milk-based one. In comparison, Novello et al. (2020) did not note any significant differences in sperm viability between diluents.

The least significant differences between stallions were in the proportion of sperm with normal morphology. For stallions III and IV the skimmed milk-based extender had the lowest values.

Figure 1 Mean values of total motility, progressive motility, viability and morphology of stallion ejaculates diluted with skimmed milk-based extender (SM), INRA 96 and BotuSemen Gold extenders

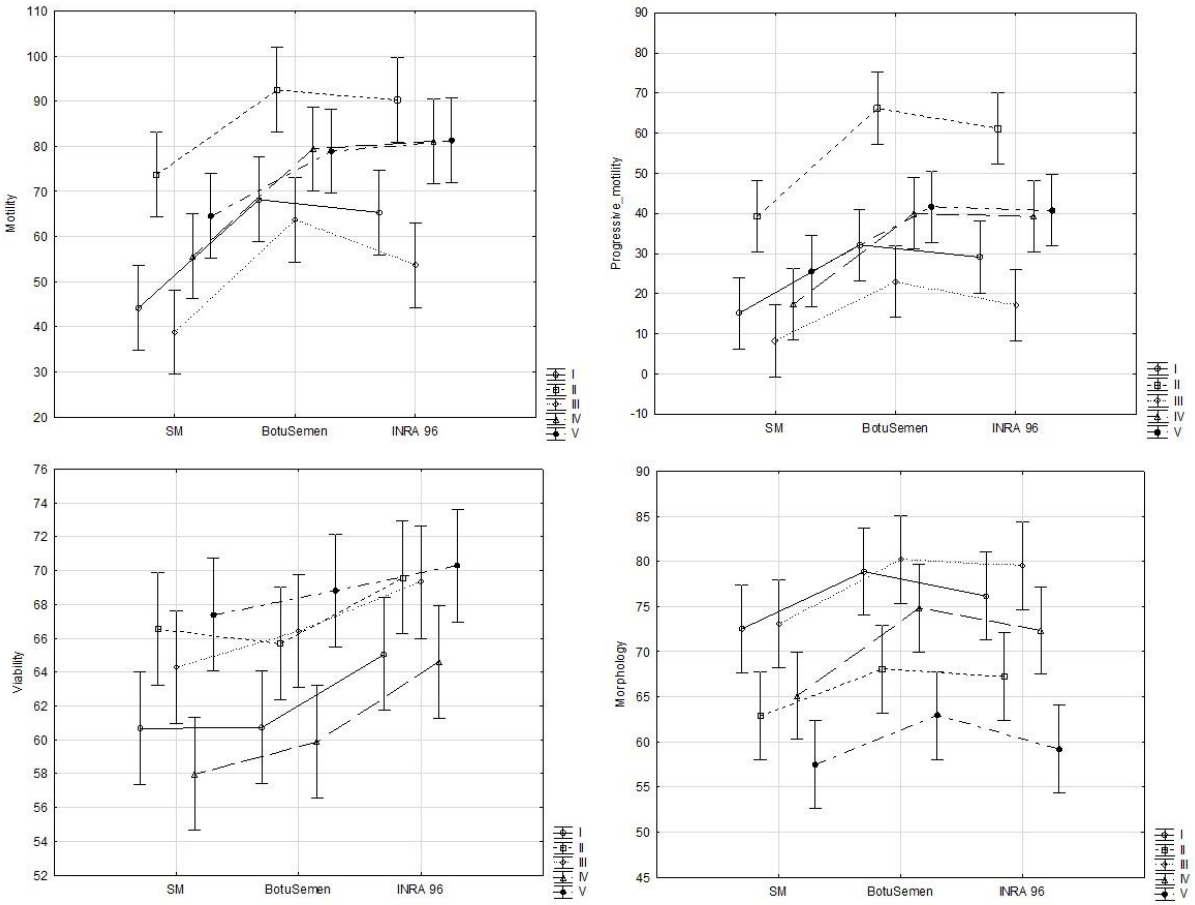

CONCLUSION

The results of our study showed differences in the response of stallion ejaculate to the diluent used during storage. This fact should be taken into consideration for individual stallions before the actual distribution of insemination doses. From the selected diluents, INRA 96 and BotuSemen Gold achieved better results than skimmed milk-based extender.

ACKNOWLEDGEMENTS

The research was financially supported by grant no. AF-IGA2020-IP066.

REFERENCES

Aurich, J.E. 2012. Artificial Insemination in Horses–More than a Century of Practice and Research. Journal of Equine Veterinary Science [Online], 32(8): 458–463. Available at: https://doi.org/10.1016/j.jevs.2012.06.011. [2021-08-18].

Aurich, J.E. 2020. Efficiency of Semen Cryopreservation in Stallions. Animals [Online], 10(6): 1033. Available at: https://doi.org/10.3390/ani10061033. [2021-08-18].

Aurich, Ch. 2005. Factors affecting the plasma membrane function of cooled-stored stallion spermatozoa. Animal Reproduction Science [Online], 89(1–4): 65–75. Available at: https://doi.org /10.1016/j.anireprosci.2005.06.025. [2021-08-18].

Aurich, Ch. 2008. Recent advances in cooled-semen technology. Animal Reproduction Science [Online], 107(3–4): 268–275. Available at: https://pubmed.ncbi.nlm.nih.gov/18524507/. [2021-08-18].

Batellier, F. et al. 2001. Advances in cooled semen technology. Animal Reproduction Science [Online], 68(3–4): 181–190. Available at: https://pubmed.ncbi.nlm.nih.gov/11744263/. [2021-08-18].

Batellier, F. et al. 1997. Effect of milk fractions on survival of equine spermatozoa. Theriogenology [Online], 48(3): 391–410. Available at: https://doi.org/10.1016/S0093-691X(97)00250-1. [2021-08-18].

Brinsko, S.P. et al. 2011. Manual of Equine Reproduction. 3. ed., Maryland Heights, Missouri: Mosby Elsevier.

Freitas, M. et al. 2014. The effect of skim milk as an equine semen extender. In Proceedings of 2014 ADSA-ASAS-CSAS Joint Annual Meeting [Online]. Kansas City, Missouri, 20–24 July, Champaign: American Society of Animal Science, pp. 599. Available at: https://www.jtmtg.org/JAM/2014/abstracts/JAM14-Abstracts.pdf. [2021-08-18].

Hartwig, F.P. et al. 2014. Use of cholesterol-loaded cyclodextrin: an alternative for bad cooler stallions. Theriogenology [Online], 81(2): 340–346. Available at: https://doi.org/10.1016/j.theriogenology.2013.10.003. [2021-08-18].

Lane, C. 2015. Equine Reproduction Part 1: Artificial Insemination. Veterinary Nursing Journal [Online], 30(5): 146–149. Available at: https://doi.org/10.1080/17415349.2015.1028770. [2021-08-18].

LeFrapper, L. et al. 2010. Comparison of Various Extenders for storage of Cooled Stallion Spermatozoa for 72 Hours. Journal of Equine Veterinary Science [Online], 30(4): 200–204. Available at: https://doi.org/10.1016/j.jevs.2010.02.007. [2021-08-18].

Morel, D. 2008. Equine Reproductive Physiology, Breeding and Stud Management 3. ed., Oxford: Oxford University Press.

Nikitkina, E. et al. 2020. Efficiency of Tris-Based Extender Steridyl for Semen Cryopreservation in Stallion. Animals [Online], 10(10): 1801. Available at: https://doi.org/10.3390/ani10101801. [2021-08-18].

Novello, G. et al. 2020. Stallion Semen Cooling Using Native Phosphocaseinate-based Extender and Sodium Caseinate Cholesterol-loaded Cyclodextrin-based Extender. Journal of Equine Veterinary Science [Online], 92(9): 103–104. Available at: https://doi.org/10.1016/j.jevs.2020.103104. [2021-08-18].

Pagl, R. et al. 2006. Comparison of an extender containing defined milk protein fractions with a skim milk-based extender for storage of equine semen at 5 °C. Theriogenology [Online], 66(5): 1115–1122. Available at: https://doi.org/10.1016/j.theriogenology.2006.03.006. [2021-08-18].

Associations of *SOST* and *TNFSF11* genes polymorphisms with bone parameters in broilers

Michala Steinerova[1], Cenek Horecky[1], Ales Knoll[1], Sarka Nedomova[2], Ales Pavlik[1]
[1]Department of Animal Morphology, Physiology and Genetics
[2]Department of Food Technology
Mendel University in Brno
Zemedelska 1, 613 00 Brno
CZECH REPUBLIC

xsteine5@node.mendelu.cz

Abstract: In modern broiler lines, increasing demands are placed on skeletal integrity, where these lines are often characterized by poor calcification and high bone porosity. Bone abnormalities, as disruption of the normal skeletal growth process and homeostasis, are usually complex and lead to increased affinity for bone damage and many bone diseases. Bone quality traits can be improved by genetic tools, given the additive genetic background of these traits. In this study, attention was focused mainly on the search for polymorphisms in selected candidate genes that play an important role in bone metabolism. We studied the associations of single nucleotide polymorphisms in several regions of two genes (*SOST* and *TNFSF11*) with selected bone parameters (bone breaking strength, length, width, bone mass) in fast (Ross 308) and slow (Hubbard M22BxJA87A) growing broilers, whereas the individual hybrid lines were also compared on the basis of the monitored bone parameters. A total of 48 animals were tested. PCR and sequencing were used to determine the polymorphisms. In selected regions of studied genes, thirteen polymorphisms have been discovered. Five of these polymorphisms were in the introns and three were synonymous. Only one polymorphism was found in selected gene regions in the experimental group of animals, which showed associations with bone breaking strength, but this polymorphism was found in the intron. Other polymorphisms, especially those found in the exon, did not show associations with the observed bone parameters.

Key Words: polymorphism, broiler, bone, *SOST*, *TNFSF11*

INTRODUCTION

Rapid growth, nutrition, and genetics are among the many factors that affect the skeletal integrity of broilers. In particular, the requirements for rapid growth, where the development of muscle mass is preferred, have led to an improvement in genetic potential. However, this can ultimately contribute to bone weakness (Mignon-Grasteau et al. 2016), problems with the legs of broilers leading to pain, lameness, infection and general discomfort (Liu et al. 2021). Many genetic mapping studies have been performed to look for important genes and processes involved in bone density, where the loci that have been identified so far do not explain most of the genetic variability (Johnsson et al. 2015).

In the process of osteoclastogenesis and osteoblastogenesis, the RANK/RANKL/osteoprotegerin and Wnt/β-catenin signaling pathways play a key role (Brunetti et al. 2019). The Wnt signaling pathway plays a very important and well-known role in bone repair and regeneration after injury, homeostasis, and overall bone development. It has the potential as a therapeutic target to enhance fracture healing, as Wnt ligands stimulate bone growth, which shows a strong regulatory role for the canonical Wnt signaling pathway just during healing (Houschyar et al. 2018). Disruption of secreted extracellular Wnt signaling antagonists can lead to osteogenic pathologies, with sclerostin being the best characterized Wnt signaling antagonist. It is secreted by osteocytes during bone remodeling and is encoded by the *SOST* gene. It uses binding to *LRP5/6* to inhibit the Wnt signaling pathway during bone formation. This leads to the completion of the negative feedback loop of osteogenesis (Kim et al. 2013). Bone remodeling, especially its regulation, is the main physiological role of the RANK/RANKL/OPG signaling pathway. It is involved in a number of bone diseases. Osteoclastic differentiation and activation is initiated by the binding of RANKL to its natural receptor (RANK), and OPG binds to RANKL, as a decoy receptor that prevents its osteoclastogenic effect (Neyro Bilbao et al. 2011).

To determine the anabolic and catabolic state of the bones, the balance between OPG and RANKL (encodes by the *TNFSF11* gene*)*, as well as the association with its RANK receptor, is crucial. RANK, which is encoded by the *TNFSF11A* gene, is determined by osteoclast differentiation and survival, which it attributes to a very important role. Any change in this complex that would cause deregulation of bone remodeling could lead to pathological conditions (García-Giralt et al. 2013).

This study aimed to screen single nucleotide polymorphisms (SNP) of selected genes (*SOST*, *RANKL*) and analyze the potential association between these genes and bone mechanical parameters in broilers. There was also a comparison of selected bone parameters within the given hybrid lines. We assume that a certain group of polymorphisms in the monitored genes affects the synthesis, activity and function of proteins essential for osteogenesis, formation and remodeling of bone tissue in broiler chickens. Bone mineral density is a predictor of many bone diseases, and the study of genes related to bone quality indicators can provide new clues to the biological processes that underlie diseases that lead to bone weakening.

MATERIAL AND METHODS

The experiment was performed on two hybrid broiler lines, for a total of 48 animals, with 24 animals from each line. Fast-growing Ross 308 hybrids and slow-growing Hubbard M22BxJA87A hybrids were tested. At 35 days of age, slaughter was performed using decapitation. Immediately after slaughter, blood was collected and stabilized with heparin. Subsequently, DNA was isolated using a commercially available DNA Lego kit (Top-Bio, Prague, Czech Republic). The following bone parameters were analyzed: bone breaking strength, bone mass, bone width, and length. The universal testing machine TIRATEST 27025 (TIRA Maschinenbau GmbH, Schalkau, Germany) was used to evaluate and analyze the bone breaking strength. Vernier calipers were used to evaluate the dimensions of the bones. According to sequences from the GenBank database (http://www.ncbi.nlm.nih.gov/genbank/) and using the OLIGO v4.0 software (Molecular Biology Insights, Inc., Colorado Springs, CO, USA), own oligonucleotide primers were designed (Table 1).

Table 1 SOST and TNFSF11 primers

Gene	Primer sequence	Product size (bp)
SOST (exon 1)	Forward: 5‘-AACCCGACAACACGAGGAG-3‘ Reverse: 5‘-CGATTCCTCCTCCATACCAAG-3‘	604
TNFSF11 (exon 2)	Forward: 5‘-TGGTGGTCATTGTGTGCTGCT-3‘ Reverse: 5‘- TCTCCATCACCATCCACTCACTG-3‘	676
TNFSF11 (exon 4 a 5)	Forward: 5‘-TTATGGGATGTGTTCTTAGCAGTG-3‘ Reverse: 5‘-GGTTTCAGGCCTCAATAGAGC-3‘	581

The following conditions were used for the PCR reaction, which was performed in a solution with a final volume of 10 µl: 94 °C for 3 min, 30 cycles at 94 °C for 1 min, 55, 56 or 58 °C for 30 s; 72 °C for 1 min, 72 °C for 10 min, then maintained at 4 °C. Annealing temperature of 55 °C was used for *TNFSF11* exon 4 a 5, 56 °C for *SOST* exon 1 and 58 °C for *TNFRSF11* exon 2. To perform PCR reactions was used an ABI Veriti thermal cycler (Life Technologies, Applied Biosystems, Foster City, CA, USA). The reaction products were visualized by 2.5% agarose gel electrophoresis at 120 V for 30 minutes, TBE buffer, and GoodView (Ecoli, ltd., Bratislava, Slovak Republic) staining was used. As molecular size marker was used the 100 bp DNA ladder (M100) (Thermo Fisher Scientific Inc., Waltham, USA). Using the BigDye® Terminator v3.1 Cycle Sequencing Kit (Applied Biosystems, Foster City, CA, USA) was carried out DNA sequencing of the PCR products. Conditions of sequencing cycle were 96 °C for 1 min, 25 cycles at 96 °C for 10 s, 50 °C for 5 s, 60 °C for 4 min, then maintained at 4 °C. For sequencing was used an ABI PRISM 3500 DNA analyzer (Life Technologies, Applied Biosystems, Foster City, CA, USA), and the results were further evaluated using SeqScape v2.7 software (Life Technologies, Applied Biosystems, Foster City, CA, USA). The Kruskal-Wallis test was used to analyze the obtained data. In terms of polymorphism testing, the genotype was chosen as the independent variable and bone breaking strength, bone length, width, and bone mass as dependent variables. In the case of a comparison of individual hybrid lines, the hybrid was an independent variable.

All statistical analyses were performed by STATISTICA 12 statistical software (StatSoft Inc., Tulsa, USA), and the overall level of statistical significance was defined as $P<0.05$.

RESULTS AND DISCUSSION

Within the studied genes, 48 samples were tested for each marker. A total of thirteen polymorphisms were found, five polymorphisms were intronic and three were synonymous.

The *SOST* gene is located, in chickens, on chromosome 27 and has two exons. In testing, exon 1 was examined, and the PCR products had a size of 604 bp. A total of six polymorphisms were found within this region, three were in exon (c.143G>A, c.164A>T, c.239G>T) and three were intronic (c.254+13T, c.254+85A, c.254+107A) (Table 2).

Table 2 Association of SOST gene polymorphisms with selected bone parameters in hybrids

Gene	SNP	Genotype (N)	Bone breaking strength	Length	Width	Bone mass
SOST	c.143G>A	AA (6)	167.85	73.91	7.54	7.75
	Hubbard	GA (8)	160.34	72.31	7.46	7.77
		GG (10)	171.26	73.14	7.47	7.89
	P-value		*0.5929*	*0.8115*	*0.6141*	*0.9726*
	c.164A>T	AA (22)	255.10	75.12	8.22	10.02
	Ross	AT (1)	241.97	69.71	8.20	9.74
		TT (1)	268.87	71.50	9.12	11.33
	P-value		*0.5934*	*0.1368*	*0.3153*	*0.3899*
	c.239G>T	GG (22)	241.97	75.12	8.22	10.02
	Ross	TG (1)	255.10	69.71	8.20	9.74
		TT (1)	268.87	71.50	9.12	11.33
	P-value		*0.5934*	*0.1368*	*0.3153*	*0.3899*
	c.254+13T	AA (10)	248.05	75.29	8.48	10.40
	Ross	AT (7)	242.83	73.60	8.02	9.74
		TT (7)	238.15	75.09	8.16	9.91
	P-value		*0.7141*	*0.6541*	*0.1992*	*0.2879*
	c.254+13T	AA (8)	166.88	73.36	7.40	7.86
	Hubbard	AT (5)	168.94	72.89	7.48	7.76
		TT (11)	165.69	72.91	7.54	7.81
	P-value		*0.9691*	*0.9647*	*0.4431*	*0.9600*
	c.254+85A	AA (11)	232.78	74.62	8.01	9.70
	Ross	AG (3)	268.73	73.33	8.37	10.28
		GG (10)	248.05	75.29	8.48	10.40
	P-value		*0.4078*	*0.7965*	*0.1399*	*0.1049*
	c.254+85A	AA (14)	*164.24*	*73.22*	*7.50*	*7.85*
	Hubbard	AG (2)	*183.99*	*70.71*	*7.69*	*7.38*
		GG (8)	*166.88*	*73.36*	*7.40*	*7.86*
	P-value		*0.5717*	*0.8217*	*0.6083*	*0.5752*
	c.254+107A	AA (10)	244.90	74.79	8.32	10.01
	Ross	AG (7)	242.83	73.60	8.02	9.74
		GG (7)	242.65	75.81	8.39	10.48
	P-value		*0.8920*	*0.5702*	*0.3434*	*0.2928*
	c.254+107A	AA (12)	163.17	73.22	7.52	7.82
	Hubbard	AG (4)	177.31	71.97	7.53	7.72
		GG (8)	166.88	73.36	7.40	7.86
	P-value		*0.4078*	*0.8973*	*0.6561*	*0.4833*

Legend: N – numbers of individuals of each genotype

The *TNFSF11* gene is located on chromosome 1 and has 6 exons. Region of exon 2, 4, and 5 were examined. The PCR products of the studied exon 2 had a size of 676 bp, and the products of the studied

region, which covered exon 4 and 5, had a size of 581 bp. A total of seven polymorphisms were found, five were in the exon. Within exons 4 and 5, there were two polymorphisms in the intron (c.137-84A, c.137-76G) and one polymorphism in the exon (c.664T>C). A total of 4 polymorphisms were found in the exon, within the studied region of exon 2 (c.248A> G, c.318C>T, c.366C>T, c.375C>T), but three of them were synonymous (c.318C>T, c.366C>T, c.375C>T) (Table 3).

Table 3 Association of TNFRSF11 gene polymorphisms (exon 2, 4 and 5) with selected bone parameters in hybrids

Gene	SNP	Genotype (N)	Bone breaking strength	Length	Width	Bone mass
TNFRSF11 (2)	c.248A>G Ross	AA (21)	244.65	74.92	8.24	10.17
		GA (2)	210.84	72.41	8.09	9.29
		GG (0)	0.00	0.00	0.00	0.00
	P-value		*0.2752*	*0.2301*	*0.7432*	*0.1017*
	c.248A>G Hubbard	AA (20)	159.71	73.10	7.45	7.81
		GA (4)	159.31	72.29	7.48	7.60
		GG (0)	0.00	0.00	0.00	0.00
	P-value		*0.8943*	*1.000*	*0.8942*	*0.5482*
	c.137-84A Hubbard	AA (22)	168.97	73.06	7.49	7.76
		AG (2)	142.46	72.97	7.41	8.40
		GG (0)	0.00	0.00	0.00	0.00
	P-value		*0.0601*	*0.9168*	*0.6381*	*0.2091*
TNFRSF11 (4, 5)	c.137-76G Hubbard	GG (22)	163.48	73.16	7.46	7.78
		GA (2)	202.92	71.90	7.77	8.23
		AA (0)	0.00	0.00	0.00	0.00
	P-value		***0.0216***	*0.2963*	*0.0756*	*0.4637*
	c.664T>C Ross	CC (22)	248.57	75.10	8.30	10.21
		CT (2)	210.84	72.41	8.09	9.29
		TT (0)	0.00	0.00	0.00	0.00
	P-value		*0.2301*	*0.1904*	*0.5851*	*0.0809*
	c.664T>C Hubbard	CC (23)	165.22	73.07	7.46	7.79
		CT (1)	202.35	72.67	7.90	8.44
		TT (0)	0.00	0.00	0.00	0.00
	P-value		*0.1293*	*0.7180*	*0.1291*	*0.4259*

Legend: N – numbers of individuals of each genotype

The values of the femur breaking strength in Hubbard M22BxJA87A broilers were from 135.47 to 203.49 N. The range of values for bone length was between 66.90 and 79.15 mm, for width 7.00 and 8.04 mm, bone mass 6.34 and 9.23 g. For Ross 308 broilers, the femur breaking strength values ranged from 170.52 to 322.21 N. The range of values for bone length was between 69.48 and 79.88 mm, for width 7.57 and 9.22 mm, bone mass 8.71 and 12.61 g. The monitored parameters of both lines were compared (Table 4).

Table 4 Comparison of observed parameters within the Ross and Hubbard hybrid lines

Hybrid	Bone breaking strength	Length	Width	Bone mass
Ross	243.64	74.74	8.25	10.07
Hubbard	166.76	73.06	7.48	7.82
P-value	*0.0001*	*0.0665*	*0.0001*	*0.0001*

As can be seen (Table 4), all observed parameters within the Ross hybrid are significantly higher compared to the Hubbard hybrid, which could be assumed because at 35 days Hubbard hybrids did not reach their peak growth, which affected the observed parameters.

Analysis of bone parameters and subsequent comparison of several broiler lines examined, for example, Mabelebele et al. (2017). They determined bone measurements in Ross 308 and Venda chicken hybrids and found that gender and hybrid combinations affected bone length, weight, and width at 90 days of age in both hybrid combinations.

In the case of the *SOST* gene, only one genotype was found in Hubbard M22BxJA87A hybrids in polymorphisms c.164.A>T and c.239G>T (*AA* genotype of c.164A>T polymorphism, and *GG* genotype of c.239G>T). Only one genotype was also found in Ross 308 hybrids, within several polymorphisms: *GG* genotype of c.143G>A in *SOST* gene; *AA* genotype of c.137-84A, and *GG* genotype of c.137-76G polymorphisms in *TNFRSF11* gene exon 4, 5; *CC* genotype of c.318C>T, c.366C>T, and c.375C>T polymorphisms in *TNFRSF11* gene exon 2.

Within the polymorphisms of the *SOST* gene no statistically significant difference was found (Table 2). The polymorphism of c.137-76G in *TNFRSF11* gene (Table 3) was significantly associated with bone breaking strength between *GG*×*GA* genotypes. The *A* allele led to stronger bone than the *G* allele. It should be noted that in the case of the *GA* genotype and the mentioned *A* allele, there were only two hybrids with this genotype in the given set. However, this polymorphism was found in the intron.

Apart from the mentioned c.137-76G polymorphism, the effect of the other studied polymorphisms on selected bone parameters within specific hybrid lines was not confirmed. Despite this fact, further, especially larger studies are needed.

Also, very few studies have been found to deal with similar topics, i.e., the analysis of polymorphisms within genes that are important in bone metabolism and the association of selected bone parameters in broilers. One of them was the study of Fornari et al. (2014), in which the g.9144C>G polymorphism in the *OPG* gene was associated with tibia weight and tibia breaking strength in broiler. Relatively more studies, which combine the analysis of polymorphisms and their association in broilers, are mainly related to the growth ability of broilers. Jin et al. (2018) studied a total of 796 hybrids from two lines, three polymorphisms were found within the *Pit-1* gene that were significantly related to some growth and feed efficiency traits in chickens. A similarly focused study of Hosnedlova et al. (2020) on two hybrid lines (Hubbard F15 and Cobb E) involved *IGF1*, *IGFBP2* and *TGFβ3* genes. A study of the same genes, that are within signaling pathways and affect bone metabolism, is reported by Steinerova et al. (2020). The *SOST* and *TNFRSF11* genes were also studied, while more polymorphisms were found in the studied group of laying hens, but without a statistically significant difference to the observed bone parameters. The study of Guo et al. (2017) also included these two genes, but in laying hens. A total of 9 polymorphisms were found to be associated with bone quality. Other studies that focus on the study of associations of polymorphisms with selected bone parameters, not only in broilers but also laying hens are Horecka et al. (2018), Raymond et al. (2018), Steinerova et al. (2019a,b).

CONCLUSION

Among the very important factors in poultry management belongs the good structure and function of the skeletal system. Bone problems that include various deformations, bone weaknesses that can lead to fractures and subsequent death, occur not only in broilers. Understanding the physiological basis of bone maturity and strength, bone parameters and genetic basis is essential to improve bone quality. The study of markers, especially those that could affect bone strength, can be used to discover new insights useful in poultry management. The discovery of these findings was the main goal of this study, which focused on the search for polymorphisms within genes that are part of one of the important signaling pathways for bone metabolism. No polymorphism was found in the exon that showed a significant association with the observed traits. Based on the results obtained, the study could be extended to new, candidate genes that play an important role in bone metabolism in human medicine.

ACKNOWLEDGEMENTS

The research was financially supported by the Internal Grant Agency of the Faculty of AgriSciences, Mendel University in Brno (AF-IGA2021-IP092).

REFERENCES

Brunetti, G. et al. 2019. An update on the role of RANKL-RANK/osteoprotegerin and WNT-β-catenin signaling pathways in pediatric diseases. World Journal of Pediatrics, 15(1): 4–11.

Fornari, M. B. et al. 2014. Unraveling the associations of osteoprotegerin gene with production traits in a paternal broiler line. SpringerPlus, 3: 682.

García-Giralt, N. et al. 2013. SNPs in the 3´UTR of the *RANK* gene determine side-dependent osteoporotic fracture. Journal of Osteoporosis and Mineral Metabolism, 5(2):85–92.

Guo, J. et al. 2017. Genetic architecture of bone quality variation in layer chickens revealed by a genome-wide association study. Scientific Reports, 7: 45317.

Horecka, E. et al. 2018. Association between single nucleotide polymorphisms of *ATP2B1* gene and bone parameters of laying hens. Avian Biology Research, 11(3): 178–182.

Hosnedlova, B. et al. 2020. Associations between *IGF1*, *IGFBP2* and *TGFβ3* genes polymorphisms and growth performance of broiler chicken lines. Animals, 10(5): 800.

Houschyar, K. S. et al. 2018. Wnt pathway in bone repair and regeneration – What do we know so far. Frontiers in Cell and Developmental Biology, 6: 170.

Jin, S. et al. 2018. Association of polymorphisms in *Pit-1* gene with growth and feed efficiency in meat-type chickens. Asian-Australasian Journal of Animal Sciences, 31(11): 1685–1690.

Johnsson, M. et al. 2015. Genetic regulation of bone metabolism in the chicken: similarities and differences to mammalian system. PLOS Genetics, 11(5): e1005250.

Kim, J. H. et al. 2013. Wnt signaling in bone formation and its therapeutic potential for bone diseases. Therapeutic Advances in Musculoskeletal Disease, 5(1): 13–31.

Liu, K. et al. 2021. Changes of lipid and bone metabolism in broilers with spontaneous femoral head necrosis. Poultry Science, 100: 100808.

Mabelebele, M. et al. 2017. Bone morphometric parameters of the tibia and femur of indigenous and broiler chickens reared intensively. Applied Ecology and Environmental Research, 15(4): 1387–1398.

Mignon-Grasteau, S. et al. 2016. Genetic determinism of bone and mineral metabolism in meat-type chickens: A QTL mapping study. Bone Reports, 5: 43–50.

Neyro Bilbao, J. L. et al. 2011. Bone metabolism regulation through RANK-RANKL-OPG system. Revista de Osteoporosis y Metabolismo Mineral, 3(2): 105–12.

Raymond, B. et al. 2018. Genome-wide association study for bone strength in laying hens. Animal Science, 96(7): 2525–2535.

Steinerova, M. et al. 2019a. The search for single nucleotide polymorphisms in genes encoding non-collagenous proteins in bone tissue of laying hens. In Proceedings of International PhD Students Conference MendelNet 2019 [Online]. Brno, Czech Republic, 6–7 November, Brno: Mendel University in Brno, Faculty of AgriSciences, pp. 490–493. Available at: https://mendelnet.cz/pdfs/mnt/2019/01/93.pdf. [2021-10-11].

Steinerova, M. et al. 2019b. Variability of selected genes in relation to the parameters of bones in laying hens: A pilot study. Journal of Microbiology, Biotechnology and Food Sciences, 9: 449–452.

Steinerova, M. et al. 2020. Study of selected signaling pathways genes that play an important role in bone metabolism in laying hens. In Proceedings of International PhD Students Conference MendelNet 2020 [Online]. Brno, Czech Republic, 11–12 November, Brno: Mendel University in Brno, Faculty of AgriSciences, pp. 424–429. Available at: https://mendelnet.cz/pdfs/mnt/2020/01/76.pdf. [2021-10-11].

TECHNIQUES AND TECHNOLOGY

Comparison of fatigue behaviour of AlSi10Mg CT samples prepared by casting and by additive technologies

Jana Dvorakova[1], Karel Dvorak[2], Michal Cerny[1]
[1]Department of Technology and Automobile Transport
Mendel University in Brno
Zemedelska 1, 613 00 Brno
[2]Department of Technical Studies
College of Polytechnics Jihlava
Tolsteho 16, 586 01 Jihlava
CZECH REPUBLIC

xdvora15@mendelu.cz

Abstract: The achieved mechanical properties influence the usability of parts prepared by additive technologies. Investigating the mechanical properties of parts and materials for additive technologies is currently one of the most up-to date topics. In this work, an electromechanical testing method is chosen, which analyzes the formation and propagation of a crack in the aluminum alloy AlSi10Mg prepared from metal powder by the additive technology DMLS (direct metal laser sintering). Testing is performed on CT (compact tension) samples according to ČSN ISO 12108 on test machine Instron Electropuls 10000, and the results are compared with values obtained by testing samples made by gravity casting from an aluminum alloy of comparable composition. 3D printing of CT samples is performed in various topologies to verify the dependence of fatigue behavior on the printing topology with the aim of applicability in determining suitable printing topologies depending on the shape of the part and the direction of stress in the practical use of parts. The research monitors the dependence of the crack formation time and its propagation speed on the print orientation of the test specimen. The results of testing determine the appropriate printing topology in order to find the ideal position of a sample during printing and assess the possible use of this 3D printed material for cyclic loaded parts.

Key Words: AlSi10Mg, additive technologies, fatigue, topology optimization, CT samples

INTRODUCTION

3D printing, through which the test samples were prepared, is an additive technology. According to the standard ISO / ASTM 52900: 2015 Additive production - general principles - Terminology, which is adopted in English into the Czech normative system under the name ČSN EN ISO 52900: 2017, additive production (AM) is a process of joining materials to obtain parts from data A 3D model is usually applied layer by layer, unlike subtractive and formative manufacturing technologies. Hidden in this definition is the essential advantage of additive manufacturing over machining or forming, which is applying the material in the desired shape, not its removal or movement. According to this definition, the advantage of additive technologies is not only saving material but also the use of a 3D model, enabling fast data transfer to remote locations, the possibility of using this data for print preparation, consisting in the most widespread additive technologies, FDM only .stl format and its conversion via freely available software tools (e.g., Cura or 3D Slicer) directly for a specific 3D printer. This advantage is also hidden in another designation of additive technology, Rapid Prototyping. This technology is an excellent benefit for rapid prototyping by printing a physical 3D model, as the name implies. Speed of prototype production is determined by the size, model complexity, and technology used.

The method of sample preparation AlSi10Mg, DMLS (Direct Metal Laser Sintering), i.e., direct sintering of metal powder (Figure 1) by a laser, belongs to the category of granular 3D printing methods. Other technologies in this category, which use a heat source such as a laser to focus energy to fuse the powder through its melting, include Electron Beam Melting (EBM), Selective Laser Melting (SLM), selective Selective Heat Sintering (SHS), and Selective Laser Sintering (SLS).

Figure 1 AlSi10Mg metal powder for additive production (ČSN EN ISO/ASTM 52907)

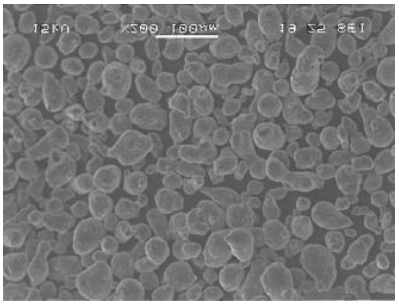

MATERIAL AND METHODS

Characterization of tested material, experimental design and testing samples

AlSi10Mg powder is made by elongated and spherical particles with smooth surface consisting mainly of aluminum with silicon of mass fraction up to 10% and less than 1% of magnesium along with other minor elements. Precipitates of Mg and Si make the alloy stronger and harder at the same time. The ČSN EN 1706 standard regulates the chemical composition and mechanical properties of aluminum and its alloys. However, this standard only regulates aluminum alloys for castings; therefore, it is used in ongoing research alloys of similar declared chemical composition only for CT samples prepared by gravity casting. Until recently, the only metal powder was considered a 3D printing material for printing metal products, which can be processed by the DMLS method, i.e., by an additive technology based on the principle of sintering of individual layers of powder using a laser. However, with the development of additive technologies, filaments (3D printing strings) based on PLA (polylactic acid) with high metal content, processable by the FDM (Fused Deposition Modeling) method, have recently started to appear. Their manufacturer declares that after firing in a sintering furnace, the result is 100% metal.

Test specimens of 3D printing aluminum alloy AlSi10Mg were prepared by the DMLS method. (Direct Metal Laser Sintering). Another research of the 3D printed aluminum alloy AlSi10Mg could examine also the material in the form of a filament, in which the aluminum alloy particles are placed on a polymeric carrier, biodegradable polylactic acid (PLA) enabling printing of the material polymer carrier. However, this research is still finding a suitable way to remove PLA without affecting the mechanical properties of the obtained components.

A significant topic of additive technologies is the orientation of components in printing (Dvorakova and Dvorak 2021, Sigmund and Maute 2013, Sedlacek and Lasova 2018). To unify the marking, the ISO / ASTM 52921 standard was issued, which regulates the marking of the coordinate system during printing and the test methodology. This standard is crucial for the uniformity of the labeling of different printing topologies, enabling a comparison of the results of research carried out by different authors.

In order to determine the load parameters during fatigue testing, basic testing using the tensile strength test method was performed as part of the preparation of this research. For samples prepared by conventional technologies, the minimum values or ranges of values are given in the standards for each alloy, the state of heat treatment and the size of the product. For additive technologies materials, the values are given in material sheets of suppliers and also differ according to the used technology of production or processing, i.e. in the case of this research also according to the performance of the laser intended for the DMLS method.

Fatigue testing is performed on CT (compact tension) samples designed by the ČSN ISO 12108 standard and prepared from AlSi10Mg metal powder by the DMLS method. We use Wöhler curves to determine the fatigue properties of the material. The Wöhler curve describes the resistance of a material to failure under cyclic loading with a constant force amplitude, which is much lower than the strength of the material found in the tensile test. He characterizes this resistance to high-cycle fatigue as the dependence of the stress amplitude σa on the number of Nf cycles. For low-cycle fatigue, (Nf is less than 10^4 cycles), it is appropriate to use the dependence between the amplitude of plastic deformation εap and Nf. The service life curve decreases with decreasing stress (Michna et al. 2005).

Therefore, aluminum alloys are characterized by a fatigue time limit for a certain number of cycles. The upper limit is usually 10^8 cycles. The fatigue life of aluminum alloys depends on the chemical composition, heat treatment, production method, nature of stress, surface quality, presence of notches, samples' case, and the amplitude of stress, environment, and shape of test specimens. In foundry alloys, the fatigue life is determined by the structure (grain size, porosity, inhomogeneity) influenced by the casting method. The fatigue properties of materials processed by additive technology depend on many factors, including surface quality, porosity, microstructure, and residual stress. Porosity and microstructure are examined, for example, by micro CT (micro-computed tomography) (du Plessis and Beretta 2020).

Defects and cracks of subcritical dimensions are commonly present in alloys, and therefore it is monitored whether the critical value of the stress intensity coefficient K, which is defined by the relationship between the nominal stress in the structure and the defect size ($K = \sigma\sqrt{(\pi a)}$) and the structure is broken.

The fracture toughness, i.e., the material's resistance to brittle failure, is characterized by the critical value of the stress intensity factor KIC under static loading by stress acting perpendicular to the opening crack.

The Instron Electropuls 10000 test machine was used for testing, and the BlueHill Universal test software records, displays, and evaluates the measured values (see Figure 2). Jaws of extensometer are placed in the groove of a sample, their opening is sensed, and during testing, crack length is determined by calculation in the machine's software. The samples are cyclically loaded with a force of 2500 N in tension with a frequency of 10 Hz. The number of cycles to crack formation and propagation is monitored.

Figure 2 Testing of CT sample using machine extensometer Instron Electropuls E 10000

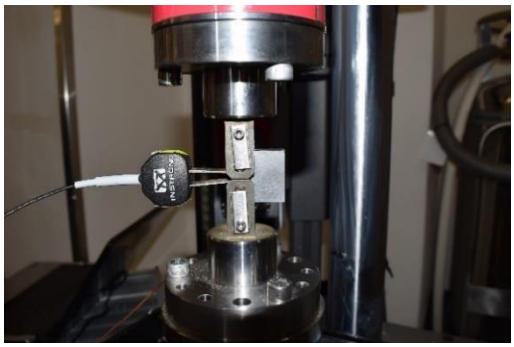

The achieved fracture surfaces of 3D printing samples and control samples made of standard alloy are further examined using a Keyence VHX digital microscope (Figure 3). In addition to Opto-digital microscopy, it is also appropriate to include the possibility of monitoring the fracture structure by electron microscopy as part of further research to investigate the crack area.

Figure 3 Fracture surface of 3D printed AlSi10Mg CT samples

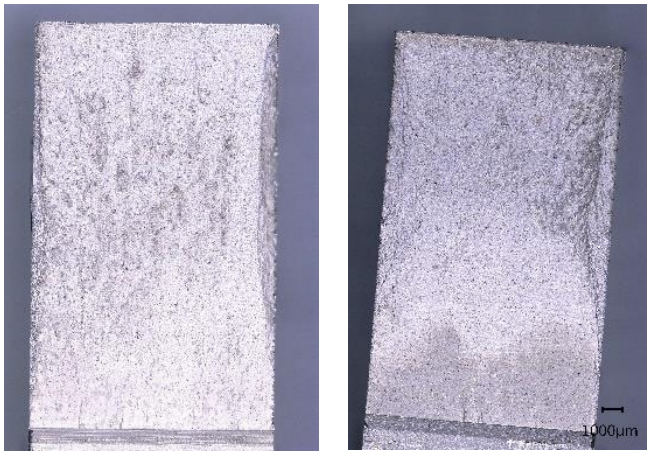

RESULTS AND DISCUSSION

Fatigue behaviour of CT samples

Research into the fatigue properties of CT samples AlSi10Mg is a current topic (Bharath et al. 2021, Lv et al. 2019). Testing on CT samples prepared by 3D printing follows the testing of mechanical properties in tension and torsion of round bars made of the same material also by DMLS published in MendelNet in 2020 in an article entitled Influence of DMLS method topology on mechanical properties of alloy AlSi10Mg.

As part of the research, the fatigue life of the AlSi10Mg alloy was tested, 5 samples for each of three 3D printing topologies were compared (Figure 4), and samples from the AlSi10Mg casting were selected as a reference material.

Figure 4 Topological orientation 1. paralel layers, 2. perpendicular layers, 3. layers at 45°

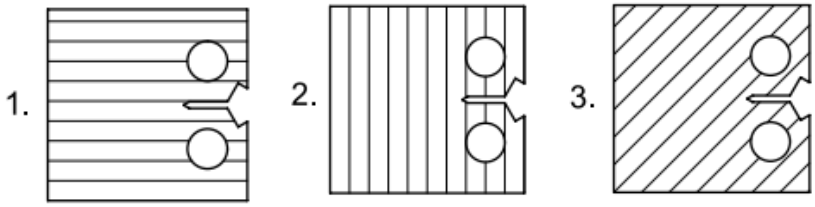

Already during the first results, a clear dependence of fatigue life on the loading speed became apparent. Using the frequency at 10 Hz, which he describes for common aluminum alloys (Matokhnyuk et al. 1988), brittle fracture occurs in the three selected printing topologies even at a low number of cycles, up to 2.5. 10^4 cycles, on the other hand, in the case of samples made of a standard alloy prepared by the gravity casting method loaded with a frequency of 1 to 2 Hz, more than 450,000 cycles have already been achieved when loaded with the same force. This shallow frequency has proved to be more effective in the number of cycles in our research than, for example, frequencies between 5 and 20 Hz, which were used in testing by other authors (Fintová et al. 2020).

Due to the comparability of the results with other authors, we chose a load frequency of 10 Hz, which appeared most frequently in the literature in the search. This frequency corresponded to lower numbers of cycles achieved (Figure 5, 6).

Statistical evaluation shown in Figure 7 proves much better fatigue behaviour of gravity casted parts compared to 3D printed parts. Paralel layers are described as DMLS 0° (Figure 4, topological orientation 1), perpendicular layers stand for DMLS 90° (Figure 4, topological orientation 2), layers at 45° means DMLS 45° (Figure 4, topological orientation31) in the Figure 7.

Figure 5 Fatigue behaviour of casted CT samples – average value

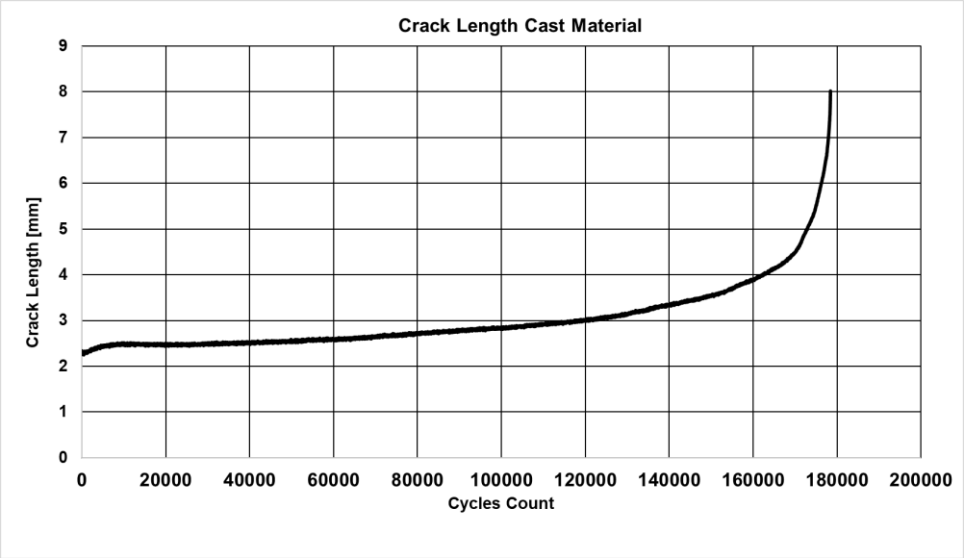

Figure 6 Comparison of fatigue behaviour of average values for three different 3D printing topologies

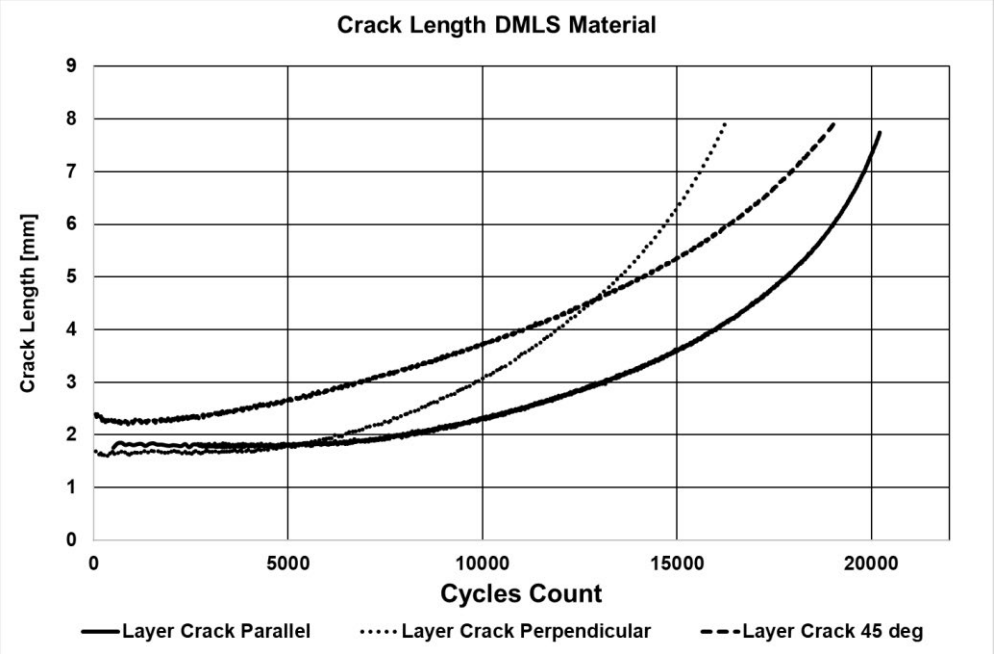

Figure 7 Statistical evaluation of samples

Material topology				
	Cast	DMLS 0°	DMLS 90°	DMLS 45°
Cycles Count to Crack Length 8 mm				
Sample 1	178517	20139	15896	18915
Sample 2	178169	20225	16251	19069
Sample 3	179147	20216	16303	18989
Sample 4	178349	20198	16495	19110
Sample 5	178171	20279	16286	19303
Avg	**178471**	**20211**	**16246**	**19077**
Std dev	362	45	195	131

The influence of surface quality of samples prepared by this method is also the subject of research by other authors (Wang et al. 2019).

Another possible direction of research is the use of the temperature chamber of the Instron Electropuls 10000 machine, enabling testing in the temperature range -100 °C to + 250 °C.

CONCLUSION

From the above results of our research, it is clear that the print topology of the DMLS method has a significant impact on mechanical properties. This knowledge can be used in practice in the preparation of models for additive technologies, with the orientation of printing of components will be chosen concerning the direction of their loading.

In the research of fatigue properties of AlSi10Mg samples, the results are obtained not only by examining the influence of print topology but also by comparison with a standard alloy, which is also tested in test batches and which is made of a material of very similar composition such as metal powder processed into CT sample by DMLS. The results of this and other follow-up research, which start, for example, with the simultaneous use of acoustic emission, will be usable for dimensioning components prepared from this material by the above method.

The fatigue tests performed on CT specimens produced by the DMLS method show brittle fracture behaviour, i.e., fracture without prior plastic deformation, which determines the limitation of their usability in applications requiring good fatigue properties. Simultaneous testing using electromechanical testing on an Instron Electropuls 10000 machine and acoustic emission will be used to investigate further the phenomena that occur just before crack initiation, comparing and detailed analysis of measured changes in the sample material we can detect events preceding crack formation and better predict its origin. As there is a significant influence on the structure of the sample and surface quality, method of ultrasonic examination of the structure of the samples will be used in further research.

From the measured data, the influence of the topology of the 3D printing DMLS material on the crack propagation rate can be judged. However, due to the overall low number of cycles achieved, the material can be considered brittle compared to the cast material. Components made of AlSI10Mg by DMLS are not suitable for cyclically highly stressed components. The orientation can improve the printing parameters when in the case of a perspective-loaded component, the printing layers and thus the horizontal position is oriented as parallel as possible to the direction of the loading force. The advantage of 3D printing technologies is the possibility of any orientation during printing, but sometimes at the cost of increased costs for additional support material in the case of complex shapes. The material in the form of casting shows a significant difference. Isotropic properties are assumed here, but the results for average quality materials may be affected by uneven homogeneity. Nevertheless, the measured data show an approximately ten times higher number of achieved load cycles.

ACKNOWLEDGEMENTS

This research was supported by the College of Polytechnics, Jihlava, Czech Republic, under Grant "Research of parameters for topological optimization of 3D printed components".

REFERENCES

Bharath, C. et al. 2021. Studies on mechanical behaviour of AlSi10Mg alloy produced by selective laser melting and A360 alloy by die casting. Materials Today: Proceedings, 45: 78–81.

Bitonti, F. 2019. 3D printing design: Additive Manufacturing and the Materials Revolutions. 1. ed., London: Bloomsburry Visual Arts.

ČSN EN ISO/ASTM 52907. Aditivní výroba - Vstupní materiály - Metody charakterizace kovových prášků. Praha: ÚNMZ, 2020.

Du Plessis, A., Beretta, S. 2020. Killer notches: The effect of as-built surface roughness on fatigue failure in AlSi10Mg produced by laser powder bed fusion. Additive Manufacturing, 35: 101424.

Dvorakova, J., Dvorak, K. 2021. Topological Optimization of a Component Made by the FDM Method. International Journal of Mechanical Engineering and Robotics Research, 10(2): 67–71.

Fintová, S. et al. 2020, Fatigue behavior of AW7075 aluminum alloy in ultra-high cycle fatigue region. Materials Science and Engineering, 774: 138922.

Lv, F. et al. 2019. Mechanical properties of AlSi10Mg alloy fabricated by laser melting deposition and improvements via heat treatment. Optik, 179: 8–18.

Matokhnyuk, L.E. et al. 1988. Fatigue resistance of aluminum and magnesium alloys at high loading frequencies. Strength of Materials, 20(7): 861–867.

Michna, Š. et al. 2005. Encyklopedie hliníku. 1st ed., Prešov: Adin, s.r.o.

Sedlacek, F., Lasova, V. 2018. Optimization of Additive Manufactured Components Using Topology Optimization. . In Proceedings of International Conference on Theoretical, Applied and Experimental Mechanics Springer, Cham, June 2018, pp. 106–107.

Sigmund, O., Maute, K. 2013. Topology optimization approaches: A comparative review. Structural and Multidisciplinary Optimization, 48(6): 1031–1055.

Wang, P. et al. 2019. Influence of manufacturing geometric defects on the mechanical properties of AlSi10Mg alloy fabricated by selective laser melting. Journal of Alloys and Compounds, 789: 852–859.

Alternative mechanical pre-treatment methods of hot-dip galvanising surface to increase of the organic coatings adhesion

Jaroslav Lozrt, Jiri Votava, Radim Smak
Department of Technology and Automobile Transport
Mendel University in Brno
Zemedelska 1, 613 00 Brno
CZECH REPUBLIC

xlozrt@node.mendelu.cz

Abstract: The content of this contribution is an evaluation of research on various mechanical pre-treatments of inorganic coating, which is part of the so-called duplex system applied to a steel sheet. In order to coating adhesion increase, the hot-dip galvanising surface was first pre-treatment using the standard light blast technology (synthetic brown corundum F40). Furthermore, pre-treatment was also carried out using alternative methods that can be used in conditions without blasting equipment – sandpaper regrinding (P40, P60, P80 and P100) and a corrosion-resistant steel brush (wire diameter 0.30 mm). Tools are designed e.g. for cleaning metal surfaces. Samples without mechanical pre-treatment and samples with blasted surface were used as a standard. The surface texture was evaluated based on the roughness height parameters Ra and Rz (according to ČSN EN ISO 4287 standard). The mechanical resistance of applied anti-corrosion protection was determined by means of a pull-of adhesion test (according to ČSN EN ISO 4624 standard). The experiment suggest results, that among the alternative methods, the use of P80 and P100 sandpapers and corrosion-resistant steel brushes seems to be the most suitable, as these tools are not as aggressive to the galvanised surface as P40 and P60 sandpapers.

Key Words: carbon steel, zinc coating, surface texture, abrasive, sweeping

INTRODUCTION

It is generally accepted that mechanical adhesion is improved by increasing surface roughness, since more active centres (anchorage points) are available. However, highly pronounced roughness can be detrimental as it can lead to local differences in the organic coating adhesion that could promote metals corrosion under the coating layer (Cabanelas et al. 2007, Votava et al. 2018). Thus, there is a critical point with an optimum roughness profile, which is particularly important for galvanized surfaces (Malone 1992). Increasing the surface roughness of galvanized steel can be achieved either naturally (by weathering) or by mechanical and chemical pre-treatment (Cabanelas et al. 2007, Votava et al. 2020). A suitable mechanical surface pre-treatment method for the application of an organic coating is the coarse removal of irregularities and lumps on the zinc coating with a coarse file, followed by a so-called sweeping with a sharp-edged abrasive (can be advantageously used especially for shape complex components – e.g. weldments) or sandpaper regrinding. The sweeping purpose is not only to achieve the desired degree of surface cleanliness, but also the necessary profile for anchoring the organic coating on the smooth zinc coating (Kuklík and Kudláček 2014, Poláková et al. 2018). Both of these factors contribute to increasing the coating adhesion to the substrate. Furthermore, blast pre-treatment also leads to an increase in the fatigue strength of metal surfaces (Hansel 1999). However, too much mechanical pre-treatment destroys and reduces zinc coating thickness or creates too much internal stress, which can later cause coating delamination. The surface pre-treatment should reduce maximum 10 µm of zinc coating (thus suitable for zinc coatings over 30 µm thickness). For this reason, the blasting air pressure should be 0.2–0.3 MPa and the distance of the nozzle end from the material surface should be 250–350 mm. However, the worker experience is also very important. The particle size for blasting galvanised steel should be between 200–500 µm (Hylák and Kudláček 2017). The authors Hylák et al. (2017) then specifically recommend brown corundum (alumina) and corrosion-resistant chromium grit for light blasting of zinc coating.

MATERIAL AND METHODS

The experiment consists of two parts. The first part is focused on the surface roughness analysis (Ra and Rz parameters) and the material removal evaluation (h parameter). The second part deals with the coating adhesion to the galvanized surface. The blasting was carried out with a BlastRazor Z-25. All alternative mechanical pre-treatments were carried out on a vertical cantilever milling machine FA 3 AV. The tools used were brand new. A total of 48 samples in 7 sets were researched. One waterborne paint and one synthetic paint were tested. The basic paint was not applied, as both of these paints are so-called self-etching ("2 in 1"). A commercially available hot-dip galvanized sheet (continuously by the so-called Sendzimir method) based on ferritic-pearlitic steel S235JRG1 was chosen. The zinc coating thickness was 35 ± 3 µm. The zinc coating thickness measurement was carried out using the Elcometer 456 non-destructive electromagnetic method in accordance with the procedure specified in ČSN EN ISO 1461 standard. The samples dimensions were 190 × 65 × 1 mm. For the samples intended for alternative mechanical pre-treatment methods, a bend was made at one end (for clamping in a vice). After surface pre-treatment, the samples length was cut to 160 mm. Table 1 then shows a breakdown of the samples number in each set.

Table 1 Samples No. in each set based on the various criteria

Set No.	Pre-treatment (grain size [µm])	Pressing force [N]	No. of samples		
			Total	Waterborne paint	Synthetic paint
1	-	-	4	2	2
2	F40 (355–500)	-	4	2	2
3	P40 (400–500)	10 ± 2	4	2	2
		40 ± 2	4	2	2
4	P60 (250–315)	10 ± 2	4	2	2
		40 ± 2	4	2	2
5	P80 (125–250)	10 ± 2	4	2	2
		100 ± 2	4	2	2
6	P100 (125–100)	10 ± 2	4	2	2
		100 ± 2	4	2	2
7	Steel brush	10 ± 2	4	2	2
		100 ± 2	4	2	2

The blasting was performed with synthetic brown corundum, the air pressure was 0.25–0.30 MPa and the nozzle distance from the surface was 300–350 mm. The sanding papers grain was always synthetic corundum with open structure, synthetic resin binder, paper substrate and 75 mm die diameter. The sandpapers clamping was done by Velcro. The steel cup brush was made of corrosion-resistant corrugated wire with a 0.30 mm diameter. The brush diameter was 75 mm. The tools clamping to the fixture was realized by means of an M14 nut with a 2.0 mm thread pitch. The jig clamping was carried out using a milling head and a clamp with a 20 mm diameter. The tool vertical movement in the jig and torque transmission was ensured by a 5 × 20 mm groove and a M5 screw. The milling table transverse travel was always 450 mm/min and the tool revolutions were always 45 1/min. The tool pressure on the workpiece was exerted by a steel coiled compression spring. The spring wire diameter was 1.6 mm, outer diameter 12 mm, free length 45 mm, number of coils 11, material EN 10270-1 SH. The spring characteristics were measured on a ZDM 5/51 universal testing machine. The pressing force setting and change was realized by vertical sliding of the milling machine table. The two different pressing forces were chosen for verification in practice (using hand tools). For the P40 and P60 sandpapers, a pressing force of only 40 ± 2 N (instead of 100 ± 2 N) had to be chosen because of the high aggressiveness of these tools (a higher pressing force would have caused the zinc layer to failure to the steel substrate) – forces were determined experimentally, as there is no standard for determining the pressing force to ensure roughness. The tools themselves exerted a force on the sample of approximately 1–2 N. This force is included in the ± 2 N tolerance. A workplace view during sample machining is shown in the Figure 1.

Figure 1 Workplace layouts during sample machining

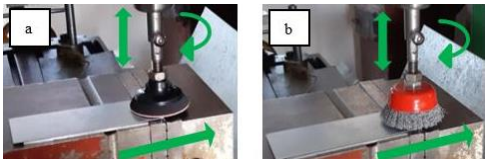

Legend: a – sandpaper; b – steel brush

The surface texture was evaluated based on the roughness height parameters Ra (average arithmetic deviation of the roughness profile under consideration) and Rz (roughness profile maximum height). The measurements were performed using a Mitutoyo SURFTEST SJ-201 mobile profilometer. The roughness profile was filtered according to ČSN EN ISO 4287 standard. Sampling length λc 2.5 mm, number of sampling lengths 5, Gauss filter, evaluation length ln 12.5 mm. The Ra and Rz parameters were measurements always parallel to the direction of workpiece movement during surface pre-treatment (approximately in the longitudinal axis – thus perpendicular to the tool grooves direction) and were carried out 100 times per set. Material removal was also evaluated. The zinc coating thickness was also measured 100 times before and 100 times after pre-treatment in one set. For low pressing forces (around 10 N), the calculation considered the zinc coating plastic deformation above the base material level, which results in the higher probe distance of the measuring instrument from the steel substrate. The material plastic deformation above the base material level (in belt grinding) is described – e.g. by Pandiyan and Tjahjowidodo (2019). Thus, the zinc coating thickness increases artificially and the actual material removal has to be determined by calculation – equation (1). It has then been verified by practical measurements that at higher pressing forces values (above 40 N) there is already a measurable decrease in the zinc coating thickness and the actual material removal needs to be determined by calculation according to equation (2):

$$h = Rz - \Delta t = Rz - (t2 - t1)\ [\mu m] \quad (1)$$

$$h = Rz + \Delta t = Rz + (t1 - t2)\ [\mu m] \quad (2)$$

Legend: h – material removal [μm]; Rz – roughness profile maximum height [μm]; Δt – zinc coating thicknesses difference before and after mechanical pre-treatment [μm]; t2 – zinc coating thickness after mechanical pre-treatment [μm]; t1 – zinc coating thickness before mechanical pre-treatment [μm]

Paints that are commonly available on the Czech market were tested. Instead of the trade name, the individual paints were designated "waterborne paint" and "synthetic paint". The main parameters of paints provided by the manufacturers are given in Table 2.

Table 2 Paints main parameters

Type of paint	Non-volatile solids [weight %]	Specific density [g/cm^3]	Emissions of volatile organic compounds [kg/kg]	$Zn_3(PO_4)_2$ [weight %]
Waterborne	50.0	1.20–1.30	0.03	-
Synthetic	43.0–48.0	1.24–1.35	0.35–0.37	≤ 5.0

The coating was applied by air spraying technology at an ambient temperature of 22 ± 1 °C. The relative humidity was 50–60%. The coating application was always carried out immediately after pre-treatment. The application interval of the individual each layers was at least 24 hours. Three coats were always applied with a tolerance of 20 ± 5 μm, so that the resulting coating thickness was always 60 ± 5 μm in total (tolerance guaranteed by air spraying application by a very experienced worker). The coating thickness was measured after it had completely dried, again using an Elcometer 456 (according to ČSN EN ISO 1461 standard). The measurements were performed 10 times on each sample. Furthermore, the samples were subjected to a pull-off adhesion test (according to ČSN EN ISO 4624 standard) immediately after the paint had completely dried. The standard test cylinder diameter was 20 mm and the two-component glue "Araldite" was used. Tensile stress analysis was carried out using an Elcometer (measuring range 0–7 MPa) – 24 hours after test cylinder gluing. Due to the limited contribution scope was realized only basic testing using by the pull-off adhesion test.

RESULTS AND DISCUSSION

Surface texture

The following graphical representation (Figure 2) shows the Ra, Rz, t1, t2 and h parameters depending on the mechanical pre-treatment and the pressing force. From Figure 2, it can be seen that the lowest average values of Ra and Rz parameters were measured on the surface without mechanical pre-treatment. Therefore, if these measured values are lower than the values optimal for maximum paint adhesion, an increase in paint adhesion to the zinc substrate can be expected (Malone 1992). It is further evident from Figure 2 that the highest average values of the Ra and Rz parameters were measured on the blasted surface. Compared to alternative mechanical pre-treatments, the blasted surface also achieves very high differences for the minimum and maximum values of the Ra and Rz parameters. This can be attributed to the variable blasting conditions. The author Hansel (1999) states that any variation in nozzle

air pressure, nozzle to surface distance or abrasive impact angle will affect the resulting profile. Authors Guzanová et al. (2014) confirm that after brown corundum blasting, the resulting surface is rated as the most dissected. This is confirmed by the values shown in Figure 2. These authors further state that the surface cleanliness is average due to the increased dustiness. From this point of view, alternative mechanical pre-treatments appear to be preferable as they produce a more homogeneous surface, which is desirable for a relatively thin zinc layer (35 ± 3 µm). Authors Cabanelas et al. (2007) reported an increase in the paint adhesion to the galvanised substrate when the Ra parameter value was increased from 0.95 ± 0.19 µm (freshly galvanised surface) to 1.87 ± 0.34 µm (low surface weathering). If Ra was further increased to 5.28 ± 1.28 µm (high surface weathering), no further increase in paint adhesion was observed. Therefore, based on the results of this publication, it can also be predicted that any mechanical pre-treatment will lead to an increase in paint adhesion (compared to a surface without pre-treatment – average Ra = 1.29 µm). At the same time, however, there will no longer be measurable differences between the blasted (average Ra = 4.92 µm) and the alternatively pre-treated surface (average Ra = 1.56–2.45 µm). Correlation of parameters Ra and Rz were not monitored.

Figure 2 Average values of Ra, Rz, t1, t2 and h parameters

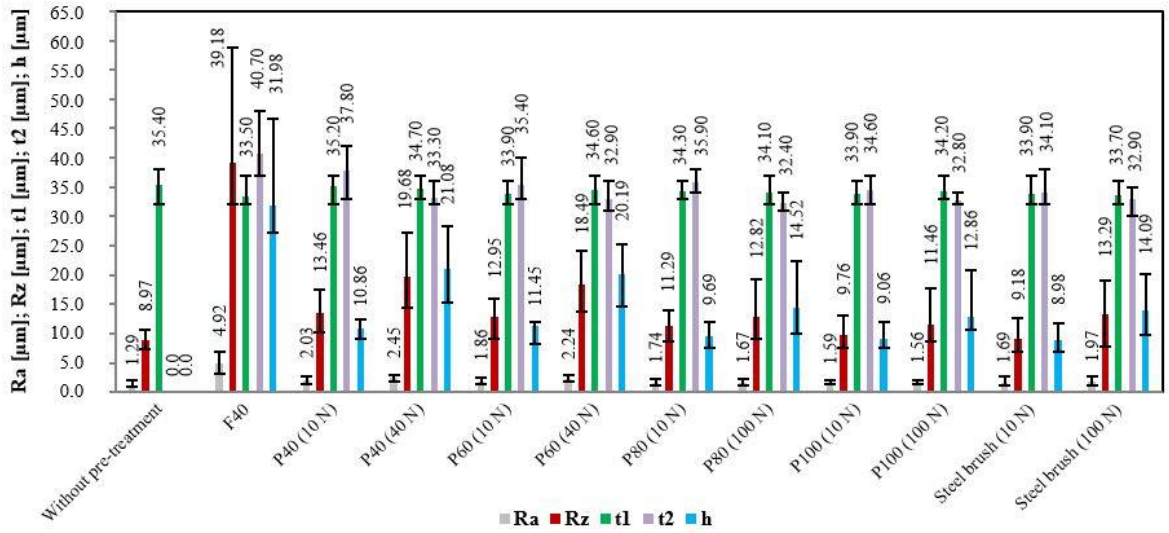

Pull-off adhesion test

The pull-off adhesion test result (Figure 3 and 4) is tensile stress necessary for the failure of the weakest interface (adhesion failure) or the weakest component (cohesion failure) of produced anti-corrosion system. Five measurements were always performed on each sample.

Figure 3 Average values of pull-off adhesion test and comparison with Ra parameter

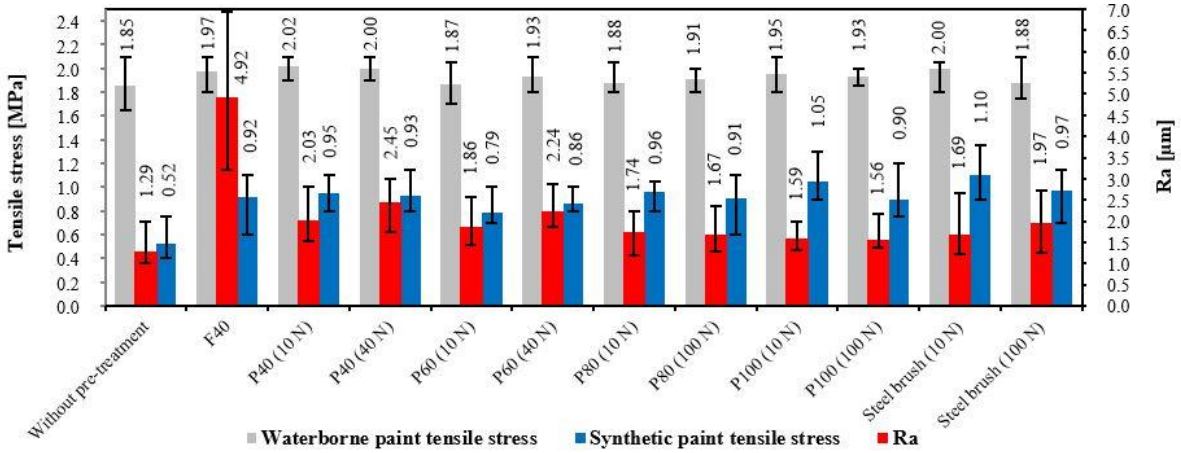

In the case of waterborne paint, only minimal increases in average tensile stress values were observed for the pre-treated surfaces (compared to the surface without pre-treatment). The surface roughness without pre-treatment is therefore sufficient. In the case of this paint, it is also important

to take into account the fact that in the vast majority of cases there is adhesion failure between the coating layers (65–80%). This finding indicates lower strength bonding layers characteristics of the paint (Hylák et al. 2017). For this reason, the implementation of any pre-treatment is also of no benefit (for this particular paint). The adhesion measurement of waterborne paint to hot-dip galvanized substrate (without pre-treatment) was also investigated by Lozrt et al. (2021) and this experiment yielded similar results (average values of 1.66–3.38 MPa). The value of 1.66 MPa was achieved by paint with the same dry matter content and specific gravity. Values of 3.38 MPa can then be justified by the higher dry matter content and specific paint gravity. In the case of synthetic paint, the mechanical pre-treatment benefit has already been statistically demonstrated. Without pre-treatment, average values of 0.52 MPa were achieved, with 90% adhesion failure between the substrate and the first layer. This finding indicates a higher level of adhesion between the paint layers, compared to the paint adhesion to the zinc substrate. The very low measured values clearly indicate incompatibility between the substrate and the paint, as the surface cleaning before paint application was always very thorough. Average values in the range of 0.79–1.10 MPa were then found during surface pre-treatment. In the case of the maximum values (1.10 MPa), adhesive failure between the paint layers (75–80%) was already detected, indicating a higher adhesion degree of paint to the substrate, compared to adhesion between paint layers and also low strength bonding layers characteristics of the paint. This finding therefore clearly confirms the positive benefit of surface pre-treatment. Similar values were also measured by Hylák and Kudláček (2017), who concluded that brown corundum blast pre-treatment increases the paint adhesion to the substrate up to twice as much (1.0 MPa without pre-treatment and 1.5–2.0 MPa with pre-treatment). However, it must be stressed that there are very large differences in the adhesion of different synthetic paints. In fact, the same authors found values in the range of 5.5–9.0 MPa with different paint, and blasting even had a negative effect on the paint adhesion here. These high values can be justified by the very good chemical paint adhesion with the zinc substrate, which leads to the formation of a very high adhesion bridge (Hylák et al. 2017). As expected the higher blasted surface roughness did not result in higher paint adhesion (compared to the alternative pre-treatments).

Figure 4 Examples of the coating failure character (test cylinder diameter 20 mm)

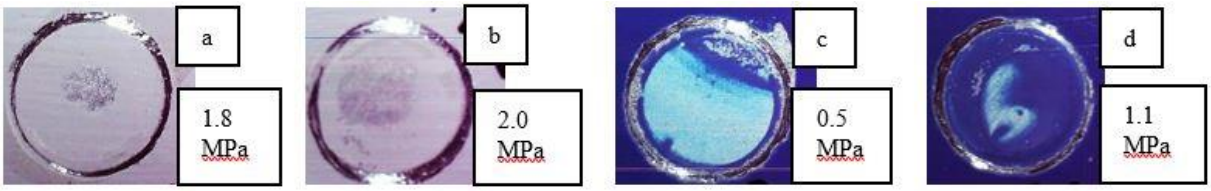

Legend: a – waterborne paint – without pre-treatment; b – waterborne paint – steel brush (10 N); c – synthetic paint – without pre-treatment; d – synthetic paint – steel brush (10 N)

CONCLUSION

In the case of waterborne paint, the mechanical pre-treatment benefit was minimal, as the zinc surface roughness without pre-treatment was near optimal. The pre-treatments use here would also be uneconomical due to the lower strength bonding layers characteristics of the individual paint layers. In this particular case, therefore, only a thorough surface degreasing before the paint application can be clearly recommended. For synthetic paint, mechanical pre-treatment can already be recommended. However, the applied synthetic paint shows low chemical adhesion to the zinc substrate. This may be due to the application of a self-etching paint ("2 in 1"). Among the alternative methods, the use of P80 and P100 sandpapers and corrosion-resistant steel brushes seems to be the most appropriate, as these tools are not as aggressive to the galvanised surface as P40 and P60 sandpapers. This fact is clearly confirmed by the measured material removal rates, e.g., P40 sandpapers achieve an average removal rate of 10.86 µm (10 N) to 21.08 µm (40 N) – thus, a fourfold increase in the pressing force results in an approximate doubling of the material removal rate. In contrast, P100 sandpapers, e.g., achieve an average removal rate of 9.06 µm (10 N) to 12.86 µm (100 N) – a tenfold increase in pressing force results in only a minimal average increase in material removal. This finding is crucial as it confirms the suitability of this technology for application in engineering practice.

ACKNOWLEDGEMENTS
The research was financially supported by the Internal Grant Agency of Mendel University in Brno, Faculty of AgriSciences. Grant project No. AF-IGA2021-IP043.

REFERENCES

Cabanelas, I. et al. 2007. Influence of galvanised surface state on the duplex systems behaviour. Corrosion Science [Online], 49(4): 1816–1832. Available at: https://www.sciencedirect.com/science/article/pii/S0010938X06003337?via%3Dihub. [2021-06-11].

Guzanová, A. et al. 2014. A study of the effect of surface pre-treatment on the adhesion of coatings. Journal of Adhesion Science and Technology [Online], 28(17): 1754–1771. Available at: https://www.tandfonline.com/doi/full/10.1080/01694243.2014.920762?scroll=top&needAccess=true. [2021-06-30].

Hansel, D. 1999. Abrasive blasting systems. Metal Finishing, 97(5): 29–55.

Hylák, K., Kudláček, J. 2017. Lehké tryskání (sweeping) žárově zinkovaného povrchu pro aplikaci nátěrových hmot. In Proceedings of Konference Studentské Tvůrčí Činnosti [Online]. Praha, Czech Republic, 20 April, Praha: Czech Technical University in Prague, Faculty of Mechanical Engineering, pp. 1–4. Available at: https://stc.fs.cvut.cz/history/2017/sbornik/papers/pdf/6595.pdf?_=1491775116. [2021-06-11].

Hylák, K. et al. 2017. Mechanické předúpravy zinkových povrchů a porovnání nátěrových hmot pro duplexní systém. In Proceedings of X. Konference Pigmenty a Pojiva [Online]. Seč, Czech Republic, 6–7 November, Pardubice: University of Pardubice, Faculty of Chemical Technology, pp. 144–148. Available at: https://docplayer.cz/90729925-Sbornik-x-konference-pigmenty-a-pojiva.html. [2021-06-14].

Kuklík, V., Kudláček, J. 2014. Žárové zinkování. 1. ed., Praha: Asociace českých a slovenských zinkoven.

Lozrt, J. et al. 2021. Duplex Anti-Corrosion Protection of Steel Using a Combination of Hot-Dip Galvanising and Water-Soluble Paints. Acta Technologica Agriculturae: The Scientific Journal for Agricultural Engineering [Online], 24(3): 129–135. Available at: https://www.sciendo.com/article/10.2478/ata-2021-0022. [2021-09-08].

Malone, J.F. 1992. Painting hot dip galvanized steel. Materials Performance, 31(5): 39–42.

Pandiyan, V., Tjahjowidodo, T. 2019. Use of Acoustic Emissions to detect change in contact mechanisms caused by tool wear in abrasive belt grinding process. Wear [Online], 436–437(1): 1–12. Available at: https://www.sciencedirect.com/science/article/pii/S0043164819305848?via%3Dihub. [2021-06-21].

Poláková, N. et al. 2018. TIG welding of stainless steel and titanium with additive AG 104. In Proceedings of International PhD Students Conference MendelNet 2018 [Online]. Brno, Czech Republic, 7–8 November, Brno: Mendel University in Brno, Faculty of AgriSciences, pp. 468–471. Available at: https://mnet.mendelu.cz/mendelnet2018/mnet_2018_full.pdf. [2021-09-08].

ÚNMZ. 1999. Geometrické požadavky na výrobky (GPS) – Struktura povrchu: Profilová metoda – Termíny, definice a parametry struktury povrchu. ČSN EN ISO 4287 (01 4450). Praha: Úřad pro technickou normalizaci, metrologii a státní zkušebnictví.

ÚNMZ. 2010. Zinkové povlaky nanášené žárově ponorem na ocelové a litinové výrobky – Specifikace a zkušební metody. ČSN EN ISO 1461 (03 8558). Praha: Úřad pro technickou normalizaci, metrologii a státní zkušebnictví.

ÚNMZ. 2016. Nátěrové hmoty – odtrhová zkouška přilnavosti. ČSN EN ISO 4624 (67 3077). Praha: Úřad pro technickou normalizaci, metrologii a státní zkušebnictví.

Votava, J. et al. 2018. Anti-corrosion systems in vehicles for the transportation and application of fertilizers. Metallic Materials [Online], 56(2): 131–136. Available at: https://doi.org/10.4149/km_2018_2_131. [2021-09-08].

Votava, J. et al. 2020. Change of Mechanical Properties of Zinc Coatings after Heat Treatment. Acta Technologica Agriculturae: The Scientific Journal for Agricultural Engineering [Online], 23(1): 7–11. Available at: https://www.sciendo.com/article/10.2478/ata-2020-0002. [2021-09-08].

Comparison of stress action of real specimens and computer model during tensile testing

Jakub Pernica[1], Michal Sustr[1], Petr Dostal[1], Matej Vodak[1], Robert Sarocky[1], Martin Brabec[2], Jaroslav Zacal[3]
[1]Department of Technology and Automobile Transport
[2]Department of Wood Science
[3]Department of Furniture, Design and Habitat
Mendel University in Brno
Zemedelska 1, 613 00 Brno
CZECH REPUBLIC

xpernic2@mendelu.cz

Abstract: The contribution focuses on the comparison of stresses in the specimen during tensile testing. The specimens were fabricated in two orientations in the printing area of a 3D printer. Digital Image Correlation method was used to measure the stress. The results were graphically evaluated and compared with each other. The graphical result of Digital Image Correlation was further compared with the computer analysis of stress action in the specimen in Autodesk Fusion 360. This comparison is very useful for realistic designing of 3D models for 3D printing of polymer materials by Fused Filament Fabrication (FFF) technology.

Key Words: additive manufacturing, tensile testing, digital image correlation, mechanical properties, ASTM D638

INTRODUCTION

Additive manufacturing is an innovative manufacturing technology that enables a different approach in the design process of parts and structures. Additive manufacturing is a very broad term. In engineering practice, a variety of additive manufacturing and material processing technologies are used, for example, polymer materials, metals, or building materials. This contribution focuses on Fused Filament Fabrication (FFF) additive manufacturing technology and the production of polymeric materials. This technology is one of the most affordable and widespread options for 3D printing, with the ability to produce fully functional parts (Hausman and Horne 2014).

The principle of FFF additive manufacturing technology is to melt a printing string, which is most often 1.75 mm in diameter. The string enters an extruder where it is heated to printing temperature and then extruded onto the bed of a 3D printer (Kloski and Kloski 2017).

The principle of the digital image correlation method is based on the principle of optical sensing. A contrasting colour is applied to the surface to be measured and a so-called pattern is superimposed. The measuring set-up usually consists of a pair of cameras, light sources and software for the evaluation of the measured data. The method is based on the principle of pattern recognition, which gradually changes its position due to the loading forces acting on the surface to be measured. Subsequent evaluation of the measurements is performed using algorithms that correlate the acquired images with a reference image. This is a very accurate and efficient method for measuring surface deformations. The method can be applied to a wide range of engineering materials and applications (Šebek et al. 2021).

The suitability of the comparison of the digital image correlation method with the finite element method was performed by Šebek et al. (2021) in the experiment Orthotropic elastic-plastic-damage model of beech wood based on split Hopkinson pressure and tensile bar experiments. In the paper, they present results comparing digital image correlation with FEM computational simulations for specimens that also exhibited anisotropic mechanical properties. Anisotropic Properties of Samples Produced by FFF Technology (FDM) Determination and Comparison of the Anisotropic Strengths of Fused Deposition Modeling P400 ABS. Fused Filament Fabrication technology is fundamentally the same as Fused Deposition Modeling technology. (Šebek et al. 2021, Wimpenny et al. 2017)

MATERIAL AND METHODS

Manufacture of samples for tensile testing

Before the additive manufacturing of the samples, heat towers were created. These are used to define the optimum nozzle temperature for 3D printing. The bore of each filament indicates the range of recommended production temperatures. Heat towers were created starting from the highest recommended nozzle temperature raised by 5 °C. The nozzle temperature was gradually reduced in 5 °C increments to the lowest recommended temperature reduced by 5 °C.

The additive manufacturing of the samples was performed in accordance with ASTM D638. A parametric 3D model was created using Autodesk Fusion 360 Education License software. The parametric 3D model was exported to .stl format. This was subsequently imported into the slicer software PrusaSlicer 2.3.0 where all manufacturing parameters were defined. For the possibility of defining the tensile strength, 100% specimen infill was chosen. The layer height was defined to be 0.2 mm and the nozzle diameter was 0.4 mm. For the ABS material, a nozzle temperature of 255 °C and a bed temperature of 110 °C were defined depending on the results of the heat towers.

The set of samples for the tensile test contains 10 samples in two sets, which differ in their position in the 3D printer print area. Five samples were oriented in the print space in the XY plane and five samples in the YZ plane.

Digital Image Correlation

For Digital Image Correlation (Figure 1), white color was applied to the selected samples in a first step. This forms the basis for applying the contrast colour. In the second step, the contrast paint was applied to the selected samples to create the so-called patterning. The patter is important for the optical sensing of the course of the applied tensile force. The instrumentation for the digital image correlation measurements consisted of a pair of AVT Stingray Cooper F-504 B CCD cameras with a transverse light-sensitive cell size of 3.45 µm and a resolution of 5 MPx. Pentax C2514-M lenses with a focal length of 25 mm were installed on the cameras. To enhance the contrast of the patterning deposited on the samples, the measurement area of the samples was supplemented with two Sobriety Cube 360 cold light sources with Luminus CSM-360 LED chips. This setup was placed next to the universal tensile machine where the tensile force loading of the samples took place. During the measurements, images were automatically recorded at a frequency of 4 Hz. Subsequent evaluation of the measured data was performed in Vic-3D version 2010. Specimens were tested using the standard ASTM D638 procedure of uniaxial tensile loading at a loading rate of 5 mm/min.

Figure 1 Measurement of samples

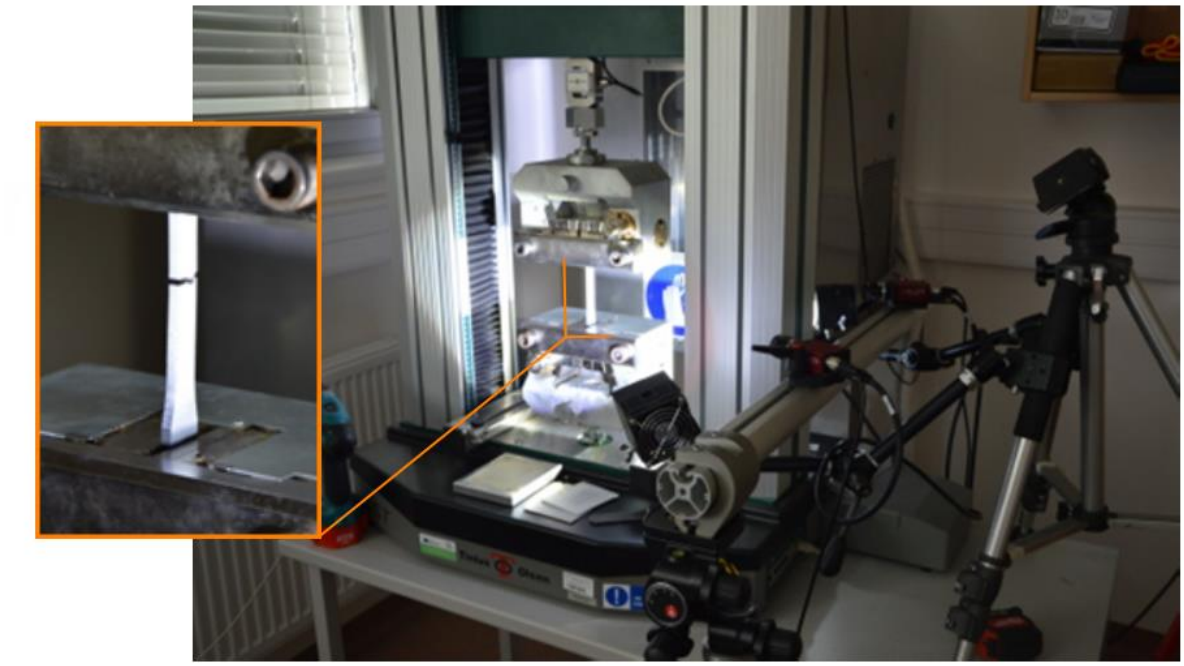

RESULTS AND DISCUSSION

Tensile strength of tested samples

The measurements confirmed the significant anisotropic properties of the tested samples. A significant decrease in tensile strength was found for the tested samples. The tensile strength was found to be 31.18 ± 1.09 MPa for the specimens oriented in XY plane. For the specimens oriented in the 3D printer space in the YZ plane, the tensile strength was found to be 16.15 ± 2.3 MPa. Thus, this is a significant decrease in the ultimate strength, which is 46.79%. The computer simulation in Autodesk Fusion 360 software evaluated the tensile strength at 19.07 MPa. The material data was applied to the Autodesk Fusion 360 plastic ABS material library. The tensile test simulation was performed at a loading force at which the safety factor was defined to be 1.

Tensile diagram

The tensile diagram corresponds to the observed values in Table 1 Results of tensile test. An interesting comparison is in the area of maximum stress. Specimens produced in the XY position show a standard pattern as conventionally machined polymeric materials (Figure 2). Similar tensile strength results were found in the laboratory of L.K. Engineering (L.K. Engineering s.r.o.). The y-axis expresses the tensile stress and the x-axis defines the elongation.

Table 1 Results of tensile test

Material	Number of samples	Plane	Tensile trength	Standard deviation	Decrease in strength limit XY -> YZ plane
			[MPa]	[MPa]	[%]
ABS	A11-A15	XY	31.18	1.09	-46.79
	A26-A30	YZ	16.59	2.30	

Figure 2 Tensile diagram – samples 3D printed XY plane

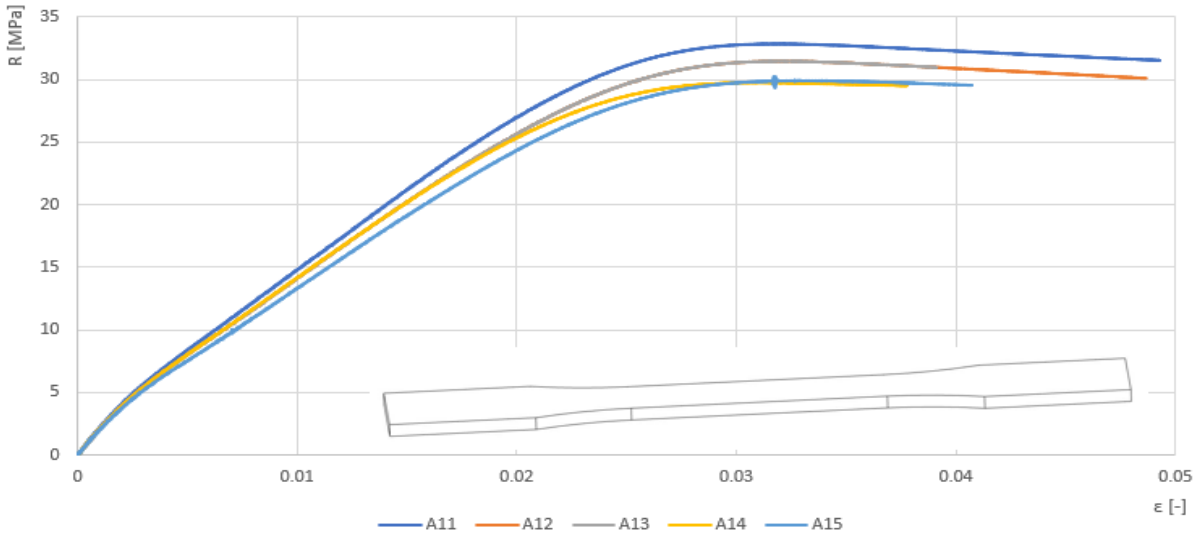

The tensile diagram for specimens that were fabricated in the YZ position (Figure 3) show a sharp fracture in the tensile strength region. In the context of the very low value of the elongation ratio, this set of specimens appears to be very brittle. The relative elongation is the ratio of the difference between the length of the specimen after breaking l and the initial length of the specimen l_0 to the initial length of the specimen l_0.

Majid et al. (2020) report a tensile strength of 35.7 MPa in their publication Mechanical behaviour and crack propagation of ABS 3D printed specimens. The publication also addresses the effect of density of infill patterns in relation to strength parameters. His results show that the higher the infill percentage, the higher the strength limits of the specimen. He presents a comparison of specimens with infill of 20%, 40%, 60% and 100% in the results graph (Majid et al. 2020).

Figure 3 Tensile diagram – samples 3D printed YZ plane

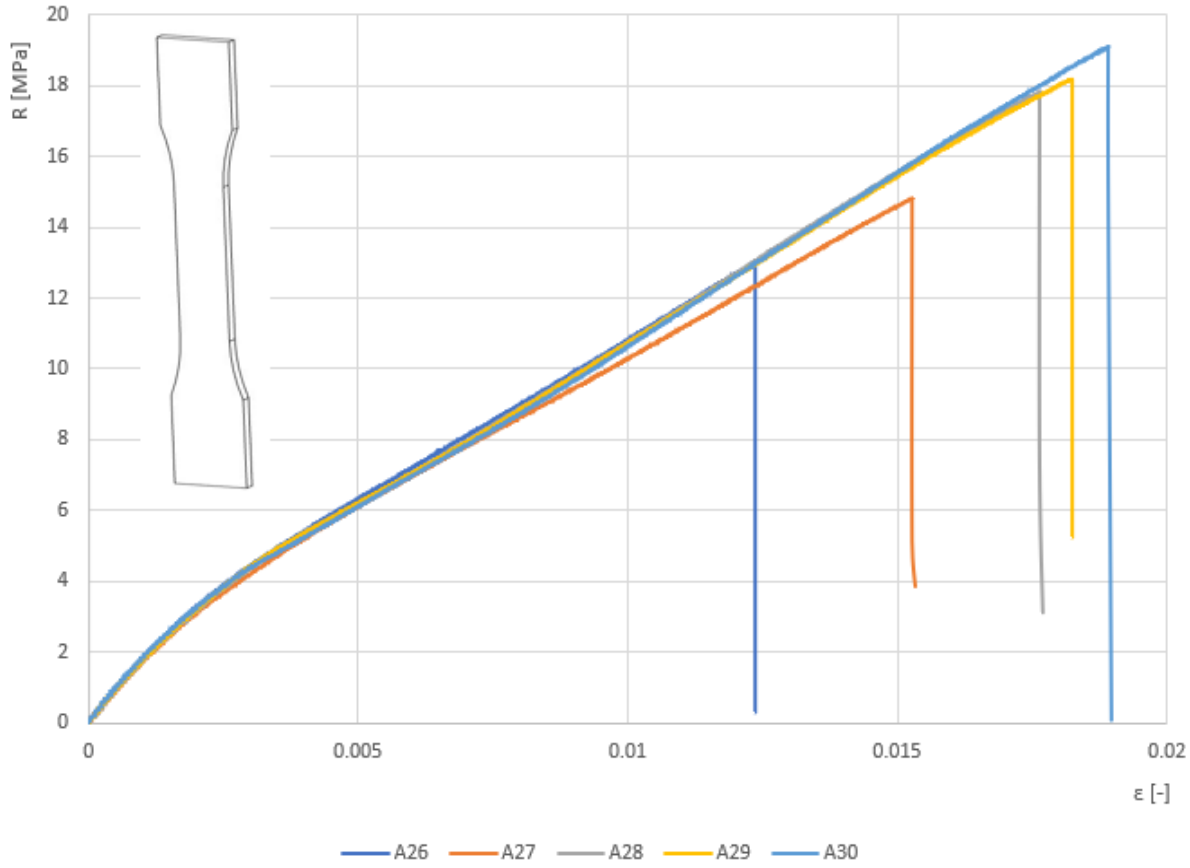

Digital Image Correlation

Digital Image Correlation yielded very interesting results. In the ABS XY sample, (Figure 4) the stress is concentrated in the middle of the sample. In addition to the stress concentration, it can be observed that the stress is transmitted along the print grid of each layer ±45°. This shows that the stress in the sample during tensile testing is transmitted along the filaments, which is characteristic of the additive manufacturing technology of Fused Filament Fabrication. In contrast, the effect of the different orientation of the sample in the 3D printer space is evident for the ABS YZ sample. Digital Image Correlation showed that the tensile test stress is transmitted through the monolayers, which are characteristic of additive manufacturing by Fused Filament Fabrication technology.

Clear differences are evident in the comparison of the tested samples with the computer simulation. From (Figure 4), it is clear that the computer simulation failed to clearly define the break point of the sample. The maximum stress and potential rupture location is shown throughout the tapered central portion of the specimen.

The publication Optimising Process Parameters of Fused Filament Fabrication to Achieve Optimum Tensile Strength verifies that computer simulation strength analysis for use in additive manufacturing Fused Filament Fabrication is a very specific and challenging area. A large number of variable factors enter into real products that can negatively affect the mechanical properties of a particular component (Weake et al. 2020).

Using FEM calculations in Autodesk Fusion 360 software for additive manufacturing applications Fused Filament Fabrication technology has its own specifics. As can be seen by comparing the digital image correlation results for real samples and the FEM calculation, the calculation model does not account for the effect of the lay-up structure that is typical in additive manufacturing (Figure 4). Therefore, the FEM calculation cannot predict the potential crack initiation location. When using the materials library, which is a supplement to Autodesk Fusion 360 software, it is also problematic to optimize the design due to the anisotropic mechanical properties that are due to additive manufacturing technology.

Figure 4 Graphical comparison of samples

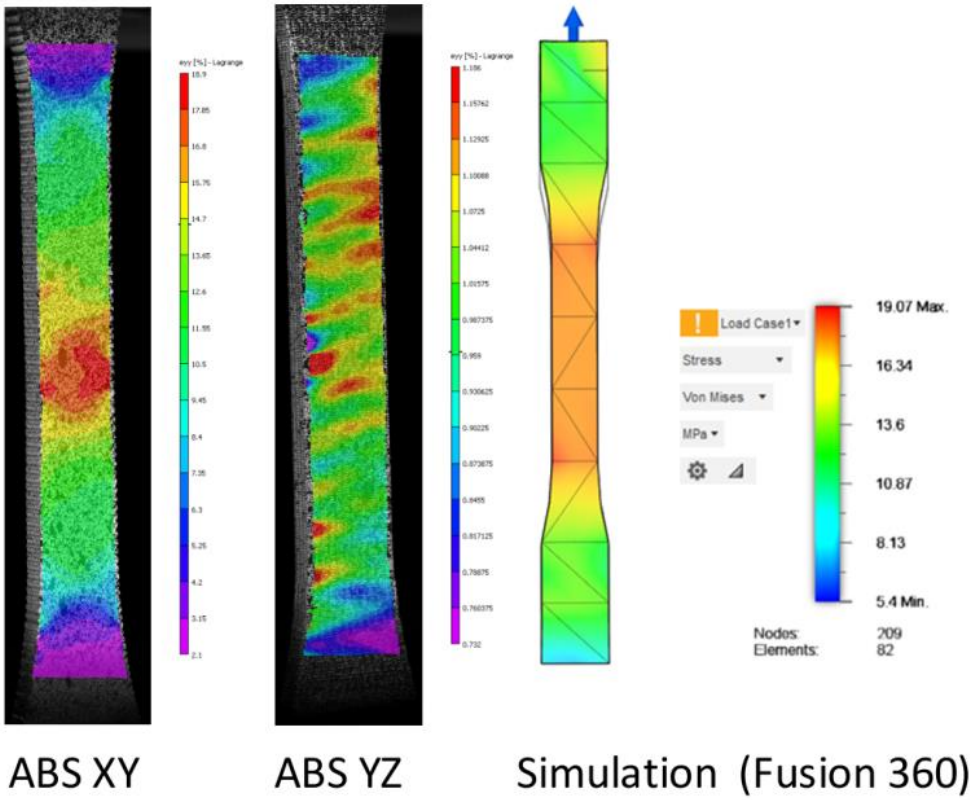

Comparison of measured data

The t-test (t-test for independent samples) was used to determine if there was a statistically significant difference between the sample groups tested. Tensile strengths for groups of specimens printed in the XY and YZ directions were compared. The test results confirmed a significant statistical difference. The calculated p-value is less than 0.001.

Box plot (Figure 5) confirmed the significant anisotropic mechanical properties of the tested samples. Specimens printed in the XY direction were found to have a higher tensile strength than specimens printed in the YZ direction.

Figure 5 Box plot – measured data

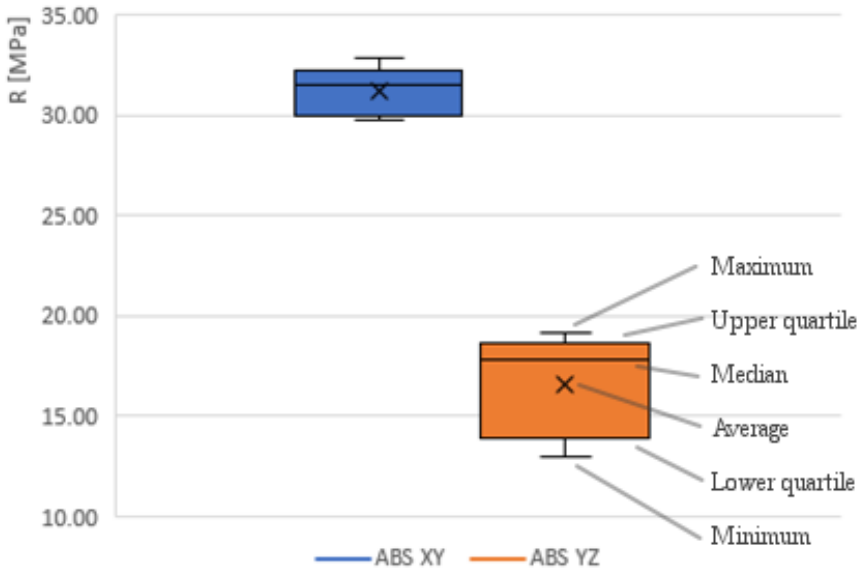

CONCLUSION

Additive manufacturing is presented as part of Industry 4.0. It is therefore evident that it is important to focus on the material and mechanical properties of the technical materials used in AM (Devezas et al. 2017).

Material properties are a very important part in the development of new products. Thanks to computational methods, it is possible to define important parameters of a product before the production and testing phase of a prototype (Shigley et al. 2010).

Comparison of computer simulation of specimen loading during tensile testing with Digital Image Correlation used during tensile testing of additive manufactured specimens showed different stress concentration regions during tensile testing. Therefore, the computer simulation can only be used for simplified analysis because the resulting concentrations may different from the actual products produced by 3D printing with Fused Filament Fabrication technology.

ACKNOWLEDGEMENTS

The research has been supported by the project TACR GAMA, Proof of Concept 2, TP01010018.

REFERENCES

ASTM. 2010. Standard test methods for tensile properties of plastics. ASTM D638. West Conshohocken: ASTM International.

Devezas, T. et al. 2017. Studies on Entrepreneurship, Structural Change and Industrial Dynamics. 1. ed., Cham: Springer International Publishing AG.

Hausman, K., Horne, R. 2014. 3D printing for dummies. 2. ed., New Jersey: John Wiley & Sons, Inc.

Kloski, W.L., Kloski, N. 2017. Začínáme s 3D tiskem. 1. ed., Brno: Computer Press.

L.K. Engineering s.r.o. ©2021. Mechanické vlastnosti materiálů pro 3D tisk. [Online]. Available at: https://www.lke.cz/cz/mechanicke-vlastnosti-materialu-pro-3d-tisk. [2021-09-05].

Majid, F. et al. 2020. Mechanical behavior and crack propagation of ABS 3D printed specimens. Procedia Structural Integrity [Online], 28(1): 1719–1726. Available at: https://www.sciencedirect.com/science/article/pii/S2452321620306491. [2021-10-04].

Shigley, J.E. et al. 2010. Konstruování strojních součástí. 1. ed., Brno: Vutium.

Šebek, F. et al. 2021. Orthotropic elastic–plastic–damage model of beech wood based on split Hopkinson pressure and tensile bar experiments. Impact Engineering [Online], 157: 1–13 Available at: https://www.sciencedirect.com/science/article/pii/S0734743X21001627. [2021-09-10].

Weake, N. et al. 2020. Optimising Process Parameters of Fused Filament Fabrication to Achieve Optimum Tensile Strength. Procedia Manufacturing [Online], 51: 704–709. Available at: https://www.sciencedirect.com/science/article/pii/S2351978920319569. [2021-09-10].

Wimpenny, D.I. et al. 2017. Advances in 3D Printing & Additive Manufacturing Technologies. 1. ed., Singapore: Springer Science+Business Media Singapore Pte Ltd.

Hyperspectral imaging LED and incandescent light source comparison for food quality inspection

Robert Rous[1], Vit Ondrousek[1], Miroslav Juzl[2]
[1]Department of Informatics
[2]Department of Food Technology
Mendel University in Brno
Zemedelska 1, 613 00 Brno
CZECH REPUBLIC

robert.rous@mendelu.cz

Abstract: Incandescent light sources are typical lighting types for Vis-NIR hyperspectral imaging. New broadband LED-based lights start to appear as a possible substitute for incandescent light sources due to the development of new LED dye types. Two light sources (Tungsten-halogen lamp and hyperspectral LED Effilux EFFI-Flex-HSI-100-SD-P2) for the Vis-NIR (400–1000 nm) hyperspectral imaging were compared on 15 samples of Gothajsky cooked salami slices. The goal was to compare these two light source technologies (old incandescent and new LED-based) in the matter of image quality. Images were scored using no-reference quality metrics (BRISQUE, NIQE, PIQE). There was a strong correlation between the mean values of the scoring metrics (BRISQUE R=0.9245, NIQE R=0.8933, PIQE R=0.9779). Results show the main advantage of the LED light is no heat stress of the samples resulting in more stable results with less glare. The main disadvantage of LED light was a lower illumination power resulting in higher exposition time needed.

Key Words: hyperspectral LED light, food quality analysis, Image Quality Assessment, machine vision

INTRODUCTION

Optical-based techniques, in general, have become more predominant for the inspection and process control of the food industry and agricultural products in a non-destructive manner in recent decades. Vis-NIR hyperspectral imaging (HSI) can extend the possibilities of the image analysis from evaluation of basic physical attributes, such as size, shape, and colour to predict the composition of sensed material and use the methods of chemometrics.

Hyperspectral cameras can sense in a wider spectral range than RGB cameras thus the light used for illuminating the scene has to contain all the frequency components the CCD sensor can measure. The usual light source used in HSI in recent years is an incandescent tungsten-halogen lamp (Özdoğan et al. 2021). This light source has bandwidth suitable for Vis-NIR HSI up to 1000 nm (Zahavi et al. 2019) but there is also a big disadvantage in the excessive heat the incandescent light source emits. This can be solved by using an LED light source but up until recent years, LED technology able to emit light in a range similar to incandescent sources was not available. Historic solutions to this problem were to use multiple LEDs for different wavelengths to piece together the spectrum similar to incandescent light. (Islam et al. 2017). Mo used this technique for a quality evaluation of pepper seeds (Mo et al. 2014). This has changed by Phosphor-converted white light-emitting diodes (pc-WLED) with CRI ≥ 95 and a broad light spectrum (Ahn et al. 2019).

This paper aims to compare a new type of hyperspectral light source (hyperspectral LED) to the incandescent light source in the meaning of image quality using different metrics. The comparison is presented on the real use case imaging cooked salami slices.

MATERIAL AND METHODS

Experiment setup

All the imaging was performed on a custom-made imaging stand pictured in Figure 1. The device consists of a line-scan hyperspectral camera with a 16 mm Edmund optics lens with adjustable focus and adjustable f-stop. Camera specifications are shown in Table 1.

Table 1 Hyperspectral camera specifications

	Photonfocus MV1-D2048x1088-HS05-96-G2
Type	hyperspectral line-scan
Resolution	2048×1088; 5 pix line-height
Spectral range	158 bands 480–920 nm

Figure 1 Imaging stand

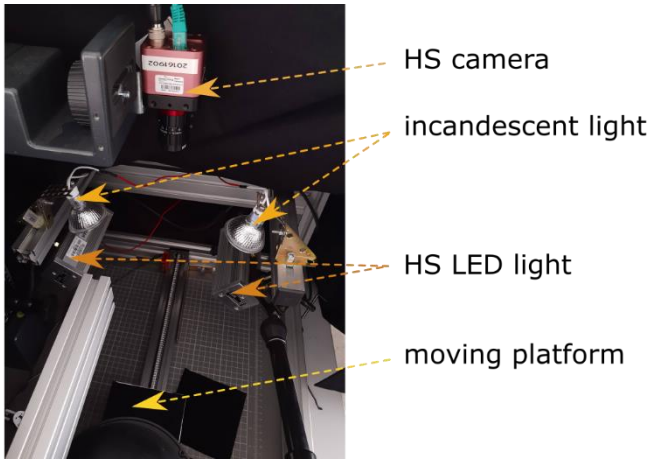

Each of the samples was imaged using the LED light and immediately after that with an incandescent light source. This order was chosen to reduce the heat stress of the samples possibly caused by the opposite order of measurement. Each sample travelled under the line-scan camera for 60 seconds to complete the imaging.

Hyperspectral camera calibration and operating conditions

The Hyperspectral imaging system was calibrated with a reflectance calibration standard before imaging according to a procedure recommended by the manufacturer. Best results were achieved by setting the exposure time set to 9.4 ms for LED light and 0.7 ms for incandescent light. The f-stop was set to 2.0 for both light sources. The imaging scene was illuminated by two types of light sources. The first consisted of two 50 W incandescent halogen spotlights (Sylvania Coolfit 50) at a 45º angle. The second illumination light was Effilux EFFI-Flex-HSI-100-SD-P2 at a 45º angle. The emission angle of the LED light was set to 10º. The temperature of the CCD chip was kept in the range from 39.0 °C to 41.0 °C according to the internal sensor by an external fan. The ambient temperature was 23 °C.

All the raw binary HSI data from the camera were processed by Photonfocus proprietary PFHySpec SDK (Photonfocus 2021) that stitches line-scan images into a resulting ENVI format hypercube.

Measured samples

In the forefront of interest were slices of a Czech cooked sausage Gothajský salám (Gothajsky salami) (Jůzl et al. 2019) prepared according to a Czech state norm recipe (ÚNMZ 1977) in laboratories of the Department of Food Technology at Mendel University in Brno. The salami was cut to slices 1.0 mm thick with an electric rotary blade slicer and cooled down to 4.0 °C before

imaging. The total number of imaged samples was 15. The diameter of each of the salami slices was 80.0 mm which is a standard size of a salami casing.

Image quality metrics

Image Quality Assessment (IQA) algorithms take an arbitrary image as an input and output a quality score. Three metrics were selected to evaluate the variance in images obtained using different light sources. All the data were processed in Matlab 2020b. All of these methods are no-reference quality metrics and thus there was no need for a reference control image. The background surrounding the salami slices was masked out with value 0 as a first step before scoring.

A) BRISQUE – Blind/Referenceless Image Spatial Quality Evaluator is a statistic-based distortion-generic IQA model that operates in the spatial domain. The algorithm only quantifies the "naturalness" (or lack thereof) in the image due to the presence of distortions (Mittal et al. 2012). Matlab implementation (*brisque()*) of this algorithm was chosen to score the images (with default model). The score Is in the range of 0 to 100 while the lower the value the better the quality of the image is.

B) NIQE – Natural Image Quality Evaluator is based on the construction of a 'quality aware' collection of statistical features based on a simple and successful space domain natural scene statistic (NSS) model (Mittal et al. 2013). Matlab implementation (*niqe()*) of this algorithm was chosen to score the images (with default model). The lower the value the better the quality of the image is.

C) PIQE – Perception-based Image Quality Evaluator relies on extracting local features for predicting quality. It estimates quality only from perceptually significant spatial regions and enables us to generate a fine-grained block-level distortion map used to score images (Venkatanath et al. 2015). Matlab implementation (*piqe()*) of this algorithm was chosen to score the images (with default model). The score Is in the range of 0 to 100 while the lower the value the better the quality of the image is.

These methods were used to score each band of the hypercube resulting in 158 values for each method in every image.

RESULTS AND DISCUSSION

Comparison of image quality metrics results

Table 2 shows the results of image quality scoring for both light sources. The standard deviation for every method is lower in every case the LED light source was used. The mean value of each of the method scores is lower (better quality) in the case of BRISQUE and higher in the case of NIQE and PIQE.

Table 2 Results for metrics

Method	Light source	Std. dev. minimum	Std. dev. maximum	Std. dev. mean	Std. dev. median	Score mean value
BRISQUE	incandescent	0.0693	3.9731	1.4992	1.4166	39.3417
BRISQUE	LED	0.0489	2.4457	1.2336	1.2532	38.8361
NIQE	incandescent	0.4071	0.7554	0.5352	0.5580	9.1174
NIQE	LED	0.2799	0.6205	0.4666	0.4651	9.4949
PIQE	incandescent	0.6124	4.1428	2.6111	2.6401	56.6812
PIQE	LED	0.2039	2.2252	1.3452	1.3115	58.3108

Figure 2 shows the mean value of each method for every frequency band and a shaded area representing standard deviation. Correlation between mean values of scores for different light sources is strong for every method. The highest correlation was for the PIQE method (R=0.9779), the second was BRISQUE (R=0.9245) and the third NIQE (R=0.8933).

Figure 3 shows images for two specific wavelengths (596.59 nm and 724.84 nm). These wavelengths were selected based on the BRISQUE method results. The first one (596.59 nm) corresponds to the largest difference between the mean values of the scoring for both lights in the BRISQUE data. The second one corresponds to a maximal standard deviation of incandescent light in the area around 730 nm where the score for both light sources is high (bad quality). The sample in Figure 3 was selected randomly from the whole set.

There is a glare on the top of the slice surface caused by melted fat due to heat stress. This is visible in the left part of the image for both wavelengths. The glare is also present in the image taken with an LED light source but in that amount as with the other light source in direct comparison. The left part of the image also shows the lighting was not even and there was a brighter part of the image.

Figure 2 Results for different methods

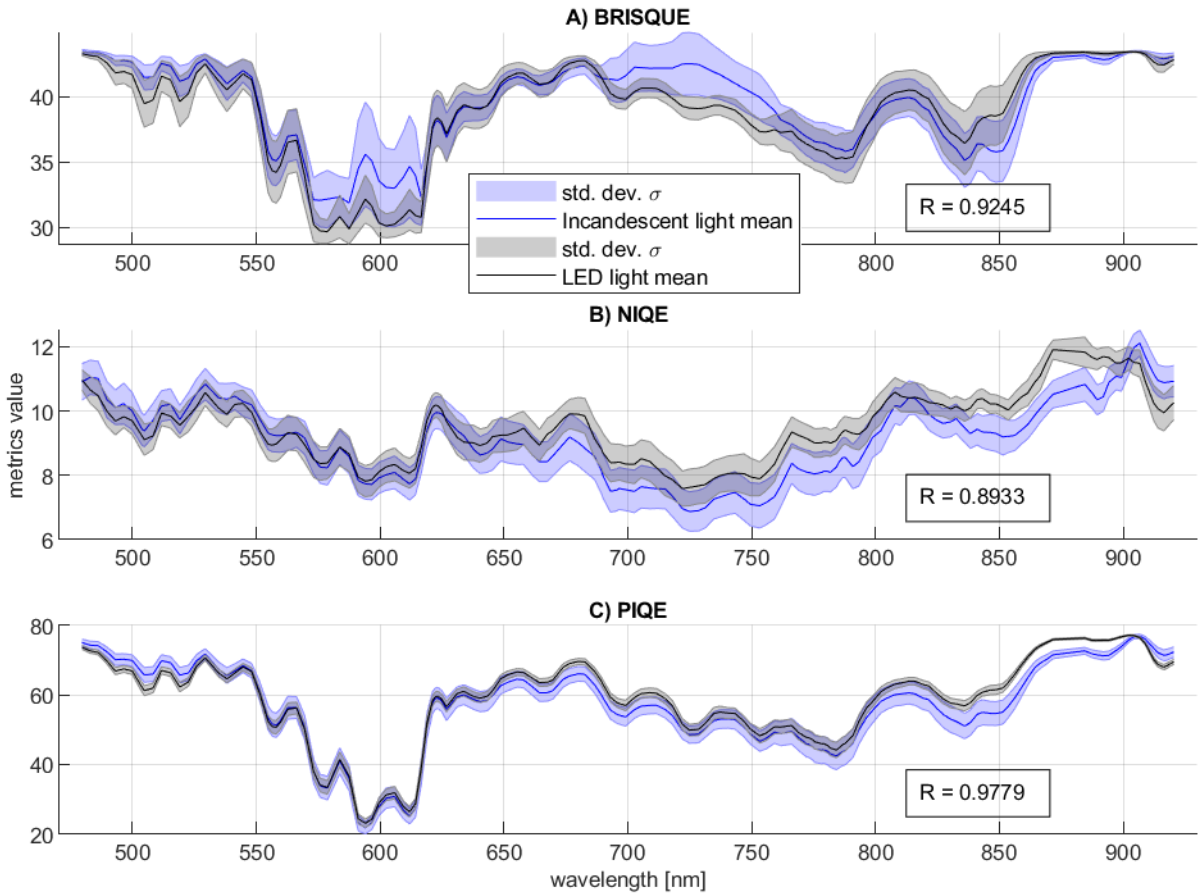

The temperature on the top of the moving platform (black cloth) was measured with a K-type thermocouple for each light source. There was a 30 °C temperature rise (from 23 °C ambient temperature to 53 °C) after 60 seconds for the incandescent light and 1 °C temperature rise for the LED light. The temperature on the top of the salami slice was measured with an IR thermometer. The temperature at the start of the measurement was 10 °C and after 60 seconds at the end of the measurement, the temperature was 26 °C for incandescent light and 17 °C for the LED light with an ambient temperature of 23 °C.

Whereas the hyperspectral LED technology is quite new and there is only one commercially available hyperspectral light up to date (Effilux light used in this experiment) there is no direct comparison published. Zahavi compares the older type of LEDs (Zahavi et al. 2019) capable of emitting the light in the range only up to 750 nm therefore not suitable for NIR region imaging.

This was not a problem with Effilux light because the spectral range of the light goes up to 1000 nm. Using multiple LED sources combined to cover the whole spectrum brings challenges in wavelength mixing and illumination uniformity as described by Islam (Islam et al. 2017). This was also not observed because the Effilux lightbar has five individual LEDs each emitting the light in the whole spectrum from 400–1000 nm.

Figure 3 Sample of the randomly selected slice under two different lights and two selected wavelengths

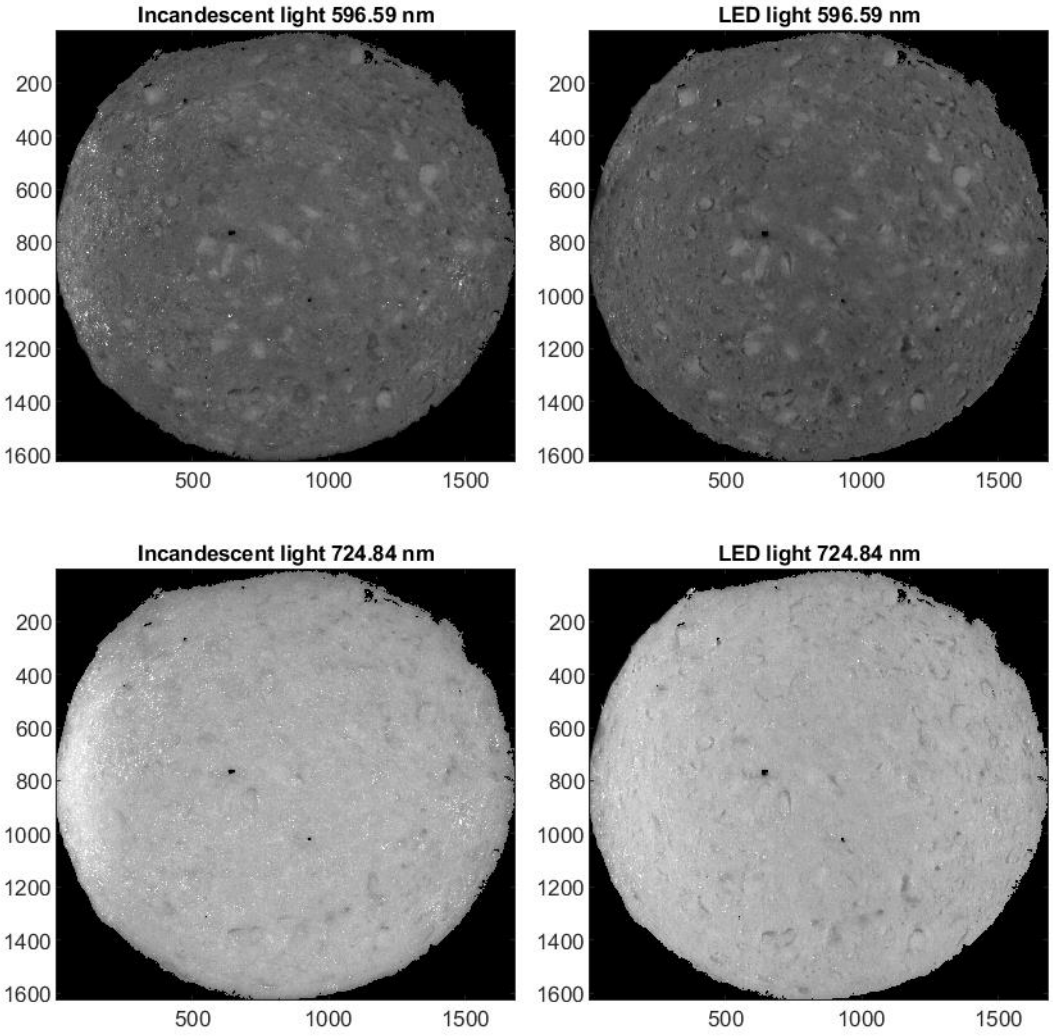

CONCLUSION

This paper shows the hyperspectral LED light source can be used in the same way the incandescent light sources were used in the past. The quality score had a strong correlation for every used method. The main advantage of the LED light source is the very low heat generated by the light source and thus no heat stressing of imaged samples and the camera. This results in a lower risk of occurrence of glares in the image created by melted fat on the top of the slice. This glare can cause pixel saturation and decrease the image quality. This is beneficial for imaging food samples or any biological sample possibly affected by a temperature change. LED light sources can also be easily diffused and the lighting of the scene can be more uniform. The standard deviation of the scores was lower for the LED lighting, i.e. it can produce more stable results. The main

disadvantage of the LED light source was low illumination power that resulted in a longer exposition time (0.7 ms vs 9.4 ms) which could introduce a higher level of noise in the image by the CCD sensor.

ACKNOWLEDGEMENTS

This research was supported by the Internal Grant Agency of the Faculty of business and economics at Mendel University in Brno. Project "Hyperspectral imaging for non-destructive detection of external food defects" number PEF_DP_2021019.

REFERENCES

Ahn, Y.N. et al. 2019. Design of highly efficient phosphor-converted white light-emitting diodes with color rendering indices (R1 - R15) ≥ 95 for artificial lighting. Scientific Reports, 9(1): 16848.

Islam, K. et al. 2017. Multi-LED light source for hyperspectral imaging. Optics Express, 25(26): 32659.

Jůzl, M. et al. 2019. Comparison of quality parameters of the cooked salami "Gothajský" in dependence on used salt content and additives. Potravinarstvo Slovak Journal of Food Sciences, 13(1): 390–395.

Mittal, A. et al. 2012. No-Reference Image Quality Assessment in the Spatial Domain. IEEE Transactions on Image Processing, 21(12): 4695–4708.

Mittal, A. et al. 2013. Making a "Completely Blind" Image Quality Analyzer. IEEE Signal Processing Letters, 20(3): 209–212.

Mo, C. et al. 2014. Non-Destructive Quality Evaluation of Pepper (Capsicum annuum L.) Seeds Using LED-Induced Hyperspectral Reflectance Imaging. Sensors, 14(4): 7489–7504.

Özdoğan, G. et al. 2021. Rapid and noninvasive sensory analyses of food products by hyperspectral imaging: Recent application developments. Trends in Food Science & Technology, 111: 151–165.

Photonfocus. 2021. HyperSpectral SDK [Online]. Available at: https://www.photonfocus.com/products/accessoriesfinder/accessory/hyperspectral-sdk/ [2021-09-10].

ÚNMZ. 1977. Gothajský salami (Gothajský salám). ČSN 577231. Praha: Úřad pro technickou normalizaci, metrologii a státní zkušebnictví.

Venkatanath, N. et al. 2015. Blind image quality evaluation using perception based features. 2015 Twenty First National Conference on Communications (NCC). Bombay, 27 February–1 March. IEEE.

Zahavi, A. et al. 2019. Influence of Illumination Sources on Hyperspectral Imaging. 2019 20th International Conference on Research and Education in Mechatronics (REM). Austria, 23–24 May. IEEE.

The evaluation of selected mechanical and physical properties of pelletized compost

Aneta Sinkova, Patrik Burg, Vladimir Masan, Alice Cizkova
Department of Horticultural Machinery
Mendel University in Brno
Zemedelska 1, 613 00 Brno
CZECH REPUBLIC

aneta.sinkova@mendelu.cz

Abstract: The production of compost and its use on agricultural land is now widespread and well known. With regard to the conditions of the changing climate (temperature fluctuations, unbalanced precipitation, etc.) and anthropogenic activities associated with soil degradation and environmental devastation, issues related to wider use of compost are being addressed within Europe. Special attention is paid to innovative modifications of compost into fertilizers with improved properties. A promising solution is also offered by the production of pellets from compost. The pellets have better utility properties, are easier and more accurately metered, and therefore it is easier to supply the required amount of organic matter to the soil. For the needs of experimental measurements carried out in 2021, connected with pelletizing, 3 variants of input raw materials were selected. These are compost itself, compost in combination with biochar and compost in combination with grape marc. Afterwards, selected mechanical-physical properties, such as bulk density (845–1 056 kg/m^3), mechanical durability (85.1–97.3%) and compressive strength (16.3–18.4 MPa) of pellets samples were evaluated. The obtained results confirmed a statistically significant difference between the evaluated samples. In particular, the results of mechanical resistance indicate their qualities. These results may ultimately be useful in eliminating risks in mechanical distribution systems, in dust generation, and in handling, applying or storing.

Key Words: sustainable technology, shaped fertilizer, compost, pellet, pelletizing, bulk density

INTRODUCTION

The production of shaped fertilizers by pelletizing represents, for sustainable agriculture, a promising method of treatment, which contributes to improving the possibility of accurate dosing, significant elimination of dust, reduction of storage, handling and transport costs and last but not least to slower the release of nutrients (Brunerová et al. 2020). The process of pelletizing raw materials is currently commonly used in the production of biofuels from waste biomass (Werther et al. 2000), or others materials (Holmes et al. 2014, Poggio-Fraccari et al. 2020).

The overall efficiency of pelletizing depends mainly on the chosen method and technology. The effect of physico-mechanical and physico-chemical processes is an increase in the density of the pelletized material. The pelletizing process itself is continuous and depends on the grain size of the input raw materials and their physical and mechanical properties (temperature, humidity, pH, etc.). The technological process of production of shaped fertilizer from compost consists of several consecutive phases. These include compost production, preconditioning processes (sieving or crushing of compost), drying and subsequent pelletizing (Lawong et al. 2011, Mieldazys et al. 2014). For pellets to be used in mechanical distribution systems, compressive strength in particular plays an important role. Compressive strength, also referred to as crush resistance or hardness, represents the maximum crushing load that a pellet can withstand before cracking or breaking. Compressive strength of densified products can be determined by using a diametric compression test (Brunerová et al. 2020).

The aim of the paper is to verify the main mechanical and physical properties of pellets made from horticultural compost in relation to their resistance when being handled, transported and stored.

MATERIAL AND METHODS

The methodology describes the basic characteristics of input raw materials, the method of pellets production and the characteristics of the pelletizing press, including the performed measurements and tests in order to determine selected mechanical and physical properties of the pellets.

Basic characteristics of raw materials

The main raw material for the production of pellets was compost made from a mixture of horticultural waste with a representation of grass, wood chips, vegetable residues, etc. which was produced by the technology of belt piles at the experimental composting plant of the Faculty of Horticulture in Lednice. Within the experimental measurements, a total of 3 variants of pellets (Figure 1) were produced in combination with bulking agents:

Var.1: compost (bulk density 650 kg/m^3)

Var.2: compost with mixture of biochar (20%), obtained from the gasification of wood residues (bulk density 350 kg/m^3)

Var.3: compost with mixture of grape marc (20%), obtained from the processing of grapes (bulk density 205 kg/m^3)

Figure 1 Variants of pellets

Characteristics of pelletizing equipment

The production of pellets was performed by using a laboratory pelletizer BONSAI 100 (Kovo Novák, Czech Republic). To extrude the incoming material, the press uses an extrusion roller with a plate die with holes, with a diameter of 6 mm. The material is pressed into a pelletizing die, where the final product is formed, which leaves a press formed into cylindrical pellets. The distance between the flat die and rollers was 0.10 mm; the rotation speed of the die was 2 800/min. The size of the applied pressing pressure was 3.5 MPa. The drive of the press is provided by an electric motor with an input of 6 kW, the efficiency of the press was at the level of 70 kg/h.

The evaluated parameters of pellets

After cooling down, the basic biometric parameters (diameter, length, weight, humidity and bulk density) of the pellets were determined. Measurements were always performed on 50 randomly selected pellets. The dimensional parameters of the pellets were determined by using a digital calliper (Dasqua IP67, Italy) with an accuracy of 0.01 mm.

The weight of the pellets was determined by using laboratory scales (Ohaus PX224, Switzerland) with an accuracy of 0.001 g. The moisture content of the pellets (%) was determined according to technical standard ISO 18134-2 (2017): Solid biofuels – Determination of moisture content – Oven dry method – Part 2: Total moisture – Simplified method. The samples were weighed fresh and dried in a laboratory oven at 105 °C for 24 hours. Bulk density of pellets was determined according to the EN ISO 18847 (2016): Solid biofuels - Determination of particle density of pellets and briquettes. The pellets were stored in a cylindrical container with a volume of 100 ml up to the top level, which was then weighed.

An important parameter expressing the properties of pellets is the compressive strength (σ). Compressive strength expresses the resistance of pellet samples to pressure effects. Compressive stress

is caused by the weight of pellets placed on top of each other during handling, storage or transport. Therefore, in practice, this parameter expresses their possible damage and has its justification in logistics. The principle of determination is based on recording the maximum load acting on the pellet sample before it disintegrates. The compressive strength of pellets was determined in the laboratory by using UTN 5000 (Research Institute of Agricultural Engineering, p.r.i., Czech Republic).

The pellet samples were compressed by a universal testing machine equipped with a force meter with a range of 0-5 000 N. The pellets were adjusted to twice the length of the diameter, i.e. 12 mm. The tests were performed by applying a compressive force acting in the vertical direction until the pellets were crushed. These tests were performed in 5 replicates on each pellet sample. The following equation was used to calculate the compressive strength:

$$\delta = \frac{Fmax}{S}$$

where: σ – compressive strength in simple pressure (MPa); Fmax – maximal load (N); S – cross-sectional area (m^2).

Another parameter evaluated was the mechanical resistance of pellets, expressing their resistance to impacts or abrasion due to handling and transport. The test sample of pellets is subjected to controlled impacts by striking the pellets against the walls of the chamber in a rotating defined test drum. From the weights of the sample remaining after separation of the abraded and finely crushed particles, the mechanical resistance is calculated. Mechanical resistance of the produced pellet samples was performed according to the mandatory standard ISO 17831-1 (2015): Solid biofuels – Determination of mechanical durability of pellets and briquettes – Part 1: Pellets. The measurements were performed by using the Pellettester equipment, type PT 500 (Research Institute of Agricultural Engineering, p.r.i., Czech Republic). The mechanical resistance of pellets is expressed by the following equation:

$$D_U = \frac{m_A}{m_E}$$

where: D_U – mechanical durability (%); m_A – weight of sieved pellets after rotating in the drum (g); m_E – weight of sieved pellets before rotating in the drum (g).

Statistical analysis

Results were reported as averages and standard deviation. Analysis of variance (ANOVA) and Tukey's honestly significant difference (HSD) tests were conducted to determine the differences among averages, using the software package "Statistica 12.0" (StatSoft Inc., USA). Analysis of variance was conducted, and the results were compared using Tukey's multiple range assay at a significance level of $\alpha = 0.05$.

RESULTS AND DISCUSSION

Table 1 shows the average values of diameter, length, weight and bulk density of evaluated pellet samples. For all evaluated samples, the diameter of produced pellets was greater than 6 mm, which corresponds to the size of matrix used. The resulting values indicate that all pellet samples experienced stress relaxation of the material after pelletizing process. Pocius et al. (2014) state that the effects of the relaxation process in pelletizing compost can be reduced by selecting the appropriate length of channels in the press die and the speed of material passage through the channel. If these parameters are not properly chosen, cracks appear on the surface of pellet due to transverse elastic deformations. The result is the disintegration of pellets and the limited possibility of their use.

The average length of pellets in the evaluated samples ranged from 14.83 to 19.49 mm, the average weight of pellets ranged from 0.68 to 0.98 g. The determined values of moisture 15.3–18.6% and bulk density ranged from 845.34–1 056.94 kg/m^3. Zafari and Kianmehr (2013) state that for fertilizer production is the optimal use of pelletizing press, which allows to achieve a balanced length of pellets, which is of great importance in terms of accurate dosing and application to the treated areas. Romano et al. (2014) dealt with the evaluation of the same parameters for pellets made from organic amendments made of swine manure solid fraction composted by itself and with three different co-formulates. The results of their evaluation show that, depending on the composition, the diameter ranged from 5.35–5.91 mm, length from 13.1–30.2 mm, humidity 4.18–12.5% and volume weight 312.2–701.1 kg/m^3

depending on the proportion of raw materials and their moisture. Bruner et al. (2020) states that in pelleted chicken litter organic fertilizer diameter 5.86 mm, length 33.03 mm, weight 1.15 g, bulk density 1 289.7 kg/m^3.

Table 1 The comparison of selected parameters of pelletized compost

Variant	The average value of monitored pellet trait				
	Caliber (mm)	Length (mm)	Weight (g)	Moisture (%)	Bulk density (kg/m^3)
1	6.01±0.11^a	19.49±4.63^a	0.98±0.26^b	18.6±0.16^a	1056.94±21.7^c
2	6.02±0.12^a	18.24±3.10^a	0.81±0.16^a	17.2±0.07^a	981.02±15.3^b
3	6.05±1.10^a	14.83±5.65^b	0.68±0.34^a	15.3±0.11^b	845.34±19.5^a

Legend: Mean values in one column followed by the same letter were not significantly different from each other by Tukey's test at $P < 0.05$.

Table 2 shows the average values of compressive strength, which in the evaluated samples range between 16.3–18.4 MPa and mechanical durability, which range between 85.1–97.3%. The results show that pellets made of compost with a proportion of grape marc (var.3) have significantly worse properties. This may be due to several factors. For example, matolins have been dried too much to prevent molding during storage. This is supported by the results from Table 2 where the pellets from grape marc have the lowest moisture. Also Benetto et al. (2015), Mieldazys et al. (2014) state that the properties of final fertilizer depend on the water content and the particle size of raw material. The origin of raw materials had a negligible influence.

Table 2 Compression strength and mechanical durability

Variant	The average value of monitored pellet trait	
	Compressive strength in simple pressure σ (MPa)	Mechanical durability (%)
1	18.4±2.4^a	97.3^a
2	18.0±3.5^a	96.7^a
3	16.3±2.2^b	85.1^b

Legend: Mean values in one column followed by the same letter were not significantly different from each other by Tukey's test at $P < 0.05$.

The values of mechanical durability do not correspond to the level of DU ≥ 97.5%, set by the technical standard ISO 17831-1 (2015): Solid Biofuels - Determination of Mechanical Durability of Pellets and Briquettes - Part 1: In this case, these standards are focused on pellets made for energy purposes, not for shaped organic fertilizers. Pawłowska et al. (2019) states that mechanical durability is the main quality indicator for both pelletized solid biofuel and fertilizer. This parameter describes the strength and resistance of the pellets to mechanical shocks that cause abrasion and damage of the pellets. These damages can be caused by storage, transport and handling of the pellets. Pocius et al. (2016) state that pelletized fertilizers can be damaged when applied to the soil surface by the centrifugal force of the spreading device.

CONCLUSION

From the resulting values of the monitored mechanical and physical properties, compost from horticultural waste can be considered as a promising raw material suitable for the production of shaped fertilizers. The compost can be used for pelletizing alone or in combination with suitable bulking agents. The performed measurements prove that the input properties of mixture intended to produce pellets significantly affect the resulting physical and mechanical properties of the produced pellets. The values of bulk density in the evaluated samples ranged from 845.34–1 056.94 kg/m^3, compressive strength in the range of 16.3–18.4 MPa and mechanical durability 85.1–97.3%. The results of the performed experiments indicate that from the point of view of ensuring the dimensional uniformity of the pellets, it will be appropriate to use pelletizing presses enabling the desired length of the pellets to be set. In operational practice, with regard to the great variability of compost mixtures, it will be necessary to solve not only the pelletizing itself but also the adjustment of moisture and grain size of compost, or the bulking agents used.

ACKNOWLEDGEMENTS

This paper was supported by the project CZ.02.1.01/0.0/0.0/16_017/0002334 Research Infrastructure for Young Scientists, co-financed by Operational Programme Research, Development and Education and the research project TA CR Nr. FW02020152 Technology for point application of organic nutrition to the permanent green root systems.

REFERENCES

Benetto, E. et al. 2015. Life cycle assessment of heat production from grape marc pellets. Journal of Cleaner Production. [Online], 87: 149–158. Available at: https://doi.org/10.1016/j.jclepro.2014.10.028. [2021-08-08].

Brunerová, A. et al. 2020. Analysis of the physical-mechanical properties of a pelleted chicken litter organic fertiliser. Research in Agricultural Engineering. [Online], 66: 131–139. Available at: https://doi.org/10.17221/41/2020-RAE. [2021-08-08].

Holmes, L.A. et al. 2014. Interactions between trace metals and plastic production pellets under estuarine conditions. Marine Chemistry [Online], 167: 25–32. Available at: https://doi.org/10.1016/j.marchem.2014.06.001. [2021-08-08].

ISO. 2015. Solid biofuels – Determination of mechanical durability of pellets and briquettes – Part 1: Pellets. ISO 17831-1. Geneva: International Organization for Standardization.

ISO. 2016. Solid biofuels – Determination of par-ticle density of pellets and briquettes. ISO 18847. Geneva: International Organization for Standardization.

ISO. 2017. Solid biofuels – Determination of moisture content – Oven dry method – Part 2: Total mois-ture – Simplified method. ISO 18134-2. Geneva: International Organization for Standardization.

Lawong, W. et al. 2011. Development of two pellet die organic fertilizer compres-sion machine. Procedia Engineering [Online], 8: 266–269. Available at: https://doi.org/10.1016/j.proeng.2011.03.049. [2021-08-08].

Mieldazys, R. et al. 2014. Evaluation of physical mechanical properties of experimental granulated cattle manure compost fertilizer. In Proceedings of 16th International Scientific Conference "Engineering for Rural Development" 2017 [Online]. Jelgava, Latvia, 24–26 May, Jelgava: Latvia University of Life Sciences and Technologies, Faculty of Engineering, pp. 575–580. Available at: https://www.tf.llu.lv/conference/proceedings2017/Papers/N113.pdf. [2021-08-08].

Pawłowska, M. et al. 2019. Influence of storage conditions on a quality of pelletized waste-derived fertilizer. Journal of Ecological Engineering [Online], 20: 226–233. Available at: https://doi.org/10.12911/22998993/99940. [2021-08-08].

Pocius, A. et al. 2014. Investigation of granulation process parameters influence on granulated fertilizer compost properties. In Proceedings of 13th International Scientific Conference "Engineering for Rural Development" 2014 [Online]. Jelgava, Latvia, 29–30 May, Jelgava: Latvia University of Life Sciences and Technologies, Faculty of Engineering, pp. 407–412. Available at: https://www.tf.llu.lv/conference/proceedings2014/Papers/69_Pocius_A.pdf. [2021-08-08].

Pocius, A. et al. 2016. Investigation of physical-mechanical properties of ex-perimental organic granular fertilizers. In Proceedings of 15th Internal Scientific Conference "Engineering for Rural Development" 2016 [Online]. Jelgava, Latvia, 25–27 May, Jelgava: Latvia University of Life Sciences and Technologies, Faculty of Engineering, pp. 1115–1120. Available at: https://www.tf.llu.lv/conference/proceedings2016/Papers/N217.pdf. [2021-08-08].

Poggio-Fraccari, E. et al. 2020. Pelletized Cu-Ni/CePr5 catalysts for H2 purification via water gas shift reaction. Fuel [Online], 271: 117653. Available at: https://doi.org/10.1016/j.fuel.2020.117653. [2021-08-08].

Romano, E. et al. 2014. Pelletization of composted swine manure solid fraction with different organic co-formulates: effect of pellet physical properties on rotating spreader distribution patterns. International Journal of Recycling of Organic Waste in Agriculture [Online], 3: 101–111. Available at: https://doi.org/10.1007/s40093-014-0070-2. [2021-08-08].

Werther, J. et al. 2000. Combustion of agricultural residues. Progress in Energy and Combustion Science [Online], 26: 1–27. Available at: https://doi.org/10.1016/S0360-1285(99)00005-2. [2021-08-08].

Zafari, A., Kianmehr, M.H. 2014. Factors affecting mechanical properties of biomass pellet from compost, Environmental Technology [Online], 35(4): 478–486. Available at: https://doi.org/10.1080/09593330.2013.833639. [2021-08-08].

Stability of intemetallic phases in the heat affected zone depending on shielding gases

Radim Smak, Jiri Votava, Jaroslav Lozrt, Adam Polcar
Department of Technology and Automobile Transport
Mendel University in Brno
Zemedelska 1, 613 00 Brno
CZECH REPUBLIC

xsmak@node.mendelu.cz

Abstract: This contribution deals with the influence of shielding gases on the parameters of MIG and MAG welds. For the experiment purposes, steels S 235 JRG1 and C45 were chosen. In the research part, welding parameters and welding conditions were proposed; based on them, a series of experiments were performed. Weld beads were subjected to metallographic analysis (samples prepared according to ČSN ISO 4967), from which the heat-affected zone and metal structure were determined. The melting bath area was not analyzed. Furthermore, in the heat-affected zone there were hardness and microhardness measured. The macrohardness of the samples was measured using the Rockwell HRB method according to ČSN EN ISO 6508 standard. The microhardness measurement was performed using Hannemann microhardness tester according to ČSN EN ISO 6507-1 standard.

Key Words: MAG, welding, depth of penetration, microstructure, hardness

INTRODUCTION

MIG (Metal Inert Gas) and MAG (Metal Active Gas) welding are currently one of the most widely used welding methods and have significant advantages over other methods, such as welding of various materials (Poláková et al. 2018). These technologies are also advantageous for the application of carbide welds (Votava et al. 2019). An important advantage of this method is the possibility of automation, which is used mainly in the car production. Other advantages are well-adjustable welding parameters, the possibility of controlled metal transfer and the possibility of combination with other welding methods, such as TIG (Tungsten Inert Gas).

To meet the required parameters of the welded joint, it is necessary to observe process parameters, such as current, voltage, torch feed rate, amount and type of used shielding gas and the metal transfer method. The choice of shielding gas is an integral part of the welding process design. The gas composition significantly affects the shape, microstructure and mechanical properties of welded joints (Boiko and Avisans 2013)

Welding is used in almost all industries; from the largest structures of bridges, buildings and ships to underwater welding, welding in space conditions and the construction of oil and gas pipelines, where high demands on the welded joint strength and tightnes are placed (Sartori et al. 2017)

The main disadvantages include influencing the microstructure and material properties in the heat-affected zone, deformation of the weldment and usually the need for further heat treatment. An important parameter in the heat treatment of weldments is the cooling rate and the cooling medium itself (Šmak et al. 2020b).

MATERIAL AND METHODS

The experimental part deals with MIG/MAG welding technology. Steel S 235 JRG1 and C45 were chosen for the production of weldments. These two materials represent standard structural steel with guaranteed weldability (S 235 JRG1), but also steel with difficult weldability (C45). The reason for difficult weldability is the higher percentage of carbon. The inert gas Argon 4.6 with a purity of 99.99% was chosen as the technical gas for the MIG method and the active gas CO_2 for the MAG

method. The research carried out (Tomc and Tušek 2013) shows that, in additionto the shielding gas composition, the shape of the weld formed by the MIG/MAG methods is also significantly affected by the nozzle geometry which forming the shielding gas stream around the forming weld pool.

Based on the performed metallographic analysis, the weldment heat-affected zone was monitored, but also the microhardness of individual structural phases was measured. The following tests were performed to determine basic characteristics of weldment:

1. measurement of base material hardness, heat affected zone and weld metal by HRB method,
2. measurement of microhardness using metallographic microscope Neophot 21 according to ČSN EN ISO 6507-1,
3. metallographic analysis of the heat affected zone.

A Picomig 180 plus TKG pulse welding unit with the following parameters was used for sample preparation:

- welding current: 170 A,
- welding voltage: 26.5 V,
- wire feed: 11.5 m/min; wire diameter: 0.8 mm.

Autrod 12.51 welding wire was chosen as an additional material for both welding technologies. The mechanical properties of the given material are given in Table 1.

Table 1 Autrod 12.51 wire mechanical properties

Welding method	Shielding gas	Rm	$R_{p0.2}$	As	KV +20°C]	KV -20 °C
MIG	Argon	540 MPa	450 MPa	25%	110 J	90 J
MAG	CO_2	560 MPa	470 MPa	26%	130 J	70 J

Characteristic of tested materials

S 235 JRG1

This steel is intended primarily for the weldments production. Its chemical composition guarantees safe weldability. It is a standard structural steel, where due to the small amount of carbon it is not possible to perform heat treatment with significant changes in structural phases. See Figure 1.

C45

This material is suitable for tempering and surface hardening. It is a structural steel with a higher percentage of carbon. Based on the metallographic analysis, see Figure 2, this material can be characterized in its natural state as a pearlitic-ferritic structure with a majority of pearlite. The pearlitic lamellae dispersity corresponds to an amount of carbon which is above 0.4%. The chemical composition of C45 steel and S 235 JRG1 steel is given in Table 2.

Figure 1Microstructure of steel S 235 RG1

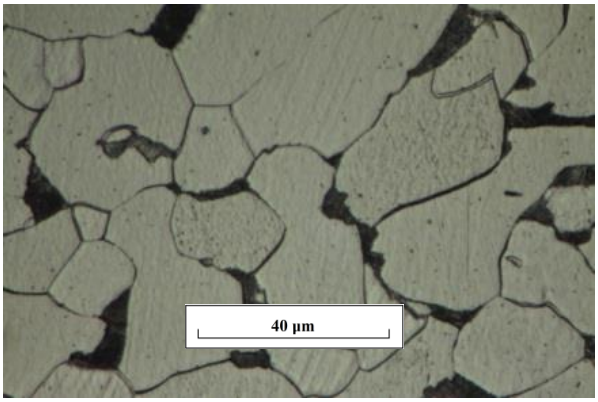

Figure 2 Microstructure of steel C45

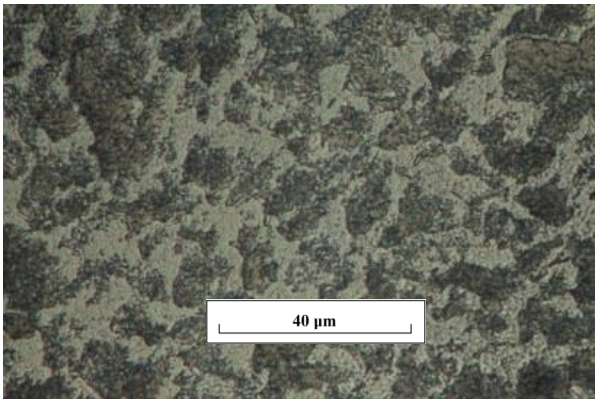

Table 2 Chemical composition of used steels

Steel	Chemical composition					
	C	CE	Mn	Si	P_{max}	S_{max}
S 235 JRG1	0.17%	0.25%	-	-	0.045%	0.045%
C45	0.45%	0.53%	0.5%	0.17%	-	-

RESULTS AND DISCUSSION

In the weld heat-affected zone, there is a greater risk of brittle structure formation, which negatively affects the mechanical properties of the steel and can also contribute with poor adhesion of inorganic anti-corrosion systems, mainly zinc coatings (Votava et al. 2018, Nascimento et al. 2012). Announced that due to exothermic reactions between O_2 and the elements contained in the electrode and the melting bath (especially iron and carbon), the arc temperature is higher for gas mixtures with higher O_2 content (active gases). In addition to this temperature increase effect, the different thermal conductivity of the shielding gases must be taken into account. This higher thermal conductivity means a greater supply of heat to the weld pool. The following changes can be identified: a decrease in the weld bead and an increase in the transition structure intensity between the weld metal and the base material. Another set of changes occurs at the microstructure level. Changes occur depending on the carbon content and cooling rate of the weldment.

Metallographic analysis

S 235 JRG1

The heat-affected zone of S 235 JRG1 steel can be characterized in both welding methods as very gradual, without enormous changes. The dendrites formed in the weld metal pass into the base material affected by plastic deformations caused by rolling. The weld metal is not affected with the base material and it can be stated that it retains a similar chemical composition as the additive material. Since these structural phases are formed from the melt, ferritic particles are particularly evident. However, the Widmanstätten structure, which was identified in the toe region created by the MAG method, can be problematic, see Figure 3. Widmanstätten structures were found in the upper layers of the weld transition area (toe) between the base material and the weld metal. With the MAG method, due to higher temperatures, carbon segregates into the form of needles. These phases are created as a result of an undesired heat-stress during the welding process or material separation by flame (Šmak et al. 2020a). These conditions do not occur with the MIG method.

Figure 3 Widmanstätten structute in heat-affected zone, S 235 JRG1 steel, MAG

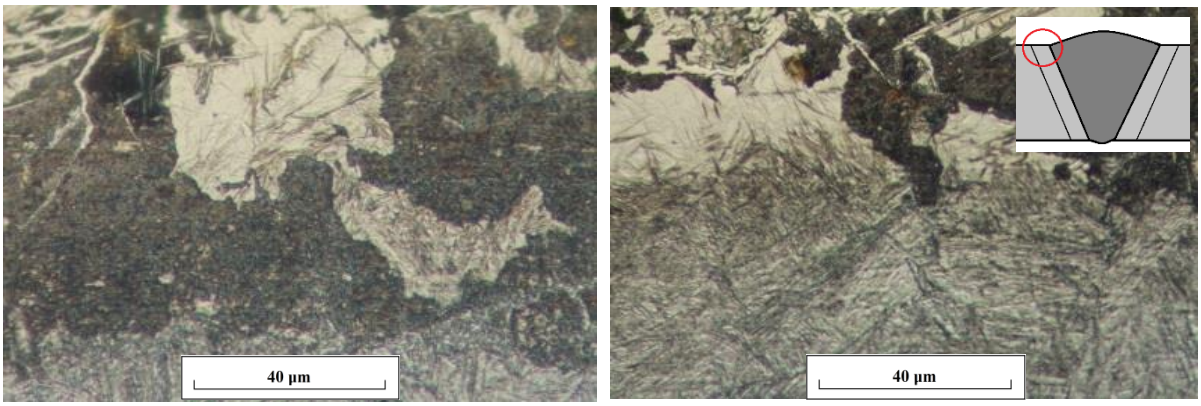

C45

When using the MIG method, the transition area is much more gradual than for MAG method. The weld metal is fundamentally affected by the content of carbon in the base material. According to the performed metallographic cuts, it is obvious that the C45 steel undergoes fundamental structural changes in the heat-affected zone. It is mainly the formation of brittle unstable phases especially bainite,

which can initiate cracks in the area. However, no pure martensitic structure was found in the samples. When using an inert gas, the transition structure consists of predominantly homogeneous fractions. The MAG method is characterized by a heterogeneous compound. In contrast, in the research performed (Ilic et al. 2020), an toughness analysis of welds performed with inert and active gases on high-strength steel S690QL was performed. Research has shown higher values of impact energy in samples welded with active gas. From this it can be clearly deduced that the resulting mechanical properties are strictly determined by both the shielding gas and the welded steel chemical composition.

Hardness measurement

Macrohardness measurements were performed using the HRB method, because with the use of this method it is possible to measure in the low range of hardnesses, when the use of the HRC method would be inappropriate, due to the low hardness of the measured materials. With this method, it is not possible to recognize changes in the microstructure, such as the Widmanstätten structure. However, the HRB method makes it possible to determine relatively accurately the overall condition of the analyzed area.

For C45 steel, an increase in values was expected due to the higher carbon content. As the base material was natural steel, the measured values are very similar to S 235 JRG1. The values measured in the heat affected zone are about 10 units higher than the value of the base material. Research performed by (Sayed et al. 2021) shows a very good resistance of C45 steel to hydrogen embrittlement and cold cracking. This effect is ensured by the use of electrodes with a low hydrogen content and controlled cooling of the weldment.

The correlation between microhardness and macrohardness values is limited. The HRB method uses a significantly higher sample area for hardness analysis. The resulting value is the summary value of hardness from the entire measured area. Microhardness measurement methods are used to measure the hardness of individual structural phases. The measured hardness values for S 235 JRG1 and C45 steel are recorded in Table 3.

Table 3 HRB measurement, S 235 JRG1 and C45 steel weldments

Welding method	Measured area	S 235 JRG1			C45		
		Average HRB	Standard deviation HRB	Var. coefficient	Average HRB	Standart deviation HRB	Var. coefficient
MIG	Weld material	79.7	2.1	2.6%	83.7	2.9	3.4%
	Heat aff. zone	81.0	2.2	2.7%	98.0	1.4	1.4%
	Base material	84.7	0.5	0.6%	86.7	2.1	2.4%
MAG	Weld material	76.7	2.1	2.7%	84.0	2.2	2.6%
	Heat aff. zone	81.7	2.5	3.1%	101.0	3.3	3.2%
	Base material	83.0	0.8	1.0%	87.0	1.4	1.6%

Microhardness measurement

Microhardness measurements were performed using a Hannemann microhardness tester. This tester is a part of the Neophot 21 metallographic microscope. The Vickers method was used for the microstructure analysis. The measurement was realised according to ČSN EN ISO 6507-1 standard.

The microhardness values of the individual areas in steels S 235 JRG1 and C45 are shown in the Figure 4. Since the basic C45 steel is already formed by a pearlitic-ferritic structure, there is also an increase in hardness values compared to the steel S 235 JRG1. According to the performed analysis, a clear increase in the structural phases microhardness in the heat-affected zone was demonstrated with values of approx. 384 $H_{V0.1}$. Although these values are not adequate to the phases of the martensitic

structure, the risk of microcracks in the heat-affected zone can be clearly predicted. (Silva Costa et al. 2020) mentions the control of weld metal transfer as a possibility to regulate the heat affected zone size.

Figure 4 Microhardness of weld areas

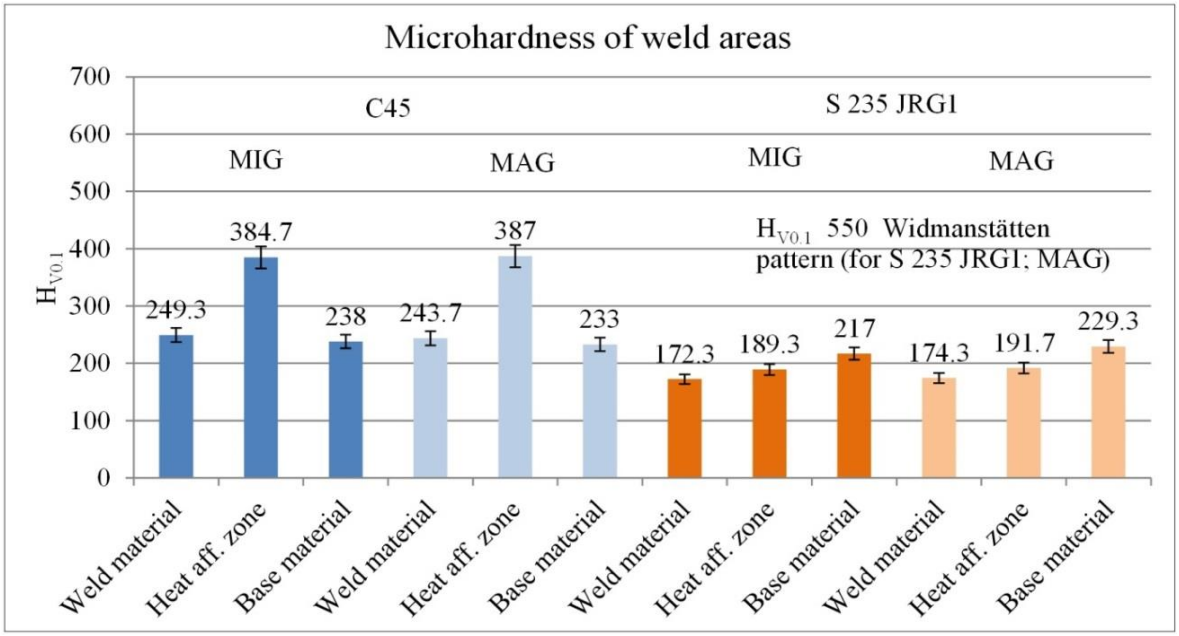

CONCLUSION

In the presented contribution, MIG and MAG methods for the production of weldments from S 235 JRG1 and C45 steel were analyzed.

Although the same additional material was used in both methods, the different mechanical properties of the weld were caused by the reaction between the shielding gas and the molten bath. Especially due to exothermic reactions between O_2 and the elements contained in the melting bath (iron and carbon), the arc temperature is higher for active gases which causes changes in the microstructure. The research clearly confirmed this.

Metallographic analysis of S 235 JRG1 steel shown the smooth dendrite flow from the melt bath into the base material. Since both the weld metal and the base material do not have a carbon content higher than 0.25%, the heat-affected zone is predominantly a ferritic compound. In the case of S 235 JRG1 steel, the presence of the Widmanstätten structure was detected using the MAG method in the heat-affected zone.

Following differences have already been noted in the analysis of C45 steel weldments. Although the influence of the shielding gas on the weldment quality itself was not proven, there is the formation of brittle bainitic structural phases not only in the weld metal itself, but especially in the heat affected zone (avg. 387 $H_{V0.1}$). Although the thickness of the weldment material guarantees sufficient heat treatment, transient structural phases with an average microhardness of approx. 384 $H_{V0.1}$ occur at the weld interface and the base material. The microhardness values for the active gas are approximately 10% higher than for the inert gas. Shielding gas for the MIG method is more expensive, but it eliminates the formation of dangerous brittle structures in the transition area.

This contribution was based mainly on the analysis of the weld microstructure. Impact testing could be performed to further describe the mechanical properties. The author considers these tests as a possibility for further research.

ACKNOWLEDGEMENTS

This project was funded by the Internal Grant Agency of Mendel University in Brno, Faculty of AgriSciences. Grant project No. AF-IGA2021-IP043.

REFERENCES

Boiko, I., Avisans, D. 2013. Study of shielding gases for MAG welding. Materials Physics and Mechanics [Online], 16: 126–134. Available at: https://www.ipme.ru/e-journals/MPM/no_21613/MPM216_04_boiko.pdf. [2021-08-15].

Ilic, A. et al. 2020. Analysis of Influence of the Welding Procedure on Impact Toughness of Welded Joints of the High-Strength Low-Alloyed Steels. Applied Sciences [Online], 10(7): 590–600. Available at: https://www.mdpi.com/2076-3417/10/7/2205/htm. [2021-07-11].

Nascimento, A. et al. 2012. Effect of waveform and shielding gas on melting rate and bead geometry for MIG/MAG-PV. Soldagem e Inspecao [Online], 17(1): 40–48. Available at: https://www.scielo.br/j/si/a/Tyv8cCzqBnJrMkYX8d99yzS/?lang=pt. [2021-08-01].

Poláková, N. et al. 2018. TIG welding of stainless steel and titanium with additive AG 104. In Proceedings of International PhD Students Conference MendelNet 2018 [Online]. Brno, Czech Republic, 07–08 November, Brno: Mendel University in Brno, Faculty of AgriSciences, pp. 468–471. Available at: https://mnet.mendelu.cz/mendelnet2018/mnet_2018_full.pdf. [2021-07-25].

Sartori, F. et al. 2017. A Comparative Analysis of Different Versions of the MIG/MAG Process Modern Variants for the Root Pass in Orbital Welding. Soldagem e Inspecao [Online], 22(4): 442–452. Available at: https://www.scielo.br/j/si/a/jHp4wLYJfNZmj7QRFsphPHm/?lang=pt. [2021-08-17].

Sayed, A. et al. 2021. Mechanical and microstructural testing of C-45 material welded by using SMAW and GMAW process. Materials Today: Proceedings [Online], 38(1): 223–228. Available at: https://www.sciencedirect.com/science/article/pii/S2214785320351142?via%3Dihub. [2021-08-18].

Šmak, R. et al. 2020a. Influence of phase structures on cutting surface quality and cutting tool degradation. In Proceedings of International PhD Students Conference MendelNet 2020 [Online]. Brno, Czech Republic, 11–12 November, Brno: Mendel University in Brno, Faculty of AgriSciences, pp. 474–479. Available at: https://mendelnet.cz/pdfs/mnt/2020/01/85.pdf. [2021-07-21].

Šmak, R. et al. 2020b. The cooling media influence on selected mechanical properties of steel. Acta Technologica Agriculturae [Online], 23(4): 183–189. Available at: https://www.sciendo.com/article/10.2478/ata-2020-0029. [2021-08-15].

ÚNMZ. 2018. Kovové materiály – Zkouška tvrdosti podle Vickerse. Část 1: Zkušební metoda. ČSN EN ISO 6507-1. Praha: Úřad pro technickou normalizaci, metrologii a státní zkušebnictví.

ÚNMZ. 2018. Kovové materiály – Zkouška tvrdosti podle Rockwella. Část 1: Zkušební metoda. ČSN EN ISO 6508-1. Praha: Úřad pro technickou normalizaci, metrologii a státní zkušebnictví.

ÚNMZ. 2015. Ocel- Stanovení obsahu nekovových vměstků – Mikrografická metoda. ČSN ISO 4967. Praha: Úřad pro technickou normalizaci, metrologii a státní zkušebnictví.

Tomc, J., Tušek, J. 2013. Description of flow of shielding gases through nozzles in MIG/MAG and TIG welding processes. Science and Technology of Welding and Joining [Online], 9(3): 260–266. Available at: https://www.tandfonline.com/doi/abs/10.1179/136217104225012184. [2021-08-20].

Votava, J. et al. 2019. Využití tvrdokovových návarů u sklízečů cukrové řepy. Listy cukrovarnické a řepařské [Online], 135(9): 297–302. Available at: http://www.cukr-listy.cz/on_line/2019/PDF/297-302.pdf. [2021-07-30].

Votava, J. et al. 2018. Anti-corrosion systems in vehicles for the transportation and application of fertilizers. Metallic Materials [Online], 56(2): 131–136. Available at: https://doi.org/10.4149/km_2018_2_131. [2021-08-19].

Mathematical models for temperature-dependent viscosity of FAME and diesel blends

Daniel Trost, Adam Polcar, Martin Fajman, Jiri Votava, Jiri Cupera, Vojtech Kumbar
Department of Technology and Automobile Transport
Mendel University in Brno
Zemedelska 1, 613 00 Brno
CZECH REPUBLIC

xtrost@mendelu.cz

Abstract: Fatty Acid Methyl Ester (FAME) is a potential alternative fuel for compensating the running out of fossil-based liquid fuels. FAME is produced from renewable sources by transesterification. It could be produced locally, in each region of usage. Furthermore, local production and no need for international fuel transportation, this method could be more ecological, and it also could bring significant savings. FAME has physical properties similar to common diesel at normal temperatures. In contrast, at low temperatures, the viscosity increases sharply. Therefore, is it mostly used in blends with diesel. The kinematic viscosity of FAME/diesel blends was investigated in this paper. Various temperature (from -10 °C up to 60 °C) and various ratios (0, 7, 10, 15, 20, 30, 85, 100 vol.%) were tested. In the experiment, the kinematic viscosity of blends was tested and compared. It was found, the Vogel model has the best result, according to the coefficient of determination R^2 and sum of squares error SSE.

Key Words: mathematical models, Vogel, viscosity, FAME, Methyl Ester, diesel, temperature

INTRODUCTION

Due to the increasing consumption of petroleum fuels and its environment-unfriendliness, research on the production and use of biofuels has been subjected to research in the past decades. Another support for the creating more ecological Europe is the 2030 EU climate & energy framework which set three key targets. One of them is to have at least a 27% share for renewables in energy consumption by 2030 (European Commission 2017). The mentioned framework annex currently used European Standard EN 590:2013+A1:2017 which specifies requirements and test methods for marketed and delivered automotive diesel fuel. It is applicable to automotive diesel fuel for use in diesel engine vehicles designed to run on automotive diesel fuel containing up to 7.0% Fatty Acid Methyl Ester (Merkisz et al. 2016). One possible way of decreasing the overall world consumption of fossil fuels is the local production of biofuels which can be made from easily accessible local sources. The expression biofuel means liquid or gaseous fuel that is produced from renewable sources like corn, canola seeds, sugar cane or sugar beet. FAME is produced by transesterification and its advantages are non-toxicity and biodegradability (Sajjadi et al. 2016). FAME at normal temperature has physical properties similar to conventional diesel. However, fatty acid methyl ester has also drawbacks in comparison to diesel including lower stability, lower cetane number, high viscosity and density specifically in low temperature. Therefore, FAME is usually mixed with diesel in various ratios. FAME/diesel blends and their properties were also subjected to research by Pexa et al. (2014) and Čedík et al. (2018).

MATERIALS AND METHODS

In this experiment was followed a similar procedure, which was already used for FAME/diesel blends in paper by Kumbár et al. (2015) and Trost et al. (2021). Fuel blends from D100 up to FAME100 were prepared. All prepared blends can be seen in Table 1. Mentioned samples were prepared from diesel without biocomponent (Čepro, Czech Republic) and FAME (Preol, Czech Republic), the sample's name is according to the volume ratio of FAME in the blend (e.g. FAME 30 contains 30 vol.% FAME and 70 vol.% diesel).

The values of the volumetric mass density of the FAME/diesel samples were measured by a digital Densito 30 PX densitometer (Mettler Toledo, USA) operating on an oscillating tube principle. All the samples were measured in temperature range from -10 to 60 °C.

To determine the dynamic viscosity, DV2T rotary viscometer (Brookfield, USA) was used. The kinematic viscosity was calculated from the dynamic viscosity and volumetric mass density using the equation: $\nu = \frac{\eta}{\rho}$, where ν is the kinematic viscosity, η is the dynamic viscosity, and ρ is the volumetric mass density.

Table 1 Composition of samples

Sample	Volume of FAME	Volume of diesel
D100	0%	100%
FAME7	7%	93%
FAME10	10%	90%
FAME15	15%	85%
FAME20	20%	80%
FAME30	30%	70%
FAME85	85%	15%
FAME100	100%	0%

In this paper three various mathematical models, for temperature dependence of kinematic viscosity were used. Part of those models were also used by Alptekin and Canakci (2008), Trávníček et al. (2013) and Peleg et al. (2017). Used models and their equations:

Exponential: $\nu = \nu_0 \cdot e^{a \cdot T}$ (1)

Where, ν is kinematic viscosity [mm^2/s], ν_0 is reference value of kinematic viscosity [mm^2/s], a is a coefficient [K^{-1}] and T is the absolute temperature [K].

Arrhenius: $\nu = \nu_0 \cdot e^{\frac{E_a}{R \cdot T}}$ (2)

Where, ν is kinematic viscosity [mm^2/s], ν_0 is reference value of kinematic viscosity [mm^2/s], R is the Universal gas constant [J/(mol·K)], E_a is the Arrhenius activation energy respectively [J/mol] and T is the absolute temperature [K].

Vogel: $\nu = \nu_0 \cdot e^{\frac{b}{c+T}}$ (3)

Where, ν is kinematic viscosity [mm^2/s], ν_0 is reference value of kinematic viscosity [mm^2/s], b and c are coefficients [K] and T is the absolute temperature [K].

All the measurements were repeated twenty times to obtain higher accuracy and relevance of the results. The values in the tables are displayed as the mean value including the standard deviation.

The suitability of mathematical models was evaluated according to the coefficient of determination R^2 and sum of squares error SSE.

RESULTS AND DISCUSSION

In the following chapter, the data obtained from the experiment are recorded in the tables. Results are ordered gradually from D100 up to FAME100. All the obtained results were processed by MATLAB R2021a (MathWorks, USA).

It can be seen from the tables above, that the kinematic viscosity of the mixtures decreases with increasing temperature. Furthermore, blends with a higher FAME content have higher viscosity similarly to results observed by Kumbár and Votava (2015).

Table 2 Values of kinematic viscosity for FAME/diesel blends, part I (mean ± standard deviation, N = 20)

Temperature [°C]	Temperature [K]	Kinematic viscosity FAME/diesel blends [mm²/s]			
		D100	FAME7	FAME10	FAME15
-10	263.15	9.076 ± 0.012	11.101 ± 0.022	11.885 ± 0.016	12.317 ± 0.034
-5	268.15	7.853 ± 0.010	9.025 ± 0.014	9.191 ± 0.014	9.686 ± 0.030
0	273.15	6.836 ± 0.012	7.427 ± 0.012	7.559 ± 0.016	7.674 ± 0.022
5	278.15	5.923 ± 0.010	6.318 ± 0.021	6.349 ± 0.011	6.423 ± 0.019
10	283.15	5.280 ± 0.011	5.457 ± 0.016	5.551 ± 0.012	5.753 ± 0.015
15	288.15	4.762 ± 0.090	4.795 ± 0.012	4.813 ± 0.010	5.036 ± 0.016
20	293.15	4.055 ± 0.012	4.298 ± 0.010	4.303 ± 0.014	4.448 ± 0.012
25	298.15	3.618 ± 0.09	3.808 ± 0.012	3.808 ± 0.011	3.988 ± 0.011
30	303.15	3.227 ± 0.011	3.386 ± 0.014	3.402 ± 0.012	3.561 ± 0.015
35	308.15	2.938 ± 0.010	3.075 ± 0.012	3.094 ± 0.012	3.230 ± 0.012
40	313.15	2.673 ± 0.011	2.819 ± 0.014	2.862 ± 0.005	2.908 ± 0.011
45	318.15	2.436 ± 0.08	2.566 ± 0.012	2.586 ± 0.011	2.684 ± 0.012
50	323.15	2.246 ± 0.09	2.385 ± 0.018	2.402 ± 0.012	2.446 ± 0.012
55	328.15	2.174 ± 0.08	2.195 ± 0.012	2.211 ± 0.005	2.249 ± 0.010
60	333.15	1.962 ± 0.07	2.029 ± 0.011	2.030 ± 0.011	2.103 ± 0.005

Table 3 Values of kinematic viscosity for FAME/diesel blends, part II (mean ± standard deviation, N = 20)

Temperature [°C]	Temperature [K]	Kinematic viscosity FAME/diesel blends [mm²/s]			
		FAME20	FAME30	FAME85	FAME100
-10	263.15	12.322 ± 0.024	12.637 ± 0.021	21.287 ± 0.052	23.001 ± 0.058
-5	268.15	9.840 ± 0.020	10.517 ± 0.018	16.708 ± 0.055	16.842 ± 0.045
0	273.15	7.925 ± 0.019	8.746 ± 0.009	12.445 ± 0.022	13.060 ± 0.017
5	278.15	6.699 ± 0.018	7.303 ± 0.004	10.509 ± 0.025	11.151 ± 0.011
10	283.15	5.831 ± 0.017	6.364 ± 0.010	8.920 ± 0.026	9.465 ± 0.011
15	288.15	5.058 ± 0.018	5.437 ± 0.005	7.702 ± 0.021	8.136 ± 0.011
20	293.15	4.499 ± 0.013	4.784 ± 0.009	6.736 ± 0.022	7.147 ± 0.011
25	298.15	4.024 ± 0.017	4.215 ± 0.012	5.968 ± 0.019	6.245 ± 0.005
30	303.15	3.615 ± 0.014	3.812 ± 0.012	5.176 ± 0.016	5.569 ± 0.011
35	308.15	3.236 ± 0.008	3.428 ± 0.005	4.727 ± 0.012	5.020 ± 0.011
40	313.15	2.923 ± 0.012	3.131 ± 0.007	4.304 ± 0.015	4.510 ± 0.014
45	318.15	2.699 ± 0.012	2.852 ± 0.016	3.852 ± 0.012	4.055 ± 0.014
50	323.15	2.468 ± 0.011	2.628 ± 0.012	3.563 ± 0.012	3.721 ± 0.012
55	328.15	2.262 ± 0.011	2.429 ± 0.011	3.250 ± 0.009	3.418 ± 0.015
60	333.15	2.108 ± 0.012	2.220 ± 0.012	2.966 ± 0.009	3.286 ± 0.013

Below this text, follow Tables 4–6 with coefficients for three various mathematical models. Model coefficients are valid for thermodynamic temperature (Kelvin unit).

In the tables above it can be seen, that the viscosity of the mixtures decreases with increasing temperature (Pelegrini et al. 2017). Furthermore, that blends with a higher FAME content have a higher viscosity similarly to results observed by Trávníček et al. (2013) and Kumbár et al. (2015). Exponential and Arrhenius model show some not statistically significant coefficients. Exponential model holds average coefficient of determination R^2 0.974, which is the lowest of all used models further followed by the biggest sum of squares error SSE 5.892 It expresses that Exponential model is the least accurate for description kinematic viscosity of FAME/diesel blends. As the second most accurate model was observed Arrhenius with average R^2 0.982 and SSE 5.402. According to the obtained results the most appropriate model for kinematic viscosity modeling FAME/diesel blends is Vogel model with R^2 0.999 and also with smallest SSE 0.393.

Table 4 Coefficients of Exponential kinematic viscosity model and its statistical indicators

Exponential	ν_0 [mm^2/s]	a [K^{-1}]	R^2	SSE
D100	4921	-0.02405	0.9926	0.5127
FAME7	1.404e+04	-0.02743	0.9784	2.22
FAME10	2.115e+04	-0.02881	0.9686	3.61
FAME15	2.263e+04*	-0.02893	0.9667	4.13
FAME20	2.276e+04	-0.0289	0.9735	3.377
FAME30	2.077e+04	-0.02835	0.9834	2.336
FAME85	1.405e+05*	-0.03375	0.9668	13.33
FAME100	1.487e+05*	-0.03377	0.9606	17.62

*Legend: *coefficient is not statistically significant*

Table 5 Coefficients of Arrhenius kinematic viscosity model and its statistical indicators

Arrhenius	ν_0 [mm^2/s]	E_a [J/mol]	R^2	SSE
D100	5.196e-06*	3.321e+04	0.9543	19.85
FAME7	0.001937	1.883e+04	0.9918	0.8441
FAME10	0.001337	1.975e+04	0.9850	1.729
FAME15	0.001333	1.983e+04	0.9833	2.067
FAME20	0.001377	1.979e+04	0.9884	1.478
FAME30	0.001740	1.939e+04	0.9948	0.7277
FAME85	0.0005912	2.283e+04	0.9831	6.789
FAME100	0.0006128*	2.286e+04	0.9782	9.732

*Legend: *coefficient is not statistically significant*

Table 6 Coefficients of Vogel kinematic viscosity model and its statistical indicators

Vogel	ν_0 [mm^2/s]	b [K]	c [K]	R^2	SSE
D100	0.6729	122	-228.2	0.9965	1.50700
FAME7	0.2568	329	-175.7	0.9997	0.02744
FAME10	0.4134	225.6	-195.8	0.9992	0.08746
FAME15	0.4505	215.4	-197.9	0.9985	0.18340
FAME20	0.3377	271.6	-187.6	0.9995	0.06189
FAME30	0.1632	456.3	-158.4	0.9998	0.03188
FAME85	0.5419	234.3	-199.4	0.9987	0.52950
FAME100	0.7695	186.4	-208.1	0.9984	0.71520

In the following section graph of mathematical models for selected blend and three-dimensional graph of kinematic viscosity/concentration/temperature are shown.

In the Figure 1 we can see that measured values which are expressed like small circles in the graph are tracked best by Vogel model. Also, it can be seen that the temperature dependence of kinematic viscosity and the effect of the FAME concentration in diesel prove a nonlinear dependence described also by Kumbár et al. (2015) and Hlaváčová et al. (2018). Furthermore, as higher FAME content in blends is as the curve slope is more significant. From the three-dimensional graph using the colour scale we can see areas with lower slope (blue) and areas with sharper slope (orange, red). It can be clearly seen that the viscosity-temperature dependence is most significant for pure FAME (FAME100) and then for FAME85 in temperatures around -5°C (~ 270 K).

Temperature-dependent viscosity of FAME/diesel blends is also described by Sajjadi et al. (2016) and Merkisz et al. (2016) with similar results. Furthermore, it was also found by Pelegrini et al. (2017) nonlinear viscosity behavior of FAME/diesel blends. Similar behavior of FAME/diesel blends in very low temperature was observed also in paper by Sirviö et al. (2019). One of the results of our paper is the fact that the Vogel model is the most appropriate for temperature-dependent viscosity description. Good results by using the Vogel model were also published by Trost et al. (2021) for biobutanol/gasoline blends.

Figure 1 Mathematical model graph for FAME 7 kinematic viscosity

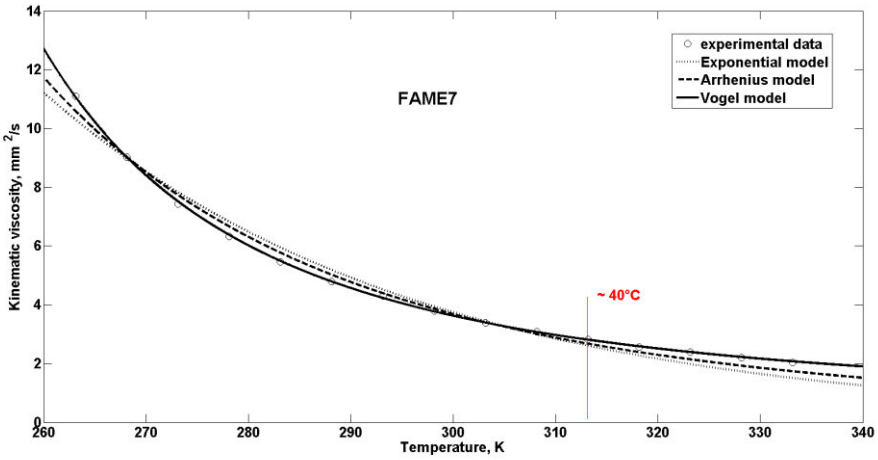

Figure 2 Three-dimensional kinematic/viscosity/temperature graph for FAME/diesel blends

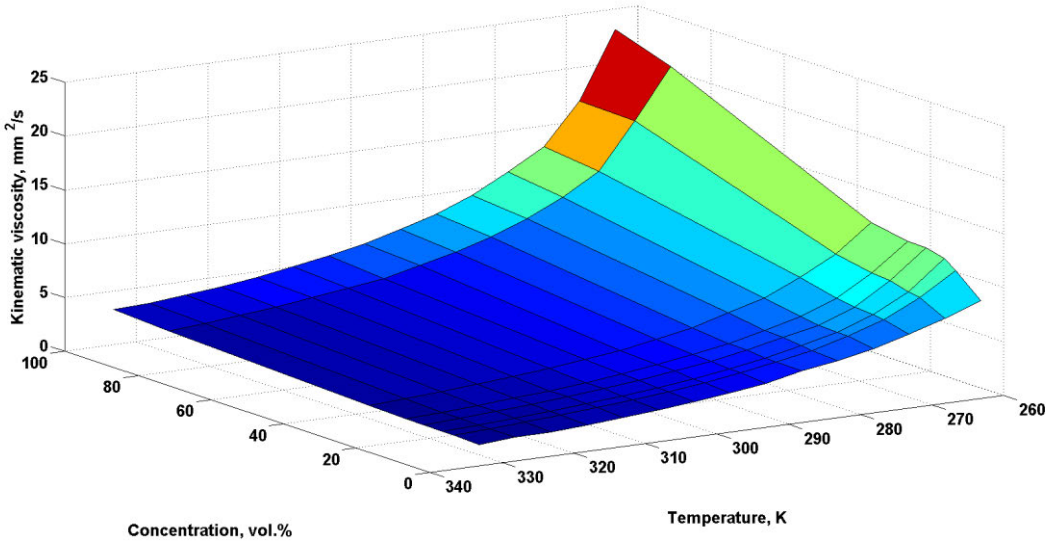

CONCLUSION

In this paper, three various mathematical equations for temperature-dependent viscosity modelling were compared. Eight fuels, six FAME/diesel blends were tested and evaluated. The results show that all used mathematical models are convenient for modelling FAME/diesel blends. Based on the obtained results partial conclusions are summarized.

- The viscosity of FAME/diesel blends decreases with increasing temperature.
- FAME/diesel blends with a higher FAME content have a higher viscosity.
- Arrhenius and Vogel model are applicable only for non-negative values of functional dependence. The Kelvin temperature scale must be used for these models. In the case of use Celsius temperature scale is Exponential model the most versatile one.
- The best results were obtained by Vogel model which reached average $R^2 = 0.999$ and smallest SSE
- It can be stated that used mathematical models were chosen appropriately, considering the coefficient of determination R^2 was ≥ 0.974.

Results obtained in this experiment might be applicable in industrial practice. For instance, the data could be used to set the car's control unit, which might be able to evaluate the exact amount of fuel needed for injection into the combustion chamber, thanks to using our published model coefficients.

REFERENCES

Alptekin, E., Canakci, M. 2008. Determination of the density and the viscosities of biodiesel–diesel fuel blends. Renewable Energy, 33(12): 2623–2630. Available at: https://www.sciencedirect.com/science/article/pii/S0960148108000773. [2021-09-14].

Čedík, J. et al. 2018. Effect of Biobutanol-Sunflower Oil-Diesel Fuel Blends on Combustion Characteristics of Compression Ignition Engine. Acta Technologica Agriculturae [Online], 21(4): 130–135. Available at: https://doi.org/10.2478/ata-2018-0024. [2021-09-14].

EN 590:2013+A1:2017. Automotive fuels. Diesel. Requirements and test methods. Finnish Petroleum and Biofuels Association.

European Commission. 2017. 2030 climate & energy framework [Online]. Available at: https://ec.europa.eu/clima/policies/strategies/2030_en [2021-09-15].

Hlaváčová, Z. et al. 2018. Selected physical properties of various diesel blends. International Agrophysics [Online], 32(1): 93–100. Available at: https://doi.org/10.1515/intag-2016-0095. [2021-09-15].

Kumbár, V. et al. 2015. Physical and Mechanical Properties of Bioethanol and Gasoline Blends. Listy cukrovarnické a řepařské [Online], 131(3): 112–116. Available at: http://www.cukr-listy.cz/on_line/2015/PDF/112-116.pdf. [2021-09-15].

Kumbár, V., Votava, J. 2015. Effect of the Rapeseed Oil Methyl Ester Component on Conventional Diesel Fuel Properties. Scientia Agriculturae Bohemica [Online], 45(4): 254–258. Available at: https://doi.org/10.1515/sab-2015-0006. [2021-09-14].

Merkisz, J. et al. 2016. Rapeseed oil methyl esters (RME) as fuel for urban transport. Alternative Fuels, Technical and Environmental Conditions [Online]. Available at: https://doi.org/10.5772/62218. [2021-09-14].

Peleg, M. 2017. Temperature–viscosity models reassessed. Critical Reviews in Food Science and Nutrition [Online], 58(15): 2663–2672. Available at: https://www.tandfonline.com/doi/full/10.1080/10408398.2017.1325836. [2021-09-14].

Pelegrini, B.L. et al. 2017. Thermal and rheological properties of soapberry Sapindus saponaria L. (Sapindaceae) oil biodiesel and its blends with petrodiesel. Fuel [Online], 199: 627–640. Available at: https://doi.org/10.1016/j.fuel.2017.02.059. [2021-09-15].

Pexa, M. et al. 2014. Mixture of Oil and Diesel as Fuel for Internal Combustion Engine. Advanced Materials Research [Online], 1030(1032): 1197–1200. Available at: https://doi.org/10.4028/www.scientific.net/AMR.1030-1032.1197. [2021-09-15].

Sajjadi, B. et al. 2016. A comprehensive review on properties of edible and non-edible vegetable oil-based biodiesel: Composition, specifications and prediction models. Renewable and Sustainable Energy Reviews [Online], 63: 62–92. Available at: https://doi.org/10.1016/j.rser.2016.05.035. [2021-09-15].

Sirviö, K. et al. 2019. Behavior of B20 fuels in arctic conditions. Agronomy Research [Online], 17(S1), 1207–1215. Available at: 9 https://doi.org/10.15159/AR.19.096. [2021-09-15].

Trávníček, P. et al. 2013. Selected physical properties of liquid biofuels. Research in Agricultural Engineering [Online], 59: 121–127. Available at: https://doi.org/10.17221/14/2013-RAE. [2021-09-15].

Trost, D. et al. 2021. Temperature Dependence of Density and Viscosity of Biobutanol-Gasoline Blends. Applied Sciences [Online], 11(7): 3172. Available at: https://doi.org/10.3390/app11073172. [2021-09-15].

The evaluation of lawn quality cut performed by a robot lawn mower

Lukas Vastik, Vladimir Masan, Patrik Burg, Pavel Zemanek
Department of Horticultural Machinery
Mendel University in Brno
Zemedelska 1, 613 00 Brno
CZECH REPUBLIC

xvastik@mendelu.cz

Abstract: The lawn areas are the dominant part of the private as well as public greenery when it comes to the size of the area and requirements on the maintenance. Their functions significantly depend on the quality and frequency of maintenance. Financial and technological conditions enabled the expansion of robot lawn mowers with autonomous mowing. As this is a relatively new technique, its effect on the quality of the lawn itself is not yet sufficiently known. Therefore, this area of technological operation was also monitored within the operating area of the Faculty of Horticulture of Mendel University in Brno. Based on the three years' experience of robot lawn mower service, a generally positive effect on the lawn have been monitored. There was a statistically significant reduction in higher weeds such as dandelion (*Taraxacum officinale*). On the other hand, it seems hard to limit lower weeds, for example Clover (*Trifolium* sp.), which leaves grow below the height of mowing, lie down to the soil surface and at these low height form inflorescences. Regular mowing did not increase the formation of lawn thatch. The mowing technology have been adapted to regular irrigation, especially during the summer.

Key Words: maintenance management, lawn maintenance technology, urban lawns, mulch, fertilizer

INTRODUCTION

Grassy and similar areas represent the predominant green areas nowadays. The share of these areas within urban greenery represents up to 70% (Niesel and Breloer 2006, Simek and Stefl 2020). According to the development, both at home and abroad, this share will constantly increase. The most numerous, time-consuming, and financially demanding maintenance intervention is by far mowing. Classic mowing, with collecting the cut material, is the most common technology applied in both urban and private sector. But there are negatives. Driving the heavy equipment with a full basket of grass causes gradual selection of more persistent and less attractive types of grass, the formation of lawn thatch, and many others.

On the other hand, mulching is becoming an alternative method. Particularly the managers of urban greenery see this method as more economic. The reason is the absence of costly collection and disposal of grass, and saving fuel (Vastik and Masan 2020, Knot et al. 2017). Mulching also reduces the need for nitrogen fertilization. The organic matter left on the ground gradually decomposes and the nutrients it contains are available for the plants again. This created biomass, which sunk to the soil surface, supports the branching of grasses, the diversity of grass species, which contributes to largening the area covered by grass and reduces weeds. A number of studies that have looked at this effect have confirmed a reduction in nitrogen requirements of 30–50%, depending on grass species and the frequency of mulching substitution for mowing (Knot et al. 2017, Liu and Hull 2006).

Recently, another new technology has been on the rise. The autonomous robot lawn mowers. The expansion of the technology itself enabled a shift in development of autonomous guidance, the necessary sensors, capacity, and battery life. A considerable reason is also the pressure to reduce greenhouse gas emissions, increase engine efficiency, the availability of skilled labour, and higher comfort in the maintenance of private lawns. Another advantage of this method is the electrical operation with immediate deployment, as the machine remains constantly on the surface and especially when in autonomous mood it operates without the need for intervention or guidance by the operator (Masek et al. 2016). The principle of robot lawn mowers is to constantly separate small increments of grass (1–

3 mm), which fall on the surface, where they subsequently decompose. This means mowing without harvesting.

The increased frequency of such mowing may evoke the higher standard of lawn, which has unfortunately not yet been verified in normal operating practice. The aim of this monitoring was to evaluate the influence of a robot lawn mower on the quality of lawn, its weeding and species composition, as well as its operating conditions.

MATERIAL AND METHODS

Characterization of locality, experimental design and mowers

The monitored lawns are in the area of the MENDELU Faculty of Horticulture campus (48°47'46.0"N 16°47'54.8"E). Two variants of mowing management were used; A-area with robot lawn mower (without collecting grass) and B-area with mowers (with collecting grass), (Figure 1). A-area has an area of 1600 m^2 and B-area has an area of 1000 m^2. The number of obstacles, fragmentation of the areas and other parameters were about the same for both areas.

Figure 1 Monitored lawns

Legend: A-area with robot lawn mower (without collecting grass) and B-area with mowers (with collecting grass).

These lawns were established in 2011 and by 2018 they were mowed only with classic lawn mower with collecting technology. Since 2019, mowing has been performed by a robot lawn mower. Mowing on the area is programmed from 7:00 to 18:00, at night the lawn is irrigated by an automatic irrigation system. The lawn is regularly scarified twice a year, with minimal herbicide treatment and twice a year fertilized with NPK fertilizer at a dose of 20 g/m^2.

The robot lawn mower (HUSQVARNA AUTOMOWER® 535 AWD) rides on the surface for about two hours, then charges for about an hour. This cycle repeats four times during the day and the entire area is mowed in about three days. The working device consists of a spinning disc lined with multiple razor blades, with a working width of 200 mm. The cutting height is set to 50 mm.

Another lawn was cut by a lawn mower tractor (SECO Starjet Exclusive UJ 102-22) and a lawn mower (HONDA HRX 537) approximately in one- or two-weeks intervals.

The evaluation of lawn condition took place before the deployment of the machine in 2018, during the spring, summer and autumn term and is repeated since then. The evaluation is performed on pre-defined areas of 1 m^2. It is based on measuring the height of the stand after mowing (observance of the set cutting height), visual evaluation of the aesthetic function of the grass area (vegetation cover, disturbing elements such as weeds, frayed stalk ends, recumbent stalks, lawn thatch), weed proportion (the area of weeds in comparison to the area of lawn) and the weed species.

It was evaluated annually, approximately from the end of April (after the first mowing) to the end of October (after the last mowing) twice a month. Five experimental plots with an area of 1 m^2 were on each variant (2x in the sun, 2x in partial shade, 1x in the shade).

Lawn involvement and weeds were measured as overgrown area in %. The height of the lawn thatch was measured with a tape measure from the soil surface. Involvement of grass and weed was measured as a percentage of coverage area.

Statistical analysis

A statistical analysis was performed using the software package "Statistics 12.0" (StatSoft Inc., Tulsa, Oklahoma, USA). Results were reported as averages and standard deviation. Analysis of variance was conducted, and the results were compared using Tukey's range test at a significance level of $P < 0.05$.

RESULTS AND DISCUSSION

Lawn quality

A frequently discussed topic when using robot lawn mowers is a different way of maintaining the lawn and its effect on the quality of lawn and the quality of mow. Regular mowing and maintaining a low mowing height should result in a higher vegetation density with a higher proportion of grasses with a narrower leaf blade. Grass species should respond to frequent mowing by better rooting in the area just above the soil.

Table 1 Effect of different mowing management on lawns parameters (n=90)

Surface	Vegetation cover (%)	Frayed stalk ends (yes/no)	Recumbent stalks (yes/no)	Lawn thatch (mm)	Weed proportion (%)
A	93.89±2.6^a	1.40^a	1.18^a	2.00±0.6^a	3.13±0.9^a
B	91.78±3.8^a	1.29^a	1.11^a	3.02±1.0^b	4.04±1.8^b

Legend: Data are expressed as means ± standard deviation; Mean values in one column followed by the same letter were not significantly different from each other by Tukey's test at $P < 0.05$.

The mentioned hypotheses were confirmed (Table 1), especially in the reduction of lawn thatch. No statistically significant differences in lawn vegetation cover, frayed stalk ends and recumbent stalks were found. On the other hand, the number of frayed grass ends and the number of lying stalks increased when the robot lawn mower was used. In our opinion, the increase in the values of these parameters is closely related to the frequency and principle of mowing by using a robot lawn mower and began to show significantly after the first year of use. This results confirmed with Grossi et al. (2016) or Pirchio et al. (2018b).

Weeds

Increasing the vegetation cover of lawn is expected to significantly reduce the area for weed germination and growth (Magni et al. 2020). More frequent mowing also assumes that weed inflorescences are cut down and that they are not sifted. In particular, the reduction of weeds is the most common monitored parameter in lawn maintenance directly influencing its aesthetics, which is becoming increasingly important due to the trend of reducing herbicides and more ecological maintenance.

The problem was weeds with harder above-ground parts that were not sufficiently mown or their cutting surface was frayed, which reduces the aesthetic value of the lawn.

A lower incidence of higher weeds has occurred such as Common dandelion (*Taraxacum officinale*). Regular mowing at shorten intervals leads to shorter reproductive organs of these weeds, which significantly limits their spread. However, it is necessary to change the knives regularly, otherwise there is no perfect mowing of harsh leaves and weeds, even with inflorescences, lie below the cutting height.

On the other hand, it is not possible to limit lower weeds, for example Clovers (*Trifolium* sp.), which develop their leaf area below the height of mowing, lie down until they crawl on the soil surface

and at this low height can even form inflorescences (Pirchio et al. 2018a). Fortunately, they are not so noticeable in the lawn, so the resulting aesthetic effect is very good.

Based on the 3 years' experience of robot lawn mower operation, a generally positive effect can be mentioned. Modern mowing technology has also an impact on maintenance of lawn. The lawn needs to be adapted for subsequent maintenance interventions. In particular, regular irrigation in the summer is needed. Otherwise, the constantly mown lawn could be exhausted and dried.

Different authors recommend, that it is necessary to apply at least a basic amount of mineral fertilizer in order to maintain the quality of the lawns, when it comes to long term period. An annual sowing is also recommended, so that no bushy species are selected in the lawn, which in the extreme case can also affect the driving of the machine, or species with coarse blades, which are less difficult to mow with this technology. An example is the use of Red fescue (*Festuca rubra*) and its cultivars (Braun et al. 2020). On the other hand, the problem is the Tall fescue (*Festuca arundinacea*), which has a wide and harsh leaf blade (± 4 mm) and is disturbing in the lawn.

From various observations, a lawn mowing height between 50 and 80 mm can be recommended. The mowed lawn has a deep and robust root system, which reduces the need for water and chemical inputs, including fertilizers, and supports the cover and thickening of the vegetation (Dobbs et al. 2014, Debels et al. 2012, Turgeon 2005, Voigt et al. 2001) This recommendation was followed during the monitored maintenance.

CONCLUSION

Within robot lawn mowers technology appear also more advanced mowing management technologies, which correspond to industry 4.0. Those simplier include measuring the resistance on knives to evaluate the density of vegetation, or the planning of mowing based on data from the weather station.

These robots appear in both, private as well as public gardens. According to the results of 3 years monitoring, the quality of mowing is better or at least comparable, although the entire area of maintenance management needs to be adapted to this technology. The deployment of technology had a positive effect on the reduction of lawn thatch and weeds. On the contrary, no statistically significant differences in lawn vegetation cover, frayed stalk ends and recumbent stalks were found.

ACKNOWLEDGEMENTS

This paper was supported by the project CZ.02.1.01/0.0/0.0/16_017/0002334 Research Infrastructure for Young Scientists, this is co-financed from Operational Programme Research, Development and Education.

REFERENCES

Braun, R. et al. 2020. Establishment of low-input turfgrass from seed with patch and repair mixtures: Mulch and starter fertilizer effects. Crop Science [Online], 60(6): 3362–3376. Available at: https://doi.org/10.1002/csc2.20266. [2021-08-08].

Debels, B. et al. 2012. Evaluation of Mowing Height and Fertilizer Application Rate on Quality and Weed Abundance of Five Home Lawn Grasses. Weed Technology [Online], 26(4): 826–831. Available at: https://doi.org/10.1614/WT-D-12-00062.1. [2021-08-08].

Dobbs, E.K., Potter, D.A. 2014. Conservation Biological Control and Pest Performance in Lawn Turf: Does Mowing Height Matter? Environmental Management [Online], 53(3): 648–659. Available at: https://doi.org/10.1007/s00267-013-0226-2. [2021-08-08].

Grossi, N. et al. 2016. Autonomous Mower Saves Energy and Improves Quality of Tall Fescue Lawn. HortTechnology [Online], 26(6): 825–83. Available at: https://doi.org/10.21273/HORTTECH03483-16. [2021-08-08].

Knot, P. et al. 2017. The impacts of different management practices on botanical composition, quality, colour and growth of urban lawns. Urban Forestry & Urban Greening [Online], 26: 178–183. Available at: https://doi.org/10.1016/j.ufug.2017.01.011. [2021-08-08].

Liu, H., Hull, R.J. 2006. Comparing Cultivars of Three Cool-season Turfgrasses for Nitrogen Recovery in Clippings. HortScience [Online], 41(3): 827–831. Available at: https://doi.org/10.21273/HORTSCI.41.3.827. [2021-08-08].

Magni, S. et al. 2020. Autonomous Mowing and Turf-Type Bermudagrass as Innovations for An Environment-Friendly Floor Management of a Vineyard in Coastal Tuscany. Agriculture [Online], 10(5): 189. Available at: https://doi.org/10.3390/agriculture10050189. [2021-08-08].

Masek, J. et al. 2016. Effect of soil tillage technologies on soil properties in long term evaluation. In Proceeding of 6th international conference on trends in agricultural engineering 2016. Prague, Czech Republic, 7–9 September, Prague: Czech University of Life Sciences Prague, pp. 391–397. Available at: https://hdl.handle.net/20.500.12259/89743. [2021-07-02].

Niesel, A., Breloer, H. 2006. Grünflächen-Pflegemanagement: dynamische Pflege von Grün; 45 Tabellen. Stuttgart (Hohenheim): Ulmer.

Pirchio, M. et al. 2018a. Autonomous Mower vs. Rotary Mower: Effects on Turf Quality and Weed Control in Tall Fescue Lawn. Agronomy [Online], 8(2): 15. Available at: https://doi.org/10.3390/agronomy8020015. [2021-08-08].

Pirchio, M. et al. 2018b. Comparison between Different Rotary Mowing Systems: Testing a New Method to Calculate Turfgrass Mowing Quality. Agriculture [Online], 8(10): 152. Available at: https://doi.org/10.3390/agriculture8100152. [2021-08-08].

Simek, P. Stefl, L. 2020. Plán péče a náklady na udržovací péči. In Inspirace. Brno: SZUZ, pp. 31–33.

Turgeon, A.J. 2005. Turfgrass Management. 7th ed., Upper Saddle River, NJ: Pearson Prentice Hall.

Vastik, L., Masan, V. 2020. Vzájomné porovnanie efektivity a nákladovosti mulčovania a kosenia trávnikov v závislosti na členitosti plochy. Agritech Science [Online], 14(1): 1–8. Available at: http://www.agritech.cz/clanky/2020-1-4.pdf. [2021-08-08].

Voigt, T.B. et al. 2001. Influence of mowing and nitrogen fertility on tall fescue turf. International Turfgrass Society Research Journal, 9: 953–956.

APPLIED CHEMISTRY AND BIOCHEMISTRY

Exploring the pH-triggerable structure of siRNA-carrying liposomal nanoparticles as tools for treatment of hepatitis B

Zdenek Kratochvil[1, 2], Tomas Do[1, 2]
[1]Department of Chemistry and Biochemistry
Mendel University in Brno
Zemedelska 1, 613 00 Brno
[2]Central European Institute of Technology
Brno University of Technology
Purkynova 123, 612 00 Brno
CZECH REPUBLIC

zdenek.kratochvil@mendelu.cz

Abstract: Gene therapy using small interfering RNA (siRNA) molecules provides silencing of undesirable genes on mRNA translational level, which eliminates potential risks related to interactions with genomic DNA of the cell. However, due to their instability, these siRNA molecules must be delivered to the site of action *via* sophisticated delivery system. In this research work, we opted for liposomal vectors modified with polyethylene glycol chains attached by a pH-sensitive linkage. These liposomal nanoparticles were monitored in different buffer and pH conditions to verify some of their physicochemical properties required for an efficient siRNA delivery. Results from light scattering methods and cryo-transmission electron microscopy revealed that higher ionic strength environment reduced the diameter and zeta potential of the nanoparticles and that mildly acidic pH (6.0) caused structural changes leading to aggregation of the nanoparticles. These findings predetermine their favourable behaviour in biological systems.

Key Words: siRNA therapeutics, lipid nanoparticles, PEGylation, oxime linkage, pH-triggerability

INTRODUCTION

The discovery of RNA interference capable of gene silencing at the mRNA translational level using siRNA molecules can be considered the most topical therapeutic breakthrough in recent gene therapy (Whitehead et al. 2009). These small double-stranded oligonucleotides are designed to interrupt the production of an undesirable protein by ultimate targeting of a particular mRNA sequence. Moreover, they do not interact with DNA, unlike gene editing tools (Hu et al. 2020, Haghiralsadat et al. 2018). Therefore, siRNA therapeutics are the subject of studies addressed to silencing of viral genes (Zhang et al. 2004, Shen et al. 2012). Their effectivity is, however, highly dependent on the smartness of a delivery system. To avoid safety risks of viral vectors, non-viral formulations such as cationic lipid-constituting liposomes have turned out to be a very encouraging option for RNA therapy (Yin et al. 2014, Safinya et al. 2014).

Since physicochemical properties of liposomes are affected by the composition of lipid formulation used during their preparation, our liposomal structures include several types of lipids, one of which allows their surface modification providing thermodynamic stability and efficient delivery to the cells of interest (Xia et al. 2016). This will be achieved using click chemistry *via* oxime linkage that is pH-sensitive and disintegrates with decreasing pH within an endosome upon cellular uptake. The exposed liposomal lipids will fuse with the endosomal membrane, resulting in the release of siRNA cargo that will cause knockdown of target gene expression (Miller 2008, Carmora et al. 2009).

This study focuses on characterization of prepared siRNA-carrying liposomal nanoparticles aimed at treatment of hepatitis B and monitoring of their pH-triggerable structure at pH conditions simulating the endosomal environment optimal for efficient endosomal escape.

MATERIAL AND METHODS

First, empty liposomes were prepared by injection of heated lipid mixture containing cationic lipid DODAG (N',N'-dioctadecyl-N-4,8-diaza-10-aminodecanoylglycine amide), neutral phospholipid DOPE (1,2-dioleoyl-sn-glycero-3-phosphoethanolamine), rigid cholesterol and coupling lipid CPA (cholesteryl-PEG^{350}-aminoxy lipid) into an excess of aqueous phase (4mM HEPES), further by evaporation of the lipid solvent and extrusion procedure to achieve a uniform size. The siRNA was passively encapsulated into the empty liposomes employing electrostatic interactions. The surface of these complexes was subsequently modified with polyethylene glycol (PEG) propionaldehyde which was coupled at pH 4 with the exposed aminooxy group of CPA lipid to form covalent oxime linkage. After the correction to the neutral pH, mass spectrometry (MALDI-TOF) was employed to confirm the surface modification with PEG (PEGylation). Nanoparticle size distribution and zeta potential were determined by light scattering techniques at three different buffering conditions.

Subsequently, the pH of PEGylated liposomal nanoparticles was adjusted to 6.2; 6.0 and 5.8 to simulate the conditions of maturing endosome including the higher ionic strength. Using dynamic light scattering, the size distributions were recorded and compared with the initial sample. To monitor the structural changes of the nanoparticles upon pH change cryo-transmission electron microscopy (cryo-TEM) was used for both low and high ionic strength samples.

RESULTS

After siRNA encapsulation and surface PEGylation, the liposomal nanoparticles got naturally larger in comparison with empty liposomes as did their zeta potential (ζ). Surprisingly, the polydispersity index (PdI) did not change significantly (see Figure 1A, left). When increasing the buffer ionic strength with 20mM HEPES, 135mM NaCl, the mean of the particle size distribution was shifted back to the initial region, however, increasing PdI. Using PBS buffer, PdI remained almost the same and the size distribution mean was reduced by more than 30 nm. In both cases, a substantial decrease of zeta potential was observable (see Figure 1B, right).

Figure 1 Impact of siRNA encapsulation, PEGylation and different buffering conditions on physicochemical parameters of liposomal nanoparticles (A), zoomed MALDI-TOF spectrum of siRNA-carrying PEGylated liposomal nanoparticles (B)

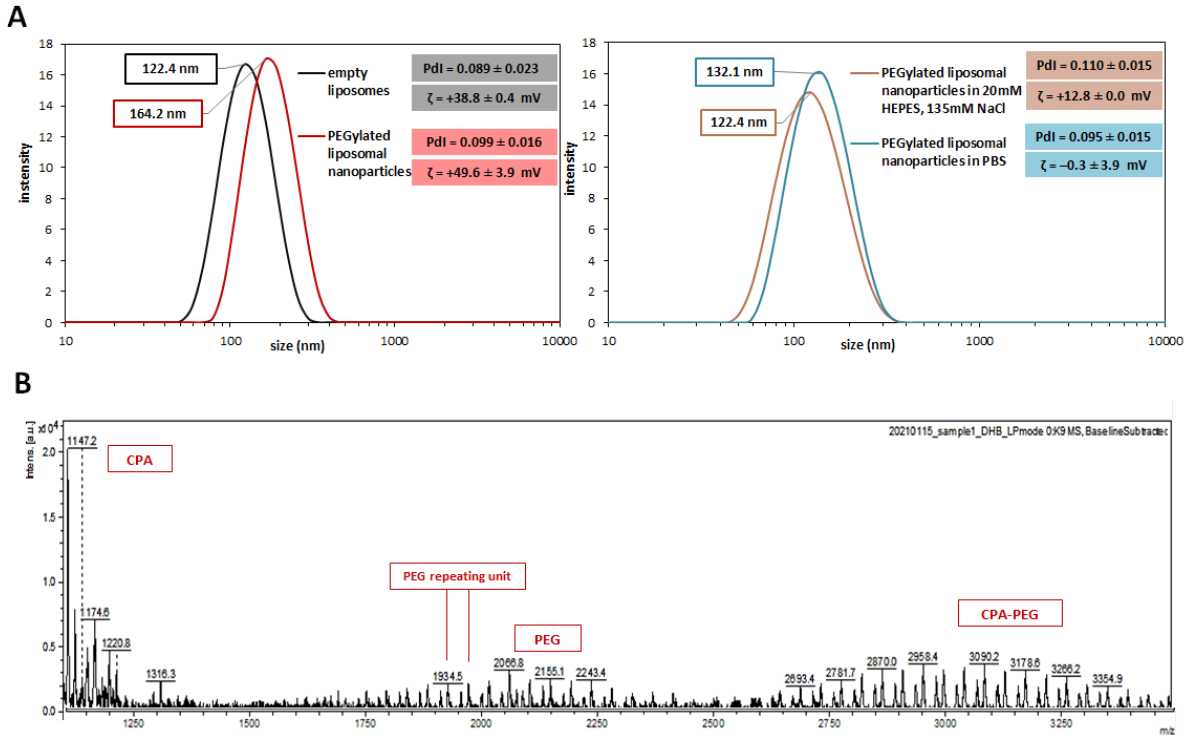

The MALDI-TOF spectrum (see Figure 1B) displays the regions of masses corresponding to CPA lipid (including its sodium or potassium adducts), PEG (also depicting the additions of the individual PEG monomers) and CPA-PEG conjugate, thus, confirming the attachment of PEG onto the liposomal surface.

Upon pH reduction at high ionic strength buffering conditions, we could notice the increase of PdI at all tested pH values, but, nevertheless, the mean of the particle size distribution remained nearly the same. However, some aggregates at about 5 µm appeared when speaking about the liposomal nanoparticles at pH 6.0 and 6.2 (see Figure 2A). The cryo-TEM images (see Figure 2B) show the real structure of siRNA-carrying PEGylated liposomal nanoparticles at various conditions. At a low ionic strength buffer, they are forming rather bilamellar structures with some ruptures at mildly acidic pH. On the other hand, there are observable multilamellar nanoparticles at a high ionic strength buffer, giving rise to large aggregated and disintegrated structures at mildly acidic pH. The diameter of particles captured by cryo-TEM matches the results obtained from dynamic light scattering.

Figure 2 Differences in liposomal nanoparticle size distribution upon pH reduction (A), cryo-TEM micrographs of siRNA-carrying PEGylated liposomal nanoparticles at various conditions (B)

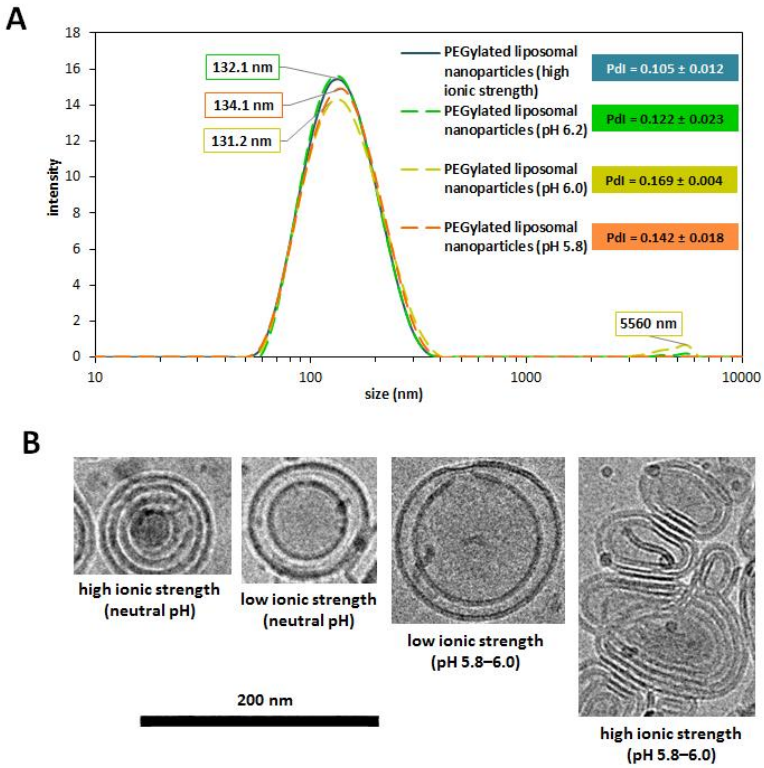

DISCUSSION

The MALDI-TOF data verified that the coupling of PEG with the liposomal surface *via* oxime linkage takes place in aqueous environment, which eliminates the need for complicated multistep synthesis and purification procedures. When transferring these modified liposomal nanoparticles into higher ionic strength conditions, they partially shrink probably due to some repulsive forces caused by higher salt concentrations. In the same way, the zeta potential is reduced significantly and the particles appear to be nearly neutral. Both these facts imply their biological benefits, since such nanoparticles become thermodynamically stable and almost invisible to the immune system, resulting in prolonged blood circulation time without any interactions with blood elements (Tirosh et al. 1998, Xia et al. 2016). On the other hand, when the PEG-coating was missing, the siRNA-carrying liposomal nanoparticles agglomerated to bigger clusters under higher ionic strength conditions most likely owing to the absence of a stabilizing component (data not shown). The data from dynamic light scattering and cryo-TEM also confirmed their pH-triggerable nature based primarily on the pH-sensitivity of formed oxime linkage which is favourable for the whole liposome structure destabilization within an endosome, efficient

endosomal escape and intracellular trafficking of therapeutic siRNA. However, the pH-threshold for destabilisation of the nanoparticle structure (in this work observed at pH values about 6.0) slightly differs from the results of the study (Kolli et al. 2013) where the pH-triggered structural changes occurred at pH 5.5. Compared to our results, such difference could be explained by the use of PEG-dialdehyde for surface modification of their nanoparticles. The reactive groups on both PEG termini could lead to the formation of polymer hairpins on the liposomal surface making the whole structure more rigid and, thus, requiring more acidic pH for its destabilization.

CONCLUSION

This study provided information on how different buffering and pH conditions affected structural behaviour of siRNA-carrying liposomal nanoparticles modified with PEG by a simple coupling reaction. The results achieved in this work anticipate great biologically beneficial characteristics of the liposomal nanoparticles that might be regarded as a serious option for non-viral delivery of therapeutic RNA molecules in clinical practice some day.

ACKNOWLEDGEMENTS

The authors gratefully acknowledge financial support from IGA MENDELU funding (AF-IGA2021-IP057) and Brno City Municipality (Brno Ph.D. Talent Scholarship). Cryo-transmission electron microscopy images were kindly provided by Jiří Nováček, Ph.D. (Cryo-Electron Microscopy and Tomography Core Facility, CEITEC, Brno, Czech Republic).

REFERENCES

Carmona, S. et al. 2009. Controlling HBV replication in vivo by intravenous administration of triggered PEGylated siRNA-nanoparticles. Molecular Pharmaceutics, 6(3): 706–717.

Haghiralsadat, F. et al. 2018. Preparation of PEGylated cationic nanoliposome-siRNA complexes for cancer therapy. Artificial Cells, Nanomedicine, and Biotechnology, 46: 684–692.

Hu, B. et al. 2020. Therapeutic siRNA: state of the art. Signal Transduction and Targeted Therapy, 5: 101.

Kolli, S. et al. 2013. pH-triggered nanoparticle mediated delivery of siRNA to liver cells in vitro and in vivo. Bioconjugate Chemistry, 24(3): 314–332.

Miller, A.D. 2008. Towards safe nanoparticle technologies for nucleic acid therapeutics. Tumori, 94: 234–245.

Safinya, C.R., et al. 2014. Cationic liposome-nucleic acid complexes for gene delivery and gene silencing. New Journal of Chemistry, 38: 5164–5172.

Shen, H. et al. 2012. Nanovector delivery of siRNA for cancer therapy. Cancer Gene Therapy, 19: 367–373.

Tirosh, O. et al. 1998. Hydration of polyethylene glycol-grafted liposomes. Biophysical Journal, 74(3): 1371–1379.

Whitehead, K.A. et al. 2009. Knocking down barriers: advances in siRNA delivery. Nature Reviews Drug Discovery, 8: 129–138.

Xia, Y.Q., et al. 2016. Effect of surface properties on liposomal siRNA delivery. Biomaterials, 79(18): 56–68.

Yin, H., et al. 2014. Non-viral vectors for gene-based therapy. Nature Reviews Genetics, 15: 541–555.

Zhang, X.N. et al. 2004. siRNA-mediated inhibition of HBV replication and expression. World Journal of Gastroenterology, 10(20): 2967–2971.

Pesticides and long-term denitrification conditions

Kristina Panikova[1], Zuzana Bilkova[2], Jitka Mala[1]
[1]Institute of Chemistry, Faculty of Civil Engineering
Brno University of Technology
Zizkova 17, 602 00 Brno
[2]RECETOX, Masaryk University
Kamenice 753/5, Pavilion A29, 625 00 Brno
CZECH REPUBLIC

kristina.panikova@vutbr.cz

Abstract: Groundwater is an important source of drinking water in many countries. Over the last decade, pesticides have been found at higher concentrations in these waters. This is potentially dangerous for people and nature. For the future, it is very important to understand the behaviour of pesticides under denitrifying conditions, which are typical for groundwaters. The aim of this study was to investigate the behaviour of atrazine, terbuthylazine and tebuconazole under denitrifying conditions during 28 days. These conditions were simulated in a semi-continuous long-term laboratory test with a single dose of the test substance at the beginning of the test. After 28 days, none of the tested pesticides showed an inhibitory effect on denitrification; on the contrary, they had a stimulating effect of up to 10% (terbuthylazine). Biotic loss was only measured in the test with atrazine (9.8%). The dominant mechanism of the loss of all tested pesticides was adsorption (terbuthylazine 68.4%, tebuconazole 82.7%, and atrazine 30.6%). The lowest residual amount of pesticide in water was measured with tebuconazole (17.3%), followed by terbuthylazine (31.6%) and atrazine (59.6%).

Key Words: groundwater, biodegradation, adsorption, triazine pesticides

INTRODUCTION

Every year, the demand for agricultural products increases greatly. As a result, more chemicals (especially pesticides) are used to protect crops and promote their growth.

The contamination of groundwater by pesticide pollutants is a very serious environmental problem which poses a risk to human health (Barra Caracciolo et al. 2009). The pollution in groundwater is persistent and seems to be related to the frequency of pesticide application as well as to rainfall, soil permeability, aquifer recharge rate and the intensity of spraying (Caldas et al. 2010).

In many European countries, monitored groundwaters are contaminated by triazines, primarily atrazine, terbuthylazine and their desethyl-degradation metabolites (Barra Caracciolo et al. 2009). In the Czech Republic, the most commonly found pesticides (more than 15%) in surface and groundwaters are the metabolites of alachlor, chloridazon, metazachlor, metolachlor, glyphosate, acetochlor, atrazine and dimethachlor (Kodeš 2019).

The triazine herbicides atrazine (ATR) and terbuthylazine (TER) are very persistent in soil, water, plants and animals. ATR has the potential to cause tremors, cardiovascular damage, gene mutations and cancer (Navarro et al. 2004). Tebuconazole (TEB) is a systemic fungicide; it is used to control a wide range of fungi on fruits and vegetables (Caldas et al. 2010). This substance has toxic effects on non-target organisms (Cao et al. 2020).

As the number of aquifers that cannot provide potable water is increasing, it is necessary to investigate their behaviour and to study methods that will allow the removal of pesticides from groundwater (Barra Caracciolo et al. 2009). However, predicting the behaviour of pesticides in groundwater, where denitrifying conditions are typical, is a complex scientific and practical problem (Navarro et al. 2004).

The presented research examined the behaviour of three selected pesticides: ATR, TER, and TEB, using a long-term (28 days) laboratory test developed and optimized by the authors (Panikova 2021).

MATERIALS AND METHODS

Chemicals and organic carrier

ATR, TER, and TEB (PESTANAL® product line) were obtained from Sigma-Aldrich (Germany) at a purity higher than 98%. Pesticide stock solutions were prepared in analytical grade methanol at a concentration of 1000 mg/l and stored in the dark at 4 °C.

Poplar wood shavings, fraction 1.0–1.5 cm, were used as the source of organic carbon. Argon gas (purity 99.996%) was obtained from Linde Gas (Czech Republic).

The long-term denitrification test

The long-term denitrification test was developed and optimized by the authors (Panikova 2021). The laboratory test was designed as a semi-continuous test with a single dose of the test substance. The long-term test lasts 28 days. The test conditions are similar to those of a previously conducted and documented batch test (Panikova et al. 2020), but NO_3-N is added at seven-day intervals to maintain denitrification conditions.

Twelve 2-litre bottles were used for the tests. 25 grams of poplar wood shavings were weighed and inserted into each bottle, after which 2000 ml of deionized water containing KNO_3 and $NaHCO_3$ were added. The contents of the bottles were purged with argon until the concentration of dissolved oxygen (DO) dropped below 0.5 mg/l. The bottles were closed and incubated at $T = 20 \pm 0.5$ °C in the dark. After 48 hours, 25 ml samples of liquid phase were taken from every bottle and concentrations of NO_X-N, pH, and DO were analysed. The bottles were divided into three groups (Table 1) and the reagents were added. After mixing, 10 ml of liquid phase was taken from samples 2 and 3. These solutions were analysed for the initial concentration of pesticide. The bottles were closed and incubated at $T = 20 \pm 0.5$ °C in the dark. Each sample had four replicates.

Table 1 Overview of the sample types

Sample	Composition of liquid medium, solution in deionised water (DIW)	Description
1	KNO_3 (15 mg/l NO_3-N), $NaHCO_3$ (0.5 g/l), methanol (0.1 ml/l)	Denitrification in progress.
2	KNO_3 (15 mg/l NO_3-N), $NaHCO_3$ (0.5 g/l), the tested pesticide (100 µg/l; solution in 0.1 ml/l of methanol)	Denitrification and biodegradation in progress.
3	KNO_3 (15 mg/l NO_3-N), $NaHCO_3$ (0.5 g/l), the tested pesticide (100 µg/l; solution in 0.1 ml/l of methanol), $HgCl_2$ (6.5 mg/l, inhibitor of biological processes)	Biological processes are stopped.

Every 7 days, 25 ml samples of liquid phase were taken from each bottle for an NO_X-N analysis. The dose of KNO_3 solution (10 000 mg/l) was calculated for every bottle so that the concentration of NO_X-N was the same as the initial concentration (15 mg/l). After the appropriate dose of KNO_3 was added, the bottles were closed and incubated.

The tests were terminated after 28 days. Immediately after opening, liquid phase from samples 2 and 3 was collected for the analysis of the tested pesticide. The remaining liquid phase was filtered through filter paper for a KA2 qualitative analysis, and concentrations of NO_X-N, NO_2-N, pH, DO and chemical oxygen demand (COD) were measured in the supernatant.

Analytical methods

The laboratory analyses were performed as follows: DO and pH with a Hach HQ40D multi meter, COD via the semi-micro method with potassium dichromate and photometric evaluation, and NO_X-N (NO_3-N+ NO_2-N) via the UV absorption method with a Hach optical Nitratax plus sc Sensor. NO_2-N values were measured using a spectrophotometer via α-naphthol.

Pesticides were extracted from the water samples using solid phase extraction cartridges. High-performance liquid chromatography analysis was performed using an Agilent 1200 chromatographic

system (Agilent, Santa Clara, CA, USA) equipped with an Agilent Triple Quad 6410 mass spectrometer (Agilent, Santa Clara, CA, USA).

Evaluation of the data

The effect of pesticides on the denitrification process was evaluated from their inhibition of the denitrification rate, which was calculated as the amount of NO_X-N removed per time unit. The effect of the tested substance was evaluated from the difference between the denitrification rates of samples 1 and 2.

The loss of the tested substance due to adsorption was assessed from the decrease in its concentration in sample 3. The decrease in the tested substance due to biodegradation was assessed by comparing the decrease in concentrations of the tested substance in samples 2 (biotic loss + abiotic loss) and 3 (abiotic loss).

RESULTS AND DISCUSSION

Test conditions

During the test, acidic substances are released from the poplar wood shavings, which can affect the pH (Panikova 2021). A dose of 0.5 g/l of $NaHCO_3$ was added to maintain optimal pH, which lies between 7 and 8 (Paul 2007). At the end of the tests, the following average pH values (sample 1 and 2) were determined for the respective tested compounds: TER 7.72 ± 0.20, ATR 7.49 ± 0.14, and TEB 7.76 ± 0.09 (Table 2). All measured pH values were in the optimal range.

Table 2 Conditions at the end of the tests (samples 1 and 2)

Parameter	TER	ATR	TEB
pH (-)	7.72 ± 0.20	7.49 ± 0.14	7.76 ± 0.09
O_2 (mg/l)	2.01	2.30	1.40
NO_2-N (mg/l)	0.067 ± 0.022	0.296 ± 0.244	0.068 ± 0.026

During the denitrification process, the removed NO_3-N is converted to the nitrite NO_2-N, which can accumulate in the system (Hu et al. 2019). No difference was found between the average NO_2-N values. The average NO_2-N for TER was 0.067 ± 0.022 mg/l, for ATR 0.296 ± 0.244 mg/l, and for TEB 0.068 ± 0.026 mg/l. For all the pesticides tested, concentrations of DO above 0.5 mg/l were measured in the analysed samples without inhibitor (samples 1 and 2) (Table 2). The higher DO values did not disturb the denitrification process, which probably continued in the micropores of the poplar wood shavings, where the DO concentration was lower, as is the case with the denitrification process inside flakes of activated sludge (Daigger et al. 2007). A COD of more than 100 mg/l was found in all test bottles. This COD value is sufficient for the denitrification process (Lahdhiri et al. 2017).

Inhibition of denitrification

The results in Table 3 indicate that the denitrifying conditions were maintained throughout all the tests. For all of the pesticides tested, a slight stimulation of the denitrification process at a concentration of 0.1 mg/l was observed. The highest value was achieved in the case of TER, namely 10.0%. In the case of ATR and TEB, the stimulation was at the same level of 6.9%. The result with ATR was in accordance with the reports of Ilhan et al. (2011), who observed that denitrification rates were not inhibited by ATR concentrations of 5 mg/l. No studies on the stimulative or inhibitive effects of TER and TEB on denitrification rates in water have yet been published in the literature.

Table 3 Average denitrification rates during tests

	r_D (mg/l/d)		
Sample	TER	ATR	TEB
1	1.09	1.10	0.98
2	1.21	1.18	1.06
Stimulation	10.0%	6.9%	6.9%

The fate of the pesticides

The degradation of pesticides involves both biotic (mediated by microorganisms or plants) and abiotic (chemical and photochemical reactions) transformation processes (Fenner et al. 2013). In our experiment, the abiotic loss was dominant in the cases with TER 68.4% and TEB 82.7% (Figure 1). The average abiotic loss with ATR was 30.6%. This is in accordance with the results of experiments by Yue et al. (2017), who observed the adsorption of ATR on different types of soil: After 24 hours, the adsorption of ATR was approximately 27.8% for laterite, 21.5% for rice field soil, and 19.3% for alluvial soil.

Figure 1 Proportion of individual processes during the denitrification process

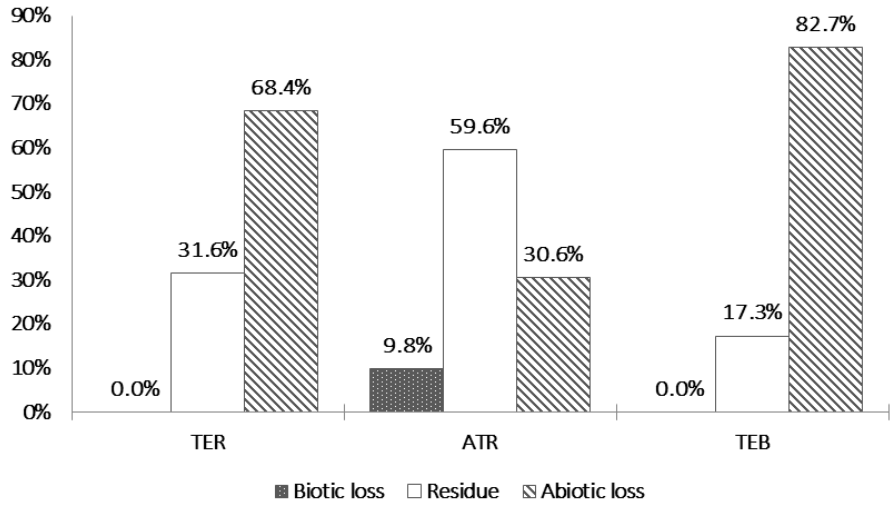

During the tests with TER and TEB, no biotic loss was observed. Navarro et al. (2004) determined the half-life of TER in groundwater as being between 263 and 366 days. This is in accordance with our results, since we did not observe any biotic loss during the tests with TER. Barra Caracciolo et al. (2009) stated that the prolonged persistence of TER in groundwater may be a sign of lower microbial activity or the absence of herbicide-degrading organisms. According to Caldas et al. (2010), after 7 days the total loss of TEB in groundwater is 50.0%. This is in accordance with our results, as we measured an abiotic loss of 82.7% after 28 days. The degradation of TEB is influenced by organic carbon content; low organic carbon contributes to decreased adsorption, and therefore encourages the microbial degradation of the fungicide (Herrero-Hernández et al. 2011). According to Jablonowski et al. (2011), ATR can persist in water and soil for decades. Our long denitrification test with this pesticide showed a significant biotic loss, namely 9.8%.

The highest residue value was measured in the case with ATR, 59.6%. This value was found to be 31.6% with TER and 17.3% with TEB.

CONCLUSION

During the 28-day semi-continuous laboratory tests with pesticide concentrations of 0.1 mg/l, the tested substances TER, ATR, and TEB had slight stimulation effects on the denitrification process, with the highest value measured for TER, namely 10%. The abiotic loss was dominant in the cases of TER (68.4%) and TEB (82.7%). The average abiotic loss of ATR was 30.6%. During the tests with TER and TEB, no biotic loss was observed. Biotic loss was found only with ATR (9.8%). The highest residual amount of pesticide in water was measured with ATR, 59.6%. This value was only 31.6% with TER and 17.3% with TEB.

The employed long-term laboratory test method for testing pesticides under denitrification conditions has proved to be suitable for the intended purposes and will be used to test other pesticide substances.

ACKNOWLEDGEMENTS

This research was financially supported by the Brno University of Technology Junior Specific Research Project FAST-J-21-7429 Behaviour of pesticides during denitrification.

REFERENCES

Barra Caracciolo, A. et al 2009. The role of a groundwater bacterial community in the degradation of the herbicide terbuthylazine. FEMS Microbiology Ecology [Online], 71(1): 127–136. Available at: https://academic.oup.com/femsec/article/71/1/127/557499. [2021-09-10].

Caldas, S.S. et al. 2010. Pesticide residue determination in groundwater using solid-phase extraction and high-performance liquid chromatography with diode array detector and liquid chromatography-tandem mass spectrometry. Journal of the Brazilian Chemical Society [Online], 21(4): 642–650. Available at: http://www.scielo.br/scielo.php?script=sci_arttext&pid=S0103-50532010000400009&lng=en&nrm=iso&tlng=en. [2021-09-10].

Cao, D. et al. 2020. Triazole resistance in Aspergillus fumigatus in crop plant soil after tebuconazole applications. Environmental Pollution [Online], 266: 115124. Available at: https://linkinghub.elsevier.com/retrieve/pii/S0269749120304218. [2021-09-10].

Daigger, G.T. et al. 2007. Diffusion of oxygen through activated sludge flocs: Experimental measurement, modeling, and implications for simultaneous nitrification and denitrification. Water Environment Research, 79(4): 375–387. Available at: https://onlinelibrary.wiley.com/doi/abs/10.2175/106143006X111835. [2021-09-10].

Fenner, K. et al. 2013. Evaluating Pesticide Degradation in the Environment: Blind Spots and Emerging Opportunities. Science [Online], 341(6147): 752–758. Available at: https://www.sciencemag.org/lookup/doi/10.1126/science.1236281. [2021-09-10].

Herrero-Hernández, E. et al. 2011. Field-scale dissipation of tebuconazole in a vineyard soil amended with spent mushroom substrate and its potential environmental impact. Ecotoxicology and Environmental Safety [Online], 74(6): 1480–1488. Available at: https://linkinghub.elsevier.com/retrieve/pii/S0147651311001072. [2021-09-10].

Hu, R. et al., 2019. Effects of carbon availability in a woody carbon source on its nitrate removal behavior in solid-phase denitrification. Journal of Environmental Management [Online], 246: 832–839. Available at: https://linkinghub.elsevier.com/retrieve/pii/S0301479719308588 [2021-09-10].

Ilhan, Z.E. et al. 2011. Dissipation of Atrazine, Enrofloxacin, and Sulfamethazine in Wood Chip Bioreactors and Impact on Denitrification. Journal of Environmental Quality [Online], 40(6): 1816–1823. Available at: https://acsess.onlinelibrary.wiley.com/doi/abs/10.2134/jeq2011.0082. [2021-09-10].

Jablonowski, N.D. et al. 2011. Still present after all these years: persistence plus potential toxicity raise questions about the use of atrazine. Environmental Science and Pollution Research [Online], 18(2): 328–331. Available at: http://link.springer.com/10.1007/s11356-010-0431-y. [2021-09-10].

Kodeš, V. 2019. Problematika pesticidů v ochraně vod – jaká data máme k dispozici a co nám říkají? In Sborník přednášek a posterových sdělení z 13. bienální konference a výstavy VODA 2019. Poděbrady, Czech Republic, 18–19 September. Brno: CzWA service s.r.o., pp. 18–25.

Lahdhiri, A. et al. 2017. Minimum COD needs for denitrification: From biological models to experimental set-up. Desalination and Water Treatment [Online], 61: 326–334. Available at: https://www.researchgate.net/publication/313374524_Minimum_COD_needs_for_denitrification_From_biological_models_to_experimental_set-up. [2021-09-10].

Navarro, S. et al. 2004. Persistence of four s-triazine herbicides in river, sea and groundwater samples exposed to sunlight and darkness under laboratory conditions. Science of The Total Environment [Online], 329(1–3): 87–97. Available at: https://linkinghub.elsevier.com/retrieve/pii/S0048969704001901. [2021-09-10].

Panikova, K. 2021. Optimalizace metodiky pro testování pesticidů. Vodovod.info - vodárenský informační portál [Online], 2021(2). Available at: http://vodovod.info. [2021-09-10].

Panikova, K. et al. 2020. Behaviour of pesticides during the denitrification process. In Proceedings of International PhD Students Conference MendelNet 2020 [Online]. Brno, Czech Republic, 11–12 November, Brno: Mendel University in Brno, Faculty of AgriSciences, pp. 543–548. Available at: https://mnet.mendelu.cz/mendelnet2020/mnet_2020_full.pdf. [2021-09-10].

Paul, E.A. 2007. Soil microbiology, ecology, and biochemistry. 3rd ed., Boston: Academic Press.

Yue, L. et al. 2017. Adsorption–desorption behavior of atrazine on agricultural soils in China. Journal of Environmental Sciences [Online], 57: 180–189. Available at: https://www.sciencedirect.com/science/article/abs/pii/S1001074216303692. [2021-09-10].

Identification of volatile compounds produced by *Laetiporus sulphureus* using OSMAC cultivation strategy

Nikola Schlosserova[1], Andrea Blahutova[1], Lucie Pompeiano Vanickova[1,2,3]
[1]Department of Chemistry and Biochemistry
[2]Department of Forest Botany, Dendrology and Geobiocenology
Mendel University in Brno
Zemedelska 1, 613 00 Brno
[3]Central European Institute of Technology
Brno University of Technology
Purkynova 464/118, 612 00 Brno
CZECH REPUBLIC

schlosserovan@gmail.com

Abstract: Basidiomycete fungus, *Laetiporus sulphureus* was analyzed for production of volatile secondary metabolites under different fermentation conditions, using the OSMAC (One Strain Many Compounds) cultivation strategy. In this study, the OSMAC strategy was based on application of three different types of media and two additional compounds - sawdust and ammonium chloride – that were added individually in the growing media prior the fermentation process. For the determination of volatile organic compounds (VOCs), two dimensional gas chromatography (GC×GC) with mass spectrometry (MS) was used with solid phase micro extraction (SPME) sample preparation (SMPE−GC×GC−MS). After the optimization process, PDMS/DVB fiber (blue) was applied for VOC preconcentration with following conditions: samples conditioning time in vials and fiber exposure to the headspace were set 30 min and 10 min, respectively. We confirmed that one fungal strain can produce a different VOCs profile depending on fermentation environment and we detected unique VOCs produced only in specific fermentation set-ups.

Key Words: Laetiporus sulphureus, OSAMC, GCxGC-TOFMS, volatile metabolites, SPME

INTRODUCTION

The *Agaricomycetes* fungi from *Basidiomycota* division are a rich source of chemical compounds with multi-directional therapeutic and pro-health effects. Currently, only a few ligninolytic fungi have practical use in medicine (Siljegovic et al. 2011). Microbial natural products are a tremendous source of new bioactive chemical entities for drug discovery, especially fungi. Fungi have the capability to produce a number of secondary metabolites, which possess multiple functions such as immune stimulating (Kawanishi et al. 2010), hypoglycemic (Han et al. 2009), or antiandrogenic activities (Dotan et al. 2011). The explorations suggest that we still haven't discovered the whole potential of these organisms and there are still compounds to be found with pharmacological effects. Secondary metabolites are synthetized by only a few common biosynthetic pathways and many of compounds are not produced at all because their genes are silent or cryptic. It means that the presence of gene coding metabolite is known nevertheless the pathway how to awake these genes and activate the translation remains unknown. On the other hand, it can be case of orphan genes for witch the corresponding metabolites is still undiscovered (Gross 2007). The microbial organic compounds with biological activities can be divided into two major groups. First are high-molecular weight molecules, obtained from extracts and products derived from the fruiting bodies of these medicinal mushrooms, and second are small organic molecules (secondary metabolites) excreted by fungi in a liquid culturing setups – fermentation (Clevenger et al. 2017). Analysis has revealed that many microorganisms contain over 30 secondary metabolite biosynthetic gene clusters (BGCs), but only a few metabolites have been detected so far. For this reason, novel techniques and approaches are needed to access the whole potential of these compounds (Onaka 2017).

Very popular method for activation of silent genes clusters is the OSMAC approach. The OSMAC strategy (see Figure 1) represents a simple tool to activate silent gene clusters to produce different

metabolites and/or enhance their production using altering stimuli for growth condition (C/N sources, temperature, pH, light, aeration) (Helge et al. 2002). This approach suggests that in different environments one strain can produce different spectrum of metabolites and could enhance production of already known products or completely new ones.

Figure 1 Scheme of OSMAC cultivation strategy

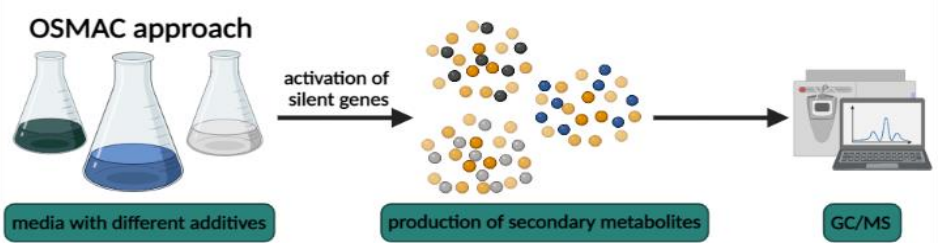

To enhance production of already known compounds represents a crucial step in natural products research because the microorganism might be able to produce bioactive compounds in very low concentrations, which means that gene expression is very low (Yi-Ming Chiang 2009). By changing chemical and physical parameters of fermentation is possible to reveal chemical diversity and to increase the concentration of compounds of interest or increase the number of new metabolites. All these changes in cultivation might trigger metabolite production as the microorganism is exposed to an unnatural environment leading to activation of the metabolic pathway under stress conditions (Romano et al. 2018) and production of VOCs as a part defense mechanism. In the present study we applied very sensitive and selective method (SMPE−GC×GC−MS), to provide a detailed analysis of VOCs metabolite changes produced by *Laetiporus sulphureus* under different fermentation conditions.

MATERIAL AND METHODS

Materials and reagents

SPME holder for manual sampling, SPME fibers, 1.5 ml glass vials with septum were purchased from Supleco (Bellefonte, PA, USA). Potato dextrose broth (PDB) and Yeast Malt Broth (YMB) from HIMEDIA, Sabouraud dextrose liquid medium (SDB) from Thermo Fisher Scientific and Sodium chloride was obtained from Sigma−Aldrich.

Biologic material and cultivation condition

The *Laetiporus sulphureus* strain used in this project was obtained from the Culture Collection of Laboratory of Environmental Chemistry and Enzymology. *L. sulphureus* was cultivated in 3 different types of liquid media (PDB, SDB, YMB) with additional additives (sawdust and ammonium chloride) for 7 days in Erlenmeyer flask at 27 °C without light. These types of media and additives were chosen based on previous screening measurements.

Sample preparation

Erlenmeyer flasks were put on ultrasonic sound for 20 minutes. After sonication 500 µl of sample were transfer to 1.5 ml glass vial with 500 µl of NaCl (200 mg/ml).

Optimization of SPME technique

The correct conditions for processing the samples were established. The individual samples were heated in a water bath at 37 °C in the glass vials sealed with the teflon septum and fungal VOCs were collected on a fiber using SPME. The selection of SPME fiber coating, incubation conditions and salting−out effect were optimized. The SPME fibers used for the method optimization were conditioned according to the manufacturer's instructions. Two different SPME fibers (gray and blue) coatings were tested. Firstly, the sample vial was conditioned for 30 min at 80 °C, and then VOCs were obtained followed by fiber exposure to the head space (HS) for 10 min at 80 °C (see Figure 2). Different conditions for the SPME incubation were tested (sample heating/VOC collection: 30min/30min, 15min/15min, 30min/15min and 15min/30min). In addition, recovery of VOCs from samples with/without NaCl (200 mg/ml) were tested.

Figure 2 Scheme of SPME technique of sample preparation

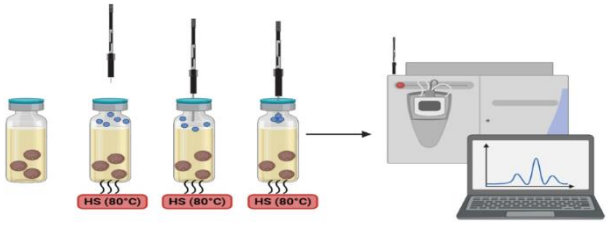

GC−MS analyses

The GC×GC−MS analyses of fungus *Laetiporus sulphurues* VOCs were carried out on a LECO Pegasus 4D instrument (LECO Corp., St. Joseph, MI). A Rtx-5Sil MS column (RESTEK, USA; 30 m × 0.25 mm × 0.25 µm film thickness) and a BPX-50 column (SGE Inc., Austin, TX; 1.18 m × 0.1 mm × 0.1 µm film thickness) were used for GC in the first and second dimensions, respectively. Helium was used as a carrier gas at a constant flow of 1 ml/min. The temperatures of the GC×GC−MS instrument were set at 250 °C at the injector, 270 °C at the transfer line, and 250 °C at the ion source. Parameters of the chromatography and mass spectrometric methods GC×GC−MS were tested and optimized (temperature of the secondary oven, modulator temperature, modulator period, cool time etc.). The mass spectrometer was operated in the electron ionization mode (EI, 70 eV).

RESULTS AND DISCUSSION

In this study, VOC profiles of *L. sulphureus* under different cultivation condition (OSMAC) were compared. Our results indicate that from all three used cultivation media, *L. sulphureus* showed the lowest metabolite production in PDB medium. In addition, Figure 3 shows that supplementation of different additives into the media resulted in production of wider VOCs profile (highlighted in red circles) (see Figure 3b and c) when compared to the control (see Figure 3a). Ammonium chloride addition in the *L. sulphureus* growing media stimulated the production of characteristic VOC metabolites (highlighted in yellow circles) in comparison with other supplements (see Figure 3b and c).

Figure 3 2D chromatograms of differences in VOC production by L. sulphureus in PDB medium

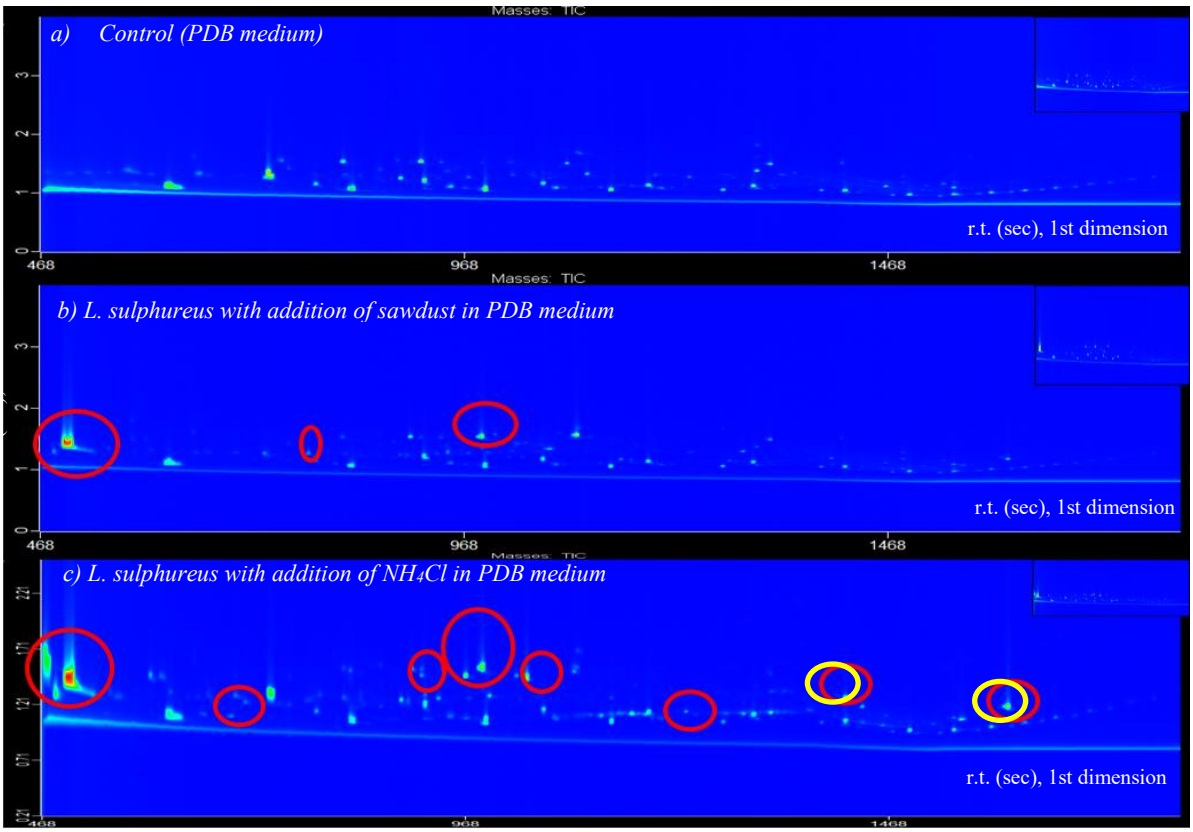

Specific VOC metabolites produced after cultivation of *L. sulphureus* in YMB medium with sawdust were detected and are highlighted in yellow circle (see Figure 4c). These metabolites are not part of the liquid medium (see Figure 4a), the fungus did not produce them while cultivating without additive (see Figure 4d) and did not produce them with NH_4Cl addition either (see Figure 4b). This result proved that the OSMAC strategy works and is possible to apply it on ligninolytic fungi to change the diversity of secondary metabolites production. In general, more metabolites were detected in SDB and YMB media than on PDB medium but in fact, cultivation with additives promote metabolite production in every single media. Scientific literature shows that the OSMAC approach was used on different types of microorganisms: bacteria, filamentous fungi, marine organisms (Pan et al. 2019) but never on ligninolytic fungi until now.

Figure 4 3D chromatograms of VOC from L. sulphureus in YMB medium with additives

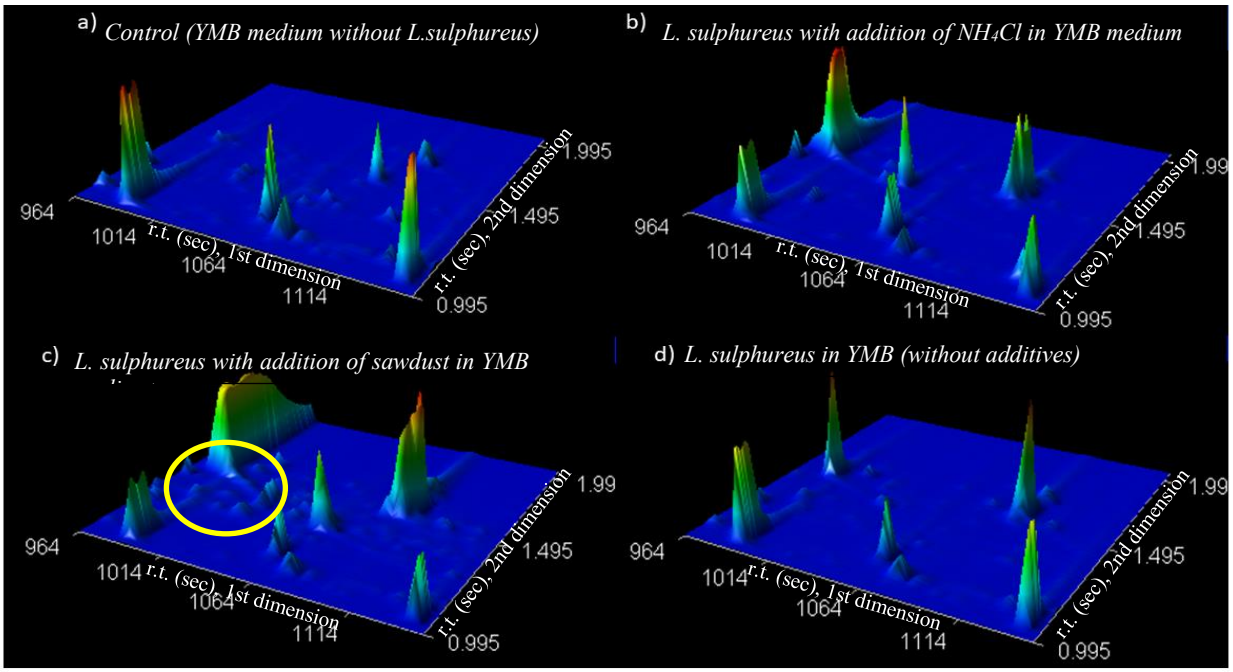

CONCLUSION

We confirmed that one fungal strain can produce a different spectrum of VOC in different cultivation environment. Unique VOCs produced only in specific fermentation set-ups were detected here by the SPME-GC×GC-MS. Further analysis will follow in order to fully characterize and identify the specific compounds and provide detailed information on the difference they make in metabolite production.

ACKNOWLEDGEMENTS

The research was financially supported by IGA grant, no. AF-IGA2021-IP028.

REFERENCES

Clevenger, K. et al. 2017. A scalable platform to identify fungal secondary metabolites and their gene clusters. Nature Chemical Biology, 13: 895–901.

Dotan, N. et al. 2011. The culinary-medicinal mushroom Coprinus comatus as a natural antiandrogenic modulator. Integrative Cancer Therapies, 10: 148–59.

Gross, H. 2007. Strategies to unravel the function of orphan biosynthesis pathways: recent examples and future prospects. Applied Microbiology and Biotechnology, 75: 267–77.

Han, C. et al. 2009. A comparison of hypoglycemic activity of three species of basidiomycetes rich in vanadium. Biological Trace Element Research, 127: 177–82.

Helge, B. et al. 2002. Big Effects from Small Changes: Possible Ways to Explore Nature's Chemical Diversity. ChemBioChem, 3(7):619–627.

Kawanishi, T. et al. 2010. Effects of two basidiomycete species on interleukin 1 and interleukin 2 production by macrophage and T cell lines. Immunobiology, 215: 516–20.

Onaka, H. 2017. Novel antibiotic screening methods to awaken silent or cryptic secondary metabolic pathways in actinomycetes. Journal of Antibiotics, 70: 865–70.

Pan, R. et al. 2019. Exploring Structural Diversity of Microbe Secondary Metabolites Using OSMAC Strategy: A Literature Review. Frontiers in Microbiology, 10: 294.

Romano, S. et al. 2018. Extending the "One Strain Many Compounds" (OSMAC) Principle to Marine Microorganisms. Marine Drugs, 16(7): 244.

Siljegovic, J. et al. 2011. Antimicrobial activity of aqueous extract of *Laetiporus sulphureus* (Bull.: Fr.) Murill. Zbornik Matice srpske za prirodne nauke, 299–305.

Yi-Ming, Ch. et al. 2009. A Gene Cluster Containing Two Fungal Polyketide Synthases Encodes the Biosynthetic Pathway for a Polyketide, Asperfuranone, in *Aspergillus nidulans*. Journal of the American Chcemical Society, 131: 2965–70.

Cross-linked-Pd^0 polyethyleneimine catalyst for bioorthogonal chemistry

Paulina Takacsova[1], Vladimir Pekarik[2]
[1]Department of Chemistry and Biochemistry
Mendel University in Brno
Zemedelska 1, 61300 Brno
[2]Department of Physiology
Masaryk University
Kamenice 753/5, 625 00 Brno
CZECH REPUBLIC

takacsovapaulina@gmail.com

Abstract: Bioorthogonal therapy represents a promising tool for controlled pro-drug activation. However, efficient catalysis in the intracellular environment mediated by organometallic compounds still poses a great challenge. Herein, we describe the preparation of a palladium-trapped cross-linked catalyst. Polycationic polymer polyethyleneimine (PEI), an efficient transfection agent, was used as a carrier for palladium catalyst. To prevent palladium leaching and undesired palladium inactivation, PEI polymer with nested palladium catalyst was cross-linked with phosphine compound tetrakis(hydroxymethyl)phosphine chloride (THPC). The catalytic activity of cross-linked-Pd-PEI catalyst was assessed by the activation of a precursor fluorescent probe. The prepared catalyst exhibited catalytic activity in cell-free conditions in a PBS environment, as well as in a cell culture medium supplemented with FBS, which simulated the cellular environment.

Key words: bioorthogonal chemistry, palladium-mediated catalysis, polyethyleneimine, tetrakis(hydroxymethyl) phosphonium chloride, nanomedicine

INTRODUCTION

Cross-linked-Pd^0 resins have shown to be a very promising tool for controlled intracellular artificial pro-drug activation. Extensive cross-linking of polystyrene carrier modified with amino groups have prevented palladium catalyst from premature leaching and enabled fluorescent labelling. However, this size of Pd^0 resins was suitable only for extracellular catalysis (Yusop et al. 2011, Weiss et al. 2014). Discrete palladium complexes face several obstacles, which lie mainly in the low efficiency of performed reaction, with substoichiometric catalytic amounts of poor cellular uptake and its toxicity (Mancuso et al. 2020). Therefore, the attention has been focused on the use of a polymer nanocarrier, which can mitigate toxic effects and facilitate cellular uptake of the palladium complex (Miller et al. 2017, Sancho-Albero et al. 2019).

In our study, cross-linked-Pd polyethyleneimine (PEI) catalyst was prepared. Branched PEI was used as a carrier. This polycationic polymer is widely used as a non-viral transfection agent that is internalized into cells by endocytosis (Pandey et al. 2016). As a cross-linking agent, tetrakis(hydroxymethyl)phosphonium chloride (THPC) was used. Previous experiments showed that THPC can reduce and stabilize noble metal precursor salts as zero-valent metallic nanoparticles (Hueso et al. 2013). THPC was also introduced as a tetra-functional cross-linking agent while reacting with primary and secondary amines of protein for hydrogels preparation (Chung et al. 2012). The catalytic activity of palladium catalysts was determined using a palladium sensitive probe based on an umbelliferone fluorophore designed for noble metals detection (Pekarik et al. 2020). The catalytic activity of molecular catalyst Pd-THPC, cross-linked-Pd polyethyleneimine of a non-reduced and reduced form containing metallic Pd(0) was compared.

MATERIAL AND METHODS

Material

All chemicals of ACS purity were obtained from Sigma-Aldrich (St. Louis, MO, USA). Propargylumbelliferone ether fluorescent probe precursor was synthesized as described earlier (Pekarik et al. 2020).

Preparation of palladium-THPC complex

Palladium-THPC complex formation was held in different organic solvents. Palladium acetate (10 µL of 100 mM solution dissolved in dimethylformamide, DMF) was diluted in DMF/acetonitrile/dioxane and then THPC (1 µL/2 µL/3 µL of 1M in DMF) were added into the reaction mixture with a final volume of 100 µL. Samples were incubated overnight at room temperature. Afterwards, fluorescent probe activation was evaluated.

Synthesis of cross-linked-palladium PEI

Palladium acetate (30 µL of 100 mM monomeric units dissolved in toluene) was diluted in 240 µL of toluene and then branched PEI (30 µL of 1M monomeric units dissolved in DMF) was added while forming a yellow-green suspension. The suspension was incubated at 80 ˚C for 10 min with shaking at 1000 RPM at thermoblock (Thermo Fisher Scientific, Waltham, MA, USA). Then, 1200 µL of toluene was added into the reaction mixture and incubated overnight at room temperature. Toluene was removed from the reaction mixture and the aggregated complex of Pd-PEI was dried at 40 ˚C to remove residual solvent. The dried Pd-PEI complex was fully solubilized in 300 µL of ethanol. Samples were divided into 50 µL aliquots. After the addition of 1 µL of THPC (1M in DMF, prepared from 80 wt% THPC in H_2O) orange-brown pellet was separated by centrifugation (10 min., 9425 × g) and washed 3× with 500 µL of ethanol (EtOH) to remove residual THPC (when tested, the solution of 1M THPC in DMF was fully soluble in 100 µL of EtOH). After each washing step, the aggregated complex was separated by centrifugation (10 min., 21206 × g). Afterwards, each aliquot was resuspended in different solvent including DMF, H_2O, acetonitrile and methanol. The catalytic activity of the prepared catalyst was then evaluated.

Samples were stored at -20 ˚C for 3 weeks. Their catalytic activity was then reevaluated for the metallic cross-linked-Pd(0) PEI complex. The reduction reaction was carried out by the addition of hydrazine (5 µL of 55% in H_2O) into 15 µL of the previously mentioned reaction mixtures, while silvery suspensions were formed.

Pd-catalyst-mediated fluorescent probe activation

The activity of each palladium catalyst was determined by the depropargylation reaction of the fluorescent probe (Figure 1). The preparation of fluorescent probe propargyl-umbelliferone ether, as well as its activation mediated by organometallic compounds, was previously described by our group (Pekarik et al. 2020). Propargyl-umbelliferone ether (0.1 µL of 100 mM in DMF) was diluted in 200 µL of PBS or DMEM/F12 cell medium supplemented with 10% FBS. Pd catalysts (1 mM in DMF or H2O) were added to the reaction mixture at final concentration of 10 µM and stirred. The suspension was placed in a 96-well plate and the fluorescent probe activation was measured on TECAN reader (excitation wavelength = 365 nm, emission wavelength = 450 nm). Results are expressed as ± standard deviation from three measurements.

Figure 1 Mechanism of propargylmbelliferone ether modified by (Pekarik et al. 2020)

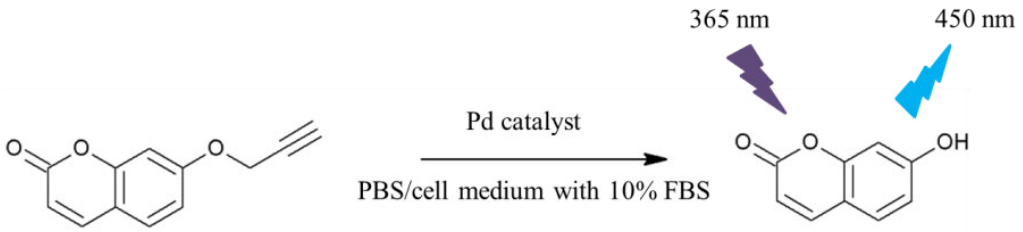

Legend: Pd=palladium, PBS=phosphate buffered saline pH 7.4, cell medium= DMEM/F12 cell medium supplemented with 10% fetal bovine serum.

RESULTS AND DISCUSSION

Controlled intracellular pro-drug activation mediated by the palladium catalyst requires biocompatible compound with sufficient cellular uptake for efficient catalysis. Herein, the initial steps leading to the preparation of the cross-linked-palladium (Pd) polyethyleneimine (PEI) catalyst, including its synthesis and evaluation of its catalytic activity in cell-free conditions, are described. A brief description of cross-linked-Pd PEI catalyst preparation procedure together with the proposed products of the reaction is shown in Figure 2. We suppose that besides primary amines depicted in Figure 2, also secondary amines were involved in THPC cross-linking, both intramolecular and intermolecular.

Figure 2 Proposed pathway for cross-linked-Pd PEI synthesis

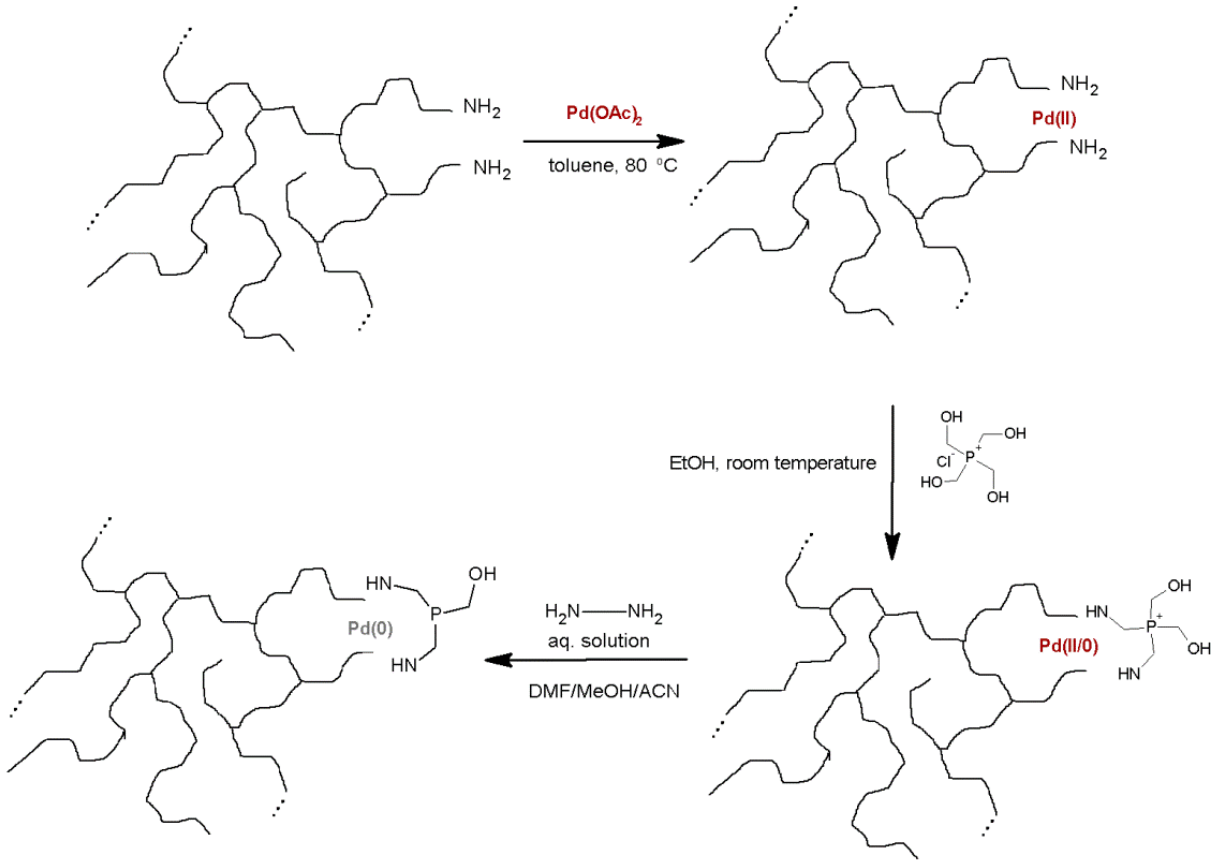

Legend: Pd(II) and Pd (II/0) in red colour represent a coordinated form of palladium. Pd(0) in silver colour represents metallic zero-valent palladium entrapped in polyethyleneimine polymer. EtOH= ethanol, MeOH= methanol, DMF= dimethylformamide, ACN= acetonitrile.

The first aim was to prepare polymeric cross-linked-Pd catalyst in an aqueous environment as previously described in studies of THPC-crosslinked hydrogel preparation (Chung et al. 2012). The study of the preparation of palladium nanoparticles manifested the reducing properties of THPC in an alkali aqueous environment (Hueso et al. 2013). However, the fluorescent probe activation study showed negligible activity of catalyst synthesized exclusively in the aqueous environment. Therefore, the preparation of palladium complex with THPC was tested in different organic solvents which are miscible with water for further cross-linking of THPC with PEI polymer in an aqueous environment. Although the formation of THPC-palladium complex was carried out in a non-aqueous environment, the further cross-linking of the complex with PEI polymer in aqueous solvent caused the diminishing of its catalytic activity. For this reason, the whole synthesis was carried out in a non-aqueous environment.

The formation of THPC-palladium complex was comparable in all three tested solvents – DMF, acetonitrile and dioxane. Since there was no difference in the behaviour of prepared catalysts in different environments, only the reaction held in DMF is shown in Figure 3. The ratio between THPC

and palladium had a significant impact on the catalytic function of the complex. When an equimolar amount of THPC and palladium were used, THPC played a role as a reductant of the metal only, while the probably oxidized product tris(hydroxymethyl)phosphine oxide lacks the coordination ability which consequently lowers the catalytic activity of palladium. The reduction into metallic Pd(0) was also manifested by the reaction mixture colour change into dark silver-black. At a higher ratio of THPC to palladium, we suppose the successful coordination complex formation suggested by the increase in catalytic activity, especially in the case of cell medium with 10% FBS. Phosphine ligand coordination can prevent palladium irreversible catalytic inactivation by thiol compounds present in cell medium with FBS addition. At the highest tested concentration of THPC, we noticed the decreased catalytic activity in the case of reaction taking place in a cell culture medium. Since the prepared complex was soluble in all prepared solvents, the separation of residual THPC from the reaction mixture was not possible. The diminished catalytic activity could be caused by the reactivity of redundant THPC.

Figure 3 Fluorescence emission intensity of precursor fluorescent probe evaluating the catalytic activity of palladium-THPC complex synthesized in dimethylformamide (DMF) using a different ratio between palladium and tetrakis(hydroxymethyl)phosphonium chloride (THPC) ligand

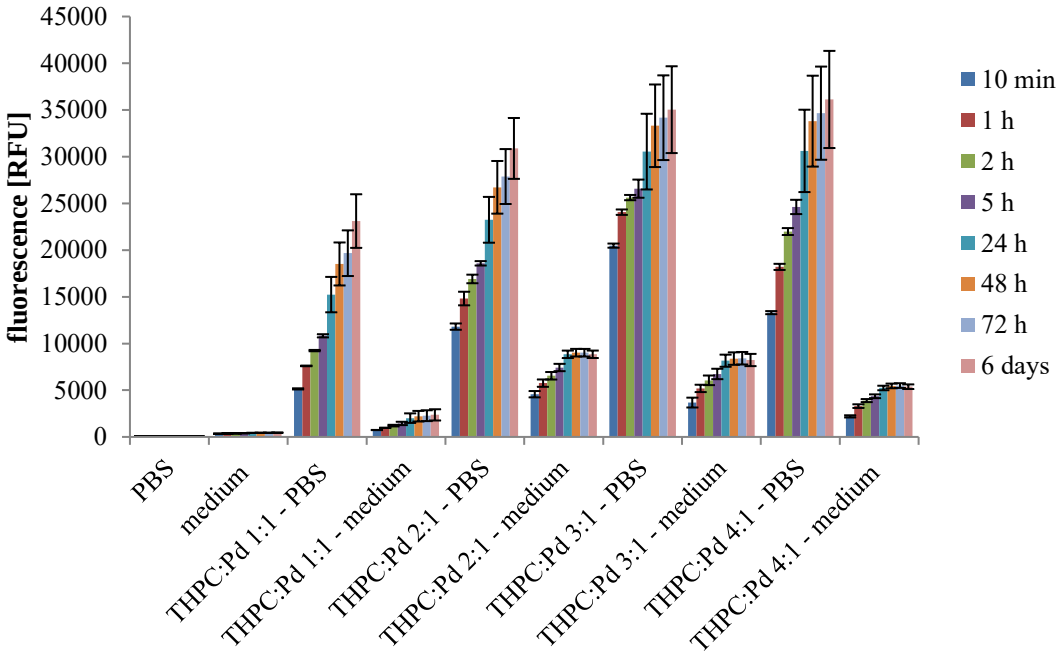

Legend: Pd=palladium, THPC= tetrakis(hydroxymethyl)phosphonium chloride, PBS=phosphate buffered saline pH 7.4, medium= DMEM/F12 cell medium supplemented with 10% fetal bovine serum. Error bars represent ± standard deviation from n = 3.

The formation of the cross-linked-Pd(II/0) PEI complex was held in toluene. The Pd(II) PEI complex prepared from palladium acetate and PEI was precipitated and separated from solvent allowing the residual palladium catalyst to be removed from the reaction mixture. In the next step, Pd(II) PEI complex was solubilized in ethanol and palladium trapped in the polymer was cross-linked and coordinated with THPC, which should ensure the protection against palladium premature release from PEI polymer and the inactivation of palladium catalysts by the components of cell medium containing thiol groups. The fluorescent probe activation study suggests that palladium-PEI complex has negligible catalytic activity on its own. When cross-linking agent THPC is added, the catalytic activity is significantly increased. This can be caused by the steric protection of palladium by the cross-linking groups and also by the donor effect of the phosphine ligand, which facilitates the oxidative addition of catalyzed depropagylation (Figure 4). We have attempted to resolubilize the cross-linked Pd(II/0) PEI complexes in various organic solvents including DMF, H_2O and methanol. The full solubility of cross-linked- Pd(II/0) PEI complex was observed in H_2O, but it was also the environment yielding the lowest catalytic activity (Figure 4).

Figure 4 Fluorescence emission intensity of precursor fluorescent probe evaluating the catalytic activity of cross-linked-Pd(II/0) PEI complex in different solvents

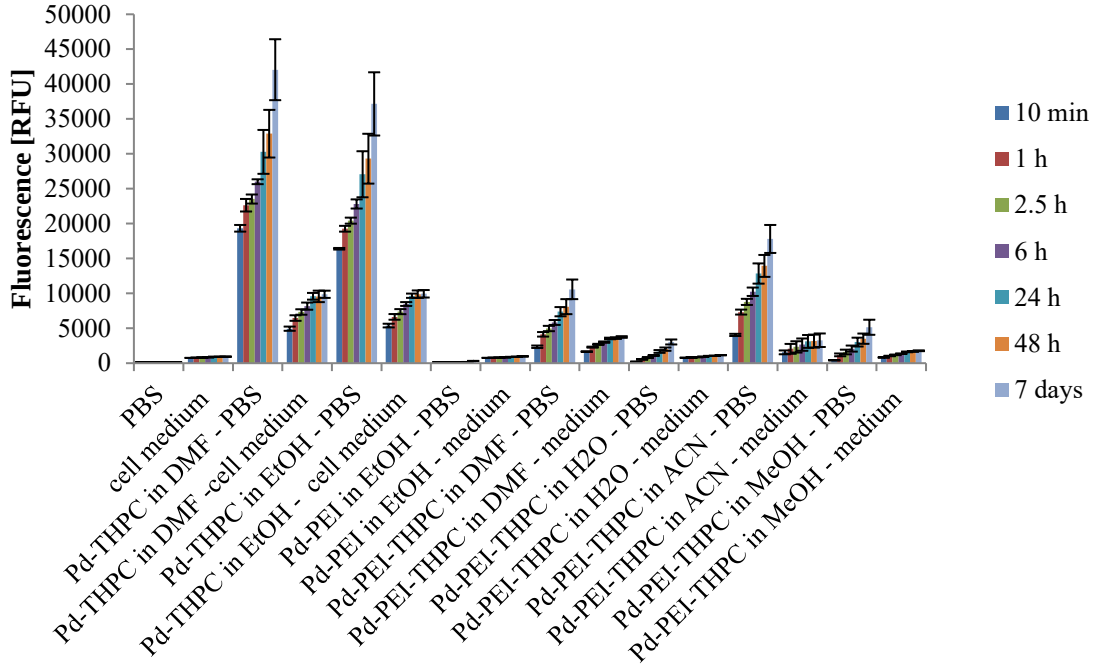

Legend: Pd=palladium, THPC= tetrakis(hydroxymethyl)phosphonium chloride, EtOH= ethanol, MeOH= methanol, DMF= dimethylformamide, ACN= acetonitrile, PBS=phosphate buffered saline pH 7.4, medium= DMEM/F12 cell medium supplemented with 10% fetal bovine serum. Error bars represent ± standard deviation from n = 3.

Figure 5 Fluorescence emission intensity of precursor fluorescent probe evaluating the catalytic activity of cross-linked-Pd(II/0) PEI complex and reduced metallic cross-linked-Pd(0) PEI

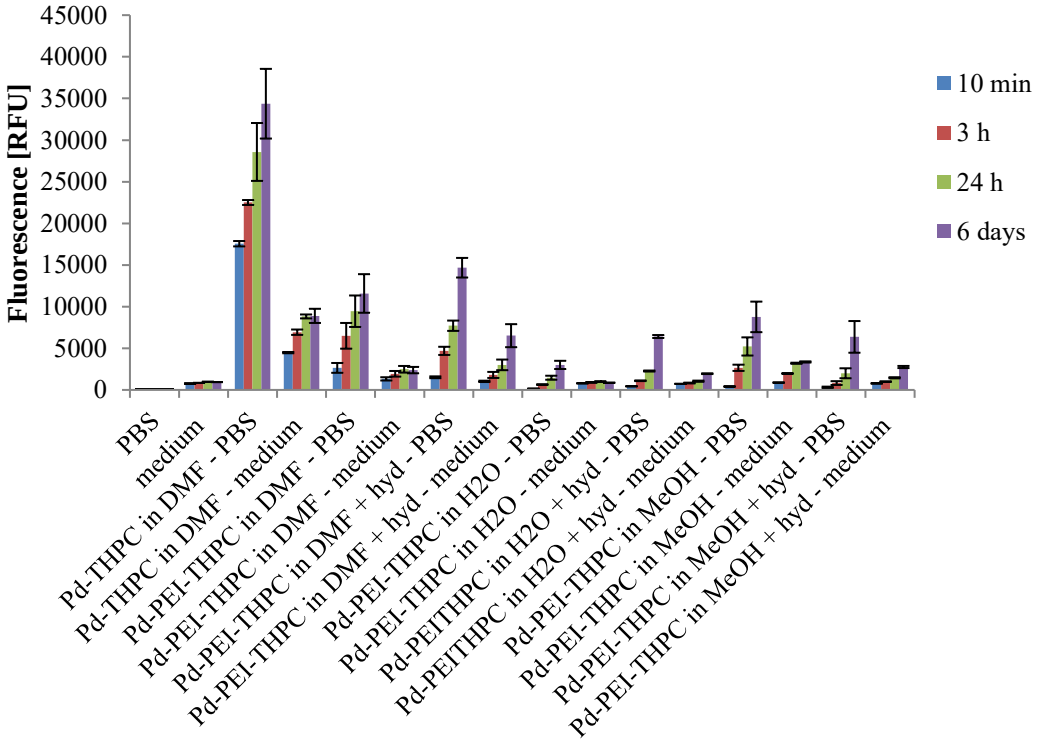

Legend: Pd= palladium, THPC= tetrakis(hydroxymethyl)phosphonium chloride, EtOH= ethanol, MeOH= methanol, DMF= dimethylformamide, PBS=phosphate buffered saline pH 7.4, medium= DMEM/F12 cell medium supplemented with 10% fetal bovine serum, hyd= hydrazine. Error bars represent ± standard deviation from n = 3.

Palladium was reduced by hydrazine into zero valent metallic Pd(0). The reduction of palladium (II/0) complex into metallic zero-valent Pd(0) was manifested by the colour change of the reaction mixture. The comparison of catalytic activity of Pd(II/0)-PEI complex with metallic Pd(0)-PEI complex is illustrated in Figure 5. To compare with the non-reduced cross-linked-Pd(II/0) PEI complex, the reduced metallic cross-linked Pd(0) PEI complex exhibited higher catalytic activity. Moreover, nanoparticles containing metallic Pd(0) showed biocompatibility towards cellular cultures and also zebrafish during embryo development (Weiss et al. 2014). To compare with the bare Pd-THPC complex, the catalytic activity of both Pd(II/0)-PEI and metallic Pd(0)-PEI catalysts was suppressed by the presence of PEI polymer, which can sterically hinder the accessibility of palladium to its substrate. During the 3-week storage, a decline in the catalytic activity of the palladium complex (II/0) catalyst has been observed. This was also caused by the presence of PEI because in the case of the Pd-THPC complex, we did not notice any decline in catalytic activity. Even so, PEI polymer represents a great advantage for cellular uptake and reduction of acute cell toxicity. The following steps will lead to a more detailed characterization of the prepared complex and the evaluation of catalytic activity in cellular culture.

CONCLUSION

The preliminary studies of fluorescent probe activation suggest that the cross-linked-Pd(0) PEI catalyst shows catalytic activity in PBS and also cell culture medium environment, which simulates cellular conditions. The reduction into zero valent metallic palladium was essential for the enhancement of catalytic activity. Although the presence of PEI caused the decrease in catalytic activity, we suppose that the entrapment of palladium into this polymer will have valuable benefits such as reducing cytotoxicity and facilitating cellular uptake.

ACKNOWLEDGEMENT

The research was financially supported by the IGA individual project AF-IGA2021-IP059.

REFERENCES

Chung, C. et al. 2012. Tetrakis(hydroxymethyl) Phosphonium Chloride as a Covalent Cross-Linking Agent for Cell Encapsulation within Protein-Based Hydrogels. Biomacromolecules, 13: 3912−3916.

Hueso, J.L. et al. 2013. Beyond Gold: Rediscovering Tetrakis-(Hydroxymethyl)-Phosphonium Chloride (THPC) as an Effective Agent for the Synthesis of Ultra-Small Noble Metal Nanoparticles and Pt-containing Nanoalloys. RSC Advances, 3: 10427.

Mancuso, F. et al. 2020. Transition-Metal-Mediated versus Tetrazine-Triggered Bioorthogonal Release Reactions: Direct Comparison and Combinations Thereof. ChemPlusChem, 85:1669–1675.

Miller, M.A. et al. 2017. Nano-palladium is a cellular catalyst for in vivo chemistry. Nature Communications, 8: 15906.

Pandey, A.P. et al. 2016. Polyethylenimine: A versatile, multifunctional non-viral vector for nucleic acid delivery. Materials Science & Engineering C-Materials for Biological Applications, 68: 904–918.

Pekarik, V. et al. 2020. Direct fluorogenic detection of palladium and platinum organometallic complexes with proteins and nucleic acids in polyacrylamide gels. Scientific Reports, 10: 12344.

Sancho-Albero, M. et al. 2019. Cancer-derived exosomes loaded with ultrathin palladium nanosheets for targeted bioorthogonal catalysis. Nature Catalysis, 2: 864–872.

Weiss, J.T. et al. 2014. Extracellular palladium-catalysed dealkylation of 5-fluoro-1-propargyl-uracil as a bioorthogonally activated prodrug approach. Nature Communications, 5: 3277.

Yusop, R.M. et al. 2011. Palladium-mediated intracellular chemistry. Nature Chemistry, 3: 239–243.

Molecularly imprinted polymers as a recognition element for the determination of disease markers

Milada Vodova, Marcela Vlcnovska, Jaroslava Bezdekova, Marketa Vaculovicova
Department of Chemistry and Biochemistry
Mendel University in Brno
Zemedelska 1, 613 00 Brno
CZECH REPUBLIC

Vodova.Milada@seznam.cz

Abstract: Molecular imprinting is a very popular technique that allows preparation of molecularly imprinted polymers (MIPs) which have the ability to recognize imprinted molecules (analytes). MIPs are highly selective for the imprinted template and are chemically very stable. In our case, pepsin was used as a template/analyte molecule as it is a marker of gastroesophageal reflux. MIPs were prepared by suspension polymerization using a mixture of functional methacrylate-based monomers. Furthermore, in this work, MIPs were used as recognition entities in the sensor using quartz crystal microbalance.

Key Words: molecularly imprinted polymers, methacrylic acid, functional monomers, quartz crystal microbalance

INTRODUCTION

Rapid identification of various diseases allows early initiation of treatment and increases the patient's chances of recovery. Nowadays, the effort is to obtain biological samples from patients, if possible, in a non–invasive way. Therefore, in recent years, the detection of diseases from breath or its condensate has gained much attention. Breath sampling is simple, time-saving, affordable, non-invasive, and detectable in real–time. In addition, the breath contains a large number of substances (volatile components, gases, non–volatile molecules or proteins) that can provide important information about the patient's medical status (Nunez–Naveira et al. 2019, Das and Pal 2020). One of the proteins contained in breath condensate can be pepsin, which occurs naturally in the stomach and digests proteins (Zhu et al. 2006, Rick 1965). In the last ten years, numerous diseases have been associated with pepsin, such as laryngopharyngeal reflux, gastroesophageal reflux etc. (Stanforth et al. 2021).

Metabolic products are present in exhaled breath in relatively low concentrations (ppm, ppb and lower). For these reasons, they are usually determined using modern and very sensitive physico–chemical methods such as gas or liquid chromatography, mass spectrometry, tandem techniques, infrared spectroscopy and biosensors (Boots et al. 2012, Amann et al. 2007, Taranenko et al. 2001, Matsuguchi and Uno 2006).

Biosensors are analytical devices consisting of a biological recognition element (receptor) and a suitable transducer connected to a data processing system. The recognition elements can be enzymes, microorganisms, cells, tissues, or other bio ligands, which are usually costly, and their lifetime on the surface of the sensor is limited. For this reason, molecularly imprinted polymers (MIPs) have been proposed as a recognition entity, thus serving as a synthetic alternative to biological receptors (Uludag et al. 2007, Myszka et al. 1998, Jha et al. 2014).

Molecular imprinting is a technique in which specific binding sites complementary to an imprinted molecule (template/analyte) are formed in crosslinked polymers. Upon completion of the polymerization, the imprinted molecules are removed using basic or acidic conditions, detergents or other solvents, resulting in cavities selective for the imprinted molecules. The selectivity of cavities is ensured by their shape, size and position of target functional groups (Feng et al. 2017, Kyzas and Bikiaris 2014). The preparation scheme is shown in Figure 1. In our case, a thermosensitive isopropylacrylamide (NIPAm) was chosen. NIPAm is able to increase its size at low temperature and decrease its size at high temperature (Zhang et al. 2017).

The great advantage of the future sensor is its simplicity and non-invasiveness in sampling. Only a small amount of sample is needed for the analysis without the need for treatment. Detection is performed in real–time and is fast and inexpensive compared to current methods for determining exhaled breath condensate.

Figure 1 Schematic showing the process for preparing MIPs: 1) interaction of the template with the polymerization mixture during which polymerization occurs, 2) removal of the template to form a cavity selective for the given imprinted molecule

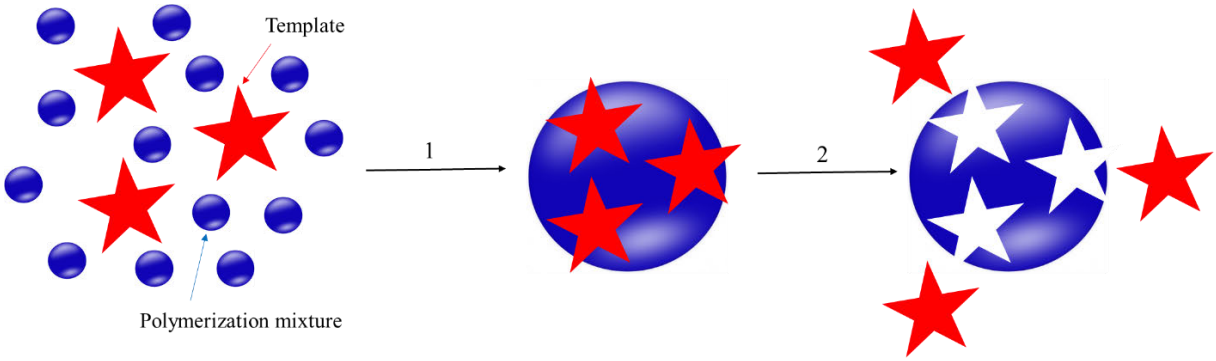

MATERIAL AND METHODS

Chemicals

Methacrylic acid (MAA) ≥ 99%, N, N, N ', N'–tetramethylethylenediamine (TEMED) ≥ 99%, ammonium persulfate (APS) ≥ 98%, sodium hydroxide ≥ 98%, N–hydroxysukcinimide (NHS) ≥ 98%, Isopropylacrylamide (NIPAm) ≥ 99%, N–tert–butylacrylamide (TBAm) ≥ 97%, N-(3-Aminopropyl) methacrylamide hydrochloride (APMA) ≥ 98%, N, N'-Methylenbis(acrylamide) (BIS) ≥ 99%, poly(ethylene glycol) 2–mercaptoethyl ether acetic acid not specified manufacturer and poly(ethylene glycol) methyl ether thiol poly(ethylene glycol) 2–mercaptoethyl ether acetic acid not specified manufacturer and poly(ethylene glycol) methyl ether thiol not specified manufacturer were purchased from Sigma–Aldrich (St. Louis, MO, USA) in ACS purity

Instrumentation

QCM (KEVA, Brno, Czech Republic), Zetasizer Nano (Malvern, Great Britain), Termoblock (Thermal shake lite, USA), Centrifuge 5424 R (Eppendorf, Germany) and Vortex (Grant–bio PV1, Great Britain)

Analysis procedure

The work is focused on the development of a sensor that will be able to non–invasively detect pepsin directly from respiratory condensate using MIPs as the synthetic receptor.

Synthesis of particle MIPs

The synthesis of MIPs consists of several steps (see Figure 2):

1. In the first step, a polymerization mixture is prepared. The mixture consists of several monomers, namely 70 mol% NIPAm, 18 mol% TBAm, 5 mol% MAA and 5 mol% NAPMA and a crosslinking agent (2 mol% BIS) dissolved in MilliQ water. Subsequently, the polymerization mixture is bubbled with nitrogen gas for 5 minutes to ensure the removal of any oxygen that inhibits the polymerization reaction.
2. In the second step, the polymerization mixture is mixed with a template (0.6 mg of pepsin). The polymerization process is initiated by the addition of the redox initiator APS (2 mg) and the TEMED molecule (2 µl) serving as its activator.
3. The polymerization step proceeds for approximately 18 hours at room temperature and is terminated by bubbling oxygen for 5 minutes. The polymerization step leads to the formation of small particles with a size of ~ 64 nm. The prepared polymer particles were washed three times with water using an Amicon 100 kDa ultra–centrifugal filter (Amicon® Ultra–0.5

Centrifugal Filter Unit, Sigma Aldrich, USA), allowing the residue of unpolymerized monomers and unpolymerized protein to be washed out.

4. In the next step, changing the solvent temperature (60 °C) for 60 minutes removes the template from the MIPs particles using a 100 kDa Amicon ultra centrifugal filter. After template removal, the cavities are formed able to selectively recognize the imprinted protein and thus serve as a synthetic antibody.
5. In the last step, the size of the polymer particles and their polydispersity were measured by dynamic light scattering (DLS) at 25 °C, and the interaction of the protein with MIPs was measured by QCM.

Figure 2 Scheme of the MIPs preparation process and subsequent use

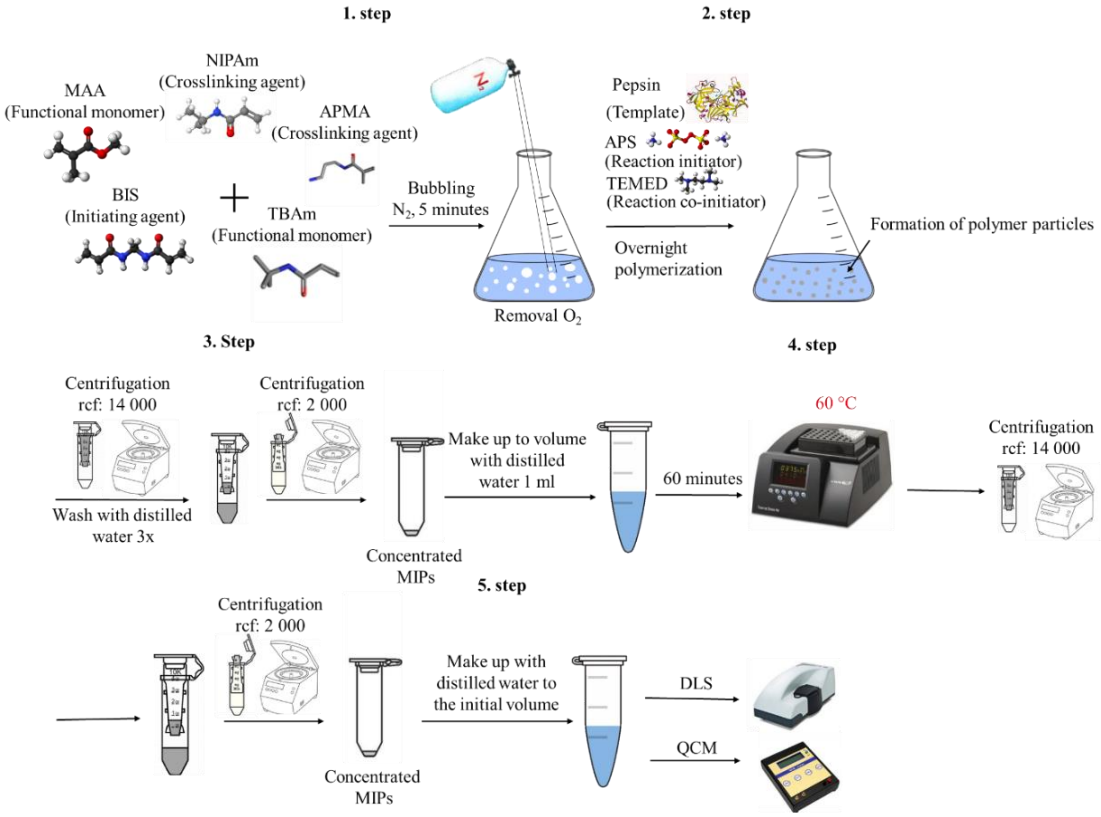

RESULTS AND DISCUSSION

Characterization of MIPs particle

The particle size and polydispersity were measured by DLS. For DLS measurements, the polymer particles were diluted ten times in distilled water. The intensity of the washed MIPs was measured. The particle size was determined to be 64.32 ± 0.27 nm as shown in Figure 3, and the polydispersity was determined to be 0.13 ± 0.01. From the measured data, it was found that the measured MIPs are monodisperse.

Preparation of the QCM chip

First, the chip was cleaned with 70% ethanol, distilled water and dried with nitrogen gas. Modification of the gold layer of the chip was performed using poly(ethylene glycol) 2-mercaptoethyl ether acetic acid and poly(ethylene glycol) methyl thiol ether in a ratio of 1: 9 dissolved in distilled water. The chip was incubated overnight (approximately 20 hours). The chip was then rinsed again with 70% ethanol, distilled water and dried with nitrogen gas. A mixture of 10 mg EDC and 50 mg NHS dissolved in 0.5 ml MilliQ water was applied to the modified chip. It was then removed and washed with phosphate buffer and covalently bound to pepsin (0.6 mg/ml) on the gold layer of the chip for 45 minutes. A scheme of the whole process is shown in Figure 4. The modified chip was placed

in a QCM cell and filled with buffer until the equilibrium was established. Subsequently, 50–fold diluted MIPs particles were dosed into the system, and a significant decrease in frequency was observed. The decline was directly proportional to the amount of particles bound to pepsin immobilized on the chip. It can be seen from Figure 5 that with increasing concentration of MIPs, there was a more significant decrease in frequency. The prepared and optimized MIPs particles are thus selective for pepsin.

Figure 3 Intensity of MIPs at 25 °C

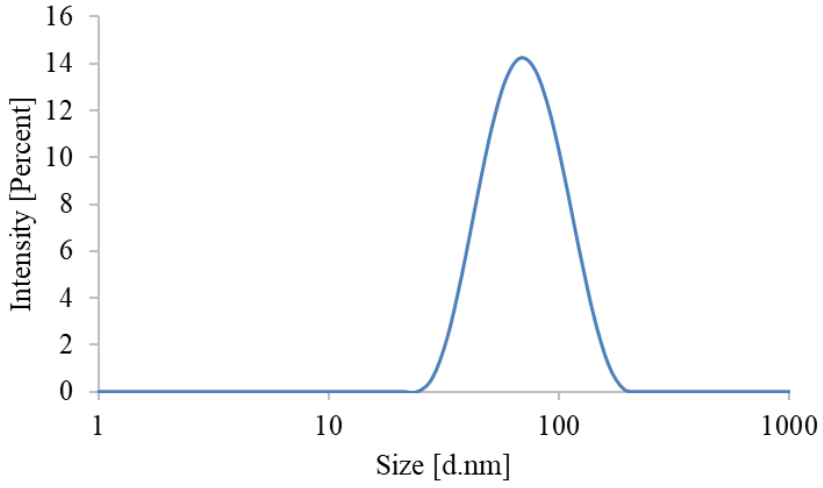

Figure 4 Binding of PEG to the gold layer of the chip and subsequent binding of the protein to the activated chip

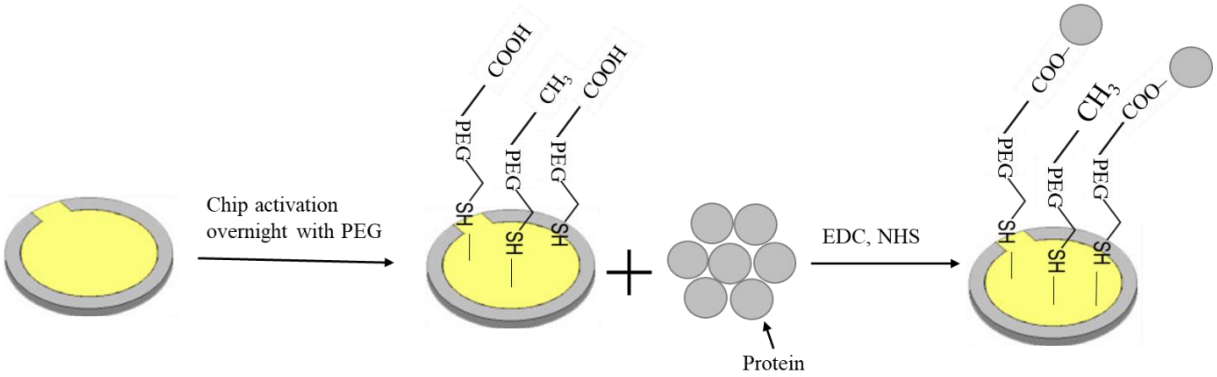

Figure 5 Observation of the interaction between MIPs and pepsin using a QCM in real–time

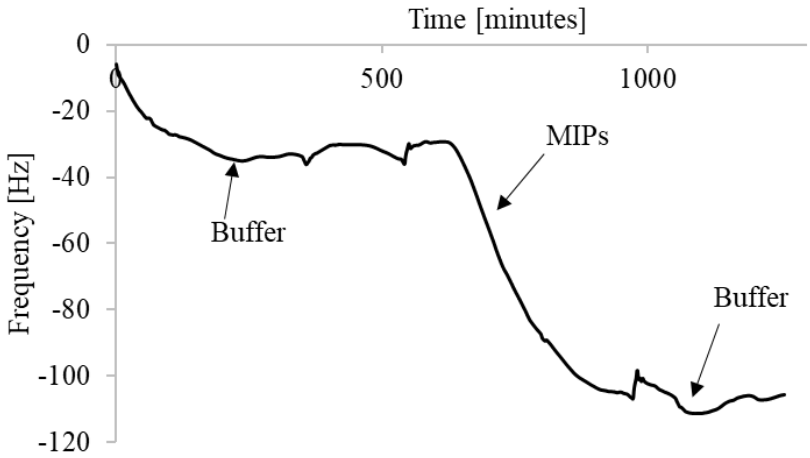

CONCLUSION

The here presented approach could be in the future adapted to measure pepsin directly from breath condensate. The great advantage of the future sensor is the simplicity and non–invasiveness of the sampling. The collected sample does not need to be pretreated, a small amount of sample is sufficient for analysis, detection is performed in real-time, it is fast and inexpensive. Therefore, it could be used in point of care analysis and in time to detect selected markers of disease.

ACKNOWLEDGEMENTS

This research was carried out under the project AF-IGA2021-IP050 with financial support from Mendel University in Brno, Czech Republic.

REFERENCES

Amann, A. et al. 2007. Breath analysis: the approach towards clinical applications. Mini Reviews in Medicinal Chemistry, 7(2): 115–29.

Boots, A.W. et al. 2012. The versatile use of exhaled volatile organic compounds in human health and disease. Journal of Breath Research, 6(2): 1–22.

Das, S., Pal, M. 2020. Review–Non-Invasive Monitoring of Human Health by Exhaled Breath Analysis: A Comprehensive Review. Journal of The Electrochemical Society, 167(3): 1–23.

Feng, Y.G. et al. 2017. Ordered macroporous quercetin molecularly imprinted polymers: Preparation, characterization, and separation performance. Journal of Separation Science, 40(4): 971–978.

Jha, S.K. et al. 2014. Molecular imprinted polyacrylic acids based QCM sensor array for recognition of organic acids in body odor. Sensors and Actuators B: Chemical, 204: 74–87.

Kyzas, G.Z., Bikiaris, D.N. 2014. Molecular Imprinting for High-Added Value Metals: An Overview of Recent Environmental Applications. Advances in Materials Science and Engineering, 2014: 1–8.

Matsuguchi, M., Uno, T. 2006. Molecular imprinting strategy for solvent molecules and its application for QCM-based VOC vapor sensing. Sensors and Actuators B: Chemical, 113(1): 94–99.

Myszka, D.G. et al. 1998. Equilibrium analysis of high affinity interactions using Biacore. Analytical Biochemistry, 265(2): 30–326.

Nunez-Naveira, L. et al. 2019. Mass Spectrometry Analysis of the Exhaled Breath Condensate and Proposal of Dermcidin and S100A9 as Possible Markers for Lung Cancer Prognosis. Lung, 197(4): 523–531.

Rick, W. 1965. Pepsin, Pepsinogen, Uropepsinogen. In Methods of Enzymatic Analysis. New York: Academic Press, pp. 819–823.

Stanforth, K.J. et al. 2021. Pepsin properties, structure, and its accurate measurement: a narrative review. Annals of Esophagus, 9: 1–9.

Taranenko, N.A. et al. 2001. Use of gas and liquid chromatography methods in studying the metabolism of organic compounds (review). Gig Sanit, (2): 6–75.

Uludag, Y. et al. 2007. Piezoelectric sensors based on molecular imprinted polymers for detection of low molecular mass analytes. Febs Journal, 274(21): 5471–5480.

Zhang, Q. et al. 2017. Thermoresponsive polymers with lower critical solution temperature: from fundamental aspects and measuring techniques to recommended turbidimetry conditions. Materials Horizons, 4(2): 109–116.

Zhu, H. et al. 2006. Bacterial killing in gastric juice–effect of pH and pepsin on Escherichia coli and Helicobacter pylori. Journal of Medical Microbiology, 55(9): 1265–1270.

Copper and zinc in dogs: impact of sex, age and diet on serum levels

Viola Zentrichova, Alena Pechova
Department of Animal Breeding, Animal Nutrition and Biochemistry
University of Veterinary Sciences Brno
Palackeho trida 1946/1, 612 42 Brno
CZECH REPUBLIC

zentrichovav@vfu.cz

Abstract: The objective of this contribution was to evaluate the impact of sex, age and diet on serum levels of copper and zinc in dogs. Samples were obtained by private veterinarians. Owners of dogs provided information about sex, age and diet, and signed informed consent. Serum was frozen until photometric analysis of copper and zinc. Eighty-one samples were analyzed, 36 from male dogs and 45 from females. Animals were of various ages (0.5–16 years) and breeds. For statistical analysis, normality was tested by Kolmogorov–Smirnov test. Depending on the outcome, either t-test or one-way ANOVA with Student-Newman-Keuls test, or Mann-Whitney U test and Kruskal–Wallis test were used. Serum concentrations of Cu ranged from 1.8 to 8.7 µmol/l (median 4.4 µmol/l). Zinc concentrations were from 4.6 to 22.3 µmol/l (median 9.7 µmol/l). Impact of sex was significant for zinc. Males had median serum level 8.6 µmol/l while females 10.6 µmol/l. Copper was affected by neuter status. Neutered male dogs had lower median (3.6 µmol/l) than intact males (5.4 µmol/l), and both neutered and intact females (4.3 and 4.3 µmol/l, respectively). Age had no impact on Zn. For Cu, young dogs (<2 years) had lower concentrations (median 4.1 µmol/l) than old dogs (>11 years, median 4.8 µmol/l). Diet did not influenced copper, but there was a numerical difference in zinc according to feeding habits. Dogs fed more than 75% of home-made food had median of serum concentrations 8.9 µmol/l, dogs fed combination of home-made and commercial food 9.5 µmol/l and animals fed more than 75% commercial diet 10.3 µmol/l. According to our findings, serum zinc is affected by sex, and there is an ascending trend with larger proportion of commercial food in diet. Copper is affected by age. Also, neuter status has impact on Cu levels in male dogs.

Key Words: home-made food, commercial food, nutrition, neuter status

INTRODUCTION

Copper and zinc are minerals essential for a dog. They both act as cofactors of many enzymes. They are needed for example for haematopoiesis, formation of bones, metabolism of saccharides and proteins, correct skin function or wound healing. In dogs, copper deficiency does not happen naturally. Copper is more discussed because of its role in chronic hepatitis and its pathological storage in liver (Fieten et al. 2012). On the other hand, zinc deficiency can be encountered. The clinical sings are formation of crusts on skin, alopecia, erythema, and sometimes pruritus (White et al. 2001). Unfortunately, up until today, there are no generally accepted reference intervals for concentration of these minerals in blood or biological tissues of dogs. Only two publications attempted to determine normal values in serum. While these authors agree on Cu levels, their reference range for zinc quite differs (Cedeño et al. 2020, Puls 1994). Also, it is not known what factors influence serum levels of these minerals. That complicates the interpretation of results and exposure of deficiencies, mainly subclinical ones. The objective of this contribution was to determine impact of sex, age and diet on copper and zinc serum levels in dogs.

MATERIAL AND METHODS

Animals

The samples were obtained from 81 dogs by privet veterinarians during preventive examinations. Animals were clinically healthy, of various ages (0.5–16 years) and breeds. All of them came from

Czech Republic. The owners signed informed consent and provided information about sex, neuter status, age, and composition of the diet. According to the age, animals were divided into four groups. Young dogs (<2 years), young adults (2–5 years), adults (5–10 years), and old dogs (>11 years). According to the composition of the diet, they were divided into three groups. Animals fed commercial diets (more that 75% of daily dose consisted of commercial food), animals fed home-made diets (more that 75% of daily dose consisted of home-made food), and animals fed combination of both types of diet. Numbers of animals are presented in Table 1.

Table 1 Characterization of animal population, n – number of animals

	Male		Female		Age (years)				Diet		
	Neutered	Intact	Neutered	Intact	<2	2–5	6–10	>11	Commercial	Home-made	Combination
n	11	25	26	19	8	37	21	15	47	20	14

Blood sampling and laboratory analyses

Samples of blood were obtained by venipuncture of *v. jugularis* or *v. cefalica antebrachii*. Tubes with no additives were used. After at least 30 minutes in the room temperature, they were centrifuged and sera were frozen at -80 °C until analysis. Zinc, copper and other biochemical parameters (ALT, AST, ALP, urea, creatinine, total protein, albumin, triglyceride, Ca, P, and Mg – data not included) were analyzed by photometry, using commercially available kits.

Statistical evaluation

All the data were statistically evaluated using UNISTAT v 6.0 (Unistat Ltd, London, United Kingdom). The basic statistical parameters for all the variables were calculated and are shown in the tables. The normality of data distribution was assessed using the Kolmogorov-Smirnov test. Depending on the outcome, either t-test or one-way ANOVA with Student-Newman-Keuls post hoc test, or Mann-Whitney U test and Kruskal–Wallis test were used. The relationship between serum copper or zinc concentrations and other biochemical parameters was evaluated by regression analysis and Spearman´s correlation coefficient is shown. The relationship between mineral levels and age was analyzed in the same way. The statistically significant level was set at $p \leq 0.05$.

RESULTS

Levels of copper and zinc in serum

Serum concentrations of Cu ranged from 1.8 to 8.7 µmol/l (median 4.4 µmol/l, mean 4.7 µmol/l). Range of zinc concentrations was very wide, 4.6 to 22.3 µmol/l (median 9.7 µmol/l, mean 10.4 µmol/l). Figure 1 shows distribution of copper levels and Figure 2 of zinc levels in the whole dataset. Results according to sex and neuter status are presented in Table 2. Table 3 presents Cu and Zn serum concentrations according to age and diet fed to the dogs. For copper, there was a statistically significant correlation with age (c = 0.267, p = 0.016).

Figure 1 Distribution of copper serum levels in dogs (n = 81)

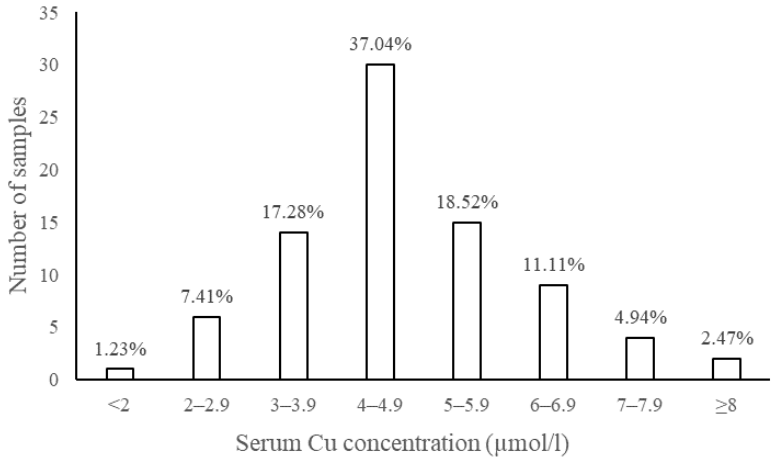

Figure 2 Distribution of zinc serum levels in dogs (n = 81)

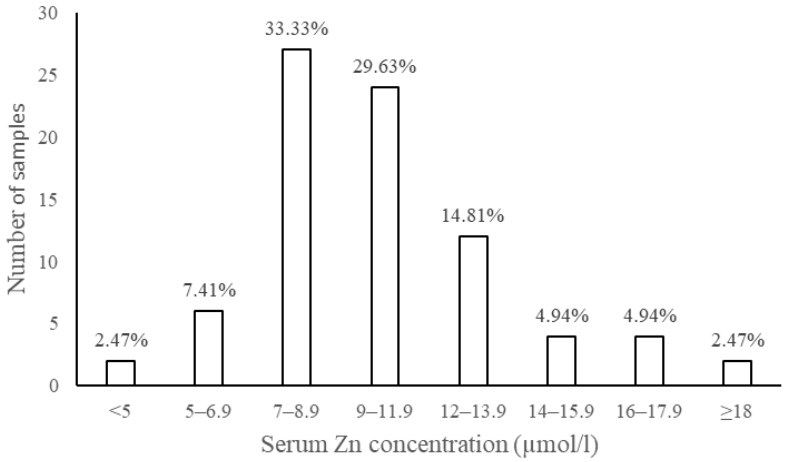

When analyzing correlations of Cu and Zn with other biochemical parameters, following relationships were statistically significant. Copper correlated positively with calcium (c = 0.401, p < 0.001), magnesium (c = 0.261, p = 0.019), albumin (c = 0.244, p = 0.028) and total protein (0.288, p = 0.009). Zinc correlated with calcium (c = 0.219, p = 0.049), magnesium (c = 0.345, p = 0.002), albumin (c = 0.465, p < 0.001) and triglyceride (c = 0.334, p = 0.002).

Table 2 Serum levels according to sex and neuter status, presented as medians

	Male			Female		
	All	Neutered	Intact	All	Neutered	Intact
Copper (µmol/l)	5.0	3.6[b,c,d]	5.4[b]	4.3	4.3[c]	4.3[d]
Zinc (µmol/l)	8.6[a]	8.6	8.7	10.6[a]	11.1	10.1

Legend: same superscripts mark statistical significance

Table 3 Serum levels according to age and diet, presented as medians

	Age (years)				Diet		
	<2	2–5	6–10	>11	Commercial	Combination	Home-made
Copper (µmol/l)	4.1[a]	4.4	4.4	4.8[a]	4.4	4.3	4.4
Zinc (µmol/l)	9.7	8.9	10.6	10.3	10.3	9.5	8.9

Legend: same superscripts mark statistical significance

DISCUSSION

Concentrations of copper and zinc in serum

Unfortunately, there are no generally recognized reference values for concentrations of copper and zinc in serum of dogs. According to our knowledge, the first one who attempted to create normal values was Puls (1994). He came with a range 3.1–12.6 µmol/l for copper and 12.7–30.6 µmol/l for zinc. In recent years, only one other reference values were made. It was by Cedeño et al. (2020). For copper, they were 2.1–11.2 µmol/l and for zinc 3.2–11.8 µmol/l (medians of all measured samples 6.0 and 7.1 µmol/l, respectively). Our results for copper are close to the lower limit of reference values of both authors. For zinc, they correspond more with the earlier study, as they are relatively high. We can also compare our result to previously released studies. For copper, serum levels measured by other authors in healthy dogs are generally higher than in our contribution. For zinc, they correspond with most of the studies. Difference could have been made by choice of analytic method, as we were the only ones using spectrophotometry. Also, geographical location animals came from could influence the results. Table 4 summarizes findings of other authors.

Table 4 Serum levels of Cu and Zn measured in previous studies

Author	Cu (µmol/l)	Zn (µmol/l)	Location	Method
(Cedeño et al. 2020)	7.1[a]	6.0[a]	Spain	ICP-MS
(Vitale et al. 2019)	7.1[a]	11.3[a]	USA	ICP-MS
(Tomza-Marciniak et al. 2012)	21.2[a]	22.9[a]	Poland	ICP-OES
(Mert et al. 2008)	13.3[b]	11.0[b]	Turkey	AAS

Legend: a – median, b – mean, ICP-MS – inductively coupled plasma mass-spectrometry, ICP-OES – inductively coupled plasma optical emission spectrometry, AAS – atomic absorption spectrometry

Impact of sex

In our contribution, female dogs had significantly higher zinc levels than male ones. That opposes findings of Tomza-Marciniak et al. (2012) who did not find any difference in Zn levels according to sex. However, they worked with a smaller number of animals (48, six of them of unknown sex).

Sex by itself had no impact on copper levels. But in male dogs, neuter status did. The reason for neutered dogs having significantly lower Cu concentrations than intact male dogs and all female dogs is unknown.

Impact of age

There was a significant difference between copper serum concentrations of young dogs (<2 years) and old dogs (>11 years). As adult dog groups had medians in between young and old dogs, there is a numerical trend of ascending with age. That again differs from the work of Tomza-Marciniak et al. (2012), as they did not find an impact of age. But our results are in agreement with human research. In men, copper increases with older age (Madarić et al. 1994).

According to our result, we found no influence of age on zinc concentration.

Impact of diet

The diet had no impact on serum levels of copper. For zinc, there was a numerical trend. Serum levels increased with amount of commercial food fed to the dogs on daily basis. That is in agreement with previous study. Dogs fed home-made food had lower Zn levels than ones fed commercial and mixed food (Tomza-Marciniak et al. 2012). Study researching composition of home-made diet for dogs came to the conclusion, that it has lower zinc content than commercial food (Pedrinelli et al. 2019). That might explain lower zinc concentrations in serum of dogs fed home-made diets. Even though the difference was not too large and none of the dogs suffered from sings of zinc deficiency, subclinical deficiency cannot be ruled out.

Correlation with other biochemical parameters

Copper correlated with calcium, magnesium, albumin and total protein. The correlation with albumin was expected. Most of the Cu in serum (40–70%) is in ceruloplasmin, but approximately 10–15% binds to the albumin (Linder 2016). Also, copper binds to other proteins, such as macroglobulin (Linder 2016). That, together with albumin and ceruloplasmin, can explain the correlation with total protein. Other correlations can be explained with albumin as well. Both calcium and magnesium bind to it (Carr 1955). Moreover, there is a positive correlation of albumin with calcium in dogs (Meuten et al. 1982). Also, dogs with low serum protein and albumin have low magnesium levels (Gurumyen et al. 2020).

Zinc correlated with calcium, magnesium, albumin and triglyceride. For the first three mentioned, explanation is similar as with copper, as Zn also binds to albumin (Masuoka and Saltman 1994). It is interesting tough, that there was not a correlation with total protein. The reason for correlation with triglycerides is not known.

CONCLUSION

According to our findings, serum zinc is affected by sex – female dogs had higher concentrations than males. There was also an ascending trend with larger proportion of commercial food in diet. Commercial food so may be a better source of zinc than home-made diets. Serum copper is not affected

by sex itself, but by neuter status. Neutered males had lower Cu concentrations than all the other groups – intact males, intact females and neutered females. Copper was also affected by age – old dogs having higher levels than young ones.

ACKNOWLEDGEMENTS

The research work for this contribution was financially supported by internal grant of University of Veterinary Sciences Brno (201/2021/FVHE).

REFERENCES

Carr, C.W. 1955. Competitive binding of calcium and magnesium with serum albumin. Proceedings of the Society for Experimental Biology and Medicine, 89(4): 546–549.

Cedeño, Y. et al. 2020. Serum concentrations of essential trace and toxic elements in healthy and disease-affected dogs. Animals (Basel), 10(6).

Fieten, H. et al. 2012. Canine models of copper toxicosis for understanding mammalian copper metabolism. Mammalian Genome, 23(1–2): 62–75.

Galan, P. et al. 2005. Serum concentrations of beta-carotene, vitamins C and E, zinc and selenium are influenced by sex, age, diet, smoking status, alcohol consumption and corpulence in a general French adult population. European Journal of Clinical Nutrition, 59(10): 1181–1190.

Gurumyen, G.Y. et al. 2020. Association of serum magnesium with haematological health indices in dogs. Animal Research International, 17(1): 3550–3558.

Linder, M.C. 2016. Ceruloplasmin and other copper binding components of blood plasma and their functions: an update. Metallomics, 8(9): 887–905.

Madarić, A. et al. 1994. Serum copper, zinc and copper/zinc ratio in males: influence of aging. Physiological Research, 43(2): 107–111.

Masuoka, J., Saltman P. 1994. Zinc(II) and copper(II) binding to serum albumin. A comparative study of dog, bovine, and human albumin. Journal of Biological Chemistry, 269(41): 25557–25561.

Mert, H. et al. 2008. Element status in different breeds of dogs. Biological Trace Element Research, 125(2): 154–159.

Meuten, D.J. et al. 1982. Relationship of serum total calcium to albumin and total protein in dogs. Journal of American Veterinary Medical Association, 180(1): 63–67.

Pedrinelli, V. et al. 2019. Concentrations of macronutrients, minerals and heavy metals in home-prepared diets for adult dogs and cats. Scientific Reports, 9(1): 13058.

Puls, R. 1994. Mineral levels in animal health: diagnostic data. 2. ed. Canada: Sherpa International: Clearbrook.

Tomza-Marciniak, A. et al. 2012. Lead, cadmium and other metals in serum of pet dogs from an urban area of NW Poland. Biological Trace Element Research, 149(3): 345–351.

Vitale, S. et al. 2019. Comparison of serum trace nutrient concentrations in epileptics compared to healthy dogs. Frontiers of Veterinary Science, 6: 467.

White, S.D. et al. 2001. Zinc-responsive dermatosis in dogs: 41 cases and literature review. Veterinary Dermatology, 12(2): 101–109.

AUTHORS INDEX

Name of publication:	MendelNet 2021 *Proceedings of 28th International PhD Students Conference*
Editors:	Assoc. Prof. Ing. Radim Cerkal, Ph.D. Ing. Natálie Březinová Belcredi, Ph.D. Ing. Lenka Prokešová
Publisher:	Mendel University in Brno Zemědělská 1665/1 613 00 Brno Czech Republic
Year of publication:	2021
Number of pages:	492
ISBN:	978-80-7509-821-4

Contributions are published in original version, without any language correction.